Lawrence Berkeley National Laboratory
LBL Publications

Title
International Collaboration Activities in Geologic Disposal Research: FY21 Progress

Permalink
https://escholarship.org/uc/item/3g10304s

Authors
Birkholzer, Jens
Faybishenko, Boris

Publication Date
2022-12-24

Peer reviewed

International Collaboration Activities in Geologic Disposal Research: FY21 Progress

Spent Fuel and Waste Disposition

Jens Birkholzer & Boris Faybishenko
Lawrence Berkeley National Laboratory (LBNL)

with contributions from:
Yves Guglielmi, Jonny Rutqvist, LianGe Zheng (LBNL)
Florie Caporuscio, Jeffrey D. Hyman, Kirsten
B. Sauer, Hari Viswanathan (LANL)
Carlos Jové-Colón, Teklu Hadgu,
Kristopher L. Kuhlman, Tara LaForce,
Yifeng Wang, Michael Nole, Edward Matteo (SNL), and
Mavrik Zavarin (LLNL)

APPENDIX E
NTRD DOCUMENT COVER SHEET 1

Name/Title of Deliverable/Milestone/Revision No.	International Collaboration Activities in Geologic Disposal Research: FY21 Progress M2SF-21LB010307012
Work Package Title and Number	Disposal Research International Coordination - LBNL SF-21LB01030701
Work Package WBS Number	1.08.01.03.07
Responsible Work Package Manager	Jens Birkholzer (signature on file)
	(Name/Signature)

Date Submitted   **09-30-2021**

Quality Rigor Level for Deliverable/Milestone[2]	☐ QRL-1 ☐ Nuclear Data	☐ QRL-2	☒ QRL-3	☐ QRL 4 Lab-specific

This deliverable was prepared in accordance with	Lawrence Berkeley National Laboratory (LBNL)
	(Participant/National Laboratory Name)

QA program which meets the requirements of

☒ DOE Order 414.1   ☐ NQA-1   ☐ Other

This Deliverable was subjected to:

☒ Technical Review   ☐ Peer Review

Technical Review (TR)	**Peer Review (PR)**
Review Documentation Provided	**Review Documentation Provided**
☐ Signed TR Report or,	☐ Signed PR Report or,
☐ Signed TR Concurrence Sheet or,	☐ Signed PR Concurrence Sheet or,
☒ Signature of TR Reviewer(s) below	☐ Signature of PR Reviewer(s) below
Name and Signature of Reviewers	**Name and Signature of Reviewers**

Boris Faybishenko (Sec. 1-5, 7) (signature on file)

LianGe Zheng (Exec. Summary, Sec. 7) (signature on file)

Jens Birkholzer (Sec. 6) (signature on file)

NOTE 1:   *Appendix E should be filled out and submitted with each deliverable. Or, if the PICS: NE system permits, completely enter all applicable information in the PICS: NE Deliverable Form. The requirement is to ensure that all applicable information is entered either in the PICS: NE system or by using the NTRD Document Cover Sheet.*

- *In some cases there may be a milestone where an item is being fabricated, maintenance is being performed on a facility, or a document is being issued through a formal document control process where it specifically calls out a formal review of the document. In these cases, documentation (e.g., inspection report, maintenance request, work planning package documentation or the documented review of the issued document through the document control process) of the completion of the activity, along with the Document Cover Sheet, is sufficient to demonstrate achieving the milestone.*

NOTE 2:   *If QRL 1, 2, or 3 is not assigned, then the QRL 4 box must be checked, and the work is understood to be performed using laboratory specific QA requirements. This includes any deliverable developed in conformance with the respective National Laboratory / Participant, DOE or NNSA-approved QA Program.*

NOTE 3:   *If the lab has an NQA-1 program and the work to be conducted requires an NQA-1 program, then the QRL-1 box must be checked in the work Package and on the Appendix E cover sheet and the work must be performed in accordance with the Lab's NQA-1 program. The QRL-4 box should not be checked*

ACKNOWLEDGEMENTS

The authors are thankful to all contributors to the FY21 annual reports of the SFWD program, which have been used as input in this overview of international activities. A complete list of the SFWD program co-authors of such feeder reports is given below. For lack of space, the title page only lists the first author of each feeder report.

LIST OF CONTRIBUTING CO-AUTHORS OF FEEDER REPORTS

LANL Reports:

H. Boukhalfa, E. Chang, S. Chu, A.R. Hoinville, K.D. Morrison, M.J. Rock, M.R. Sweeney, K. Telfeyan, J. Zouabe

LBNL Reports:

S. Babhulgaonkar, S. Borglin, C. Chang, C. Chou, P. Cook, P. Dobson, C. Doughty, P. Fox, M. Hu, L. Lammers, P. Li, S. Nakagawa, P. Nico, L. Peruzzo, N. Subramanian, E. Singer, L.F. Soom, C. Steefel, C. Tournassat, C.-F. Tsang, H. Xu, M. Whittaker, Y. Wu (all LBNL); A. Niemi, C. Juhlin, H. Lorenz, B. Dessirier, A. Tatomir, F. Basirat, E. Lundberg, B. Almqvist (all Uppsala University, Sweden), J.-E. Rosberg (Lund University, Sweden)

LLNL Reports:

C. Atkins-Duffin, W. Bourcier, S.F. Carle, E. Chang, R. Kaukuntla, J. Zouabe

SNL Reports:

E. Basurto, J. Bean, K.W. Chang, C. Choens, E.N. Coker, T. Dewers, M. Gross, C. Herrick, T.A. Ho, R. Jayne, J. Kruichak, R. Leone, C.M. Lopez, M.M. Mills, M. Nemer, H.D. Park, M. Paul, F.V. Perry, B. Reedlunn, S. Russo, A.C. Sanchez, S. Sobolik, A. Salazar, E.R. Stein, T.A. Tuan, Y. Xiong (all SNL), P.C. Lichtner (OFM Research), and G.E. Hammond (PNNL)

EXECUTIVE SUMMARY

Background and Main Objective

This report describes the FY21 status of international collaboration regarding geologic disposal research in the Spent Fuel and Waste Disposition (SFWD) Campaign. Since 2012, in an effort coordinated by Lawrence Berkeley National Laboratory, SFWD has advanced active collaboration with several international geologic disposal programs across the world. Such collaboration has allowed the SFWD Campaign to benefit from a deep knowledge base in regards to alternative repository environments developed over decades and has provided a framework for active peer-to-peer research participation in international groups which conduct, analyze, and model performance-relevant processes. Via international collaboration, the SFWD Campaign also benefits from substantial international investments in research facilities (such as underground research laboratory testing and modeling) and achieves cost savings via joint funding of expensive field experiments. To date, SFWD's International Disposal R&D Program has established formal collaboration agreements with multiple international initiatives and various international partners, and national lab scientists associated with SFWD have conducted a large number of specific collaborative R&D activities that align well with its R&D priorities. Guiding principles for selection of collaboration options and activities have been as follows:

- Focus on activities that align with the strategic direction of the SFWD campaign and complement ongoing disposal R&D (e.g., the science and engineering tools developed in SFWD are tested in comparison with international experiments).

- Select collaborative R&D activities based on technical merit, relevance to safety case, and cost/benefit, and strive for balance in terms of host rock focus and repository design.

- Emphasize collaboration that provides access to and/or allows for participation in field experiments conducted in operating underground research laboratories in clay, crystalline, and salt host rock, which are not currently available in the U.S.

- Focus on collaboration opportunities for active R&D participation of U.S. researchers and close collaboration with international scientists on specific R&D projects relevant to both sides.

Key Issues Tackled in Current and Planned Portfolios

The current work conducted within international activities centers on the following key research questions:

- **Engineered Barrier Integrity:** What is the long-term stability and retention capability of backfills and seals? Can bentonite be eroded when in contact with water from flowing rock fractures? How relevant are interactions between engineered and natural barrier materials, such as metal-bentonite-cement interactions? Is gas pressure increase and gas migration a concern for barrier integrity?

- **Near-Field Perturbation:** How important are thermal, mechanical, and other perturbations to a host rock (such as argillite/clay/shale, crystalline rock, and salt), and how effective is healing or sealing of the damage zone in the long term? How reliable are existing predictive models for the strongly coupled thermal-hydrological-mechanical and chemical behavior of clay and salt formations?

- **Flow and Radionuclide Transport:** What is the effect of high temperature on the diffusion and sorption characteristics of clay materials (i.e., considering the heat load from dual-purpose canisters)? What is the potential for enhanced transport with colloids? Can transport in diffusion dominated formations (i.e., clay, bentonite, salt) and advection dominated systems (i.e., fractured granite) be predicted with confidence?

- **Integrated System Behavior and Performance Assessment:** Can the early-time behavior of an entire repository system, including all engineered and natural barriers and their interaction, be measured and demonstrated? Can this integrated behavior be reliably predicted? Are the planned construction and emplacement methods feasible? Which monitoring methods are suitable for performance confirmation? How reliable are performance assessment models?

Collaboration Opportunities Provided by International Initiatives (Section 3 of this report)

Since 2012, SFWD has joined several multinational collaboration initiatives as a formal partner, and has established a balanced portfolio of selected R&D projects collaborating with international peers.

- *Mont Terri Project*

  The Mont Terri Project is an international research partnership (currently 22 partners) for the characterization and performance assessment of a clay/shale formation. The partnership provides open access to an existing underground research laboratory (URL) in Switzerland, the Mont Terri URL. Partner organizations can conduct experiments in the URL, can participate in experiments conducted by others, and have access to all project results from past and ongoing efforts. In the current phase, the Mont Terri Project comprises about 40 separate experiments that are relevant to all phases in the lifetime of a repository. The annual budget for the *in-situ* work amounts to several million U.S. dollars, complemented by the interpretation, analyses, and modeling work conducted by the partners. The U.S. Department of Energy (DOE) joined the Mont Terri Project in July 2012. Since then, SFWD researchers have engaged in several projects ranging from large-scale heater tests to damage zone, diffusion and fault slip experiments. A significant extension of the Mont Terri URL has recently been undertaken, providing significantly more space for new experiments, some of which have now started. This extension ensures the long-term future of the Mont Terri Project.

- *DECOVALEX Project*

  The DECOVALEX Project (DEvelopment of COupled Models and their VALidation Against EXperiments) is an international research collaboration and model comparison activity for coupled processes simulations in geologic repository systems (currently 17 partners). The project has been active and running for almost 30 years, and is aimed at the development of modeling test cases based on experimental data sets from international Underground Research Laboratories (URLs). Typically, these experimental test cases are proposed by one of the project partners, and are then collectively studied and modeled by all DECOVALEX participants. During this reporting year, DOE scientists participated in a broad range of relevant modeling tasks associated with the current DECOVALEX Project phase referred to as DECOVALEX-2023, which was initiated in early 2020 and will run through December 2023. These tasks include *in-situ* tests on thermal and gas fracturing in argillite, gas migration in bentonite, a full-scale demonstration test in a clay host rock, a full-scale engineered barrier experiment, and a more fundamental task involving laboratory experiments fluid flow, shear, thermal and reaction processes. Furthermore, SFWD scientists are serving as task leads for two additional tasks, one focusing on brine migration in heated salt, and one on performance assessment.

- *Colloid Formation and Migration (CFM) Project*

  The CFM Project is an international research project for the investigation of colloid formation, bentonite erosion, colloid migration, and colloid-associated radionuclide transport. This collaborative project (currently six partners) is one of several experimental R&D projects associated with the Grimsel Test Site (GTS) in the Swiss Alps, a URL situated in sparsely fractured crystalline host rock and one of few facilities underground that permits radionuclide studies. The CFM project conducts radionuclide migration experiments in a fracture shear zone in the GTS, complemented by laboratory and modeling studies. DOE joined the CFM Project in August 2012, but decided to end its official membership in 2015. However, SFWD researchers continue to collaborate with CFM researchers, currently by supplementing the field interpretation with targeted laboratory experiments on thermal alteration and erosion of bentonite colloids.

- *FEBEX Dismantling Project*

  The Full-scale Engineered Barriers EXperiment (FEBEX) experiment at GTS, an *in-situ* full-scale heater test focusing on bentonite backfill in a crystalline host rock, started in 1997 and ended in 2015 after 18 years of operation at a maximum bentonite temperature of about 100°C. A related international collaboration project, referred to as FEBEX Dismantling Project (FEBEX-DP), was initiated

in June 2014 to make optimal use of the long-term test. The objective of FEBEX-DP was to carefully dismantle the test site, perform a post-mortem analysis of engineered and natural barrier components, and conduct joint analysis of the integrity of these barriers. DOE joined the FEBEX-DP Project as one of the initial partners (currently 12 partners). The project has now officially ended, but continues to provide a unique opportunity for better understanding of the performance of barrier components that underwent continuous heating and natural saturation for a significant period. Therefore, some of the project partners, including SFWD researchers, have remained informally involved in collaborative research, for example by additional post post-dismantling characterization and testing of the FEBEX samples, or by continued improvements of interpretative models of the FEBEX in-situ test.

- ***HotBENT (Studying the Effects of High Temperatures on Clay Buffers/Nearfield)***

   Several international organizations (including U.S. DOE) initiated a new collaboration project in 2018 referred to as HotBENT (currently ten partners). Under leadership of NAGRA, the Swiss waste management organization, the project addresses research needs related to the performance of clay buffers and near-field rock at temperature from 150°C to 200°C, which is higher than the 100°C maximum temperature generally assumed for clay-based repository materials. Substantial cost savings can be achieved in the design of a repository if the maximum temperature can be raised without drastic performance implications. However, higher temperatures may lead to potentially detrimental physicochemical changes of engineered and natural materials and may induce complex moisture transport processes. Because the impact of such alterations and processes on the performance of a repository cannot be realistically assessed at the smaller laboratory scale, the objective of HotBENT project is to conduct a full-scale high-temperature heater experiment at the GTS in Switzerland. As of writing this report, the construction and installation of HotBENT has been finalized and the *in-situ* experiment has officially started with the onset of heating on September 9, 2021. The test is set up in a modular fashion, with individual test segments along the experimental tunnel section insulated from each other, so that part of the experiment may be ended and excavated after 5 years, while the remainder of the test keeps running for up to 20 years. Meanwhile, the newly established HotBENT modeling platform provides an opportunity for model improvements and validation through comparative modeling efforts from multiple international teams.

- ***SKB (Swedish Nuclear Fuel and Waste Management) Task Forces***

   The SKB Task Forces are a forum for international collaboration in the area of conceptual and numerical modeling of performance-relevant processes in natural and engineered systems (currently 12 partners). One task force focuses on flow and radionuclide migration processes in naturally fractured crystalline rock (Groundwater Flow and Transport Task Force, Sweden (GWFTS) Task Force); another task force tackles remaining challenges in predicting the coupled behavior of the engineered barrier system (EBS Task Force). While historically both task forces have centered on experimental work conducted at the Äspö Hard Rock Laboratory (HRL) situated in crystalline rock, there have been more and more tasks in recent years that are of generic nature or bring in experiments and data from other URLs. DOE joined both Task Forces in January 2014, and has been actively engaged since. In the GWFTS Task Force, SFWD researchers are currently studying modeling approaches to predict flow channelized flow and reactive transport in fractured crystalline rock. In the EBS Task Force, DOE/SFWD researchers (1) have taken leadership of Task 11, which inolves joint modeling of the HotBENT Column Test conducted at LBNL, and (2) are participating in Task 12 on modeling cement-bentonite interaction experiments.

Above collaborative initiatives all foster active research projects, provide access to field and laboratory data, and/or may allow for participation in field experiments in URLs. Complementing these activities, DOE or its national laboratories have also engaged in collaboration opportunities provided by the Nuclear Energy Agency (NEA) or by certain European Union research programs, where the nature of the engagement is less on active research collaboration rather than on the exchange of information or shared approaches. Examples include NEA's Clay Club, Salt Club, Crystalline Club, Thermochemical Database Project, REPMET, and the Information, Data and Knowledge Management (IDKM) Project.

Bilateral Collaboration Opportunities (Section 4 of this report)

In addition to its extensive cooperation with multiple international organizations under the umbrella of above-listed initiatives, the SFWD program has also explored direct bilateral opportunities for active research collaboration, and has selected additional R&D activities with potential for substantial technical advances. The status of selected opportunities and activities is described below.

- Germany has emerged as one of the most important partners for active research collaboration. SFWD and German partners have a long history of collaborating on model benchmarking and data exchange for salt repositories in bedded salt (at the Waste Isolation Pilot Plant, WIPP, in New Mexico) and domal salt (at the Asse Mine in Germany). The U.S.-German collaboration on salt currently comprises a range of topics, from temperature influence on the deformation behavior of rock salt, to geotechnical barriers in salt formations, and the coupled behavior of crushed rock salt. These topics are all of particular importance for the design, operation, and evaluation of the long-term safety of underground repositories for disposal of high-level radioactive waste in salt. Beyond the salt-focused collaborations, there are many other opportunities for joint research, as Germany like the U.S. is now considering a broad range of host rocks and repository designs. One active collaboration involves, for example, the joint research with the German Helmholtz Zentrum Dresden Rossendorf on surface complexation modeling and development of related thermochemical databases. ES.

- DOE and the National Radioactive Waste Management Agency of France (ANDRA) have established a Memorandum of Understanding (MoU) regarding collaborative work in clay/shale disposal research at the LSMHM Underground Laboratory near Bure (also referred to as Bure URL), which is co-located with the French disposal site Cigeo in Meuse/Haute-Marne in the east of France. (LSMHM stands for Laboratoire de recherche Souterrain de Meuse/Haute-Marne, meaning an underground laboratory in the Meuse/Haute-Marne region in France.) While there are currently no direct bilateral activities involving active research collaboration, ANDRA and U.S. researchers have been closely cooperating under the umbrella of the DECOVALEX Project. ANDRA is leading a new task in the current DECOVALEX-2023 Project, which focuses on the potential for thermal and gas-pressure related fracturing of the argillite host rock at the Bure URL.

- Collaboration with a scientific deep drilling project in Sweden referred to as COSC (Collisional Orogeny in the Scandinavian Caledonides) has provided a valuable opportunity for field testing of site characterization techniques in crystalline host rocks. Since 2017, SFWD scientists have conducted two major field campaigns using the deep borehole to (1) identify deep flowing fracture zones in crystalline rock with new fluid logging techniques, and (2) to probe the coupled hydromechanical and chemical processes in fracture zones, comparing transmissive and not transmissive fractures. International collaboration on best practices and technologies for site selection and characterization is listed as a longer-term goal in the SFWD campaigns 5-Year Plan (Sassani et al. 2020; 2021).

- The Korea Atomic Energy Research Institute (KAERI) Underground Research Tunnel (KURT) is a generic underground research laboratory in a shallow tunnel in granite host rock, located in a mountainous area near Daejeon, Republic of Korea. In collaboration with the Korean Atomic Energy Institute, SFWD researchers in past years collaborated with KAERI colleagues to develop improved techniques for characterizing groundwater flow in a fractured formation and for evaluating the hydrogeological properties of the damage zone around a deep borehole. However, these activities have now ended and there are currently no research activities of SFWD scientists related to KURT.

- Other potential opportunities exist with several disposal programs, such as those from Japan, Belgium, Finland, Czech Republic and China. The Horonobe (sedimentary) and Mizunami (crystalline) URLs in Japan are accessible for SFWD participation under the JNEAP (Joint U.S.–Japan Nuclear Energy Action Plan) agreement. Belgium and Finland have strong R&D programs in geologic disposal and a long history of work in underground research laboratories (HADES URL in Belgium and Onkalo URL in Finland). The Czech Republic has an internationally oriented nuclear waste disposal program, and since 2017 has conducted *in-situ* testing in its Bukov Underground

Research Facility in an existing mine in crystalline rock. Meanwhile, China has launched an ambitious long-term URL R&D plan and has just started construction of its Beishan URL also situated in crystalline host rock. All these countries are open to collaborate with SFWD scientists.

SFWD Research Activities Associated with International Collaboration (Section 6)

Starting in 2012, SFWD has established a balanced portfolio of international R&D activities in disposal science, addressing relevant R&D challenges in fields like engineered barrier integrity, near-field perturbation, RN transport, integrated system behavior and performance assessment. These now form a considerable portion of SFWD disposal research, and significant advances have been made over the past few years across different host rock types and engineered barrier research challenges. Figure ES-1 gives a visual overview of the major international field experiments that SFWD researchers have participated in since 2012, either as active members of the experimental team, or as researchers involved in the interpretative evaluation and model interpretation of the experimental data (see list of experiments in Table ES-1). The figure tries to graphically illustrate the balance and focus of SFWD's international program over the past years. There are a few notable observations:

- Going from the center outward, one can see that SFWD's research is well balanced between EBS focus, near-field focus and far-field emphasis.

- Several experiments address at the same time EBS behavior and near-field processes, which comes as no surprise because *in-situ* experiments in URL tunnels by design have near-field host rock impacts even if the main emphasis may be on the engineered barrier behavior.

- There are many activities related to argillite and crystalline host rock, whereas less international work has been conducted for salt. This can be explained by the U.S. program having its own salt URL in the bedded salts at the Waste Isolation Pilot Plant (WIPP) in New Mexico, so there is less need for international research outside of the U.S.

- The topic of "Integrated System Behavior" features only one experiment with SFWD participation, the Full-Scale Emplacement Experiment (or FE Heater Test) as a demonstration experiment. Given the current status of the U.S. disposal program where R&D is currently generic (i.e., not site-specific) it does make sense to place less emphasis on demonstration experiments.

Overall, the focus on international collaboration has allowed deep engagement of U.S. researchers with the international waste management R&D community in terms of best practices, new science advances, state of the art simulation tools, new monitoring and performance confirmation approaches, lessons learned, etc. The joint R&D with international researchers, the worldwide sharing of knowledge and experience, and the direct access to relevant data/experiments from a variety of URLs and host rocks has helped SFWD researchers significantly improve their understanding of the technical basis for disposal in a range of potential host rock environments. Comparison with experimental data has contributed to testing and validating predictive computational models for evaluation of disposal system performance in a variety of generic disposal system concepts. Comparison of model results with other international modeling groups, using their own simulation tools and conceptual understanding, have enhanced our confidence in the robustness of predictive models used for performance assessment. The possibility of linking model differences to particular choices in conceptual model setup provides guidance into "best" modeling choices and understanding the effect of model uncertainty. Such advances in the ability to make long-term predictions of complex coupled THMC and flow and transport processes contribute directly to improving post-closure performance assessments (PA) models. Selected highlights of recent SWFD research advances related to international collaboration are given below:

Coupled Processes and Alterations in Bentonite-Based Engineered Barrier Systems

Collaborations with the international FEBEX-DP and HotBENT projects involve experimental and modeling studies to better understand temperature-dependent perturbations and alterations in engineered barrier materials. These activities have provided valuable insights as to how repository performance may be affected by these perturbations and alterations.

- Participation in the large scale FEBEX *in-situ* heater and its comprehensive dismantling effort after 18 years of operation has significantly enhanced the understanding of the thermal alteration of EBS materials at moderate disposal temperatures (up to 100ºC), and has led to the development of validated THMC simulation tools for long-term EBS integrity predictions.

- Continued analysis of post-mortem FEBEX-DP bentonite samples provided a sound basis for understanding potential EBS property changes as a result of THMC alterations. Furthermore, microbial experiments conducted on those samples determined whether bentonite materials collected from the FEBEX experiment possess microbial communities capable of metabolizing H_2, and how thermal alterations impact those capabilities.

- After years of planning, preparation and construction, the full-scale HotBENT field experiment started its heating phase on September 9, 2021. HotBENT will test bentonite behavior at much higher temperatures (up to 200ºC) relative to those that were achieved in the FEBEX heater test, to examine whether the maximum temperature in a bentonite-backfilled repository can be raised to this this level without strong performance impact.

Alterations at the Interface Between EBS and Host Rock Materials

Several international collaboration studies made important progress in evaluating interfacial reactions between EBS components and host rock materials. Materials alterations in the vicinity of these interfaces can affect repository performance in multiple ways, for example by changing the flow and transport properties for radionuclides to migrate from the engineered into the natural barrier systems. Interfacial reactions are most prominent early in the lifetime of a repository when EBS materials such as bentonite, metal containers, and cementitious materials have just been emplaced and when thermal-hydrological perturbations remain strong.

- Hydrothermal laboratory studies were conducted to evaluate high-temperature impacts on interfacial processes and alterations, considering multiple EBS materials in contact with crystalline rock (Grimsel granodiorite from the Grimsel Test Site), argillaceous rock (Opalinus Clay from Mont Terri), and carbonate rocks (limestone and marl from Israel).

- Reactive transport simulations were initiated to interpret interfacial reactions and their impact across aged bentonite, concrete/cement, and clay rock interfaces. This activity is aligned with the international CI experiment, which probes diffusive transport across materials emplaced about 14 years ago in a borehole at the Mont Terri URL.

THM Processes in Heated Argillaceous Rock

Through access to several *in-situ* heater experiments, SFWD scientists made significant scientific advances in understanding and predicting the thermo-hydro-mechanical (THM) perturbations occurring in argillaceous host rock after emplacement of heat-emanating radioactive waste.

- The full-scale FE heater test at Mont Terri, now in its 6th year of heating, continues to provide valuable data for comparative THM model testing and validation at a relevant scale.

- High-performance modeling approaches were developed as part of a DECOVALEX-2019 task that allow for simulations of THM processes at the scale of an entire repository while ensuring that the computational load remains manageable. Working with their international partners, SFWD scientists demonstrated that most THM model input parameters for argillite host rock can be up-scaled from laboratory data, but certain parameters, such as those for the excavation disturbed zone, are best characterized *in-situ*.

- The ability to simulate processes and mechanisms of fracture initiation and growth in claystone has been identified as an emerging modelling challenge due to the potential for gas-pressure or thermal damage. These processes now being tested in a new task of the international DECOVALEX-2023 project. The primary focus of this task is predictive and interpretative modeling of a recent *in-situ* fracturing experiments conducted at ANDRA's Bure URL.

Gas Transport in Bentonite and Clay-Based Host Rock

Gas generation from canister corrosion and other processes can impact the performance of a geological disposal facility in several ways: the gas-water interfaces serve as an important vehicle for the transport of radionuclides and microorganisms due to channelized flow and preferential sorption, whereas trapped gas bubbles can cause accumulation or immobilization of radionuclides. Local pressure build-up due to gas production and accumulation can trigger mechanical responses such as deformation or fracturing in low-permeability materials like bentonite and clays. Significant progress was made in understanding the short- and long-term processes involved in the generation and migration of repository gases.

- Modeling studies of gas migration laboratory experiments on compacted clay were conducted under the umbrella of the international DECOVALEX-2019 project. International teams including SFWD scientists compared a suite of novel phenomenological models and approaches for gas migration and identified which ones could best capture the complex phenomenological behavior of gas flow through bentonite.

- With promising simulation methods developed and tested against laboratory experiments, SFWD scientists and their international partners are now testing their predictive capabilities at the field scale, under the umbrella of a new gas-migration task in the DECOVALEX-2023 project.

Coupled Processes, Fluid Flow and Transport in Fractured Crystalline Rock

Because crystalline formations are often fractured, repository performance assessment studies require an understanding of (1) the impact of stress changes and other perturbations on fracture properties, and (2) the large-scale transport patterns of radionuclides migrating in fracture networks from the repository to the biosphere. Two international collaboration activities have made great progress in addressing these challenges.

- Task G of the DECOVALEX-2023 project involves hydromechanical modeling of fracture contact mechanics. International teams are simulating laboratory-scale experiments to link micro-scale THMC effects acting on fracture surfaces with emergent fracture properties such as permeability.

- Under the umbrella of the SKB Task Forces, SFWD scientists performed discrete fracture network (DFN) modeling efforts to characterize the impact of network structure on flow, transport, and fluid-fluid reactive transport. The ability to conduct reactive transport simulation at large fracture network scales has been enabled by the development of new high-performance computing methods.

Coupled Processes in Salt

A broad portfolio of international collaboration has resulted in significant advances regarding the understanding of complex mechanical, hydrological, thermal and chemical processes in domal and bedded salt.

- Collaborative research with German institutions included: (1) the analysis of drift closure in the joint project WEIMOS, (2) the assessment of geotechnical barriers in salt in the collaborative project RANGERS, and (3) the improvement of THM modeling of crushed salt (used as backfill for repository tunnels) in the joint KOMPASS project.

- SFWD scientists are now leading a new task in the international DECOVALEX-2023 project which comprises several modeling steps associated with the Brine Availability Test in Salt (BATS) at WIPP. This will allow SFWD to benefit from the engagement of international partners in the analysis and modeling of brine migration in heated salt.

Characterization of Faults as Potential Transport Pathways

Via field-based and simulation-based research, SFWD scientists made important advances in understanding whether faults in low-permeability host rock can become potential radionuclide migration pathways upon activation from thermal pressurization or gas pressure increase.

- SFWD scientists continued their advanced numerical analysis of the 2015 and 2020 fault reactivation experiments conducted at the Mont Terri URL to explore the link between fault zone complexity,

fault deformation, and permeability change. The close integration of *in-situ* experiments and modeling resulted in important model improvements and provided a better understanding of the hydromechanical behavior of minor faults and fractures.

- Several international partners contributed to new investigations of fault deformation in the Mont Terri URL to investigate the long-term sealing and healing of faults after an initial activation and permeability increase.

Characterization of Fractured Crystalline Rock

A key concern relating to geologic disposal is fractured crystalline rock is the presence of potentially conductive fractures that could result in transport of radionuclides. There is a need for improved hydrological, geophysical, and geochemical site characterization techniques, especially to detect flowing fractures and their hydrogeologic properties, as this will allow for the development of better constrained discrete fracture network (DFN) models.

- In a research cooperation with the "Collisional Orogeny in the Scandinavian Caledonides" (COSC) project in Sweden, a deep borehole was used as a testbed for an advanced downhole probe developed by SFWD scientists. The probe, referred to as SIMFIP, allows identifying flowing fractures, evaluating their hydromechanical properties, and estimating the state of stress in the subsurface.

- The workflow for the characterization of fractured rock via borehole studies as demonstrated at COSC provides a promising blueprint for *in-situ* testing across various potential repository sites, in particular in crystalline host rock.

Performance Assessment

Recognizing the importance of building confidence in the models, methods, and software used for performance assessment (PA) of deep geologic repositories, SFWD researchers have increased their international collaboration in this area.

- In Task F of the DECOVALEX 2023 project, confidence in performance assessment models and methods is enhanced by comparing PA modeling results from ten international disposal programs applied to the same reference cases, one involving a repository in a fractured crystalline host rock and another featuring a repository in a bedded salt formation.

- Radionuclide transport simulations are a central component of any performance assessment model, as these evaluate transport from the repository to the biosphere for dose calculations. Continued collaboration with the international research community led to significant improvement of thermodynamic and thermochemical databases and models for radionuclide transport simulations.

Outlook for International Collaboration (Sections 5 and 7)

SFWD's international research portfolio has evolved, and continues to evolve, as research priorities change and new collaboration opportunities emerge. The campaign routinely reviews, assesses, and develops such opportunities in close integration with international partners, evaluates the technical merit and alignment with the SFWD objectives, and makes revisions to the portfolio of international R&D activities as appropriate. Given its importance within the overall portfolio of disposal research activities, any such planning and prioritization is done in tight integration with all other disposal research areas, e.g., the host-rock specific research portfolios, the EBS research portfolio, and the performance assessment research portfolio. This report identifies several additional opportunities for international collaboration which the campaign may consider going forward, such as field experiments addressing gas transport in engineered and natural barriers, diffusion experiments, studies with focus on microbial processes, experiments testing sealing elements for tunnels, shafts and boreholes, bentonite degradation and erosion experiments, corrosion studies and last not least collaborative studies to develop best practices and technologies for site selection and characterization. International collaboration also provides ample opportunity of training/educating junior staff well suited to move the U.S. disposal research program forward into the next decades, a promising avenue for developing a next generation workforce of disposal scientists.
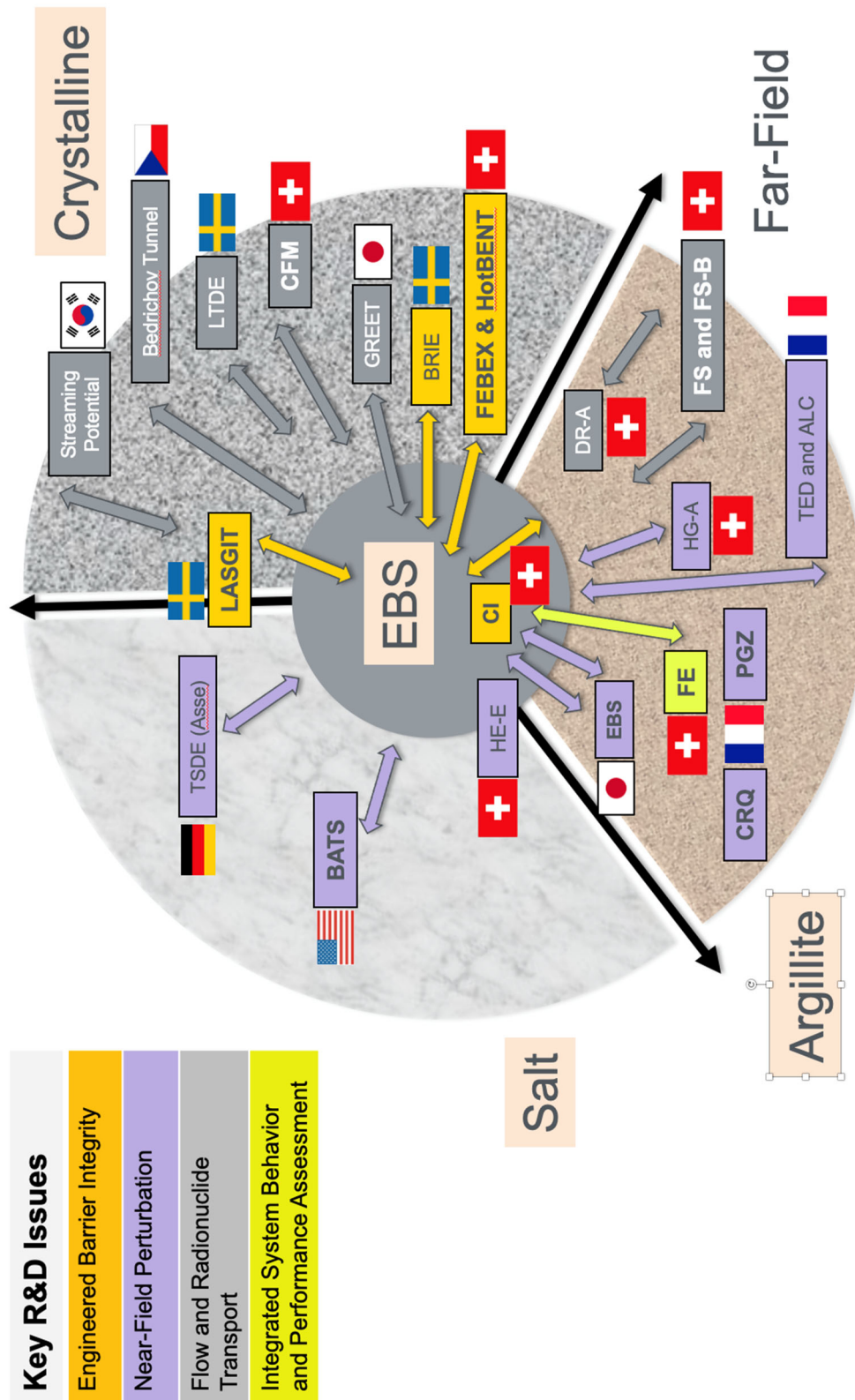
Figure ES-1. High-level overview of the major field international URL experiments conducted in various countries that SFWD researchers have participated in since 2012. Experiments in bold denote currently active collaborations. See Table ES-1 for more information on each experiment. Status: September 2021.

International Collaboration Activities in Different Geologic Disposal Environments

Table ES-1. High-level overview of the major international URL experiments conducted in various countries that SFWD researchers have participated in since 2012. Status: September 2021.

Key Topics	International Experiment	URL	Main R&D Focus
Engineered Barrier Integrity	Cement Clay Interaction (CI) Experiment	Mont Terri, Switzerland	Chemical interaction between host rock and engineered barrier materials
	Bentonite-Rock Interaction Experiment (BRIE)	Äspö HRL, Sweden	Understand the impact of flowing fractures in crystalline rock on bentonite saturation, integrity and erosion
	Engineered Barrier System (EBS) Experiment	Horonobe, Japan	Studies of the thermo-hydro-mechanical-chemical (THMC) behavior of the EBS
	Full-Scale Engineered Barrier Experiment - Dismantling Project (FEBEX-DP)	Grimsel Test Site, Switzerland	Dismantling and sampling of long-term test evaluating the long-term integrity and performance of heated bentonite
	HotBENT Experiment	Grimsel Test Site, Switzerland	Complex THMC behavior of EBS materials up to 200 degrees C at the canister/bentonite interface
	Large-scale Gas Injection Test (LASGIT)	Äspö HRL, Sweden	In situ monitoring of gas migration processes in bentonite buffer
Near-Field Perturbation	Heater Experiment E (HE-E)	Mont Terri, Switzerland	Bentonite/rock interaction to evaluate sealing and clay barrier performance at elevated temperature, micro-tunnel
	Thermal Experiment (TED) / Full-scale Emplacement Test (ALC)	Bure, France	Upscaling THM simulations from lab tests to repository scale
	Gas Path Though Host Rock Experiment (HG-A)	Mont Terri, Switzerland	Evaluation of flow paths through the near-field damage zone and specifically along seals
	Thermal Simulation for Drift Emplacement (TSDE)	Asse Mine, Germany	Model benchmarking studies for thermal-hydrological-mechanical behavior salt heater test
	Brine Availability Test in Salt (BATS)	WIPP, USA	Monitoring brine distribution, inflow, and chemistry from heated salt using geophysical methods and direct liquid & gas sampling
	Fault Slip Experiments FS and FS-B	Mont Terri Switzerland	Fault reactivation due to repository-induced effects and permeability generation
	CRQ Thermal Fracturing Experiment	Bure, France	Testing the behavior of argillite host rock to a thermal fracturing stress regime
	PGZ Gas Fracturing Test	Bure, France	Testing the behavior of argillite host rock upon high-pressure gas injection
Flow and Radionuclide Transport	Bedrichov Tunnel Experiment	Bedrichov, Czech Republic	Interpretation of water inflow patterns and tracer transport behavior in fractured granite
	Fault Slip (FS) Experiment	Mont Terri, Switzerland	Evaluation of pressure increase impacts on reactivation of faults
	GREET (Groundwater Recovery Experiment)	Mizunami, Japan	Evaluation of early resaturation behavior in crystalline rock looking at flow behavior and chemical-biological interactions upon resaturation
	Long-Term Sorption Diffusion Experiment (LTDE)	Äspö HRL, Sweden	Monitoring the diffusion behavior in fractured crystalline rock
	DR-A Experiment (Diffusion Retention and Perturbation Test)	Mont Terri, Switzerland	Ion diffusion through compacted clay where electro-chemical charges affect transport behavior
	Colloid-Facilitated Radionuclide Migration Test (CFM)	Grimsel Test Site, Switzerland	RN transport of bentonite colloids compared in a shear zone in fractured granite
	Streaming Potential Test	KURT, Korea	Site characterization techniques (in situ borehole characterization)
Integrated System Behavior	Full-scale Emplacement Experiment (FE)	Mont Terri, Switzerland	Full-scale demonstration experiment, one of the largest and longest-duration heater tests

TABLE OF CONTENTS

LIST OF FIGURES

LIST OF TABLES

LIST OF ACRONYMNS/INSTITUTIONS

AD	Air-dried
ALC	Full-scale Emplacement Experiment, Bure URL, France
ANDRA	National Radioactive Waste Management Agency, France
BASE	Federal Office for the Safety of Nuclear Waste Management, Germany
BATS	Brine Availability in Salt Experiment, WIPP, New Mexico
BBM	Barcelona Basic Model
BExM	Barcelona Expansive Model
BCV	Czech Bentonite (BCV) from Cerny Vrch deposit (north western region of the Czech Republic)
BGE	Federal Company for Radioactive Waste Disposal, Germany
BGR	Federal Institute for Geosciences & Natural Resources, Germany
BGS	British Geological Survey
BMT	Benchmark Test
BMWi	Ministry for Economy and Labor, Germany
BRIE	Bentonite Rock Interaction Experiment, Äspö HRL, Sweden
BRIUG	Beijing Research Institute of Uranium Geology
C-A-S-H	Calcium Silicates Hydrates with Limited Substitution of Al for Si
CASSM	Continuous Active-Source Seismic Monitoring
CDFs	Arrival Time Distributions
CCDFs	Complement of the Cumulative Distributions
CEC	Cation Exchange Capacity
CFD	Computational Fluid Dynamics
CFM	Colloid Formation and Migration Project, Grimsel Test Site, Switzerland
CFT	Colloid Facilitated Transport
CI	Cement Interaction Test, Mont Terri, Switzerland
CIEMAT	Centro Investigaciones Energéticas Medioambientales y Tecnológicas, Madrid, Spain
CNL	Constant Normal Load
CNS	Constant Normal Stiffness
COSC	Collision Orogeny in the Scandinavian Caledonides
COVID	Coronavirus
COX	Callovo-Oxfordian Claystone
CPU	Central Processing Unit
CRIEPI	Central Research Institute of Electric Power Industry, Japan
CRR	Colloid and Radionuclide Retardation Project, Grimsel Test Site, Switzerland
C-S-H	Calcium Silicate Hydrate
CT	Computed Tomography
CTD	Closure Test Drift
DECOVALEX	DEvelopment of COupled Models and their VALidation Against EXperiments
DFN	Discrete Fracture Network
DI	Deionized

DITF	Drilling-Induced Tensile Fractures
DLVO	Derjaguin, Landau, Vervey, and Overbeek
DOE	Department of Energy, USA
DPC	Dual Purpose Canister
DR-A	Diffusion, Retention, and Perturbation Experiment, Mont Terri, Switzerland
DR-C	Thermal Diffusion Test, Mont Terri, Switzerland
DRZ	Disturbed Rock Zone
DSC	Differential Scanning Calorimetry
DSS	Distributed Brillouin Strain Sensing
EB	Engineered Barrier
EBS	Engineered Barrier System
EC	Electrical Conductivity
EDL	Electrical Double Layer
EDRAM	International Association for Environmentally Safe Disposal of Radioactive Waste
EDS	Energy Dispersive X-ray Spectroscopy
EDZ	Excavation Damage Zone (or Excavation Disturbed Zone)
EG	Ethylene Glycol
EMP	Electron Microprobe
ENRESA	National Radioactive Waste Corporation, Spain
ENSI	Swiss Federal Nuclear Safety Inspectorate, Switzerland
EPA	U.S. Environmental Protection Agency
ERT	Electrical Resistivity Tomography
ESEM	Environmental Scanning Electron Microscopy
ETH	Swill Federal Institute of Technology Zurich
FANC	Federal Agency for Nuclear Control, Belgium
FDM	Finite Difference Method
FE	Full-scale Emplacement Experiment, Mont Terri, Switzerland
FEBEX	Full-scale Engineered Barrier Experiment
FEBEX-DP	FEBEX Dismantling Project
FEM	Finite Element Method
FEPs	Features, Events, and Processes
FFEC	Flowing Fluid Electrical Conductivity
FRAM	Feature Rejection Algorithm for Meshing
FS	Faults Slip Hydro-Mechanical Characterization Experiment, Mont Terri, Switzerland
GAST	Gas Permeable Seal Test, Grimsel Test Site, Switzerland
GBM	Granular Bentonite Material
GC	Gas Chromatography
GREET	Groundwater REcovery Experiment in a Tunnel
GT	Gas Transport Experiment, Mont Terri, Switzerland
GTS	Grimsel Test Site, Switzerland
GWFTS	Groundwater Flow and Transport Task Force, Sweden

HADES	High Activity Disposal Experimental Site, Mol, Belgium
HE-E	Heater Experiment in Micro-tunnel, Mont Terri, Switzerland
HG-A	Gas Path through Host Rock and Seals Experiment, Mont Terri, Switzerland
HLM	High-Level Radioactive Waste
HM	Hydro-Mechanical
HMC	Hydro-Mechanical-Chemical
HPC	High-Performance-Computing
HRL	Hard Rock Laboratory
IAEA	International Atomic Energy Agency
i-BET	In Situ Bentonite Erosion Test, Grimsel Test Site, Switzerland
IfG	Institute für Gebirgsmechanik
IGSC	Integration Group for the Safety Case
IRSN	Institut de Radioprotection et de Sûreté Nucléaire, France
JAEA	Japan Atomic Energy Agency, Japan
JNEAP	U.S.–Japan Nuclear Energy Action Plan
KAERI	Korea Atomic Energy Research Institute, Republic of Korea
KIT	Karlsruhe Institute of Technology, Karlsruhe, Germany
KTH	Royal Institute of Technology, Stockholm, Sweden
KURT	KAERI Underground Research Tunnel, Republic of Korea
LANL	Los Alamos National Laboratory, USA
LASGIT	Large-Scale Gas Injection Test, Äspö HRL, Sweden
LBNL	Lawrence Berkeley National Laboratory, USA
LIT	Long-term *In-situ* Test, Grimsel Test Site, Switzerland
LLNL	Lawrence Livermore National Laboratory, USA
LXO	LeachXS/Orchestra
LSMHM	Laboratoire de recherche Souterrain de Meuse/Haute-Marne
LSP	Liquid-Solid Partitioning
LTD	Long-Term Diffusion, Grimsel Test Site, Switzerland
LTDE	Long-Term Diffusion Sorption Experiment, Äspö HRL, Sweden
MA	Microbial Activity Test, Mont Terri, Switzerland
MACOTE	Materials Corrosion Test, Grimsel Test Site, Switzerland
MC	Monte Carlo
MD	Molecular Dynamics
MoU	Memorandum of Understanding
MWCF	Major Water Conducting Feature
Na-MMT	Na-Montmorillonite
NAGRA	Swiss Waste Management Organization
NBS	Natural Barrier System
NE	Nuclear Energy
NEA	Nuclear Energy Agency
NTS	Nevada Test Site
NUMO	Nuclear Waste Management Organization of Japan

NWMO	Nuclear Waste Management Organization, Canada
OBAYASHI	Construction, Engineering and Management Company, Japan
OPA	Opalinus Clay
OPC	Ordinary Portland Cement
PA	Performance Assessment
PNNL	Pacific Northwest National Laboratory
POSIVA	Nuclear Waste Management Organization, Finland
QXRD	Quantitative X-Ray Diffraction
RBSN	Rigid-Body-Spring Network
R&D	Research and Development
REPRO	Rock Matrix Retention Properties, Onkalo URL, Finland
RH	Relative Humidity
ROK	Republic of Korea
RWM	Radioactive Waste Management Limited, UK
SCK/CEN	Belgian Nuclear Research Centre, Belgium
SET	Borehole Sealing Test, Grimsel Test Site, Switzerland
SEM	Scanning Electron Microscopy
SFWD	Spent Fuel and Waste Disposition
SIMFIP	Step-Rate Injection Method for Fracture *In-situ* Properties
SKB	Swedish Nuclear Fuel and Waste Management, Sweden
SNF	Spent Nuclear Fuel
SNL	Sandia National Laboratories, USA
SOTA	State of the Art
SP	Streaming Potential
SSM	Swedish Nuclear Waste Regulator
SURAO	Radioactive Waste Repository Authority, Czech Republic
SW-A	Sandwich Experiment, Mont Terri, Switzerland
swisstopo	Federal Office of Topography, Switzerland
TC	Test Case
TDB	Thermochemical Database
TDE	Through Diffusion Experiment, Onkalo URL, Finland
TDRW	Time Domain Random Walk
TED	Thermal Experiment, Bure URL, France
TEM	Transmission Electron Microscope
TGA	Thermogravimetric Analysis
TH	Thermo-hydro
THC	Thermo-hydro-chemical
THM	Thermo-hydro-mechanical
THMC	Thermo-hydro-mechanical-chemical
TSDE	Thermal Simulation for Drift Experiment, Asse Mine, Germany
TUC	Clausthal University of Technology, Germany
UFD	Used Fuel Disposition

UFZ	Umweltforschungszentrum Leipzig-Halle, Germany
UPC	Polytechnic University of Catalonia, Barcelona, Spain
URL	Underground Research Laboratory
VSG	Gorleben Repository
WIPP	Waste Isolation Pilot Plant, New Mexico, USA
WPDE	Water Phase Diffusion Experiment
XRD	X-Ray Diffraction
XRF	X-Ray Fluorescence

1. INTRODUCTION

Since 2012, in an effort coordinated by Lawrence Berkeley National Laboratory (LBNL), the Spent Fuel and Waste Disposition (SFWD) Campaign has advanced active collaboration with several international geologic disposal programs in Europe, North America, and Asia. Such collaboration has allowed the SFWD Campaign to benefit from a deep knowledge base in regards to alternative repository environments developed over decades and has provided a framework for active peer-to-peer research participation in international groups which conduct, analyze, and model performance-relevant processes. Via international collaboration, the SFWD Campaign also benefits from substantial international investments in research facilities (such as underground research laboratory testing and modeling) and achieves cost savings via joint funding of expensive field experiments. To date, SFWD's International Disposal R&D Program has established formal collaboration agreements with six international initiatives and various international partners. National lab scientists associated with SFWD have participated in a balanced portfolio of international R&D activities in disposal science, addressing relevant R&D challenges in fields like near-field perturbation, engineered barrier integrity, RN transport, and integrated system behavior. These form a considerable portion of SFWD disposal research and significant advances have been made over the past years. The current international activities center on the following key research questions:

- **Engineered Barrier Integrity**: What is the long-term stability and retention capability of backfills and seals? Can bentonite be eroded when in contact with water from flowing fractures? How relevant are interactions between engineered and natural barrier materials, such as metal-bentonite-cement interactions? Is gas pressure increase and gas migration a concern for barrier integrity?

- **Near-Field Perturbation:** How important are thermal, mechanical, and other perturbations to a host rock (such as argillite/clay/shale, crystalline rock, and salt), and how effective is healing or sealing of the damage zone in the long term? How reliable are existing predictive models for the strongly coupled thermal-hydrological-mechanical and chemical behavior of clay and salt formations?

- **Flow and Radionuclide Transport**: What is the effect of high temperature on the diffusion and sorption characteristics of clays (i.e., considering the heat load from dual-purpose canisters)? What is the potential for enhanced transport with colloids? Can transport in diffusion dominated (i.e., clay, bentonite, salt) and advection dominated systems (i.e., fractured granite) be predicted with confidence?

- **Integrated System Behavior and Performance Assessment**: Can the early-time behavior of an entire repository system, including all engineered and natural barriers and their interaction, be measured and demonstrated? Can this integrated behavior be reliably predicted? Are the planned construction and emplacement methods feasible? Which monitoring methods are suitable for performance confirmation? How reliable are performance assessment models?

International collaboration has allowed engagement of U.S. researchers with the international waste management R&D community in terms of best practices, new science advances, state of the art simulation tools, new monitoring and performance confirmation approaches, lessons learned, etc. The joint R&D with international researchers, the worldwide sharing of knowledge and experience, and the access to relevant data/experiments from a variety of Underground Research Laboratory (URLs) and host rocks has helped SFWD researchers significantly improve their understanding of the current technical basis for disposal in a range of potential host rock environments. Comparison with experimental data has contributed to testing and validating predictive computational models for evaluation of disposal system performance in a variety of generic disposal system concepts. Comparison of model results with other international modeling groups, using their own simulation tools and conceptual understanding, have enhanced our confidence in the robustness of predictive models used for performance assessment. The possibility of linking model differences to particular choices in conceptual model setup provides guidance into "best" modeling choices and understanding the effect of model uncertainty. International collaboration also provides opportunities for training/educating junior staff well suited to move the U.S. disposal research program forward into the next decades. Promising avenues exist for further expansion of the international program.

International Collaboration Activities in Different Geologic Disposal Environments

This annual report describes the FY21 status of international collaboration regarding geologic disposal research in the SFWD. The focus of the report is on opportunities that provide access to field data (and respective interpretation and modeling), and/or allow participation in ongoing and planned field experiments. The report is an update to earlier annual reports summarizing SFWD's international activities (Birkholzer, 2012, 2014, 2015, 2016; Birkholzer et al., 2017, 2018, 2019a, 2020).

2. STRATEGY FOR INTERNATIONAL COLLABORATION

Recognizing the benefits of international collaboration toward the common goal of safely and efficiently managing the back end of the nuclear fuel cycle, DOE's Office of Nuclear Energy (NE) and its Office of Spent Fuel and Waste Research and Development (formerly Used Fuel Disposition, UFD) have developed a strategic plan to advance cooperation with international partners (UFD, 2012). International geologic disposal programs are at different maturation states, ranging from essentially "no progress" in some countries to select sites to pending license applications in others. The opportunity exists to collaborate at different levels, ranging from providing expertise to those countries "behind" the U.S. to sharing information and expertise with those countries that have mature programs. Working with other countries optimizes limited resources by integrating knowledge developed by researchers across the globe.

SFWD's strategic plan lays out two interdependent areas of international collaboration (UFD, 2012). The first area is cooperation with the international nuclear community through participation in international organizations, working groups, committees, and expert panels. Such participation typically involves conference and workshop visits, information exchanges, reviews, and training and education. Examples include multinational activities, such as under International Atomic Energy Agency (IAEA) (e.g., review activities, conference participation, and education), OECD/Nuclear Energy Agency (NEA) (e.g., participation in annual meetings, Integration Group for the Safety Case membership, NEA Thermochemical Database, NEA's Clay Club, NEA's Salt Club, NEA's Crystalline Club), and EDRAM (International Association for Environmentally Safe Disposal of Radioactive Waste). DOE also actively supports several bilateral agreements for international information exchanges and other collaboration purposes. SFWD will continue participation in and/or support of ongoing international collaborations in this first area, will assess their benefits, and will identify the need for expanding or extending their scope. New activities and agreements may be developed with an eye toward the objectives and R&D needs of the United States (UFD, 2012).

The second area of international collaboration laid out in the strategic plan involves active R&D participation of U.S. researchers within international projects or programs (UFD, 2012). Active collaboration means in this report that U.S. researchers work closely together with international scientists on specific R&D projects relevant to both sides. With respect to geologic disposal of radioactive waste, such active collaboration provides direct access to information, data, and expertise on various disposal options and geologic environments that have been collected internationally over the past decades. Many international programs have been operating underground research laboratories (URLs) in clay/shale, granite, and salt environments, in which relevant field experiments have been and are being conducted. Depending on the type of collaboration, U.S. researchers can participate in planning, conducting, and interpreting experiments in these URLs, and thereby get early access to field studies without having *in-situ* underground research facilities in the United States.

SFWD considers this second area, active international R&D, to be particularly beneficial to the program, helping to efficiently achieve the program's key disposal research goals, such as the short- and medium-term research objectives as described in *Update of the Used Fuel Disposition Campaign Implementation Plan (FCRD- UFD-2014-000047, September 2014* (Bragg-Sitton et al., 2014)). For example, the Campaign Implementation Plan called for achieving a "comprehensive understanding of the current technical basis for disposal of used nuclear fuel and high-level nuclear waste in a range of potential disposal environments to identify long-term R&D needs" and developing "advanced, predictive computational models, with experimental validation, for evaluation of disposal system performance in a variety of generic disposal system concepts and environments." It was decided in 2012 that the SFWD campaign priority should focus on advancing and utilizing such active international collaboration in disposal research. Coordinated by LBNL, a focused effort was made to collect information on international opportunities that complement ongoing disposal R&D within the SFWD, help identify those activities that provide the greatest potential for substantive technical advances, interact with international organizations and programs to help advance specific collaborations, and initiate specific R&D activities in cooperation with international partners.

Active collaboration can be achieved under different working models. One option is informal peer-to-peer interaction with international R&D organizations. Many U.S. scientists involved in SFWD research activities

have close relationships with their international counterparts, resulting from workshops and symposia meetings, or from active R&D collaboration outside of SFWD. Continued SFWD support for participation of U.S. researchers in relevant international workshops, meetings, conferences and symposia helps foster discussion and expand such relationships. Other working models for active international collaboration require that DOE becomes a formal member in multinational initiatives. Since the launch of the international disposal research collaboration program in 2012, DOE has joined six international cooperation initiatives as a formal partner, the DECOVALEX Project, the Mont Terri Project, the Colloid Formation and Migration Project (2012 through 2015), the Full-scale High-Level Waste Engineered Barriers Experiment Dismantling Project (FEBEX-DP), the SKB (Swedish Nuclear Fuel and Waste Management) Task Forces, and recently the HotBENT Project, a high-temperature Engineered Barrier System (EBS) experiment to be conducted at the Grimsel Test Site in Switzerland. All of these provide access to field data from URLs and/or allow participation in ongoing and planned URL field experiments. Section 3 of this report gives a comprehensive overview of these initiatives and describes the various opportunities arising from DOE's membership. Outside of the above initiatives, SFWD scientists also collaborate with individual international disposal programs, which may or may not require formal bilateral agreements. Section 4 presents an overview of the international disposal programs that are open to bilateral collaboration with U.S. researchers. Both of these sections describe relevant collaboration opportunities that the SFWD campaign has already engaged with as well as others that are promising for potential engagement.

The benefit of international collaboration needs to be evaluated, and periodically reevaluated, in the context of the open R&D issues that can be addressed through collaborative scientific activities. Section 5 points out that a reassessment of SFWD's international research portfolio has been conducted routinely in lieu of changing research priorities and boundary conditions and the development of new opportunities for collaboration. The sections start with the first planning exercise for the international portfolio conducted by SFWD in FY11 and FY12, which led to the initial selection of a set of R&D activities that align with current goals, priorities, and funded plans of SFWD, and follows with a description of annual replanning activities. A thorough "deep dive" reassessment was recently conducted as part of a broad SFWD campaign roadmap update, described in Sevougian at el. (2019). The purpose of this roadmap update was to summarize the progress of ongoing generic disposal R&D activities since 2012, to re-assess R&D priorities, and to identify new activities of high priority, such as R&D on disposal of dual-purpose canisters (DPCs) which now contain a significant fraction of the Nation's commercial spent fuel activity. In FY20, the DOE requested development of a formal plan for activities in the disposal research in SFWD for the next five-year period, which resulted in a strategic guidance document that also includes a five-year direction for the international collaboration tasks. Results from these recent reassessments are briefly described and plans for better alignment of international modeling activities with new performance assessment modeling are discussed in Section 5.

Finally, Section 6 provides brief summaries of all international collaboration research activities conducted by SFWD researchers in FY21 (including some relevant activities from FY20 or earlier). Example R&D results are presented, albeit without exhaustive explanations, since these are provided in several referenced feeder reports. Each research activity in Section 6 provides a pointer back to the specific international initiative or bilateral cooperation described in Section 3 and 4 that has provided the opportunity for collaboration.

3. MULTINATIONAL COOPERATIVE INITIATIVES

This section gives a comprehensive overview of the six international cooperation initiatives that DOE has joined as a formal partner. These are the Mont Terri Project, the DECOVALEX Project, the Colloid Formation and Migration Project (CFM), the FEBEX Dismantling Project, the HotBENT Project, and the SKB Task Forces. Table 3.1-1 lists the international waste disposal organizations currently participating in these initiatives, sorted by country. The table demonstrates the high level of cooperation between nuclear nations. As mentioned before, the focus of DOE's international collaboration strategy is on initiatives that foster active research with other international disposal programs, provide access to field data (and respective interpretation/modeling), and/or may allow participation in ongoing and planned field experiments in URLs (Sections 3.1 to 3.4). Section 3.5 briefly touches on other international collaboration initiatives organized by the Nuclear Energy Agency (NEA) or by certain European Union initiatives where the nature of our engagement is less focused on active collaboration and more on the exchange of information and shared approaches. Note that this section describes both cooperation opportunities that SFWD scientists are already participating in as well as some others where future engagement could be beneficial

3.1. Mont Terri Project

3.1.1. Introduction to the Mont Terri Project

The Mont Terri Project is an international research project for the hydrogeological, geochemical, and geotechnical characterization of a clay/shale formation suitable for geologic disposal of radioactive waste (Zuidema, 2007; Bossart and Thury, 2007). The project was officially initiated in 1996, and has been conducted in a clay-rock underground rock laboratory, which lies north of the town of St-Ursanne in northwestern Switzerland. The URL is located at a depth of ~300 m below the surface in argillaceous claystone (Opalinus Clay). The rock laboratory resides in and beside the security gallery (initially the reconnaissance gallery) of the Mont Terri motorway tunnel, which was opened to traffic at the end of 1998. The rock laboratory consists of the security gallery with small niches excavated in 1996, Gallery 98 with 5 lateral niches, excavated in 1997/98, a gallery for the EZ-A experiment, excavated in 2003, Gallery 04 with 4 lateral niches excavated in 2004, and Gallery 08 with side galleries for the Mine-by Test and Full-scale Emplacement Experiment excavated in 2008 (Figure 3.1-1). An additional excavation was conducted recently and has significantly expanded the URL, providing ample space for additional experiments. More information can be found at https://www.mont-terri.ch.

The Mont Terri Project operates as a collaborative program providing open access to an existing URL and the results of investigations. The research program consists of a series of individual experiments divided into annual project phases, running from July 1 in one year to June 30 the next year. The Swiss Federal Office of Topography, swisstopo, helps conduct the operation and maintenance of the rock laboratory, and provides the operational management and experimental support. Organized as a consortium, the partner organizations (currently 22) fund the experiments and the related technical work. Partner organizations can select to conduct experiments, can participate in experiments conducted by others, and have access to all project results from past and ongoing efforts, which are available in reports and a project-owned web-based database. Planning, steering, and financing is the responsibility of all partners participating in a given experiment.

Over the years, the organizations involved in the Mont Terri Project have provided substantial financial investments. Additional support has been contributed by the European Community and by the Swiss Federal Office for Science and Education. It is not surprising, therefore, that the Mont Terri Project has been very successful, and a wide range of experimental studies on clay/shale behavior (including backfill/buffer behavior) have been conducted. In recognition of the Mont Terri Project's 20th anniversary in 2016, a Special Issue of the Swiss Journal of Geosciences provided a range of publications describing key experiments and achievements of the Mont Terri Project (Bossart et al., 2017).

Table 3.1-1. Participation of International Programs in Cooperative Initiatives Related to URLs: Status September 2021.

Nuclear Nation	Organizations	DECOVALEX 2023	Mont Terri	Colloid Formation And Migration	FEBEX-DP	HotBENT	SKB Task Forces
Belgium	SCK/CEN		×				
	FANC		×				
Canada	NWMO	×	×			×	×
	CNSC	×					
China	CAS	×					
Czech Republic	SURAO	×			×	×	×
France	ANDRA		×		×		
	IRSN		×				
	Total		×				
Finland	POSIVA		×		×		×
Germany	BASE	×	×				
	BGE	×	×	×		x̶	×
	BGR	×	×		×	×	×
	GRS		×	×			×
	BMWi/KIT						
	Helmholtz Ass.	×	×				
Japan	JAEA	×	×				×
	CRIEPI		×				×
	Obayashi		×		×	×	
	NUMO			×		×	
Netherlands	COVRA	×					
Rep. of Korea	KAERI	×		×	×	×	×
Spain	ENRESA	×	×		×	×	×
	CIEMAT				×		
Sweden	SKB	×			×	×	×
	SSM	×					×
Switzerland	NAGRA	×	×	×	×	×	
	ENSI		×				
	ETH		×				
	swisstopo		×				
Taiwan	TaiPower	×					
United Kingdom	RWM	×	×	×	×	×	×
United States	DOE	×	×	(x)	×	×	×
	Chevron		×				×

6

Figure 3.1-1. 3D schematic of the Mont Terri URL with side galleries and drifts. This schematic does not show the recently finalized expansion of the URL. Abbreviations point to some of the key experiments conducted at Mont Terri.

In 2011, the DOE leadership recognized that membership in the Mont Terri Project could be highly beneficial to SFWD's R&D mission, and in early 2012 decided to formally apply for membership. DOE's partnership started officially with Phase 18 of the project, which ran from July 1, 2012 through June 30, 2013. Today, DOE is one of 22 partners from nine countries of the Mont Terri Project, namely from Switzerland (swisstopo, ENSI, NAGRA, ETH), Belgium (SCK/CEN, FANC), Canada (NWMO), France (ANDRA, IRSN, Total), Germany (BASE, BGE, BGR, GRS, Helmholtz Association), Japan (OBAYASHI, JAEA, CRIEPI), Spain (ENRESA), United Kingdom (RWM), and the U.S. (Chevron, DOE). Participation in the project provides an unlimited access to an operating URLs in a claystone environment, with several past and ongoing experiments that are highly relevant to SFWD's R&D objectives. The DOE's membership has given SFWD researchers an access to relevant field data and project resulting from all past Mont Terri phases. More importantly, SFWD researchers have been working collaboratively with international scientists on selected experimental studies, which include the design, characterization, modeling, and interpretation aspects related to field experiments. DOE also has an opportunity to propose and eventually conduct its own experiments at the Mont Terri URL, which could be an option for project future phases.

Figures 3.1-2 and 3.1-3 show an overview of key experiments conducted at the Mont Terri URL as described in the 2016 Special Issue of the Swiss Journal of Geosciences (see Bossart et al., 2017 and other publications in the Special Issue). The timeline in Figure 3.1-2 places these experiments in the context of relevance to different phases in the lifetime of a repository: (1) Experiments related to initial conditions and repository construction, (2) Experiments related to early-time perturbations, (3) Experiments related to transient- to late-time post-closure phase of a repository. For comparison, the figure also shows two features that are important for the repository evolution: (1) the temperature variations in the buffer (red curve) indicating the thermal loading of the disposal system canister emplacement, and (2) the transient changes in buffer saturation (blue curve) indicating the slow process the bentonite buffer reaching fully saturated conditions. Figure 3.1-3 shows the same key experiments in a plan view.
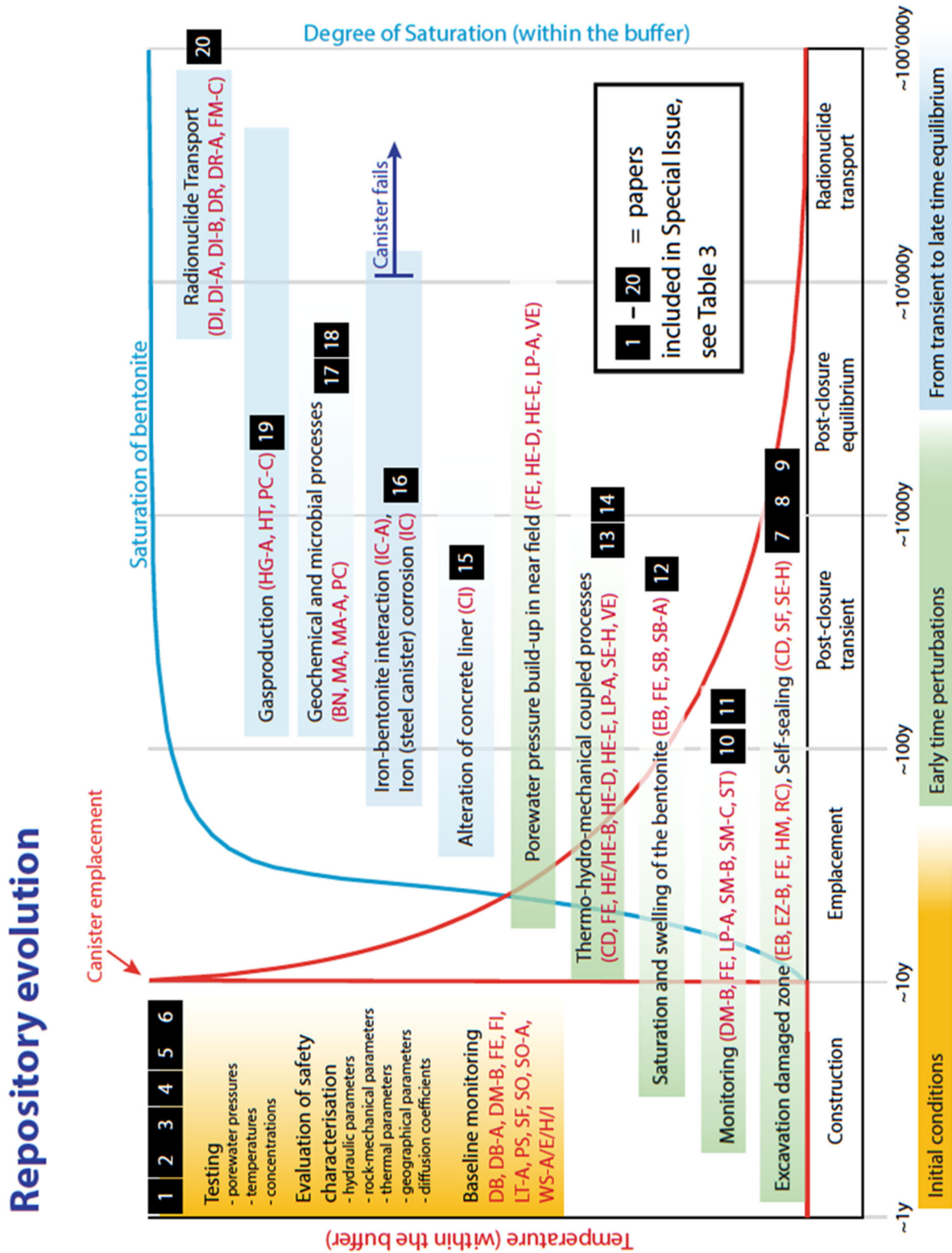
Figure 3.1-2. Major Mont Terri URL experiments as described in Bossart et al. (2017), displayed with respect to repository phases. Only a subset of the full Mont Terri experimental portfolio is shown here. Number 1-20 in black point to publications in the 2016 Special Issue of the Swiss Journal of Geosciences.
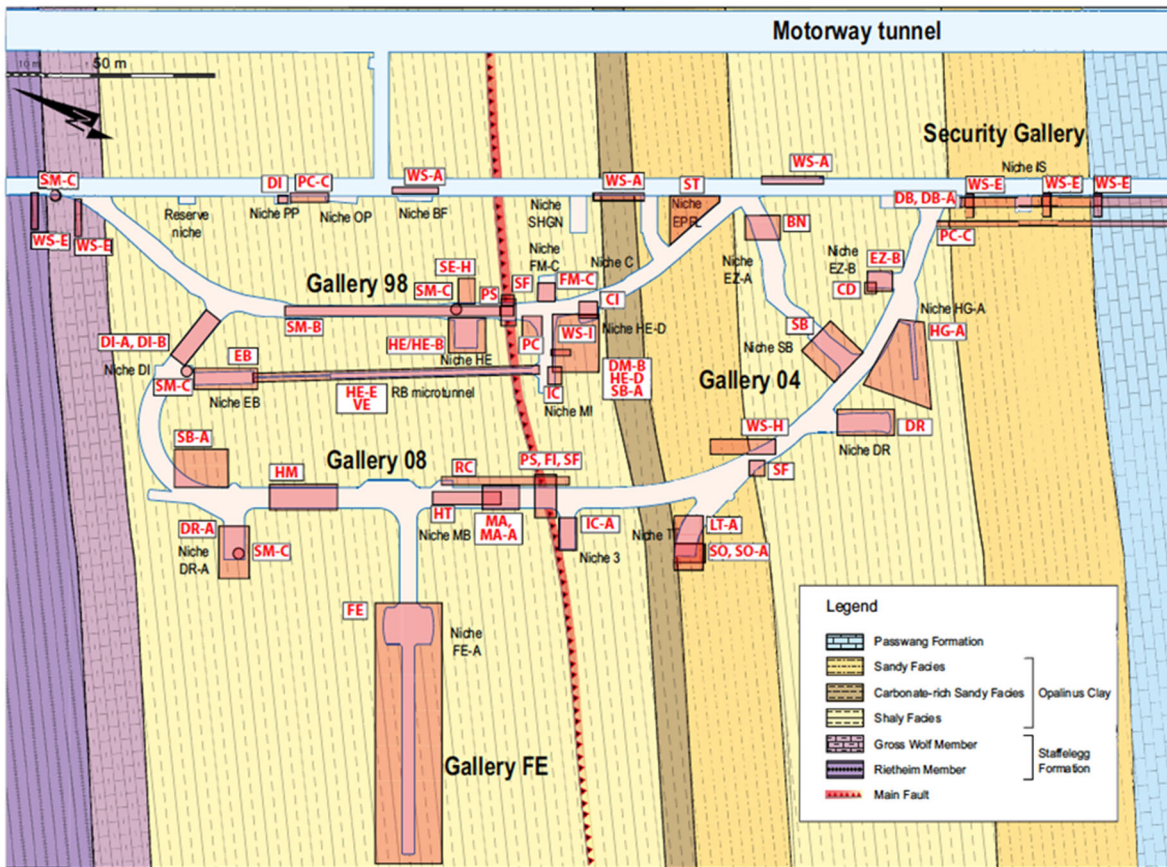
BN	Bitumen-nitrate-clay interaction	**HT**	Hydrogen transfer
CD	Cyclic deformations	**IC**	Iron corrosion of Opalinus Clay
CI	Cement-clay interaction	**IC-A**	Corrosion of iron in bentonite
DB	Deep inclined borehole through the Opalinus Clay	**LP-A**	Long-term monitoring of parameters (porewater pressures)
DB-A	Porewater characterisation-Benchmarking	**LT-A**	Clay properties, analyses of labtesting
DI	Diffusion in rock	**MA**	Microbial activity in Opalinus Clay
DI-A	Long-term diffusion	**MA-A**	Modular platform for microbial studies
DI-B	Long-term diffusion	**PC**	Porewater chemistry
DM-B	Long-term deformation measurements	**PC-C**	Gas porewater equilibrium
DR	Diffusion and retention experiment	**PS**	Petrofabric and strain determination
DR-A	Diffusion, retention and perturbations	**RC**	Rock mass characterisation
EB	Engineered barriers	**SB**	Selfsealing barriers clay - sand mixtures
EZ-B	Fracture generation	**SB-A**	Borehole sealing experiment
FE	Full scale emplacement demonstration	**SE-H**	Self-sealing with heat (Timodaz)
FI	Fluid-mineral interactions in Opalinus Clay during natural faulting and heating	**SF**	Self-sealing of tectonic faults
FM-C	Flow mechanism (tracer)	**SM-B**	High resolution seismic monitoring
HE/HE-B	Heater experiments I and II	**SM-C**	Permanent nanoseismic monitoring
HE-D	THM behaviour of host rock (heater test)	**SO**	Sedimentology of Opalinus Clay
HE-E	In-situ heater test in VE microtunnel	**SO-A**	Palynology of the Opalinus Clay
HG-A	Gas path host rock & seals	**ST**	Seismic transmission measurements
HM	Experimental lab investig. on HM-coupled properties & behavior Opalinus Clay	**VE**	Ventilation test
		WS-A/E/H/I	Porewater profiles, wet spots

Figure 3.1-3. Plan view of the Mont Terri URL with key experiments and selected list of relevant experiments. Gallery FE indicates the area of the FE Heater test, which is currently the largest subsurface heater experiment worldwide (Bossart et al., 2017). This schematic does not show the recently finalized expansion of the URL.

Many experiments shown in Figure 3.1-2 and 3.1-3 are long-running tests that have carried on into the current Phase 26 (July 2021 through June 2022) of the Mont Terri Project, and that will continue into future project phases. While a few experiments at Mont Terri are relevant to other subsurface applications, such as geologic carbon sequestration, the majority of activities is related to geologic disposal of radioactive waste or has cross-cutting relevance including waste disposal. Since 2012, DOE has engaged in several such experiments, such as the HE-E (*In-situ* Heater Experiment in Micro-tunnel) Heater Test, the EB Engineered Barrier Experiment, the Mine-by Test, the HG-A Experiment (Gas Path through Host Rock and Seals Experiment), and the DR-A Diffusion, Retention, and Perturbation Experiment. Currently, SFWD scientists are participating in, or utilizing data from, three major tests at Mont Terri: the FE Heater Test, the FS and FS-B Fault Slip Experiments, and the CI-D Cement-Clay Interaction Experiment. General information about the experiments in which DOE is currently involved is given in Sections 3.1.2 through 3.1.5, and summaries of SFWD research activities related to these experiments are provided in Section 6. Almost all of these field experiments are further supported by laboratory and modeling tasks.

The collaborative nature of the Mont Terri project allows for efficient initiation and planning of new experimental works. At each Technical Meeting, which is held in the January or February months, partner organization(s) may give a brief presentation of any new proposed work to be annually conducted in the upcoming Mont Terri project phase(s). The proposing partners need to present the technical scope and merits of the proposed work, give a rough cost estimate, and then invite other partner organizations to consider joining the new task. In some cases, the proposing partners could provide a direct financial contribution to the experiment, and in other cases, may invite partners to conduct monitoring or modeling analysis complementing their proposal. They will then write a short project description prior to the next Mont Terri Steering Committee Meeting (which is typically held a few months following the Technical Meeting), where ongoing and new experiments are selected. The experimental program for the next project phase is then finalized, including the consideration of financial contributions of partners, at the second Steering Committee Meeting held just before the start of the new phase. Partners can be found if the proposed work aligns with the interest of other Mont Terri organizations. It is important to note that the existing infrastructure at Mont Terri makes developing and conducting experiments very easy, even if the proposing partner is located far away from the URL. Swisstopo can handle many of the organizational details, if needed, and there is a long list of experienced contractors available to conduct the actual experimental work.

In the Spring of 2018, the Mont Terri Project started construction on a significant extension of the URL, which has now been finalized and provides a significant additional working space for new large-scale experiments. As shown in Figure 3.1-4, extension of the URL was achieved via a tunnel loop excavated in a southwestward direction. Prior to and during the excavation, the project leads held several planning exercises to brainstorm how the new experimental space should be used. About 45 proposals for new experiments were submitted, of which about 60% were nuclear waste related. Some of these have now been initiated or are in final planning stages. These offer promising opportunities for DOE to engage (see some examples in Section 3.1.5).

Section 3.1.2 through 3.1.5 below describe selected experiments conducted at Mont Terri, starting with some that DOE is already involved with followed by other potentially relevant new opportunities for engagement.
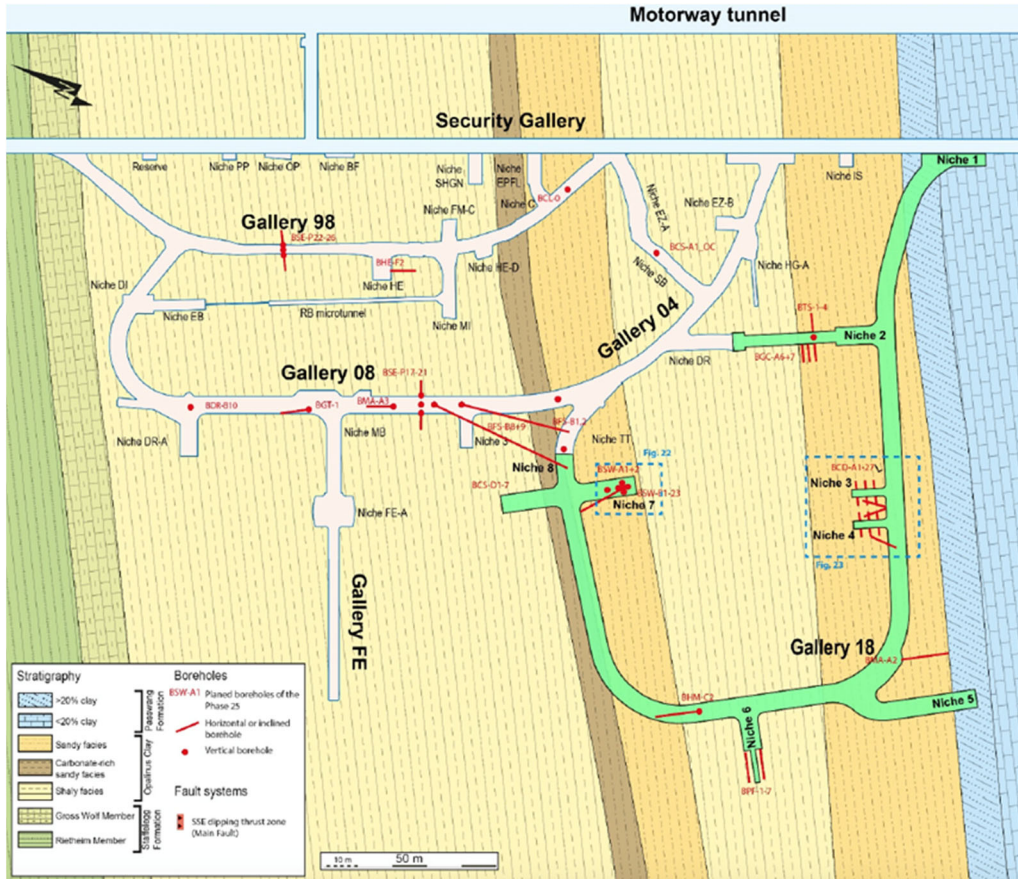
Figure 3.1-4. Plan view of the Mont Terri URL after extension of the URL in mostly southwestward direction. The green coloring shows the added tunnels and niches.

3.1.2. FE Heater Test

The Full-Scale Emplacement Experiment (FE Heater Test) is one of the largest and will likely be the longest-duration subsurface heater tests ever conducted. This heater experiment has been designed by NAGRA as a long-term test for the performance of geologic disposal in Opalinus Clay, with focus on both EBS components and host-rock behavior. Mont Terri partners collaborating with NAGRA in this experiment are ANDRA, BGR, GRS, NWMO, and, starting from July 2012, DOE. As shown in Figures 3.1-5 through 3.1-7, the FE Heater Test is conducted in a side niche and gallery at Mont Terri, excavated along the claystone bedding plane for this purpose, with 50 m length and about 2.8 m diameter. Heating from emplaced waste is simulated by three heat-producing canisters of 1500 W maximum power. A sophisticated monitoring program was planned and implemented, including dense pre-instrumentation of the site for *in-situ* characterization, dense instrumentation of bentonite buffer and host rock, and extensive geophysical monitoring. A thermo-hydro-mechanical (THM) modeling program is conducted in parallel with the testing and monitoring activities.

After years of preparation and construction, including installation of the heaters, the bentonite buffer, and instrumentation, the heaters were turned on in February 2015 (Figure 3.1-8). During the preparation phase, predictive THM models of the anticipated FE Heater Test behavior had been developed by some project partners (among them SFWD scientists from LBNL), for the support of the design and instrumentation planning, as well as for the comparison of "blind predictions" with measured THM effects. In the final design, a staged heating approach was employed in which the three heaters were turned on subsequently (Figure 3.1-9). This ensured that the models for predicting the maximum temperature in the buffer were validated against early temperature data from one heater before running all three heaters at the same time.
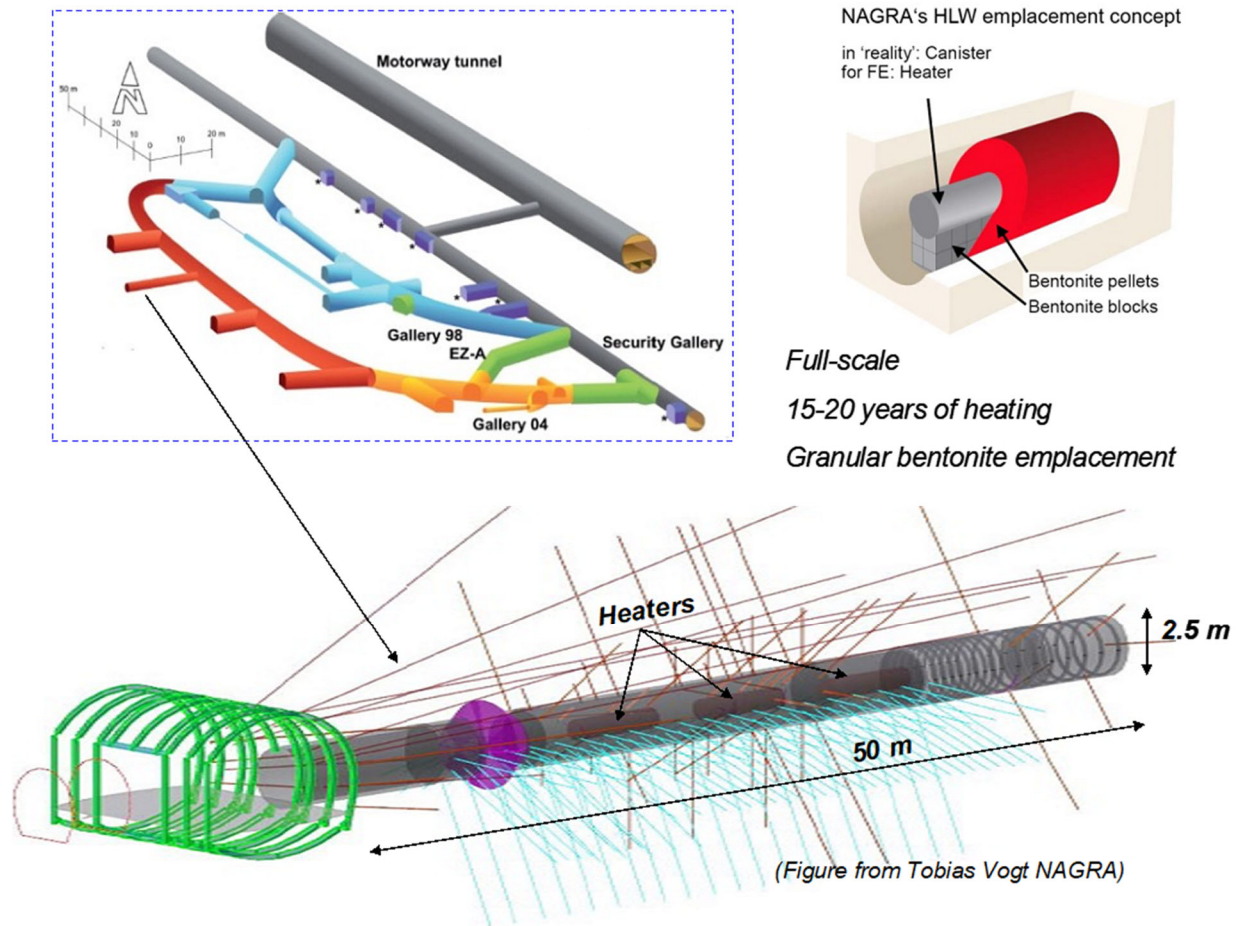
Figure 3.1-5. FE Heater Test at Mont Terri URL: experiment setup and borehole layout (Zheng et al., 2015)

After now more than 6.5 years of heating, the experiment has already provided valuable data for the validation of THM coupling effects regarding the processes in the host rock, while accounting for (and examining) the expected conditions in the emplacement tunnel (temperature, saturation, stress pressure, and swelling pressure). Due to the 1:1 scale of the experiment, it is possible to achieve realistic temperature, saturation, and stress gradients. The experiment also allows for the testing of backfilling technology with granular bentonite, as well as an application of lining technology with shotcrete, anchors, and steel ribs, and provides an ample opportunity for examining the suitability of various monitoring methods. Processes examined in the test cover many aspects of the repository evolution, such as the EDZ (Excavation Damage Zone, or Excavation Disturbed Zone) creation and desaturation during tunnel excavation and operation (including ventilation for about one year), reconsolidation of the EDZ, resaturation, thermal stresses, and thermal pore-pressure increase after backfilling and heating (heating and monitoring period > 10 years). Monitoring data from the FS Heater Test are now being utilized in a THM modeling task in the DECOVALEX-2023 project (see Section 3.2.3.3). SFWD researchers and their international partners continue to work on the interpretative modeling of the first several years of monitoring data from the FE Heater test. Specifically, two modeling teams from LBNL and SNL respectively are participating in the DECOVALEX-2023 task featuring the FE Heater Test; a brief summary of these modeling activities is given in (Section 6.3.1).
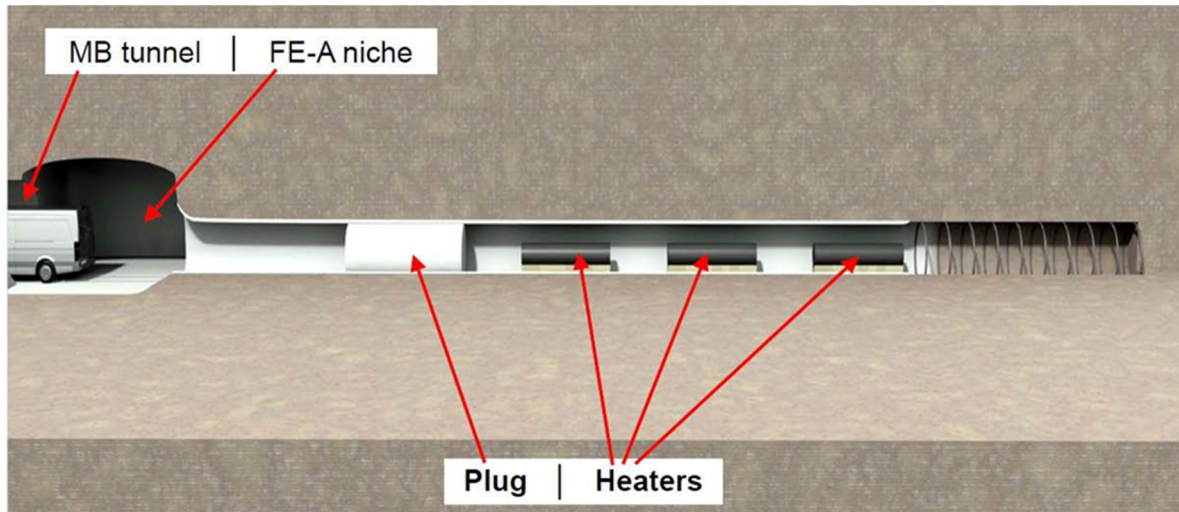
Figure 3.1-6. FE Heater Test: Side view of the experiment setup and the heater layout (Garitte, 2010).

Figure 3.1-7. View from the FE gallery into the heater tunnel during final installation (Bossart, 2014).
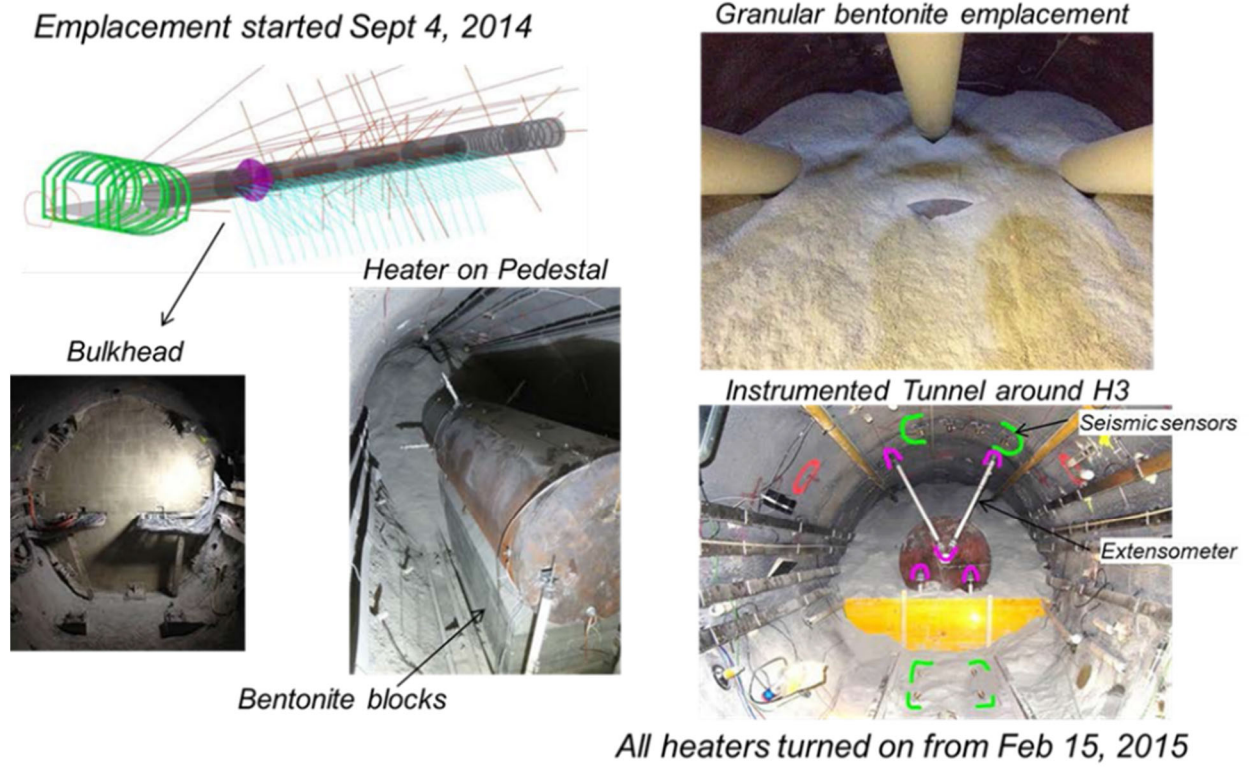
Figure 3.1-8. Images from the construction and installation of heaters, bentonite buffer and plugs (Zheng et al., 2016).
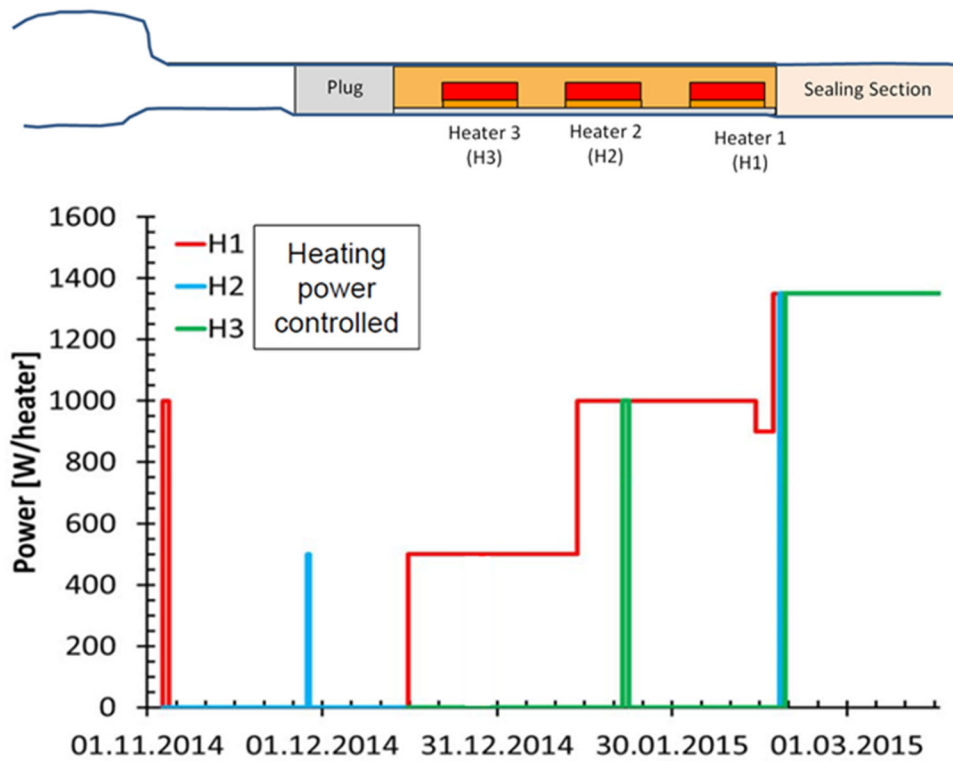
Figure 3.1-9. Heat power applied to Heaters H1, H2 and H3 during the start-up of heating at the Mont Terri FE experiment

3.1.3. FS and FS-B Fault Slip Experiments

Text As shown in Figure 3.1-10, the Mont Terri URL is transected by an intermediate-scale fault which provides intriguing opportunities for *in-situ* testing of fault activation and fault slip caused by pressure and stress changes. In geologic repositories for nuclear waste, such changes could be triggered, for example, by thermal stresses or gas pressure increases. In 2015, researchers at Mont Terri conducted a first fault activation experiment referred to as the Fault Slip (FS) Test, which was aimed at understanding: (i) the conditions for slip activation and stability of clay faults, and (ii) the evolution of the coupling between fault slip, pore pressure and fluids migration. Results obtained by the experiment are crucial for defining mechanisms of natural and induced earthquakes, their precursors and risk assessment, and for a better understanding of a possibility of the loss of integrity of natural low permeability barriers. Recent studies suggest that slow slip of faults may be a dominant deformation mechanism of shale during hydraulic stimulation or other large subsurface injection activities (Zoback et al., 2012). The same mechanism may be important in case of the stress perturbation, which may reactivate a pre-existing fault and eventually enhance rock permeability, for example due to drilling of a network of underground galleries for radioactive waste emplacement. Of similar concern may be the fault slip caused by the pore pressure increase due to heating from the high-level waste or from the generation of gas due to steel corrosion. Hence, the possibility of increasing permeability caused by fault slip and generation of potential pathways in the host rock or in an upper sealing formation could cause a major risk for the long-term safety of a repository.

The key idea of the 2015 FS experiment at Mont Terri was to conduct controlled fault-slip experiments via localized pressurization in a packed-off section of a borehole drilled through the Mont Terri main fault zone (Figures 3.1-10 and 3.1-11). Water was injected between inflatable packers at increasing flow rates to progressively decrease the effective stress until fault destabilization occurs, while monitoring injection flow rate, pore pressure, fault slip and normal displacement evolution from the stable to the unstable fault states. Monitoring was performed with a new device called the SIMFIP probe (Guglielmi et al., 2013a,b), which is capable of measuring slip velocities and slip deformation at unprecedented spatial resolution (Figure 3.1-12). The probe allows for simultaneous high-frequency monitoring of full 3D-deformations of the borehole wall, fluid pressure, and injection flow rate within a 1.5m long injection chamber set between two inflatable packers. The accuracy of measurements is very high, with a measurement resolution of 10^{-6} for deformations, 10^{-3} Pa for pressure, and 0.1 L/min for flow rate.

Two experimental test sequences using the SIMFIP probe in the main fault zone were conducted in May and October 2015. Both test sequences involved injection into different test intervals in two separate boreholes (Figure 3.1-13). Prior to active testing, the detailed three-dimensional geology of the main fault was characterized and the regional state of stress was determined. The aim of the analysis was to estimate how the fault zone structural heterogeneity controls the fault slip activation and what would be the effect on pore pressures. Indeed, as shown in Figure 3.1-11, the Mont Terri fault displays a high structural heterogeneity characterized by solitary slickensides, millimeter-thin gouges associated with scaly clay having contrasted hydraulic and mechanical properties, which could generate complex shear stress concentrations and hydromechanical couplings.

Figure 3.1-14 shows typical monitoring results from the Mont Terri controlled-release injection test, here depicted for four different borehole intervals. Three of the intervals in or near the fault damager zone are characterized by an initial pressure increase without significant flow followed by a sudden increase in the flow rate occurring without any significant increase of pressure, indicating that the tested fault segment is opening to accept fluid (Fracture Opening Pressure—FOP). In contrast, no clear flow rate variation was observed in the fault core (Test 44.65 m), suggesting that different parts of the fault have different hydromechanical behavior. (Most of the flow rate transients depicted on the figure are related to pumping artifacts.) Results from these tests were utilized as a modeling task in the DECOVALEX-2019 project (see Section 3.2.2).
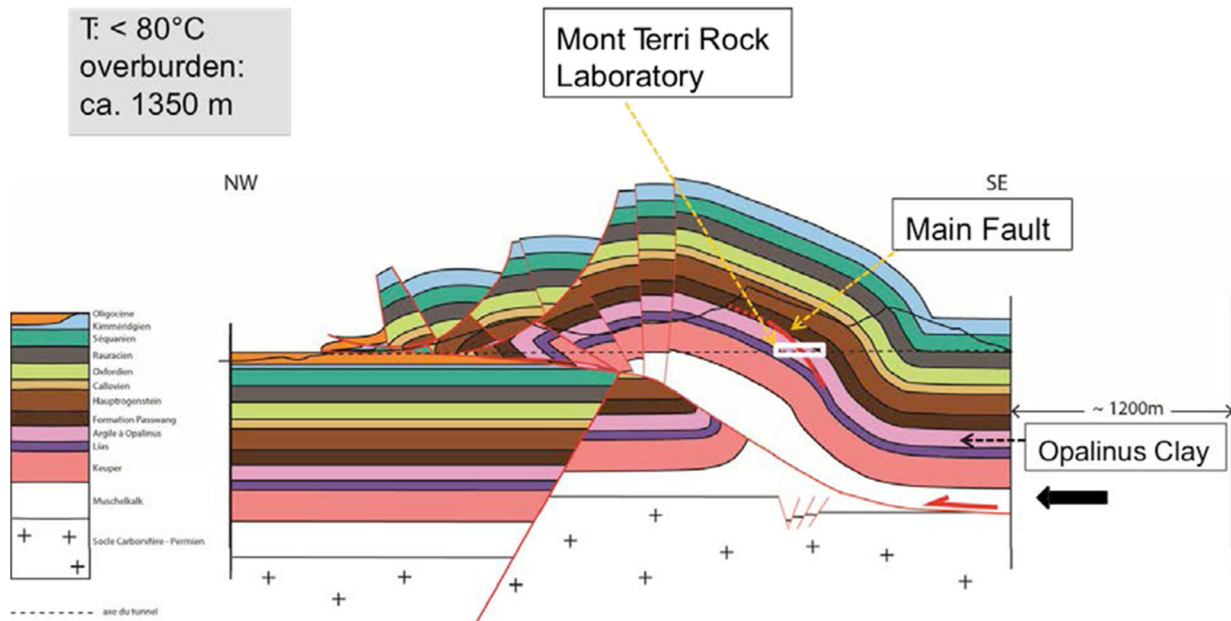
Figure 3.1-10. Geologic setting showing Mont Terri URL and location of main fault (Guglielmi et al., 2015c).
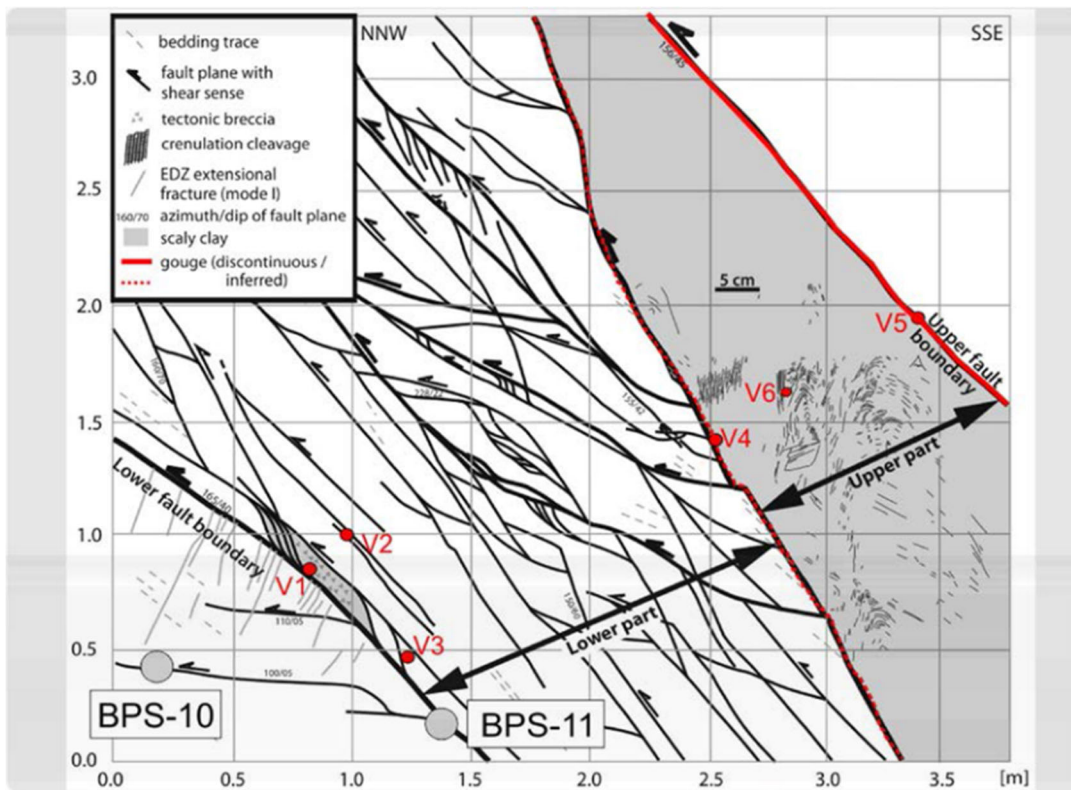
Figure 3.1-11. Detailed fault geometry at Mont Terri (Guglielmi et al., 2015c).
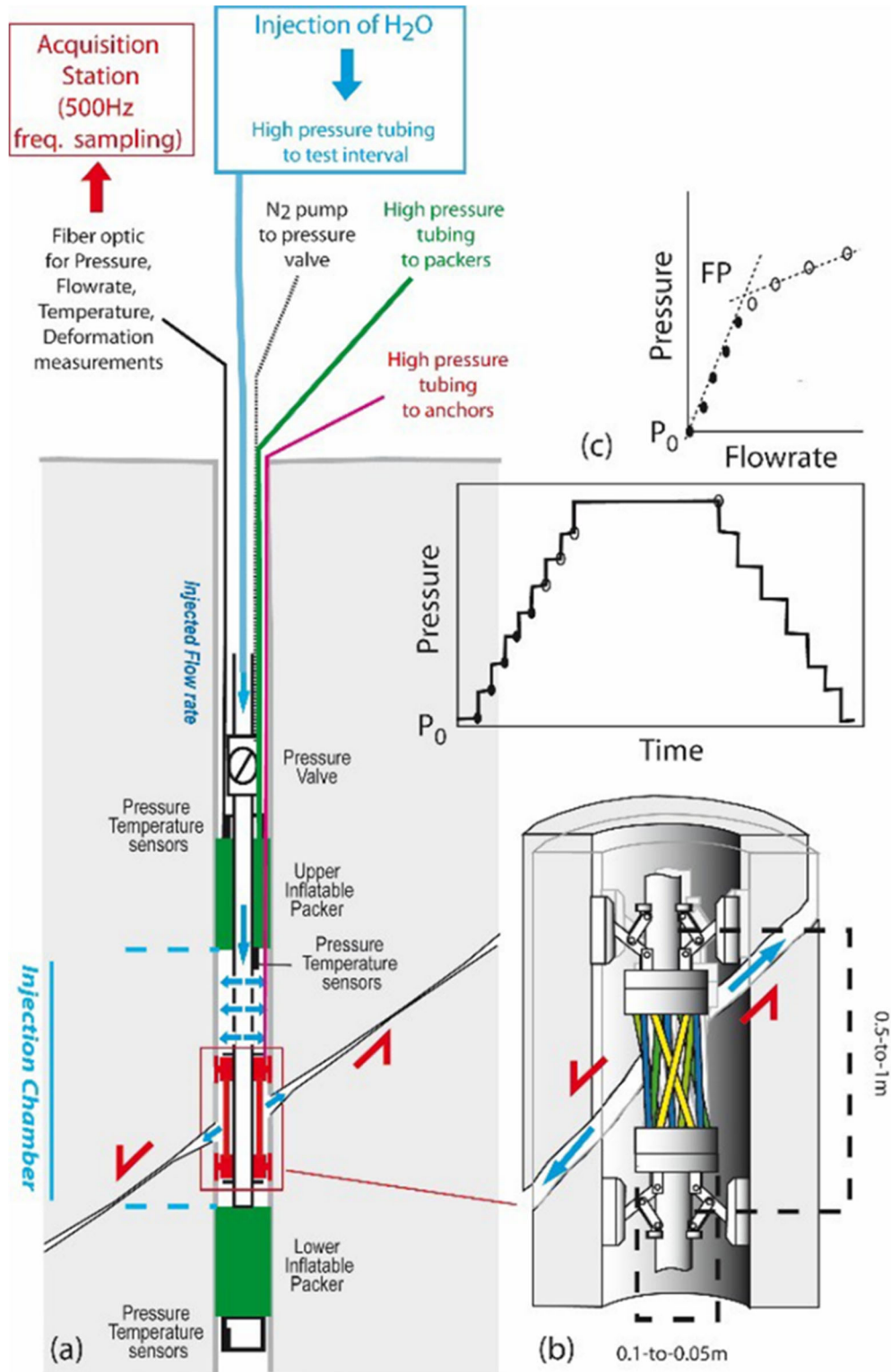
Figure 3.1-12. (a) Fault slip test equipment setup; (b) Schematic view of the three-dimensional deformation unit. Tubes are differently colored to show that they display different deformations when there is a relative movement of the rings anchored to the borehole wall across the activated fracture; (c) Typical Step-Rate Test protocol (Guglielmi, 2016).
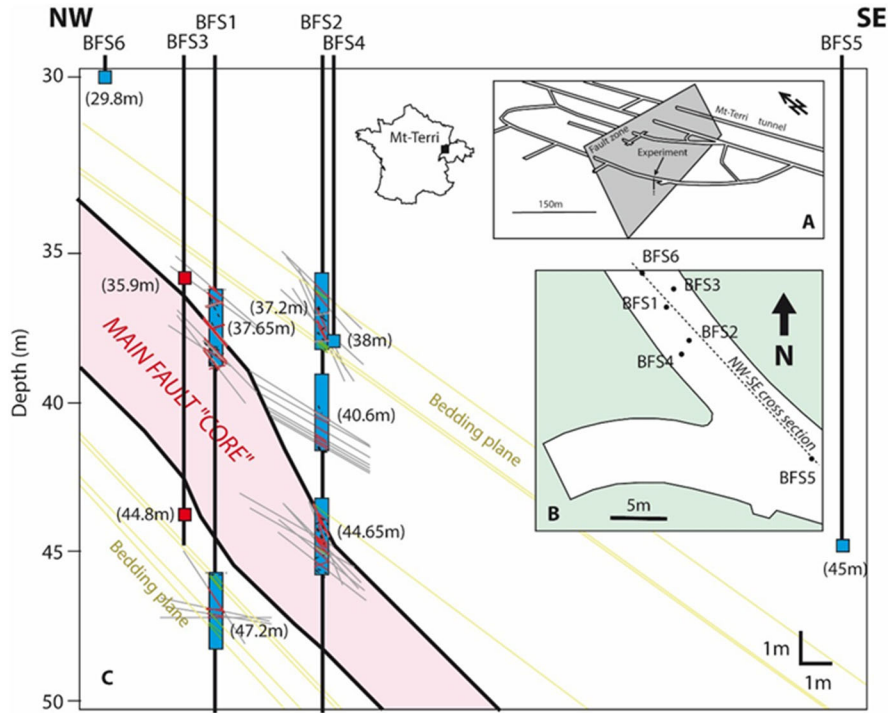
Figure 3.1-13. Test intervals across the Mt-Terri Main Fault (red squares are seismic sensors, blue squares are piezometers, blue rectangles are injection and monitoring intervals); A – Experiment location in Mt-Terri URL; B – Map of the borehole geometry in the FS experiment zone; C – Cross section showing the different testing intervals.
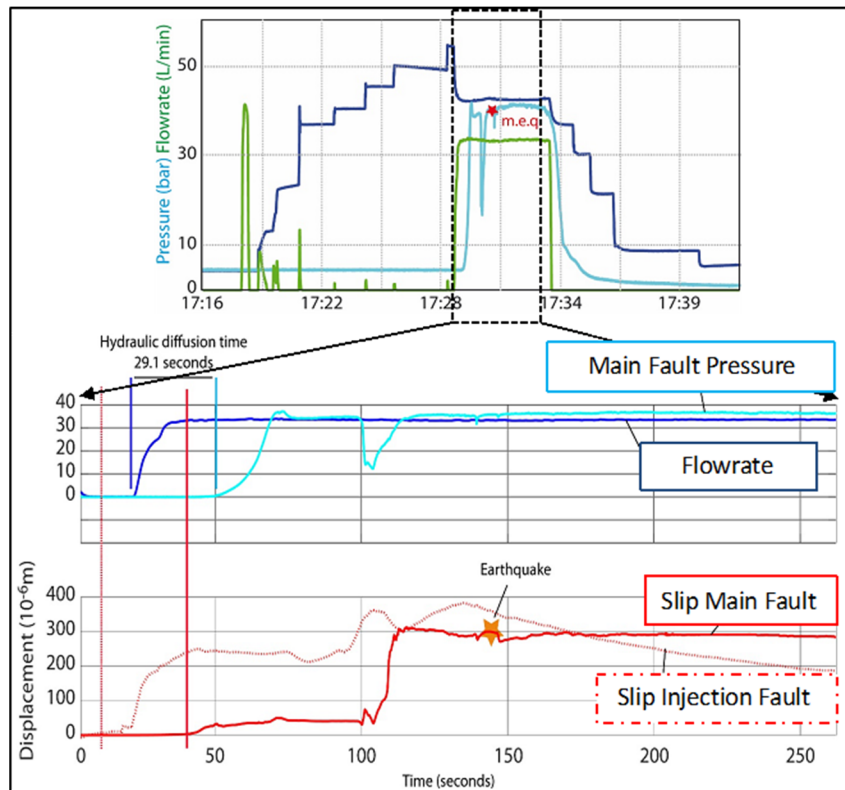
Figure 3.1-14. Pressure, injected flowrate, and displacements monitored observed in one of the injection tests (40.6 m). Top plot: Dark blue is pressure in the injection interval, light-blue is pressure in the monitoring interval, and green is injection flowrate, m.e.q. indicates micro-earthquakes. Bottom plot zooms in on the timeline.

Several Mont Terri partner organizations, including DOE, partnered in 2018 to plan and develop a larger-scale fault testbed for follow-on experiments, referred to as FS-B (Imaging the Long-Term Loss of Faulted Host Rock Integrity). FS-B features a similar controlled-injection fault reactivation program as the previous FS test, but activates a much larger fault patch and uses an upgraded version of the SIMFIP tool. The FS-B testbed is located near the location of the previous FS experiment, at the intersection between Gallery 4 and the new tunnel of the rock lab extension (Figure 3.1-15). The objective of FS-B is to understand longer-term impacts and processes during and after the fault activation; therefore, several activation and monitoring periods are planned over a multi-year time span. FS-B also involves an active seismic imaging of fluid flow and stress variations using a cross-well design that straddles the activated fault. In 2019 and 2020, the partners concluded all preparatory activities for FS-B, including drilling of several boreholes into and along the fault, and installation of the monitoring equipment. The first fault reactivation test was initially planned for March 2020 but had to be postponed to November 2020 due to Covid-19 related restrictions. Figure 3.1-15 and 3.1-16 show the setup of tilted boreholes that straddle the fault and allow for cross-well seismic imaging with a semi-continuous monitoring approach referred to as CASSM, or Continuous Active Seismic Source Monitoring, in combination with fiber optics cables for distributed acoustic and strain sensing (DAS and DSS).
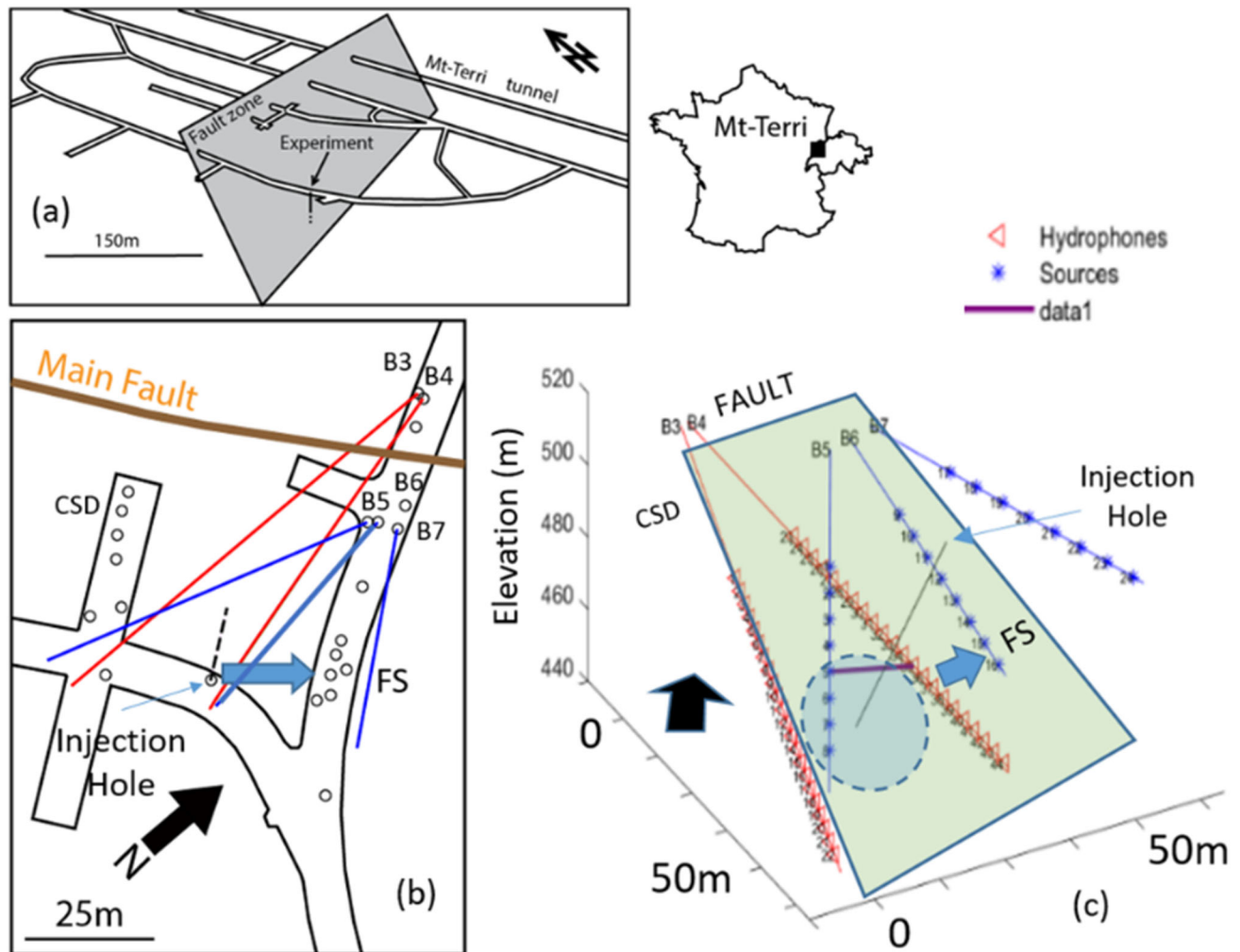
Figure 3.1-15. Location of the FS-B experiment and setup for the active seismic imaging across the fault. (a) Experiment location in the Mont Terri underground laboratory. (b) Map view of the FS-B experiment (circles indicate vertical boreholes crosscutting the fault). Colored lines are the inclined boreholes instrumented with CASSM. Blue arrow shows the hydraulic connection between injector and monitor during the experiment. (c) 3D view of the CASSM setting (fault is simplified as the green plane). The receiver boreholes, B3, B4, are in the footwall and the source boreholes, B5, B6, B7, are in the hanging wall. The injection borehole is 30-40° inclined with the fault plane.
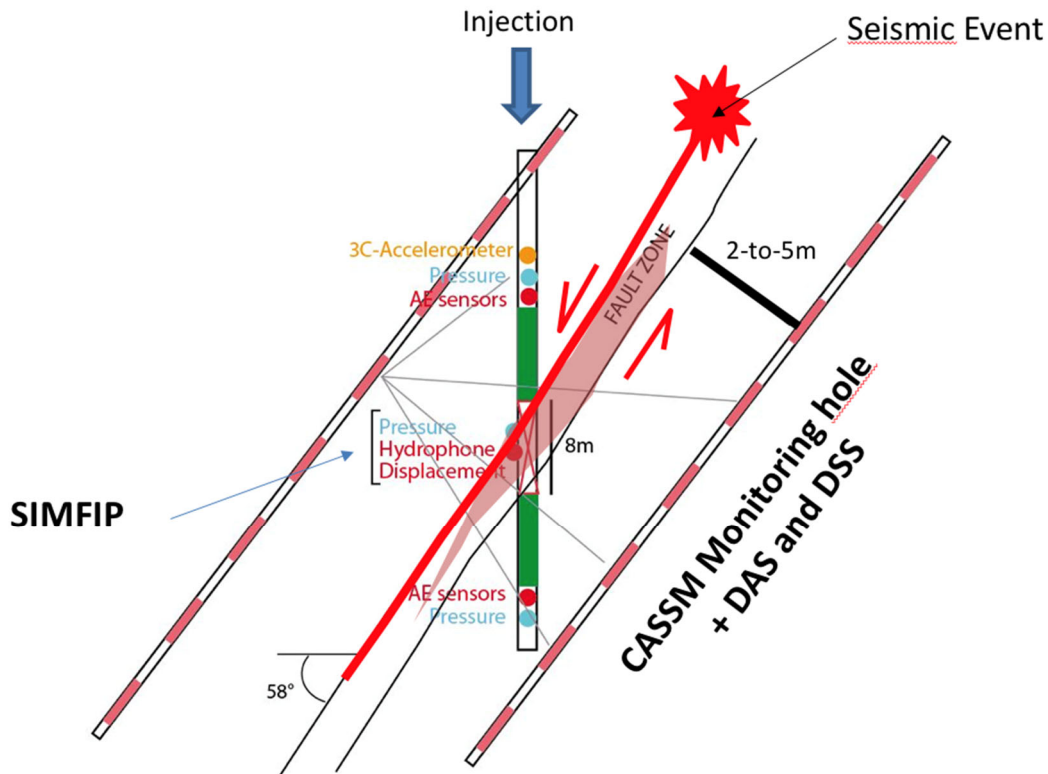
Figure 3.1-16. Vertical cross-section showing a schematic of tilted boreholes for cross-well geophysical monitoring of the dynamic fault behavior upon activation.

As mentioned above, the first FS-B fault stimulation experiment took place on November 21, 2020. Six consecutive injections were successfully conducted in a borehole at 40.4 m depth below the Mont Terri galleries, through a 1 m long interval set across the top of the Main Fault zone. The fault hydraulically opened when injection pressure was between 5 and 6 MPa. At some point during the injection cycles, when the cumulated injected volume reached 178 liters, a hydraulic connection was established between the injection and a monitoring borehole in Gallery 2008, a distance of 15–18 m away along the strike of the fault (Figure 3.1-17). No clear hydraulic connection was observed in other boreholes intersecting the fault. These results show an apparent heterogeneity in the fault leakage behavior. Preliminary results of the time-lapse seismic imaging (CASSM = Continuous Active-Source Seismic Monitoring) conducted during the first FS-B injections are shown in Figure 3.1-18. Although processing of the data is ongoing, first results confirm that changes in p-wave velocities across the fault are measurable, and that such changes correlated to changes in effective stress and deformations induced during and after the injection. The seismic imaging confirms that the leakage volume is local within the fault zone. Instantaneous changes in the seismic signals relate to fracture opening while delayed changes might highlight some irreversible shear damage following activation.

SFWD scientist are key participants in the FS and FS-B activities, contributing to the monitoring, analysis, and modeling of the tests. The main activities and key findings in FY21 are summarized in Section 6.7.
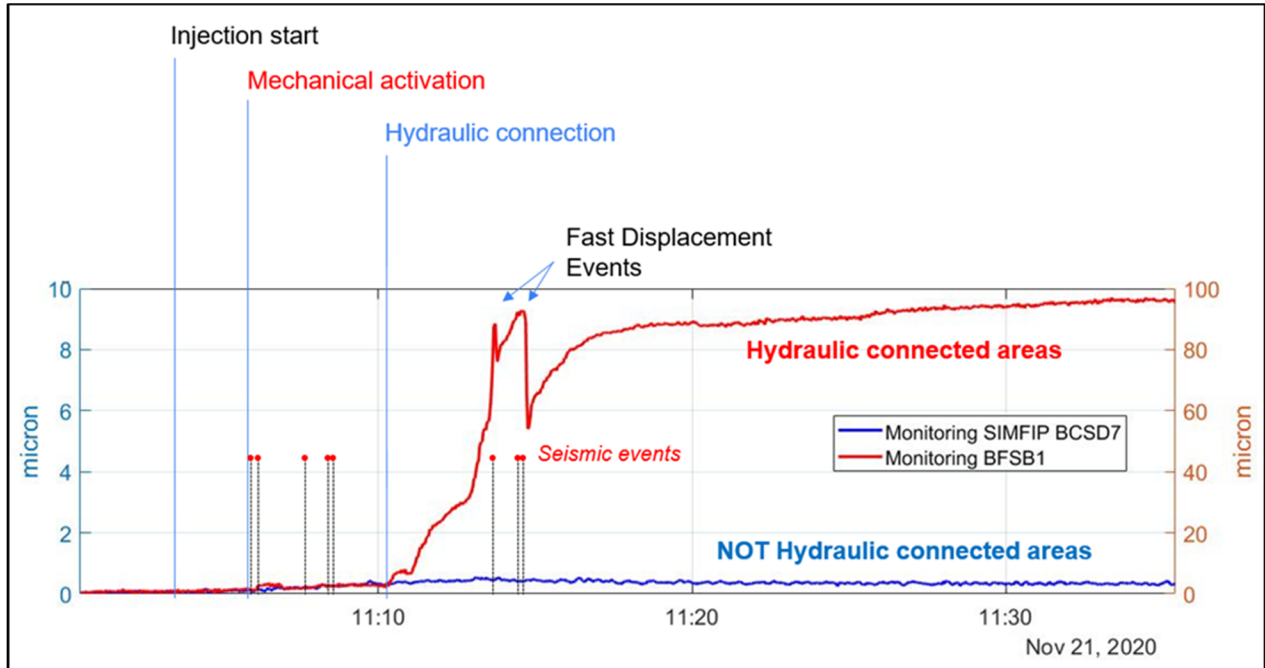
Figure 3.1-17. Shear displacement measured in two monitoring boreholes. Red line shows deformation in borehole BFSB1, which became hydraulically connected during one of the injection cycles. Blue line shows deformation in borehole BCSD1, which did not show hydraulic connection.
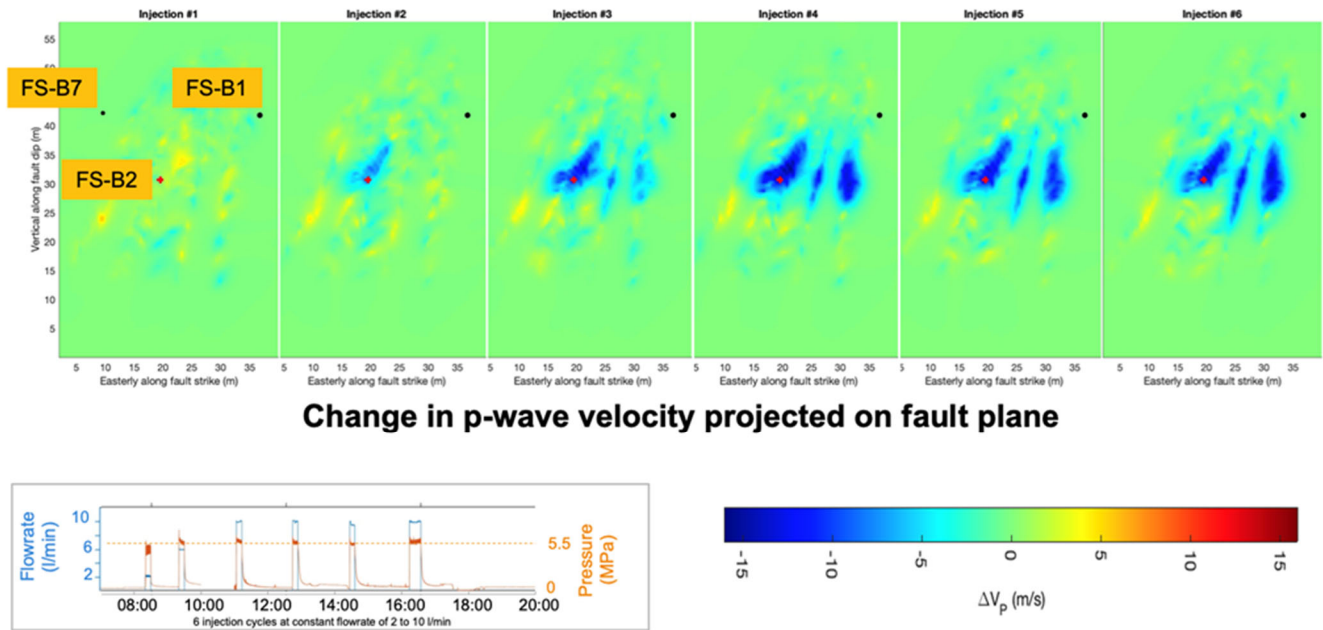
Figure 3.1-18. Preliminary time-lapse analysis of p-wave velocities across the fault from CASSM measurements. Blue zones indicate reduction of p-wave velocity linked to fault opening and fluid migration.

21

3.1.4. CI-D Experiment

The CI-D Experiment is a newly started activity at Mont Terri that is closely linked to a long-term test that has been conducted at Mont Terri since about 2007, the so-called CI Cement Clay Interaction Experiment. As shown in Figure 3.1-19, CI was set up 12 years ago with two vertical boreholes in Gallery 98 that have multiple segments with bentonite and concrete/cement materials in interaction with the argillite host rock. Since then, several sampling campaigns have been conducted in 2009, 2012, 2015, and 2017 where slanted boreholes were carefully drilled into the vertical boreholes to retrieve core materials with interfaces between bentonite, concrete/cement, and clay rock. The objective of these past campaigns was to characterize these interfacial regions with regards to time-dependent mineralogical, chemical or textural changes.

The idea of CI-D is to go beyond characterization of interfaces with various imaging approaches to direct *in-situ* testing of transport properties and processes across the interfaces. Starting in May 2019, a cocktail of water with radionuclide tracers was released in a pilot borehole drilled into the vertical borehole in a Portland cement/concrete section. The tracer cocktail has since been allowed to migrate outwards mainly by diffusion across the interface and into the argillite host rock. It is expected to continue the *in-situ* migration process for another two years or so and then to overcore the affected volume. Results from CI-D will provide valuable answers to questions about whether an aged concrete/claystone interface impedes diffusive transport of water and solutes. Or in other words whether a "skin" may form which may impede radionuclide transport (a beneficial effect) or cause delays in bentonite saturation (un unwanted effect). CI-D also comprises parallel laboratory studies and has just initiated a joint modeling effort in which SFWD scientists plan to participate. The modeling task of the CI and CI-D experiment was kicked off last year and LBNL scientists have since joined the collaborative modeling work (see Section 6.2.3).
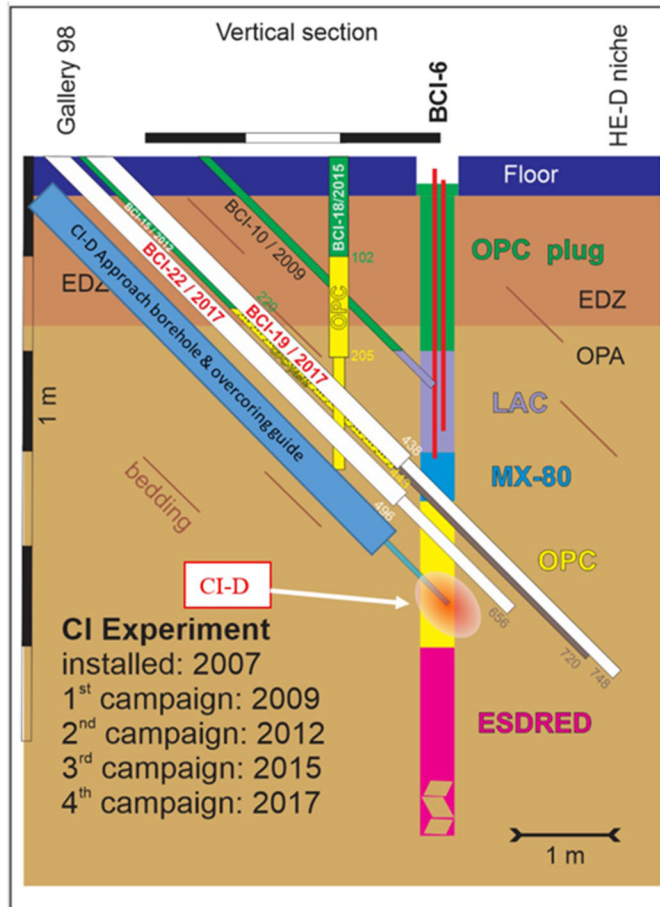
Figure 3.1-19. Schematic of CI-D experiment (Maeder and Martin, 2020).

3.1.5. Other Experiments at Mont Terri Summary

3.1.5.1. MA-A Experiment

Microbial processes can have significant impact on the long-term performance of a disposal site. In the near-field and in particular with regards to engineered barrier behavior, microbial processes can enhance the corrosion of containment systems like the waste packages; microbial activity may also alter migration properties of radionuclides in the near-field rocks. At later stages, microbial activity may have beneficial effects because microbes can consume the hydrogen gas generated from long-term corrosion of canisters. The aim of the MA-A experiment at Mont Terri is to answer questions related to the characterization of microbial communities in the pore water of the Opalinus Clay. The experiment is set up to allow for surface access to collect samples and decoupling of the downhole from the surface equipment. The technical design is as follows: Borehole BMA-A1 serves to obtain characteristics of unaltered Opalinus Clay porewater, including microbiota developed in the borehole since drilling. (Drilling was conducted using disinfected drills). Because there are only water lines designed for an outflow of accumulated water, no disturbance of the developed microbiota is expected. When necessary, an inert argon gas phase was introduced, using sterile filtered argon gas. In close proximity, in the alcove next to the Mont Terri gallery, a laboratory space was designed with a glovebox to provide controlled anoxic conditions (Figure 3.1-20). Ease of accessibility enables the utilization of Opalinus Clay porewater for types of microbial analysis and scientific experiments. Because the design was focused on ensuring anoxic conditions (with oxygen sensors installed between the packer and the gallery ceiling, shielding of water lines, and the anoxic glovebox), experiments can be conducted under realistic reducing environment of Opalinus Clay rock. SFWD researchers are currently considering participation in the analysis of MA-A data.

Figure 3.1-20. Borehole BMA-A1 (top) and glovebox in side alcove (bottom) of MA-A experiment.

3.1.5.2. GT Experiment

The purpose of the GT Experiment is to evaluate gas transport models and the behavior of clay rocks under gas pressure. Conventional theory suggests that as the gas pressure increases up to the capillary entry pressure, the gas phase starts to displace water from the pore system. Upon further gas pressure increase, the system will be successively drained as the gas phase displaces the wetting phase from smaller pores. When finally, a continuous non-wetting phase has developed (gas breakthrough) through the pore network, viscous gas flow is initiated. However, in initially saturated clay-rocks with extremely narrow interparticle spaces, the capillary threshold pressure required to initiate gas flow can be too large for the gas to be able to penetrate and desaturate the clay (Horseman et al., 1999). In a clay-rich host formation there is major uncertainty as to whether gas can escape through the host rock without the pressure rising to a level at which fractures occur and create preferential pathways, potentially leading to groundwater transport. The focus of the GT Experiment is on the characterization of the physical phenomena describing the gas transport and its mechanical interaction with the surrounding barriers and in particular to further understand the creation of micro and macro fractures based on experimental work and whether they could be a hazard for the long-term safety of a repository for radioactive waste.

This experiment is conducted in a stepwise approach starting with laboratory experiments using samples of Opalinus Clay (OPA) from Mont Terri to a field-scale rock laboratory experiment that has now been designed based on the results of the laboratory experiment. In 2019, samples of OPA taken from Mont Terri were tested in a triaxial permeameter cell and analyzed with the help of micro-imaging techniques. Strain data obtained during these experiments (see example in Figure 3.1-21) support process understanding, helping to differentiate between visco-capillary and dilatant gas flow mechanisms. Laboratory tests were performed parallel and perpendicular to bedding to evaluate anisotropy in the material response. Meanwhile, installation of the field experiment is progressing: all monitoring wells and the central injection well have been drilled (Figure 3.1-22). After an initial hydraulic testing campaign, the experiment is now ready for the step rate hydraulic testing sequence and subsequent gas injection below the gas fracking pressure. Injection will be conducted into a number of packed-off intervals and the response of the formation will be monitored in a series of parallel observation boreholes that are arranged in a radial array. It is foreseen to model the results of the experiment with numerical codes taking into account both visco-capillary and dilatant processes to elicit which behavior predominates. SFWD researchers are not currently engaged in the GT Experiment, but given the importance of this topic future participation may be considered in upcoming reprioritization exercises.
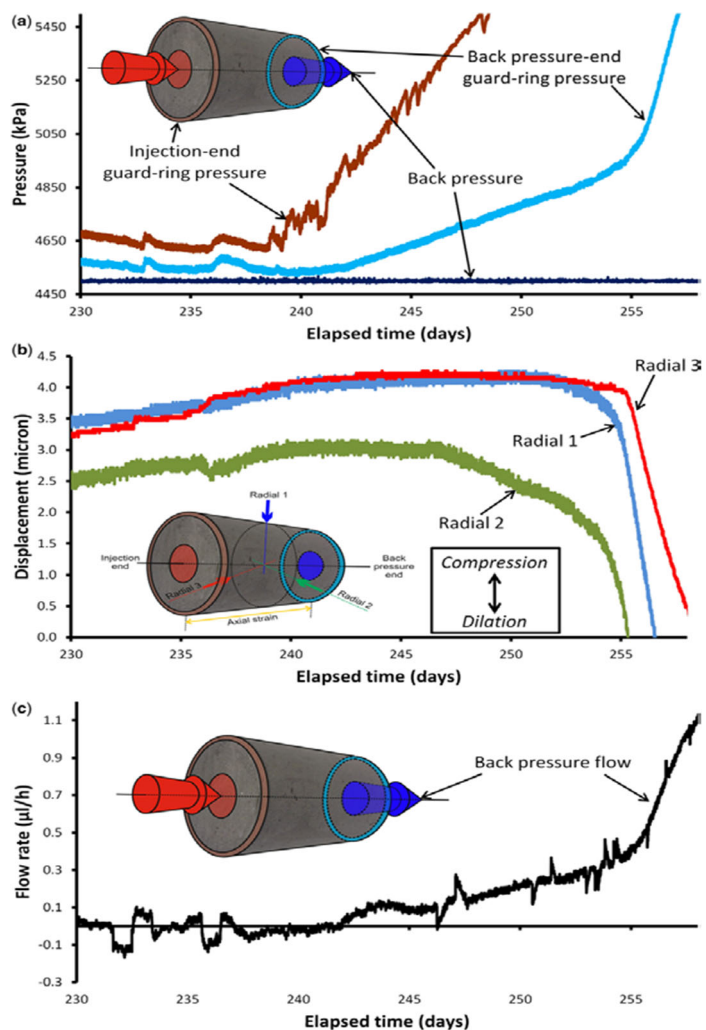
Figure 3.1-21. Data from a triaxial test report by Cuss et al. (2014) showing the response of a claystone sample at the onset of gas flow: (a) pressure response; (b) radial deformation; (c) outflow from the sample.

24
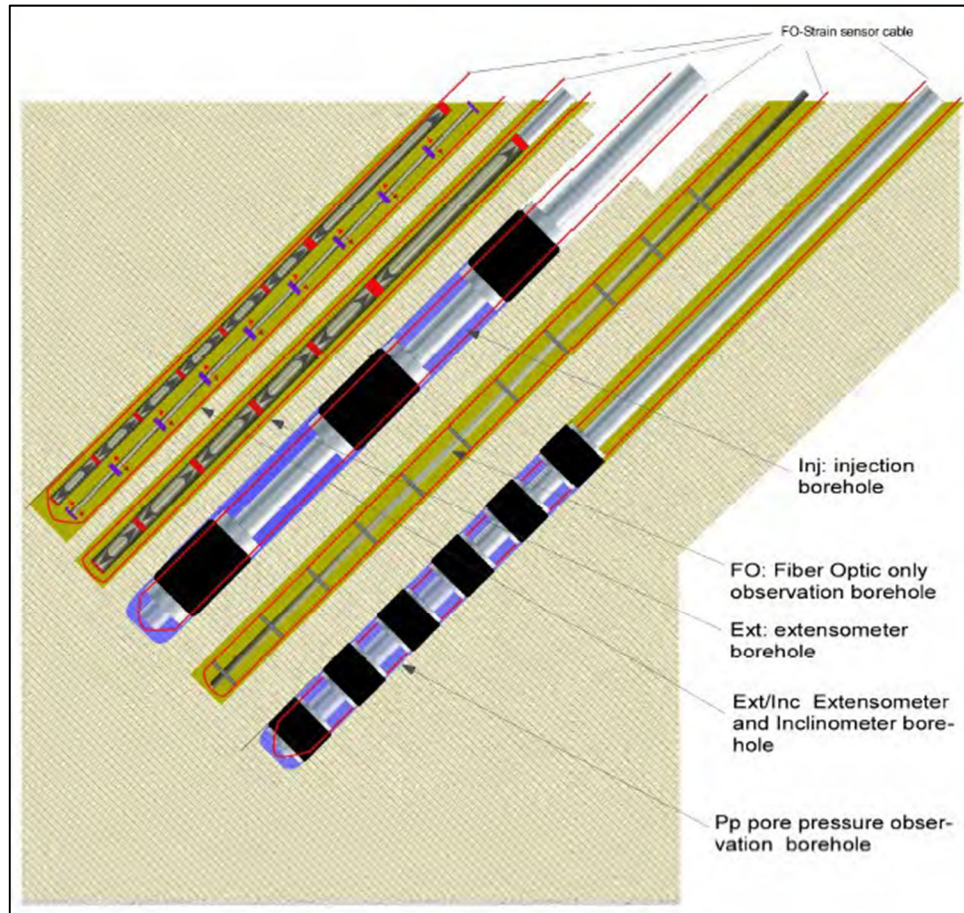
Figure 3.1-22. Schematic showing the field test design with central gas injection borehole surrounded by monitoring boreholes.

3.1.5.3. DR-C Experiment

The DR-C Experiment is one of several experiments enabled by the recent rock lab extension. Installed in 2021 in the new Gallery 18, DR-C has the following objectives: (1) understand the *in-situ* diffusion behavior in Opalinus Clay in the presence of a thermal gradient, and (2) assess the *in-situ* effect of temperature and temperature gradients on the diffusion of selected radionuclides. Such assessment is important for any radionculide release scenario early enough to have RN transport coincide with the presence of a thermal gradient, such as in certain early canister failure scenarions. The experimental setup includes a central injection borehole drilled vertically below a Mont Terri gallery, surrounded by a few monitoring boreholes nearby. Two separate experimental setups are being installed in the sandy facies of the Mont Terri rock lab, one heated setup with temperature up to 80ºC and one at ambient temperature as a reference test for comparison (Figure 3.1-23). To date, three monitoring boreholes have been drilled for baseline monitoring. Two boreholes have been equipped with FBG strain/temperature sensors and one borehole with a pore pressure monitoring system. The central injection well, of the heated setup, as well as the ambient injection borehole, are planned for early 2022 and the injection of the radioactive tracer cocktail in a thermal field is planned for Phase 28 (second half of 2022). The field experiments are accompanied by a suite of lab diffusion experiments. At this point, the lead organization for the DR-C experiment, the Belgium regulator FANC, has expressed interest in participation from additional partners, such as DOE, but no decision has been made in this regard by the SFWD campaign. Figure 3.1-24 shows the results of first scoping simulations indicating the important effect of bedding-plane related anisotropy on tracer diffusion in the Opalinus Clay.
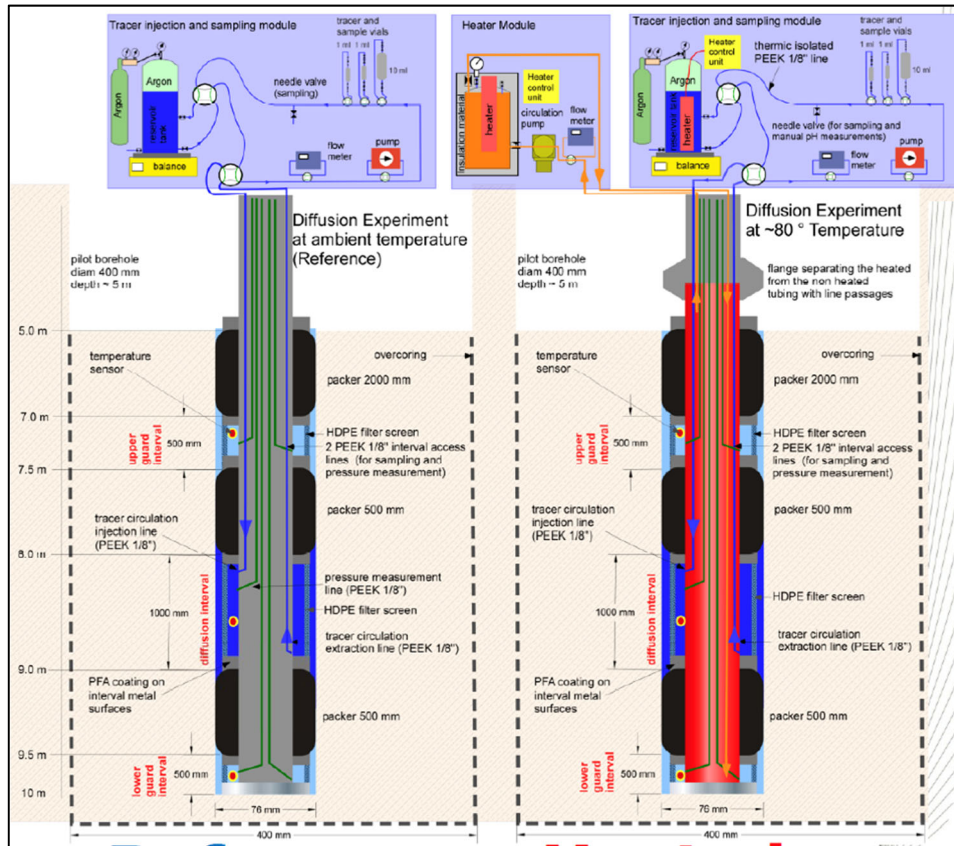
Figure 3.1-23. Schematic showing DR-C design with heated (right) and unheated(left) setups (Bernier and De Canniere, 2020).
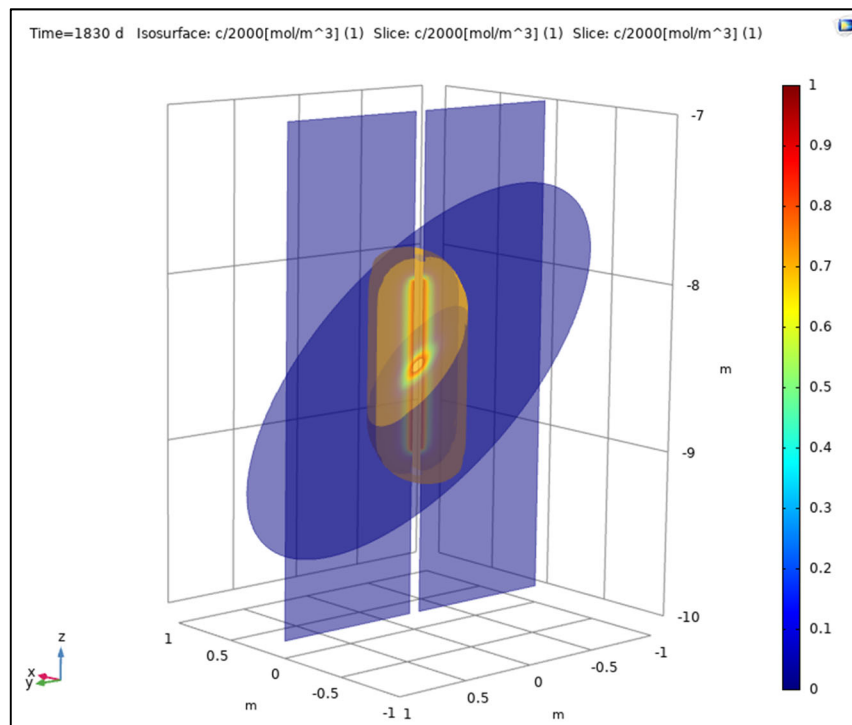
Figure 3.1-24. Scoping simulations of tracer diffusion in heated Opalinus Clay as per DR-C design (Bernier and De Canniere, 2020).

3.1.5.4. SW-A Sandwich Experiment

The SW-A Sandwich Experiment, to be conducted in a new niche in the extended rock lab (Gallery 18), is one of a few currently planned new experiments that address questions about suitable sealing approaches for a geologic repository, in this case the sealing of vertical shafts in an argillite host rock. The Sandwich seal consists of highly conductive equipotential layers emplaced in alternation with sealing layers, in order to obtain a more homogeneous resaturation of the seal. The system was successfully tested at the small and medium lab scale, demonstrating that the alternating layers of sealing segments and equipotential segments adsorbs potential seal bypass and fingering as well as high hydraulic loads. SW-A involves a large-scale field experiment to test the sandwich seal system in a natural rock environment (Figure 3.1-23). Two experimental shafts of 1.2 m diameter have been excavated. The first (primary) shaft has been fully backfilled as planned (i.e., equipped with the designed alternating sandwich seals) and extensive instrumentation of the shafts and surrounding rock was installed. The seals are now being resaturated via slanted boreholes from the shaft bottom. After some initial problems with leakage along some cables, the pressurization is about to begin while the seal evolution and rock response will be monitored in terms of saturation, pore pressure, stress and deformation. The second (backup) shaft will be backfilled end of 2022/early 2023. The lead organization for the DR-C experiment, the German GRS, has expressed interest in participation from additional partners, such as DOE, but no decision has been made in this regard by the SFWD campaign. However, the topic of developing and testing suitable sealing elements for tunnels, shafts, and boreholes in different host rocks is an important one and thus participation in SW-A may be considered in upcoming reprioritization exercises.
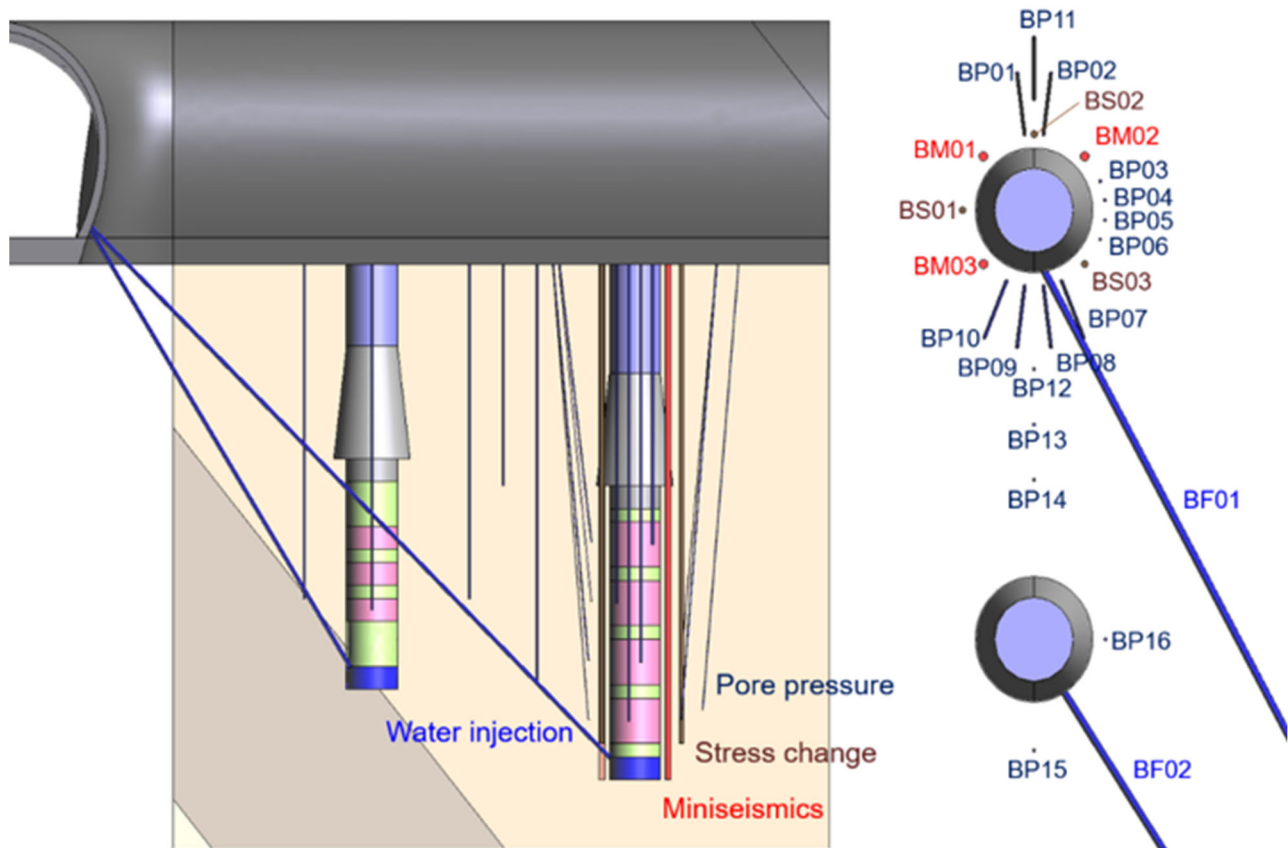
Figure 3.1-23. Design of SW-A experiment with two vertical shafts and planned monitoring approach (Hesser and Wiezcorek, 2020).

3.1.6. Mont Terri Summary

Benefits of Participation:

- Access to experimental data from the URL in clay/shale host rock, with many past, ongoing and future experiments addressing various FEPs,

- Opportunity to participate directly in international research groups that conduct, analyze, and model experiments (e.g., more direct involvement than in the DECOVALEX Project, see Section 3.2), and

- Opportunity to plan and conduct own research experiments

Status of Participation:

Effective July 1, 2012, DOE formally joined the Mont Terri Project as a partner organization. A substantial part of DOE's partnership fee was provided as an in-kind contribution by DOE researchers, i.e., by having SFWD researchers conduct work related to ongoing Mont Terri experiments. Specifically, the in-kind contribution of DOE included participation of LBNL researchers in the design and prediction/interpretative modeling of the FE Heater Test, which is now a long-term ongoing research activity. In addition to the FE Heater Test, SFWD researchers have in prior years participated in several other tests, such as the Mine-by Test, the HE-E Heater Test, the HG-A Experiment, and the DR-A Diffusion Experiment, and, as part of DECOVALEX-2019, have been participating in the collaborative modeling of the EB Experiment and the FS Fault Slip Test. In addition to the FE Heater Test, SFWD scientists are currently participating in, or utilizing data from, the FS-B Fault Slip Experiment and the CI-D Cement-Clay Interaction Experiment. Overall, participation of SFWD researchers in the Mont Terri Project has been extremely beneficial.

Outlook:

SFWD researchers will continue to stay involved in relevant experiments, in particular in the long-term FE Heater Test, and will keep abreast of new opportunities in the URL as they evolve. Eventually, DOE/SFWD may propose its own experiments to be conducted at the site. A significant extension of the Mont Terri URL, just finalized, now provides significantly more space for new experiments), which ensures the long-term future of the collaborative Mont Terri Project. SFWD researchers should evaluate whether some of new opportunities pointed out in this section (e.g., MA-A Experiment, GT Experiment, DR-C Experiment, SW-A Sandwich Experiment) would offer important new scientific direction and is worth pursuing as a new collaboration opportunity.

Contact Information:

DOE Contact:
Prasad Nair, DOE-NE (R&D)

SFWD Contact:
Jens Birkholzer, LBNL

Mont Terri Project Contact:
Christophe Nussbaum, Director, swisstopo, Switzerland
David Jaeggi, Project Manager, swisstopo, Switzerland

3.2. DECOVALEX Project

3.2.1. Introduction to the DECOVALEX Project

The DECOVALEX Project is a multinational research collaboration for advancing the understanding and mathematical modeling of coupled thermo-hydro-mechanical (THM) and thermo-hydro-chemical (THC) processes in geologic and engineered systems associated with geologic disposal of radioactive waste. DECOVALEX is an acronym for "Development of Coupled Models and their Validation against Experiments." Since 1992, the project has made important progress and played a key role in the development and validation of advanced numerical models and in-depth knowledge of the complex THM and THC behavior of different host rock formations and buffer/backfill materials. The knowledge accumulated from this project, in the form of a large number of research reports and international peer-reviewed journal and conference papers in the open literature, has been applied effectively in the implementation and review of national radioactive-waste-management programs in the participating countries. The project has been conducted by research teams from a large number of radioactive-waste- management organizations and regulatory authorities, from countries such as Canada, China, Finland, France, Japan, Germany, Spain, Sweden, UK, Republic of Korea, Czech Republic, and the USA. A good overview of the project is provided on the DECOVALEX Project web site (www.decovalex.org).

The DECOVALEX Project has generally been conducted in separate four-year project phases. Seven project phases were successfully concluded between 1992 and 2019, results of which have been published in a series of Special Issues in the International Journal of Rock Mechanics and Mining Sciences (Vol. 32(5) in 1995, Vol. 38(1) in 2001, and Vol. 42(5-6) in 2005), in the Journal of Environmental Geology (Vol. 57(6) in 2009), in the Journal of Rock Mechanics and Geotechnical Engineering (Vol. 5(1-2) in 2013), in the Journal of Environmental Earth Sciences (Vol. 77 in 2018), and in the International Journal of Rock Mechanics and Mining Sciences (Virtual Issue, DECOVALEX-2019, https://www.sciencedirect.com/journal/international-journal-of-rock-mechanics-and-mining-sciences/special-issue/10RM99KRN7V). The publications included in these Special Issues provide an in-depth overview of the collaborative research efforts conducted in the DECOVALEX Project and how these have advanced the state of the art of understanding and modeling coupled THMC processes over a more than 25-year period. Useful summaries of the history and achievements of the DECOVALEX Project are also given in Tsang et al. (2009) and Birkholzer et al. (2019b). The currently active DECOVALEX Project phase, referred to as DECOVALEX-2023, will run through the end of 2023.

Each DECOVALEX phase features a small number (typically three to seven) of modeling tasks of importance to radioactive waste disposal. Modeling tasks can be either Test Cases (TC) or Benchmark Tests (BMT). TCs are laboratory and field experiments that have been conducted by one of the project partners and are then collectively studied and modeled by DECOVALEX participants. BMTs involve less complex modeling problems, often targeted at comparing specific solution methods or developing new constitutive relationships. Numerical modeling of TCs and BMTs, followed by comparative assessment of model results between international modeling teams, can assist both to interpret the test results and to test the models used. While code verification and benchmarking efforts have been undertaken elsewhere to test simulation codes, the model comparison conducted within the DECOVALEX framework is different, because (a) the modeling tasks are often actual laboratory and field experiments, and (b) DECOVALEX engages model comparison in a broad and comprehensive sense, including the modelers' choice of interpretation of experimental data, boundary conditions, rock and fluid properties, etc., in addition to their choice of simulators. Over the years, a number of large-scale, multiyear field experiments have been studied within the project (e.g., the Kamaishi THM Experiment in Japan, the FEBEX heater test at Grimsel Test Site in Switzerland, the Yucca Mountain Drift-Scale Heater Test, or the FE Heater Test at the Mont Terri URL). Thus, the project provides access to valuable technical data and expertise obtained by DECOVALEX partner organizations; this is particularly useful in disposal programs that are starting their research on certain disposal or repository environments and have no URLs. DECOVALEX has a modeling focus, but with a tight connection to experiments.

To participate in a given DECOVALEX phase, interested parties—such as waste management organizations or regulatory authorities—need to formally join the project and pay an annual fee that covers the cost of

administrative and technical matters. In addition to this fee, participating (funding) organizations provide funding to their own research teams to work on some or all of the problems defined in the project phase. Representatives from the funding organizations form a Steering Committee that collectively directs all project activities. DOE had been a DECOVALEX funding organization for several past project phases. In 2007, DOE decided to drop out due to the increasing focus on the license application for Yucca Mountain. When the radioactive waste disposal program shifted to other disposal options and geologic environments, a renewed DOE engagement with DECOVALEX was suggested in 2011 (Birkholzer, 2011) as a logical step for advancing collaborative research with international scientists. In 2011, DOE evaluated the benefits of joining the upcoming DECOVALEX phase for the years 2012 through 2015, referred to as DECOVALEX-2015. SFWD leadership realized that a renewed DECOVALEX participation would provide SFWD researchers an access to relevant field data from international programs and would allow them to work collaboratively with international scientists on analyzing and modeling these data. More specifically, the modeling test cases and experimental data sets proposed for DECOVALEX-2015 were highly relevant to SFWD's R&D objectives. A decision was made in early 2012 that DOE would formally join the DECOVALEX project as a funding organization, and SFWD researchers were involved in two of the three main modeling tasks in the DECOVALEX-2015 phase.

DOE has since continued to be an official and active funding organization in the DECOVALEX project. In 2016, Jens Birkholzer from LBNL became the new Chairman of the DECOVALEX project. At the same time, DECOVALEX moved into the next project phase with seven modeling tasks for the years 2016 through 2019, referred to as DECOVALEX-2019 (Bond and Birkholzer, 2020). DOE researchers participated in several of these DECOVALEX-2019 tasks, as briefly summarized in Section 3.2.2. The current DECOVALEX Project phase started in April 2020, again with DOE participation in multiple new tasks and DOE leadership of two new tasks (Section 3.2.3). This new phase, referred to as DECOVALEX-2023, will end in December 2023.

3.2.2. Brief Summary of DECOVALEX-2019 Tasks and Achievements

DECOVALEX-2019, the most recent completed project phase, started in the spring of 2016 and ended in December 2019. Thirteen funding organizations were participating in this phase as follows (Table 3.2-1). As DOE's substantial task participation ended in FY20, we will provide a brief overview of DECOVALEX-2019 below, but will not give any details on specific task contributions by SFWD scientists. These were provided in the last annual report in Birkholzer et al. (2020).

Table 3.2-1. Funding Organizations Involved in DECOVALEX-2019.

ANDRA	French National Radioactive Waste Management Agency	France
BGR/UFZ	Federal Inst. for Geosciences & Natural Resources (BGR) and Umweltforschungszentrum Leipzig-Halle (UFZ)	Germany
CNSC	Canadian Nuclear Safety Commission	Canada
DOE	Department of Energy	United States
ENSI	Swiss Federal Nuclear Safety Inspectorate	Switzerland
IRSN	Inst. for Radiological Protection & Nuclear Safety	France
JAEA	Japan Atomic Energy Agency	Japan
KAERI	Korean Atomic Energy Research Institute:	Korea
RWM	Radioactive Waste Management Limited	Great Britain
NWMO	Nuclear Waste Management Organization	Canada
SSM	Swedish Radiation Safety Authority	Sweden
SURAO	Radioactive Waste Repository Authority	Czech Republic
TaiPower	Taiwan Power Company	Taiwan

Seven tasks were conducted in DECOVALEX-2019. As is generally the case in DECOVALEX, most of the modeling tasks involved data from experiments conducted in URLs.

- **Task A:**

  ENGINEER: Modeling Advective Gas Flow in Low Permeability Sealing Materials (Task Lead: BGS, United Kingdom)

  The purpose of Task A in DECOVALEX-2019 was to better understand the processes governing the adjective movement of gas in low permeability clay barrier materials (Harrington 2016). Special attention was given to understanding the mechanisms and controlling factors such as gas entry and flow, as well as pathway stability and sealing, which will affect barrier performance. The modeling task utilized a series of well-instrumented small-scale laboratory experiments that were conducted by the British Geological Survey (BGS). Task participants were testing new model representations in comparison to a variety of tests that were conducted under different conditions and dimensionalities, ranging from 1D gas flow under isotropically stressed samples to spherical gas flow point under constant volume conditions. Eight international modeling teams participated in ENGINEER using nine different modeling approaches and simulators; SFWD researchers from LBNL and Sandia National Laboratories (SNL) participated as DOE's modeling teams in this task. A summary of the collaborative research work conducted in this DECOVALEX task is given in Tamayo-Mas et al. (2021).

- **Task B:**

  Modeling the Induced Slip of a Fault in Argillaceous Rock (Task Lead: ENSI, Switzerland, with technical support from LBNL, USA)

  This modeling task evaluated the conditions for slip activation and stability of faults in clay formations and in particular addressed the complex coupling between fault slip, pore pressure, permeability creation, and fluid migration. This subject is of great importance to many subsurface applications where injection of fluids leads to pore-pressure increase and reduction of effective normal stresses on faults, which in turn can cause fault reactivation. Regarding radioactive waste emplacement, increases in pore pressure could be caused by release of heat from the high-level waste or by the generation of gas due to steel corrosion. The possibility of an increased permeability caused by fault slip and generation of potential pathways in the host rock or in an upper sealing formation could be a major risk for the long-term safety of a repository. The central element of this modeling task was the FS Fault Slip Experiment conducted at Mont Terri (Section 3.1.3), which utilized a novel experimental setup for controlled fault slip testing in realistic underground settings at field scale. SFWD researchers from LBNL helped lead this modeling task and were also participating as DOE's modeling team. A summary of the collaborative research work conducted in this DECOVALEX task is given in Graupner et al. (2020) and Rutqvist et al. (2021a).

- **Task C:**

  GREET: Modeling Hydro-mechanical-chemical-biological Processes During Groundwater Recovery in Crystalline Rock (Task Lead: JAEA, Japan)

  This modeling task centered on the GREET test, a full-scale experiment recently conducted in the Japanese Mizunami URL (crystalline rock) to evaluate the processes and implications of natural resaturation of the repository near-field environment after construction and before repository closure. The goals of GREET were as follows: (1) to understand the water recovery processes and mechanisms of the geological environment during facility closure, (2) to verify coupled hydrological-mechanical-chemical and -biological simulation methods for modeling these processes, and (3) to develop monitoring techniques for the facility closure phase and appropriate closure methods taking recovery processes into account. Modeling teams looked at the three major stages in the GREET Experiment: (1) excavation of the closure test drift (CTD), (2) hydrological recovery during filling of the CTD, and (3) evaluation of the long-term steady-state recovery conditions. SFWD researchers from SNL

participated as DOE's modeling team. A summary of the collaborative research work conducted in this DECOVALEX task is given in Iwatsuki (2020).

- **Task D:**

  INBEB: Hydro-mechanical (HM) and THM Interactions in Bentonite Engineered Barriers (Task Lead: Polytechnic University of Catalonia (UPC), Spain)

  The objective of the INBEB modeling task was the interpretation and modeling of the performance of an initially inhomogeneous bentonite barrier using two full-scale long-term experiments. These are the isothermal Engineered Barrier experiment (EB), which ran for over ten years at the Mont Terri URL, and the non-isothermal FEBEX experiment, which has been conducted for over 18 years at the Grimsel Test Site. INBEB assessed the evolution from an installed unsaturated engineered system to a fully functioning barrier, using HM and THM model predictions in comparison to experimental data. This requires an increased understanding of material behavior and properties, an enhanced understanding of the fundamental processes that lead to barrier homogenization, and improved capabilities for numerical modeling. SFWD researchers did not participate in INBEB. A summary of the collaborative research work conducted in this DECOVALEX task is given in Gens (2020) and Gens et al. (2021).

- **Task E:**

  Upscaling of Heater Test Modeling Results (Task Lead: ANDRA, France)

  The purpose of this modeling task was to evaluate upscaling approaches for THM modeling, from small size experiments (some cubic meters) to real scale emplacement cells (some ten cubic meters) all the way to scale of a waste repository (cubic kilometers). The task was closely aligned with the French repository program, which focuses its R&D on the Callovo-Oxfordian claystone (COx) formation near Bure in the east of France. A comprehensive research program was conducted in the Meuse/Haute-Marne URL near Bure to investigate the THM response of the COx to thermal loading from parallel microtunnels, through laboratory and *in-situ* experiments. The *in-situ* experimental program consists of a step-by-step approach ranging from small-scale heating boreholes (TED experiment) to full-scale experiments (ALC experiment). Results from these heater experiments were utilized in Task E. SFWD researchers from LBNL participated as DOE's modeling team. A summary of the collaborative research work conducted in this DECOVALEX task is given in Plúa et al. (2020), Seyedi et al. (2021), and Plúa et al. (2021).

- **Task F:**

  FINITO: Fluid Inclusion and Movement in the Tight Rock (Task Lead: BGR, Germany)

  The purpose of this modeling task was to refine and compare modeling approaches for the behavior of fluid inclusion in tight low-permeability rock, such as salt or clay. Fluids including liquid and gas phases can be found within the crystal structure or along grain boundaries in all types of sedimentary rock and were formed by accumulating and reacting of different mineral and/or organic particles under pressure and temperature conditions during the genesis. These small inclusions range in size of several micrometers and are usually invisible in detail without microscopic studies. However, these fluids usually dispersed in a very low amount can form local accumulations in a rock volume up to some cubic meters. Teams involved in this task collaborated to improve process understanding and model concept development. Researchers from SNL and LBNL participated on behalf of the SFWD campaign. A summary of the collaborative research work conducted in this DECOVALEX task is given in Shao et al. (2019).

- **Task G:**

  EDZ Evolution: Reliability, Feasibility, and Significance of Measurements of Conductivity and Transmissivity of the Rock Mass (Task Lead: SSM, Sweden)

The objective of this modeling task was to improve our understanding of the formation of an excavation damage zone (EDZ) in crystalline rock and its impact on change of hydraulic properties of the host rock mass near the excavations of spent fuel repositories. A specific focus was on the challenges and uncertainties for measurement and monitoring of rock mass permeability evolution during construction and operation of a repository hosted in granitic rock in Sweden. A good knowledge of the hydraulic property evolution of the EDZ is a key item of Safety Assessment (SA)/Performance Assessment (PA) of repositories in such host rocks. SFWD researchers did not participate in this task. A summary of the collaborative research work conducted in this DECOVALEX task is given in Meier and Backers (2020).

In summary, DECOVALEX-2019 successfully explored some common themes across a range of complex modeling tasks (see further discussion of themes below), yielding new insights but also encountering common issues that remain to be resolved (Bond and Birkholzer, 2020). Significant progress was achieved by research teams of all tasks involved in DECOVALEX-2019. Modeling teams adopted advanced modeling approaches using different numerical methods and computer codes and were generally able to achieve good agreement, both with the experimental observations and with alternative modeling approaches. In cases where differences remained, task leads and modeling teams made an effort in isolating the reasons for them and discussed what could to be done to improve. Overall, the achievements and outstanding issues obtained from the seven tasks formed a good step forward for better understanding of the scientific/technical issues of importance for safe geological disposal of radioactive wastes in different host rocks, with complex geological conditions and increasing environmental challenges. Major progress was made in four common areas as discussed below:

- **Novel Representations of Complex Processes**

  Both Tasks A and F dealt with the extremely complex issues of highly non-linear fluid migration within very low permeability formations. Observed experimental behaviors are often strongly stochastic and therefore it can be very difficult to rationalize the core physical behavior (i.e., identify what experimental features are reproducible under different circumstances) and successfully interpret the experiments. In addition, the experimental setup can be very important in determining the result, hence careful representation of the experiment (e.g., the injector apparatus in Task A) can be key to building a successful model. In this context, the DECOVALEX working model of close integration between experiment and modeling is an important one. For example, the model comparison in Task A was coordinated by the very scientist who conducted the series of experiments. In the case of Task A, the primary concern was advection of pressurized gas in compacted bentonite, while Task F mainly considered migration of inclusions in salt formations. While superficially quite distinct, there are a number of commonalities, and indeed the SNL research team used similar approaches in both tasks to characterize and represent the experiment. For Task A, it was shown that conventional two-phase flow approaches are largely inadequate to represent the system in a convincing fashion, taking into account all the known features of the experimental results (e.g., very low gas saturations at breakthrough). Hence the inclusion of implicit or explicit features to represent the dilation process is essential. Similarly, for Task F, explicit treatment of fluid migration along the halite grain boundaries, also by a dilation process under strongly deviatoric stress conditions, was found to be a good representation of salt inclusion migration. Both tasks have illustrated the importance of micro-scale control on macro-scale phenomena and novel approaches for bringing the micro-scale understanding into the meso- and macro-scale have been put forward.

- **Complexities of Fault and Fracture Representation**

  Tasks C and G both dealt with the problem of interpreting groundwater flows and (in the case of Task C) transport within discrete fracture networks (DFNs). This is an area of long-standing study within DECOVALEX and the tasks have encountered many of same issues, albeit from a different perspective. Both tasks illustrated that producing models that can successfully represent net tunnel inflows is possible with plausible DFN based on geological observation, with some calibration and some teams using an equivalent continuum porous medium (EPCM) approach. However, both tasks

struggled when looking at more complex aspects of the problem. In the case of Task C, successfully modeling the wide range of observed chloride concentrations in the tunnel was particularly problematic. Producing a convincing representation of the transport required manual intervention in the DFN/EPCM to create large-scale heterogeneity to allow the excavated tunnel to connect to vertically distant higher and lower concentrations of chloride. Task G showed a similar issue at a much smaller scale, whereby the interference tests in the TAS04 experiment were very hard to interpret and model when using intersection of identified planar fracture surfaces identified in the EDZ. Both tasks concluded that channelization with the fracture network could be the cause of the difficulties in modeling the observations, nothing that large scale heterogeneities in the DFN network for Task C could also be a factor.

- **Complex Hydro-Mechanics with Wider Applications**

  For Task B, the problem was focused on a single fault-zone in an argillite rather than a DFN system in a crystalline potential host rock. Here the work focused on the numerical issues of a good representation of an extremely well-characterized fault system that was stimulated using fluid injection. The highly non-linear nature of the hydro-mechanical response meant that different numerical methods were found to have different strengths and weaknesses. This necessitated different modeling strategies and conditioning of the models with respect to the known data, depending on the numerical approach. Nonetheless, after considerable effort, consistent and coherent results for the experiment have been produced. A useful next step to build confidence would be predictive studies of small-scale fault reactivation. This task is also of interest outside of the radioactive waste management arena, being of direct relevance to other sub-surface geo-engineering applications (e.g., geothermal, underground gas/air storage, oil and gas etc.)

- **THM Processes in Clays**

  Task D and E both considered THM processes in clays or clay-based materials such as bentonite, albeit from different perspectives. Task E demonstrated that good blind predictions of pore-pressure and temperature can be obtained for heat-generating disposal analogues using heat diffusion and conventional elastic poro-mechanics. There was some evidence of surprising local heterogeneity in the Callovo-Oxfordian clay which meant some recalibration was required when moving between experiments. This work clearly illustrated the impact of variability and heterogeneity on pore pressure. The teams were also able to upscale their models in to represent the whole repository, and use these models to investigate the sensitivity of uncertainty and variability on key metrics (pore pressure and implied effective stress) that could impact the safety case. In understanding the details of the experiments, it was clear that the development of the EDZ, and the resulting effective hydraulic and mechanical properties of the EDZ, were important to calibrate the models to the observations. This remains a complex exercise and differing approaches were taken by the teams, but no fully mechanistic model was used by any team. While the task was a clear success, the treatment of mechanical damage and the resulting change in the argillite properties, remains an area of significant uncertainty. Task D was focused on compacted and pelleted bentonite used as a buffer material in two very different experiments. While teams were able to obtain good agreement with the measured thermal and hydraulic responses, a complete representation of the plastic mechanical deformation – in this case focused on the homogenization of the bentonite during heating and resaturation – remains challenging. This was not helped by non-trivial uncertainties in some of the *in-situ* data. It was noted that highly simplified mechanical models could be used in some circumstances, depending on the modeling objectives. Both tasks encountered similar issues in terms of treatment of the plasticity of clays (Task D – homogenization, Task E – damage), albeit from different perspectives. This perhaps indicates the direction for future work in argillites from a coupled processes perspective.

3.2.3. Modeling Tasks in the Current DECOVALEX-2023 Phase

DECOVALEX-2023 is the current phase of the DECOVALEX Project; this phase started in early 2020 and will end in late 2023. To identify suitable tasks for DECOVALEX-2023, the project organized several planning sessions during workshops in 2018 and in 2019. At the end of this process, prospective funding organizations decided on seven relevant and interesting tasks to be included in DECOVALEX-2023. A total of 17 funding organizations are participating in DECOVALEX-2023, including DOE. Jens Birkholzer from LBNL continues to serve as the Chairman of the DECOVALEX Project.

A list of the DECOVALEX-2023 funding organizations is given in Table 3.2-2 below. The seven modeling tasks are briefly summarized in Table 3.2-3; more information is given in Sections 3.2.3.1 through 3.2.3.7. Table 3.2-4 shows which funding organizations (and their research organizations) are participating in the seven tasks. SFWD scientists serve as task leads for two tasks, namely Task E and Task F, and they are currently involved in all but one of the seven tasks (with participation of LBNL, SNL, and LANL scientists).

Table 3.2-2. Funding Organizations Involved in DECOVALEX-2023.

ANDRA	French National Radioactive Waste Management Agency	France
BASE	Federal Office for the Safety of Nuclear Waste Management	Germany
BGE	Federal Company for Radioactive Waste Disposal	Germany
BGR	Federal Inst. for Geosciences & Natural Resources	Germany
CAS	Chinese Academy of Sciences	China
CNSC	Canadian Nuclear Safety Commission	Canada
COVRA	Central Organisation for Radioactive Waste	Netherlands
DOE	Department of Energy	United States
ENRESA	Radioactivity and Radioactive Waste Management	Spain
ENSI	Swiss Federal Nuclear Safety Inspectorate	Switzerland
JAEA	Japan Atomic Energy Agency	Japan
KAERI	Korean Atomic Energy Research Institute:	Korea
NWMO	Nuclear Waste Management Organization	Canada
RWM	Radioactive Waste Management Limited	Great Britain
SSM	Swedish Radiation Safety Authority	Sweden
SURAO	Radioactive Waste Repository Authority	Czech Republic
TaiPower	Taiwan Power Company	Taiwan

Table 3.2-3. Modeling Tasks for DECOVALEX-2023 (Bond and Birkholzer, 2019)

Task ID	Short Name	Title	Organization	Processes	Primary Material Type
A	HGFrac	Heat and Gas Fracturing	Andra	THM + gas	Argillite
B	MAGIC	Modeling Advection of Gas in Clays	BGS	HM + gas	Engineered Clay
C	-	THM Modeling of the FE Experiment	ENSI/Quintessa	THM	Argillite
D	-	Full-scale Engineered Barrier System Experiment at Horonobe URL	JAEA	THM(C)	Sedimentary
E	BATS	Brine Availability Test in Salt	DOE (SNL)	THMC	Evaporitic Salt
F	-	Performance Assessment (PA)	DOE (SNL)	PA – THMC	Crystalline and salt
G	SAFENET	Safety Implications of Fluid Flow, Shear, Thermal and Reaction Processes within Crystalline Rock Fracture Networks	UFZ, UoE, DynaFrax	THMC	Crystalline focus plus greywacke

Table 3.2-4. Task Participation by Funding Organization and Planned Number of Research Teams

Funding Organisation	Task A: HGFrac	Task B: MAGIC	Task C: FE Experiment	Task D: EBS Experiment	Task E: BATS	Task F: Performance Assessment	Task G: SAFENET
Task Lead	ANDRA	BGS	ENSI, Quintessa	JAEA	SNL	SNL	UFZ, UoE, DynaFrax
ANDRA	2	1	0	0	0	0	0
BASE	0	0	0	0	0	1	1
BGE	0	0	1	0	0	0	0
BGR	1	1	2	1	2	2	0
CAS	0	0	1	1	0	0	1
CNSC	0	0	0	0	0	1	1
COVRA	0	0	0	0	1	1	0
DOE	1	2	1	0	1	1	2
ENRESA	1	0	0	0	0	0	0
ENSI	1	0	1	0	0	0	0
JAEA	0	0	0	1	0	0	0
KAERI	0	0	1	1	0	1	1
NWMO	1	0	1	0	0	1	0
RWM	1	0	0	0	1	0	1
SSM	0	0	0	0	0	1	1
SURAO	0	0	0	0	0	1	0
Taipower	0	0	0	1		1	0
Total Number of Research Teams	8	4	8	5	5	11	8

3.2.3.1. Heat and Gas Fracturing (HGFrac) – Task A

The overall objective of this DECOVALEX-2023 Task A is to improve the ability of models to predict the processes and mechanisms of fracture initiation and growth in claystone due to a rapid increase of heat or gas overpressure. Based on heat and gas fracturing tests conducted at the Bure URL in France, HGFrac will enhance the understanding of fundamental processes and the improvement of capabilities for numerical modeling of these processes. Several tests have been designed and conducted by ANDRA to reach the rupture of claystone under either a rapid heat load or strong gas pressure increase. The task is divided into two main sub-tasks that will be undertaken in parallel, one on heat-driven and one on gas-pressure driven fracturing. Both steps have similar structure: (1) definition of conceptual models and initial benchmark exercises involving laboratory experiments, (2) blind prediction and numerical reproduction of *in-situ* experiments in the Callovo-Oxfordian claystone (Cox) at Bure, and (3) application at the repository scale. For heat-driven fracturing, ANDRA has so far provided results from laboratory triaxial extension tests which feature a fast-heating phase and an automatic confining control under constant vertical total stress (see Figure 3.2-1). This initial modeling phase is now being followed by blind prediction of a field experiment referred to as CRQ, which was specifically designed to test the behavior of claystone exposed to a thermal fracturing stress regime (Figure 3.2-2). For gas-pressure driven fracturing, teams have started modeling a series of benchmark exercises with increasing degrees of difficulty. This will be followed by the simulation of several gas injection tests (PGZ) performed *in-situ* at Bure. These tests use a multi-packer system installed in a small diameter borehole drilled in the COx. The test interval consists of an inner tube, a stainless-steel filter with porosity of 30%, and an annular space between the stainless-steel filter and the rock mass (Figure 3.2-3). SFWD researchers from LBNL are participating as DOE's modelling team in Task A, so far with focus on the thermal fracturing topic (Section 6.3.2).
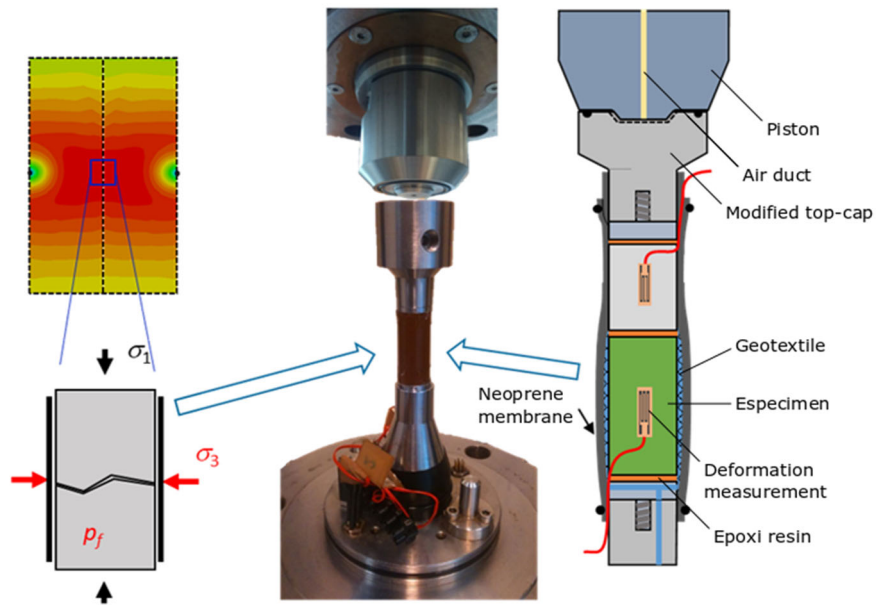
Figure 3.2-1. Schematic representation of two micro-tunnels in the HLW area with possible fracturing in the center (left) and illustration of triaxial extension experiments designed to reproduce the stress path expected in the middle between two micro-tunnels (right) (Plúa and Armand, 2020).
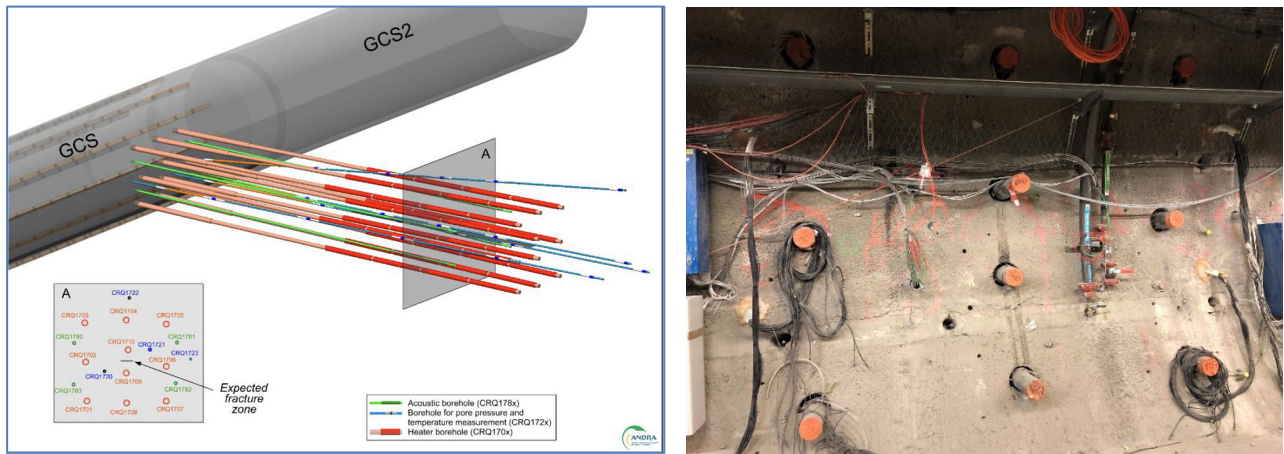
Figure 3.2-2. CRQ thermal fracturing experiment. Rendering on the left shows the overall borehole setup. The photo on the right shows boreholes drilled into the wall of the test tunnel at Bure URL (Bond and Birkholzer, 2019).
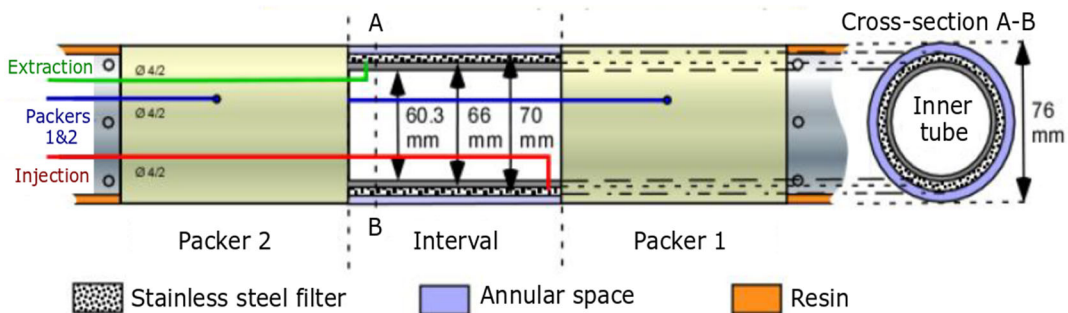
Figure 3.2-3. Multi-packer system for gas and water injection tests (Plúa and Armand, 2020).

3.2.3.2. *Modeling Advection of Gas in Clays (MAGIC) – Task B*

The objective of this task is to understand the processes and mechanisms governing the advective movement of gas in compacted bentonite and natural clay-based materials, improve physics-based models of these systems, and hence support the development of performance and safety assessment models. As an extension of the Task A from DECOVALEX-2019 (Section 3.2.2), which was based solely on laboratory data, the current DECOVALEX-2023 Task B centers on a field test with bentonite backfill situated in fractured crystalline hard rock. After some benchmarking and blind predictions, research teams will be provided data from the large-scale gas injection test (LASGIT) at Äspö HRL in Sweden which is based around a mock waste canister, encapsulated in bentonite/pellets, and placed within a vertical deposition hole (Figure 3.2-4). The bentonite has been allowed to hydrate since 2005 after a two-year construction phase ended with the closure of the deposition hole. Since then, gas injection tests have been conducted occasionally from a number of filters embedded along the surface of the canister. The test is highly instrumented: Sensors continually monitor variations in the relative humidity of the clay, the total stress and porewater pressure at the borehole wall, the temperature, any upward displacement of the lid and the restraining forces on the rock anchors. Dismantling of the test planned for October 2020 will provide additional data for ground-truthing of the simulation results. SFWD researchers from LBNL and SNL are participating as DOE's modelling teams in this gas migration task, continuing their previous work in the related DECOVALEX-2019 Task A. Further information on LBNL's contributions so far is provided in Section 6.4.3.
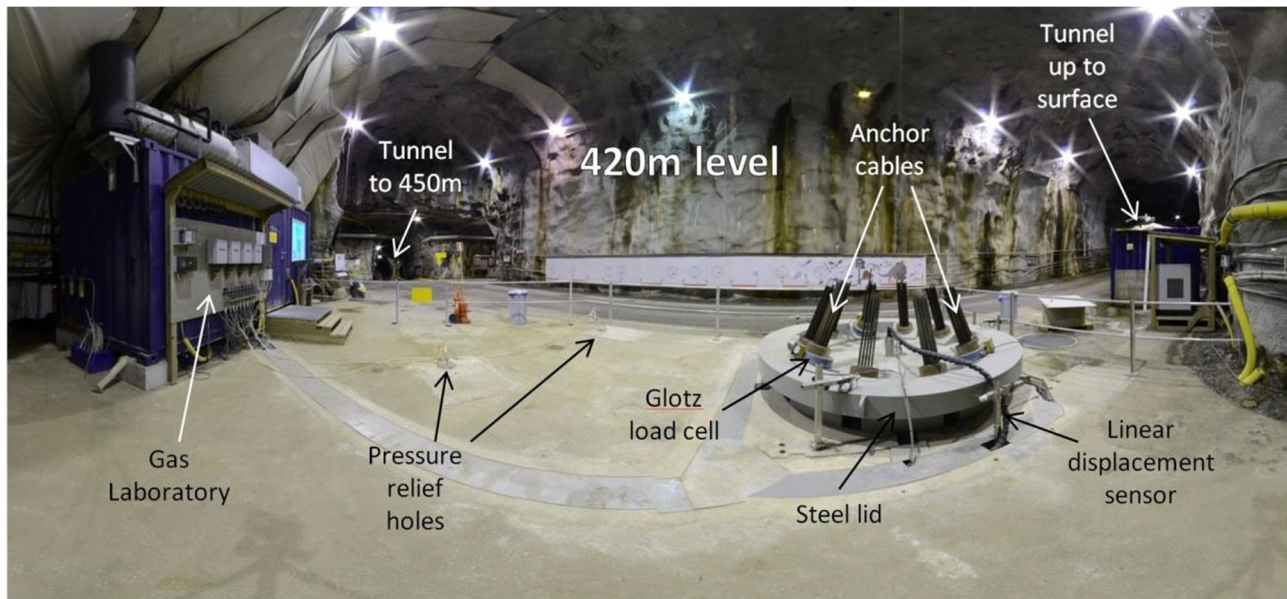
Figure 3.2-4. Large-Scale InjectionTest LASGIT at Äspö HRL (Harrington and Tamayo-Mas, 2020).

3.2.3.3. *THM Modeling of the FE Experiment – Task C*

The objective of this task is to model THM processes in the Opalinus Clay using data from the Full-Scale Emplacement (FE) heater experiment in Mont Terri. The focus is to understand pore pressure development in the host rock and how this is affected by heating, engineering factors (e.g., shotcrete, tunnel shape) and damage due to tunnel construction and thermal effects. As described earlier in Section 3.1.2, a large dataset from the FE experiment is already available including time series data from construction of the tunnel, ventilation of the tunnel, and the on-going heating phase. The data include temperature, pore pressure, relative humidity, displacement and inclination measurement at high spatial and temporal resolution (Figure 3.2-5). The FE experiment was designed to test both engineering capabilities for construction, waste emplacement and backfilling and the early-stage evolution of thermal, hydraulic, mechanical and chemical processes of a geological disposal facility. This provides an opportunity to consider how the engineering of the experiment

impacts the THM evolution of the system. The task has been structured into several steps, starting with a preparation and benchmarking phase, followed by modeling of the FE heating and ventilation phases, and finally a phase involving several sensitivity studies (Thatcher and Graupner, 2020). SFWD researchers from LBNL and SNL are participating as DOE's modelling teams in this task (Section 6.3.1).
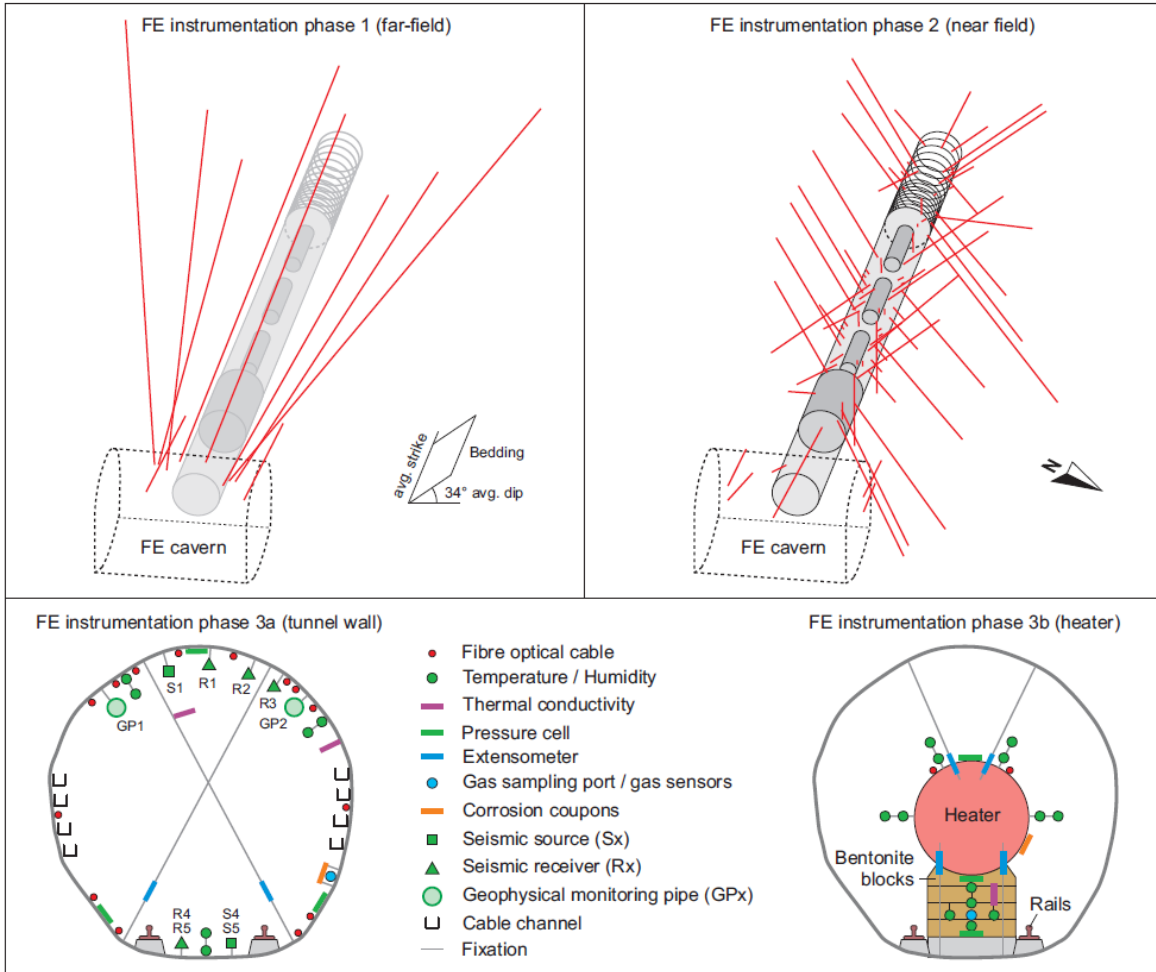
Figure 3.2-5. Diagram showing instrumented boreholes within the FE experiment and sensor locations within two cross-sections of the tunnel (Bond and Birkholzer, 2019).

3.2.3.4. *Engineered Barrier System Experiment at Horonobe URL – Task D*

The objective of this task is to better understand and be able to simulate the coupled THMC processes occurring in and around an engineered barrier system as designed in the Japanese disposal concept (see Figure 3.2-6). The Horonobe EBS experiment is a full-scale mock-up of this concept, which comprises the waste package and overpack, bentonite buffer, a mixed bentonite-soil backfill, and a low-alkaline cement plug. The heating phase, which started in 2015, will soon be followed by a monitored three-year cooling phase. Over one hundred sensors were placed in the buffer, backfill and the surrounding rock mass during the installation of the experiment to monitor the coupled THMC processes, including temperature, total pressure and pore pressure, water content, resistivity, displacement, and strain (Figure 3.2-7). JAEA designed several modeling steps for this task, including modeling several laboratory tests, an *in-situ* isothermal mock-up test, and finally the actual EBS heater experiment (Sugita, 2020). In support of the Horonobe EBS experiment, LANL plans to conduct laboratory experiments to study potential temperature-related reactions between EBS materials (Kunigel bentonite, low carbon steel) and the mudstone host rock (Caporuscio et al., 2020), see Section 6.2.1.3.
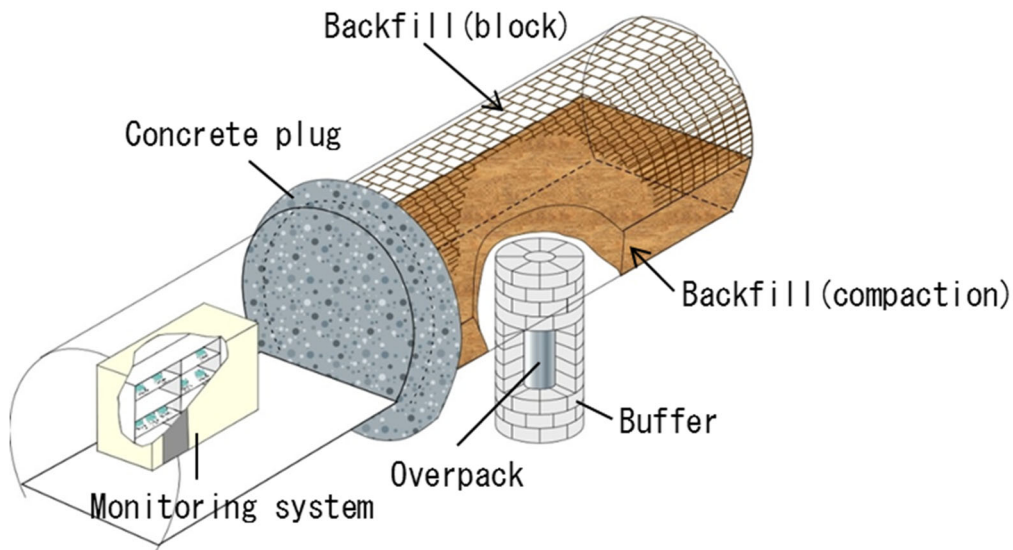
Figure 3.2-6. Schematic view of the Horonobe full scale *in-situ* EBS experiment (Bond and Birkholzer, 2019).
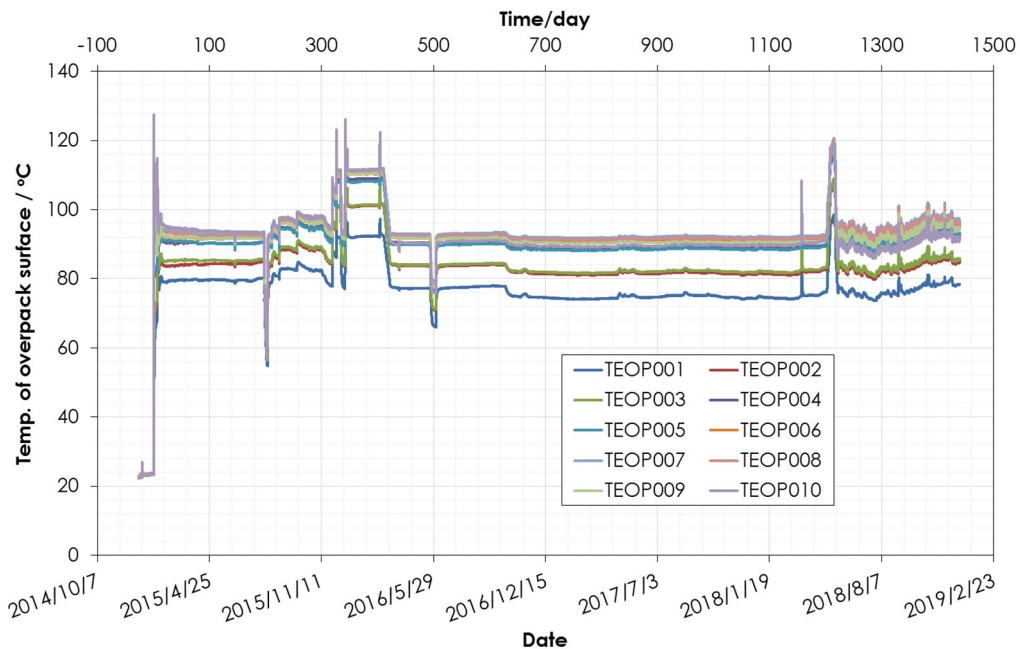
Figure 3.2-7. Temperature Evolution in the EBS experiment (Sugita, 2020).

3.2.3.5. *Brine Availability Test in Salt (BATS) – Task E*

The objectives of this task are to observe and predict the coupled processes governing the availability of water to heated excavations in geologic salt. Brine availability strongly impacts the long-term performance of salt repositories for heat-generating radioactive waste. The task utilizes data from the ongoing BATS tests at WIPP to (1) confirm the strengths and types of coupled THMC processes (i.e., thermal, hydrologic, mechanical, and chemical – THMC) that govern preferential brine flow paths and canister corrosion (e.g., Figure 3.2-8), and (2) develop and validate numerical and constitutive models for coupled processes and salt migration in bedded salt. Kris Kuhlman from SNL serves as the task lead.

The BATS field tests are conducted in short horizontal boreholes at the repository level (~650 m depth) in the US Department of Energy's Waste Isolation Pilot Plant (WIPP). So far, the following test activities have been conducted (Kuhlman et al., 2021a,b):

- A preliminary "shakedown" test was conducted in summer 2018 to compare heater designs and test equipment in the salt environment, completed in boreholes cored in 2013 (BATS "1s"). Brine inflow was quantified by circulating dry N2 gas behind a packer and through desiccant (i.e., grams water per day) and temperature data (thermocouples) were collected during several sequential multi-day heating episodes at different heater power levels. These results provide a first dataset to test numerical modeling approaches.

- A second test series was conducted from January to March 2020 (Phase 1a), in two parallel and nearly identical test arrays drilled specifically for BATS, one heated with a source borehole maintained at ~96ºC (2 weeks pre-heating data, 1 month of heated data, 2 weeks cool-down data) (Figure 3.2-9), the other unheated. The tests provided data on volumetric flowrate and composition of fluids (e.g., brine and steam) and tracers entering the boreholes through time. Geophysical data (i.e., electrical resistivity tomography, acoustic emissions, ultrasonic wave velocity, temperature, fiber-optic distributed temperature and strain) complement solid (i.e., cores around seals and heaters before and after testing), liquid (i.e., samples of brine with natural and added tracers), and gas (i.e., stable water isotopes and gas chemical composition) sampling (Figure 3.2-10). Fluid samples and geophysical data have been collected before, during, and after the heating phases.

- Despite Covid related testing and travel restriction, the BATS experimental program and analysis has made good progress in the past year. BATS Phases 1b and 1c began in January 2021 and involved addition of gas (1b) and liquid (1c) tracers in the same heated and unheated boreholes of the BATS Phase 1a location.

- Subsequent tests in the same boreholes will be conducted at higher heater power levels and with additional data collection. Seals have been emplaced into boreholes as part of the heated and unheated arrays, while monitoring stress and temperature in the plugs. The seals and surrounding salt will be overcored and removed after extended exposure to compare against complementary laboratory tests on seal materials being conducted at GRS.

For SFWD, a joint modeling team has been formed to participate in Task E, consisting of the organizations conducting the BATS test (SNL, LANL, LBNL). In terms of the task structure and schedule, Task E incorporates elements of:

- **Benchmarks**: Relatively simple simulations, either synthetic or well-constrained experiments to act as a 'warm-up' for participants and allow codes and process models to be compared.

- **Test Cases**: More complex modeling, with detailed comparisons against field and laboratory experimental data. A logical step here is to start with simulating brine migration under ambient conditions, and then to move to modeling brine production under multi-phase heated conditions (including production changes during heating and cooling), building on the previous step.

- **Uncertainty and Parameter Sensitivity**: Quantification of model-data uniqueness and model parameter sensitivity helps build understanding to balance complexity of added processes and non-linearities.

To date, teams have been going through a series of joint benchmarking exercises, and a preparing for the full complexity of the heat test modeling.
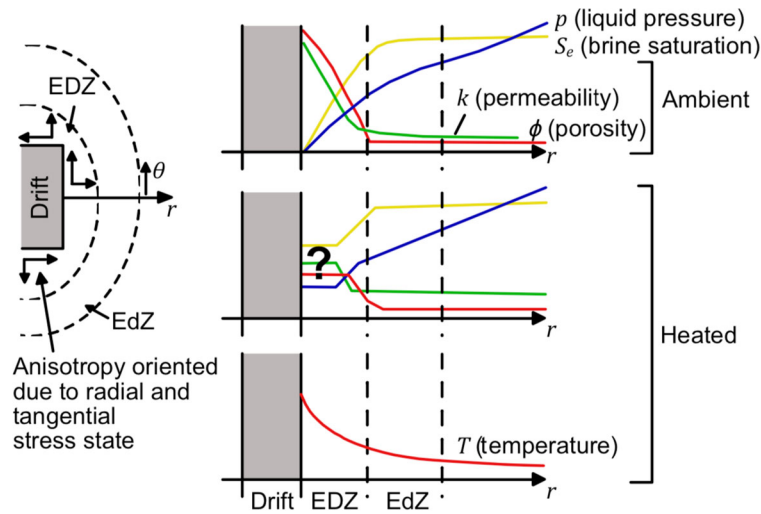
Figure 3.2-8. Schematic trends in hydrological properties and state variables from an excavation in salt to the far field under ambient (top) and heated (bottom) conditions (Kuhlman, 2020)
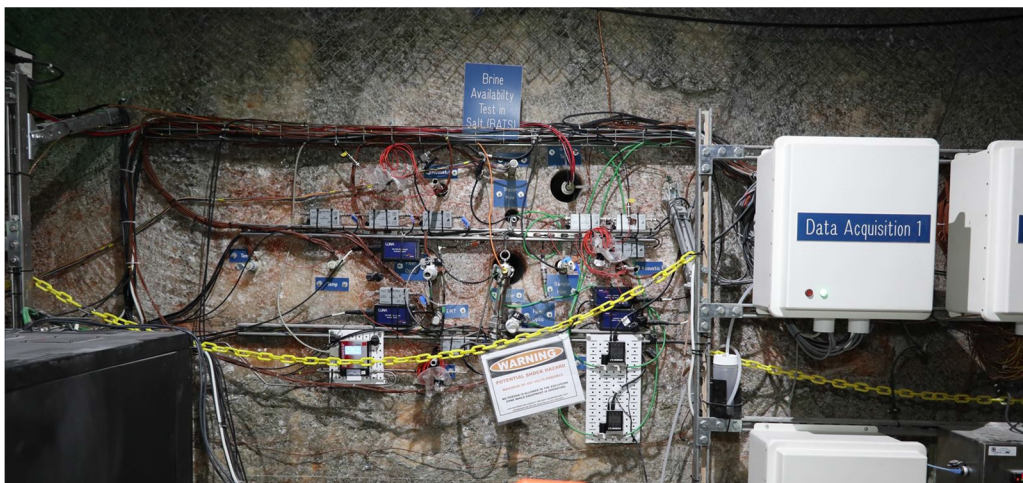
Figure 3.2-9. BATS heated array at the beginning of Jan – March testing (Kuhlman, 2020)
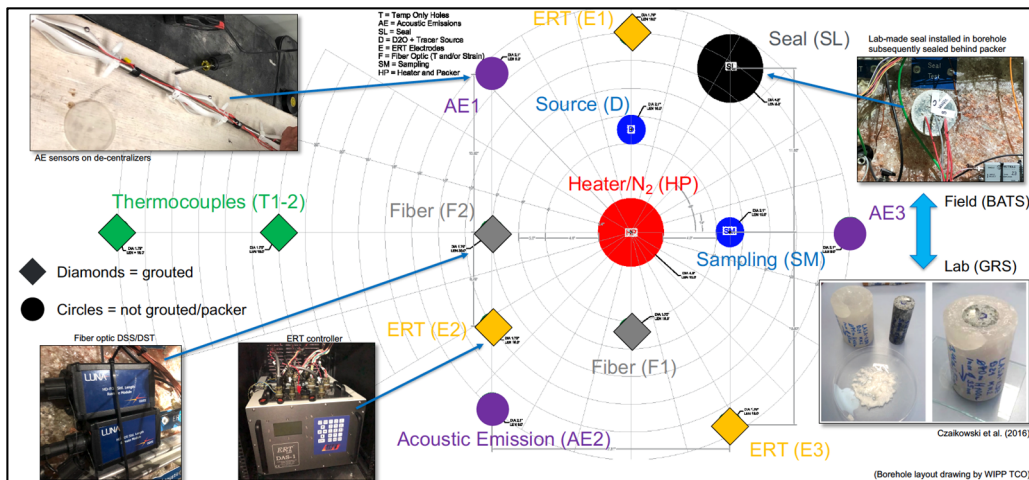
Figure 3.2-10. Borehole layout with central heater borehole and satellite monitoring boreholes in vertical cross-section perpendicular to heater element (Kuhlman, 2020).

3.2.3.6. *Performance Assessment (PA) – Task F*

The ultimate objective of this DOE-proposed task is to build confidence in the models, methods, and software used for performance assessment (PA), or safety assessment, of deep geologic repositories, and/or to bring to the fore additional research and development needed to improve PA methodologies. To achieve this objective, Task F involves a staged comparison of models and methods used in different PA frameworks, including: (1) coupled-process submodels (e.g., waste package corrosion, spent fuel dissolution, radionuclide transport, etc.) comprising the full PA model, (2) deterministic simulation(s) of the entire PA model for defined reference scenario(s), (3) probabilistic simulations of the entire PA model, and (4) uncertainty quantification (UQ) and sensitivity analysis (SA) methods/results for probabilistic simulations of defined reference scenario(s). The task will focus on performance measures indicative of the ability of the repository system to isolate radionuclides from the biosphere through containment and retardation. Performance measures are related to (1) the overall performance of the repository system, such as radionuclide concentrations in groundwater some distance from the repository and (2) the performance of individual components of the engineered or natural system, radionuclide flux from one component of the system to another. Emily Stein from SNL serves as lead for this task.

Task F investigates two generic reference cases in parallel: a repository for commercial spent nuclear fuel (SNF) in a fractured crystalline host rock and a repository for commercial SNF in a salt formation (Stein et al., 2020). Teams may choose to participate in the comparison for either or both of the reference cases. Although a direct comparison cannot be made between simulations of a crystalline repository and simulations of a salt repository, it is expected that lessons learned regarding, for instance, methods of coupling process models, propagating uncertainty, or conducting sensitivity analysis will be transferable between concepts.

Over the past several years, SFWD has developed a suite of reference cases to conduct 3D probabilistic performance simulations of generic repositories in a variety of host rocks (see example in Figure 3.2-11). The DOE crystalline and salt reference cases have been used as valuable starting points to define the two DECOVALEX test cases. Specific features and characteristics of the natural and engineered systems for inclusion in the generic DECOVALEX test cases have been discussed with all participating teams in order to create performance assessment challenges that are of interest to all participants. More details on the current status of Task F and the modeling work for Task F conducted by the SNL team are provided in Section 6.9.2.
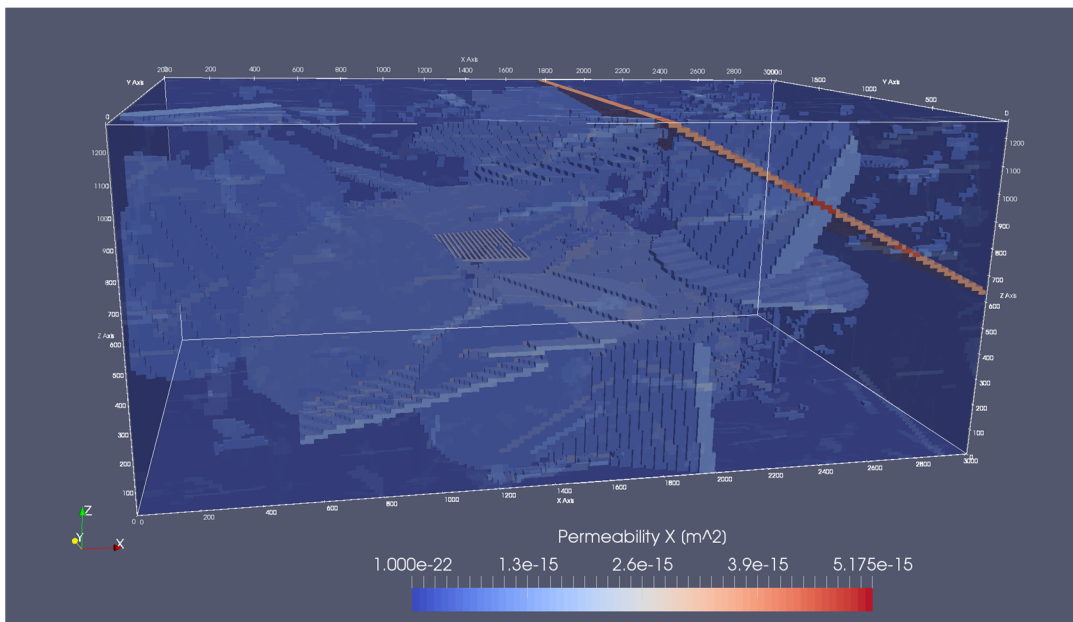
Figure 3.2-11. Generic reference case for a crystalline repository as developed by the SFWD campaign. The figure shows emplacement 3,360 waste packages in 168 drifts place 20 m apart, with a fracture network based on Forsmark (Sweden) fracturing characteristics (Stein, 2020).

3.2.3.7. *Safety ImplicAtions of Fluid Flow, Shear, Thermal and Reaction Processes within Crystalline Rock Fracture NETworks (SAFENET) – Task F*

Understanding of shear reactivation of pre-existing discontinuities for brittle host rocks is an area of considerable interest for radioactive waste disposal. The potential for existing features to undergo shear displacements and related changes in permeability as the result of coupled thermal, mechanical, hydrological and chemical effects can have significant impacts on repository safety functions (e.g., creating permeable pathways or, for very large displacements, mechanical damage of waste packages). The purpose of this task is to improve our quantitative understanding of fracturing processes in brittle rocks caused by mechanical (shear), hydraulic (fluid injection), and thermal (heating) processes, via the following task activities (Figures 3.2-12 and 3.2-13):

- Evaluation of mechanical (M) results derived from constant normal load (CNL) direct shear tests and constant normal stiffness (CNS) direct shear tests as well as high-resolution fracture surface scans (TU BA Freiberg) (Step 1). This step will elucidate the mechanics of rough fractures and how they are affected by shear and normal displacement.

- Investigation of hydro-mechanical (HM) results obtained with the GREAT cell (University of Edinburgh) with focus on fundamental shear processes under complex 3D stress states (Step 2). Building on Step 1 and using the same rock samples, this step will elucidate controls on fracture fluid flow under repository *in-situ* conditions, with a focus on deformation, fracture normal stress, shear stress and fluid pressure.

- Investigation of thermo-mechanical (TM) results obtained from tri-axial tests conducted at KICT with focus on shear processes triggered by thermal stresses (Step 3). Building on Steps 2 and 3, this step will answer the following key scientific question: Can shear slip of a stressed fracture be induced by long-term heating effects, and if so, what are the factors that mostly influence the shear slip process?

- Evaluation of impacts of coupled THM processes and upscaling to near-field scale. This step will be further defined during the course of the project and may involve some creative combination of Step 2 and 3 towards a new THM benchmarking study (Figure 3.2-14).

The focus of this task is at the laboratory scale, using well-designed experiments as listed above, to link micro-scale THMC effects acting on fracture surfaces and asperity contacts with emergent fracture properties such as permeability. The experiments are conducted on typical granite samples with pre-existing well-characterized discontinuities. It is expected that research teams will apply and develop existing constitutive models for fracture characterization and hence improve fundamental physical understanding of these complex processes as well as improving modeling predictive capabilities.
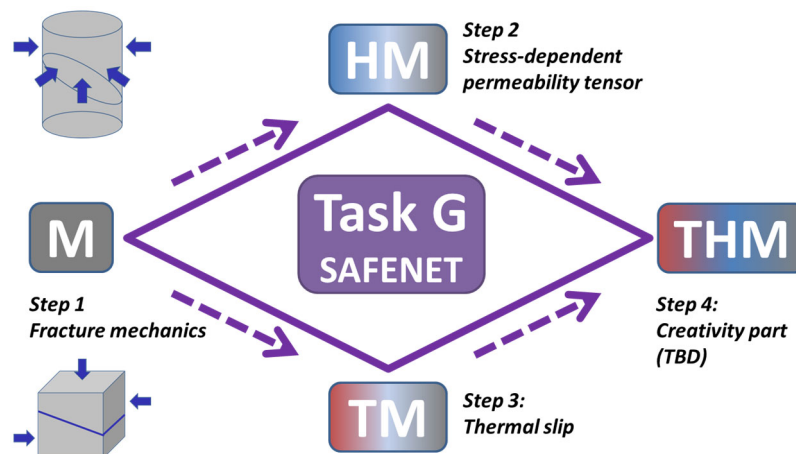
Figure 3.2-12. Task G structure (Kolditz et al., 2020)
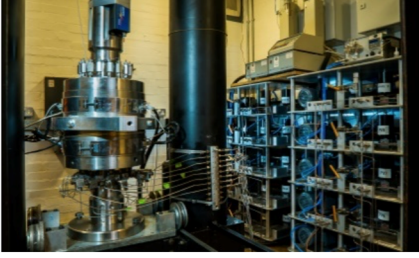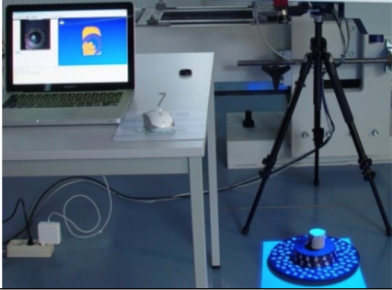
Figure 3.2-13. Experimental facilities used in this task (Kolditz et al., 2020).
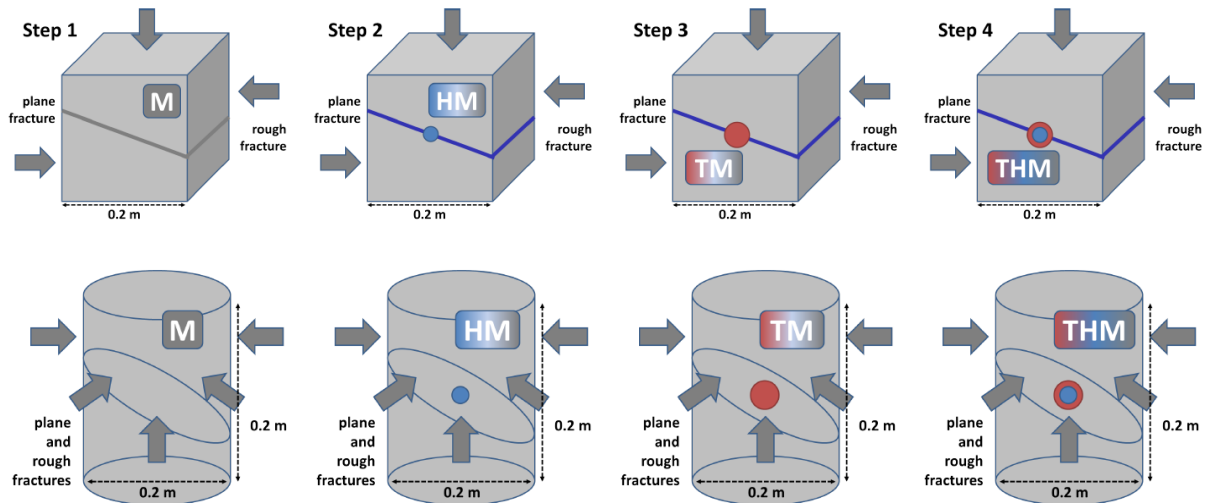
Figure 3.2-14. Task G benchmarking ideas (Kolditz et al., 2020).

What makes this task novel is that it is focused on understanding fundamental processes, based in part from previous DECOVALEX work, but also makes an attempt at linking these processes to key safety performance functions in radioactive waste disposal facilities. The wide range of high-quality experiments and conditions being examined allows for process understanding to be developed and robustly tested using state of the art approaches.

In FY21, task participants from multiple international modeling groups started with a first benchmark simulation to set the stage for more complex blind-prediction modeling of laboratory experiments. This first benchmark investigates the mechanical behavior rough fractures before and after mechanical shear. Shearing of a single fracture in a rectangular domain exposed to a differential (shear) load is simulated and the results are compared with an analytical solution. First modeling results and findings from the two SFWD teams participating in this task (LBNL and SNL) are summarized in Section 6.5.1.

3.2.4. DECOVALEX Summary

Benefits of Participation:

- Access to four to seven sets of experimental data from different URLs and different host rock environments

- Opportunities for modeling and analysis of existing data in collaboration with other modeling groups (typically less direct interaction with the project teams that run or interpret the experiments)

- Opportunity to suggest and/or lead modeling test cases of interest to DOE.

Status of Participation:

DOE formally joined the DECOVALEX project in 2012, with the start of the DECOVALEX-2015 phase. During this reporting year, DOE scientists participated in several modeling tasks associated with the DECOVALEX Project phase referred to as DECOVALEX-2023, which was initiated in early 2020 and will run through December 2023. These tasks include studies on heat and thermal fracturing of low-permeability rocks, bentonite gas migration studies, two full-scale heater tests in an argillite and a mudstone respectively, a brine migration field test in salt, a task focusing on performance assessment methods, and finally a fundamental task on shear activation in brittle host rocks.

Outlook:

As discussed in Section 3.2.3, many of the seven new DECOVALEX-2023 tasks are of high relevance for SFWD, and given the relatively small annual membership fee, the benefit of participating in DECOVALEX is very high. Two of the seven new tasks were proposed by DOE scientists and are now led by task leads from SNL (Kris Kuhlman for Task E, Emily Stein for Task F). Also, Dr. Jens Birkholzer of LBNL continues to serve as Chairman of the DECOVALEX project, which will help ensure that DECOVALEX tasks continue to be of importance to DOE's R&D goals.

Contact Information:

      DOE Contact:
      Prasad Nair, DOE-NE

      SFWD Contact:
      Jens Birkholzer, LBNL

      DECOVALEX Contact:
      Jens Birkholzer, Chairman of DECOVALEX-2019, LBNL, USA
      Alex Bond, DECOVALEX Technical Coordinator, Quintessa, United Kingdom

3.3. Grimsel Test Site Projects

The Grimsel Test Site (GTS) is a URL situated in sparsely fractured crystalline host rock in the Swiss Alps. The URL was established in 1984 as a center for underground R&D supporting a wide range of research projects on the geologic disposal of radioactive waste (Figure 3.3-1). GTS provides an environment, analogous to that of a repository site, thus allowing the development and testing of equipment, methodology, and models under fully realistic conditions (www.grimsel.com). GTS is a research facility and not a potential repository site, though investigations may utilize a wide range of radioactive tracers. NAGRA, as the site operator, has organized the majority of experimental activities in the URL as multinational collaborative projects, which typically include several partners from Europe, Asia, and North America. Participation in these collaborative projects requires formal project agreement between NAGRA and its partners. As discussed below, DOE has been quite involved with GTS activities. For example, DOE was a partner in the Colloid Formation and Migration Project (CFM) at GTS from 2012 through 2015 (Section 3.3.1), participated in the FEBEX Dismantling Project (FEBEX-DP) at GTS until its official close in 2018 but continues informal collaboration for further analysis and modeling (Section 3.3.2), and is currently one of several international partner organizations engaged in the high-temperature heater test (HotBENT) which just started operating its heaters after years of planning and installation (Section 3.3.3). GTS also offers other collaboration opportunities that SFWD has not currently tapped into. Examples are the Gas Permeable Seal Test (GAST) and the Materials Corrosion Test (MACoTE), both of which have been ongoing for a while and are moving into interesting project phases, as well as the Borehole Sealing Test (SET), which is currently in its pre-test preparation phase. These three examples are further described at the end of this section (Section 3.3.4).
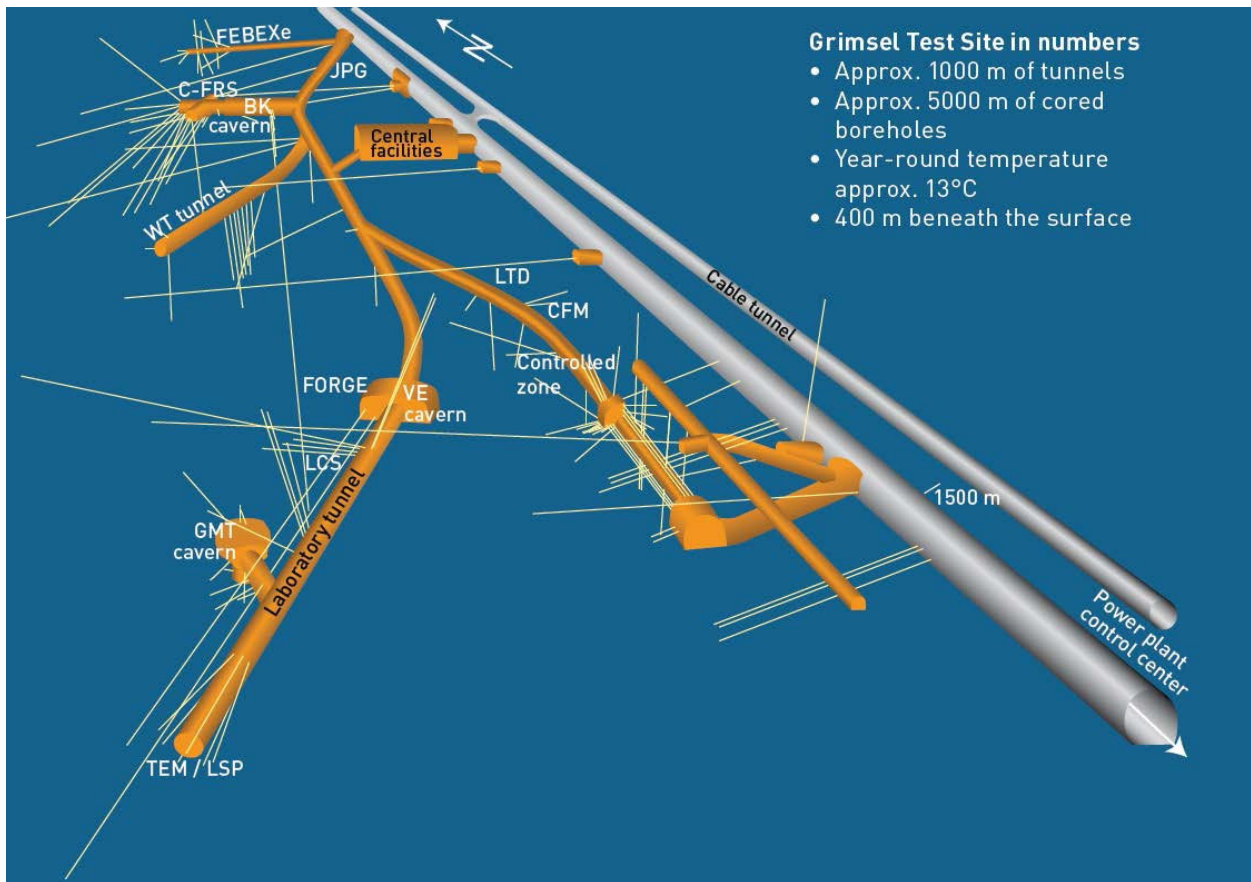
Figure 3.3-1. 3D view of layout of the Grimsel Test Site in Switzerland (NAGRA, 2010).

3.3.1. Colloid Formation and Migration Project

3.3.1.1. Overview of the CFM Project

The Colloid Formation and Migration (CFM) Project is a long-term international research project for the investigation of colloid formation due to bentonite erosion, colloid migration, and colloid-associated radionuclide transport. Colloid-related R&D at GTS comprises *in-situ* migration experiments conducted between boreholes in a fracture shear zone; these field experiments are complemented by laboratory and modeling studies. The main R&D objectives are as follows:

- To examine colloid generation rates and mechanisms at the EBS–host rock boundary under *in-situ* conditions

- To study the long-term geochemical behavior (mobility, mineralization, colloid formation, etc.) of radionuclides at the EBS–host rock interface

- To evaluate the long-distance migration behavior of radionuclides and colloids in water- conducting features in a repository-relevant flow system (i.e., with a very low flow rate/water flux)

- To examine reversibility of radionuclide uptake onto colloids

- To gain experience in long-term monitoring of radionuclide/colloid propagation near a repository.

The CFM project was preceded by the Colloid and Radionuclide Retardation (CRR) project, conducted at the Grimsel Test Site from 1997 to 2003. Twenty-seven field tracer tests were conducted during the CRR, including seven that involved short-lived radionuclides, one involving a suite of long-lived radionuclides with isotopes of U, Np, Am, and Pu, and one involving a suite of radionuclides (including Cs, Sr, Tc, U, Np, Am, and Pu isotopes) injected with bentonite colloids. Colloid-facilitated radionuclide transport was quantified by comparing the breakthrough curves of the radionuclides in the latter two tests (with and without the colloids). Similar tests with and without colloids were also conducted using nonradioactive homologues of actinides—e.g., stable isotopes of thorium (Th), hafnium (Hf), and terbium (Tb). All of the CRR tests were conducted as weak-dipole tests between boreholes completed in a fracture shear zone, with the tests involving radionuclides being conducted between boreholes separated by 2.2 m.

The CFM project was initiated in 2004 and has since been operating in four major phases (Figure 3.3-2). While similar in many respects to the CRR project, the CFM project aimed to improve or expand upon CRR in two key areas: (1) increase tracer residence times in the fracture shear zone to allow interrogation of processes that may not be observed over the very short time scales of the CRR tests (e.g., colloid filtration, radionuclide desorption from colloids), and (2) directly evaluate the performance of bentonite backfill with respect to swelling, erosion, and colloid generation, by emplacing a bentonite plug into a borehole completed in the fracture shear zone. To accomplish these objectives, a "tunnel packer" system was planned and installed during CFM Phases 1 and 2 (2004 – 2014) to seal off the entire access tunnel (Figures 3.3-3) where it was intersected by the shear zone. With this packer system, the flow rate from the shear zone into the tunnel could be throttled back from a natural rate of ~700 mL/min to any desired value, and the water from the shear zone could be collected in a controlled manner. Boreholes penetrating the shear zone could then be used as injection boreholes for tracer tests or for emplacement of the bentonite plug, with the tunnel packer effectively serving as an extraction location.

Using this novel setup, the CFM team conducted a total of 30 tracer tests between 2006 and 2013 in the controlled flow field in and near the shear zone. Early tests were conducted with conservative (nonsorbing) tracer tests at various shear zone flow rates and using different boreholes as injection holes to test the tunnel packer system and to evaluate tracer residence times that could be achieved. Tracer transport pathways from these tests and in from previous CRR tests are depicted in Figure 3.3-4, which shows the locations of several boreholes relative to the main tunnel within the shear zone. Borehole CFM 06.002, drilled in 2006 for the CFM project, was later established as the primary injection borehole to be used in subsequent tracer testing involving colloids, homologues, and radionuclides. Tests were conducted with injections of tracer solutions into borehole CFM 06.002 while extracting water from the Pinkel surface packer located at the tunnel wall ~6.2 m from the

injection interval. In 2008, an additional tracer test was conducted in which a bentonite colloid solution with homologues presorbed onto the colloids was injected into CFM 06.002. This test was followed immediately with a conservative tracer test in the same configuration. Based on lessons learned from these tests, five more tests were performed in 2009 and 2010, three of these with conservative tracers, two with bentonite colloids and homologues in addition to conservative tracers (Test 10-01 and 10-03). Finally, in 2012 and 2013, the CFM Project conducted two tests (12-02 and 13-05) involving the injection of a radionuclide-colloid cocktail including the actinides Pu(IV) and Am(III) into injection interval CFM 06.002. These experiments evaluated the transport of bentonite colloids with radionuclides from the source to the extraction point at the tunnel wall.
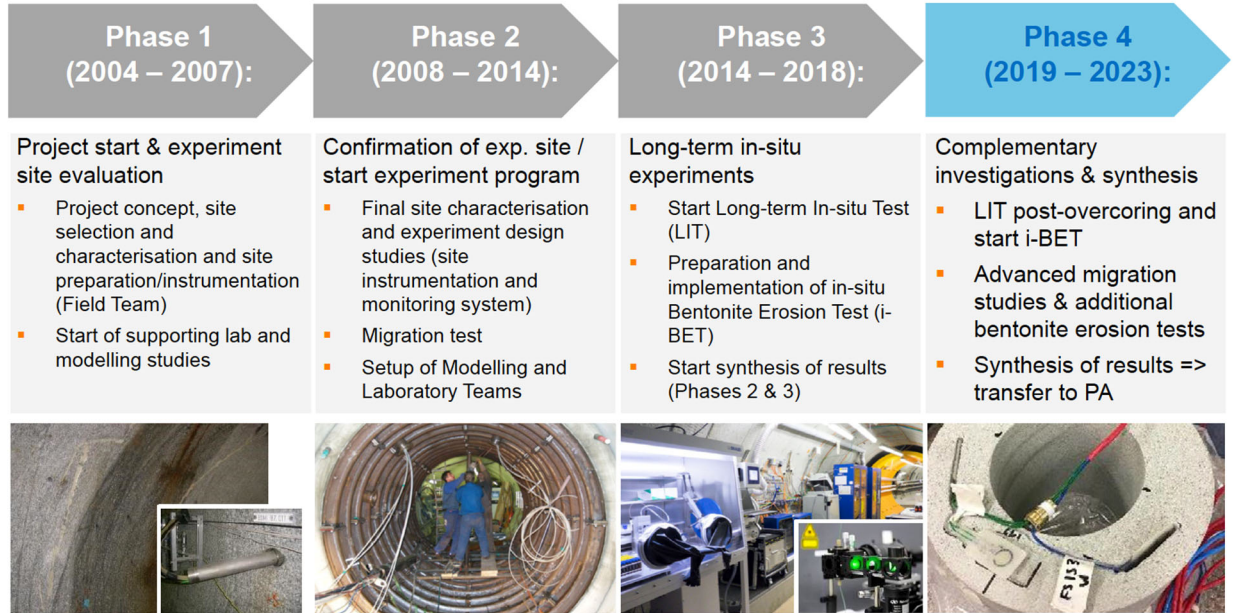
Figure 3.3-2. CFM Project Phases 1 to 4 (Blechschmidt et al., 2021).
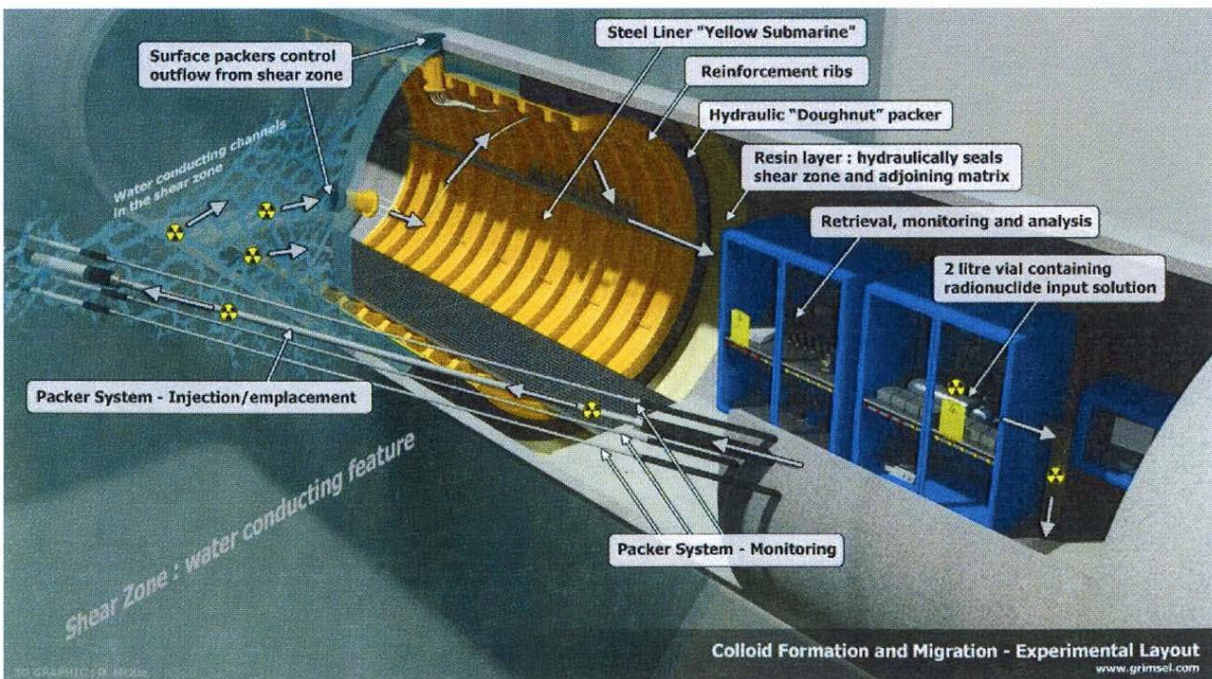
Figure 3.3-3. Schematic illustration of the CFM field test bed at Grimsel Test Site (Reimus, 2012).
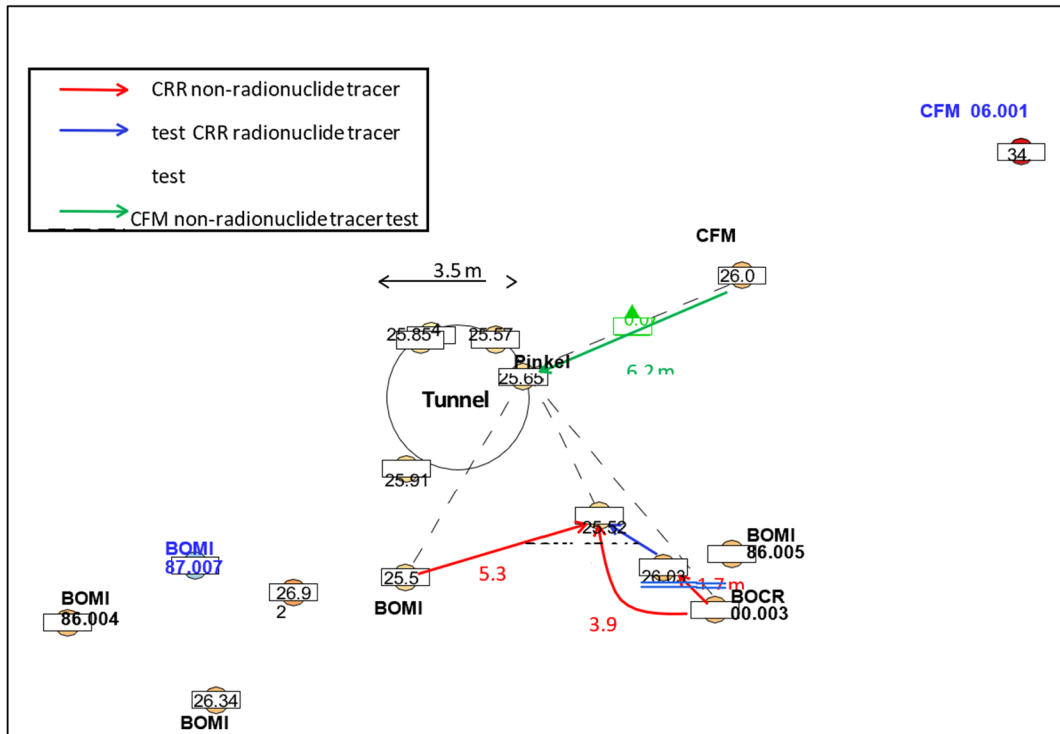
Figure 3.3-4. CFM field test bed at Grimsel Test Site: Borehole layout and test locations for all tracer tests 2001-2012 (Reimus, 2012).

3.3.1.2. Long-Term In-situ Test (LIT)

The CFM project entered its Phase 3 in 2014 with the emplacement of a radionuclide-doped bentonite plug into the same injection interval CFM 06.002 intersecting the flowing shear zone at the GTS. This experiment is referred to as the Long-term *In-situ* Test, or LIT. Three smaller diameter boreholes, CFM 11.001, 11.002, and 11.003, were drilled through the shear zone in roughly a triangular pattern around CFM 06.002 to serve as near-field monitoring boreholes during the LIT (Figure 3.3-5). Starting in 2014, the radionuclide-doped bentonite plug was emplaced in the flowing shear zone for about five years, until 2019 when the ensemble of four boreholes was overcored (shown as dashed lines in Figure 3.3-5). Samples obtained from the overcoring are currently used in a comprehensive post-mortem evaluation of the LIT to determine the disposition of both bentonite and radionuclides in the shear zone at the end of the experiment (see example in Figure 3.3-6). Results from detailed analysis of the overcored materials should be available soon.

3.3.1.3. In-situ Bentonite Erosion Test (i-BET)

The current CFM Phase 4 centers on the i-BET experiment, or "*In-situ* Bentonite Erosion Test. The project goal is to study bentonite swelling, colloid generation, and radionuclide migration in fractured crystalline rock. addresses a scenario where waste package breach allows radionuclides to sorb onto bentonite backfill, which in turn may erode into flowing fractures and may carry radionuclides away on colloids. The experimental setup involves bentonite rings emplaced into a borehole around a steel mandril and sealed at both ends with packers (see Figure 3.3-7). During installation of i-BET in late 2018, all bentonite rings were equipped with multiple sensors to monitor the swelling pressure and the water content. Additional boreholes were drilled to monitor the groundwater composition around the source and detect potential bentonite erosion. The experiment has been in a hydration and monitoring phase for almost two years and stable hydraulic conditions have established, as shown in the pore pressure monitoring data. Similar to the LIT, the project partners envision overcoring of the central borehole, likely in late 2022 or early 2023. i-BET may be an opportunity for SFWD researchers to consider.
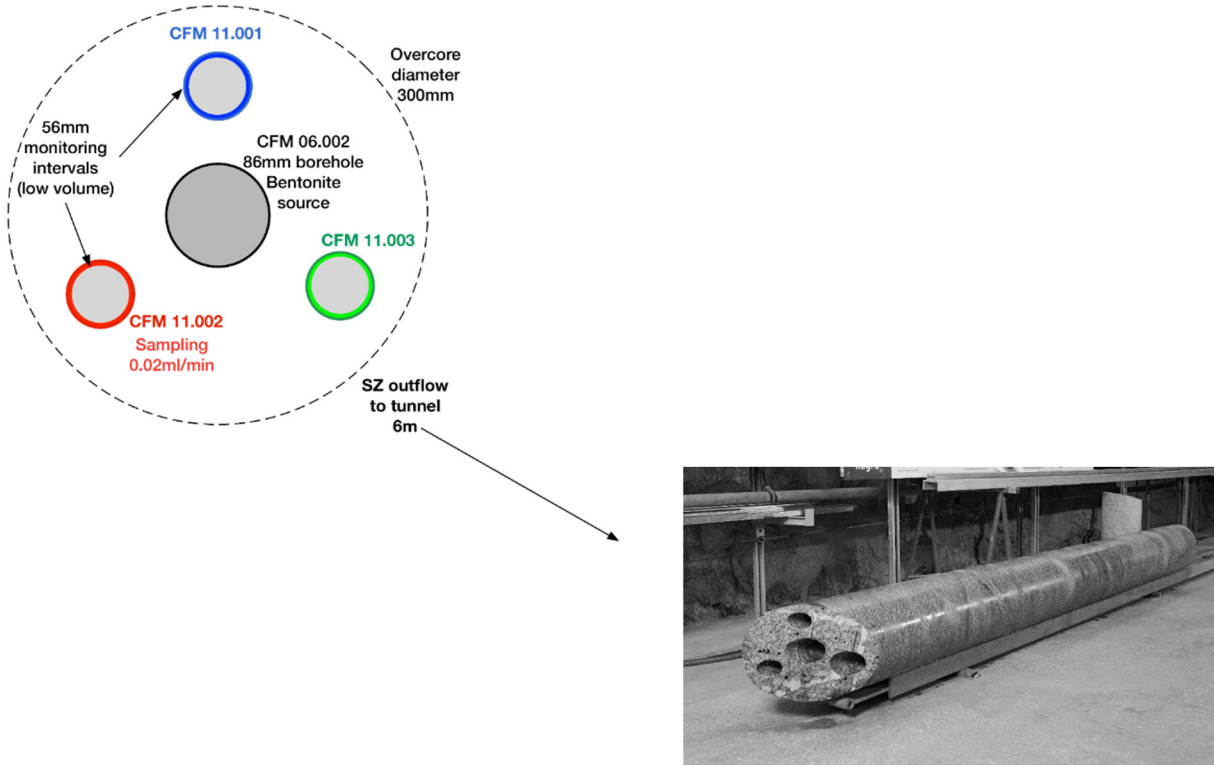
Figure 3.3-5. Plan view of the borehole configuration for the LIT showing the diameter of the overcoring (top left) and photo showing the overcored column (bottom right).
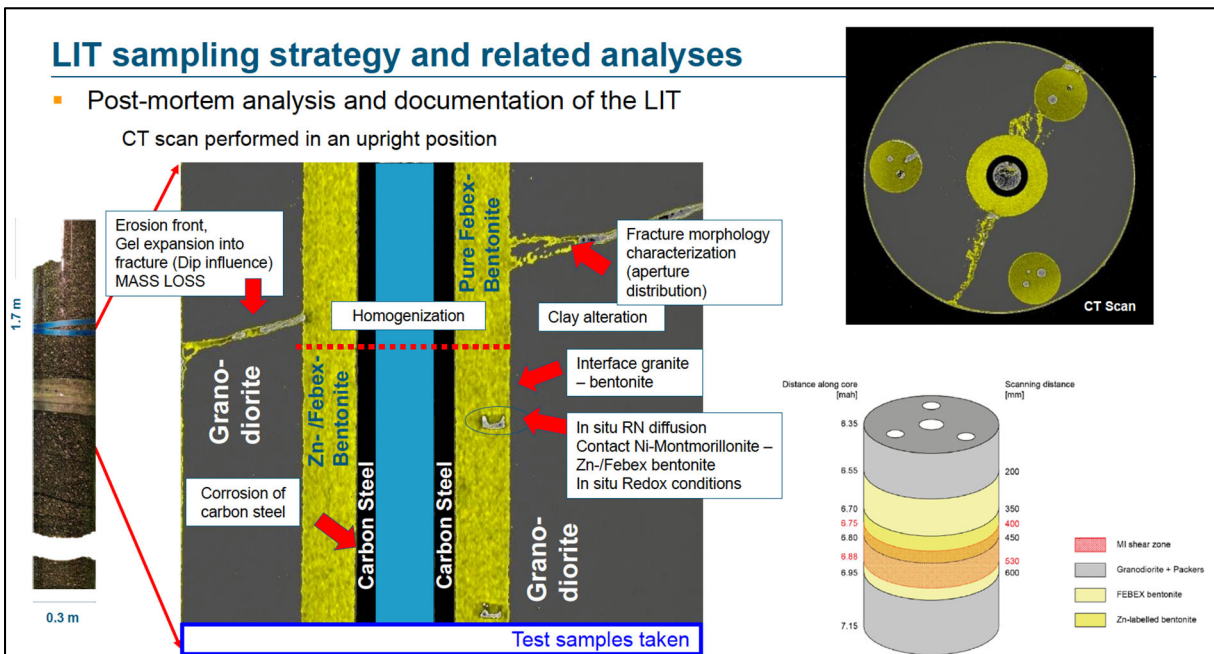
Figure 3.3-6. Example for sampling and analysis of LIT overcore column, here showing results from CT scanning (Blechschmidt et al., 2021).
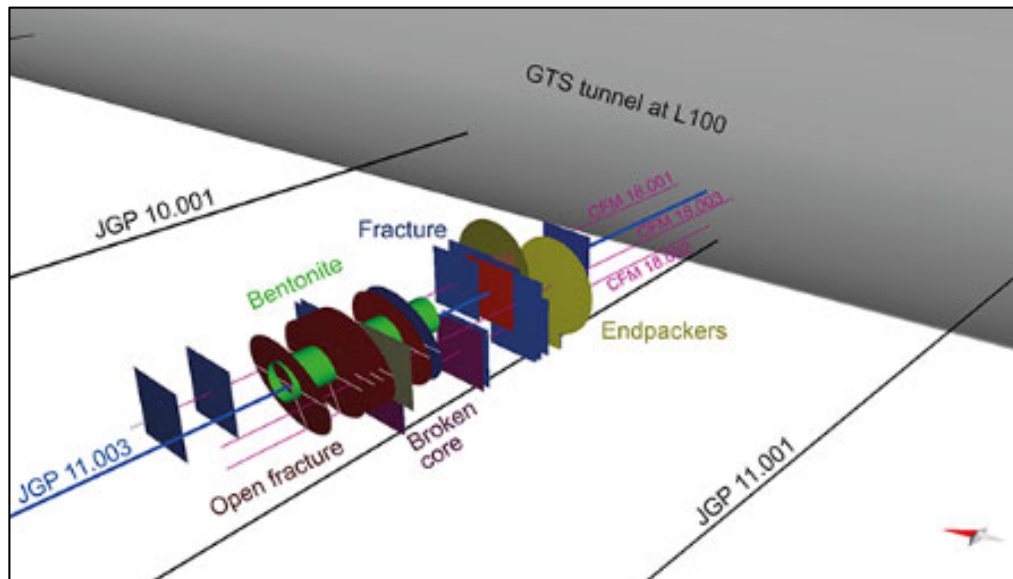
Figure 3.3-7: 3D picture showing the design of the I-BET experiment with the bentonite source and the fractures mapped along the surrounding boreholes. Monitoring boreholes are shown in pink.

3.3.1.4. SFWD Participation in CFM

The CFM experiments are unique in that they evaluate colloid-facilitated radionuclide transport in a field setting intended to mimic a high-level nuclear waste repository scenario. Realizing the benefit of becoming a formal partner, DOE in early 2012 formally applied for partnership in the CFM Project and was accepted as a new partner in August 2012. Partnership gave DOE and affiliated National Laboratories exclusive access to all experimental data generated by CFM. More importantly, it allowed SFWD researchers to work collaboratively with international scientists in ongoing experimental and modeling studies, and it involves them in the planning of new experimental studies to be conducted in the future. Like the Mont Terri Project, this type of international collaboration goes beyond the mostly modeling focus of DECOVALEX.

In contrast to both the DECOVALEX project and the Mont Terri project, which comprise a range of experiments covering a wide spectrum of relevant R&D issues, the CFM has a relatively narrow focus, i.e., colloid-facilitated radionuclide migration. In part because of this narrow focus and the comparably high membership fee relative to other international initiatives, DOE decided in 2015 to cancel its participation in the CFM Project. In FY16, a comprehensive synthesis of the current state of knowledge of colloid-facilitated radionuclide transport from a nuclear waste repository risk-assessment perspective was assembled in an overview report by Reimus et al. (2016). The report draws heavily on findings from the extensive and carefully controlled set of colloid-facilitated solute transport experiments conducted at GTS. Even without an official membership in the project, SFWD researchers from Los Alamos National Laboratory, USA (LANL) and Lawrence Livermore National Laboratory, USA (LLNL) continue to informally collaborate with their international partners in CFM. For example, LANL scientists in FY20 and FY21 conducted batch and column transport experiments to address two potential alterations to bentonite that could have strong impact on colloid transport: (1) high temperature impacts on bentonite colloids, and (2) swelling and/or erosion of bentonite pellets (Section 6.1.4). The current CFM project partners are from Germany (BMWi/KIT, BGE), Japan (NUMO), Great Britain (RWM), Republic of Korea (KAERI), and Switzerland (NAGRA). SFWD researchers should evaluate whether the ongoing i-BET experiment would offer important new scientific direction and is worth pursuing as a new collaboration opportunity, in which case renewing the previous partnership makes sense.

3.3.1.5. Colloid Formation and Migration Summary

Benefits of Participation:

- Access to experimental data from a suite of past, ongoing, and future experiments on colloid-facilitated migration at Grimsel, more narrow focus than other initiatives (Note the CFM membership does not provide access to other experiments at Grimsel)

- Opportunity to participate directly in international research groups that conduct, analyze, and model migration experiments (more direct involvement than DECOVALEX)

- Opportunity for participating in and steering ongoing or planned experiments as well as conducting own experiments

Status of Participation:

DOE formally joined the CFM Project in August 2012. As part of the CFM Project, SFWD researchers were involved in the interpretation and analysis of several colloid-facilitated tracer tests and conducted batch and column transport experiments to refine a colloid-facilitated transport model and to provide insight into potential colloid-facilitated transport of Cs isotopes in a crystalline rock repository. DOE ended its participation in the CFM project in December 2015, but continued informal collaboration with CFM partner organization. For example, LANL scientists in FY20 and FY21 conducted batch and column transport experiments to address two potential alterations to bentonite that could have strong impact on colloid transport: (1) high temperature impacts on bentonite colloids, and (2) swelling and/or erosion of bentonite pellets. A comprehensive synthesis report by Reimus et al. (2016) summarizes the current state of knowledge of colloid-facilitated radionuclide transport as derived from CFM and other activities.

Outlook:

DOE discontinued its participation in the CFM project in 2015, in part due to resource constraints but also because the scientific focus of the CFM Project is narrower than other initiatives discussed in this section. Informal collaboration is expected to continue. SFWD researchers should evaluate whether the new I-BET experiment would offer important new scientific direction and is worth pursuing as a new collaboration opportunity.

Contact Information:

       DOE Contact:
       Prasad Nair, DOE-NE

       SFWD Contact:
       Jens Birkholzer (LBNL), Paul Reimus (LANL)

       CFM Contact:
       Ingo Blechschmidt, Head of Grimsel Test Site, NAGRA, Switzerland

3.3.2. FEBEX Dismantling Project

3.3.2.1. Overview

The FEBEX heater test is a full-scale Engineered Barrier System (EBS) test that was operating under natural resaturation conditions for almost two decades (Figures 3.3-8). The overall objective of the heater test was to evaluate the long-term performance of the EBS and, to a lesser degree, of the near-field crystalline rock, with emphasis on the thermal evolution and resaturation of bentonite backfill surrounding a heated waste package. With heating initiated in 1997 and the heaters turned off in 2015, the FEBEX experiment was the longest running full-scale heater experiment in the world, providing a unique data set for the transient behavior of a heated repository. A fixed temperature of 100°C had been maintained at the heater/bentonite contact during this time, while the bentonite buffer had been slowly hydrating with the water naturally coming from the rock. As shown in Figure 3.3-8, the test comprised two individual heater sections, placed horizontally into a short tunnel at GTS. In total, 632 sensors of diverse types were installed in the bentonite barrier, the rock mass, the heaters, and the service zone to measure the following variables: temperature, relative humidity, total pressure, stress, displacement, and pore pressure.

Partial dismantling of the *in-situ* test was carried out during 2002, after five years of heating. The first one of the two heaters was removed, and the materials recovered (bentonite, metals, instruments, etc.) were analyzed to investigate the different types of processes undergone, while the second heater continued to operate (Figure 3.3-9). The samples recovered from this first heater experiment provided valuable information on the long-term condition of heated EBS materials (Lanyon et al., 2013).

In FY15, about 13 years after the first partial dismantling, NAGRA launched the FEBEX Dismantling Project (FEBEX-DP), which removed the second heater and recovered relevant EBS and host rock materials. This provided a unique opportunity for analyzing samples from an engineered barrier and its components that underwent continuous heating and natural resaturation for 18 years. DOE joined the FEBEX-DP Project as one of the initial partners, together with NAGRA, SKB, POSIVA, ENRESA, CIEMAT, KAERI, OBAYASHI, ANDRA, RWM and SURAO. The objective of FEBEX-DP project was to provide data and to improve understanding of the long-term THMC performance of the EBS components and their interactions with the host rock. This in turn increases confidence in the models required for predicting the long-term evolution of the engineered barriers and how their natural environment affects these. The FEBEX-DP Project thus focused on the collection of the following primary data/objectives (Gaus and Kober, 2014; NAGRA, 2014):

- Key physical properties (density, water content) of the bentonite and distribution
- Corrosion on instruments and coupons under evolving redox conditions and saturation states
- Mineralogical interactions at interfaces and potential impacts on porosity
- Integration of monitoring results and modeling

The dismantling project was initially scheduled to finish by the end of 2016, but then was extended till the end of 2018 to allow for further sample analysis and interpretative modeling. The project has now officially ended, while the valuable data set continues to provide a unique opportunity for better understanding of the performance of barrier components that underwent continuous heating and natural resaturation for a significant period. Therefore, some of the project partners, including SFWD researchers, remain informally involved in collaborative research to further the post-dismantling analysis and modeling interpretation (Section 6.1.2). Until recently, selected joint THM and THMC modeling activities were also coordinated in the context of the SKB EBS Task Force (see Section 3.4.3) as well as within Task D of the DECOVALEX-2019 Project (Section 3.2.2.4), but both of these activities have now ended. Key researchers from the previous FEBEX-DP team are in the final stages of publishing a comprehensive synthesis report on FEBEX-DP data synthesis and interpretation (expected by the end of 2021).
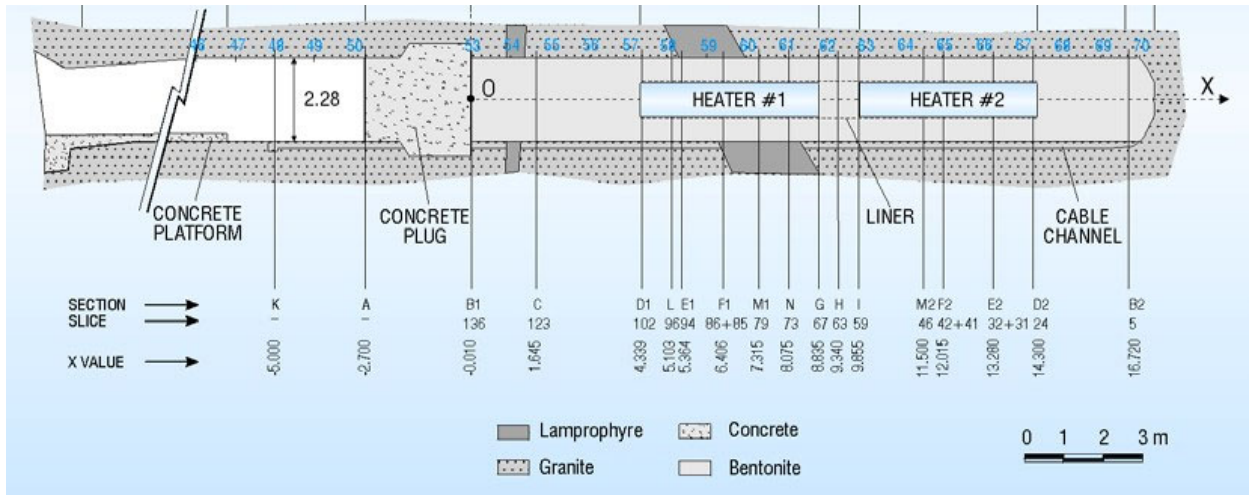
Figure 3.3-8. Schematic cross section of the FEBEX Test at Grimsel Test Site (NAGRA, 2014).
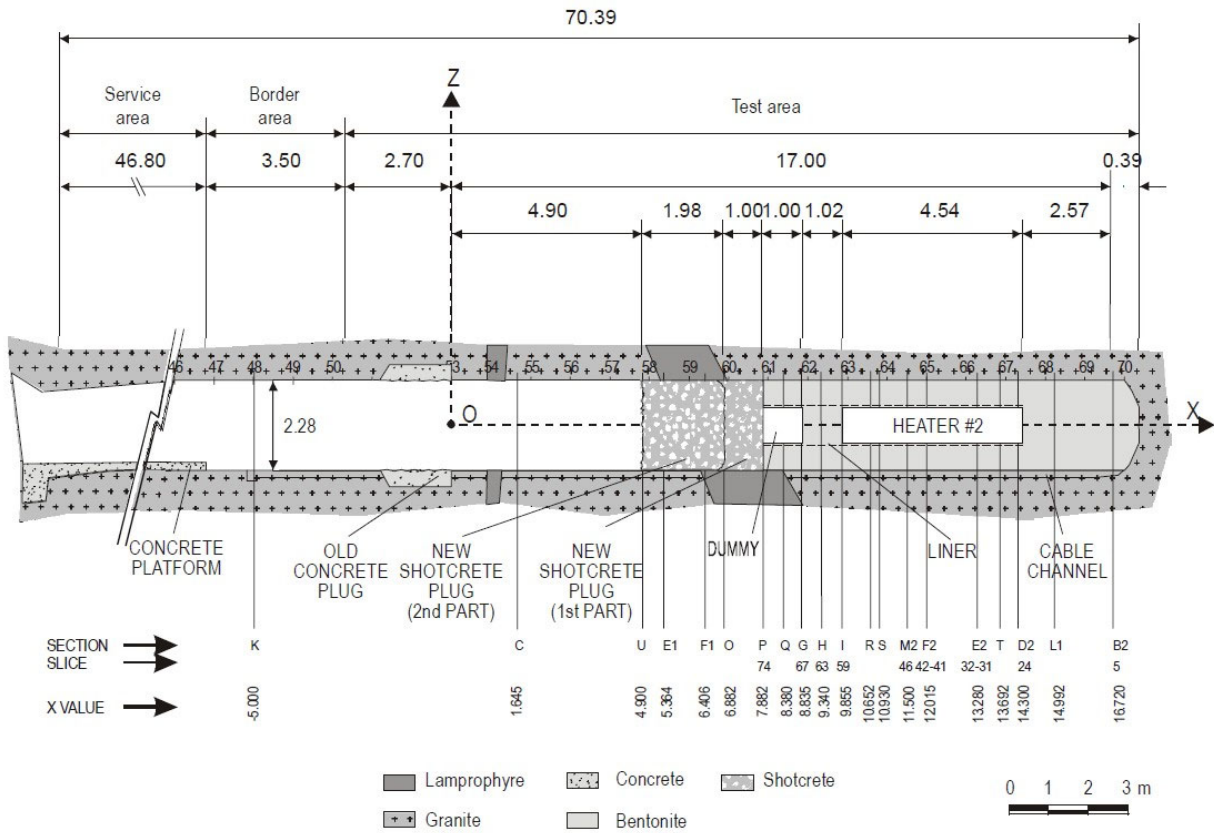
Figure 3.3-9. *In-situ* test configuration following dismantling of Heater 1 (Huertas et al., 2005).

55

3.3.2.2. Brief Review of FEBEX-DP Findings

Dismantling of the FEBEX experiments was conducted in a highly structure and organized manner. Figure 3.3-10 shows the configuration of multiple dismantling sections. In February 2015, drilling was conducted through the concrete plug and parts of the bentonite to get access to the heater test area, and in about two weeks of dismantling, the dismantling crew retrieved several overcores with intact shotcrete/bentonite interface. Then the concrete plug was demolished and sampling of the bentonite sections was finished by August of 2015. Figure 3.3-11 shows an example of several core samples drilled out of one dismantling section, Section 62. Details about the dismantling of the second heater are given in García-Siñeriz et al. (2017). The samples were then distributed to the various partners of FEBEX-DP for THMC and biological characterization and further experimental study. Starting in early FY16, FEBEX-DP partners embarked on a broad portfolio of laboratory analyses to characterize the hydrological, mechanical and chemical properties bentonite samples, followed by a modeling campaign focusing on various aspects of the diverse data set.

Overall, the FEBEX dismantling confirmed that the EBS in the FEBEX study performed largely as expected and predicted. THM and THC parameters and properties measured suggest that long-term safety requirements were fulfilled. The FEBEX-DP provided a number of valuable data sets, results, insights and outcomes for the confirmation and partial further development of repository concepts and safety requirements. Main findings are briefly summarized below, mostly describing the results from the 2015 dismantling campaign but also at times referring to the earlier 2002 dismantling (Kober, 2017a); a high-level synthesis is also given in Figure 3.3-12. Several NAGRA Working Reports (NAB) have been published over the course of project, and as mentioned above, a major technical synthesis report summarizing the major findings and outcomes of the FEBEX-DP Project is currently in the final preparation stages.
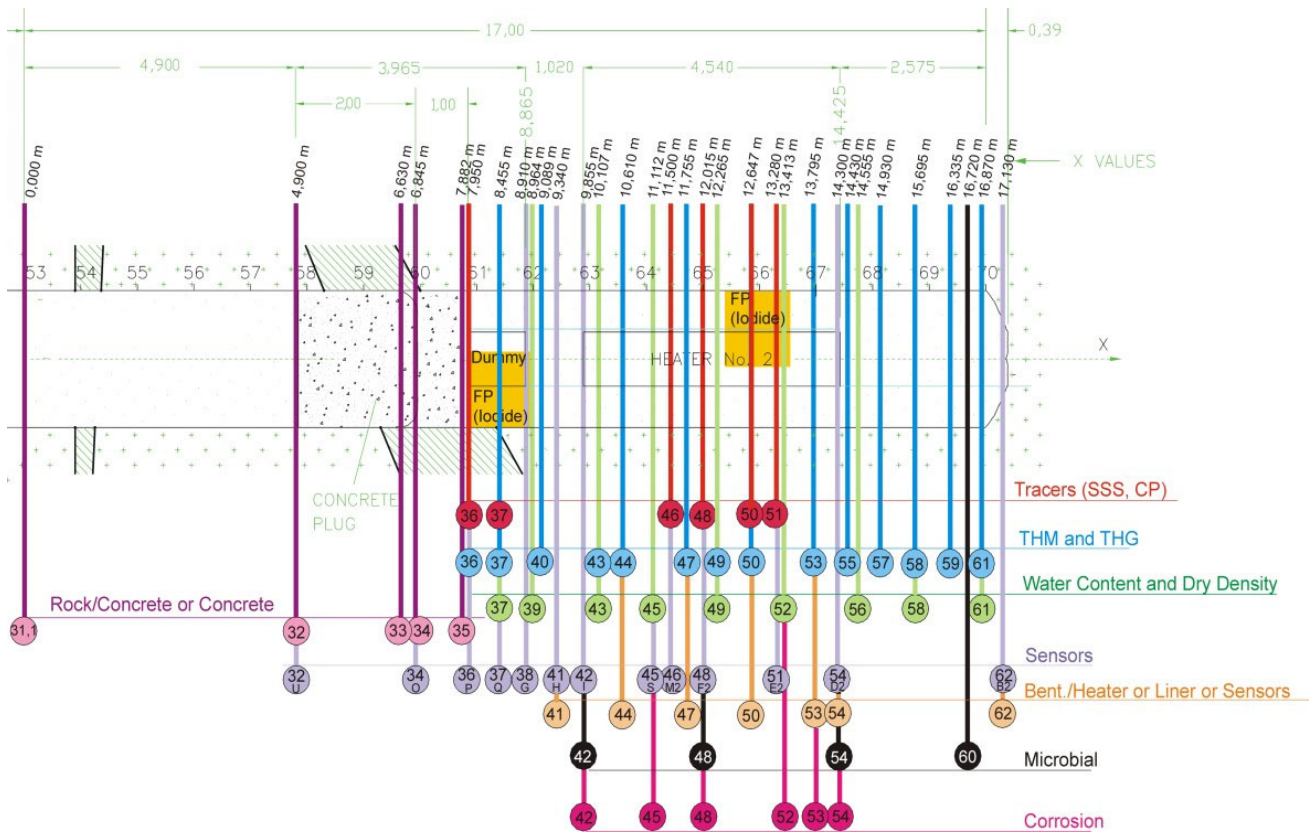
Figure 3.3-10. Sampling cross-sections (numbers in circles are cross-section numbers) for FEBEX-DP Project (NAGRA, 2014).

Figure 3.3-11. The front of dismantling section 62 with core samples taken for microbiological studies, the blue bar prevents the partially detached bentonite from collapsing (García-Siñeriz et al., 2017).

Safety relevant attributes (NTB 14-12; Leupin et al. 2014)	FEBEX/FEBEX-DP contribution (depending on organizational requirements)
Low hydraulic conductivity	Properties not altered, diffusion dominated ($10^{-12} - 10^{-14}$ m/s)
Chemical retention of RN	Sorption properties unlikely altered (no mineral transformation)
Sufficient density	Density gradients evolved, mean 1.59 g/cm^3
Sufficient swelling pressure (avoid EDZ extension)	~6 MPa (for 1.6 g/cm^3); lab-scale confirmed in 1:1 experiment
Mechanical support (canister sinking, stress buffering)	Sufficient support ($\uparrow$ 6; $\downarrow$ -17; $\leftrightarrow$ 6 mm - liner, with low confidence)
Sufficient gas transport capacity (gas transport without compromising hydraulic barrier)	not relevant
Minimise microbial corrosion	No indication of MIC on canister, No unambiguous indication of MIC on instruments
Resistance to mineral transformation	No significant transformations detected
Sufficient heat conduction	As predicted

Figure 3.3-12. Synthesis of FEBEX-DP findings in safety context (Kober, 2017b).

Bentonite Properties: The direct measurements of key physical properties (water content, dry density, degree of saturation) in 2002 and 2015 provided valuable information on the hydration patterns under the influence of heating, which have been relatively symmetric, yielding differences along the gallery axis related to the temperature during operation and to the initial inhomogeneity of the barrier. Expected gradients evolved away from the heater and towards the gallery. During dismantling in 2015, the water content varied between 17% (near the heater) up to 34% (bentonite- rock interface), inverse to dry density values of about 1.75 g/cm^3 and

1.43 g/cm^3, respectively. Average best estimates for the whole barrier excavated in 2015 after 18 years of heating and hydration around Heater 2 were a water content of 25.5%, a dry density of 1.59 g/cm^3 and a saturation of 97%, evolving from respective 2002 values of 22.2%, 1.58 g/cm^3 and 85% (Villar et al., 2005). Generally, a homogeneous pattern of hydration occurred despite some host rock heterogeneities with zones of higher permeability (see example pattern of saturation in Figure 3.3-13). Thus, the resaturation process was driven by the suction of the bentonite rather than by the availability of water in the rock, especially in the early phase, with the water content in the buffer close to the heater slowly increasing over the years.
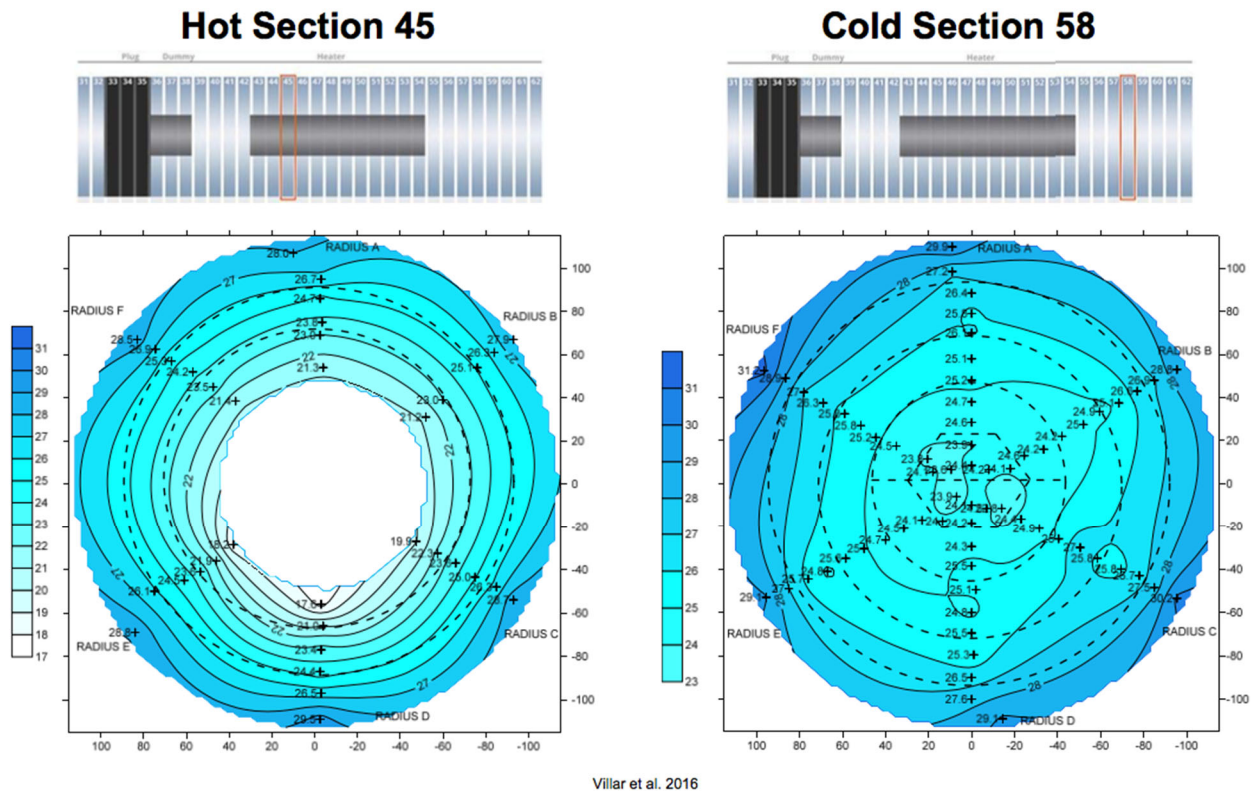
Figure 3.3-13. Spatial distribution of water content in two cross sections (Kober, 2017b).

Bentonite Mineralogy: The changes observed in bentonite mineralogy and crystal-chemical related properties were minor, with only small evidence of increase in total layer charge of the smectite near the heater, along with Mg enrichment towards the heater. No changes in the cation exchange capacity with respect to the original bentonite were observed, whereas the changes in the pore water composition were remarkable. The hydro-mechanical properties of the barrier were linked mainly to dry density. The water retention capacity was not altered by operation and no substantial changes in hydraulic conductivity or swelling capacity with respect to the reference bentonite were observed. The thermal conductivity was quite homogeneous in the barrier and mostly between 1.2 and 1.3 W/mK, in accordance with the high degree of saturation of the bentonite. The concrete plug had a limited impact on the bentonite, affecting a thickness of 1-2 mm, while changes in the concrete matrix by interaction with bentonite extended up to 5 cm (Alonso et al., 2017).

Corrosion Processes: Corrosion phenomena related to carbon steel-based materials (heater, perforated liner, various sensors) were localized and influenced by the variable moisture evolution in the test and potentially some partial dismantling perturbation. Thus, the thickness of corrosion affecting the bentonite occurred in layers that varied from almost zero to several cm, where the extent of the surrounding Fe-enriched bentonite varied proportionally to the corrosion layer thickness. The dominant corrosion products formed were Fe(III) oxides (e.g. goethite) which indicates that corrosion occurred mainly under aerobic conditions. However, the formation of magnetite and siderite, and reduced iron species in the clay are evidences of anaerobic corrosion

occurring upon oxygen depletion in the experiment. Mass balance considerations suggest that the oxic phase was prolonged because of air ingress during the experiment. In general, a temporal and spatial evolution in redox state of the experiment can be concluded.

SFWD Participation in FY21: With regards to sample characterization of the experiment, SFWD scientists from SNL in FY21 continued studying the micro-structure of the FEBEX-DP bentonite samples to better understand potential heat-induced chemical and mechanical alterations (Sections 6.1.2.3). Using bentonite samples from the FEBEX-DP test, LBNL researchers investigated the potential for heating-related mineral alterations impacting the radionuclide diffusion and sorption properties in bentonite (see Section 6.1.2.4) and are also looking at the effect of heating on microbial communities (see Section 6.1.2.5). LBNL scientists also conducted THMC modeling of the FEBEX test evolution to interpret the dismantling data and provide validated simulation methods for long-term PA studies (Section 6.1.2.1). As a participant in Task 9 of the SKB EBS Task Force, SNL finalized in FY21 a TH and THM modeling exercise using the FEBEX experiment as an example (Section 6.1.2.2).

3.3.2.3. FEBEX-DP Summary

Benefits of Participation:

- Access to experimental samples and laboratory investigations from a long-term heater experiment with focus on engineered barrier components, more narrow focus than other initiatives (Note that FEBEX-DP membership does not provide access to other GTS experiments)

- Opportunity to participate directly in international research groups that analyze samples and conduct modeling work on coupled THM and THC behavior

- Opportunity for designing sampling plans as well as conducting own laboratory experiments

Status of Participation and Outlook:

The FEBEX-DP Project has now officially ended. However, some project partners, including SFWD scientists, are informally continuing their collaboration to further data analysis and modeling interpretation. Lessons learned from the FEBEX-DP characterization and simulation studies are being applied to the planned high-temperature HotBENT heater test discussed in Section 3.3.3. Note also that some THM and THMC modeling activities related to the FEBEX-DP experiment have been embedded in other international initiatives, like the SKB EBS Task Force and the DECOVALEX-2019 Project, though both of these have now ended.

Contact Information:

> DOE Contact:
> Prasad Nair, DOE-NE
>
> SFWD Contacts:
> Jens Birkholzer (LBNL), Carlos Jové-Colón (SNL), and Liange Zheng (LBNL)
>
> FEBEX-DP Contact:
> Florian Kober, NAGRA, Switzerland

3.3.3. HotBENT – A Full-Scale High-Temperature Heater Test

3.3.3.1. Overview

Several international disposal programs have recently initiated a research program motivated by the desire to understand if clay-based barriers can withstand temperatures higher than the 100°C threshold for bentonite performance usually assumed in advanced repository designs. For example, the SFWD campaign has investigated the feasibility of direct geological disposal of large spent nuclear fuel canisters (the so-called dual-purpose canisters, or DPCs) currently in dry storage (Hardin et al., 2014), which would benefit from much higher emplacement temperatures. The performance of bentonite barriers in the <100 °C temperature range is underpinned by a broad knowledge base built on laboratory and large-scale *in-situ* experiments. Bentonite parameter characterization above 100°C is sparser (especially for pelletized materials); although up to 150°C no significant changes in safety-relevant properties are indicated. At temperatures above this threshold, it is possible that a potentially detrimental temperature-driven physicochemical response of materials (cementation, illitization) may occur, the characteristics of which are highly dependent on, and coupled with, the complex moisture transport processes induced by strong thermal gradients. The impact of such complex processes on the performance of a repository cannot be realistically reproduced and properly (non-conservatively) assessed at the smaller laboratory scale. Such an assessment needs to be conducted by large *in-situ* experiments in underground research laboratories (URLs), where the most relevant features of future emplacement conditions can be adequately reproduced.

Starting in 2015, options for a targeted high-temperature experiment (150°C to 200°C) in a fractured rock environment were actively pursued under the leadership of NAGRA with several international partners, including DOE (Vomvoris et al., 2015). In FY16, NAGRA and partners proposed a new collaboration effort referred to as the HotBENT experiment, a full-scale high-temperature heater test using the well-characterized FEBEX drift at the Grimsel Test Site, which has been empty since the FEBEX dismantling in 2015. The benefit of such a large-scale test, accompanied by a systematic laboratory program and modeling effort, is that the temperature effects can be evaluated under realistic conditions of strong thermal, hydraulic and density gradients, which cannot be reproduced in the laboratory. This will lead to improved mechanistic models for the prediction of temperature-induced processes, including chemical alteration and mechanical changes, which can then be used for performance assessment (PA) analysis of high-temperature scenarios. The key question is whether higher repository temperatures would trigger mechanisms that compromise the various barrier functions assigned to the engineered components and host rock. If the barrier function is (partially) compromised, PA analysis can evaluate whether the reduced performance of a sub-barrier (or parts thereof) would still give an adequate performance. DOE's participation in this collaborative effort is expected to be extremely beneficial; substantial cost savings would be achieved in the design of a repository if HotBENT the maximum temperature of bentonite backfill can be raised without drastic performance implications.

In FY16 through FY19, NAGRA held several planning meetings to discuss the interest of potential partners in the project and to develop a plan/design for the HotBENT project. Potential partners agreed on a common set of objectives as follows: (1) Increase data base (monitoring, sampling, lab-analysis) and understanding on buffer behavior at high T conditions (up to 200°C conditions at the canister surface), (2) Assessment of buffer performance at realistic scales and gradients compared to small scale laboratory tests and modeling, (3) Evaluate effects and impacts of microbial activities / corrosion processes / gas evolution, and (4) Integrate modeling (e.g. THMC) and lab activities (e.g. mock-up experiments). The partners decided on a modular design with several modules that would differ mainly in terms of type of bentonite and canister, temperature range, design with/without concrete liner, etc. LBNL actively participated in the project planning and design from the very beginning and used THMC modeling work to help facilitate the final design of the experiment. A comprehensive report was completed by LBNL scientists to determine the extent of coupled geochemical alterations expected in HotBENT and whether these would lead to measurable changes in bentonite properties (Zheng et al., 2018a). The official HotBENT Project start was in 2018 once all agreements with the partner institutions had been in place. In addition to DOE and NAGRA, the joint project has four other full partner institutions (Surao, RWM, NUMO, and BGE) and four associated institutions (NWMO, BGR, ENRESA, and Obayashi).

3.3.3.2. *HotBENT Design and Status*

The following description and figures provide an overview of the design and status of the HotBENT experiment. In the two years following the official start of the project, the test was constructed at the end of the FEBEX gallery (drift) that starts at the northern entrance of the Grimsel Test Site (Figure 3.3-14). The gallery is geologically, hydraulically and geophysically well characterized (Huertas et al., 2005) and has proven realistic conditions for saturation (Villar et al., 2017a,b). The experimental concept builds on previous experiments and large-scale heater tests in granitic and claystone host rock, such as FEBEX at the Grimsel Test Site, EB, HE-E and FE at the Mont Terri Underground Research Laboratory. The experiment is designed in a modular fashion, whereby a module represents a heater rested on a bentonite block pedestal and encapsulated by a granular bentonite backfill (Figure 3.3-15). Modules differ in their design temperature, bentonite type, experimental duration, and whether a liner is used or now. The two modules deepest in the drift are separated from the others by an insulation plug to enable earlier excavation (i.e., after 5 years) of part of the experiment with minimal perturbations to the remaining modules (which may run as long as 20 years).
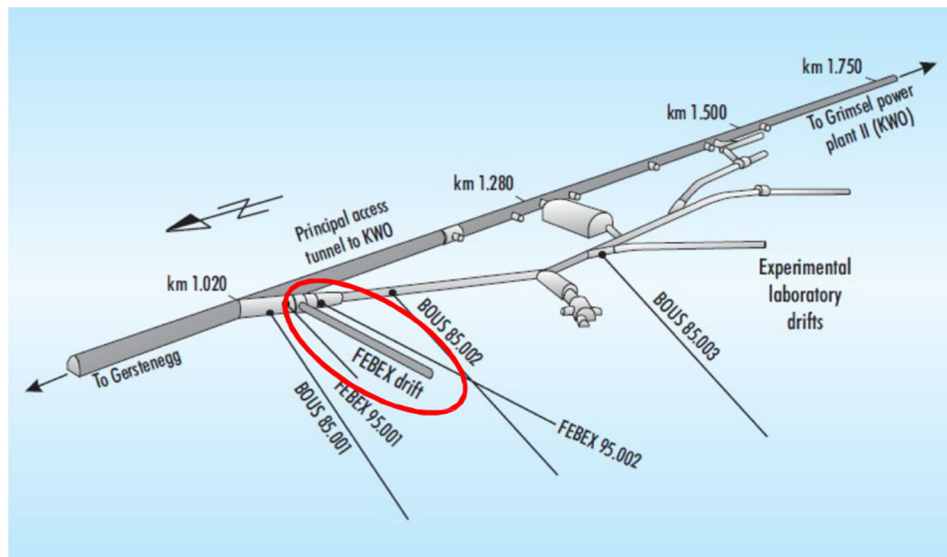
Figure 3.3-14. Location of the FEBEX Drift at the Grimsel Test Site (NAGRA, 2017)
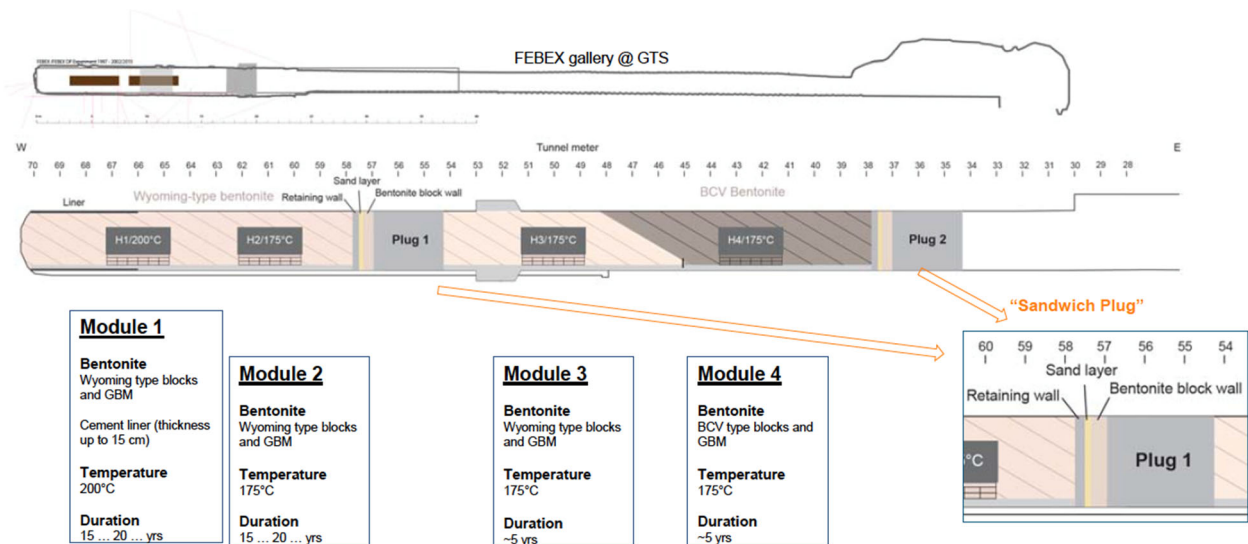
Figure 3.3-15. Final HotBENT design with individual modules (Kober, 2020).

HotBENT features a dense and broad portfolio of monitoring and instrumentation equipment. The THMC evolution of the engineered barrier and the surrounding host rock will be tracked with ~4100 instruments arranged in 28 monitoring segments along the tunnel axis, measuring properties such as temperature, mechanical pressure, hydraulic pressure, water content, saturation, and humidity, displacements, gas concentration and gas pressure. HotBENT also includes corrosion studies with metal coupons distributed near the heaters and plans to for microbiological characterization. The photo in Figure 3.3-16 shows the complex arrangement of the heater and the sensor equipment before backfilling of the tunnel with granular bentonite. Note that four boreholes have been drilled in the host rock along-side the heated tunnel which are equipped with multiple packers for segmented forced hydration of the experimental testbed.
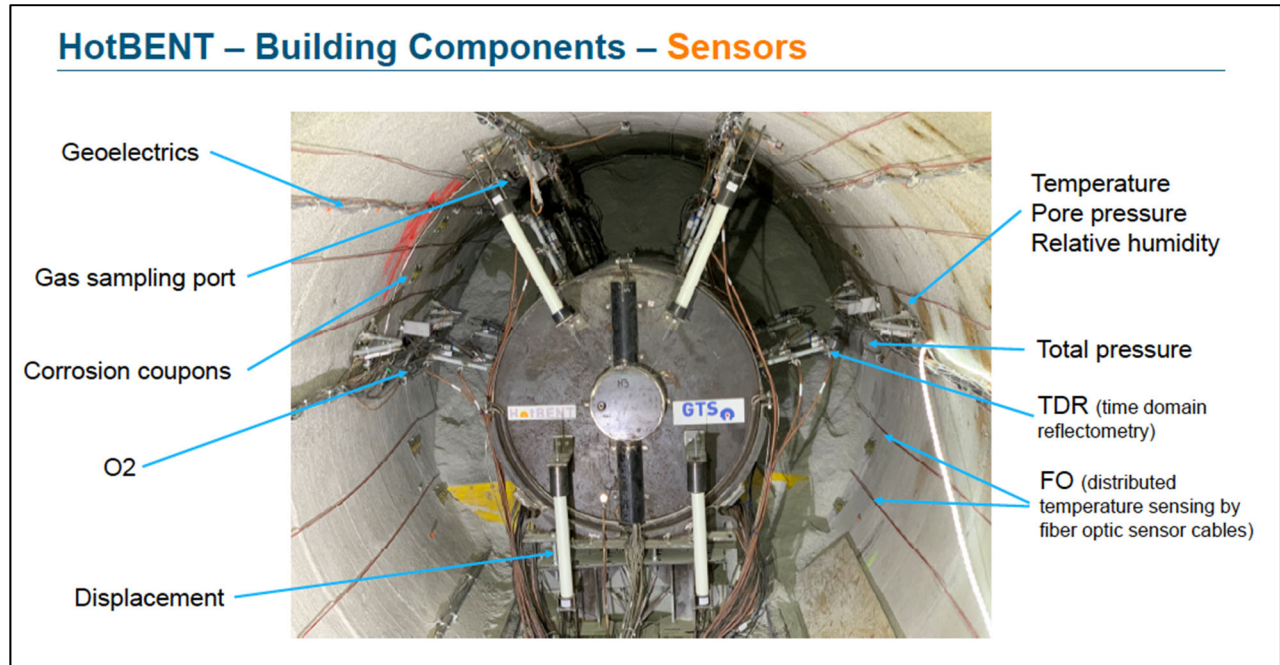
Figure 3.3-16. Phot showing the heater and sensor equipment in the HotBENT tunnel (Kober, 2021).

In parallel with the construction, NAGRA and partners launched a HotBENT Modeling Platform, which will include modeling groups associated with the individual partner organizations that are working on interpretative modeling of the test data. The multi-institutional group is structured so as to (a) increase the support provided to the HotBENT experiment and its interpretative evaluation, (b) broaden questions being addressed to advance fundamental understanding, and (c) address modeling issues, specifically the quantification of conceptual uncertainties. All partners encourage the Modeling Platform to pursue a broad spectrum of alternative conceptual models that address a common question or support a decision to be made jointly by the HotBENT participants. In addition, specific expertise and skills of the modeling groups can be used to examine particular aspects raised by the data collected as part of the HotBENT experiment, or to make specific predictions. SFWD scientists from LBNL and possibly SNL plan to participate in the Modeling Platform. Pre-test predictions from LBNL's THMC simulations are summarized in Section 6.1.2.3.

A detailed timeline for the experiment is given in Figure 3.3-17. After on-site and off-site preparatory work since 2018, the construction of the field test started in February 2020. The construction was completed in August 2021 and on September 9 2021 at 09:30 all heaters were switched on to an initial power of 300 W per heater. Following this initial stage, the heaters will be ramped up to full power in three roughly 6-week long interim steps. Figure 3.3-18 illustrates the first measurements showing elevated temperature as a result of heating.
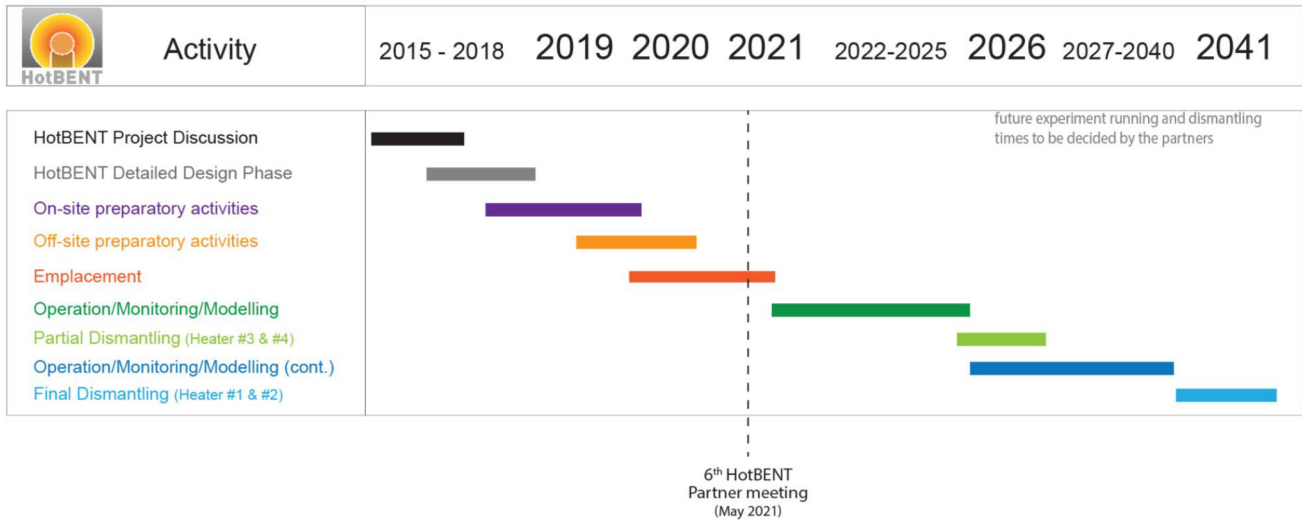
Figure 3.3-17. Planned timeline for HotBENT experiment (Kober, 2021).
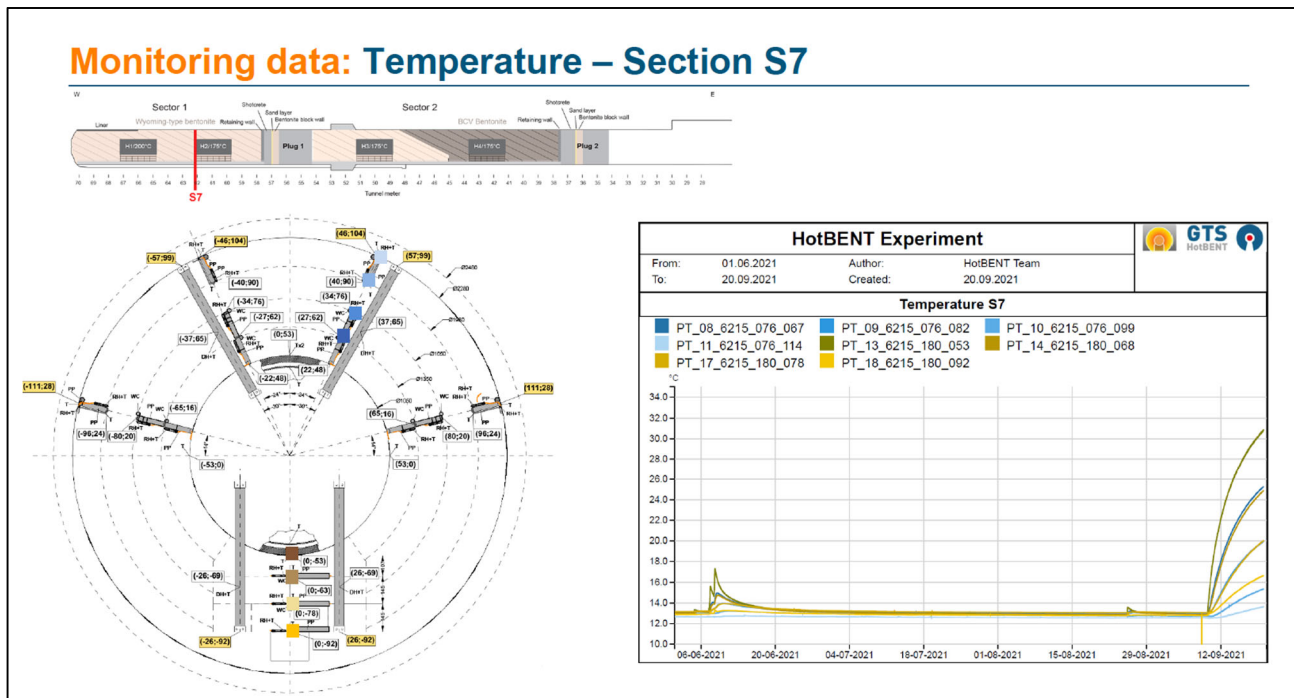
Figure 3.3-18. Temperature evolution in monitoring section 57 (Kober, 2021).

3.3.3.3. HotBENT Column Test

In addition to being the primary THMC modeling group supporting the HotBENT experiment, LBNL started in June 2019 a bench-scale laboratory experiment featuring a pressure column constructed to reproduce realistic heating and hydration conditions of the field-scale experiment (the so-called HotBENT Column test, or HotBENT Lab, see Section 8 in Zheng et al., 2020). To better separate the effects of heating and hydration, the experiment involved two identical test columns, with the control column undergoing only hydration, and the experiment column experiencing both heating up to 200ºC and hydration (Figure 3.3-19). The laboratory experiment, designed to specifically image potential THMC perturbations in the bentonite column, has various embedded sensors for temperature and electrical resistivity measurements (ERT), and also allows for time-

lapse CT scans (see Section 6.1.3.3). Both column tests were dismantled in December 2020 after running for 564 days and extensive characterization of heated versus unheated samples was conducted (see Chapter 7 in Zheng et al., 2021). Figures 3.3-20 shows resistivity maps from ERT inversion of the column tests. Results from the HotBENT Column Test are now used as Task 11 in SKB's EBS Task Force (see Section 3.4.3.4).
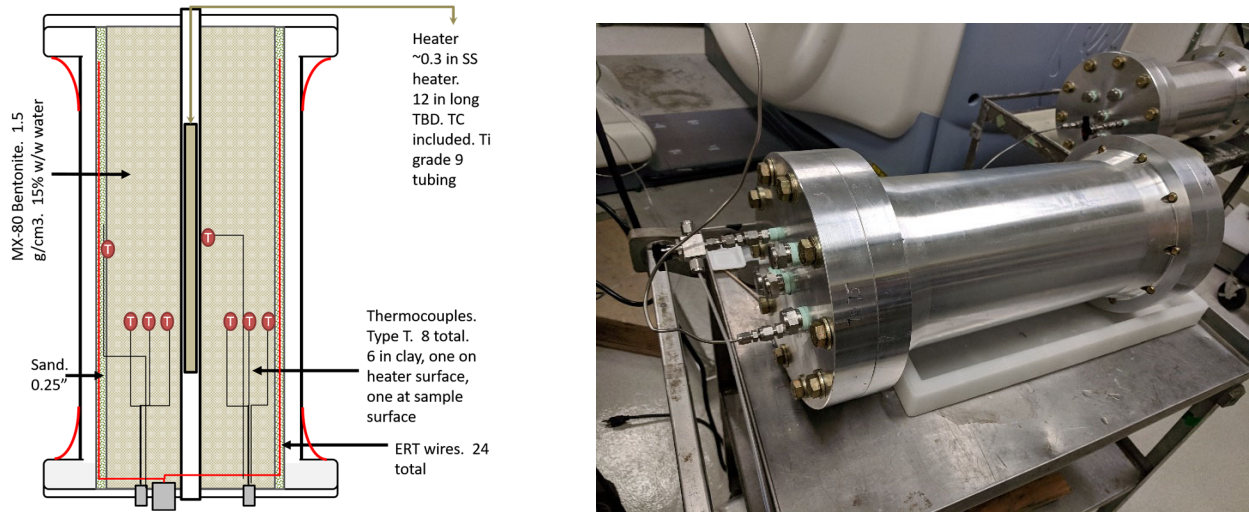
Figure 3.3-19. High-temperature column experiment: left shows test design as a schematic, right shows actual test column at LBNL (Zheng et al., 2020).
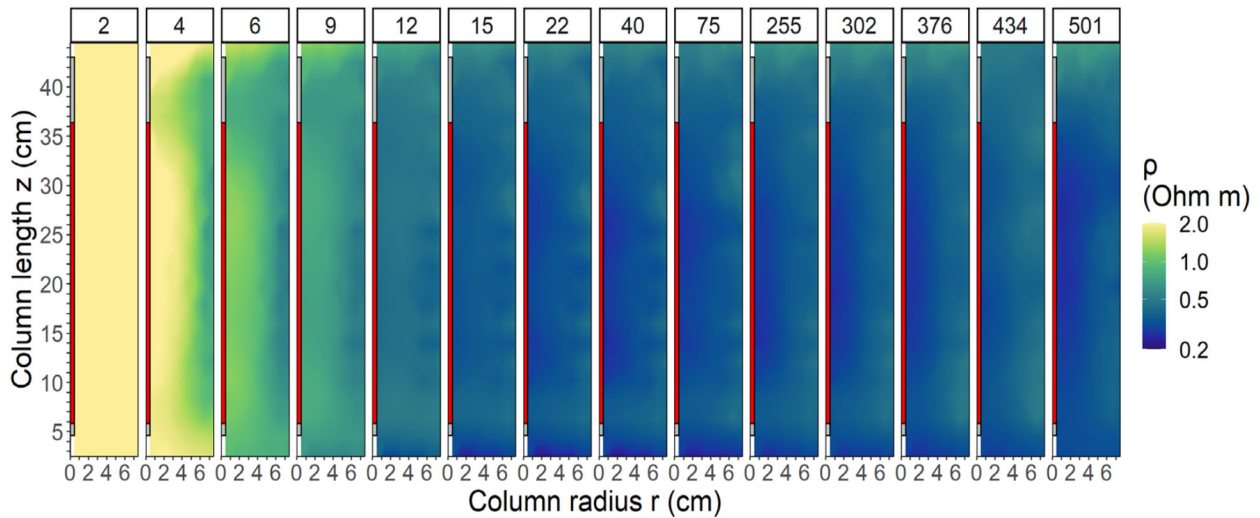
Figure 3.3-20. Radial resistivity map of the heated column (C1) after flow started (day 2 to 501). The red rectangle at the center is the location of the heater. The color bar is log-scaled from 0.2 to 2.0 Ωm. (Zheng et al., 2021)

3.3.3.4. HotBENT Summary

Benefits of Participation:

Access to experimental results, samples and laboratory investigations from a long-term full-scale heater experiment with focus on high-temperature disposal of radioactive waste (up to 200ºC). This temperature range is important if DOE was to pursue direct disposal of large dual purpose waste canisters.

- Opportunity to participate directly in international research groups that analyze monitoring data and conduct modeling work on coupled THM and THC behavior in EBS and NBS materials.

- Opportunity for designing the field experiment to DOE specific needs as well as conducting own laboratory experiments

Status of Participation and Outlook:

The HotBENT experiment has just entered into its heating phase on September 9, 2021, after years of planning, design, construction and implementation. The field test is designed in a modular fashion, with individual segments insulated from each other so that part of the experiment may be ended and excavated after 5 years while the remainder of the test keeps running for up to 20 years. Thus, HotBENT will provide valuable data on heat-induced perturbations and alterations in the EBS and NBS of a high-temperature repository for years to come. SFWD scientists have participated in the HotBENT planning from the very beginning and DOE has been one of the founding partners of the HotBENT consortium. SFWD scientists are also participating in the collaborative HotBENT Modeling Platform, and LBNL has been conducting a series of bench-scale laboratory experiments featuring a pressure column constructed to reproduce realistic heating and hydration conditions of the field-scale experiment (the so-called HotBENT Column test).

Contact Information:

DOE Contact:
Prasad Nair, DOE-NE

SFWD Contacts:
Liange Zheng (LBNL)

FEBEX-DP Contact:
Florian Kober, NAGRA, Switzerland

3.3.4. Other Experiments at GTS

Besides the CFM, the FEBEX-DP Project and the HotBENT test, other collaboratively conducted experiment at the Grimsel Test Site (GTS) may also be of interest to DOE/SFWD. Below we briefly introduce three such current opportunities, the Gas Permeable Seal Test (GAST), and the Materials Corrosion Test (MACoTE), both of which have been ongoing for a while and are moving into interesting project phases, as well as the Borehole Sealing Test (SET), which is currently in its pre-test preparation phase.

3.3.4.1. Gas Permeable Seal Test (GAST)

The Gas-Permeable Seal Test (GAST) investigates the performance of bentonite-sand mixtures for increased gas transport capacity (to mitigate pressure buildup from long-term gas generation as a result of canister corrosion) within the backfilled underground structures, without compromising the radionuclide retention capacity of the engineered barrier system (Figure 3.3-21). The objective of the test are as follows:

- Demonstrate the effective functioning of gas permeable seals

- Validate and improve current conceptual flow models for sand / bentonite

- Determine up-scaled water and gas permeabilities of sand / bentonite

Designed and constructed in 2011, the full-scale *in-situ* experiment has been in a slow saturation phase for almost ten years and is finally reaching full saturation and good homogenization. Figure 3.3-22 shows (a) the dense sensor network within the bentonite-sand mixture, arranged in segments along the test tunnel axis and layers from top to bottom and (b) the distribution of pore pressure as of May 2021, suggesting that most layers have fully hydrated with the exception of the top layer. As such, the project is now gearing up for the first gas injection tests to be conducted, likely starting in early 2022 until late 2023. Predictive modeling suggests that the breakthrough of gas from one end of the experiment to the opposite end could take about 1.5 years, but there is significant uncertainty about this estimate. Careful dismantling of the bentonite-sand mixture is planned in 2024.

NAGRA as the project lead is now discussing to kick-start a GAST Modeling Group, which would invite modeling teams from interested partner organizations to conduct predictive and interpretative modeling of gas migration and gas breakthrough behavior. DOE has been asked to participate with its own modeling groups, and such participation is currently discussed within the SFWD campaign.
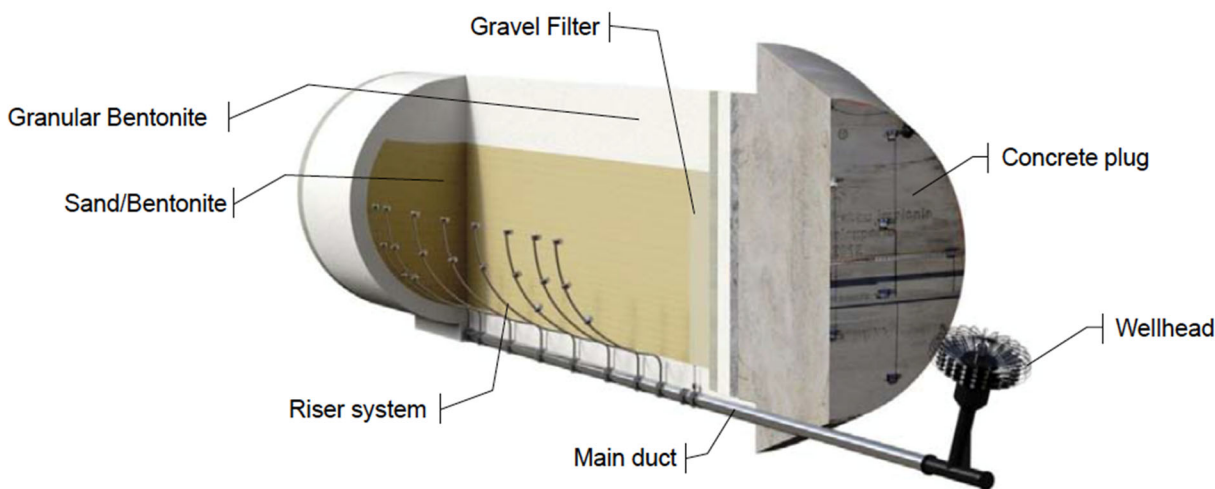
Figure 3.3-21. Schematic illustration of Gas Permeable Seal Experiment at GTS (Reinicke et al., 2020).

66
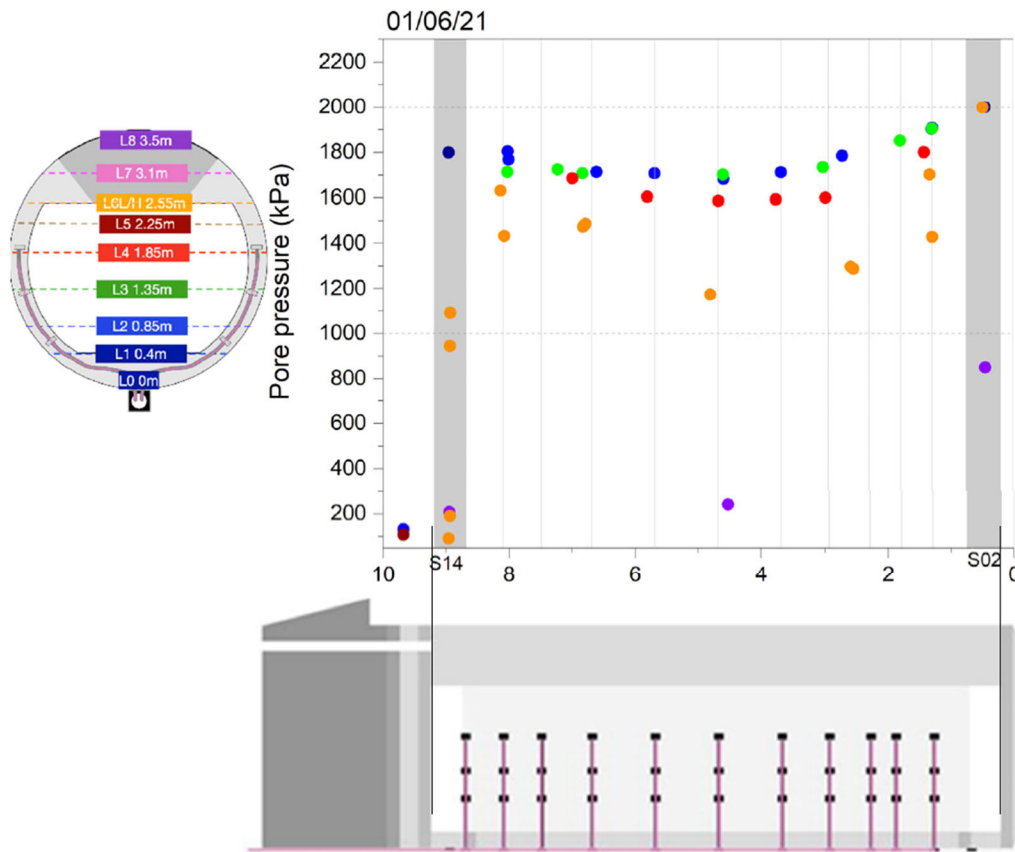
Figure 3.3-22. Pore pressure measurements in the GAST in May 2021 (Reinicke et al., 2021).

3.3.4.2. Borehole Sealing Test (SET)

The Borehole Sealing Test (SET) is a new activity at Grimsel Test Site led by the Japanese NUMO that is currently in the planning and preparation stage. The purpose of the test it to explore the performance of borehole seals in a geologic repository. NUMO envisions SET to be conducted at realistic scale using their Kunigel bentonite as sealing material. Two vertical boreholes – accessible from both ends – will be used for testing a 0.5m Kunigel V1 plug. The seals in each borehole will be identical, but one borehole will be equipped with multi-modal monitoring devices (e.g., fiber optics) while the other will be left almost free of any instrumentation to make sure that one test is conducted at almost undisturbed conditions (Figure 3.3-24). Instrumented packer equipment and high precision pumps allow for artificial saturation and execution of different hydraulic characterization procedures. The test aims at characterizing the saturation development, the swelling pressure and the hydraulic conductivity of the borehole seal in a vertical setting within bedrock. Regarding the timeline, the boreholes will be drilled and the bentonite emplaced in early 2022, followed by a seal saturation phase roughly through the end of 2022. Hydraulic testing of the seals will be conducted in 2023. NUMO intends to invite international teams to partner in the experiment and support the project by predictive and interpretative HM modeling.
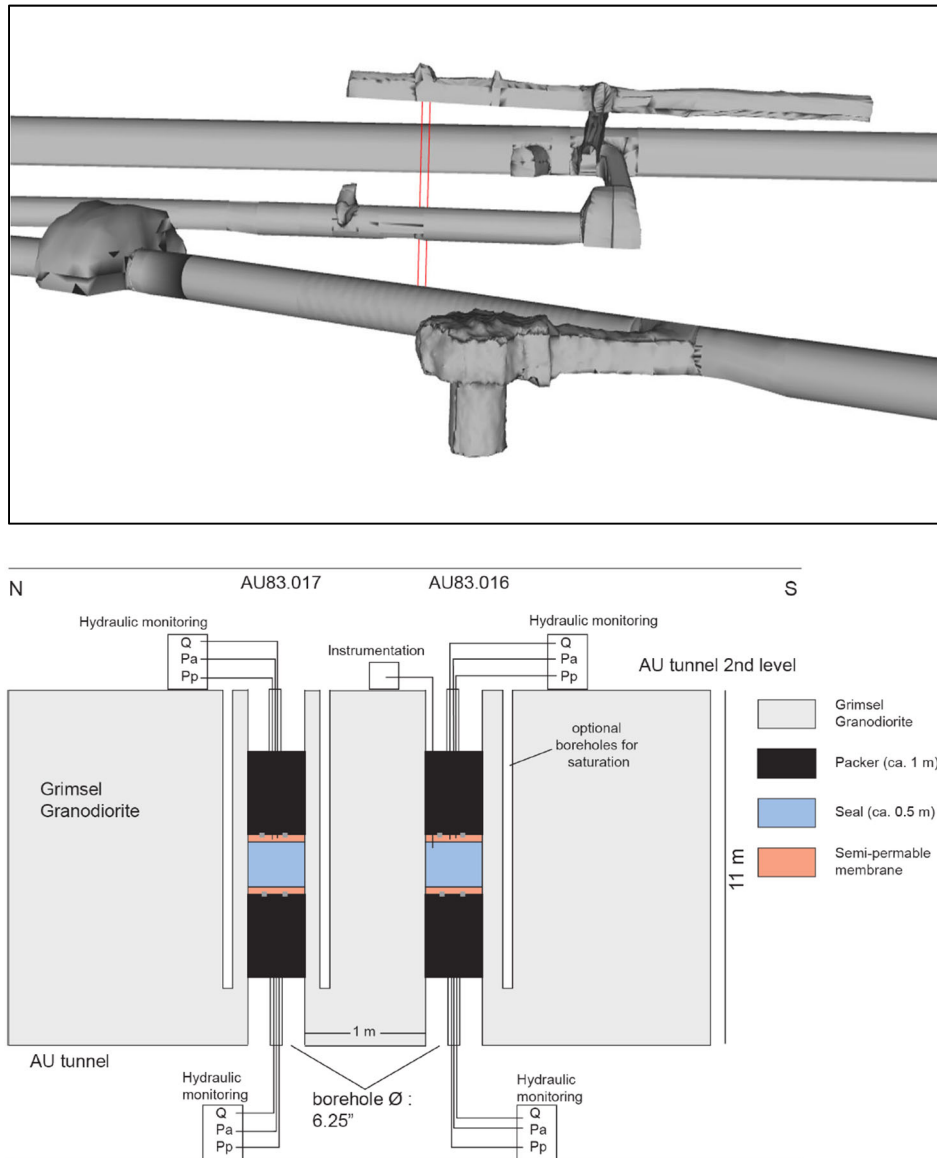
Figure 3.3-23. Schematic illustration of SET Experiment at GTS (Kunimaru et al., 2020). The top graph shows the 3D setup of the boreholes with access from the top and the bottom. The bottom schematic shows the setup of the plugs within each borehole.

3.3.4.3. Materials Corrosion Test (MACOTE)

The Material Corrosion Test (MaCoTe) at the GTS consists of non-heated and heated experiments to study *in-situ* corrosion of candidate canister materials embedded in bentonite. Two broad aims are as follows:

- Provide confirmation of the long-term anaerobic corrosion rate of carbon steel, stainless steel and copper in compacted bentonite under repository-relevant environmental conditions,

- Provide evidence of corrosion products and material interactions (copper-bentonite, steel-bentonite),

- Provide experimental evidence of the inhibiting effect of the bentonite buffer on microbial activity and microbially-influenced corrosion.

The ongoing *in-situ* experiment is made up of a series of specially designed modules (0.3 m long) that are inserted into a 10 m long vertical borehole and sealed with a double packer system. Each module contains 12

specimens embedded in bentonite with dry densities of either 1.25 or 1.5 Mg/m^3 (Figure 3.3-25). Different bentonite types and densities are used, mostly MX-80 bentonite from Wyoming and the Czech BaM lime-magnesium bentonite. Starting in 2014, metal samples have been periodically removed for destructive and non-destructive testing (after 1, 2, 3, and 4 years). Others have remained for longer-term exposure (e.g., for 7 years or longer), and some new ones have been added to the ongoing experiment.

At this point, the experiment offers to DOE/SFWD researchers a rich and growing dataset for evaluation of corrosion processes in an anaerobic bentonite environment, at ambient and under heated conditions. Additional samples will be retrieved according to a pre-defined schedule that currently runs through 2023 (Project Phase 2). The current experimental partners (seven) are open to additional organizations joining. The experiment will possibly offer the option of adding material specimens of particular interest to new partners.
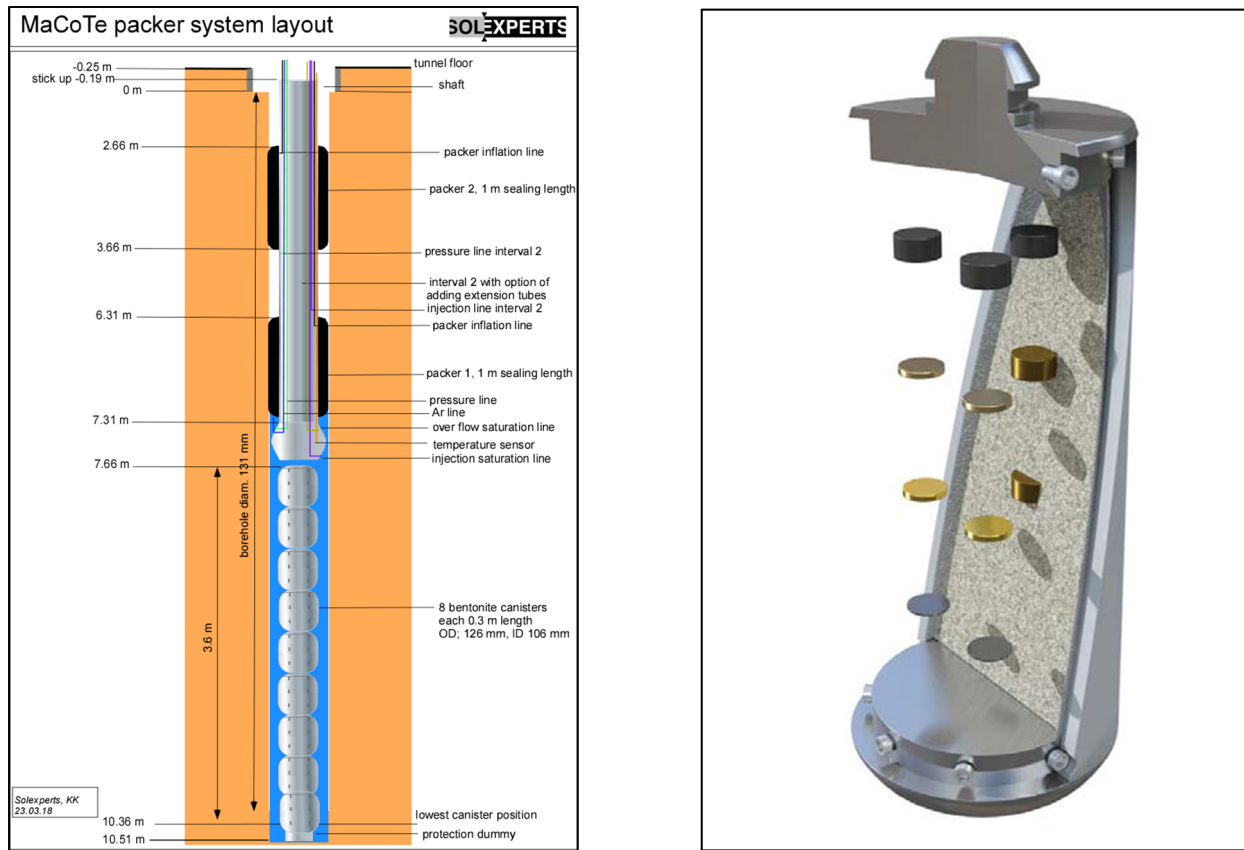
Figure 3.3-25. Schematic illustration of MACOTE Experiment at GTS (Martin, 2021). The graphic on the left shows specially designed modules (0.3 m long) with specimens inserted into a 10 m long vertical borehole. The right schematic shows the module design with 12 specimens each.

Figure 3.3-26 shows the complex and careful process of taking modules out of the boreholes without causing sample contamination. Figure 3.3-27 provides some early characterization results, indicating that the corrosion rate decreases significantly with time (i.e., from 1 year to 4.5 years). Results also suggest evidence of non-uniform or localized corrosion, reasons for which are still being investigated.

Figure 3.3-26. Photo showing retrieval of modules from borehole (Martin, 2021).
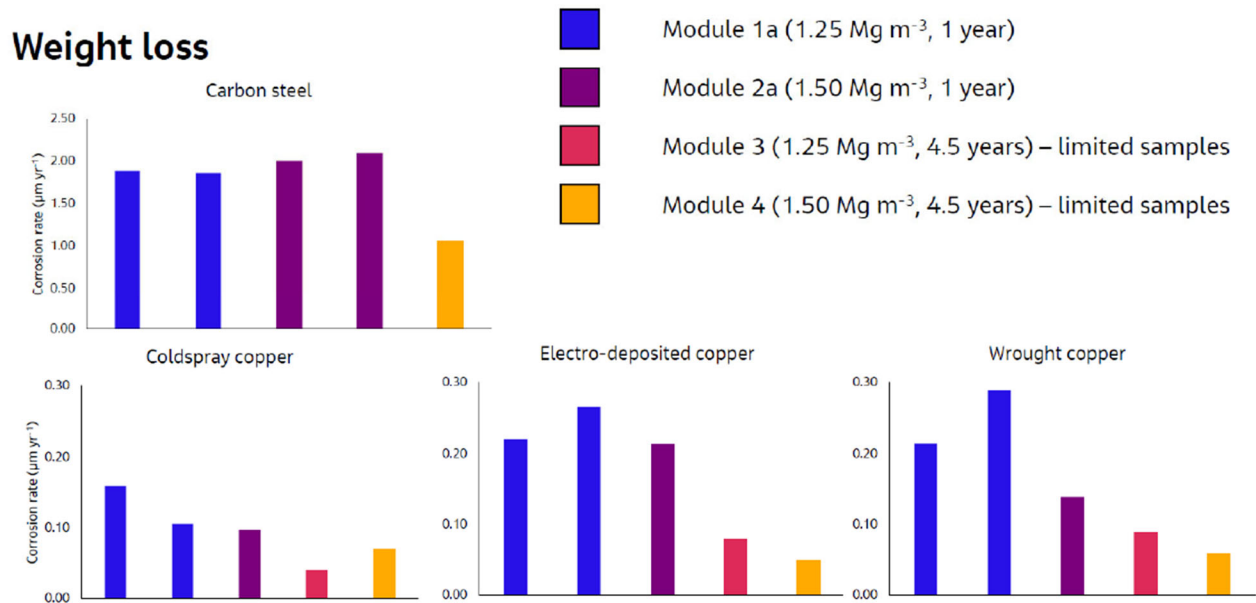
Figure 3.3-27. Corrosion rates for 1-year and 4.5-year retrieval of unheated samples (Martin, 2021).

3.4. SKB Task Forces

3.4.1. Introduction to SKB Task Forces

SKB, the Swedish Nuclear Fuel and Waste Management Company, has been organizing task forces as a forum for international organizations to interact in the area of conceptual and numerical modeling of performance-relevant processes in natural and engineered systems. There are two task forces: The Groundwater Flow and Transport (GWFTS) Task Force initiated in 1992, and the Engineered Barrier Systems (EBS) Task Force initiated in 2004. The GWFTS Task Force is led by Björn Gylling of SKB. The EBS Task Force has two parts, one for THM processes (led by Antonio Gens from UPC in Spain), and the other for THC processes (led by Urs Maeder of University of Bern). Different modeling tasks are being addressed collaboratively, in the past often involving experiments carried out at SKB's Äspö Hard Rock Laboratory (HRL) situated in crystalline rock near Oskarshamn in Sweden. The Äspö HRL consists of a main tunnel that descends in two spiral turns to a depth of 460 m, where various tests have been and are being performed in several side galleries and niches (Figure 3.4-1). SKB collaborates closely with the Finnish repository program; thus, in some cases, SKB Task Force modeling tasks use experiments conducted at the Onkalo URL in Finland (Section 4.6). In recent years, the task forces have moved to include relevant modeling tasks unrelated to the Äspö and Onkalo URLs.
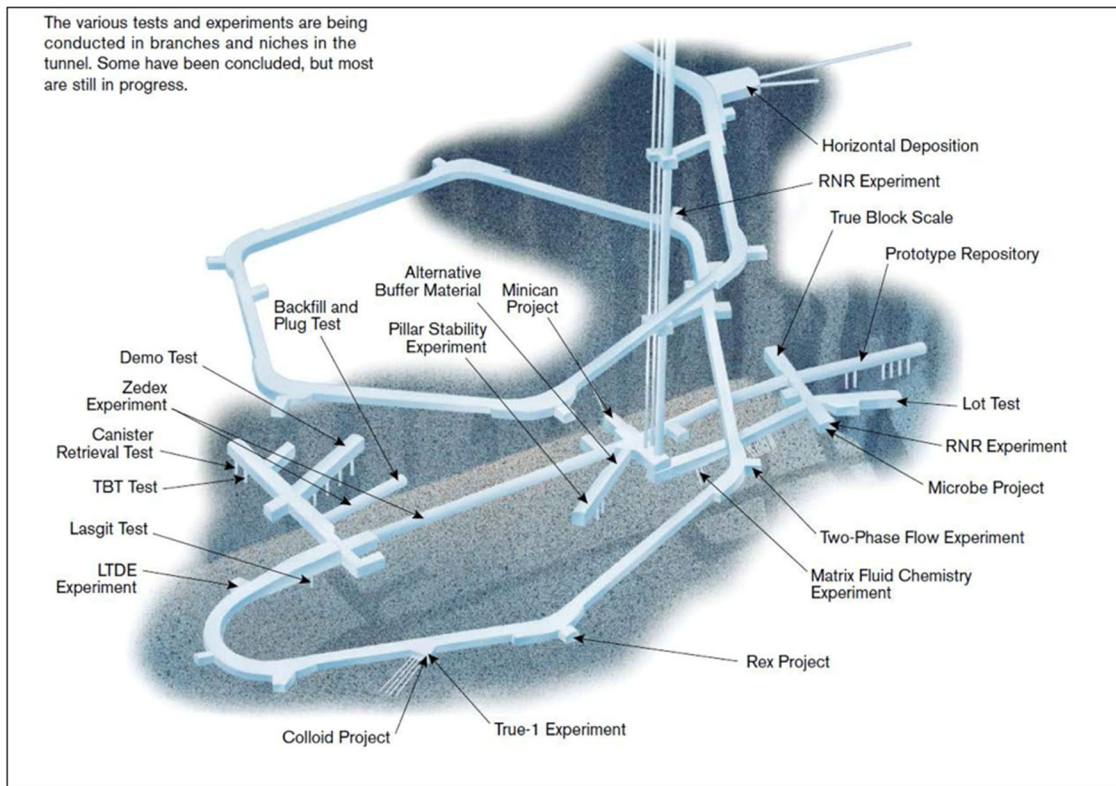
Figure 3.4-1. Layout of Äspö HRL and location of main experiments (Birkholzer, 2012).

Similar to the other collaborative initiatives introduced earlier in this report, participation in SKB in the Task Forces requires a formal membership agreement. Each participating organization is represented by a delegate; the modeling work is performed by modeling groups associated with these organizations (not unlike the DECOVALEX framework). The task forces meet regularly about once to twice a year. Task force members interact closely with the principal investigators responsible for carrying out experiments at Äspö HRL. Much emphasis is put on building of confidence in the approaches and methods in use for modeling of groundwater flow and migration, as well as coupled THM and THC process, in order to demonstrate their use for performance and safety assessments.

DOE eventually joined both the GWFTS and EBS Task Forces task forces in January 2014 and hosted a joint task force meeting in Berkeley in December 2014. Other participating organizations in the GWFTS and/or EBS Task Forces are SKB, POSIVA, KAERI, CRIEPI, JAEA, NAGRA, BMWi/KIT, RWM, NWMO, and SURAO. In terms of the GWFTS task force, SFWD researchers initially engaged in and conducted simulation work supporting the interpretation of the Bentonite Rock Interaction Experiment (BRIE) at Äspö HRL, Sweden experiment (FY14 and FY15). In FY17, SFWD's focus shifted to another GWFTS modeling task, which involved diffusion and sorption experiments conducted at the Äspö HRL, Sweden, and the Onkalo URL, Finland (Section 3.4.2.1). This effort has been winding down in FY20 and instead, SFWD researchers have started participating in a new GWFTS Task 10, which addresses modeling challenges related to multi-scale flow channelization in fractured crystalline rock and validation of fracture network models. With regards to the EBS Task Force, SFWD researchers initially focused on a full-scale demonstration experiment at Äspö HRL, the so-called Prototype Repository. In FY20, SFWD's participated in the collaborative THM analysis and modeling of the FEBEX-DP experiment, a continuation/expansion of the THMC modeling conducted for the FEBEX-DP Project while it was still active (Section 3.3.2). Also, DOE proposed to the EBS Task Force leadership to include the HotBENT Column Test as a new modeling task (Section 3.3.3). This proposal was accepted as a new EBS Task 11 which is now led by LBNL researchers and has seven participating modeling teams. As pointed out in Section 3.4.3 below, a few additional EBS tasks have recently been developed which might also be of interest to SFWD researchers.

3.4.2. GWFTS Task Force

The main objective of the GWFTS Task Force is to develop and apply appropriate methods for investigating flow and transport in fractured crystalline rock, in particular to obtain better understanding of the retention of radionuclides transport in crystalline rock, and to improve the credibility of simulation models. The task force also provides a platform for interaction in the area of conceptual and numerical modeling of groundwater flow and solute transport in fractured rock.

For the first few years of DOE's participation, the main modeling task conducted in the GWFTS task force was Task 8: Modeling of the BRIE at Äspö HRL. The BRIE experiment was a joint task shared between the GWFTS and the EBS Task Forces. The objective of the BRIE experiment was to enhance the understanding of the hydraulic interaction between the fractured crystalline rock at Äspö HRL and the unsaturated bentonite used as backfill. The experiment was subdivided into two parts: the first part involving the selection and characterization of a test site and two central boreholes, the second part handling the installation, monitoring, and later overcoring of the bentonite-rock interface. Modeling groups, including a group of SFWD scientists, were able (a) to gain a better understanding of water exchange at the bentonite-rock interface, and (b) to obtain better predictions of bentonite wetting in a fractured rock mass. Task 8 (BRIE) ended in FY17 and Task 9 was initiated, which involved modeling of two diffusion/sorption experiments: the Long-Term Diffusion Experiment at Äspö HRL and the REPRO (Rock Matrix Retention Properties) Experiment at Onkalo URL in Finland. Details on Task 9 are given below in Section 3.4.2.1. As Task 9 is now in the final evaluation and reporting stage, an additional Task 10 was developed and officially introduced in 2020, with a focus on flow channelization in fractured rock ranging from the small (within a single fracture) to large (small fracture network) scale (Section 3.4.2.2).

3.4.2.1. Modeling Two Diffusion and Sorption Experiments in Crystalline Rock

Task 9 of the GWFTS task force focused on the modeling of coupled matrix diffusion and sorption in heterogeneous crystalline rock matrix at depth. This was done in the context of inverse and predictive modeling of tracer concentrations measured in two *in-situ* experiments performed within Long-Term Diffusion and Sorption Experiment (LTDE-SD) at the Äspö HRL in Sweden as well as within the REPRO project at Onkalo URL in Finland (see Section 4.6. The ultimate aim was to develop models that in a more realistic way represent retardation in the natural rock matrix at depth. Researchers from LANL participated in Task 9 in past years but in FY20 moved on to focus on the new Task 10 (Section 6.5.2).

LTDE-SD, the Long-Term Diffusion Sorption Experiment was completed in 2010. The experiment was designed to examine diffusion and sorption processes in both matrix rock and a typical conductive fracture identified in a pilot borehole. A telescoped large-diameter borehole was drilled subparallel to the pilot borehole, in such a way that it intercepts the identified fracture some 10 m from the tunnel wall, and with an approximate separation of 0.3 m between the circumferences of the two boreholes (Figure 3.4-4). A cocktail of nonsorbing and sorbing tracers was circulated between the boreholes in packed-off sections for a period of 6 ½ months, after which the borehole was overcored and the extracted rock analyzed for tracer penetration and fixation. The specific objectives of LTDE-SD were to:

- Obtain data on sorption properties and processes of individual radionuclides, and their effect on natural fracture surfaces and internal surfaces in the rock matrix.

- Investigate the magnitude and extent of diffusion into matrix rock from a natural fracture *in-situ* under natural rock stress conditions and hydraulic pressure and groundwater chemical conditions.

- Compare laboratory-derived diffusion constants and sorption coefficients for the investigated rock fracture system to the sorption behavior observed under natural conditions.

The illustration in the lower right of Figure 3.4-2 shows the location of LTDE-SD in the Äspö HRL tunnel system. In the center of the figure, the local tunnel section is depicted together with the different boreholes drilled from the site. These boreholes include the LTDE-SD borehole and a closely located pilot borehole. These two boreholes intersect a water-conducting natural fracture at a distance of 11 m from the tunnel wall, which is the experiment's target fracture. The LTDE-SD borehole was drilled with a large diameter down to the fracture intersection, and a small diameter beyond the fracture planed, so that it could later be overcored. This is simplistically illustrated in the lower left of Figure 3.4-2. The borehole is indicated by the solid black line and the intersected fracture is indicated by the curved blue line. Orange areas indicate packed-off volumes, whereas blue areas indicate volumes of the tracer cocktail. The red arrows symbolize in-diffusion of tracers from the large-diameter borehole through the fracture surface and into the altered rock matrix. They also symbolize diffusion into the unaltered rock matrix from the small-diameter borehole. The dashed black line indicates the rock volume that was overcored at the end of the tracer test.
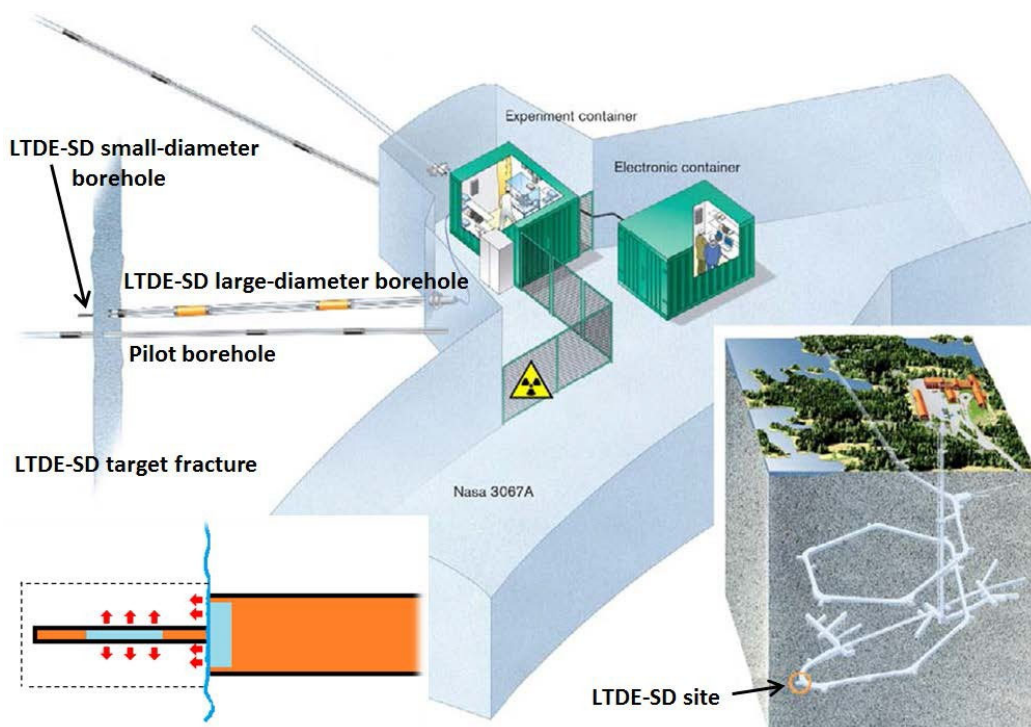
Figure 3.4-2. Schematic layout of LTDE-SD at Äspö HRL.

The tracers injected were Na-22, S-35, Cl-36, Co-57, Ni-63, Se-75, Sr-85, Nb-95, Zr-95, Tc-99, Pd-102, Cd-109, Ag-110, Sn-113, Ba-133, Cs-137, Gd-153, Hf-175, Ra-226, Pa-233, U-236, and Np-237. Tracer concentrations as well as other environmental parameters were monitored during the 200-day tracer test. After that the surrounding rock volume was overcored, and from the overcored volume a number of smaller drill cores were excavated, as illustrated on the left in Figure 3.4-3. Here, the natural fracture surface is located on the right-hand side of the overcored rock volume. A large number of the core samples were cut into subsamples as indicated to the right in Figure 3.4-3, which were used to obtain tracer penetration profiles. Tracer concentrations (or activities) in the rock were measured by a number of analysis methods, including autoradiography on intact samples, direct activity measurements on intact and crush samples, and leaching or dissolution of intact and crush samples, followed by water phase measurements.
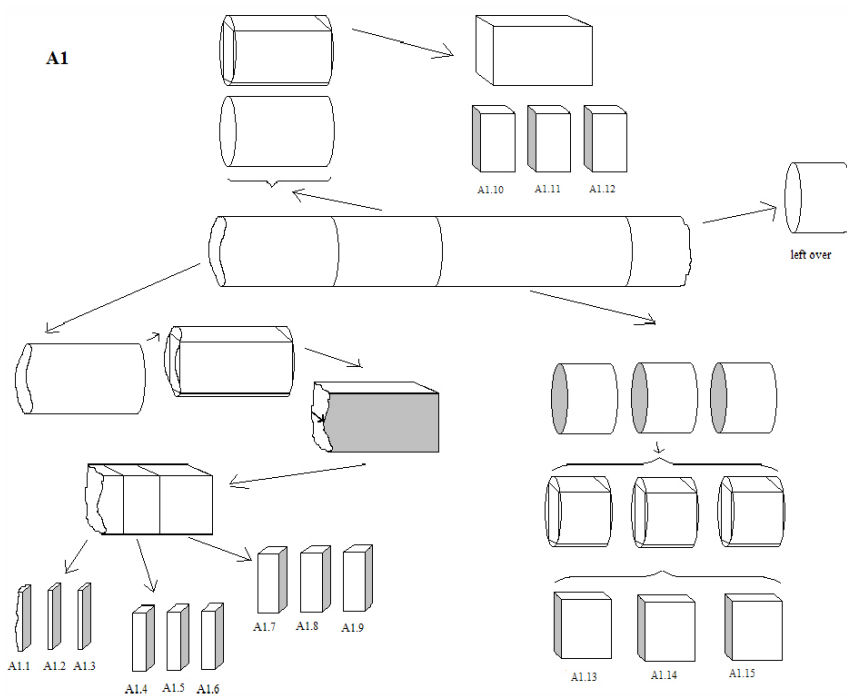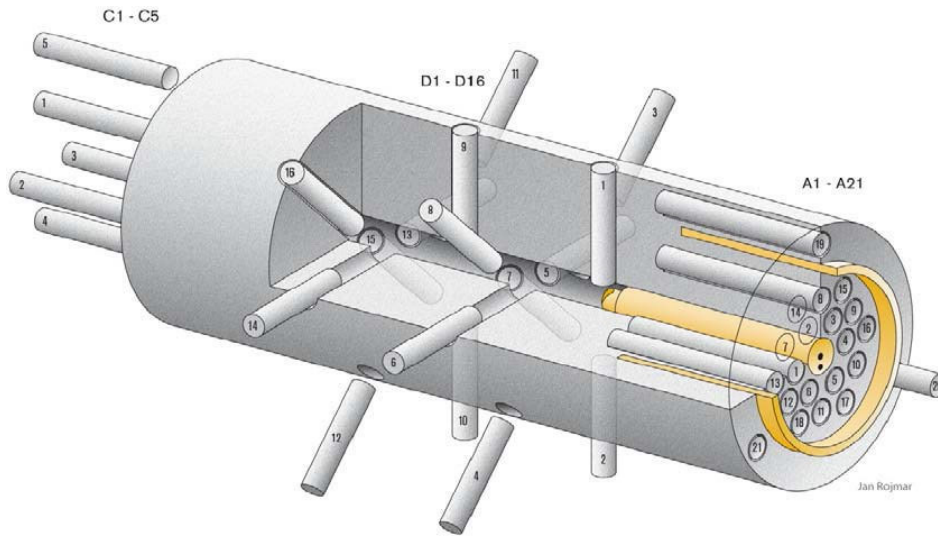
Figure 3.4-3. Illustration of the sampling of the overcored rock volume in LTDE-SD.

Results from the overcoring rock volume in LTDE-SD provide concentration profiles in the rock matrix that were not fully understood initially. Figure 3.4-4 shows experimental concentration profiles of two tracers compared to predictive model results, with obvious discrepancies in the curve shapes. These may be a result of heterogeneities in the rock matrix or may be related to inappropriate model assumptions related to Fickian diffusion or equilibrium sorption. One aim of Task 9 was to increase realism in the diffusion-sorption predictions of the LTDE-SD. It turned out, however, that the apparent deep penetration of some of the tracers into the rock matrix was caused by sample contamination. Work has been done since to investigate possible contamination mechanisms and develop guidance on detection limits and contamination "risk levels."
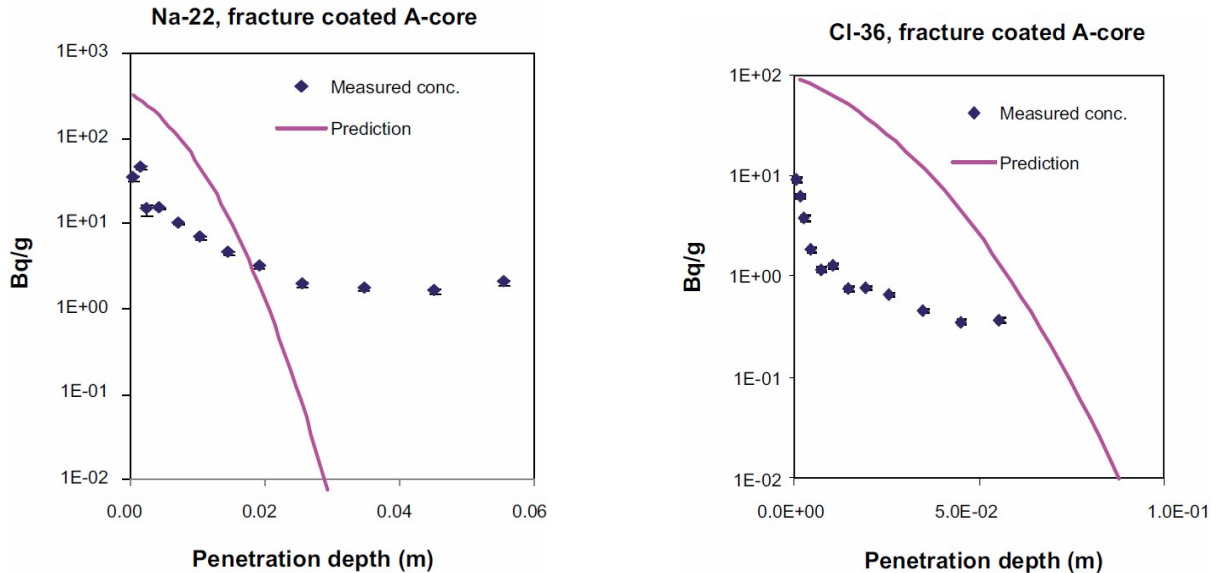
Figure 3.4-4. Results from the *in-situ* in-diffusion experiment LTDE-SD through a natural fracture surface. Modeled Na-22 and Cl-36 penetration profiles (solid curves) are compared to the measured profiles (diamonds). Na-22 activities in the rock matrix were obtained on intact of crushed rock slices and Cl-36 activities were obtained by leaching of intact or crushed slices (Viswanathan et al., 2016).

The REPRO experiments at Onkalo URL in Finland were the other important element of Task 9. REPRO involved a number of boreholes that have been drilled into the non-fractured rock matrix from a working niche at the Onkalo underground rock characterization facility, at about 400 m depth (see Figure 3.4-5). Borehole ONK- PP323 was utilized for the Water Phase Diffusion (WPDE) series of experiments, which are advection diffusion-sorption tests carried out between ~18-20 m from the tunnel wall. A 1.9 m long section was packed off, and in this section a dummy has been placed. Its diameter is 54 mm whereas the borehole diameter is 56 mm, leaving a 1 mm gap between the borehole wall and the dummy. This gap is regarded as an artificial fracture of relatively well-defined geometry. A very low steady state water flow was applied in this gap, directed towards the tunnel. This was achieved by injecting the water at the far end of the packed-off section, as shown to the upper right in Figure 3.4-7. In this water flow, the tracers HTO, Na-22, Cl-36, and I-125 were injected in WPDE-1, and HTO, Na-22, Cl-36, Sr-85 and Ba- 133 in WPDE-2. Injection was made as a few hours long pulse at the far end of the experimental section. As the pulse traveled with the water flow, its tracers diffused into the rock matrix. As the pulse passed, the concentration gradients were reversed and the tracers diffused out of the rock matrix and into the flowing water.

Another REPRO experiment, referred to as Through Diffusion Experiment (TDE), was carried out between three parallel boreholes situated perpendicular to each other, in 1 m long packed-off sections, at a distance of about 11 to 12 m from the tunnel wall. Borehole ONK-PP326 was used as the injection hole and boreholes ONK-PP324 and ONK-PP327 were used as observation holes (see Figure 3.4-5, upper left corner). The distances between the boreholes were between 10 and 15 cm. Advective flow between the boreholes was insignificant, as the experiment takes placed in a rock volume that lacks in water-bearing fractures. Different

tracers such as HTO, Na-22, Cl-36, Ba-133, and probably Cs-134 were injected. The decreasing and (expected) increasing tracer concentrations in the injection hole and observations holes, respectively, were analyzed, both in the laboratory, by liquid scintillation counting and High-Resolution x-ray spectroscopy as well as directly in the injection hole and observation holes by a High Performance Germanium detector and a Na(Tl)I-scintillation detector, respectively.
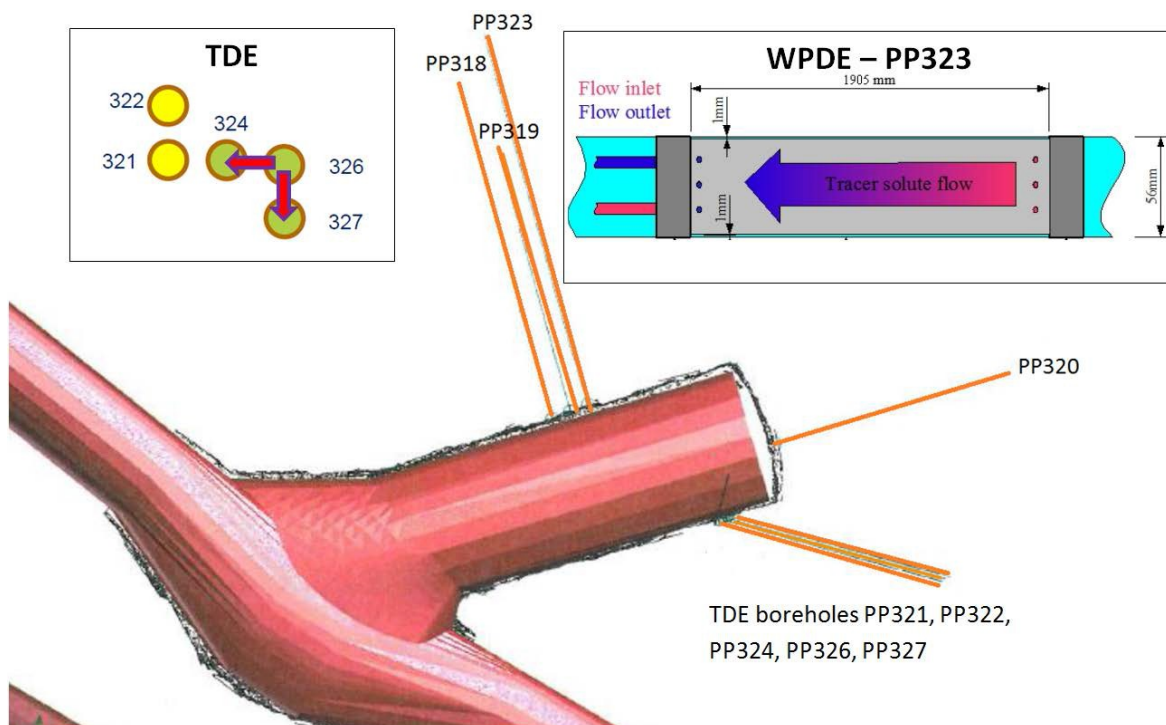
Figure 3.4-5. The REPRO Niche at the 401 m level at ONKALO with nine boreholes drilled from the niche. Borehole PP323 is utilized for WPDE-1&2, and boreholes PP324, PP326, and PP327 for TDE (Viswanathan et al., 2016).

In addition to the modeling of the *in-situ* experiments described above, Task 9 leads decided to advance the relatively small-scale modeling of radionuclide retention in comparison with URL data into an expanded Task 9D, which took the lessons learned and applied them to a semi-synthetic safety assessment exercise. Questions addressed were, for example, how the more complex behavior observed in the experiments would scale to safety assessment conditions and timescales, and what consequences would be expected when neglecting micro-scale heterogeneity (which was important to consider when matching experimental data) in larger-scale safety assessment simulations. Task 9 has now been finalized with completion of all larger-scale simulations, and final publications and reports are in development.

3.4.2.2. Flow Channeling and Discrete Fracture Network Modeling

The title of the new GWFTS Task 10, officially started in May 2020, is "Validation Approaches for Groundwater Flow and Transport". The focus on (1) improving our understanding of multi-scale flow channelization in fractured crystalline rock, and (2) validating of fracture network models and other models that can account for such channelization. While previous GWFTS tasks typically involved experiments, the main interest in Task 10 is on modeling methodologies and approaches, with emphasis on validation and conceptual model uncertainty. Experiments are still needed, but in this task they are more a means to assess validation strategies rather than the central element of the task. Figure 3.4-6 shows the structure of Task 10, starting with development of a White Paper on pragmatic model validation methods, followed by testing of such methods at three different scales from single fracture to small network to block scale. As illustrated in Figure 3.4-7, hydromechanical laboratory experiments conducted on natural rock joints will be used in Task 10.2 to examine validation approaches for flow within a single fracture with hydromechanical coupling.

76

Structure of Task 10
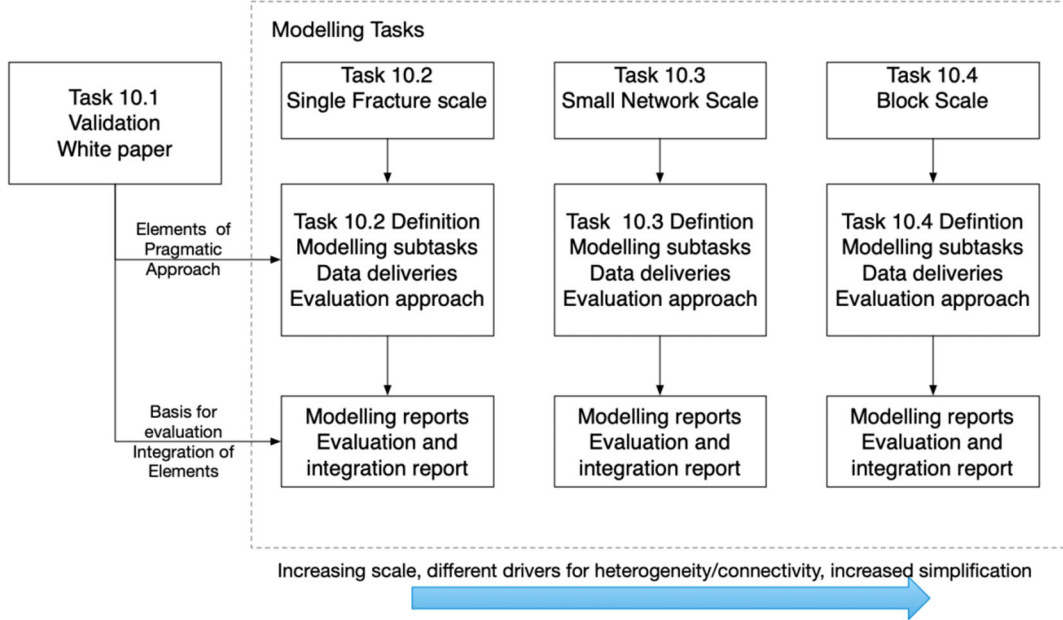
Figure 3.4-6. Structure of GWFTS Task 10 (Lanyon, 2021).
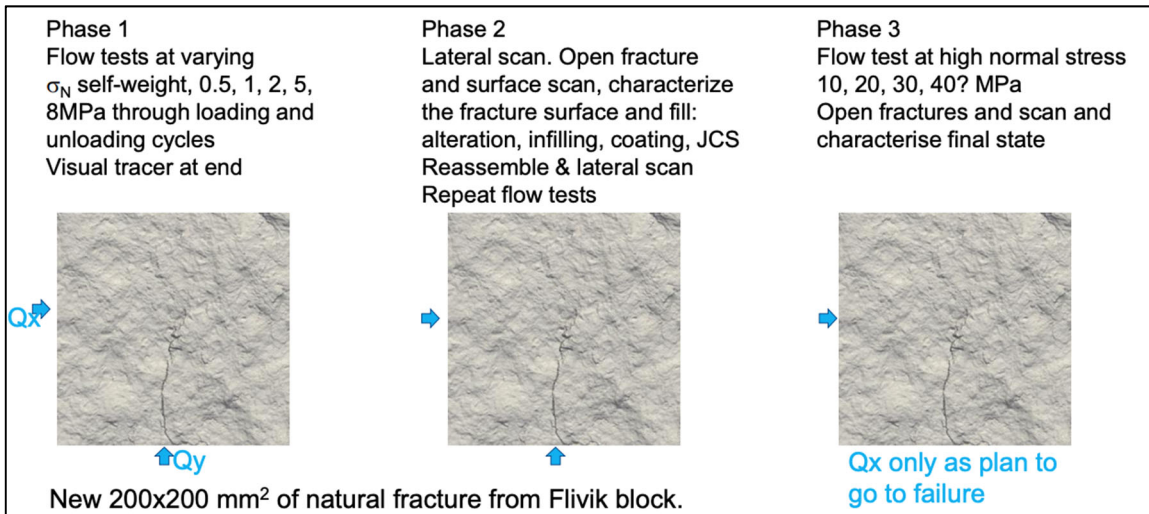
Figure 3.4-7. Hydromechanical testing planned for Task 10.2 (Bruines and Lanyon, 2021).

LANL researchers are currently working with other members of the GWFTS task force team to finalize the White Paper on DFN model validation, as a framework document for model validation and as a reference planning document for the Task 10 validation activities. The finalized White Paper is expected by end of 2021 or early 2022. In parallel, LANL scientists started to develop capabilities to simulate channelized flow and transport in individual fractures and fracture networks. In FY20, this work comprised initial simulations of transport in fractured rock, taking into account surface asperities and textures with different connectivity structures (Birkholzer et al., 2020, Section 6.5.2). Full details of the second goal, model validation, are yet to be finalized; current discussions center on the availability of adequate data sets for validation of discrete fracture network models. In FY21, LANL scientists started including irreversible kinetic reactions to their discrete fracture network transport calculations since repository performance assessment studies will require considering reactive transport of radionuclides potentially migrating from a repository (Section 6.5.2).

3.4.3. EBS Task Force

As mentioned above, the EBS Task Force essentially has historically involved two distinct focus areas, one is on THM processes referred to as EBS-THM (led by Antonio Gens from UPC in Spain), and the other is on chemical processes referred to as EBS-C (led by Urs Maeder of University of Bern). The main goal of the EBS-THM Task Force is the development and application of general and effective tools for the advanced coupled THM analysis of buffer and backfill materials, and their interactions with a saturated fractured host rock environment. Specific goals are as follows: (1) to verify the capability to model THM processes in unsaturated as well as saturated bentonite buffer and backfill materials, (2) to validate and further develop material models and computer codes by numerical THM modeling of laboratory and field tests and compare modeling results with measured results, and (3) to evaluate the influence of parameter variations, parameter uncertainties and model imperfections. During the past few years, the EBS-THM Task Force has been in a transition phase with various tasks ending and new tasks being developed. More specifically, six main modeling tasks that had been running for several years were finalized in FY18 and FY19: The Prototype Repository (Task 4), the Homogenization Task (Task 5), the Sensitivity Analysis of Bentonite (Task 6), and the BRIE experiment (Task 3) that was shared with the GWFTS Task Force. Two other more recent tasks ended in FY20 and FY21, respectively: Task 7 (Gas Transport in Bentonite) and Task 9 (FEBEX *In-situ* Test). Currently active are Task 10 (Water Transport in Pellet Filled Slots) and two recently added tasks: Task 11 (Berkeley High-Temperature Column Test, or HotBENT Column Test), and Task 13 (Unsaturated Homogenization). Below, we will briefly review the recently finalized and currently ongoing tasks in the EBS-THM Task Force, namely Tasks 7, 9, 10, 11 and 13.

As aforementioned, the EBS Task Force used to have the EBS-C focus area, led by Urs Maeder from the University of Bern (Switzerland) and Martin Birgersson of Clay Technology in Lund (Sweden). EBS-C aimed at advancing the fundamental understanding of physicochemical processes in clay or bentonite materials relevant to various aspects of safety assessment. The two EBS sections on THM and C were traditionally working on different modeling tasks, and EBS Task Force meetings were jointly held but in separate sessions for THM and C. In addition, in contrast to the EBS-THM section, which usually has a tight connection between models and experiments, the "chemical" task force had been mainly working on conceptual model development and benchmark/modeling studies of varying complexity. After conducting a range of benchmark simulations and simplified modeling studies for several years, the EBS-C task force has recently been through a major overhaul: as a result, all the benchmarking tasks have ended and its remaining task focusing on modeling physicochemical processes at the cement-bentonite interface was renamed as Task 12 of an integrated EBS Task Force line-up. Below, Task 12 is briefly described along with the other EBS-THM tasks. We assume that this major reorientation will in the future lead to a more tightly coordinated portfolio of THM and C tasks in a joint EBS Task Force.

3.4.3.1. Gas Transport in Bentonite (Task 7)

This task involved development and testing of new phenomenological models for gas transport in bentonite applied to a series of well-defined benchmarks (Romero et al., 2017). Subtask 1 involved calibration of hydro-mechanical models to the various aspects of the behavior of unsaturated bentonite, including water retention behavior, compaction curves, MIP, swelling pressure tests, and oedometric tests at different suctions and confining stress levels (individual processes). Subtask 2 involved verification and validation of coupled hydro-mechanical response of bentonite during water saturation and gas injection under oedometer conditions (system behavior). The data were interpreted by a HM model developed by EPFL (Ecole Polytechnique Federale de Lausanne) focusing on the pressure dissipation phase and a multiphase flow model by INTERA using TOUGH-MINC. The research topic and objective of this task are similar to that of Task A of the DECOVALEX-2019 phase and also related to Task B of the current DECOVALEX-2023 phase (Section 3.2). Since researchers from LBNL and SNL had already been participating in these DECOVALEX modeling tasks, it was decided that the EBS Task 7 would not be joined by SFWD researchers. Task 7 was completed by the end of 2020.

3.4.3.2. FEBEX In-situ Test (Task 9)

This task involved a coordinated and collaborative model comparison to further analyze and evaluate the THM response measured in the FEBEX-DP experiment (Section 3.3.2). The organizers of the FEBEX-DP Project, which officially ended in late 2018, designated the SKB EBS Task Force to provide the framework for such coordinated analysis. In FY20, LBNL scientists continued their THMC modeling of the FEBX Experiment, starting with a validated THMC model for the test and then using it to predict the long-term evolution of engineered-natural barrier behavior (Section 6.1.2.1). In a complementary effort, SNL researchers also participated in this task, focusing on TH Modeling with PFLOTRAN and related sensitivity studies (Section 6.1.2.2). Because of the lack of interest and capability of simulating coupled THMC processes, there were no other modeling teams besides LBNL and SNL that joined this task. In the 31st EBS Task Force meeting in November 2020, the Task Force decided to close this task and refocus THM and THMC modeling efforts on the new High-Temperature Column Test defined in Task 11 (Section 3.4.3.5).

3.4.3.3. Water Transport in Pellets-filled Slots (Task 10)

Task 10 involves modeling of water transport in pellet filled laboratory chambers, which would aim to develop new material models for the time-dependent evolution of pelletized buffer material properties. This is an important topic because the saturation and hydration behavior of pelletized bentonite depends very much on a correct constitutive model for water transport. A series of laboratory experiments have been conducted measuring the water transport in different pellet fillings with varying boundary and inflow conditions and at different temperature situations (e.g., Figure 3.4-8). Modeling teams are jointly simulating: (1) water consumption as a function of time, (2) relative humidity evolution at measuring points, (3) water content as function of distance from bottom at the three times and at test termination and (4) density and degree of saturation as function of distance from bottom. The task involves different experimental setups evaluated in Subtask A (1D-tests with water freely available), Subtask B (constant water inflow rate from point inflow, see example results in Figure 3.4-9) and Subtask C (1D-tests with water redistribution in a temperature gradient). Subtask A and CB have been completed. Subtask B was expected to be finished in 2021 with a final evaluation. However, the final evaluation was delayed due to the postponement of the group meeting. SFWD scientists are not involved in this task.
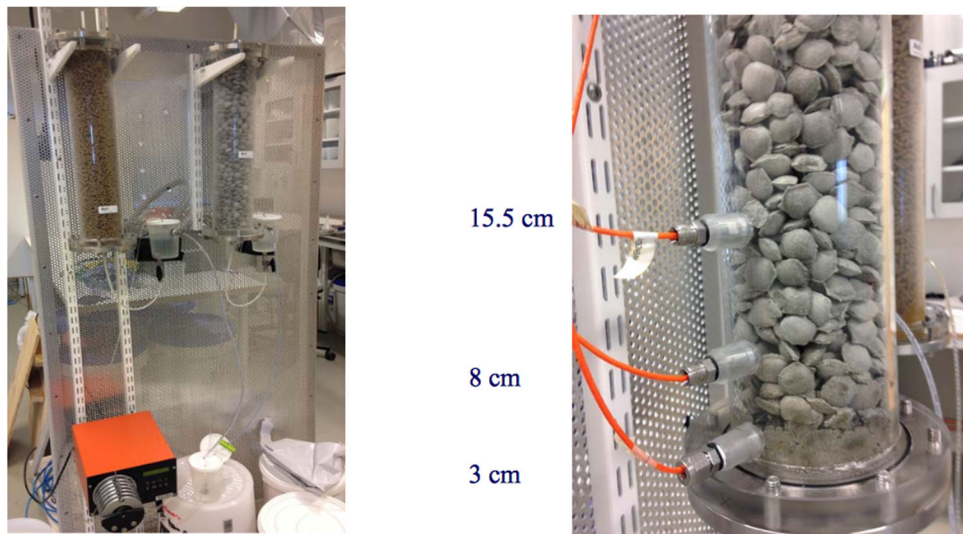
Figure 3.4-8. Column experiments conducted to determine time-dependent water uptake in different types of pelletized bentonite (Börgesson and Akesson, 2016).
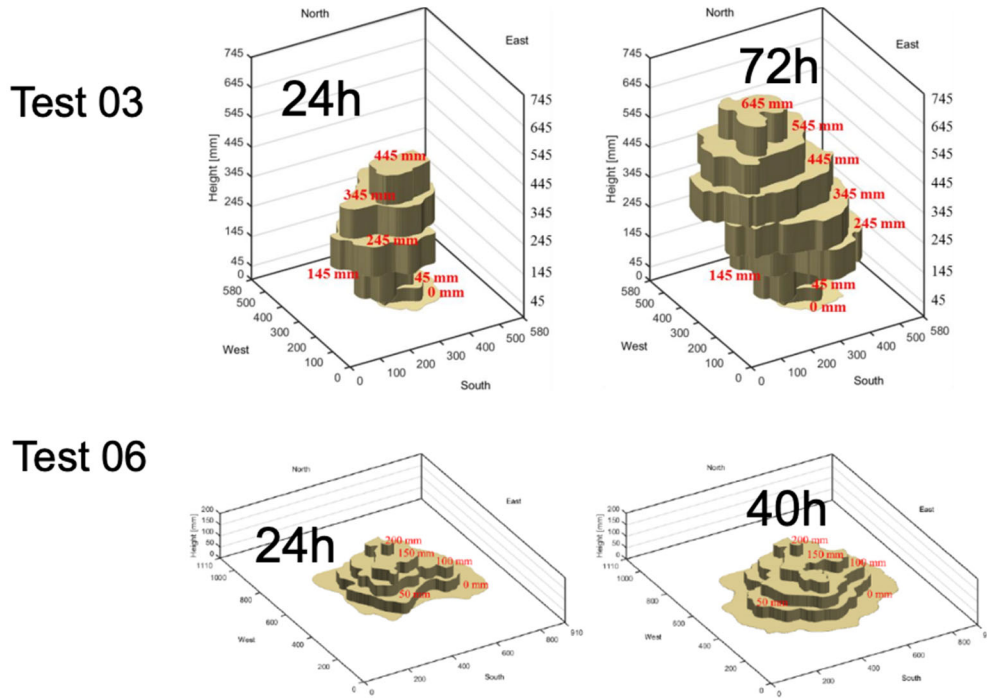
Figure 3.4-9. Wetting patterns observed in Subtask B. Test 03 features injection from the center with a surface load applied at the top. Test 06 features inflow from the bottom with no surface load. (Akesson, 2021).

3.4.3.4. Berkeley High-Temperature Column Test (Task 11)

Task 11 involves the HotBENT Column Test (or HotBENT Lab) conducted at LBNL, a mock-up bench-scale experiment specifically designed to provide time-lapse CT and ERT images of THMC perturbation of a hydrating bentonite sample heated to a maximum temperature of 200ºC (Section 3.3.3). The task description was provided by LBNL and is now available on the SKB task force website. Seven teams from various organizations (LBNL, SNL, Clay Tech, NAGRA, POSIVA, RWM, and SKB) expressed interest in Task 11 and have now started simulating the high-temperature heating and hydration experiment. LBNL has initiated development of a THMC model to interpret the data from the HotBENT Column Test (Section 6.1.3.3). SKB finished a 1-D model using the Comsol Multiphysics software, focusing on the TH aspect of the heated column. Clay Technology developed a 2-D model for the heated column and provided a decent match of the temperature and density data. Further model improvement is expected when the group will meet next in early 2022.

3.4.3.5. Cement-Bentonite Interaction (Task 12)

In Task 12, modeling teams collaboratively simulate long-term reactions occurring at cement-bentonite interfacial regions with regards to time-dependent mineralogical, chemical, or textural changes. Details on how these reactions occur in space and time define whether an aged cement/bentonite interface may impede radionuclide transport (a beneficial effect) or cause delays in bentonite saturation (an unwanted effect). Teams started with three modeling benchmark cases for different types of bentonite, cement, temperature (non-isothermal versus isothermal), and saturation conditions (unsaturated in bentonite versus saturated). Teams will later move to simulate relevant experiments. Data from the Cl project at Mont Terri may be used for this purpose (Section 3.1.4). Because it is uncertain whether data from the Cl project can be used for the EBS Task Force, LBNL scientists resorted to the data collected from the FEBEX *in-situ* test to constrain a continuum-scale reactive transport model for the interfacial area between cement and bentonite (see Section 6.2.3 below; more detail in Section 9.3 in Zheng et al., 2021). Moreover, considering the limit of continuum scale reactive transport model to describe the change in pore structure and the resulting permeability change, LBNL scientists also attempted to use a pore- to mesoscale model based on the Lattice Boltzmann Model (LBM) approach to simulate the cement-bentonite interface area. LBM may be suitable to describe the change in pore structure

and the resulting permeability change with a feasible computation load for a scale of 10-20 cm. In FY21, LBNL scientists started with capability development adding a reactive transport module to an existing LBM simulator for multiphase flow (see Chapter 9 in Rutqvist et al., 2021a). The next step will be to verify the LBM model against the continuum reactive transport model and start simulating the scenarios described in Task 12.

3.4.3.6. *Unsaturated Homogenization (Task 13)*

This task involves a series of laboratory tests on bentonite homogenization conducted by CIEMAT (Villar et al., 2020). The question asked is to which extent bentonite would be capable of swelling into a gap or void and if so what the resulting bentonite properties would be. In this test program, FEBEX bentonite samples were compacted inside stainless steel rings and a gap was left at the top. The granulated bentonite was initially compacted with its hygroscopic water content (14%) at a target dry density of 1.7 g/cm^3. These samples were hydrated and later dismantled after different time periods. The final water content and dry density of the bentonite at different levels of the sample were measured, as well as the incremental bentonite intrusion into the gap (see example results in Figure 3.4-10) and the resulting pore size distribution. The tests were conducted as part of a European Union Project called BEACON (Section 3.6), which aims to develop and test the tools necessary for the assessment of the mechanical evolution of a bentonite barrier and the resulting sealing ability of the barrier. Activities under this task have started in 2021; SFWD participation is not currently considered.
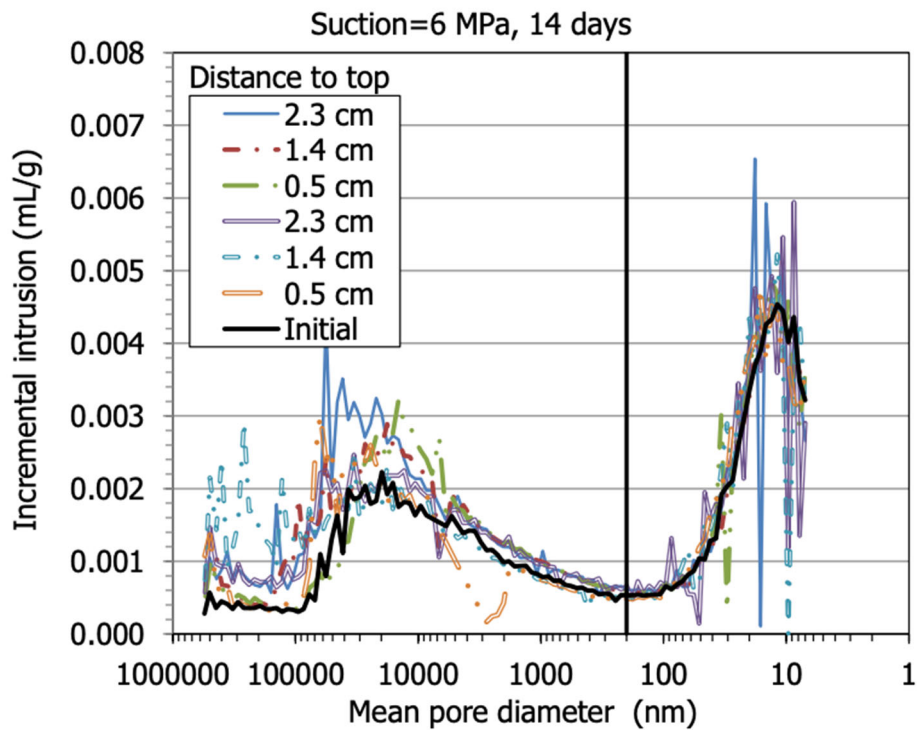
Figure 3.4-10. Incremental intrusion of pelleted bentonite swelling into a gap (Gens, 2021).

3.4.4. SKB Task Force Summary

Benefits of Participation:

- Access to several sets of experimental data from URLs in crystalline rock

- Opportunity to perform modeling and analysis of existing field and laboratory data in collaboration with other modeling groups (typically less direct interaction with the project teams that run or interpret the experiments)

Status of Participation:

DOE joined both Task Forces in January 2014. Under the umbrella of the GWFTS Task Force, SFWD researchers recently finalized their involvement in GWFTS Task 9 (diffusion and sorption experiments), which is winding down, and have since started working on a new Task 10 which focuses on flow channelization in fractured crystalline rocks and validation of discrete fracture network models (Section 3.4.2.2). In regards to the EBS Task Force, DOE/SFWD researchers have taken leadership of a new Task 11 which focuses on joint modeling of the HotBENT Column Test conducted at LBNL (Section 3.4.3.4), and are participating in Task 12 (Cement-Bentonite Interaction) with two alternative model approaches (Section 3.4.3.5).

Outlook:

SFWD's participation in the SKB task forces has recently been redirected to three exciting new tasks, namely Task 10 in the GWFTS Task Force, and Tasks 11 and 12 in the EBS Task Force. In regards to latter, the SFWD campaign sees a lot of value in leading this task related to the high temperature laboratory test currently conducted at LBNL. Having multiple international teams contribute to the interpretative modeling of the high-temperature column test is a win-win for SFWD and its international partners.

Contact Information:

DOE Contact:
Prasad Nair, DOE-NE

SFWD Contact:
Hari Viswanathan, LANL (GWFTS Task Force)
Carlos Jové-Colón, SNL, and Liange Zheng, LBNL (EBS Task Force)

SKB Contact:
Patrik Vidstrand, Executive Secretary, Technical-Scientific Council, SKB, Sweden
Björn Gylling, Secretary of GWFTS Task Force, SKB, Sweden
Antonio Gens, EBS Task Force for THM, from UPC, Spain
Urs Maeder, EBS Task Force for THC, University of Bern, Switzerland

3.5. NEA's Cooperative Initiatives

The previous sections describe initiatives that foster active research with other international disposal programs, provide access to field data, and/or may allow participation in field experiments in URLs (Sections 3.1 to 3.4). Here we briefly touch on NEA's international collaboration initiatives and certain European Union research initiatives where the nature of the engagement is less on active collaboration rather than on the exchange of information and shared approaches.

3.5.1. NEA's Clay Club

In 1991, the Nuclear Energy Agency (NEA) established a "Working Group on the Characterization, the Understanding and the Performance of Argillaceous Rocks as Repository Host Formations," known more commonly as the "Clay Club." Since 2000, the Clay Club has operated under the umbrella of NEA's Integration Group for the Safety Case (IGSC), an international forum on confidence building in repository technical safety cases and on the underlying methodological and scientific bases for the purpose of decision-making in repository development. The Clay Club promotes the exchange of information and shared approaches and methods to develop and document an understanding of clay media as a host rock for a repository, and provides advice to the IGSC on major and emerging issues related to the understanding of the multi-scale characterization, numerical model simulation, and barrier performance of argillaceous media. In particular, the Clay Club addresses recommendations, trends and information gaps concerning issues such as:

- Current knowledge regarding the long-term barrier integrity of argillaceous rock as relevant to establishing a deep geological repository safety case on time frames of one million years;

- The development of best international practice with respect to multi-disciplinary laboratory, borehole and *in-situ* characterization of argillaceous sediments necessary to understand far-field phenomena governing repository evolution, behavior and long-term performance;

- The refinement of the understanding of repository-induced effects in argillaceous rocks during excavation, operation and post-closure phases.

The work program and modus operandi of the Clay Club emphasize the pooling of resources, the sharing and synthesis of understanding and experiences, and the communication of findings to various audiences. Clay Club projects are established most often at the initiative of the members; work may also be undertaken on specific topics at the request of the IGSC. The topics of work reflect issues of common interest, considering the experience, progress and challenges of national program. Decisions on projects are made on a consensus basis, thereby taking into account the importance and urgency of the issue, the breadth of interest (i.e., the number of national programs for whom the issue is considered a key issue), and the necessary resources and schedules to accomplish the work proposed. Communication within the group takes place through plenary meetings, which occur on at least an annual basis.

The Clay Club chooses among a variety of mechanisms for its work program, including, for example: to install task-oriented expert groups; to organize workshops; to hire dedicated consultants and specialists; to collaborate in conferences; or a combination of these. The Clay Club is composed of senior technical experts with experience in assembling or reviewing the understanding of argillaceous media as host rocks for deep geologic disposal projects. Members represent waste-management agencies, regulatory authorities, academic institutions, and R&D institutions. Each member organization sends a representative to the annual meetings and provides a report on ongoing activities. Clay Club members are expected to: (1) promote Clay Club activities in their own organization; (2) provide relevant data and bibliographic material to support Clay Club initiatives; and (3) make human or financial resources available to the Clay Club initiatives as appropriate and on an ad hoc basis. In contrast to other international initiatives (such as the Mont Terri Project, DECOVALEX, or SKB's Task Forces), the Clay Club is not about active R&D collaboration, but rather about having a regular forum for in-depth discussion and information exchange. Current members are institutions from Belgium, Canada, France, Germany, Hungary, Japan, Netherlands, Spain, Switzerland, United Kingdom, and USA (LBNL).

3.5.2. NEA's Salt Club

The Salt Club brings together nations currently considering rock salt as a candidate medium for deep geologic disposal of High-Level Waste (HLW) and long-lived radioactive waste. The club's mission is to develop and exchange scientific information on rock salt as a host rock formation for deep geologic repositories. By promoting information and knowledge exchange, the Salt Club also intends to stimulate interest in other nations with appreciable rock salt deposits to consider rock salt as a viable repository medium. In addition to the technical aspects, the working group also aims at transferring obtained knowledge to programs at different phases of development, fostering education and training of future subject-matter experts in the field of rock salt, and cooperating with other NEA working groups (e.g., the Forum on Stakeholder Confidence, FSC) to engender public acceptance and building stakeholder confidence. The Salt Club working group is composed of senior technical experts with experience in assembling or reviewing the understanding of salt formations as host rock for deep geologic disposal projects. Members represent waste management agencies, regulatory authorities, academic institutions, and research and development institutions. Salt Club members have a level of seniority in their organizations such that they are able to mobilize resources to contribute to Salt Club initiatives. DOE is a current member of the Salt Club; other members are SNL, LANL, RESPEC, as well as several institutions from Germany, the Netherlands, Poland, Romania, the United Kingddom.

The club started in 2011 as an NEA working group, comprised of scientists and experts in developing disposal solutions in geologic rock salt formations. The official kick-off meeting for the Salt Club took place on April 20, 2012, at the OECD NEA headquarters in Paris to discuss initial work activities, schedules and other project details; since then, the members have met roughly once a year. The Salt Club has the following areas of interest:

- Geomechanical issues (coupled processes, excavation damaged zone (EDZ) behavior, rock mechanic issues, backfilling, sealing and plugging of rooms, drifts, shafts)

- Brine and gas migration

- Actinide and brine chemistry

- Microbial activities in rock salt

- Geochemical issues (radionuclide chemistry, modeling, natural analogs)

- Technical/technological and engineering issues (construction, operation, closure)

- Performance of geotechnical barriers

- Contributions to the Safety Case (e.g., FEP catalog, scenarios, performance assessment issues, uncertainties, use of natural analogs).

- Similar to the Clay Club, the Salt Club is not about active R&D collaboration, but rather about providing a regular forum for in-depth discussion and information exchange.

3.5.3. NEA's Crystalline Club

The Crystalline Club is the most recent addition to NEA's radioactive waste disposal working groups. Recognizing the mutual benefits of joint international research efforts and also the successes of the NEA Clay Club and Salt Club, delegates from the Czech Republic, Germany, Japan, Russian Federation, Spain, Romania, Switzerland, and the United States requested that the NEA establish a similar group for the study of crystalline rocks. Among the different geological formations considered suitable for hosting geological repositories, crystalline rocks are characterized by high strength, thereby providing cavity stability, low heat sensitivity, permeability and dissolution properties. Although fractures are common in crystalline rocks, the resulting fracture permeability can be resolved by engineered barriers such as waste containment and bentonite backfill. Although an advanced scientific and geotechnical understanding of crystalline rocks has been accumulated by the dedicated research carried out by several countries, there are research areas in which member countries may benefit from knowledge exchange, in-depth discussions, and joint R&D efforts.

The club started in December 2017 with its first face-to-face meeting in Prague, Czech Republic. The work program and modus operandi of the Crystalline Club is coordinated by a Crystalline Club Bureau which is consisting of six experts. Project topics are driven by common interest among members. The mode of cooperation is by plenary meetings, periodic general workshops and the use of electronic media. The club was set up to have a representative from each participating country serve as a chair or vice chair. Paul Mariner of SNL, nominated by DOE to participate in the Crystalline Club, became the club's vice chair.

3.5.4. NEA's Thermochemical Database Project

The purpose of the international Thermochemical Database Project (TDB) is to make available a comprehensive, internally consistent, quality-assured and internationally recognized chemical thermodynamic database of selected chemical elements, in order to meet the specialized modeling requirements for safety assessments of radioactive waste disposal systems (https://www.oecd-nea.org/dbtdb/). The unique feature of the TDB project is that the data are evaluated and selected by teams of leading experts drawn from universities and research institutes around the world, through a critical review of the existing primary experimental sources. Detailed TDB reports document the process leading to the selected values. Participating countries are as follows: Belgium, Canada, Czech Republic, Finland, France, Germany, Japan, Spain, Sweden, Switzerland, United Kingdom, and the United States. A 2015 report on the history of NEA TDB activities summarizes the accomplishment of the project since its inception in 1984 (Ragoussi and Brassinnes 2015). DOE has been participating in the TDB Project for a while (Zavarin et al., 2016; 2018; 2019; 2020) and is represented by Cindy Atkins-Duffins from LLNL, who serves as the SFWD campaign's representative for the international thermodynamic database development effort and was elected to the Executive Group of the project. This close engagement with the NEA TBD Project ensures that the generic disposal system modeling conducted by SFWD researchers is aligned with internationally accepted practices for repository performance assessment calculations. FY21 research activities conducted by SFWD scientists in support of the NEA-TDB project are described in Section 6.9.3 (based on the report by Zavarin et al., 2021b).

The TDB project has operated in five phases over almost two decades; a sixth phase was officially started in February 2019. During the initial phases of the project, a high priority was assigned to the critical evaluation of the data of inorganic compounds and complexes of the actinide's uranium, americium, neptunium, and plutonium, as well as the inorganic compounds and complexes of technetium. The second phase supported radioactive waste management programs by updating the existing database and applying the TDB methodology to new elements present in radioactive waste (as fission or activation products): nickel, selenium and zirconium, and simple organic complexes. The third phase started in 2003, with three new reviews on thorium, tin, and iron (Part 1), and with the constitution of an expert team for the preparation of guidelines for the evaluation of thermodynamic data for solid solutions. The fourth phase (2008-2014), started the second portion of the iron review (Part 2), a review of molydenum, and a review of auxiliary data which includes species and compounds necessary to describe aqueous chemistry of aluminum and silicon, data on inorganic species and compounds of elements such as iodine, boron, magnesium, calcium, strontium, and barium. Phase 5 of the NEA-TDB program, conducted from 2014-2019, took on a second update to actinide and fission product volumes, and two State-of-the-Art reviews--Cement Minerals and High Ionic Strength Aqueous Systems. Finally, the project initiated the design and development of a new TDB electronic database that is compatible with PHREEQC.

In 2017, NEA-TBD leads started discussing options for continuing the TDB effort into a Phase 6. The NEA-TBD Executive Committee invited international participation to a planning workshop held April 11-12, 2017. Mavrik Zavarin and Cindy Atkins-Duffin from LLNL as well as Carlos Jové-Colón from SNL attended and participated in the workshop discussions. There was overwhelming consensus that the NEA-TDB project remains an important asset to the international nuclear waste research community, and in November 2017 the Program Management Board took the decision to continue the Program. Phase 6 started officially in February 2019, with all participating member parties having signed the Framework Agreement. The First Meeting of the Management Board (MB) and the Executive Group (EG) were held at the NEA in Paris February 19-20, 2019. Projects from Phase 5 that were still in progress were brought forward to Phase 6. The current status of the Phase 6 program and the associated reviews are as follows:

- Iron (Part II) Volume – Published online (NEA TDB website) in January, 2020.

- 2nd Update of the Actinides Volume – Published online (NEA TDB website) in October, 2020

- Ancillary Data Volume – The volume is in the final stages of editing and production, expected publication (NEA TDB website) by the end of 2021. Carlos Jové-Colón (USA) is one of the peer reviewers.

- Molybdenum Data Volume – This review continues to struggle with delivery of information from the team to the NEA and to other teammates. Several rescoping and personnel assignments have been put into place. The EG has taken a more visible management role in this project. The current planned publication (NEA TDB website) by the end of 2022.

- Cements State of the Art Report – Considerable discussions were conducted by the TDB MB and EG regarding the pace of this review. The review team as asked to provide a realistic schedule to complete the project. The team provided a new schedule to the EG. The NEA Project Coordinator and the EG liaison (Cindy Atkins-Duffin, USA) convened quarterly meetings with the review team to monitor the review teams progress to their schedule. Progress has been steady with a planned publication (NEA TDB website) by the end of 2022.

- High Ionic Strength Solutions State of the Art Report – Progress continues to be slow on this project. The next deliverable, first single author drafts, and internal reviews of the text are due soon. The publication of NEA TDB website is currently planned for the end of 2022.

- Organics Update – The initiation report work was delayed and is now underway.

- Lanthanides Volume – The initiation team submitted their final report by the end of June. There was considerable discussion about the initiation report (strategy and approach) at the fall 2020 EG and MB meetings. Several small discussions and a meeting of the Initiators and the EG was convened. Contracting of the review team complied with the new OECD procurement processes and was initiated in early March 2021. Deliverable dates are under discussion.

- High Temperature State of the Art Report – The initiators have submitted a document containing a synopsis of the topics that will be covered and the organization of their initiation report. A panel of experts to review the identified material is being constructed. Once identified the remaining review scheduled can be planned and contracting initiated.

- TDB course – The in-person course planned for Paris in November 2020 was cancelled. An online option was presented as a substitute. 75 people participated and reviewed the opportunity favorably. The possibilities of continuing online presentation of this material either as side event to the in-person meeting or as a separate promotional event are under consideration. The September 2021 course (adjacent to Migration '21) was postponed.

- TDB Electronic Database – In November 2020 the electronic version of the NEA database was upgraded to include the release of a search engine and the inclusion of the SIT1 and SIT2 coefficients. Work is underway at this time to add the data from the recently released Ancillary review data and continue with bug fixes.

The NEA has announced there will be no "in person" meetings convened for NEA projects through this calendar year. Plans are in progress to convene the annual meeting in November of the Management Board and the Executive Group by virtual means.

3.5.5. NEA's Repository Metadata (RepMET) Project

From 2014 to 2019, NEA conducted the Radioactive Waste Repository Metadata Management initiative (RepMet) under the auspices of the Integration Group for the Safety Case (IGSC) technical body. The objective was to create a metadata registry that can be used by national programs to manage their repository data and records in a way that is harmonized internationally and is suitable for long-term management and utilization (McMahon 2017, 2018, 2019). Furthermore, the initiative that involved over ten different countries developed a consistent set of guiding principles for capturing and generating metadata, recommending a shortlist of selected relevant standards and guidelines on international good practices.

National radioactive waste repository programs require a large amount of data across multiple disciplines (e.g. geoscience, radioactive waste management, engineering) that increase as these programs proceed in number, type and quality for multiple reasons and goals (e.g.: site characterization, licensing, safety case elaboration, etc.). Considering these boundary constraints, the core idea of long-term data management is that "data are being collected and managed for others to use". Next generations of data-users have to be able to understand and access the information that the preserved data represent. Individual scientists and research teams, as well as managers and communications specialists, need to be aware of this and document their work accordingly. RepMet facilitated this task by bringing about a better understanding of a key aspect of the modern data management within the field of radioactive waste disposal, namely the identification and management of metadata. The initiative has analyzed the metadata implementation both from the high-level point of view (i.e., methodologies, approaches, organisation policies) and from a more technical one (i.e., recommendation and application of selected metadata standards, data modeling techniques and implementation of controlled dictionaries).

RepMet has now officially ended and produced five inter-related documents as listed below:

- RepMet/01 – Metadata in Radioactive Waste Management provides an overview of metadata and its application within RWMOs, discusses issues around the implementation of metadata, and outlines the outputs of RepMet and how they may be used. It also provides specific recommendations concerning metadata for RWMOs.

- RepMet/02 – Site Characterisation Library deals with data and related metadata that are considered during the characterisation of a site investigated and surveyed for suitability for radioactive waste disposal purposes.

- RepMet/03 – Waste Package Library deals with data and related metadata about packaged waste and spent nuclear fuel that, after proper treatment and conditioning processes, are ready for final disposal at the repository.

- RepMet/04 – Repository Library deals with data and related metadata relating to the engineered structures and waste acceptance requirements of radioactive waste repositories.

- RepMet/05 – RepMet Tools & Guidelines supports the libraries, providing a number of tools, methods, guidelines and approaches that were either used in developing the libraries or will be useful for RWMOs when adopting and implementing the libraries.

The documents discuss key aspects of data and related metadata for selected scientific and technical topics involved in the lifecycle of a radioactive waste repository. The reports include, and are underpinned by, three technical libraries, containing high-level conceptual data models, descriptions of data entities, attributes, associated metadata and other relevant information, and are ready to support the activities of RWMOs. The major report summary report on the Metadata Initiative has been published by NEA and is available for download at their web site (NEA, 2018). SNL researchers have been participating in this NEA sponsored project for the last few years, and have helped create conceptual data models for waste-package, HLW/SNF (Spent Nuclear Fuel) repository, and geoscience.

3.5.6. NEA's Data and Knowledge Management Group (IDKM)

After officially ending RepMET, NEA's Radioactive Waste Management Committee (RWMC) continued to demonstrate commitment in the data sciences area. Under RWMC's auspices, the Expert Group on Waste Inventorying and Reporting Methodology (EGIRM), the Radioactive Waste Repository Metadata Management (RepMet) initiative, and the Preservation of Records, Knowledge and Memory (RK&M) across Generations initiative have all developed valuable products related to information, data and knowledge management within the field of radioactive waste management. Following completion of these initial activities, the RWMC has now created a working group dedicated to Information, Data and Knowledge Management (IDKM) in the RWM field (https://www.oecd-nea.org/jcms/pl_29865/idkm-of-radioactive-waste-management). This group extends the objectives of the previous groups to holistically cover all RWM phases from cradle to grave while preserving the awareness of disposed wastes and its repository for future generations (McMahon 2019, NEA 2019, 2019a, 2019b).

To that end, a IDKM planning workshop took place in January 2019 in the NEA offices in Boulogne-Billancourt (Paris), France, with the following scope: (1) to advertise and present publicly the outcomes of the EGIRM, RepMet and the RK&M groups; (2) to further explore the current needs, expectations and challenges in the IDKM area for radioactive waste management organizations (RWMOs), regulators and other stakeholders; and (3) to develop recommendations for RWMC in the definition and planning of future NEA activities in the area of IDKM. The workshop was open to IDKM specialists in RWM and non-RWM fields, including engineers and scientists in RWMOs involved with data and information management, and knowledge managers and social scientists involved with knowledge management on extended timescales (up to hundreds of years). DOE was represented at this workshop by SNL scientists.

In FY20, planning efforts for the NEA Knowledge Management effort continued, with a planning meeting in January 2020. The official kick-off meeting for IKDM was held virtually on September 15-17, 2020, with 42 representatives from 12 NEA member countries and the European Union (EU). DOE was represented by SNL scientists (Camphouse, 2020). The participating working group members agreed to create subsidiary ad hoc expert groups in four working areas: (i) safety case, (ii) knowledge management, (iii) archiving, and (iv) awareness preservation, as illustrated in Figure 3.5-1 below.
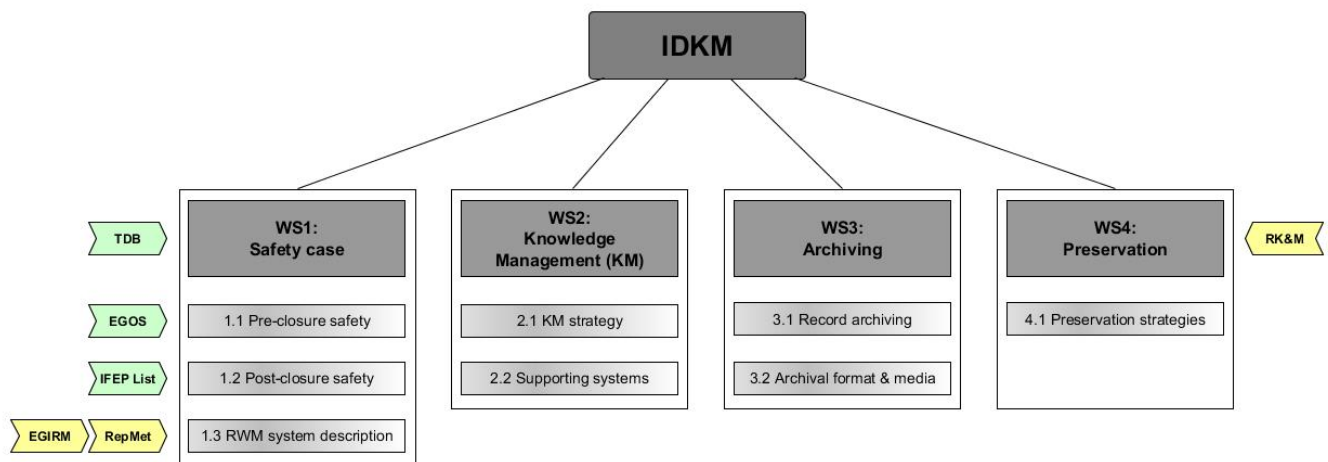
Figure 3.5-1. Main working areas envisioned by the NEA IDKM working group (from McMahon, 2019)

3.6. European Union Research Programs

The European Union supports substantial long-term research and innovation programs, the most recent one the Horizon 2020 program with nearly €80 billion of funding available over 7 years (2014 to 2020). One of the themes in Horizon 2020 is H2020-Euratom-1.2 entitled: "Contribute to the development of solutions for the management of ultimate nuclear waste." Several relevant long-term research projects have been conducted under this theme, such BEACON: Bentonite Mechanical Evolution, DISCO: Modern Spent Fuel Dissolution and Chemistry in Failed Container Conditions, CEBAMA: Cement-Based Materials, Properties, Evolution, Barrier Functions, MODERN-2020: Development and Demonstration of Monitoring Strategies and Technologies for Geological Disposal, and MIND: Development of the Safety Case Knowledge Base About the Influence of Microbial Processes on Geological Disposal of Radioactive Waste. European Union projects are often open to external collaboration, and thus offer valuable cooperation opportunities for SFWD researchers. Here is more information on two of the projects mentioned above that just ended this fiscal year.

BEACON (ongoing)

The overall objective of the BEACON Project was to develop and test the tools necessary for the assessment of the hydro-mechanical evolution of an installed bentonite barrier and its resulting long-term performance (https://cordis.europa.eu/project/id/745942). This was done by close cooperation between design, engineering, science and performance assessment. The evolution from an installed engineered system to a fully functioning barrier was also assessed. BEACON was coordinated by SKB, and, as is typical for European Union projects, had multiple participants from various countries (Czech Republic, Finland, France, Spain, Germany, United Kingdom, Belgium, Lithuania, Switzerland, and Sweden). The project ran from 2014 through May 2021.

DISCO (ongoing)

The development of robust safety cases for geological disposal of spent nuclear fuel requires a solid understanding of its dissolution over very long timescales (https://cordis.europa.eu/project/id/755443). The spent fuel dissolution is the main source term for the release of radionuclides under repository conditions, and it will control the release of radioactivity in the environment surrounding the engineered barriers (the near field) of a disposal facility once the engineered barrier system (EBS) has degraded and groundwater comes into contact with the spent fuel. The DISCO Project goal is to fill the gap of knowledge on spent fuel dissolution arising from the development and use of novel types of fuel (Cr- doped and MOX). As such, DISCO represented a logical follow-up of earlier Euratom projects (such as SFS, NF-PRO, MICADO, REDUPP and FIRST-Nuclides) which focused on dissolution and radionuclide release from conventional UO_2 spent fuels. Specific objectives of DISCO can be summarized as follows:

- To enhance our understanding of spent fuel matrix dissolution under conditions representative of failed containers in reducing repository environments;

- To assess whether novel types of fuel (mixed oxide fuels such as MOX, or Cr/Al-doped) behave like the conventional ones.

DISCO started in 2017 and ran through May 2021. There were 16 participants from eight countries, including Sweden, Finland, Germany, Belgium, Switzerland, France, United Kingdom, and Spain.

The expected knowledge gain is essential for Waste Management Organizations and is of interest for a wider range of potential users (e.g., research organizations). Therefore, the project aims to disseminate the new knowledge gained through different channels in order to reach a wider community. One of these channels is the organization of regular Annual Meetings that are open to everyone. To leverage technical information from European collaborators, researchers from Pacific Northwest National Laboratory (PNNL) participated in the 3rd Annual DISCO Meeting, which was held virtually on April 23, 2020 (Asmussen and Hanson, 2020). PNNL scientists will also join the final meeting of the DISCO Project in October 2021. This final meeting aims to provide a forum to facilitate the discussion of project results, as well as to communicate with the broader scientific community on research findings and remaining challenges.

4. BILATERAL COLLABORATION OPPORTUNITIES

Access to data from international field experiments and participation of SFWD researchers in collaborative field studies can also be facilitated via direct informal or semi-formal agreements between national laboratories and international partners. Several SFWD scientists have close relationships with their international counterparts, resulting from workshops and symposia meetings, or from collaboration outside of SFWD's scope. International disposal programs benefited from collaboration with SFWD scientists and are generally quite open to including them in their ongoing research teams. This may require preparation of Memorandum of Understandings (MoU) or other types of bilateral agreements. The U.S. DOE has several such bilateral agreements in place, among those the Joint Fuel Cycle Studies (JFCS) agreement with the Republic of Korea, with the German Federal Ministry of Education and Research (BMWi), with Japan under the JNEAP (Joint U.S.–Japan Nuclear Energy Action Plan) agreement, and with France as a result of a MoU with ANDRA. The subsections below give a short description of selected bilateral collaboration opportunities providing access to valuable data and major field experiments. Some of the opportunities described (e.g., Republic of Korea, Germany, Sweden, Israel) have already resulted in close collaborative research work between SFWD scientists and their international counterparts; the others describe opportunities for active research collaboration in the future. This list is being amended and updated as new opportunities arise.

4.1. Collaborations with KURT URL, Republic of Korea

Several years ago, a formal commitment to collaboration on the management of nuclear fuel was established between the United States and the Republic of Korea (ROK). The bilateral agreement between DOE and the Republic of Korea (ROK) Ministry of Science, ICT and Future Planning (MISP) has led to a broad collaborative research program regarding the utilization of civilian nuclear energy and the nuclear fuel cycle (McMahon 2017). The two countries set up the Spent Fuel Management Working Group (SFMWG) to discuss/plan collaboration the storage, transportation and disposal of spent nuclear fuel. In terms of active research elements centered on disposal science, the bilateral R&D has focused on the KURT URL in Korea. KURT stands for KAERI Underground Research Tunnel, with KAERI being the Korea Atomic Energy Research Institute.

KURT is a generic underground research laboratory hosted by a shallow tunnel in a granite host rock, located in a mountainous area near Daejeon, Republic of Korea. Using KURT, KAERI intends to obtain information on the geologic environment and the behavior and performance of engineered barriers under repository conditions. KURT has a total length of 255 m with a 180 m long access tunnel and two research modules with a total length of 75 m. The maximum depth of the tunnel is 90 m from the peak of a mountain. The horseshoe shape tunnel is 6 m wide and 6 m high (Figure 4.1-1). The tunnel construction at KURT started in March 2005 and was completed in November 2006. An expansion of the tunnel completed in 2014 is shown in Figure 4.1-2, which allowed for additional several hundred meters of tunnel length for further site characterization and *in-situ* testing. The host rock is granite, which is one of the potential host rock types for an HLW disposal repository in Korea. The utilization of radioactive material in KURT is not allowed.

Compared to other URLs, including those discussed in Section 3, KURT is a relatively new facility. The first research phase started in 2006 after successful completion of the facility. Past or current research works has included (1) geologic characterization and long-term monitoring, (2) development and testing of site investigation techniques, (3) solute and colloid migration experiments, (4) EDZ characterization, (5) borehole heater tests, and (6) investigation of correlation between streaming potential and groundwater flow (Figure 4.1-3). Later phases comprised additional site characterization work related to the tunnel expansion and also included *in-situ* long-term performance tests on a 1/3 scale engineered barrier system at KURT. The focus of the site characterization work was on a major water-conducting feature (MWCF), which was initially identified from surface boreholes and which will soon be accessed from the new expansion tunnels.

The KURT site offers one unique feature in regards to *in-situ* borehole characterization and deep borehole disposal R&D. The site hosts an existing deep (1 km) borehole drilled into granitic bedrock, which provides a unique opportunity for developing and testing techniques for *in-situ* borehole characterization in fractured

crystalline rocks. The DB-2 borehole was drilled from the surface to a depth just outside of the KURT facility (Figure 4.1-4) to better understand the deep geologic, hydrogeological, and chemical characteristics around the KURT site, and to specifically explore the MWCF. The deep borehole offers valuable possibilities of collaboration regarding deep borehole characterization and deep borehole disposal concepts. The Republic of Korea and KAERI are interested in further exploration of such concepts.
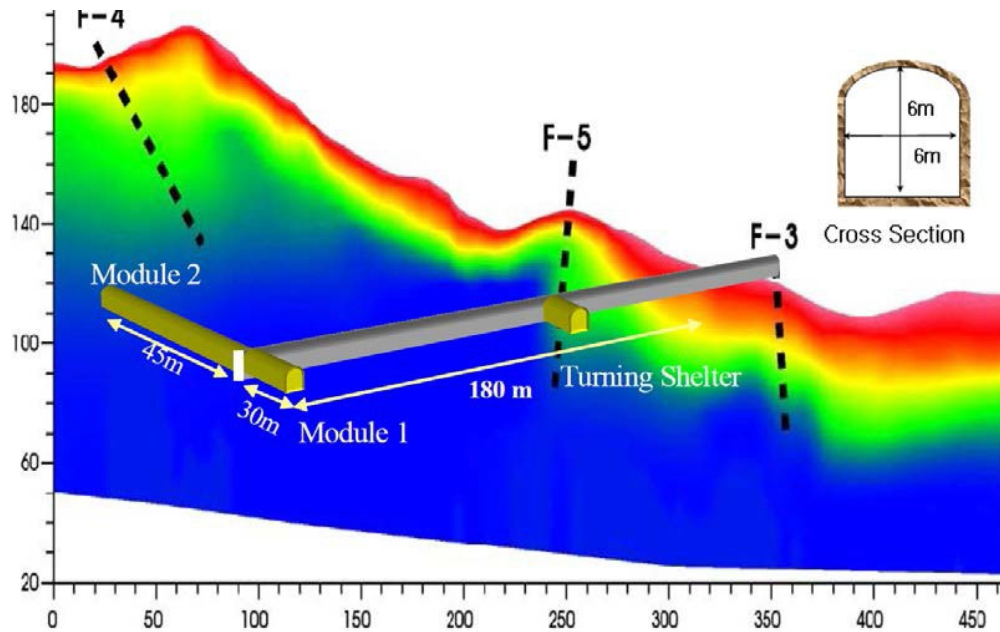
Figure 4.1-1. Layout of the KURT URL in Daejeon, Korea before extension (KAERI 2011).
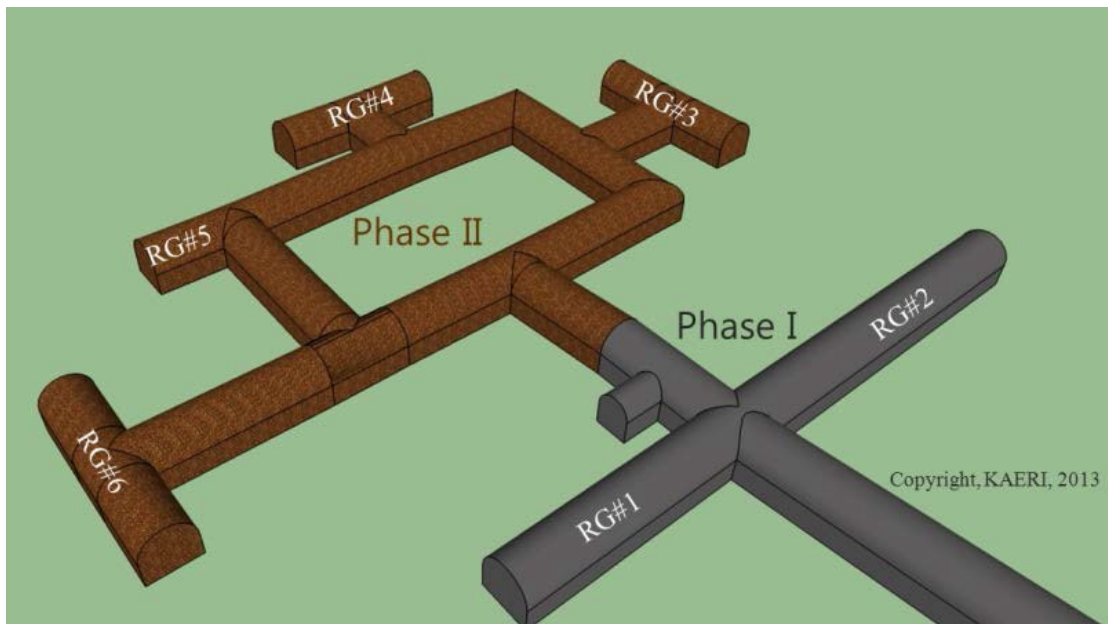
Figure 4.1-2. Layout for tunnel extension of KURT (Wang et al., 2014).
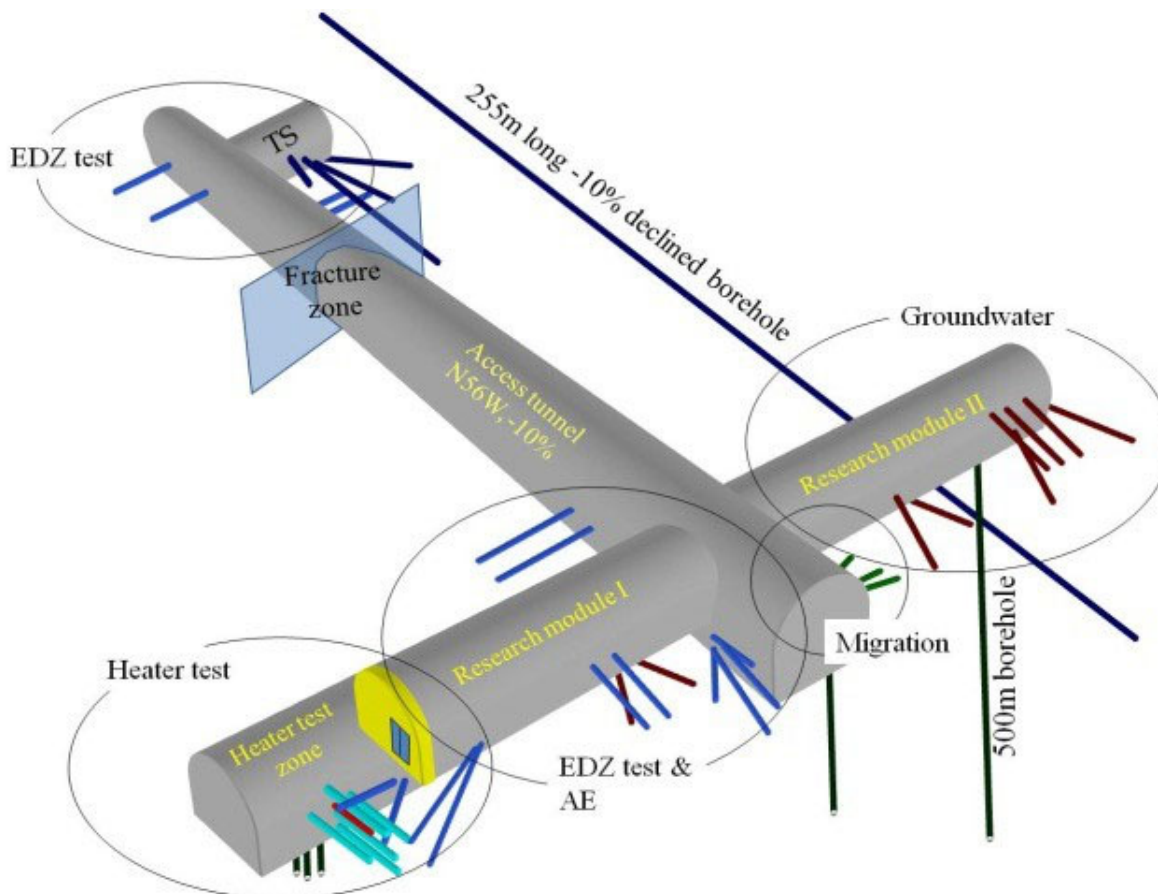
Figure 4.1-3. Location of *in-situ* tests and experiments at KURT (from Wang et al., 2014).
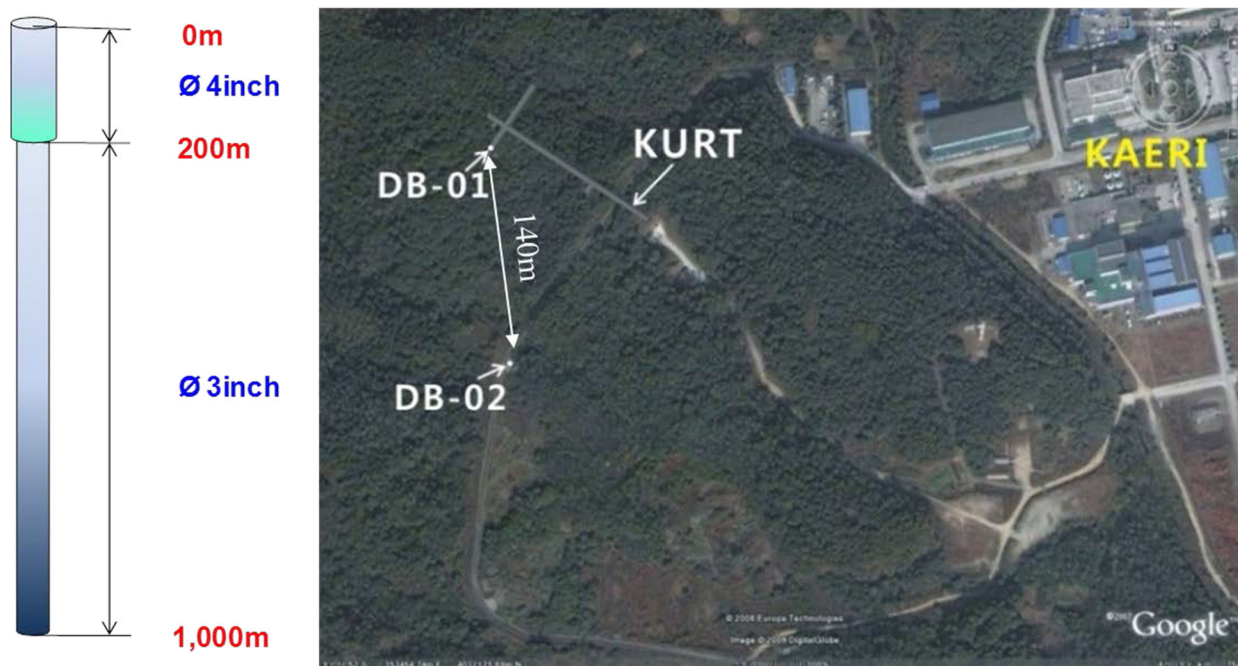
Figure 4.1-4. Specification of DB-2 borehole and its location near KURT site (from Wang et al., 2014).

As part of their joint activities in the Spent Fuel Management Working Group, researchers at SNL and KAERI developed a multi-year plan in 2015 for joint field testing and modeling to support the study of high-level nuclear waste disposal in crystalline geologic media, which includes sharing of KURT site characterization data. Three specific collaborative tasks were defined, as follows: (1) streaming potential (SP) testing regarding correlation with groundwater flow, (2) technical data exchange regarding site characterization and buffer material specifications, and (3) technique development for *in-situ* borehole characterization. The first two tasks were completed in FY16, and the results are documented in Wang (2016). Regarding *in-situ* borehole characterization, KAERI and SNL in FY16 and FY17 worked on the development of *in-situ* hydrological and geochemical measurements in deep boreholes, with the specific objective of better characterizing the hydrogeological properties of the damage zone around a deep borehole and understand its possible role in the migration of nuclides. The damage zone is defined as the zone around a borehole where flow and transport properties are significantly changed from hydromechanical and geochemical modifications. The plan was that new approaches to assess borehole damage zones would be tested in existing boreholes at KURT; however, this collaborative research task did not continue since the deep borehole R&D has now been discontinued in the U.S. program. Currently, there are no research activities of SFWD scientists related to KURT; however, KAERI remains open to future collaboration on a variety of topics.

4.2. Collaborations with Germany

Germany has a long history of research and exploration work with focus on radioactive waste disposal in domal salt. However, the Gorleben site became a highly contentious political issue in the 80's and 90's, and a moratorium on further development of the site was imposed in 2000, mostly due to political reasons. Germany's program for permanent disposal of high-level waste hit a reset button and essentially started from scratch again. In July 2013, Germany adopted a new Act on the Search and Selection of a Site for a Repository for Highly Radioactive Waste (StandAG). As a first step, the newly created law was evaluated by a joint federal/state committee of members representing different interests, the "Commission on the storage of high-level radioactive waste". Among other things, the Commission developed criteria and recommendations for the selecting a repository site that ensures the best possible security for the period of one million years. On the basis of the commission's final report, the further developed Site Selection Act (StandAG) was amended in May 2017. In a new multi-phase, science based comparative procedure, the site is to be selected by 2031 and approved by a resolution of the Federal Parliament. According to the Site Selection Act, all regions in Germany with suitable geologies such as rock salt, clay rock and crystalline rock (such as granite) must be taken into account in the site selection procedure.

Germany also redefined responsibilities for radioactive waste disposal. BGE, the Federal Company for Radioactive Waste Disposal, is entrusted with the task of implementing site selection procedures for a final repository, particularly for heat-generating radioactive waste. BASE, the Federal Office for the Safety of Nuclear Waste Management, is the regulator. BASE performs regulatory, licensing and supervisory tasks when it comes to disposing of and storing, handling and transporting high-level radioactive waste. BASE also regulates the site selection procedure for a disposal site for radioactive waste, is monitoring the completion of the process, and is organizing public participation in the search for a site. Meanwhile, BGR, the Federal Institute for Geosciences and Natural Resources (i.e., the German Geological Survey), is tasked to provide the German Government with independent and neutral advice on all geoscientific and geotechnical issues involved in the Federal Government's nuclear repository projects.

With the start of the site selection procedure in September 2017, Germany's nuclear waste disposal program needed to begin considering a broad range of host rock options, just like the U.S. program had done when in 2011 it stopped proceeding with the Yucca Mountain site. Germany, like the U.S., became strongly engaged in various international collaboration initiatives, many of which are the same as DOE has been partnering with. For example, BGE, BASE, and BGR all joined the DECOVALEX2-2023 Project and are partners in the Mont Terri Project. BGE is also a partner in the HotBENT Project and the CFM Project. BGR participates in the SKB Task Forces and the HotBENT Project. In addition, there are several research organizations with strong international relationships. GRS, the Gesellschaft für Anlagen- und Reaktorsicherheit, carries out research and analysis in its fields of competence, namely reactor safety, radioactive waste management as well as radiation

and environmental protection (Mont Terri Project). And the Helmholtz Centers (perhaps best described the German equivalent of DOE's National Laboratories) have long-running research programs focused on safety issues relating to nuclear waste management, including the long-term safety of final storage repositories (DECOVALEX-2023 Project, Mont Terri Project).

Given that the two countries are in a similar stage in terms of nuclear waste disposal, with a broad focus on a range of suitable geologies, it is no surprise that there are several ongoing collaboration projects conducted by SFWD researchers and their German counterparts, both under the umbrella of above-mentioned multi-partner initiatives or in direct bilateral collaborations. As to the latter, much of this collaboration is centered on salt research, as described in Section 4.2.1 below. Other ongoing research collaborations are briefly discussed in Section 4.2.2 and Section 6.6.

4.2.1. Salt Research Collaborations

DOE/SFWD scientists and their German colleagues in academia and other research laboratories collaborate closely on various R&D issues related to disposal of radionuclide waste in salt. A MoU was signed several years ago between DOE and the German Federal Ministry of Economics and Technology (BMWi) to cooperate in the field of geologic disposal of radioactive wastes (MoU date: November 2011). Also, eleven U.S.–German Salt workshops have been held so far to advance collaboration, starting with a preparatory workshop on May 25–27, 2010, in Jackson Mississippi, followed by Peine, Germany, (November 2011), Albuquerque, New Mexico (October 2012), Berlin, Germany (September 2013) (Hansen et al., 2013), Santa Fe, New Mexico (September 2014) (Hansen et al., 2015), Dresden, Germany (September 2015), Washington D.C. (September 2016), Nieuwdorp, Netherlands (September 2017), Hanover, Germany (September 2018), and Rapid City, South Dakota (May 2019) (Buchholz et al., 2019). The 2020 workshop was scheduled for May 2020 in Braunschweig, Germany, but the meeting had to be postponed due to the Covid-related travel restrictions. The 11th US/German Workshop was finally held in virtual mode on February 2, 2021, June 17, 2021, and September 8-9, 2021. The overriding premise of the U.S.-German collaboration is to advance the scientific basis for salt repositories. Over the past ten years or so, scientists from both countries have engaged in several cooperative activities, including joint experiments, coupled-salt-mechanics modeling and benchmarking.

Germany has a long history of salt R&D. The country started in 1979 to conduct exploration work at the Gorleben salt dome to evaluate its suitability for waste disposal (Figure 4.2-1). While the moratorium on Gorleben has been lifted, R&D activities at Gorleben have not yet resumed, and it is questionable whether and when further underground testing at this URL might be conducted. Another mine, the Asse II Mine, was also used as a research facility in the past, between 1965 and 1995, where some major experiments such as the long-term TSDE (Thermal Simulation for Drift Emplacement) experiment were carried out. As shown in Figure 4.2-2, the TSDE experiment comprised of two parallel drifts, each of which housing three electrical heaters to simulate emplacement of heat-producing waste. A significant amount of data was collected over several years in 20 monitoring cross sections: temperature, stress changes, displacement, convergence, and porosity of crushed salt, among others. Data from the TDSE experiment have been used by SFWD scientists to validate the large-scale applicability of coupled THM models (Rutqvist et al., 2016). Previously, the joint projects between Germany and the U.S. on salt R&D primarily focused on domal salt (e.g., Gorleben) rather than bedded salt (e.g., the Waste Isolation Pilot Plant (WIPP) facility). This changed with the onset of the collaborative KOSINA Project which ended in 2018, as well as several ongoing joint projects (WEIMOS, RANGERS, COMPASS, SaltFEP) which are further described below.

Figure 4.2-1. View of one of the underground tunnels at Gorleben at the 840 m level (BMWi 2008).
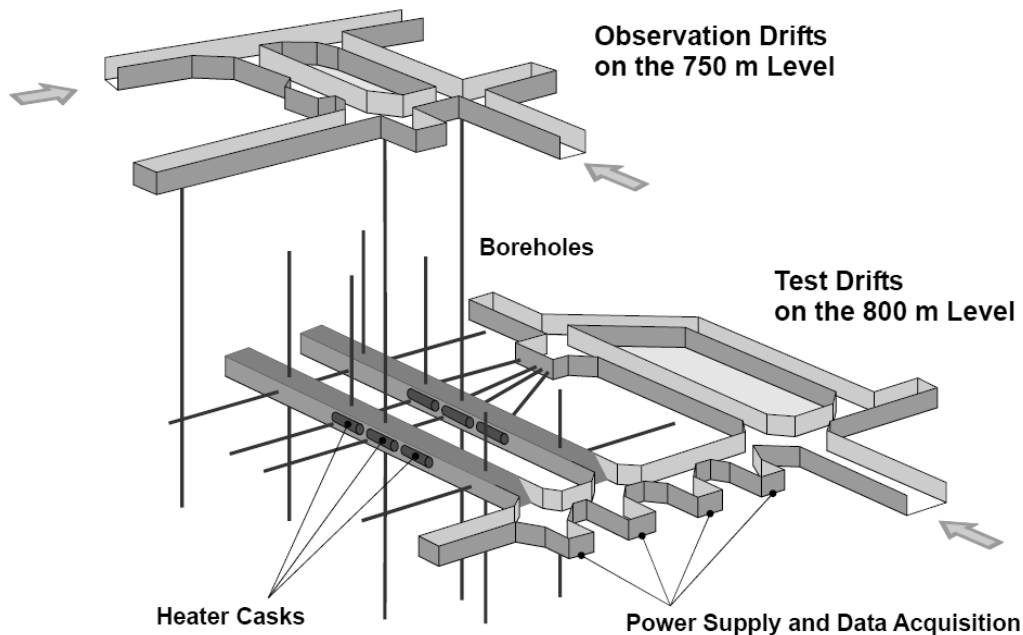
Figure 4.2-2. Schematic view of the two drift tests used in the TSDE experiment (800 m level of the Asse salt mine) (Rutqvist et al., 2015).

4.2.1.1. WEIMOS Project

WEIMOS is a collaboration of German and U.S. researchers seeking to improve thermo-mechanical modeling of salt repositories. The group primarily focuses on improving constitutive models for rock salt, but the partners also undertake extensive laboratory test programs and refine methods for simulating the evolution of underground structures. Typically, the laboratory tests help inform and calibrate the partners' constitutive models, which are then benchmarked against underground experiments. After translating to English, the acronym WEIMOS stands for "Further Development and Qualification of the Rock Mechanical Modeling for the Final High-Level Waste Disposal in Rock Salt". The WEIMOS partners include Hampel Consulting (Mainz, Germany), Institute für Gebirgsmechanik (Leipzig, Germany), Leibniz University (Hannover, Germany), Technical University of Braunschweig (Germany), Technical University of Clausthal (Germany), and SNL (Albuquerque, USA). The three joint projects that preceded WEIMOS substantially improved the

current state-of-the-art models and also helped identify the following work packages that together comprise WEIMOS:

1. Deformation behavior at small deviatoric stresses.

2. Temperature and stress dependence of damage reduction and healing.

3. Deformation behavior resulting from tensile stresses.

4. Influence of inhomogeneities (layer boundaries, interfaces) on deformation.

5. Virtual demonstrator.

More detail on SFWD research activities conducted in the context of WEIMOS is given in Section 6.6.2. Further descriptions are provided in Kuhlman et al. (2021a,b).

4.2.1.2. RANGERS Project

The objective of the joint U.S.-German RANGERS project is to develop a "Design and Integrity Guideline for Engineered Barrier Systems for a HLW Repository in Salt". Despite extensive knowledge and experience about geotechnical barriers in salt formations, there is no guideline for the design and verification of such structures for a high-level radioactive waste repository. Thus, the project between SNL and BGE Technology aims at developing a guideline for the planning and the design of geotechnical barriers in salt formations. This guideline will serve as a reference manual for the conceptualization of a HLW repository in Germany or the USA. It summarizes the state of the science and art available today in a single report and gives an outlook about the technologies, which will impact the development of geotechnical barrier systems in the future. Recommendations for the design and verification of geotechnical barriers based on the state of the art in science and technology will be formulated and an overview of new concepts, building materials and technologies that will shape the state of the art of tomorrow will be given. Four sub-goals are formulated for this purpose:

1. Compilation of existing knowledge and experience for the design and construction of geotechnical barriers and compilation of new concepts and technologies on the subject of geotechnical barriers.

2. Development of a guideline based on the state of the art in science and technology for the design and verification of geotechnical barriers.

3. Preliminary design and verification of the geotechnical barrier system for selected repository systems based on the developed guideline.

4. Comparison of design results according to the new guideline with results of previous design and assessment.

The project is divided in six work packages, which are described in Kuhlman et al. (2021a,b). The outcome of the project KOMPASS – another binational project between Germany and the US (see Section 4.2.1.3 below) – about the compaction of crushed salt as a key element of a sealing system in a salt high-level waste repository will be exploited in this project. More detail on SFWD research activities conducted in the context of RANGERS is given in Section 6.6.3.

4.2.1.3. KOMPASS Project

KOMPASS is a collaboration of German and American researchers seeking to improve thermo-hydro-mechanical models for crushed salt (i.e., run-of-mine or granular salt). The project is similar to WEIMOS but focuses on crushed salt: partners conduct experiments to understand crushed salt behavior and further develop, calibrate, and validate models for crushed salt. After translating to English, the acronym KOMPASS stands for "Compaction of Crushed Salt for Safe Enclosure." The KOMPASS partners are BGE, Institute für Gebirgsmechanik (Leipzig, Germany), Technical University of Clausthal (Germany), GRS, and BGR on the German side, and SNL on the U.S. side.

The project involves the following four work packages:

1. Benchmarking existing constitutive models

2. Thermal-hydraulic-mechanical (THM) characterization experiments

3. Analysis of microstructural mechanisms

4. Develop a sequel to the KOMPASS project

The first phase of the KOMPASS project was completed in 2020, with a comprehensive final report by Czaikowski et al. (2020). During this phase, experimental techniques for consolidation were thoroughly evaluated to produce adequate pre-compacted and compacted samples under various conditions, which included characterizing sufficient reference material. The second phase of the project officially began in July 2021. Based on results from the first phase, a systematic test series has been planned to further establish reproducible and predictable correlations between stress, duration of compaction, moisture states, and respective target porosity. More detail on SFWD research activities conducted in the context of KOMPASS is given in Section 6.6.4. Further description of each work package is given in the report by Kuhlman et al. (2021a,b).

4.2.1.4. Salt FEPs Catalog and Salt Scenarios

Researchers from SNL and from the German GRS have collaborated on the development of a comprehensive Features, Events and Processes (FEPs) catalogue and FEP database for a high-level waste repository at a generic salt site. The salt FEP catalogue was developed using a matrix approach that classifies FEPs using a two-dimensional structure consisting of a Features/Components axis and a Processes/Events axis. The FEP catalog builds upon prior work at SNL and at GRS, and supports the Nuclear Energy Agency (NEA) Salt Club Mandate. The "SaltFEP" database archives information from the catalog and from other supporting documentation into a user-friendly format that is easy to search. The generic salt repository FEPs include consideration of relevant FEPs from a number of U.S., German, and international FEP lists and should be suitable for any repository program in bedded or domal salt formations. In FY20, a number of changes were made to the existing salt FEP catalog, including an improved description of the thermal-mechanical and thermal-hydrological FEPs, the use of more generalized process descriptions that allow the FEP catalog to be extended to other types of geologic media, and creation of a crosswalk from the list of matrixes FEPs to the NEA list of IFEPs. Freeze et al. (2020) issued a final report on the bilateral US-German Salt FEPs project, which is now linked to from the NEA Salt Club website. An effort was made since then to broaden this FEP work and publish it as an NEA report, see more details in Section 6.6.5 of this report and in Kuhlman et al. (2021a,b).

4.2.2. Other U.S.-German Collaborations

As an example of other bilateral U.S.-German collaborations, LLNL researchers have for a long time engaged in close collaborations with the German Helmholtz Zentrum Dresden Rossendorf (HZDR) on surface complexation modeling and in particular the development of a surface complexation/ion exchange database. Two components of database development are pursued. First, a primary sorption data capture effort is focused on radionuclide (e.g., Cs, Sr, U, Np, and Pu) sorption to clay minerals (with particular focus on bentonite/montmorillonite). Second, methodologies for development of a surface complexation/ion exchange constant database from the primary sorption data are being pursued. A key component of this effort is the integration of commercially available fitting routines (e.g., PEST) that can be linked to surface complexation/ion exchange codes (e.g., PHREEQC) and produce optimized constants and associated parameter uncertainties. A new component of this effort that was initiated in FY20 and continued this year is the application of machine learning and data science techniques to this database effort. The combination of machine learning approaches with more traditional PEST/PHREEQC data fitting approaches provides flexibility to performance assessment modeling efforts (e.g., use of mechanistic surface complexation/ion exchange models versus smart Kd lookup tables). More information on recent work and achievements is provided in Section 6.9.3.4 and in Zavarin et al. (2021b).

4.3. Collaboration with COSC, Sweden

The "Collisional Orogeny in the Scandinavian Caledonides" (COSC) project in Sweden is a scientific deep drilling project whose objective is to gain insights into the tectonic evolution of the area, characterize present and past deep fluid circulation patterns, determine current heat flow to constrain climate modeling, and characterize the deep biosphere. Another objective of this project is to calibrate high quality surface geophysics through deep drilling. The project is centered on the drilling of two deep boreholes (each to depth of ~2.5 km) into crystalline rock in Sweden. The first hole (COSC-1) was completed on August 26, 2014 to a depth of 2495.8 m: core recovery was greater than 99%. The COSC-1 borehole was drilled though the Seve Nappe, which contains high-grade metamorphic rocks indicative of deep (100 km) crustal levels (Figure 4.3-1). The main lithologies encountered consist of felsic, amphibolite, and calc-silicate gneisses, amphibolite, migmatites, garnet mica schist, with discrete zones of mylonite and microkarst. There is a transition from gneiss into lower grade metasedimentary rocks that occurs between 2345 and 2360 m, which likely marks a structural boundary between different nappes. In addition to drilling the well and collecting core, the research team also conducted pre-drilling and post- drilling seismic and other geophysical surveys, borehole geophysical logs, conducted on-site measurement on recovered cores, carried out systematic X-ray fluorescence (XRF) measurement on all cores at 10 cm intervals for key chemical compositions, and performed downhole spectral gamma ray (SGR) logging to determine U, Th and K contents all along the borehole.
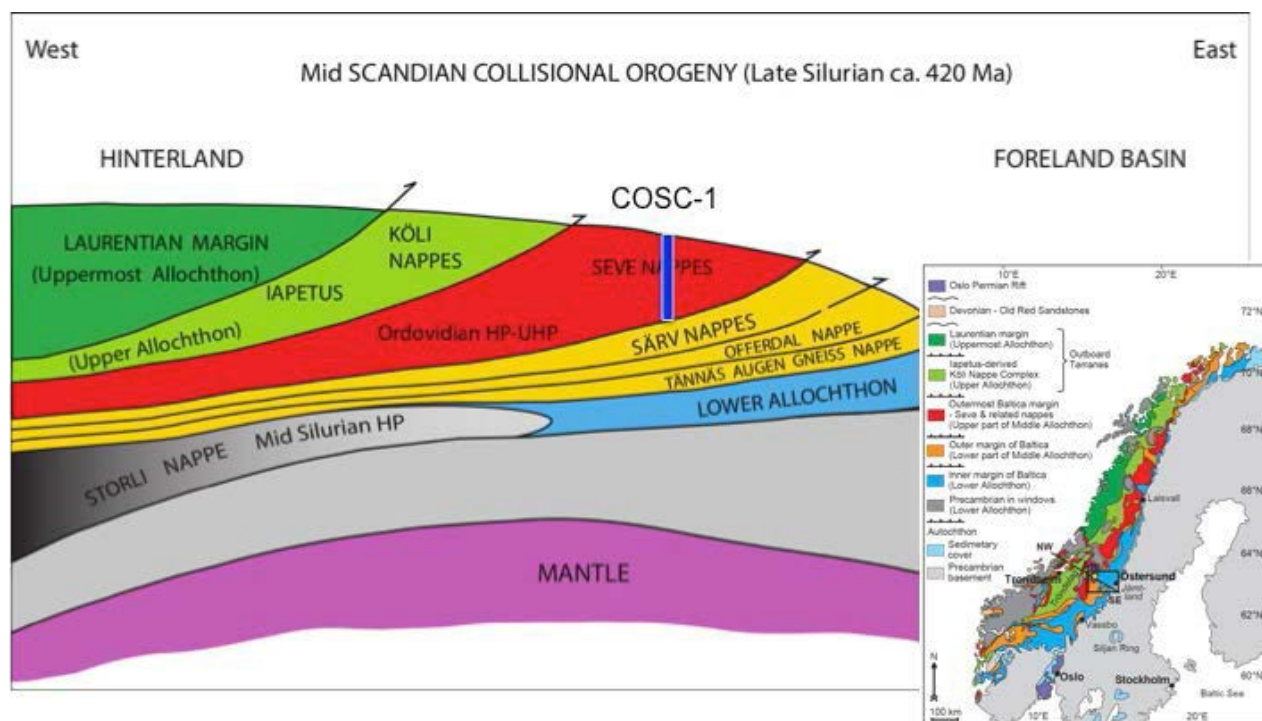
Figure 4.3-1. Location of COSC-1 deep borehole (Dobson et al., 2016).

It was recognized by SFWD that the COSC project provided a valuable opportunity to test characterization techniques for crystalline host rocks. In FY15, LBNL initiated a joint R&D program centered on fluid-logging testing using the first COSC borehole. The main objective of the joint research was to develop a better understanding of what information can be obtained from core and borehole measurements and how best to characterize the deep subsurface environment in granitic and other crystalline rocks in the context of nuclear waste disposal. LBNL gained key insights on the use of the flowing fluid electrical conductivity (FFEC) logging tool to identify deep flowing fracture zone in crystalline basement. In FY17, LBNL conducted laboratory measurements of transmissivity of fractured core samples from the COSC-1 well as a function of controlled stress. These fractured core samples were spatially correlated with fluid flow zones in the same well

that were identified by flowing fluid electrical conductivity (FFEC) logs. In FY18 through FY209, LBNL researchers further examined the hydraulic properties of crystalline rock cores from the COSC-1 well using a unique laboratory-scale apparatus that allowed for measuring the multi-directional transmissivity to assess fracture anisotropy under confining stress conditions.

In the summer of 2019, LBNL together with its Swedish partners conducted a new field-testing campaign in the COSC-1 well to probe the coupled hydromechanical and chemical processes in selected fracture zones, comparing transmissive and not transmissive fractures (Guglielmi et al., 2019). This work was done using an innovative downhole fracture characterization device, the Step-rate Injection Method for Fracture *In-situ* Properties (SIMFIP) tool, which can be used to measure real-time 3D mechanical deformation of a borehole interval, containing one or more fractures, together with measurements of the injection water flow rate, pressure, temperature and water electric resistivity. The following field tests were carried out: pressure buildup tests, pressure falloff tests, and constant flow rate tests for each of the three intervals. In FY21, LBNL continued its a comprehensive analysis and interpretation of the field testing results (Section 6.7.2). The following tasks were performed: (1) interpretation of the observed fracture displacements during stimulation, (2) evaluation of stress perturbations and their impact on fracture aperture at the borehole scale, and (3) study on stress perturbations and their impact on fracture flow at the network scale (Guglielmi et al., 2021). These analyses provided insights into the stress state for the borehole intervals, as well as how the fractures responded to hydraulic stimulation. The field data analysis was complemented by data analyses and numerical modeling of laboratory testing on cores taken from the COSC-1 well (Sections 6.8.3 and 6.8.4). The Swedish COSC team is currently drilling a new deep borehole (COSC-2), so there may be additional opportunities for conducting tests in this new well.

4.4. Collaboration with Israel

The Israel Atomic Energy Commission is examining the possibility of locating a geological waste disposal site within the carbonate Ghareb and Nezer Formations in the northern Negev, Israel (Klein-BenDavid et al., 2019). A research program is underway in Israel which includes studies to better quantify and predict chemical interactions along interfaces between cementitious materials and the carbonate host rocks. Such interactions may lead to chemical and structural alteration of both the cement and the host rock caused by diffusion and reaction driven by gradients in porewater pH and composition, pore structure, and mineralogical differences between the different materials. As described in Section 6.2.2 and in Matteo et al. (2020a), researchers from the Nuclear Research Center of the Negev in Israel and of SNL conducted a joint study to simulate the long-term performance of interfaces between cementitious materials (CEM I, selected as a bounding case for alkali cement-rock interactions, and a low pH cement) with carbonate geologic strata (limestone, chalk, marl, oil shale, low organic phosphorite and high organic phospharite). For the U.S. program, this collaboration provides insights into the specific challenges of using carbonate rocks as host rocks for permanent disposal or interim storage. Also, the methods for long-term predictions of interfacial reactions between cement and carbonate are relevant for other interfacial materials as well.

4.5. Collaboration Opportunities at ANDRA's LSMHM URL, France

The major underground disposal research facility in France is ANDRA's LSMHM (Laboratoire de recherche Souterrain de Meuse/Haute-Marne) URL sited near Bure in the Meuse and Haute-Marne districts in the east of France, co-located with the proposed French disposal site Cigeo. R&D at Bure aims at studying the feasibility of reversible geologic disposal of high-level and long-lived intermediate-level radioactive waste in the Callovo-Oxfordian clay formation. This facility was licensed in August 1999, and its construction (access shafts, basic drift network with underground ventilation) was finalized in 2006. As shown in Figure 4.5-1, the URL consists of two shafts sunk down to a depth of about 500 m. A network of about 900 m of tunnels and drifts is used for various scientific experiments, engineering technological demonstrations, and the testing of industrial solutions for construction and operation (Figure 4.5-2). DOE and ANDRA have a Memorandum of Understanding (MoU) which covers any bilateral research collaboration on clay/shale disposal and use of the LSMHM. This would be in addition to the collaborative work of U.S. and French scientists under the umbrella

of the DECOVALEX Project. As mentioned earlier, ANDRA leads Task A of the current DECOVALEX-2023 phase, with focus on field experiments on thermal and gas fracturing at the Bure URL (Section 3.2.3.1).
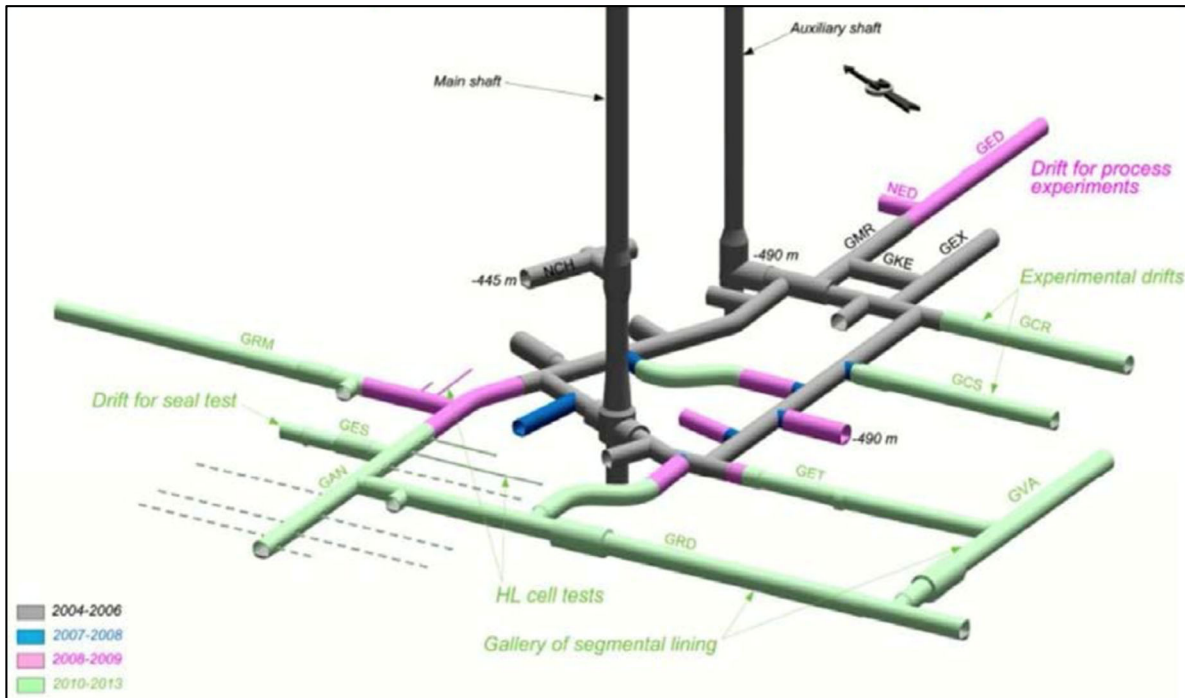
Figure 4.5-1. Layout of the LSMHM URL at Bure, France (Lebon 2011).

Figure 4.5-2. LSMHM URL at Bure, France
(from http://www.andra.fr/download/andra-international- en/document/355VA-B.pdf).

4.6. Collaboration Opportunities with JAEA's URLs in Japan

Opportunities for active collaborative R&D in underground research laboratories in Japan exist at the Horonobe URL in sedimentary rock and at the Mizunami URL in crystalline rock (Figure 4.6-1). Japan and the United States entertain close collaboration on issues related to nuclear energy under the JNEAP (Joint U.S.–Japan Nuclear Energy Action Plan) agreement. JNEAP has a Waste Management Working Group that meets in regular intervals to discuss joint R&D on, among other topics, waste disposal issues. Japanese research institutions are also a frequent partner in many of the cooperative initiatives that DOE has joined in recent years (Section 3, Table 3.1-1), and both nations have collaborated for several years on the DECOVALEX Project. In the current DECVOVALEX-2023 phase, JAEA leads a modeling task related to EBS behavior at the Horonobe URL based on a full-scale *in-situ* experiment (Section 3.2.3.4).
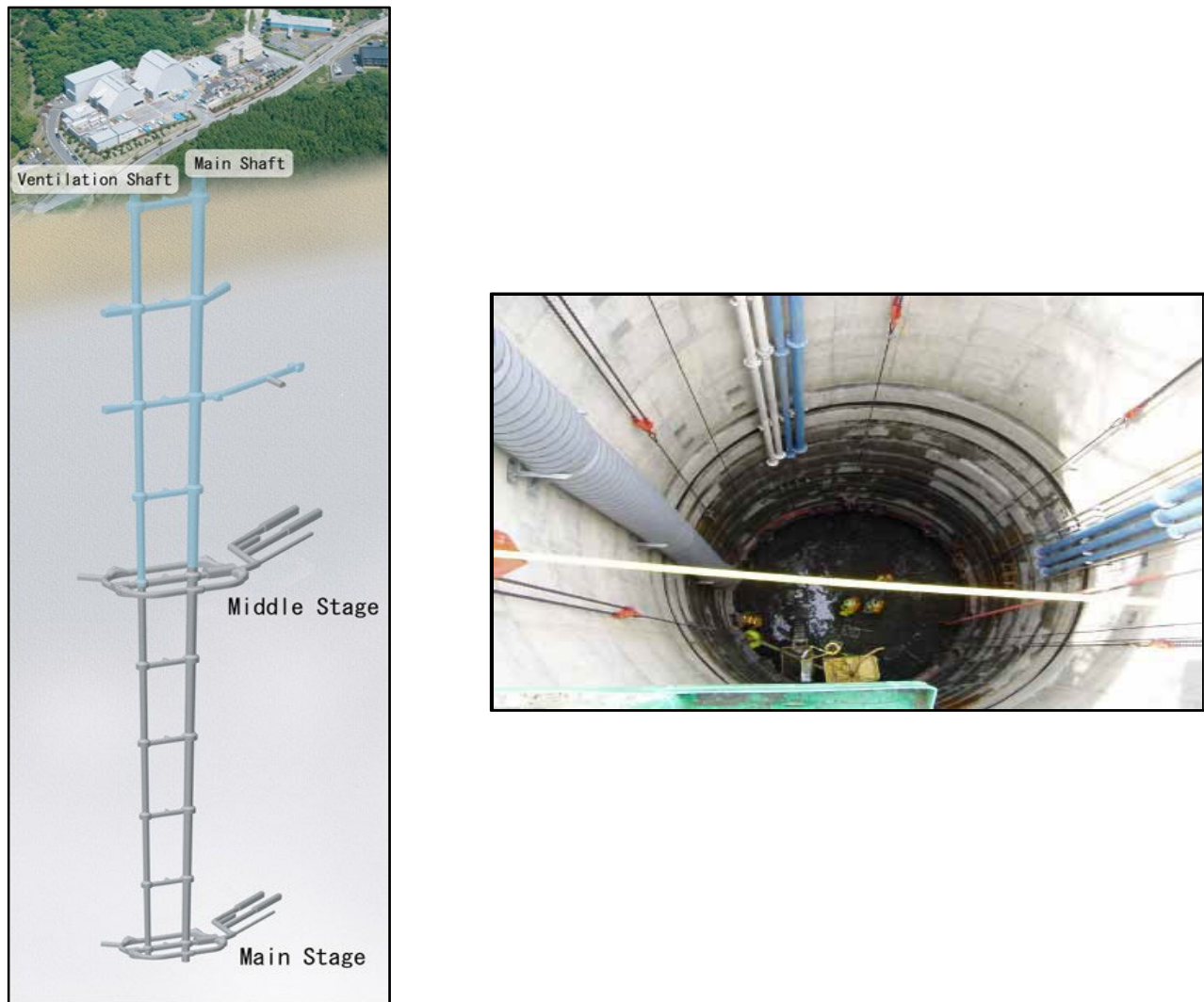
Figure 4.6-1. Layout of the Mizunami Underground Research Laboratory in Japan, and photo of tunnel shaft construction.

4.7. Collaboration Opportunities at HADES URL, Belgium

Belgium is another country with a strong R&D program in geologic disposal and a long history of experimental work in an underground research laboratory. The HADES (High Activity Disposal Experimental Site) URL is located in a secured area belonging to one of Belgium's nuclear power plants, which also hosts other nuclear research facilities. HADES is essentially a several-hundred-meter-long tunnel in the soft Boom Clay rock formation, accessible by two shafts located at each end (Figure 4.7-1). The tunnels were drilled in stages, starting with a first section in 1982, followed by additions in 1987 and 2001. Each of these sections was secured with different types of ground support, reflecting increased knowledge about the structural behavior of the host rock. Most interesting to DOE's program is probably the PRACLAY heater experiment, and, to a lesser degree, the long-term clay diffusion experiments, both of which are discussed in more detail below. The Belgium organizations involved in conducting and interpreting these experiments have long-standing relationships with DOE/SFWD scientists; they are open to participation with SFWD research groups and have already invited researchers to provide THM modeling expertise to the PRACLAY project team. However, there are currently no joint activities related to the HADES URL.
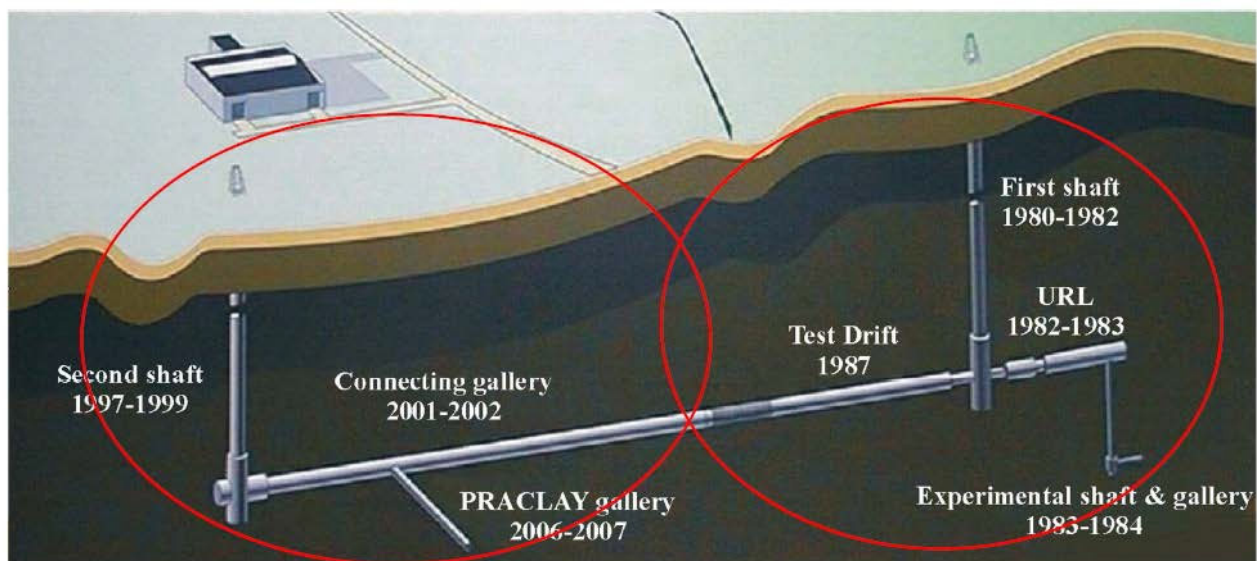
Figure 4.7-1. Layout of the HADES URL in Mol, Belgium (Li 2011).

4.7.1. PRACLAY Test

The PRACLAY Heater Test is a full-scale validation and confirmation experiment conducted at the HADES URL, excavated at 223 m depth in Boom Clay, a tertiary clay formation in Mol, Belgium. The heater test involves a 30 m gallery section to be heated for 10 years with many monitoring sensors (Figures 4.7-2, 4.7-3, and 4.7-4), for the purpose of investigating the thermo-hydro-mechanical (THM) behavior of near-field plastic clay under the most "mechanically critical" conditions that may occur around a repository (Van Marcke and Bastiaens 2010). For plastic clay under the influence of temperature change, these are undrained conditions, which then generate a higher pore-pressure increase and a higher possibility of near-field damage. For this objective, a hydraulic seal has been installed at the intersection between the planned heated and unheated sections of the gallery. The heating phase of the test started in January 2015. Once the heating phase is over (probably around 2024) and the entire experiment has been dismantled, scientists will spend time analyzing all the data and drafting their final conclusions. The results of the PRACLAY experiment will refine existing knowledge about the behavior of the Boom Clay when subjected to heat. The main objective is to confirm that heating does not impair the clay's ability to physically contain the radioactive waste. It is therefore a crucial step in the process of developing and implementing a repository in soft clay rock.
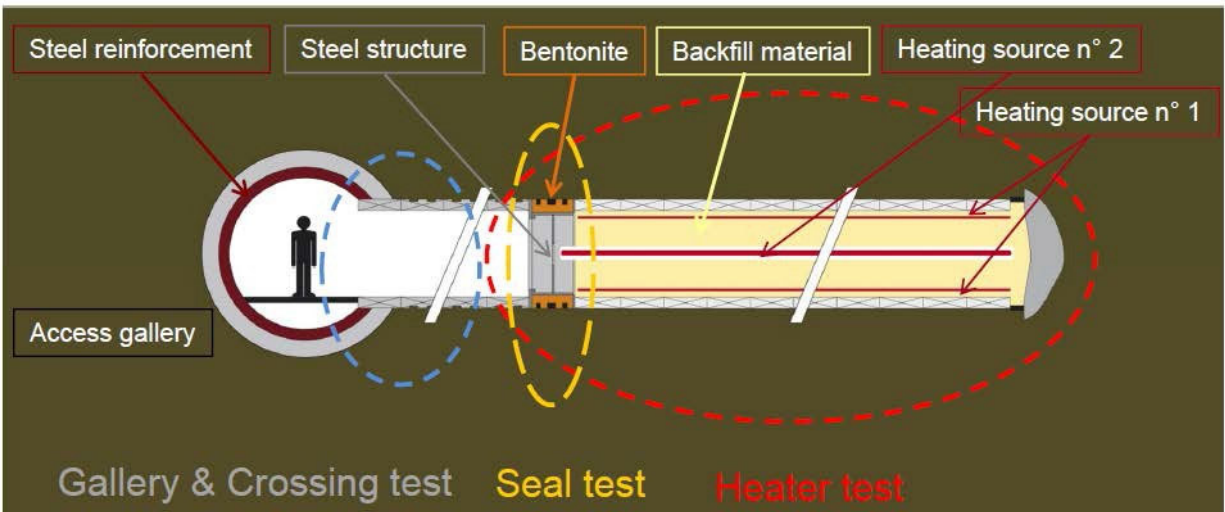
Figure 4.7-2. Layout of the PRACLAY *in-situ* experiment at HADES URL (Li 2011).
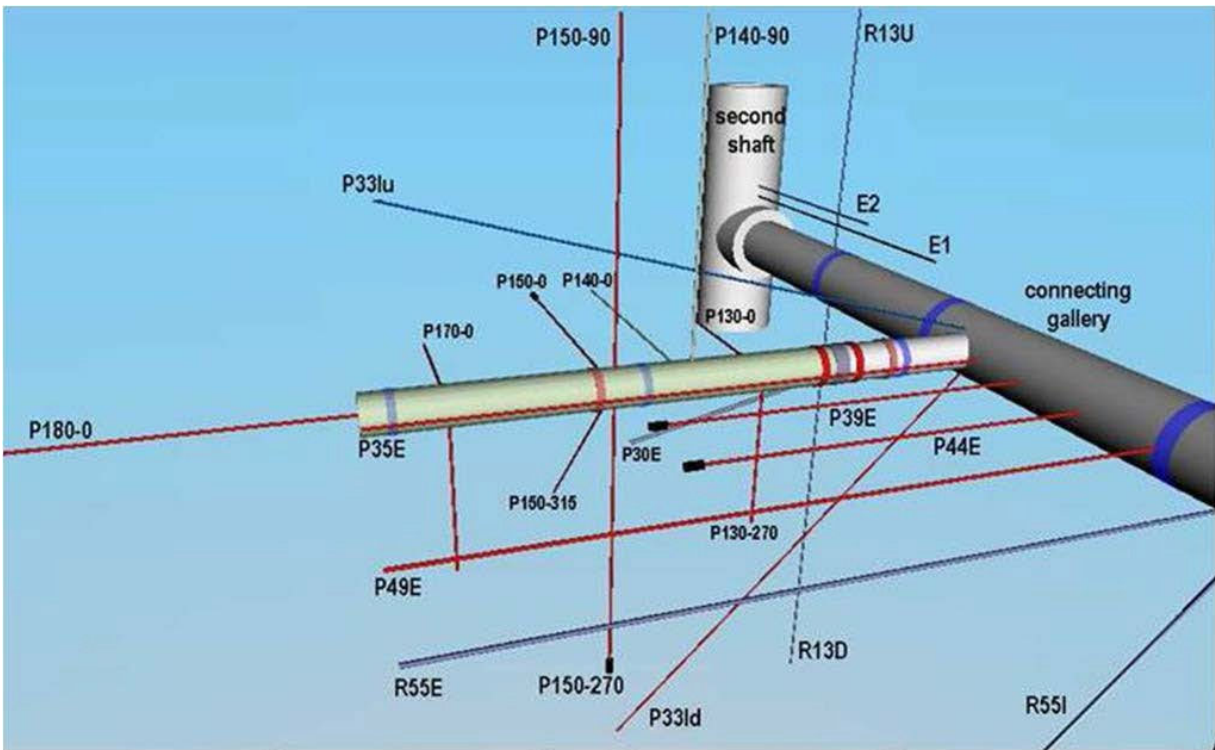
Figure 4.7-3. PRACLAY *in-situ* experiment at HADES URL: Configuration of boreholes for pressure, stress, displacement, and water chemistry measurements (Li, 2011).
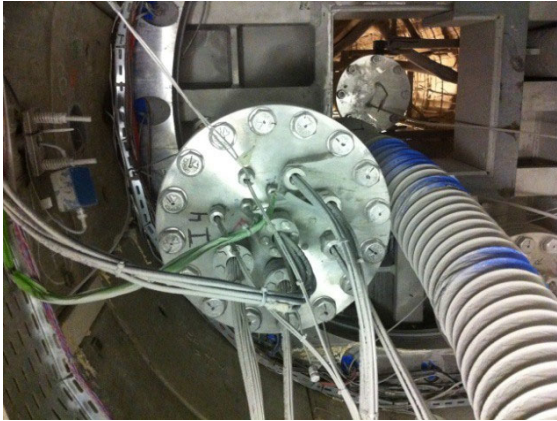
Figure 4.7-4. PRACLAY *in-situ* experiment at HADES URL: Photo on left shows hydraulic seal from the outside, with an access hole to the right, which soon will be closed. Photo on right was taken from access hole into the heater gallery section, which is currently being backfilled.

4.7.2. Radionuclide Migration Experiments

The Belgium waste management program has been conducting a suite of long-term radionuclide migration *in-situ* experiments in dense clays at their HADES URL near Mol. Two of these experiments, named CP1 (Figure 4.7-5) and Tribicarb-3D, have been ongoing for decades and offer valuable data on the slow diffusion-controlled migration of radionuclides in clay rock. Because of their duration, they offer unique test cases for model and process validation. Recently, two other ongoing large-scale migration experiments were initiated at HADES. The TRANCOM test involves colloid transport with C-14 labeled humic substances. The RESEAL shaft seal experiment investigates transport of iodine-125 through the disturbed zone and the interface between Boom Clay and bentonite.
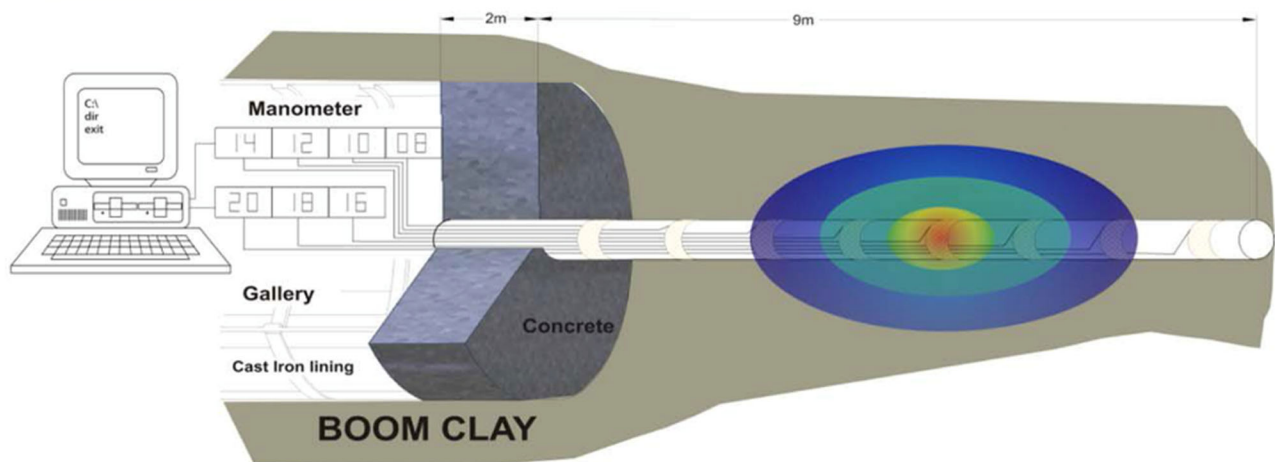
Figure 4.7-5. Schematic of CP1 Diffusion Experiment at HADES URL (Maes et al., 2011).

4.8. Collaboration Opportunities at Onkalo URL, Finland

The Onkalo URL in Finland is located at a site chosen to co-host a geologic repository. Thus, it is not only an underground research laboratory, but also an underground characterization and waste disposal facility. The URL is constructed in crystalline bedrock to the anticipated repository depth of 430–440 m. Construction began in 2004 and is ongoing, but actual underground tests were already started in 2007. Figure 4.8-1 shows the layout of the URL, with an access tunnel and three shafts. The access tunnel takes the form of a spiral on an

approximately 1 in 10 incline downward, and reaches the technical facilities level at about 437 m. The three shafts consist of one personnel shaft and two ventilation shafts. Details may be found in Posiva (2011) and Aalto et al. (2009). There are currently no direct bilateral research activities between DOE and the Finnish waste management program related to the Onkalo URL. However, in past years researchers from both countries have been participating in the modeling interpretation of the REPRO diffusion experiment at Onkalo, which was a modeling task conducted under the umbrella of the SKB GWFTS Task Force (see Section 3.4.2.1).
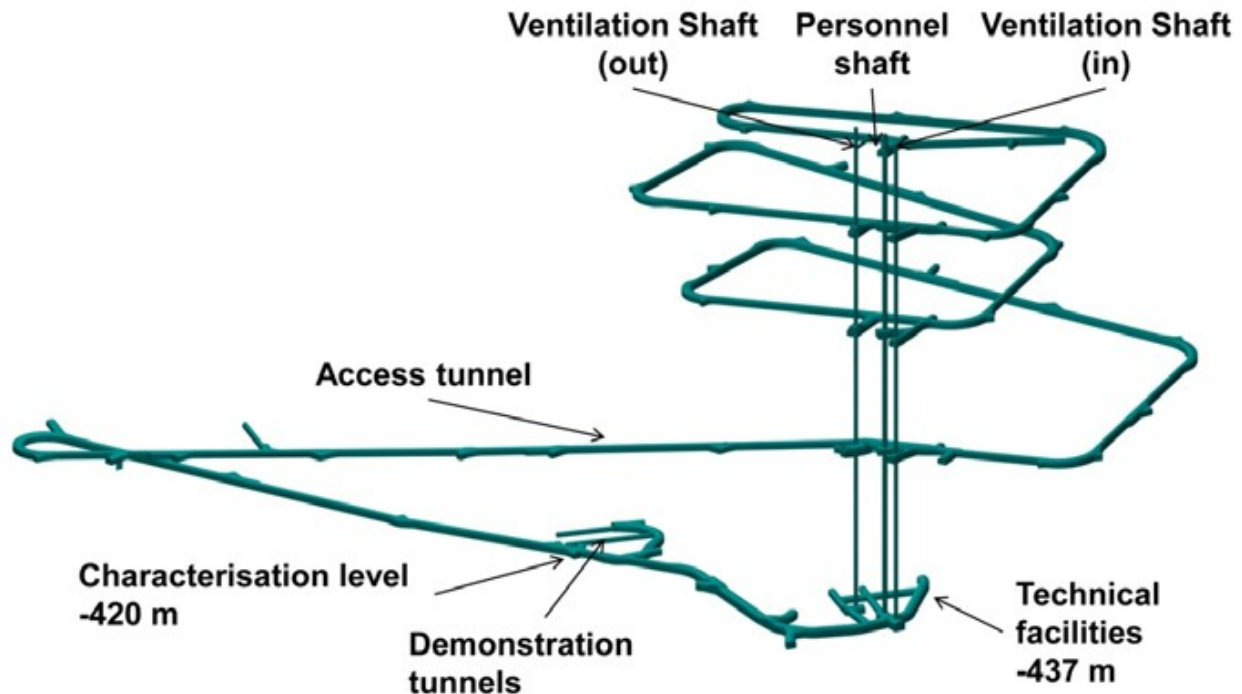
Figure 4.8-1. Layout of the Onkalo URL in Finland (Äikäs 2011).

4.9. Collaboration Opportunities at Bukov URL, Czech Republic

SÚRAO, the radioactive waste management authority of the Czech Republic, has an ambitious geologic disposal program focusing on the nation's granitic host rock environments. Czech researchers working on disposal issues are well connected international; SÚRAO has been a member of DECOVALEX for several years and is also a partner in FEBEX-DP, the HotBENT Project, and the SKB's task forces.

About a decade ago, SÚRAO identified the Bukov Underground Research Facility (URF), located at a depth of 550 meters below the surface, as an ideal site for the research and evaluation of the geological environment as part of the deep geological repository development program. As with similar facilities of its type, it makes use of a pre-existing underground mine infrastructure, namely the former Rožná I uranium mine. The underground areas of the URF are located on the 12th level close to the B-1 shaft and are made up of a system of crosscuts, drifts and experimental niches (Figure 4.9-1). Construction started in 2013 and was finished in 2017, followed by a site characterization phase (2015 through 2017). The construction phase included the use of various technological methods and mine working dimensions in such a way that the testing of different solutions in different geological environments helped to determine the final design. SÚRAO has now embarked on a comprehensive experimental phase at Bukov. The experimental program is divided into the following topical areas:

- Geological characterization

- Testing of long-term monitoring methods

- Testing groundwater flow and radionuclide transport models

- Testing of engineered barriers

- Testing of the origin and development of the of the damaged zone in the vicinity of an underground working

- Testing of technological procedures for the construction of underground working

- Demonstration experiments

SÚRAO is actively reaching out to the international community for potential partnerships as the experimental research program in the URL is being executed over the next years and decades.

Figure 4.9-1. Impression from the URF research galleries in the Bukov URF.

4.10. Collaboration Opportunities with Planned URL in China

As a major nuclear nation with a long-standing geological disposal program, China has embarked on an ambitious plan to develop area-specific underground research laboratories in representative rock formations (Wang, 2014). China is moving swiftly with URL site selection and characterization plans; the current idea is that the country would focus on a granite site first, followed by a clay formation. The granite formations in the Beishan area, located in northwestern China's Gansu Province, have been selected as the most suitable area for a high-level waste repository in China. This is based on an abundance of favorable host rock geologies, with eight large granite intrusions identified as suitable subareas. The Beishan area has other advantages as well: the region has favorable socio-economical and natural conditions, characterized by extremely sparse population, no useful farm land, lack of mineral resources, and generally poor economic potential. At the same time, Beishan can be easily reached with convenient transportation options. In terms of potential clay sites, China focuses on two regions of potential interest. These are the Tamusu and the Suhongtu regions within the Bayingebi Basin, located in the Inner Mongolia region. China's geological disposal program is managed by

the Beijing Research Institute of Uranium Geology (BRIUG), which is open to international cooperation. In fact, with the IAEA coordinating, BRIUG over the past decade has closely worked with several countries, including the U.S., for technical guidance and practical advice related to their URL program, for example related to on early siting criteria, site selection approaches, and specific site characterization techniques.

In 2021, China started construction of its first underground research laboratory in the Beishan area. According to the current design, the URL will have a large expandable research space at two main working levels (240 m and 540 m below surface), accessed by a ramp and a personnel shaft (Figure 4.10-1). Research to be conducted will include site characterization activities, testing of engineering technologies and engineered barriers, and safety assessment activities such as monitoring of radionuclide release and migration behaviour. It is expected that underground *in-situ* testing will take place until 2050. The final stage – the construction of the disposal facility – is planned to take place from 2041 to 2050, assuming the *in-situ* testing confirms the area's suitability (Carter and Nieder-Westermann, 2021).
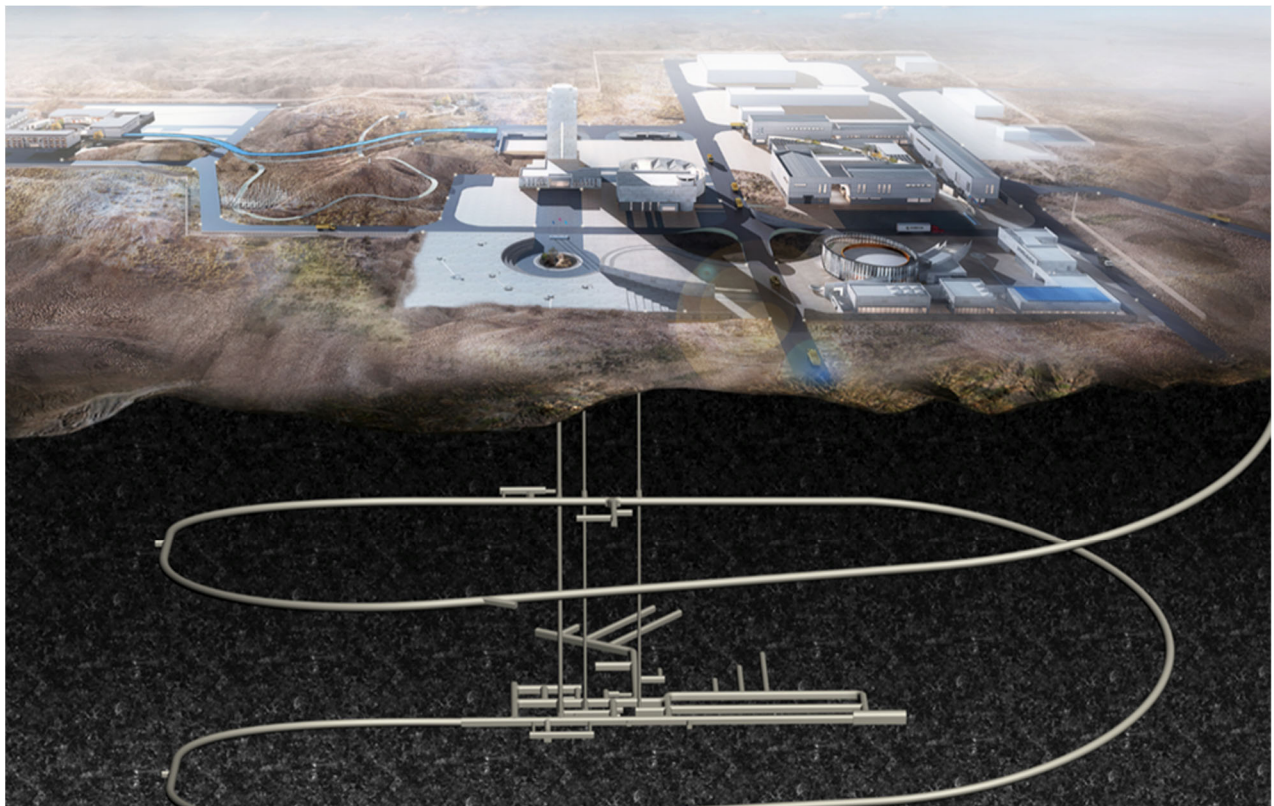
Figure 4.10-1. Design of the planned URL in Beishan, China (Carter and Nieder-Westermann, 2021).

5. SELECTION AND RE-EVALUATION OF INTERNATIONAL COLLABORATION TASKS

5.1. Collaboration Planning and Re-Evaluation

Starting in 2012 with an emphasis on international collaboration, DOE became a formal partner in several multinational initiatives that promote active joint research, often with specific focus on URL field experiments and related data: the DECOVALEX project, the Mont Terri Project, the Colloid Formation and Migration Project (until July 2015), the FEBEX-DP Project, the SKB Task Forces and recently the HotBENT Project. As a result, SFWD researchers have been in a position for several years now that allows for participation in planning, conducting, and interpreting the many past and ongoing field experiments associated with these initiatives, and they do so in close collaborative partnership with international scientists. DOE also reached out to—and explored options of collaboration with—individual international disposal programs, such as from the Republic of Korea, Germany, France, Japan, Belgium, Sweden, Israel, Czech Republic, and Finland (Section 4), which have led to several bilateral joint R&D.

In FY12, when SFWD made the decision to focus on active international collaboration as a strategic emphasis for DOE's disposal research, the campaign first developed a set of guiding principles for selection of collaboration options and activities, as follows:

- Focus on activities that complement ongoing disposal R&D within SFWD (e.g., the science and engineering tools developed in SFWD are tested in comparison with international experiments) and that align with goals, priorities, and funded plans of the SFWD program.

- Select collaborative R&D activities based on technical merit, relevance to safety case, and cost/benefit, and strive for balance in terms of host rock focus and repository design.

- Emphasize collaboration that provides access to and/or allows participation in field experiments conducted in operating underground research laboratories not currently available in the U.S. (i.e., clay, crystalline).

- Focus on collaboration opportunities for active R&D participation (i.e., U.S. researchers work closely together with international scientists on specific R&D projects relevant to both sides).

Starting from these principles, the campaign initiated a planning exercise to identify the most relevant and promising international opportunities, and to select and develop a set of activities that align with the goals, priorities, and funding plans of the SFWD. In a general sense, the benefits of international collaboration are obvious: SFWD can gain substantial value from the knowledge, data, and modeling capabilities that international partners have developed over decades of research. In terms of specific activities, however, the benefit of international collaboration needs to be evaluated in the context of the open R&D issues that can be addressed through collaborative scientific activities. The SFWD campaign had identified such open R&D issues in several planning exercises, as summarized for example in Wang (2010) and Jové-Colón et al. (2010), and in a roadmap exercise prioritized them by importance to the safety case (Nutt, 2011, Tables 7 and 8).

As part of the initial planning exercise, SFWD management and scientists developed a comprehensive table of international opportunities to provide a basis for selection of international activities. The table listed the most relevant ongoing or planned field experiments conducted in international URLs, provided information on how SFWD participation can be achieved, which research areas would be the main benefactor (generally either the Engineered barrier System, EBS, or Natural Barrier System, EBS), the key FEPs addressed (including a link to roadmap and FEPs importance ranking; using the Used Fuel Disposition Campaign Disposal Research and Development Roadmap, FCRD-USED-2011-000065 Rev 0, March 2011 [Nutt 2011]), and finally information on the experimental schedules. Detailed planning of an initial set of international activities was then conducted in three workshops held in FY11 and FY12. The objectives of these workshops were (1) to inform DOE leadership and SFWD scientists about existing or future international opportunities, and (2) to align SFWD work package activities with opportunities for international collaboration. The first workshop was a session held in conjunction with the SFWD Working Group Meeting in Las Vegas in July 2011, at this point mostly

for informative purposes. The second workshop, held in Las Vegas in April 2012, was a full-day meeting to review the current and planned work scope within SFWD work packages for possible leveraging with the international programs, and to develop an initial set of R&D activities that align with goals, priorities, and funded plans of the SFWD program. A third workshop was held in conjunction with the SFWD Working Group Meeting in Las Vegas in May 2012, to inform SFWD researchers about the outcome of the full-day planning workshop, to present them with the collaboration options, and to initiate active R&D participation.

As research priorities changed over the years and new opportunities for collaboration have emerged, SFWD's international research portfolio evolved and it will continue to evolve in the future. Therefore, SFWD has made a targeted effort to re-evaluate its international collaboration activities, in a process similar to the initial planning phase in 2012. Planning sessions were held in conjunction with the SFWD Working Group Meetings in Las Vegas in June 2015, June 2016, May 2017, May 2018, May 2019 and May 2021 (the meeting in 2020 was canceled due to Covid-19 restrictions) to review existing and emerging opportunities for international collaboration, evaluate their technical merit and cost/benefit ratio, to align these opportunities with the current and planned work scope within SFWD work packages for possible leveraging, and to develop a revised portfolio of international R&D activities that align with goals, priorities, and funded plans of the SFWD program. For example, as a result of this process, SFWD decided in FY15 to end its participation in the CFM Project because of its relatively narrow focus and relatively high participatory cost.

In FY18 and FY19, the SFWD campaign initiated a detailed re-planning effort to ensure that all disposal research activities were aligned with and of high relevance to the safety case. Starting at the SFWD Working Group Meetings in Las Vegas in May 2018 and continued/finalized at a dedicated R&D Roadmap Update Workshop in Las Vegas in January 2019, all ongoing and planned research activities were discussed in the context of their priority score, which in turn was evaluated by answering two important questions: (1) how important is the knowledge gained from a given research activity in terms of the three safety case elements (pre-closure safety analysis, post-closure safety assessment, confidence enhancement) and its technical basis, and (2) what is the state of the art level that the research activity would support (in other words, a given research activity would be most important when it addresses fundamental gaps in methods or data). The former was measured with the so-called ISC score (Importance to Safety Case), ranging from low importance (ISC = 1) to high importance (ISC = 5). The latter was evaluated using the so-called SAL score (State of the Art Level), ranging from well understood (SAL = 1) to fundamental knowledge gaps (SAL = 5). Priorities were then assigned by a score matrix that combined both scores, with the highest priorities assigned to research activities that were both important to the safety case and still had fundamental knowledge gaps. Detailed results from this roadmap update are given in the report by Sevougian at el. (2019), which summarizes the progress of ongoing disposal R&D activities since 2012, re-evaluates R&D priorities for all existing activities, and identifies new activities of high priority.

International collaboration activities, and their integration with other generic research tasks, were included in this broad activity-based priority assessment conducted in 2018. In addition to reviewing the benefits of ongoing activities, the participating experts evaluated several new international collaboration opportunities, e.g., the new tasks proposed for the upcoming DECOVALEX-2023 phase, and some planned Mont Terri, Grimsel Test Site, or SKB experiments. Priority scoring considered emerging R&D needs recognized by the international community (e.g., the issue of gas pressure buildup in response to gas generation from corrosion) or emerging priorities in the SFWD campaign, such as R&D on disposal of dual-purpose canisters (DPCs) which now contain a significant fraction of the Nation's commercial spent fuel activity. The resulting expert scores for international activities are given in Table 5.1-1 below, categorized into "high-priority," "high- to medium priority," and "medium priority" (Sevougian et al., 2019). As shown in the table, the highest-scoring items include research activities on high-temperature impacts in bentonite and clay, gas generation and transport, fault slip and development of flow paths, and coupled processes in salt. None of the international activities, current or planned, scored lower than "medium." The SFWD campaign has since refined its international portfolio based on the prioritization provided in Sevougian et al. (2019) and it will continue to do so in the future. It should be noted that though much has been accomplished since 2012, through R&D in the U.S. and through international collaborations, the 2019 R&D Roadmap Update reflects the need for continuing R&D on many of the 2012 R&D Issues, plus some obvious new priorities.

Table 5.1-1. Priority scores for international activities based on 2019 R&D Roadmap (Sevougian et al., 2019)

High Priority	
I-04	Experiment of bentonite EBS under high temperature, HotBENT
I-06	Mont Terri FS Fault Slip Experiment
I-08	DECOVALEX-2019 Task A: Advective gas flow in bentonite
I-12	TH and THM Processes in Salt: German-US Collaborations (WEIMOS)
I-13	TH and THM Processes in Salt: German-US Collaborations (BENVASIM)
I-16	New Activity: DECOVALEX Task on Salt Heater Test & Coupled Modeling
I-18	New Activity: DECOVALEX Tasks on Large-Scale Gas Transport

Medium-High Priority	
I-02	FEBEX-DP Modeling: Dismantling phase of the long-term FEBEX heater test - Modeling
I-03	FEBEX-DP Experimental Work: Dismantling phase of the long-term FEBEX heater test
I-07	DECOVALEX-2019 Task E: Upscaling of modeling results from small scale to one-to-one scale based in heater test data in Callovo-Oxfordian claystone (COx) at MHM underground research laboratory in France.
I-09	DECOVALEX-2019 Task C: GREET (Groundwater REcovery Experiment in Tunnel) at Mizunami URL, Japan
I-14	TH & THM Processes in Reconsolidating Salt: KOMPASS
I-21	New Activity: SKB Task 10 Validation of DFN Modeling

Medium Priority	
I-01	Radionuclide Transport as Pseudocolloids, Grimsel
I-05	Mont Terri FE (Full-scale Emplacement) Experiment
I-10	SKB GWFTS Task Force: Long-term Diffusion Experiment LTDE-SD at the Äspö HRL
I-11	Microbial Processes Affecting Hydrogen Generation/Uptake: FEBEX-DP and Mont Terri Studies
I-15	Geotechnical Barriers in Salt: RANGERS
I-17	New Activity: DECOVALEX Task on GDSA, PA, SA, UQ
I-19	New Activity: DECOVALEX Task on Thermal Fracturing
I-20	New Activity: Planned Mont Terri Task on Gas Transport (GT) in Host Rock

In FY20, the DOE requested development of a formal plan for activities in the SFWD disposal research portfolio over a five-year period. SFWD campaign leadership then worked across several control accounts to discuss the five-year direction of the campaign and developed a report that serves as a strategic guide to the work within the disposal research R&D technical areas (i.e., the control accounts), focusing on the highest priority technical thrusts (Sassani et al., 2020). The five-year plan, and its FY21 update (Sassani et al., 2021), distinguishes the near-term (i.e., the more certain 1- to 2-year) timeframe) and the longer term (less certain 3- to 5-year) timeframe. The near-term emphasis can be viewed as a representation of the present R&D portfolio with modest modifications that reflect emerging priorities and funding levels. In contrast, the 3- to 5-year period represents a longer-term vision of where the SFWD disposal research portfolio is heading provided there is no major external change to the program direction. According to this plan, international collaboration will remain an important cross-cutting campaign activity over the next five years, in particular with regards to opportunities involving *in-situ* experiments in underground research laboratories across a range of geologic systems. Below is a short synopsis of the 1-2 year and 3-5year planning elements defined for international collaborations in disposal research (Sassani et al., 2020; 2021).

Near-Term Topics (Next 1- to 2-year period)

- *Continue participation within international R&D in underground research laboratories for a range of geologic systems*

  As mentioned above, the current international research portfolio, which spans across several technical areas including Engineered Barrier System R&D, Argillite Disposal R&D, Crystalline Disposal R&D, Salt Disposal R&D, and Geologic Disposal Safety Assessment, has been re-evaluated and re-

prioritized in 2019 as part of a broad activity-based priority assessment across the campaign (Sevougian at el., 2019). As such, the five-year plan suggests that this revised portfolio will remain largely intact over the next two years or more. The current key activities either involve long-term *in-situ* experiments that will continue for years to come (e.g., the full-scale FE Heater Test at Mont Terri, the recent fracture network modeling task related to the SKB Task Forces), or they are multi-year collaborations that have recently been initiated based on the revised 2019 roadmap (e.g., the HotBENT experiment at Grimsel Test Site, or the new collaborative tasks defined in the DECOVALEX-2023 Project).

- *Continue assessment of new international opportunities*

Ongoing evaluation of existing and emerging opportunities for international collaboration is a key responsibility of the international collaborations control account. The campaign will continue to review, assess, and develop such opportunities in close integration with international partners, will evaluate technical merit and alignment with the SFWD objectives, and will make revisions to the portfolio of international R&D activities as appropriate. This FY21 International Collaboration Status report mentions several new opportunities for international collaboration which the campaign may consider going forward, such as additional field experiments addressing gas transport in engineered and natural barriers (such as the GT Experiment in Section 3.1.5.2 and the GAST in Section 3.3.4.1), additional diffusion studies (such as the DR-C Experiment in Section 3.1.5.3), studies with focus on microbial processes (see MA-A Experiment in Section 3.1.5.1), experiments testing sealing elements for tunnels, shafts and boreholes (see SW-A Experiment in Section 3.1.5.4 and SET in Section 3.3.4.2), bentonite degradation and erosion experiments (see I-BET in Section 3.3.1.1), and corrosion studies (see MACOTE in Section 3.3.4.3). See a summary description of such opportunities and their current status in Table 5.1-2 below.

- *Contribute to integration and confidence building for Generic Disposal System Analysis (GDSA)*

The international research activities, with their focus on modeling and comparative analysis for complex *in-situ* experiments, ultimately lead to better predictive models and thus directly contribute to confidence building for post-closure performance assessments (PA) models. In the SFWD campaign, the work packages for international collaboration, for generic research on EBS and host-rock specific topics, and for GDSA need to be well integrated to make optimal use of improved process models leading to better safety assessments models. The international technical area can contribute to this goal. Confidence in PA models can also be enhanced by comparing PA methods to international standards, or by benchmarking PA studies against international data sets. Under leadership of SFWD scientists, the new performance assessment task in DECOVALEX-2023 compares PA methodologies for generic salt and generic crystalline repositories across multiple international disposal programs (Section 3.2.3.6).

Longer-Term Topics (Next 3- to 5-year period)

International collaboration will continue to be a central element of SFWD Campaign's disposal R&D over the next five years and beyond. And as research priorities change and new opportunities for collaboration present themselves, the international research portfolio will be re-prioritized as appropriate. Many of the two-year themes discussed above will continue to drive the campaign planning. In addition, depending on the direction of the campaign and the progress made, international collaboration could be expanded to in several ways to serve other objectives. Here are two examples:

- *Develop best practices and technologies for site selection and characterization*

The current campaign focus in disposal research is to (1) provide a sound technical basis for multiple viable disposal options in the U.S., (2) to assess suitability and geographic distribution of host rock types, (3) to increase confidence in the robustness of generic disposal concepts, and (4) to develop the science and engineering tools needed to support disposal concept implementation. As the campaign evolves, a suitable goal for international collaboration may be to support site characterization for site

screening and site selection, via engagement with countries that currently go through such efforts at varying execution stages: Germany for example is in the early stages of a comprehensive site selection effort considering a broad range of host rocks (Section 4.2). Other countries are currently in a down selection process from multiple possible sites to one (e.g., Switzerland or Canada). And a few countries have already selected a repository site and are undergoing detailed characterization (e.g., Sweden). At a minimum, international collaboration would involve close observation and information exchanges, to gain a better understanding of best practices for different host rocks and different site selection stages. On the technology side, the campaign could be actively embedded in ongoing international site characterization efforts, for example, via joint development and testing of surface- and borehole-based characterization tools. SFWD's international collaborations with the Swedish COSC program are a good example of joint research efforts on site characterization methods that benefit both partners (Section 6.8).

- *Utilize international activities for training/education of junior staff*

International collaboration has provided extremely valuable data sets from underground testing that are not only relevant to the SFWD's campaign R&D objectives but also provide for complex scientific challenges of high interest to young researchers. The campaign could make a dedicated effort to use international collaboration activities as an opportunity to recruit and train early-career scientists to become the next-generation workforce for disposal research in the U.S. SFWD scientists recently developed a concept paper for a pilot program at LBNL and SNL that would attract a broad talent pool by providing interesting learning/research challenges and attractive work-abroad opportunities in conjunction with SFWST's multiple international collaboration partners (Birkholzer et al., 2021).

Table 5.1-2. Summary descriptions of selected international collaboration opportunities related to field experiments in URLs that should be considered by the SFWD campaign in future prioritization efforts.

Research Theme	Name	Description	Status
Gas Migration	GT	Gas migration in clay-rich host rock, lab and field tests at Mont Terri URL. Section 3.1.5.2.	Field gas injections to start in late 2021 or early 2022.
Gas Migration	GAST	Performance of bentonite-sand mixtures for increased gas permeability. Grimsel Test Site, Section 3.3.4.1.	Hydration is ending. Gas injections to start in early 2022.
RN Diffusion	DR-C	Planned experiment at Mont Terri URL to understand diffusion behavior in Opalinus Clay in the presence of a thermal gradient. Section 3.1.5.3.	Test is being installed right now. Injection of RN tracer cocktail planned for late 2022.
Microbial Processes	MA-A	Characterization of microbial communities in the pore water of the Opalinus Clay. At Mont Terri URL. Section 3.1.5.1.	Ongoing experiment.
Sealing Elements	SW-A	Field testing of a novel multilayer seal for shafts at Mont Terri URL. Section 3.1.5.4.	Installation is done, hydration of seals is ongoing. Testing of seals expected in 2022.
Sealing Elements	SET	Field test at Grimsel Test Site to evaluate performance of borehole seals in repositories. Section 3.3.4.2.	Installation and bentonite saturation in 2022. Hydraulic testing in 2023.
Bentonite Erosion	i-BET	Field test at Grimsel Test Site to study erosion of bentonite and impact on colloid transport. Section 3.3.1.3.	Installed in 2019. Ongoing right now. Overcoring is envisioned for late 2022 or early 2023.
Material corrosion	MACOTE	Ongoing *in-situ* experiment at Grimsel Test Site testing canister materials embedded in heated and unheated bentonite. Section 3.3.4.3.	Project Phase 2 is ongoing. Short-term samples have been retrieved and tested. Long-term samples remain in place for removal in 2023.

The five-year plan in Sassani et al. (2020; 2021) also calls for DOE to consider moving from a mostly participatory role in ongoing *in-situ* experiments conducted by other nations to a more active role in conducting its own experimental program in international URLs. The advantage of active planning is obviously that the experimental focus and design can be better tailored to the campaign needs. While there are no immediate plans for DOE to conduct its own experiments in international URLs of opportunity, SFWD's disposal program has already started taking a much more active approach in shaping the future R&D portfolio of the international initiatives it has joined as a partner. For example, with Jens Birkholzer of LBNL now the Chairman of the DECOVALEX-2019 Project, SFWD scientists have been very influential in the project's task selection for DECOVALEX-2023, and are now leading two of the new modeling tasks, one focusing on the BATS heater test at WIPP and one comparing different performance assessment approaches (see Sections 3.2.3.5 and 3.2.3.6, respectively). SFWD researchers are also leading a new modeling task in the SKB EBS Task Force, which at its center has a high-temperature column experiment conducted at LBNL (Section 3.4.3.5). In addition, DOE has co-developed with international partners the planning and design of the HotBENT Project, the full-scale high-temperature heater experiment planned at the Grimsel Test Site (Section 3.3.3.1).

More such active collaborations can be considered in the future. It should be pointed out in this context that collaborative initiatives like the Mont Terri Project or the Grimsel Test Site definitely provide the opportunity for any of the partners, such as DOE, to conduct their own experimental projects if that is desired in the future. The existing infrastructure in these URLs developing and conducting experiments very easy, even if the proposing partner is located far away from the URL. At Mont Terri for example, swisstopo can handle many of the organizational details if needed, and there is a long list of experienced contractors that are available to conduct the actual experimental work. Community URLs like Mont Terri or Grimsel Test Site allow the U.S. disposal program to perform *in-situ* fieldwork in representative host rocks, even though there are currently no operating underground research laboratories in clay or crystalline host rock environments in the U.S.

We note that the U.S. Nuclear Waste Technical Review Board (NWTRB recently released a report to the U.S. Congress and the Department of Energy entitled "Six Overarching Recommendations for How to Move the Nation's Nuclear Waste Management Program Forward" (NWTRB, 2021). One of the six recommendations is to continue and expand engagement with the international community, and in particular to sustain active engagement in international programs given the tangible benefits derived from close involvement. The Board also recommended to continue and expand participation in collaborative international URL activities, which is at the center of DOE's international collaboration activities in disposal research. On a related note, the NWTRB report suggests to establish one or more dedicated domestic URLs that will provide the necessary opportunities for researchers and students to conduct *in-situ* investigations into subsurface processes at scale, test models, and advance international collaboration. The Board recognizes that if DOE develops one or more domestic URLs, it should encourage international participation, which could benefit the DOE program by incorporating broader perspectives and expertise.

5.2. Overview of International Collaboration Portfolio

Today, more than nine years after its initiation, the international disposal program within SFWD has established a balanced portfolio of selected collaborative R&D activities in disposal science, addressing relevant R&D challenges and open research questions as follows:

- **Engineered Barrier Integrity**: What is the long-term stability and retention capability of backfills and seals? Can bentonite be eroded when in contact with water from flowing fractures? How relevant are interactions between engineered and natural barrier materials, such as metal-bentonite-cement interactions? Is gas pressure increase and gas migration a concern for barrier integrity?

- **Near-Field Perturbation**: How important are thermal, mechanical, and other perturbations to a host rock (such as clay and salt), and how effective is healing or sealing of the damage zone in the long term? How reliable are existing predictive models for the strongly coupled thermal-hydrological-mechanical behavior of clays and salts?

- **Flow and Radionuclide Transport**: What is the effect of high temperature on the diffusion and sorption characteristics of clays (i.e., considering the heat load from dual-purpose canisters)? What is the potential for enhanced transport with colloids? Can transport in diffusion dominated (clays, bentonites) and advection dominated systems (fractured granites) be predicted with confidence?

- **Integrated System Behavior and Performance Assessment**: Can the early-time behavior of an entire repository system, including all engineered and natural barriers and their interaction, be measured and demonstrated? Can this integrated behavior be reliably predicted? Are the planned construction and emplacement methods feasible? Which monitoring methods are suitable for performance confirmation? How reliable are performance assessment models?

Figure 5.2-1 gives a visual overview of the major international experiments conducted in various countries that SFWD researchers have participated in since 2012, either as active members of the experimental team, or as researchers involved in the interpretative evaluation and model interpretation of the experimental data (see list of experiments in Table 5.2-1). Experiments in bold denote currently active collaborations. The figure tries to graphically illustrate the balance and focus of SFWD's international program over the past years. There are a few notable observations:

- Going from the center outward, one can see that SFWD's research is well balanced between EBS focus, near-field focus and far-field emphasis.

- Several experiments address at the same time EBS behavior and near-field processes, which comes as no surprise because *in-situ* experiments in URL tunnels by design have near-field host rock impact even if the main emphasis may be on the engineered barrier behavior.

- There are many activities related to argillite and crystalline host rock, whereas less international work has been conducted for salt. This can be explained by the U.S. program having its own salt URL in the bedded salts at the Waste Isolation Pilot Plant (WIPP) in New Mexico, so there is less need for international research outside of the U.S.

- The topic of "Integrated System Behavior" features only one experiment with SFWD participation, the Full-Scale Emplacement Experiment (or FE Heater Test) as a demonstration experiment. Given the current status of the U.S. disposal program where R&D is currently generic (i.e., not site-specific) it does make sense to place less emphasis on demonstration experiments.

Figure 5.2-1: High-level overview of the major international URL experiments conducted in various countries that SFWD researchers have participated in since 2012. Experiments in bold denote currently active collaborations. See Table 5.2-1 for more information on each experiment. Status: September 2021.

Table 5.2-1. High-level overview of the major international URL experiments conducted in various countries that SFWD researchers have participated in since 2012. Experiments in bold denote currently active collaborations. Acronyms are explained in the list of Acronyms/Institutions on page xxx. Status: September 2021.

Key Topics	International Experiment	URL	Main R&D Focus
Engineered Barrier Integrity	**Cement Clay Interaction (CI) Experiment**	**Mont Terri, Switzerland**	**Chemical interaction between host rock and engineered barrier materials**
	Bentonite–Rock Interaction Experiment (BRIE)	Äspö HRL, Sweden	Understand the impact of flowing fractures in crystalline rock on bentonite saturation, integrity and erosion
	Engineered Barrier System (EBS) Experiment	**Horonobe, Japan**	**Studies of the thermo-hydro-mechanical-chemical (THMC) behavior of the EBS**
	Full-Scale Engineered Barrier Experiment - Dismantling Project (FEBEX-DP)	**Grimsel Test Site, Switzerland**	**Dismantling and sampling of long-term test evaluating the long-term integrity and performance of heated bentonite**
	HotBENT Experiment	**Grimsel Test Site, Switzerland**	**Complex THMC behavior of EBS materials up to 200 degrees C at the canister/bentonite interface**
	Large-scale Gas Injection Test (LASGIT)	**Äspö HRL, Sweden**	***In situ monitoring of gas migration processes in bentonite buffer***
Near-Field Perturbation	Heater Experiment E (HE-E)	Mont Terri, Switzerland	Bentonite/rock interaction to evaluate sealing and clay barrier performance at elevated temperature, micro-tunnel
	Thermal Experiment (TED) Full-scale Emplacement Test (ALC)	Bure, France	Upscaling THM simulations from lab tests to repository scale
	Gas Path Though Host Rock Experiment (HG-A)	Mont Terri, Switzerland	Evaluation of flow paths through the near-field damage zone and specifically along seals
	Thermal Simulation for Drift Emplacement (TSDE)	Asse Mine, Germany	Model benchmarking studies for thermal-hydrological-mechanical behavior salt heater test
	Brine Availability Test in Salt (BATS)	WIPP, USA	Monitoring brine distribution, inflow, and chemistry from heated salt using geophysical methods and direct liquid & gas sampling
	Fault Slip Experiments FS and FS-B	**Mont Terri Switzerland**	**Fault reactivation due to repository-induced effects and permeability generation**
	CRQ Thermal Fracturing Experiment	**Bure, France**	**Testing the behavior of argillite host rock to a thermal fracturing stress regime**
	PGZ Gas Fracturing Test	**Bure, France**	**Testing the behavior of argillite host rock upon high-pressure gas injection**
Flow and Radionuclide Transport	Bedrichov Tunnel Experiment	Bedrichov, Czech Republic	Interpretation of water inflow patterns and tracer transport behavior in fractured granite
	Fault Slip (FS) Experiment	Mont Terri, Switzerland	Evaluation of pressure increase impacts on reactivation of faults
	GREET (Groundwater Recovery Experiment)	Mizunami, Japan	Evaluation of early resaturation behavior in crystalline rock looking at flow behavior and chemical-biological interactions upon resaturation
	Long-Term Sorption Diffusion Experiment (LTDE)	Äspö HRL, Sweden	Monitoring the diffusion behavior in fractured crystalline rock
	DR-A Experiment (Diffusion Retention and Perturbation Test)	Mont Terri, Switzerland	Ion diffusion through compacted clay where electro-chemical charges affect transport behavior
	Colloid-Facilitated Radionuclide Migration Test (CFM)	**Grimsel Test Site, Switzerland**	**RN transport of bentonite colloids compared in a shear zone in fractured granite**
	Streaming Potential Test	KURT, Korea	Site characterization techniques (in situ borehole characterization)
Integrated System Behavior	**Full-scale Emplacement Experiment (FE)**	**Mont Terri, Switzerland**	**Full-scale demonstration experiment, one of the largest and longest-duration heater tests**

116

6. GEOLOGIC DISPOSAL RESEARCH ACTIVITIES ASSOCIATED WITH INTERNATIONAL COLLABORATIONS

Section 6 provides summaries of ongoing international R&D activities conducted by SFWD scientists in collaboration with researchers from other countries. These activities involve participation of U.S. researchers in experiments conducted in URLs, analysis of laboratory experiments, benchmarking studies, development of thermodynamic databases, advances in site characterization and monitoring methods, and comparison of PA models.

The summaries of current R&D activities are prepared based on the FY21 milestone reports provided by SFWD researchers from LANL, LBNL, LLNL, and SNL (see a list of FY21 milestone report in Section 8). Examples of R&D activities with international involvement are presented, albeit without providing exhaustive explanations, with the intent to illustrate scientific and technical advances achieved in various areas, and to demonstrate the value of having access to international data and expertise. Specific details of these activities can be found in the references cited in the text and listed in Section 8. The structure of Section 6 is as follows:

- Section 6.1 presents the summaries of experimental and modeling investigations focused on understanding of coupled THMC processes affecting bentonite-based EBS. Research activities are aligned with two full-scale EBS heater experiments, both of which are international projects hosted at the Grimsel Test Site (GTS) in Switzerland: the FEBEX-DP experiment and the HotBENT experiment. A detailed summary of the modeling and experimental analysis of the FEBEX-DP Experiment is given in Section 6.1.2, including development and application of various types of THMC Models, microstructural analysis of FEBEX bentonite samples using XRF and TGA studies, experimental investigations of U(VI) adsorption and diffusion experiments using FEBEX bentonite, and laboratory studies to understand the fate of microbial communities in heated and unheated FEBEX bentonite. Research related to the HotBENT field experiment (Section 6.1.3) includes pre-test THMC modeling of the field test and ongoing column heater experiments referred to as HotBENT-Lab. SFWD scientists also conducted laboratory experiments with focus on bentonite alteration and erosion to better understand implications for colloid transport (Section 6.1.4), in collaboration with the international CFM.

- Section 6.2 describes SFWD research activities dedicated to better understand interactions between EB and host rock materials. Section 6.2.1 summarizes experiments designed to study geochemical and mineralogical interactions between EBS components and, respectively, Mont Terri and GTS rock samples. Section 6.2.2 includes the results of investigations, conducted in a collaboration with Israel, of the processes occurring near interfaces between cement and carbonate rocks (limestone and marl). Finally, Section 6.2.3 provides first results from recently started reactive transport modeling studies to interpret the evolution of the CI-D experiment at Mont Terri, which focuses on the long-term interaction between cement, bentonite and Opalinus Clay.

- Section 6.3 focuses on R&D activities related to heater experiments conducted in argillaceous rock, including summaries of THM modeling of the full-scale Mont Terri FE Experiment in Switzerland (Section 6.3.1) and the Thermal Fracturing Experiment at the Bure URL in France (Section 6.3.2). As opposed to the experimental and modeling described in Sections 6.1 and 6.2, the emphasis in these experiments is more on the host rock than on the EB. Participating in these international activities provides data for model validation for two different claystone host rocks and for two different repository design concepts, the emplacement in horizontal tunnels with bentonite backfill (Swiss concept) and emplacement in micro-tunnels extending from the walls of larger tunnels (French concept).

- Section 6.4 provides results of modeling of gas migration in compacted clay-based sealing materials, such as clay rock or bentonite, to develop a better understanding of the fate of repository gases generated over long periods from canister corrosion or radioactive decay of the waste. This is done under the umbrella of the international DECOVALEX Project. Section 6.4.2 summarizes the findings from SFWD participation in Task A of the DECOVALEX-2019 phase, which was focused

117

on comparative modeling of a series of laboratory experiments on gas transport in bentonite. When Task A ended in late 2019, SFWD researchers migrated to Task B of the current DECOVALEX-2023 phase, which in addition to new laboratory experiments comprises modeling of a full-scale field experiment referred to as LASGIT (Section 6.4.3).

- Section 6.5 summarizes two international collaboration activities on modeling of coupled processes, fluid flow and transport in fractured crystalline rock. An effort related to the DECOVALEX-2023 Project involves micro-scale hydromechanical modeling of fracture contact mechanics upon shearing (Section 6.5.1). Focusing on larger scales, Section 6.5.2 highlights DFN modeling efforts to characterize the impact of network structure on flow, transport, and fluid-fluid reactive transport. These latter activities provide new understanding and capabilities to support international collaboration under the umbrella of the SKB Task Forces, namely the GWFTS task force and its ongoing Task 10 work.

- Section 6.6 focuses on international collaboration activities related to coupled processes and brine migration in salt as a host rock, including investigations related to drift closure analysis (joint project WEIMOS), behavior of EBs in salt repositories (RANGERS project), development of improved THM models for crushed salt (KOMPASS project), and modeling of the BATS test at WIPP as a DECOVALEX-2023 task under SFWD leadership.

- Section 6.7 provides a summary of ongoing international studies on faults as potential radionuclide pathways. Most of the activities revolve around controlled-injection fault experiments conducted in 2015 and 2020 at the Mont Terri URL. SFWD scientists continued their advanced numerical analysis of the 2015 fault slip test to explore the link between fault zone complexity, size of the leakage volume, and induced seismicity (Section 6.7.2). In addition, Section 6.7.3 describes analysis of the long-term fault activation induced by the excavation of a new Mont Terri gallery in 2018. Finally, SFWD scientists started collecting and analyzing data from the new fluid injection experiment conducted in November 2020 which occupies a much larger fault testbed and features additional monitoring methods such as time-lapse seismic imaging of fault movements and fluid leakage (Section 6.7.4).

- Section 6.8 summarizes the development and testing of advanced characterization and monitoring techniques conducted in cooperation with the Collisional Orogeny in the Scandinavian Caledonides (COSC) project, a deep drilling project in a crystalline formation in Sweden. Section 6.8.2 provides an update on the field-based activities, which demonstrated new workflows for improved identification of flowing fractures and better estimates of the state of stress in the subsurface. Section 6.8.3 summarizes a laboratory testing effort that complements the field studies, and Section 6.8.4 describes a new numerical model to reproduce the laboratory results.

- Section 6.9 describes collaborative activities to improve post-closure PA modeling. Task F of the current DECOVALEX 2023 Project involves a staged comparison of models and methods used in different international PA approaches. Section 6.9.2 summarizes recent progress in defining and modeling two PA reference cases for crystalline rock and salt. Because an important component of PA is the ability to conduct radionuclide transport simulations while accounting all relevant equilibrium and kinetic reactions, Subsection 6.9.3 includes an update on international activities to improve thermodynamic and thermochemical databases under the umbrella of the NEA.

The references to the FY21 International reports by the SFWD scientists used in preparation of Section 6 are cited at the beginning of each subsection of this report.

6.1. Coupled Processes and Alterations in Bentonite-Based Engineered Barrier Systems

6.1.1. Introduction to Studies of Thermally Induced Coupled Processes and Alterations in Bentonite

Most disposal options in deep geological repositories currently under investigation consider using clay-based materials (i.e., bentonite) as candidates for engineered barriers (EB) due to their low hydraulic conductivity and high adsorption capacity for radionuclides (e.g., Altmann, 2008; Altmann et al., 2012; Delay et al., 2007; Guyonnet et al., 2009; SKB, 2011; Tournassat et al., 2015). The repository concepts typically impose a temperature limit of about 100°C in the bentonite buffer, with elevated temperature persisting on the order of thousands of years (e.g., Johnson et al., 2002; Wersin et al., 2007; Zheng et al., 2015). However, elevated temperature may impose changes to hydrological and mechanical properties of clay (Cuadros and Linares, 1996; Wersin et al., 2007; Zheng et al., 2015), as well as lead to biogeochemical composition. Recently, several international programs have initiated R&D activities to determine whether the 100°C temperature limit could be raised to perhaps 175°C or even 200°C, which would allow for significant cost savings due to tighter spatial arrangement of the waste canisters in the repository. DOE is one of the programs strongly interested in this research, due to the programs interest in direct disposal of dual-purpose canisters in geologic repositories.

This section comprises summaries of SFWD's modeling and experimental international activities conducted to better understand temperature-dependent perturbations and alterations in EB materials, with focus on bentonite as an important buffer material. The goal is to provide insights as to how repository performance may be affected by these perturbations and alterations. Several relevant activities by SFWD scientists were centered around *in-situ* testing at GTS, in particular the FEBEX-DP experiment, a long-term heater test conducted at 100°C temperature maximum temperature (Section 6.1.2 below and Section 3.3.2) and the HotBENT experiment as a follow-on high-temperature test (Section 6.1.3 below and Section 3.3.3). These tests evaluate temperature-induced effects, such as chemical alteration and mechanical damage of bentonite, under realistic conditions in the field. In a parallel effort, SFWD scientists conducted laboratory experiments to investigate if thermal alterations of bentonite would impact the potential for bentonite erosion and related colloid transport (Section 6.1.4 below); via the selection of experimental conditions and materials, these are also linked to international collaboration efforts such as the Colloid Formation and Migration Project (Section 3.3.1) and the FEBEX-DP Project (Section 3.3.2).

6.1.2. Research Activities Related to FEBEX-DP Experiment

The FEBEX *in-situ* experiment was conducted to study the behavior of components of EBS in the near-field for a high-level radioactive waste (HLW) repository in crystalline rock at the Grimsel URL, Switzerland, from 1997 until 2015, with partial dismantling in 2002, and the final dismantling in 2015 (the latter referred to as FEBEX-DP, or FEBEX Dismantling Project, see Section 3.3.2). The FEBEX test was comprised of bentonite blocks (at 1650 kg/m^3 dry density) placed in a radial arrangement around two underground heaters and heated to a maximum temperature of 100°C (ENRESA, 2000). The FEBEX-DP dismantling activities involved detailed characterization and testing of a large number of samples of the barrier bentonite, steel liner, sensors, embedded metallic components (e.g., metal coupons), and near-field sections with tracer components. Data from sensors embedded in the test together with results from the post-mortem characterization of samples provide a unique opportunity for interpretative modeling of coupled processes in the EBS and the validation of respective simulation tools. Figure 6.1-1 shows a schematic configuration of sampling zones for the FEBEX-DP project, and Figure 6.1-2 depicts a schematic diagram of sampling locations for the FEBEX-DP dismantling of Section 49. Section 49, which is located in the center of Heater 2, is exposed to the highest temperatures along the heated tunnel.
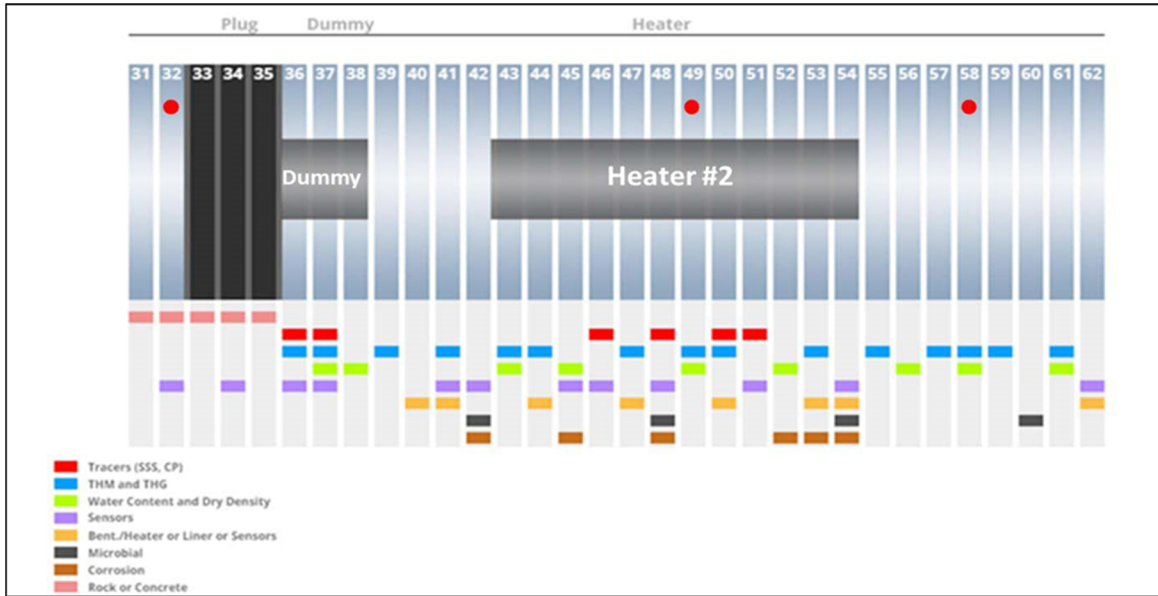
Figure 6.1-1. Schematic configuration of sampling zones (indicated by vertical light blue bars) for the FEBEX-DP project. Filled red circles indicate zones for samples obtained by SNL (Jové-Colón et al., 2021).
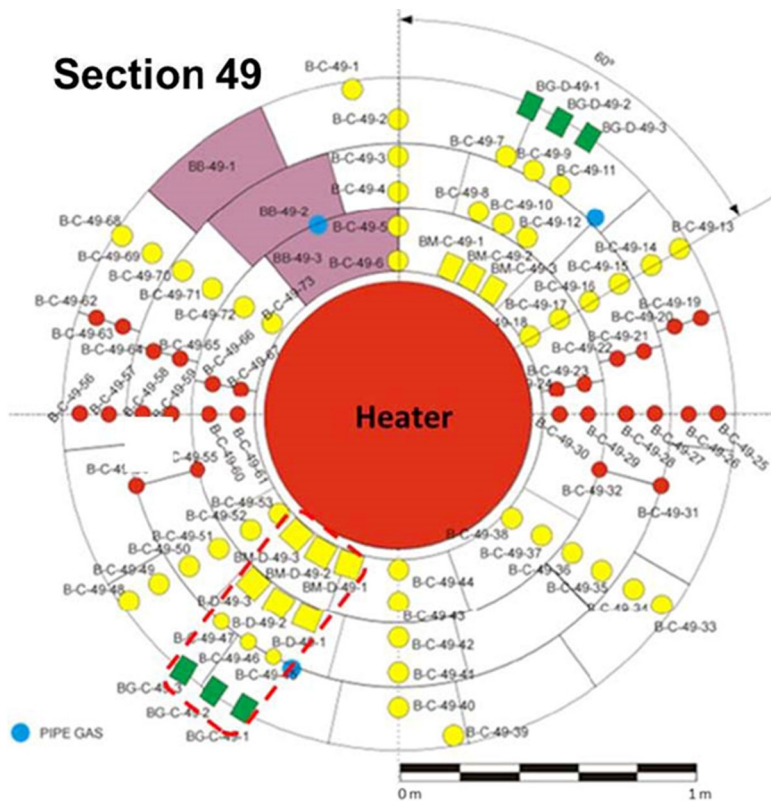
Figure 6.1-2. Schematic diagram of sampling locations for the FEBEX-DP dismantling of Section 49. The red-dashed line delineates the locations of samples analyzed with XRD, XRF and TGA/DSC studies.

The valuable data set and samples from FEBEX and FEBEX-DP have been used for advanced THMC modeling and bentonite sample testing by DOE SFWD scientists. Several sub-sections below include summaries of the following types of FY21 research related to the international FEBEX-DP Project:

- Section 6.1.2.1 describes results of interpretative THMC modeling for the FEBEX experiment, including the development of a suitable THMC modeling framework and the results of detailed THMC simulations over the 18 years of heating (based on the reports by Zheng et al., 2020; 2021).

- Section 6.1.2.2 provides results from TH and THM modeling activities related to the FEBEX test as part of SKB's EBS Task Force activities, including sensitivity and uncertainty analysis (based on the report by Matteo et al., 2020a,b).

- Section 6.1.2.3 includes results of microstructural analysis and molecular dynamics modeling of FEBEX bentonite samples as reported in Jové-Colón et al. (2021).

- Section 6.1.2.4 presents the results of core experiments related to diffusion of ^{3}H and SE in clay materials (Zheng et al., 2021).

- Section 6.1.2.5 includes the results of experiments to determine if bentonite materials collected from the FEBEX experiment possess microbial communities capable of metabolizing H_2, and how the thermal treatment impacted those capabilities (Zheng et al., 2021).

6.1.2.1. THMC Modeling of FEBEX Experiment

6.1.2.1.1. Model Development

Since FY16, the LBNL researchers have been involved in the development of coupled THMC models to predict the long-term thermal, hydrological, mechanical and chemical processes in bentonite exposed to heating. In FY17 and FY18, LBNL used early versions of coupled-processes models to match observational THMC data obtained from the 2002 and 2015 FEBEX dismantling campaigns. The model interpretation of the FEBEX *in-situ* test started from a simple TH model and gradually increased the level of complexity until a fully coupled THMC model was developed. In FY19, modeling efforts focused on the refinement of the chemical model to obtain a better understanding of chemical data based on the aqueous concentrations in bentonite. In FY20, Zheng et al. (2020) applied the calibrated THMC model for the FEBEX test to predict the long-term evolution of engineered-natural barrier systems, in particular, to assess the effect of high temperature on mineralogical alterations of clay minerals, because illitization could potentially lead to decreasing the swelling capacity or reducing the adsorption potential of bentonite. In FY21, Zeng et al. (2021, Section 9.2)) conducted simulations to predict a process of the long-term, up to 10,000 years, alteration of bentonite under conditions similar to the FEBEX *in-situ* test, and also developed a 1D reactive transport model to explain the data collected at the bentonite/concrete interface. Although the model was able to reproduce some data, there were discrepancies between the model and data, which warranted further refinement of the model.

Initial numerical simulations were conducted with TOUGHREACT- FLAC^{3D} , which was used to sequentially couple the multiphase fluid flow and reactive transport simulator TOUGHREACT V2 (Xu et al., 2011) with the finite-difference geomechanical code FLAC^{3D} (Itasca, 2009). In FY18, the code TOUGHREACT V2 (Xu et al., 2011) was upgraded to TOUGHREACT V3.0-OMP (Xu et al., 2014). The application of the OpenMP parallelization of chemical routines on multi-core shared memory computers allowed for decreasing the computation time. In FY20, Zheng et al. (2020) transitioned to a new simulator – TReactMech (Sonnenthal et al., 2015; 2018) with new libraries, which modified the coupling strategy from iterative two-way coupling to a sequential coupling method.

The base THMC model of the FEBEX test uses a radial-symmetrical mesh that accounts for the three relevant EBS components: heater, bentonite and granite (Figure 6.1-3). The simulations were conducted for the period from February 27, 1997 to July 1, 2015, a total of 6,698 days (18.3 years). The initial conditions applied throughout the model domain were: temperature of 12ºC and the bentonite water content of 14% (gravimetric), corresponding to the saturation of 55% and a suction of 1.11×105 kPa. The following boundary conditions were applied: a temperature of 100ºC and a no-flow condition at the heater-bentonite interface, and a temperature of 12ºC and a liquid pressure of 7 MPa at the external boundary (r = 50 m).
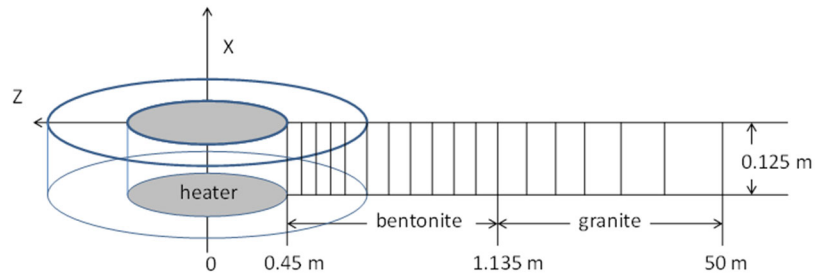
Figure 6.1-3. Schematic of the modeling mesh used for the model, not to the scale.

6.1.2.2. FEBEX Simulations with Base THMC Model

From FY16 to FY19, the simulations for the FEBEX *in-situ* test evolved from a TH model (Zheng et al., 2016) to a THMC model that can reasonably interpret the coupled THMC data collected at the test site (Zheng et al., 2018b; 2019a,b; 2020). Because the TH model overestimated the relative humidity data and water content data (Zheng et al., 2016), additional processes were added seeking better match between data and model. First, mechanical effects, using the state surface approach, were added to the model to simulate the swelling of bentonite, expanding the model from a TH to a THM model. As a result of swelling, the porosity and permeability od the bentonite are changing. Variable permeability as a function of dry density was used. Second, another coupled process, thermal osmosis, was added to the model, using a calibrated thermal osmotic permeability.

The final THMC model, referred to as the Base THMC model, was able to provide a good match to various data from the FEBEX test, such as temperature (Figure 6.1-4), relative humidity (Figure 6.1-5), stress (Figure 6.1-6), and the chloride concentration (Figure 6.1-7). This confirmed the necessity of using a THMC model to explain the hydrological behavior of bentonite. THM processes strongly affect the geochemical evolution, but usually not vice versa, which is why a great deal of effort was dedicated to have a sound THM model that can match the THM data. Once the THM processes are relatively well established, before studying the possible chemical reactions, the model of transport processes needs to be constrained. While the advection of chemical species is fixed in the THM model, diffusion has to be calibrated in the chemical model. Because chloride is only controlled by transport processes, its temporal and spatial evolution is a good indicator of the transport processes. The THMC model nicely fit the data near the heater (Figure 6.1-7), indicating that the chloride concentration could be fairly high at the canister-bentonite interface. If such a trend persists for an extended time period until the canister is fully corroded, the high chloride concentration might significantly affect the degradation of waste. As granite pore water (which has much lower chloride concentration than bentonite pore water) penetrates into the bentonite, it dilutes significantly the bentonite pore water, and the chloride concentration is reduced near the granite at the radial distance between 0.8 m and 1.1 m. Meanwhile, bentonite pore water pushed towards the heater by advection and evaporation causes an increase in the chloride concentration there, as manifested by the high chloride concentration near the heater.

The base THMC model (Zheng et al., 2018b; 2019a; 2020) showed that the key processes required to match THM data and chloride concentration include vapor diffusion, porosity change due to swelling, permeability change as a function of dry density, and thermal osmosis. The concentration profile of pH, bicarbonate and sulfate is largely determined by chemical reactions. Because of the buffer by surface protonation, the spatial profile of pH is fairly flat, except in the area near the granite and the heater (Figure 6.1-8). The increase in pH in bentonite pore water at the heater vicinity is related to the dissolution of montmorillonite (Figure 6.1-9). The evolution of clay minerals, namely smectite and illite, has great implications to the long-term stability of the bentonite barrier. Laboratory heater tests are often too short to show significant change in clay minerals or conditions in the laboratory tests are very different from the *in-situ* conditions. In contrast, the mineral characterization of the samples collected after the final dismantling of FEBEX-DP provides insight into the possible change of clay minerals after long-term heating and hydration. Unfortunately, given the large variation of the illite fraction in the illite/smectite mixed layer between samples, it is impossible to delineate if there is

any increase or decrease of the illite mass fraction by comparison with the reference bentonite. Models show illitization near the heater, as manifested by illite precipitation and montmorillonite dissolution, but on the order of less than 1%, which cannot be proved or disapproved by the short-term test data.
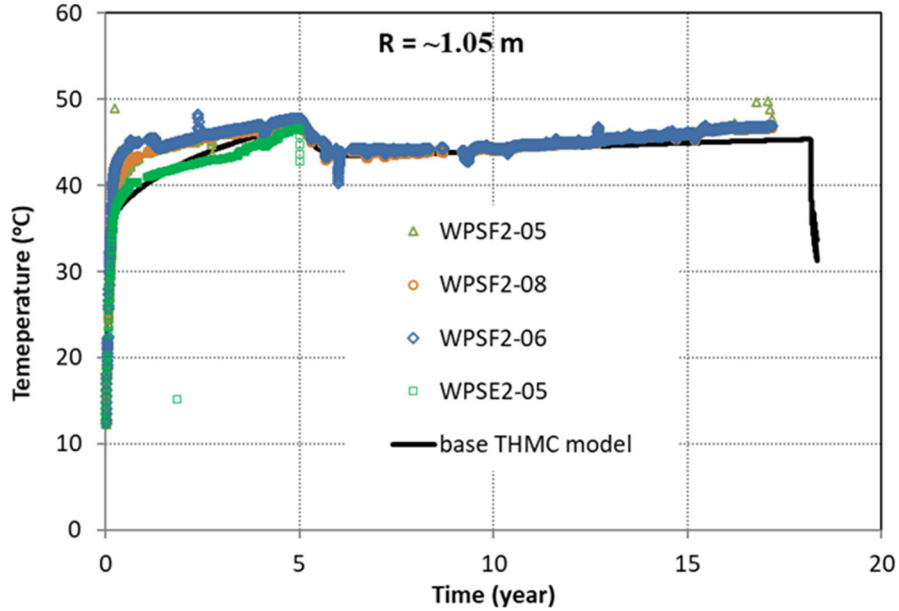
Figure 6.1-4. Measured temperature by sensors at different locations, but the same radial distance (1.05 m) and results from the base THMC model.
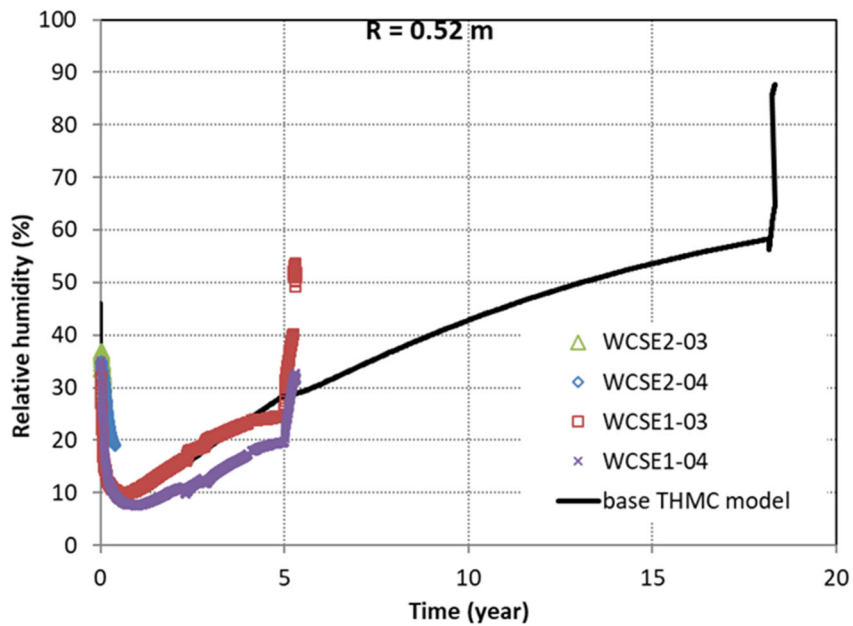
Figure 6.1-5. Relative humidity data measured from sensors at different locations, but the same radial distance (0.52 m), and model results from the base THMC model.
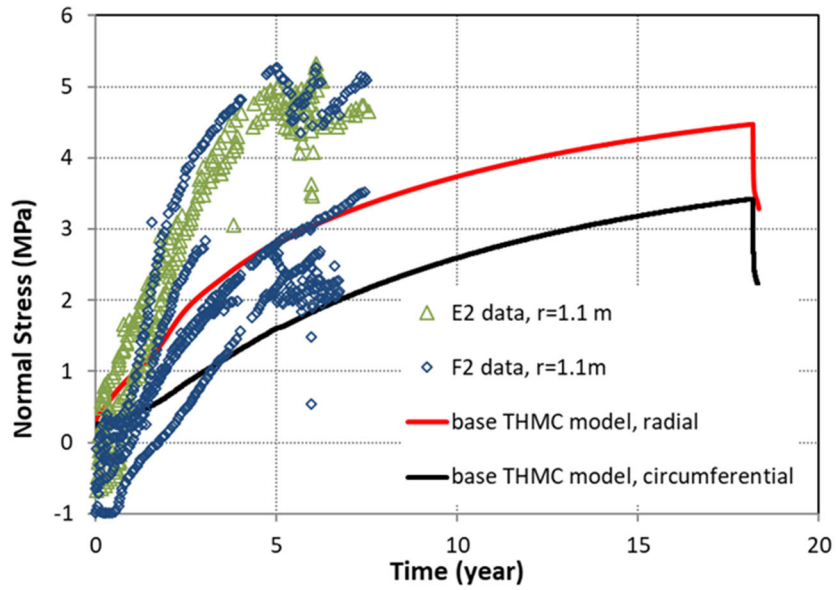
Figure 6.1-6. Measured stress by sensors at different locations (from sections E2 and F2, see ENRESA, 2000), but the same radial distance (1.1 m), and results from the base THMC model.
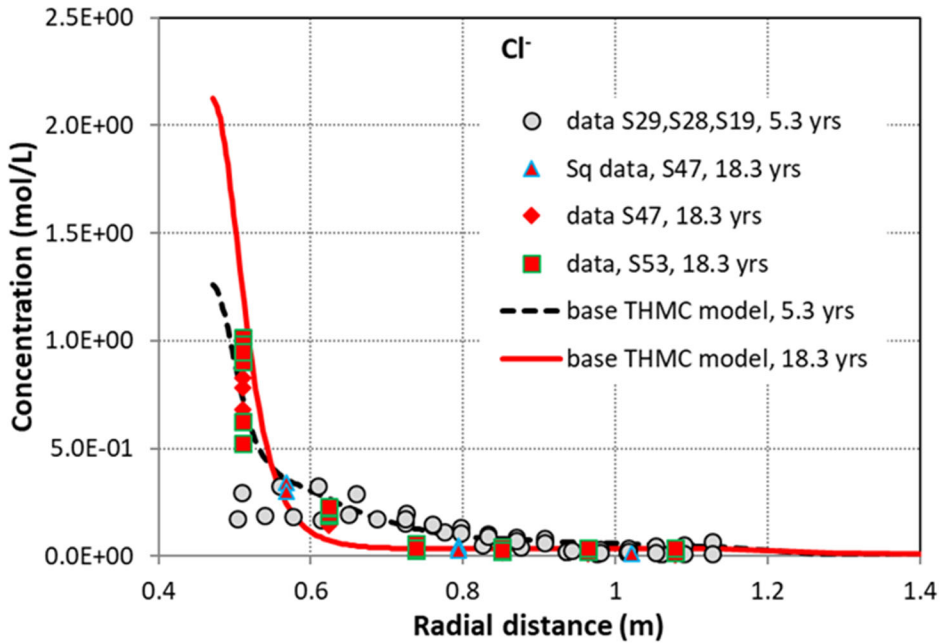
Figure 6.1-7. Calibrated chloride concentration data at 5.3 years from aqueous extract test for Sections 29, 28, and 19 (Zheng et al., 2011), calibrated chloride concentration data at 18.3 years from aqueous extract test for Section 47 ("data S47, 18.3 years") and Section 53 ("data S53, 18.3 years"), chloride concentration data from squeezing test for Section 47 ("Sq data, S47, 18.3 years"), and model results from the base THMC model.
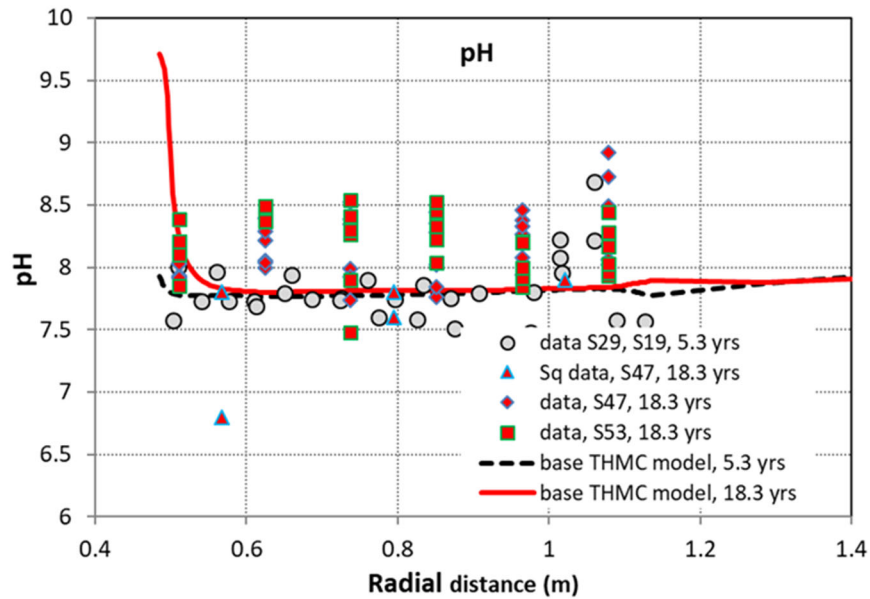
Figure 6.1-8. Calibrated pH data at 5.3 years from aqueous extract test for Sections 29, 28, and 19 (Zheng et al., 2011), calibrated chloride concentration data at 18.3 years from aqueous extract test for Section 47 ("data S47, 18.3 years") and Section 53 ("data S53, 18.3 years"), chloride concentration data from squeezing test for section 47 ("Sq data, S47, 18.3 years"), and model results from the base THMC model.
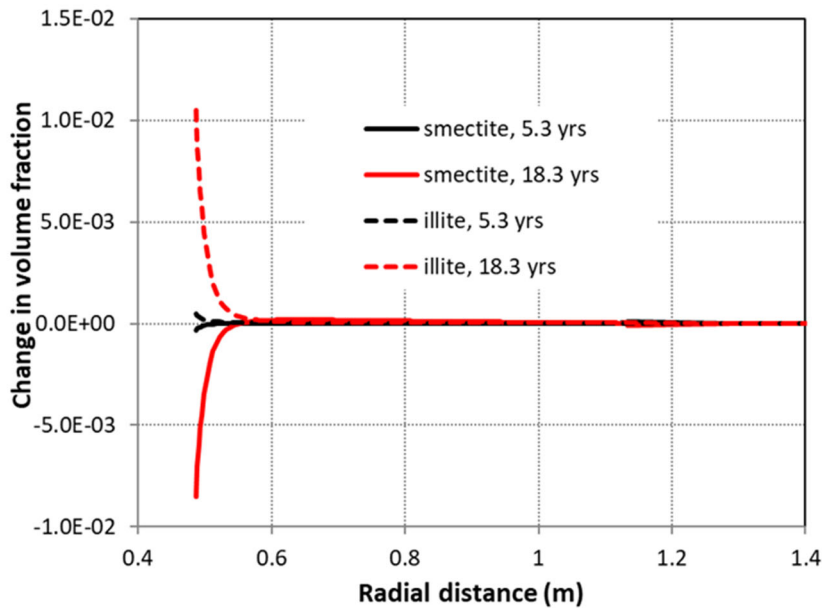
Figure 6.1-9. Model results of smectite and illite volume fraction change at 5.3 years and 18.3 years. Negative values mean dissolution, and positive values means precipitation.

6.1.2.2.1.　　Using the Calibrated FEBEX THMC Base Model for Long Term Predictions

As discussed in the previous section, the Base THMC model was able to provide a reasonable interpretation of the FEBEX behavior. Simulations using the Base THMC model for the FEBEX *in-situ* test showed a relatively small amount of illitization (due to dissolution of smectite and precipitation of illite) at an area near the heater after 18 years of heating and hydration. The question is of course whether there will be a more significant amount of illitization over the much longer time periods relevant for nuclear waste disposal. To

125

evaluate the possible amount and impact of illitization over the lifespan of a repository, LBNL in FY21 conducted long-term THMC simulations (Zheng et al., 2021, Section 9). For this purpose, the Base THMC model was run for 20,000 years, keeping all other conditions the same except for the heat output defined at the heater. The shape of the heat decay function is similar to that used in Rutqvist et al. (2011) for a 2-D model, but the magnitude is scaled down so that the temperature in the EBS close to the heat source is around 100ºC, as shown in Figure 6.1-10. After 10,000 years, the temperature returns to the ambient temperature. This long-term model is called the "L-THMC model." Examples findings are presented below.
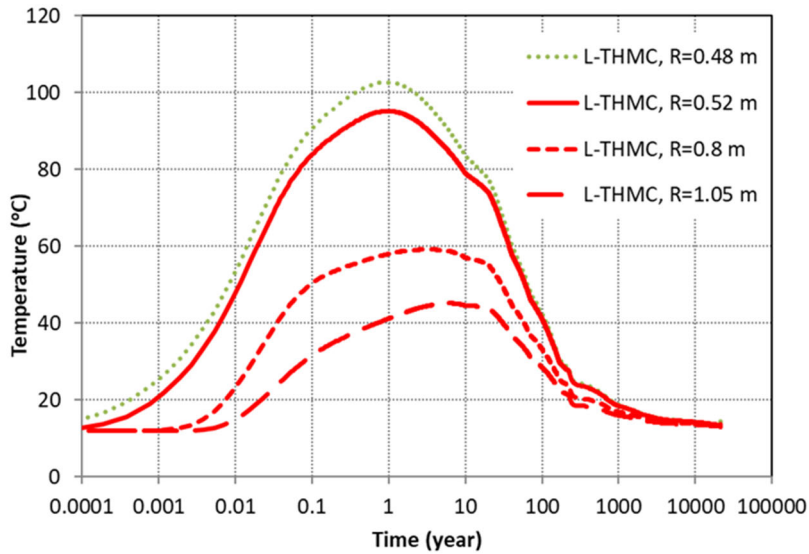
Figure 6.1-10. Temporal evolution of temperature at several radial distances in the "L-THMC model."

Modeling with the L-THMC model showed that in the bentonite barrier near the heater/canister, the temporal evolution of relative humidity goes through three phases. An early desaturation phase lasts for about one year, causing a sharp decrease of relative humidity, followed by a rapid re-saturation phase that ends after 35-40 years. Then, the bentonite barrier enters into a slow re-saturation phase, with the relative humidity close the heater (at R = 0.48 m) increasing from 92% at 35 years to 97% at 200 years, and 99% at 10,000 years in the "L-THMC" model (Figure 6.1-11). However, the water saturation reaches 100% after about 50 years (Figure 6.1-12).
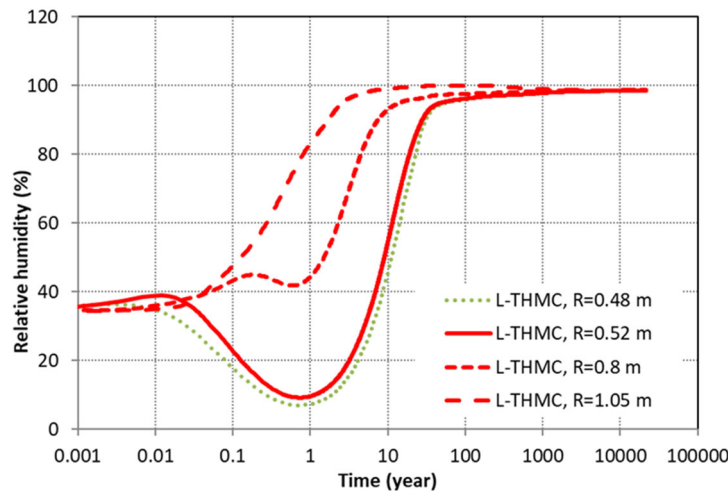
Figure 6.1-11. Temporal evolution of relative humidity at several radial distances in the "THMC model."
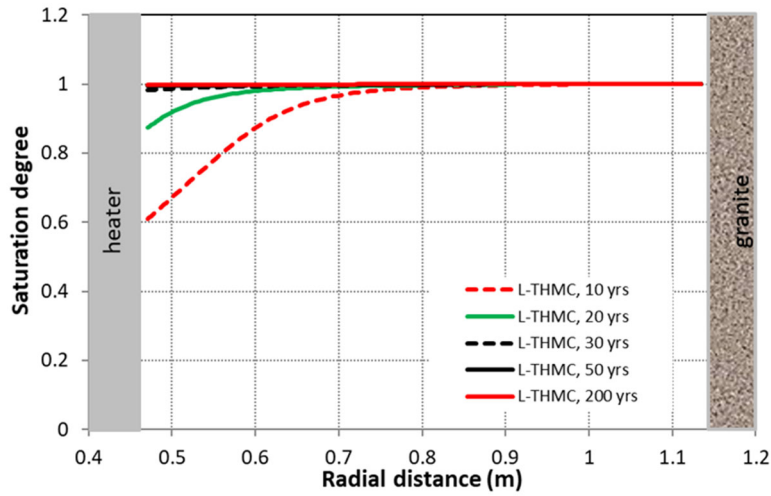
Figure 6.1-12. Spatial distribution of water saturation at different times in the "L-THMC model."

In the FEBEX *in-situ* test, a relatively high ion concentration was observed in the pore water of the bentonite. LBNL's long-term modeling shows that the chloride concentration can reach about 2 mol/L near the heater (Figure 6.1-13) because of evaporation during the early heating phase. Later, when the bentonite barrier becomes fully saturated, a chloride concentration of about 0.1 mol/L is almost evenly distributed in the bentonite barrier, which is slightly lower than the initial chloride concentration in the pore water of bentonite (0.16 mol/L).
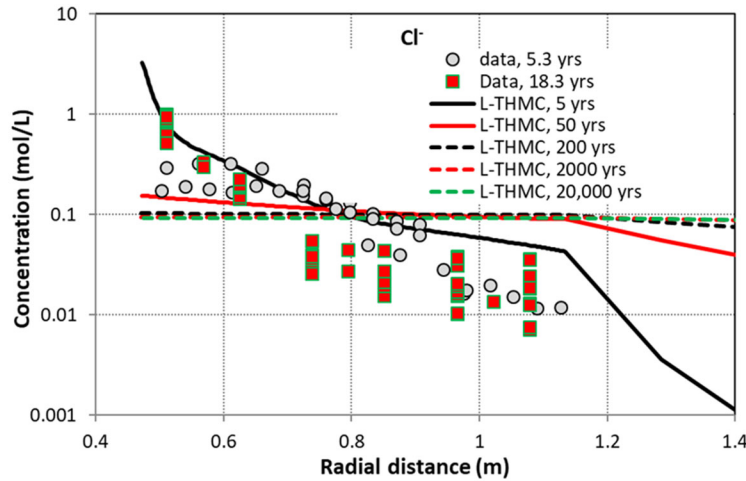
Figure 6.1-13. Spatial profiles of chloride concentration at several time points in the "L-THMC model."

As it was shown in previous modeling work for the FEBEX test (e.g., Zheng et al., 2016; 2017), the concentration profiles of cations (calcium, potassium, magnesium, and sodium) were largely shaped by transport processes despite their concentration levels being affected by mineral dissolution/precipitation and cation exchange. In terms of long-term spatial trends, just like chloride, the spatial profile of potassium flattens out in the bentonite barrier: at 2,000 or 20,000 years, the concentration near the heater is just slightly higher than that near the granite rock interface. As an example, Figure 6.1-14 shows profiles of potassium concentration at several time points in the "L-THMC model."
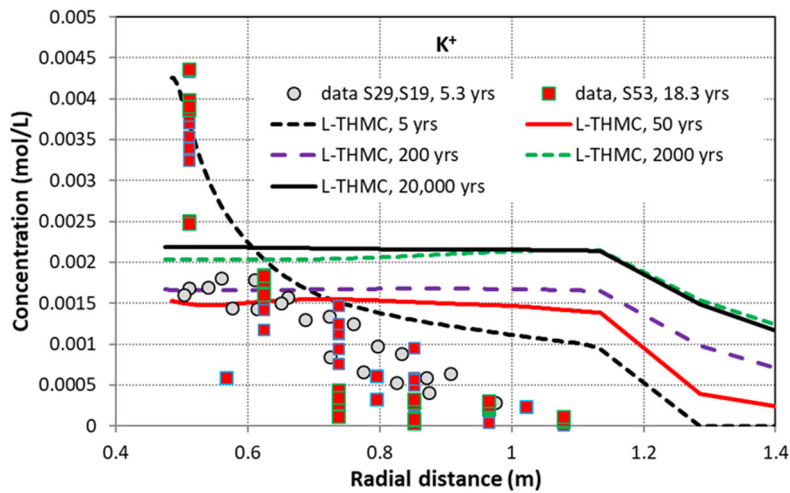
Figure 6.1-14. Spatial profiles of potassium concentration at several time points in the "L-THMC model."

Illitization (transformation of montmorillonite to illite) is one of the major concerns throughout the world that has led to the establishment of a thermal limit of 100ºC for argillite and crystalline repository with bentonite barrier (Zheng et al., 2015). The Base THMC model for the FEBEX test showed that montmorillonite dissolves and illite precipitates (illitization is usually expressed as the dissolution of montmorillonite and precipitation of illite, but here we only display the dissolution of montmorillonite) in the bentonite near the heater with an amount less than 1% after 18 years. This finding was neither disapproved nor approved by the experimental data because the measurements for the mineral phase were too scattered (Zheng et al., 2018). The long-term THMC simulation using the "L-THMC" model (Figure 6.1-15) shows that dissolution of montmorillonite does not progress further. Instead, at 20,000 years, only 0.5% mass fraction of montmorillonite dissolves on average. The model furthermore shows that there is about 2% dissolution of montmorillonite at the granite/bentonite interface. Also, there is precipitation of montmorillonite across the bentonite barrier at 20,000 years.
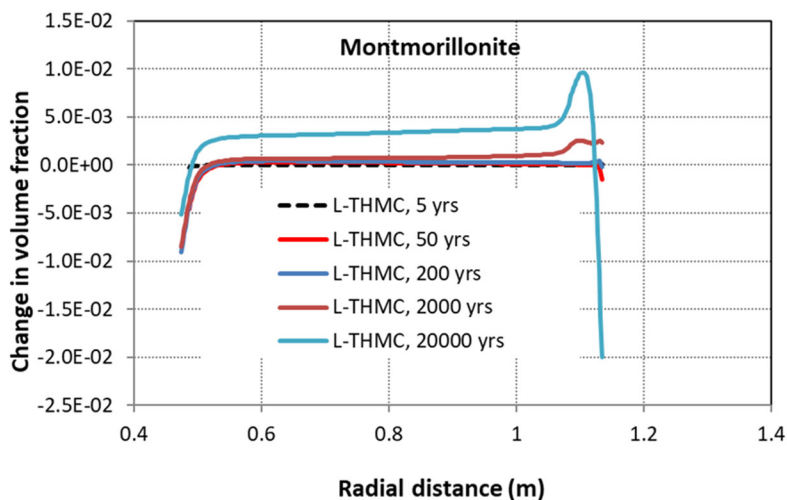
Figure 6.1-15. Model results for montmorillonite volume fraction change at several times in the "L-THMC model."

In the long run, when bentonite passes the initial high temperature and unsaturation-to-saturation transition time, the chemical change at the granite/bentonite interface becomes more pronounced. For example, there is strong calcite dissolution on the bentonite side and strong calcite precipitation on the granite side of the granite/bentonite interface (Figure 6.1-16). The long-term results indicate the importance of understanding the

geochemical changes across interfacial areas, which will be discussed in Section 6.1.2.1.4 below for concrete-bentonite interface samples from the FEBEX test and more generally in Section 6.2 for various other interfaces.
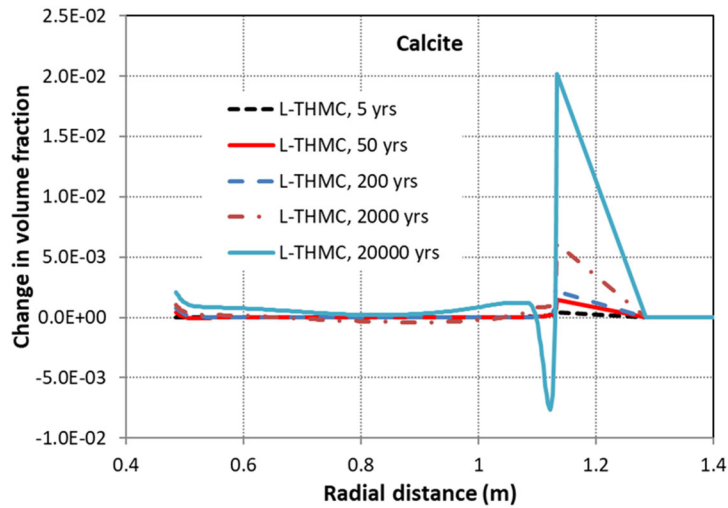
Figure 6.1-16. Model results for calcite volume fraction change at several time points in the "L-THMC model."

6.1.2.3. Modeling the Concrete/Bentonite Interface in the FEBEX In-situ Test

This section of the report summarizes modeling activities described in the report by Zheng et al. (2021, Section 9.3). After dismantling of Heater 1 of FEBEX in 2002, a concrete plug was constructed between the open tunnel of the FEBEX galley and the heater/bentonite ensemble of the remaining Heater 2. During the final dismantling in 2015, a series of cores were taken at the interfacial area (see Figure 6.1-17) to determine geochemical properties of concrete and bentonite and to understand the long-term (13 years) interaction of concrete and bentonite under *in-situ* heated conditions.
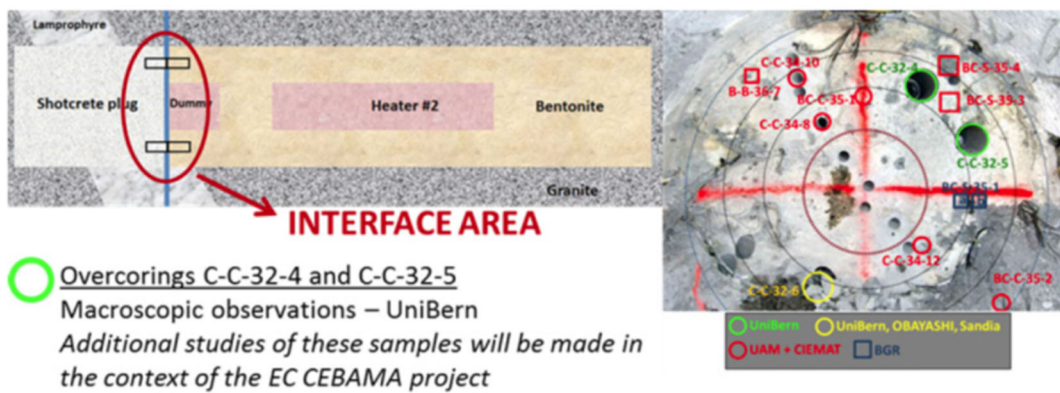
Figure 6.1-17. Overcoring at the concrete/bentonite interface during the final dismantling of the FEBEX *in-situ* test (Turrero and Cloet, 2017).

Comprehensive characterization of the physical and geochemical properties of bentonite and concrete around the concrete/bentonite interface was conducted by various institutions, as documented in Turrero and Cloet (2017). Some general observations are as follows: Within the concrete, the concentrations of sulfate, sodium, and potassium decreased at the bentonite interface, and the calcium concentration increased. Within concrete, precipitation of ettringite was observed both far and near the interface, and dissolution of portlandite at the interface was observed by XRD, which was depleted within 2 mm from the interface. There was an increase in specific surface area on both sides of the interface, indicating there might be pore size/structure changes

caused by mineral dissolution and precipitation in both concrete and bentonite. Specifically, chloride content is an order of magnitude lower in the first 5 cm of bentonite, and chloride diffuses into the concrete plug and Friedel's salt precipitates on the concrete side of the interface. Na+ concentration in aqueous extracts from bentonite and concrete samples is lower than that from the reference FEBEX bentonite or the reference concrete. K+ concentration increased significantly in the first 2 mm of the bentonite. Ca2+ from portlandite diffuses towards the bentonite, where an increase in concentration is observed in the first centimeters compared to the FEBEX original. Soluble Mg2+ gets accumulated in the first 2 cm from the interface in concrete. In bentonite, Mg2+ in aqueous extracts is negligible, due to precipitation of Mg silicates.

A 1D reactive transport model was developed by LBNL to simulate the interaction between bentonite and concrete (Figure 6.1-18). The model simulated a time period of 13 years representing the time from 2002, when Heater #1 was dismantled and the concrete plug was installed, to 2015, when Heater #2 was dismantled. The model extends 30 cm on each side of the interface and no-flux boundary conditions are imposed such that there is only diffusive flux across the interface. Preliminary simulations were conducted using the porosity of 0.125 for concrete and 0.41 for bentonite, assuming no changes due to mineral precipitation/dissolution, the porosity remains constant, and the effective diffusion coefficient is 2×10^{-10} m2/s.
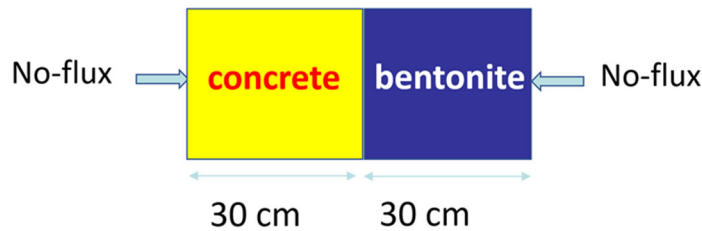
Figure 6.1-18. Setup of the 1-D reactive transport model

The model considered aqueous complexation, mineral dissolution/precipitation, cation exchange, and surface complexation. Modeling was conducted taking into account that bentonite had been reacting with granite for 5.3 years prior to constructing the concrete plug (from 1997 to 2002). To determine initial conditions for pore water and minerals, modeling was conducted for 1,000 years to reach static long-term equilibrium conditions. These results were used as the initial conditions for concrete in the reactive transport model. Table 9.4 in the report by Zheng et al. (2021) lists the pore water composition for concrete, and Tables 9.5 and 9.6 list the minerals and their saturation index for bentonite and concrete, respectively.

Preliminary results from the interfacial model are briefly shown below. Diffusion and reactions shape the concentration profiles at the end of the simulation, i.e., after 13 years. Conservative species such as chloride are controlled by a diffusion process following the concentration gradient whereas concentrations of highly reactive species are largely controlled by reactions Examples of computed concentrations of chloride, carbonate, sulfate, and pH at the end of the simulation are shown in Figure 6.1-19. At present time, detailed model validation is ongoing and more work is needed. For example, the model does not consider precipitation of Friedel's salt, which may significantly decrease the concentration of chloride around the interfacial area.
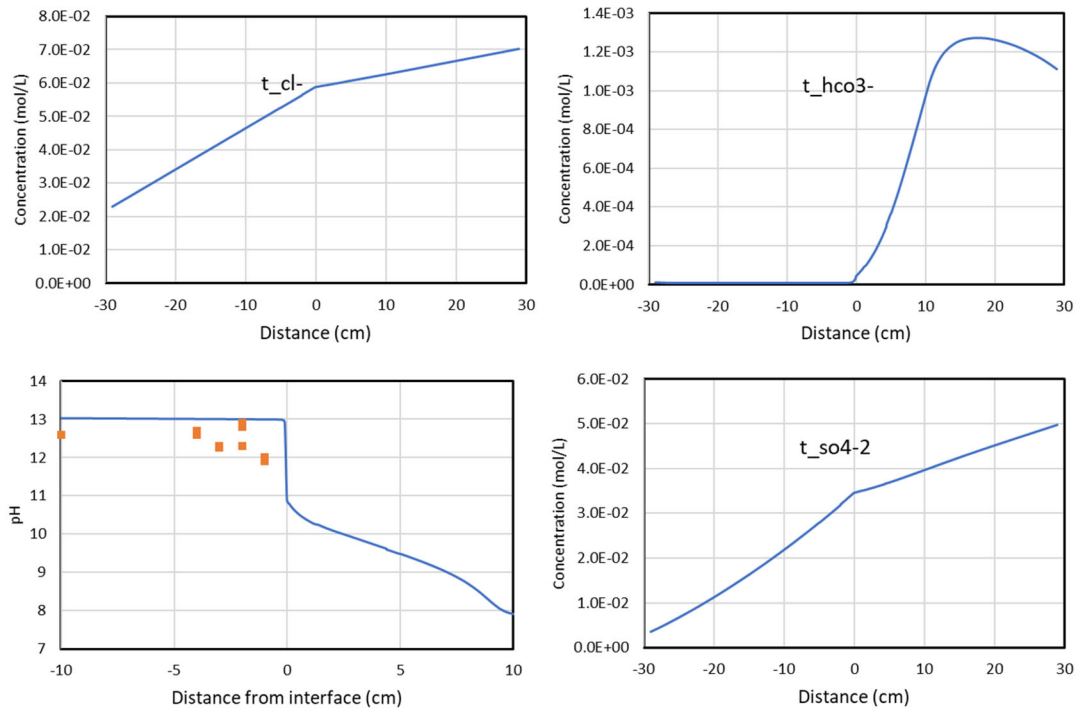
Figure 6.1-19. Computed total concentrations of chloride, carbonate, sulfate, and pH at the end of the simulation. Also shown are measured pH in concrete. The interface locates at X=0, negative values are on the concrete side and positive values are on the bentonite side.

Regarding mineralogical changes, pH and calcium changes cause changes in minerals like portlandite, ettringite, calcite, and C-(A)-S-H. Turrero and Cloet (2017) reported that on the concrete side, portlandite dissolves, and losing Ca destabilizes ettringite, and there is decalcification in about 15 mm from the interface and formation of C-(A)-S-H. The model confirms the dissolution of portlandite (Figure 6.1-20a) and ettringite (Figure 6.1-20b). However, the model shows precipitation of calcite (Figure 6.1-20c) instead of decalcification as data suggest, which is probably why the model does not show noticeable precipitation of CSH (see Figure 6.1-20d). On the bentonite side of the interface, the model and data are consistent in terms of precipitation of calcite which is caused by the diffusion of calcium from concrete to bentonite because of the dissolution of portlandite in concrete. The model also confirms the observation of the dissolution of montmorillonite (Figure 6.1-20e) due to silicate depletion. The preliminary model explains the behavior of some species and mineral, but some discrepancies need to be resolved by revising the model.

6.1.2.3.1.   Summary and Future Work

The FEBEX *in-situ* test, which lasted more than 18 years, is extremely valuable for validating the coupled THMC model and deepening our understanding of the evolution of the bentonite barrier throughout heating and hydration. The ultimate goal of LBNL's FEBEX modeling is to use THMC data from FEBEX-DP to validate models for long-term THMC processes and alterations in bentonite. After the THMC model provided a coherent explanation of the THMC data collected at the FEBEX *in-situ* test, LBNL scientists used the well-calibrated THMC model to conduct exploratory simulations of repository behavior. The simulations conducted in FY21 addressed questions about the long-term alteration of bentonite, up to 20,000 years, under conditions similar to the FEBEX *in-situ* test.

In FY21, LBNL also developed a 1D reactive transport model to explain data collected at the bentonite and concrete interface of the FEBEX test. The model was able to reproduce some data, but there were also discrepancies between model and data, which warrant further model refinement. In the future, LBNL will modify the model by firstly adding new secondary minerals and refining the thermodynamic and kinetic

database to resolve the discrepancies between measured aqueous concentration and model results, and secondly introducing the effect of changing porosity on tortuosity and diffusion coefficients to understand the effect of mineral dissolution/precipitation on the transport process at the interface.
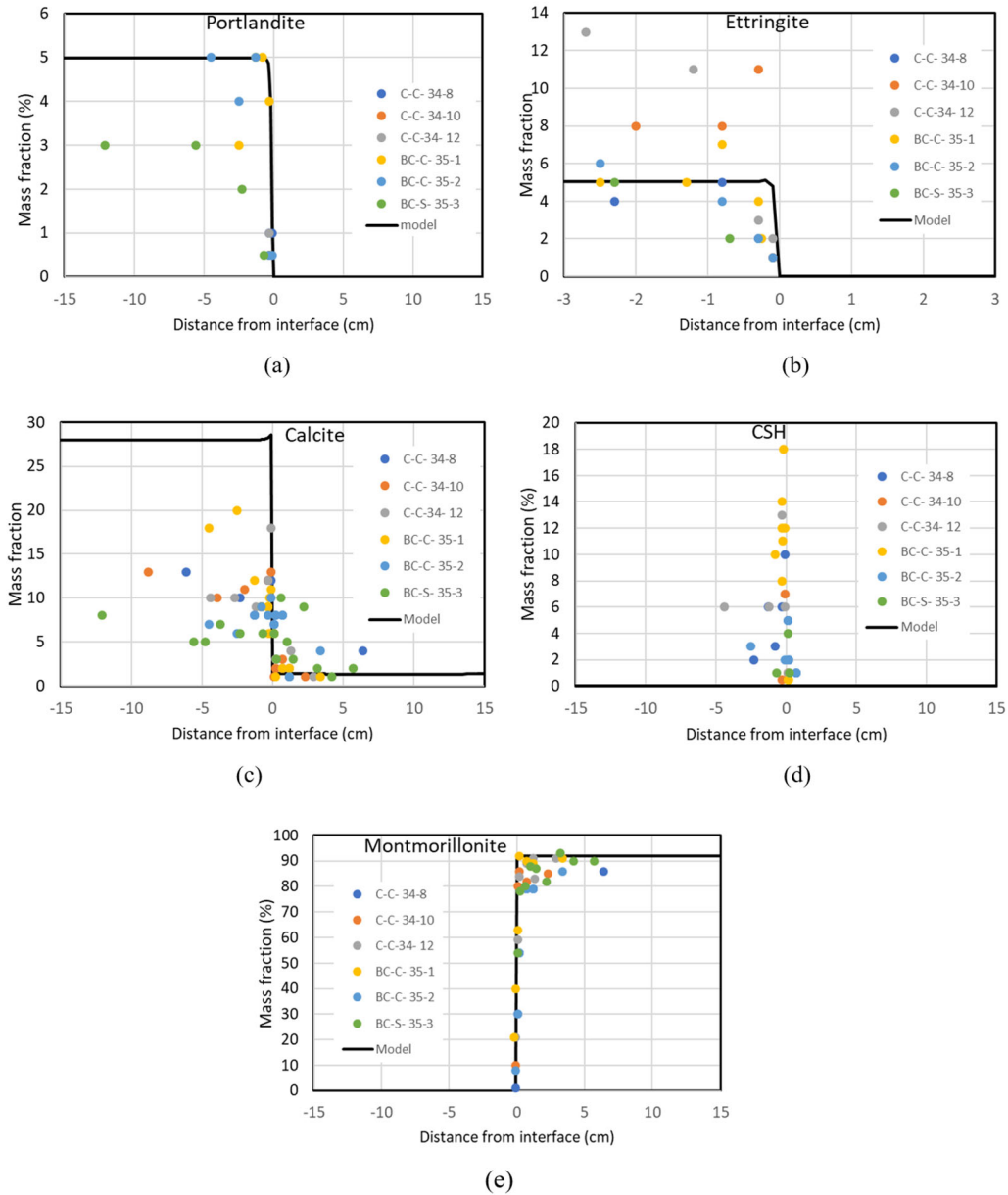
Figure 6.1-20. Computed mass fraction of portlandite, ettringite, calcite, CSH, and montmirillonite at the end of the simulation.

6.1.2.4. *TH and THM Modeling of FEBEX Test in the Context of SKB Task Forces*

Complementary to LBNL's modeling with focus on coupled THMC and bentonite mineral alterations, SNL simulated the FEBEX heater test as part of Task 9 of the SKB EBS Task Force activities. SNL's work aimed at interpretation of the larger-scale TH and THM behavior of the FEBEX experiment (Matteo et al., 2021, Chapters 2 and 3), with a focus on three subtasks of Task 9, namely: (1) Modeling with Coupled CFD and Porous Flow: Effects of Barrier Gaps, (2) TH Modeling: Uncertainty Quantification and Parameter Estimation with PFLOTRAN, and (3) Modeling of Gas Transport in Visco-elasto-plastic Soft Materials. Preliminary results of these tasks were presented at the SKB Task Force meeting in Barcelona in May 2019, and updates on sub-tasks were presented at the meeting in Baden, Switzerland, in November 2019. As discussed in Section 3.4.2.1, Task 9 was slowly winding down in 2020 and has now effectively ended, after years of modeling studies of the FEBEX test by many notable modeling teams (Gens et al., 2009; Sánchez et al., 2010; 2012; Samper et al., 2008; Matteo et al., 2019; Zheng et al., 2020). SNL's modeling activities with regards to the FEBEX test also ended in FY21. Below is a brief summary of the results from SNL's TH modeling activities with PFLOTRAN and related sensitivity studies.

6.1.2.5. *TH Modeling with PFLOTRAN*

In FY20, SNL's scientists performed modeling of FEBEX Stages 1 (5 years of heating until the first dismantling) and 2 (the remaining time between the first and the second dismantling), taking into account 3D flow and transport processes, gravity and asymmetric wetting and drying out of the bentonite barrier. Modeling was conducted using the PFLOTRAN THC code with massively parallel computational methods, which is an open source, state-of-the-art, massively parallel subsurface flow and reactive transport code operating in a high-performance computing environment (Hammond et al., 2014). Matteo et al. (2020) presents the modeling approach and associated results, as well as a comparison of those modeling results to the field results. The approach in this model is different from other Task 9 modeling. A Forscheimer approximation, including Navier-Stokes plus Brinkman corrections, was used, which allows for matching flux conditions between gaps and porous media, and a discontinuity in fluid pressure at bentonite boundaries. The model uses the gas pressure and the molar density of water component as persistent variables for the compositional portion of the model, which allows continuous representation of the compositional model in the tunnel, cement, bentonite, and any open gaps during initial wetting up and dry out near heaters. The focus is on gas flux and the influence of gaps and homogeneity in wetting up of the bentonite, and on the impact on thermal conductivity near the heaters. The 3D CFD model uses a tetrahedral mesh to solve the coupled TMH equations. The constitutive models for bentonite shrinking/swelling and thermal conductivity in particular have been validated against experimental data.

The TH simulations were conducted using a 3D modeling domain with dimensions of $60 \times 20 \times 40$ m in the x, y and z directions, respectively. The simulation domain included various regions representing different materials–granite, disturbed rock zone (DRZ), bentonite buffer, heaters, plug, liner, micro-annulus, lamprophyre and a fracture at back of test area. An axisymmetric boundary condition was applied. The geometry of the mesh is shown in Figures 6.1-21 and 6.1-22. Different meshes were used for Stage 1 and Stage 2 modeling. The mesh size for Stage 1 comprised 125,824 grid blocks. It was assumed that the DRZ, lamprophyre dikes, and fracture zones have the same properties as the granite domain. Upon the bentonite buffer emplacement, a pressure of one atmosphere and a liquid saturation of 0.36 were applied. At the beginning of the heating phase the bentonite saturation was assumed to 0.65 due to hydration from the formation. Hydrostatic pressure boundary condition was assigned on the sides of the modeling domain with a pressure of 0.7 MPa at the top of the domain. A 1,200 W heat was applied at the two heaters for the first 20 days, and the power of each heater was raised to 2,000 W between Days 20 and 60. For the rest of the simulation time in Stage 1, time varying heat was applied at the two heaters to maintain a temperature of 100°C. Modeling of Stage 2 was performed with a different domain geometry and a different 3D mesh to incorporate the geometry changes that occurred due to the first dismantlement. For Stage 2, modeling was performed for 18 years with only Heater 2 operating. The mesh size for Stage 2 was 329,828 grid blocks (Figure 6.1-23).
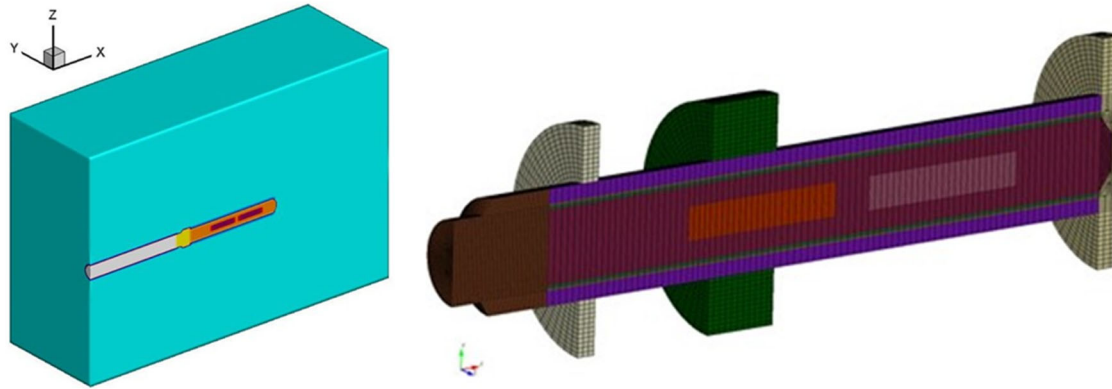
Figure 6.1-21. 3D modeling domain with axisymmetric meshing for Stage 1.
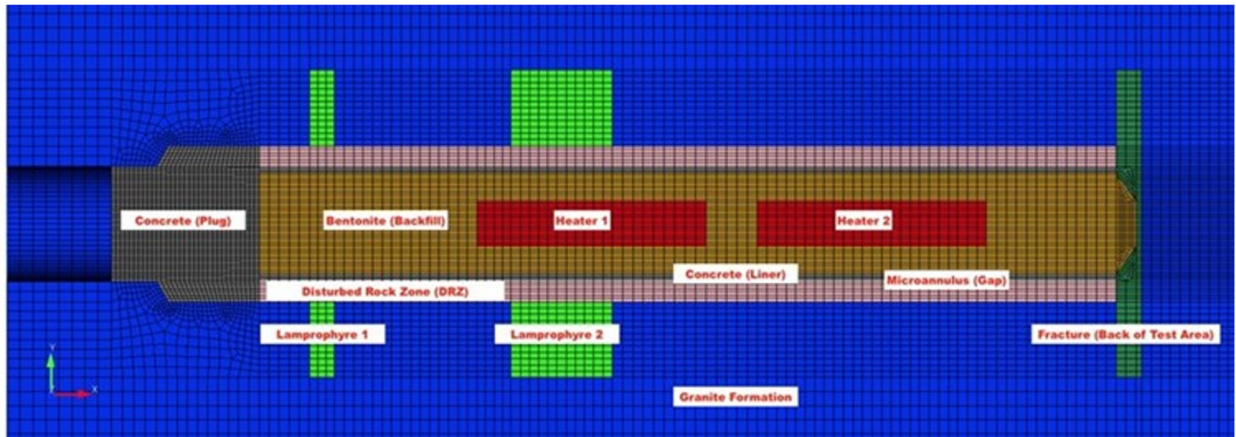
Figure 6.1-22. Meshing of the TH modeling domain for Stage 1.
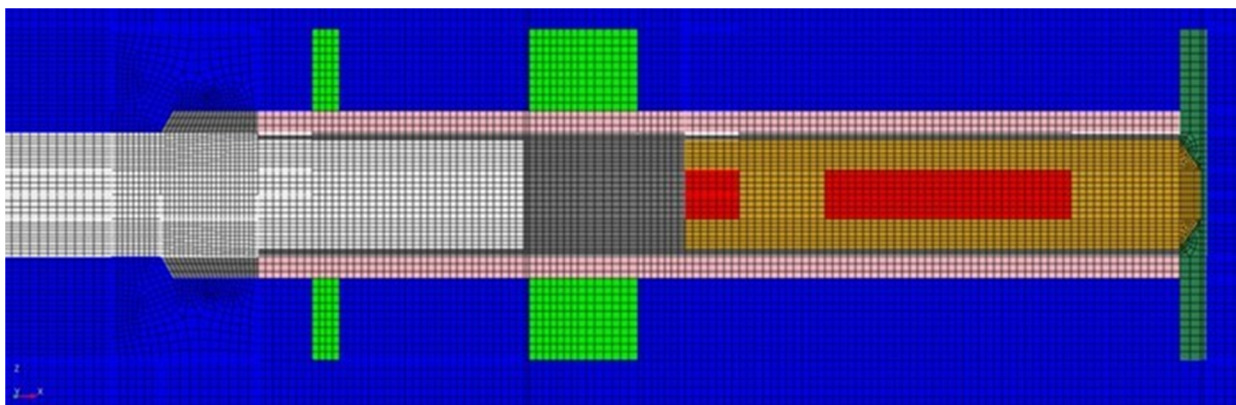
Figure 6.1-23. Meshing of the TH modeling domain for Stage 2.

A detailed analysis of simulation results and comparison with experimental data for Stages 1 and 2 are given in the report by Matteo et al. (2020). As examples of TH modeling results, Figure 6.1-24 (left) shows the distribution of temperature along the axis of the tunnel, a perpendicular cross-section at the location of Heater

1 and a horizontal cross-section, indicating penetration of heat into the buffer and host rock. Figure 6.1-24 (right) shows the corresponding distribution of liquid saturation. Figure 6.1-25 demonstrates that predictions of temperature are close to the measured temperature along the axial segment AS2 at 90 days and 1,800 days for Stage 1. As expected, temperature was higher close to the heater and decreased with distance from the heaters. Figure 6.1-26 shows an example of the predicted distribution of liquid saturation along radial segments on Section 31 after dismantling the first heater. The numerical simulations were able to capture general trends of temperature and liquid saturation.
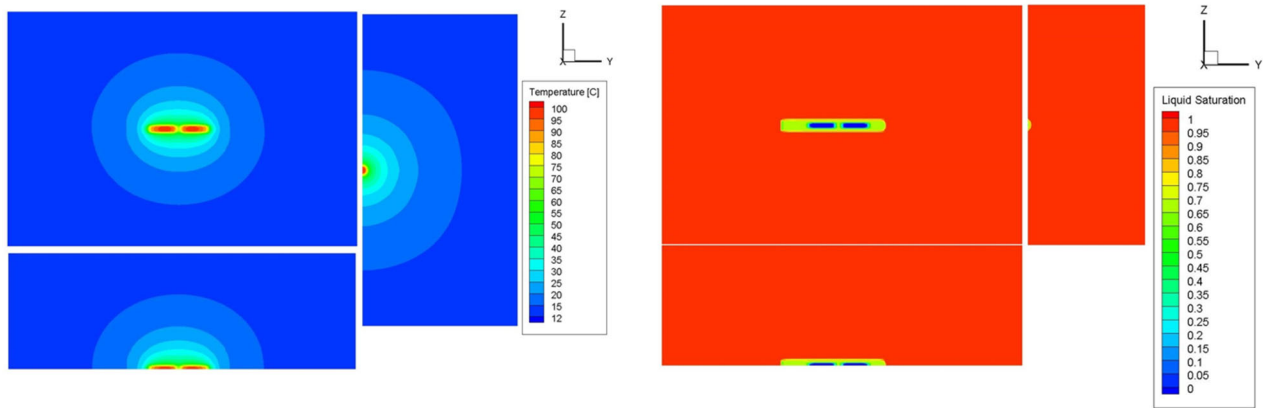
Figure 6.1-24. Predicted temperature (left) and liquid saturation (right) distribution for Stage 1 at 1,800 days.
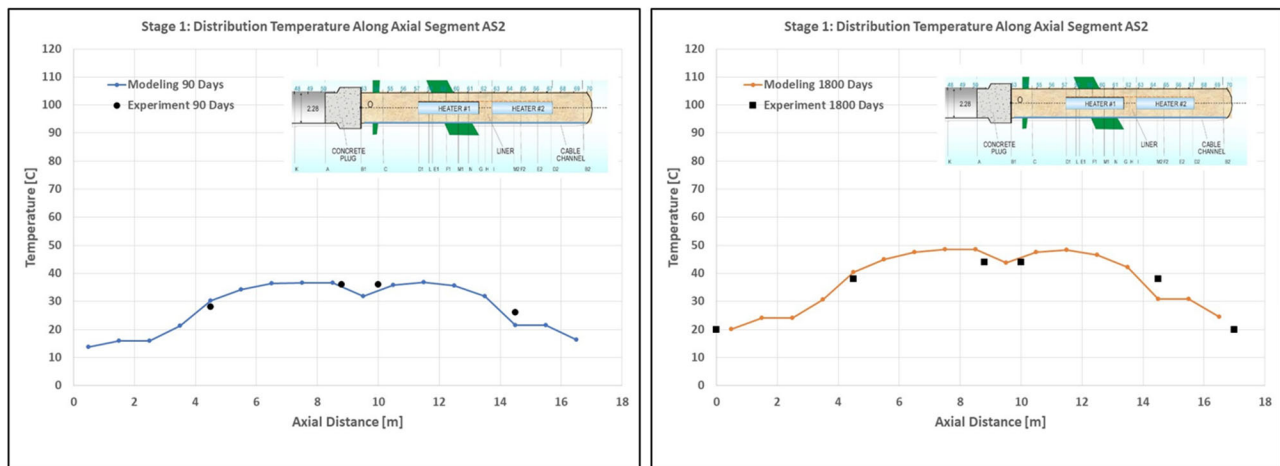
Figure 6.1-25. Comparison of predicted and measured temperature along axial segment AS2 at 90 days (a) and 1,800 days (b) for Stage 1.
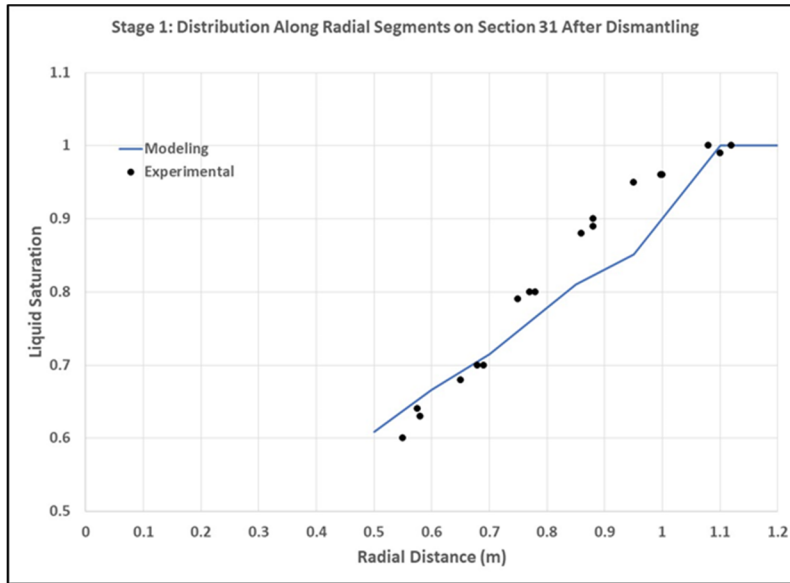
Figure 6.1-26. Predicted and measured liquid saturation along radial segments on Section 31 after dismantling of the first heater (Stage 2).

6.1.2.5.1. *Preliminary Sensitivity and Uncertainty Analysis*

To complement the results of the 3D thermal-hydrologic simulations conducted by the SNL team (Hadgu et al., 2020; Matteo et al., 2021, Chapter 2), preliminary sensitivity and uncertainty analyses were conducted for Stage 1 of the FEBEX *in-situ* test (Matteo et al., 2021, Chapter 3). The goal was to determine parameters that are important to define thermal-hydrologic conditions in the bentonite buffer and the host rock. To allow for multiple simulations, a 2D model with a reduced mesh size was used. TH simulations were made using PFLOTRAN to match experimental data. For Stage 1, simulations were run for a total of 1800 days with both heaters operating and using parameter values described in the report by Matteo et al. (2020).

Preliminary sensitivity analysis and uncertainty quantification were conducted by wrapping PFLOTRAN with an uncertainty quantification and optimization code (DAKOTA) as shown in Figure 6.1-27. The analysis was performed for ten input parameters listed in Table 6.1-1.
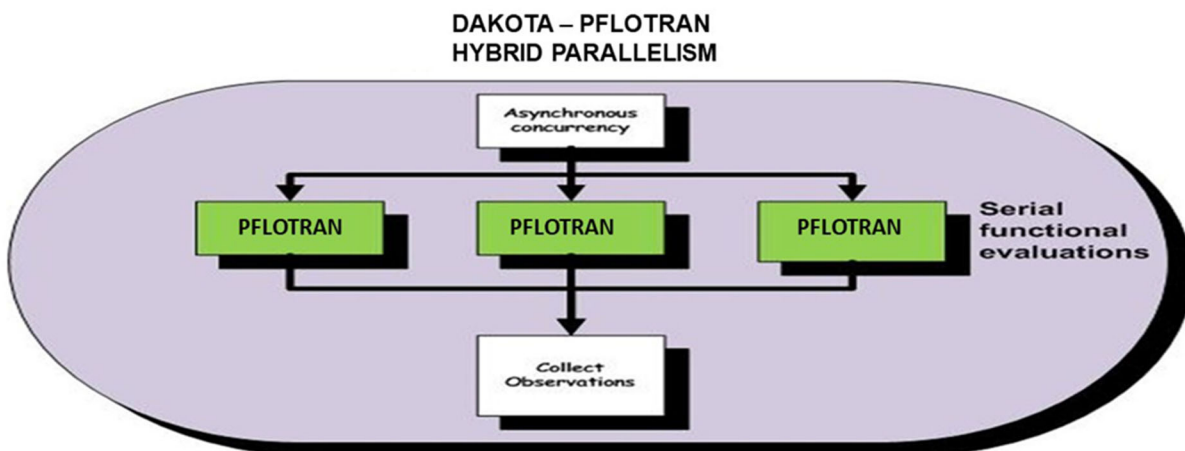
Figure 6.1-27. Schematic diagram of DAKOTA-PFLOTRAN hybrid parallelism.

Table 6.1-1. Ranges of the values of uncertain input parameters.

Input Parameter	Distribution Type	Value
Granite permeability, m²	lognormal	Mean: −18.0; Stand. Dev.: 1.0
Buffer permeability, m²	lognormal	Mean: −20.0; Stand. Dev.: 1.0
Plug permeability, m²	lognormal	Mean: −20.0; Stand. Dev.: 2.0
Po, MPa	uniform	Range: 20.0–200.0
van Genuchten α	uniform	Range: 0.1–0.3
Heater Power, W	uniform	Range: 1740.0–2390.0
Granite thermal conductivity, W/(m·K)	lognormal	Mean: 3.0; Stand. Dev.: 0.5
Buffer thermal conductivity dry, W/(m·K)	lognormal	Mean: 0.7; Stand. Dev.: 0.3
Buffer thermal conductivity wet, W/(m·K)	lognormal	Mean: 1.5; Stand. Dev.: 0.3
Plug thermal conductivity, W/(m·K)	lognormal	Mean: 3.0; Stand. Dev.: 0.5

Simulations showed a strong correlation between Heater 1 temperature and power, because the power directly controls the temperature. A good correlation was also found between the relative humidity and the unsaturated hydraulic parameters of the buffer. The relative humidity is very sensitive to the values of the inverse of the air entry pressure. Practically no correlation was found for the relationship between the dry thermal conductivity of the buffer and temperature.

6.1.2.5.2. Summary and Future Work

TH modeling of the Stage 1 and Stage 2 FEBEX *in-situ* experiment using the massively parallel reactive transport code PFLOTRAN was accomplished using HPC facilities at SNL. For the TH modeling, shrink/swell aspects and other structural deformational aspects of the bentonite barrier were neglected. Nonetheless the simulation results show a good agreement with some FEBEX measurements, while some disagreement with some others. In general, the modeling under-calculated humidity measurements, which may have been a consequence of the spatially constant initial conditions for bentonite wetting assumed in the modeling.

As to future work, the SNL team decided in FY21 to move away from further FEBEX modeling and deploy the massively parallel modeling framework to the new DECOVALEX-2023 Task C, which focuses on model interpretation and comparison for the FE Heater Test at Mont Terri. These activities are described in Section 6.3 below.

6.1.2.6. *Microstructural Analysis of FEBEX Samples, Hydration-Dehydration Effects, and Molecular Dynamics Simulations*

The 2015 disassembling of the FEBEX-DP provided DOE with a large number of samples of heat-exposed bentonite, steel liner, sensors, embedded metallic components (e.g., metal coupons), and their respective interfaces with other EBS and natural materials, which have since been used by SFWD scientists for further analysis and characterization. SNL scientists continued in FY21 their microstructural analyses of FEBEX samples in order to identify spatial heterogeneities of barrier materials near and far from EBS interfaces. These data can be used to obtain parameters for reactive transport models, which can be used to simulate the extent of chemical variations and heterogeneities (e.g., reaction fronts) at EBS interfaces and bulk barrier materials, and ultimately to evaluate the potential for long-term chemical-mechanical alterations in heated EB materials. The extent of barrier alteration due to interactions with fluids and other materials can cause porosity enhancement and reduction (i.e., clogging) of EB materials and associated interfaces. These interactions mainly involve mineral dissolution and precipitation along with transport, which has been a topic of investigation particularly in the assessment of EB alteration in reactive-transport models (Marty et al. 2015; Wilson et al. 2015; Xie et al. 2015).

In FY18 and FY19, SNL scientists conducted microstructural analysis on bentonite samples from FEBEX Section 49, using X ray Fluorescence (XRF), X-ray diffraction (XRD), and thermogravimetric analysis (TGA/DSC) analytical techniques (Jové-Colón et al., 2018; 2019a,b). In FY20, SNL scientists studied the FEBEX-DP bentonite samples to evaluate the effects of thermal loads over the distance from the heater (Jové-Colón et al., 2020). In FY21, SNL scientists conducted additional thermal analysis (DSC) with controlled hydration/dehydration cycles on FEBEX-DP bentonite samples at temperatures of 85°C and 150°C. The report by Jové-Colón et al. (2021) provides data for the dehydration steps and *in-situ* XRD analysis under controlled conditions with a defined dew point of ~58°C at a temperature of 85°C. The report also describes the results of molecular dynamics (MD) simulations of Na-Montmorillonite (Na-MMT) dehydration focusing on water transport at the smectite interlayer. This modeling effort was motivated by the TGA/DSC, water adsorption isotherm experiments, and more recently *in-situ* XRD analyses on FEBEX-DP bentonite samples to evaluate mechanism of water transport at the molecular level. A summary of these activities is given below.

6.1.2.6.1. *Thermogravimetric (TGA/DSC) Analyses of Bentonite Hydration*

Water adsorption/desorption behavior in expansive clay is key to this material swelling phenomena but also to water transport during hydration/dehydration processes. Thermal loads in deep geological nuclear waste repositories control RH conditions in the disposal galleries where bentonite is used as backfill barrier material. Therefore, chemo-mechanical responses and mechanisms of bentonite hydration/dehydration to changes in RH and temperature are crucial to the EBS performance. Cyclical TGA/DSC analyses under controlled RH and temperature supply important information on the kinetics of expansive clay hydration/dehydration and also provides insights on the hysteretic behavior of this process.

In FY20 and FY21, SNL conducted TGA/DSC experiments to evaluate the potential effect of grain size and duration of the hydration cycle for the FEBEX bentonite sample on the cyclical hydration/dehydration profiles, using samples with 2 μm, 38 μm and 75 μm (Jové-Colón et al., 2020; 2021). Appendix A of Jové-Colón et al. (2020) provides detailed results of studies of adsorption/desorption for bentonite close and far from the heater surface, and Figures 6 to 8 of Jové-Colón et al. (2020) show temporal TGA/DSC profiles of water adsorption and desorption cycles at 60°C as a function of time for the less than 2 μm, 38 μm and 75 μm bentonite samples.

Thermal analysis (thermogravimetric analysis, TGA, and Differential Scanning Calorimetry, DSC) were conducted using an STA 449 F3 Jupiter (Netzsch, Germany) with MHG humidity generator (ProUmid, Germany). The bentonite sample (ca. 20 mg), which was placed in a platinum crucible and loaded into the thermal analyzer, was subjected to a drying process prior to humidity cycling. Under a constant flow of dry nitrogen (200 ml/min) the specimen was heated to 150°C at 10°C/min and held for 30 minutes, then cooled to 85°C and held for about 60 minutes to ensure a dry starting point for analysis. Bentonite hydration was carried out under a flow of 200 ml/min humid nitrogen (dewpoint 58°C); and dehydration occurred under a 200 ml/min flow of dry nitrogen. After each hydration-dehydration cycle at 85°C, the specimen was dried by heating to

150°C under 200 ml/min dry N2 and holding for 30-60 minutes before cooling to 85°C and beginning the next cycle. The hydration-dehydration tests at temperature of 150°C were conducted using the procedure, but with no additional drying steps between each cycle.

Cyclical hydration/dehydration was provided to obtain key information about the adsorption/desorption rates of water, quantity of water adsorbed, and energetics of hydration/dehydration reaction. For the cyclical TGA/DSC analyses under controlled Relative Humidity (RH) and temperature of 60°C, bentonite samples were initially exposed to dry N2 heated at a rate of 10°C/min to 100°C holding this temperature for 30 minutes. Still under dry N2, the temperature was increased (10°C/min) to 150°C for another 30 minutes. Subsequently, the temperature was decreased to 60°C for 60 minutes to the expose the bentonite to a succession of dry and humid cycles (60% RH in the generator; 50% RH close to the sample) by flowing water-wet and dry N2 atmospheres to hydrate and dehydrate the samples. Figure 6.1-28a shows a representative temporal TGA/DSC profile of water adsorption/desorption cycles at 60°C as a function of time for the less than 2 μm sample.
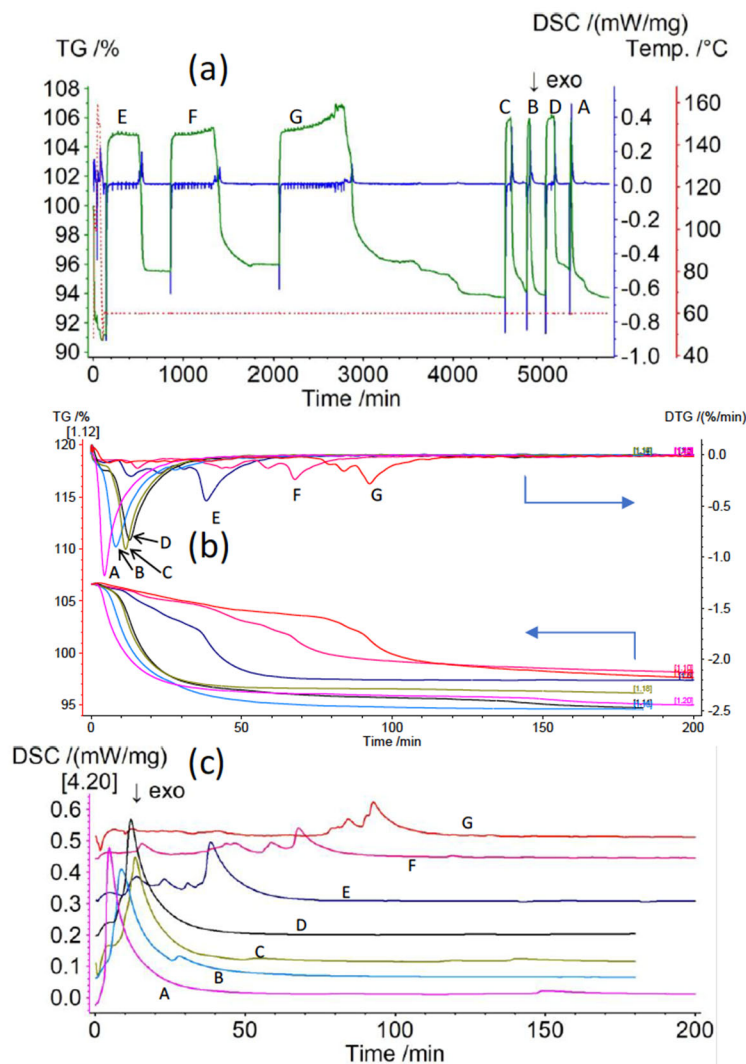
Figure 6.1-28. TGA, DTA, and DSC curves as a function of time for water adsorption/desorption cycles at 60°C for the <2 μm bentonite sample. (a) The green curve represents the thermogravimetric analysis (left y-axis). The blue curve stands for the DSC analysis (right y-axis). The red dotted line signifies the temperature (2nd right y-axis). The period of hydration was varied for each cycle, as depicted by the curve labels; A = 15 min, B = 30 min, C = 1 hour, D = 1.5 hours, E = 6 hours, F = 8 hours, and G = 12 hours. (b) TGA (lower) and DTA (upper) curves for the dehydration steps only, plotted against dehydration time. Curve labels identical to panel (a). (c) DSC measurements as a function of elapsed time for the dehydration steps; curves have been offset arbitrarily on the y-axis for clarity (Jové-Colón et al., 2021).

139

The green line Figure 6.1-28a depicts the mass of the sample as it responds to changing RH during water adsorption/desorption cycles. Figures 6.1-28b,c depict the desorption steps only, represented by TGA and differential TGA (or DTA) and DSC. These plots show that the dehydration behavior is dependent on the duration of preceding hydration. As the duration of the hydration step increases beyond two hours (curves E-G in Figure 6.1-28c), however, the subsequent dehydration becomes a more complex process, with a changing slope in the TGA curve and clearly shown as negative peaks in the DTA plots. Note that the DTA and DSC traces are essentially mirror images, since any loss of mass of the sample (DTA) is accompanied by a heat flow signal that is proportional (DSC). Similar data were obtained for the <75 μm bentonite samples at 60°C but for the dehydration steps only. Figure 6.1-28 shows an overall trend of increasing hydration time periods, in particular, with regards to endothermic peaks in the DSC thermograms. Jové-Colón et al. (2021) also demonstrated that the DSC curves as a function of time for the <2 μm bentonite sample for the dehydration steps at 85°C and 150°C are similar to those at 60°C up to a hydration time period of 120 minutes.

6.1.2.6.2. *Molecular Dynamics Modeling of Transport-Mechanical-Chemical Coupling Effects During Clay Dehydration*

Expansive clays such as those used in bentonite are phyllosilicate minerals that can adsorb a large quantity of water into interlayers resulting in very complex chemo-mechanical behavior in many environmental, geological (energy resources), and industrial systems – including the EBS in deep-geological nuclear waste repositories. Understanding THMC coupling effects during clay swelling/shrinking is key to the behavior of backfill bentonite material and water transport in the near-field environment. Molecular simulations provide a feasible approach to model the deformation of materials coupled with molecular behaviors of simulated systems. Unfortunately, most molecular dynamics simulations studying clay hydration/dehydration focus on structural and dynamics properties of water/ion in the clay interlayers at a certain hydration state. The deformation of materials from one hydration state to another, coupling with chemical alteration and water transport in the interlayer, remains not well understood. Furthermore, our knowledge regarding the thermodynamic state (e.g., gas, liquid, ice-like) and transport mechanism of water molecules in the clay interlayers and its effect on swelling/shrinking is unfulfilled, compared with the knowledge acquired for other layered materials such as graphene and graphene oxide. To address this knowledge gap, SNL researchers in FY21 continued to sue a combination of molecular dynamics (MD) simulations with the experimental approaches described above (i.e., thermogravimetric analysis (TGA), differential scanning calorimetry (DSC), and XRD experiments) to probe the atomic resolution dynamics of the dehydration process. Their results provide a molecular picture of the coupling nature of water transport mechanism and pathway, and the collapse of clay hydrated structure (Jové-Colón et al., 2021).

Figure 6.1-29 gives an example image of the MD simulation setup used to study the water transport mechanism in the interlayer and structural transformation of hydrated Na-MMT during the dehydration process. The Na-MMT particle, with 10 interlayers in total, has 2 edges facing the vacuum. The method to build the Na-MMT particle can be found in previous work (Ho et al., 2020). The MD simulations demonstrated that clay dehydration is a two-stage process. In the first stage, water transport exhibits an advection mechanism as mass loss is linear with time. The first stage is associated with the evacuation of water molecules from the hydrophobic sites and also with the fast removal of the first few water molecules from the Na+ ion hydration shell. The second stage represents the slow desorption of the last 1-2 water molecules from the Na+ ions. Movement of water molecules through the interlayer in the second stage follows a diffusion mechanism. These conclusions are supported by the results obtained from the TGA/DSC calorimetry and *in-situ* XRD experiments reported in Section 6.1.2.4.1.
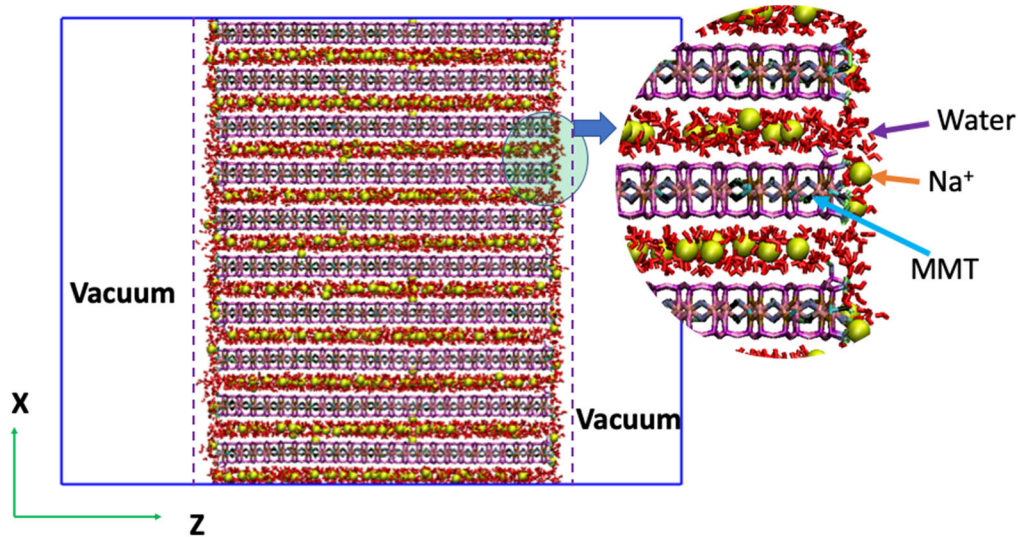
Figure 6.1-29. Simulation system used to study the dehydration process of Na-MMT. The simulation box size is 150 × 31.06 × 200 Å3. When applying periodic boundary conditions for all directions, the Na-MMT particle becomes infinite in the x and y directions and finite in the z direction (Jové-Colón et al., 2021).

6.1.2.6.3. *Planned Future Work on FEBEX Sample Analysis*

SNL's planned work for FY22 on FEBEX-DP samples includes the following activities:

- Continuation of cyclical thermal analyses conducted at higher temperature and controlled moisture conditions to evaluate the effect on hydration/dehydration profiles and *in-situ* XRD analyses under controlled moisture and temperature conditions as soon as the equipment setup becomes available.

- Extending thermal analyses into other types of bentonite clay material.

- Expanding MD simulations on dehydration phenomena at the clay interlayer.

- Expand the work on montmorillonite dehydration in the presence of K+ and Ca++

- Evaluate the effects of surface charge density on montmorillonite dehydration and water transport

- Exploratory studies of H_2(gas) adsorption and transport/mobility in the interlayer of clay (wet, or dry) through MD simulations

- Thermodynamic analysis of clay hydration and dehydration from MD simulations

6.1.2.7. Diffusion Experiments of FEBEX Bentonite Samples

In past years, LBNL scientists used bentonite samples from heated and unheated parts of the FEBEX heater test to investigate potential effects of temperature-related alterations on diffusion and sorption properties (Zheng et al., 2020, Section 3). The focus in FY20 was on the diffusion U(VI) through compacted smectite, comparing samples from field-heated (95°C, 18-years) and cold-zone (20°C) FEBEX bentonite under different chemical conditions. In FY20, diffusion experiments were conducted with 95°C heated and 20°C cold-zone purified FEBEX bentonite at a bulk density of 1.25 kg/L. The experiments were conducted at a constant ionic strength (0.1 M NaCl) at pH 7 in the presence of 0.1 mM Ca or 2 mM Ca. The average normalized ^{3}H flux at steady state ($\geq$50-hr) for ^{3}H through-diffusion was not significantly different across samples, with values ranging from $1.38 \pm 0.13 \times 10^{-3}$ m/day to $1.73 \pm 0.17 \times 10^{-3}$ m/day. U(VI) in-diffusion experiments conducted in the presence of 2 mM Ca showed the diffusive loss of U(VI) from the high concentration reservoir was indistinguishable for the heated and cold-zone bentonite and U(VI) traveled less than 1 mm into the clay over the 30-day diffusion period. While lower U(VI) adsorption was previously measured on the heated-zone FEBEX bentonite compared to the cold-zone bentonite, it is possible that differences in U(VI) diffusion due to differences in adsorption may only become apparent over much longer time periods.

In FY21, LBNL launched a new diffusion testing campaign with focus on selenium (Zheng et al., 2021). While present at lower total amounts than U, ^{79}Se is a major driver of the safety case for nuclear waste disposal due to its long half-life (3.3×10^5 yr) and presence as relatively mobile anionic species under a range of chemical conditions (e.g., HSe$^-$, SeO$_3^{2-}$, SeO$_4^{2-}$). Se redox chemistry is complex, with oxidation states ranging from -II to +VI over environmentally relevant conditions. While Se(-II) and Se(0) are relatively immobile due to the formation of low solubility precipitates, Se(IV) and Se(VI) exist as the oxyanions selenite (SeO$_3^{2-}$) and selenate (SeO$_4^{2-}$) and are highly mobile in water due to their high solubility. Se adsorption to clay minerals is quite low compared to other important radionuclides such as U. K$_d$ values for selenite adsorption to smectite are in the range of 1^{-10} L/kg (compared to values up to 10^4 for U(VI)).

6.1.2.7.1. Experimental Design and Results

Experimental results from ^{3}H and Se(VI) through-diffusion experiments through a well-characterized, purified montmorillonite source clay (SWy-2) are provided in Zheng et al. (2021, Section 5). Instead of using FEBEX samples as before, the clay materials were obtained from the Clay Minerals Society. Experiments were conducted under a single ionic strength (0.1 M) and three different electrolyte compositions representing pure Na, pure Ca, and a Na-Ca mixture in order to probe the effects of electrolyte composition on clay microstructure, Se(VI) aqueous speciation, and ultimately diffusion. The montmorillonite was purified in order to remove minor impurities (quartz, feldspars, and calcite). The remaining clay fractions were combined into a glass beaker, dried at 60°C and ground in ball mill with tungsten carbide balls. Diffusion experiments were conducted with purified, pre-equilibrated montmorillonite at a dry bulk density of approximately 1.3 kg/L using the diffusion cell design shown in Figure 6.1-30. The diffusion cells used for experiments were machined in-house at LBNL, which are based on the design of (Van Loon et al., 2003), with dimensions adjusted to accommodate smaller samples.

Experiments were conducted under a single ionic strength (0.1 M) and three different electrolyte compositions: 0.1 M NaCl, 0.033 M CaCl2, and 0.085 M NaCl + 0.005 M CaCl2, representing pure Na, pure Ca, and a Na-Ca mixture, respectively. All experiments were performed at room temperature at pH 6.5 in equilibrium with atmospheric conditions (~20% O$_2$ and 400 ppm CO$_2$). The diffusion experiment was conducted in three phases: (1) saturation, (2) tritiated water (^{3}H) diffusion, and (3) Se(VI) diffusion. The clay was saturated by circulating 200 mL of background electrolyte at both ends of the cell at approximately 1 mL/min using a peristaltic pump for 40-42 days. After the saturation period, the ^{3}H through-diffusion phase was started by replacing the background electrolyte solutions with a high ^{3}H reservoir containing background electrolyte spiked with 30 nCi/mL ^{3}H (200 mL) at one end and a low ^{3}H reservoir containing only background electrolyte (20 mL) at the other end. The high concentration reservoir was sampled at the beginning and the end of the ^{3}H diffusion experiment and did not change significantly over that time period. The low ^{3}H reservoir was changed at time intervals of 3-36 hr, and the ^{3}H concentration was measured in the low reservoir samples by liquid scintillation

counting. An in-house built autosampler using a 3D printer (Creality Ender 3Pro) as the base was used to change the low reservoir samples at regular time intervals. The ^{3}H concentration in the low reservoir never exceeded 0.5% of the concentration in the high reservoir. The ^{3}H diffusion was continued for 16 days. After this period, the high concentration reservoir was replaced with a Se(VI)-spiked solution containing 1.0 mM sodium selenate in background electrolyte with a total volume of 190 mL, marking the start of the Se(VI) diffusion experiment. The low concentration reservoirs containing only background electrolyte (5-10 mL) were changed at time intervals of 12-48 hours for the first 44 days, then 48-170 hours for the remaining 33 days and Se concentrations were measured by ICPMS. Se concentrations in the low reservoir never exceeded 1% of the concentration in the high reservoir. Subsamples of the high concentration Se(VI) reservoir were collected at the beginning and end of the experiment and did not change significantly over the experiment. At the end of the Se(VI) diffusion period, the diffusion cells were disassembled and the clay plug was extruded using the PEEK packing rod and sliced into thin slices. The thickness of the clay slices was measured using a digital caliper with a precision of 0.1 mm. Samples were analyzed for Se by ICP-MS (Perkin-Elmer Elan DRC II) after acidification and dilution with ultrapure (ultrex grade) 0.15 M nitric acid and internal standard addition.
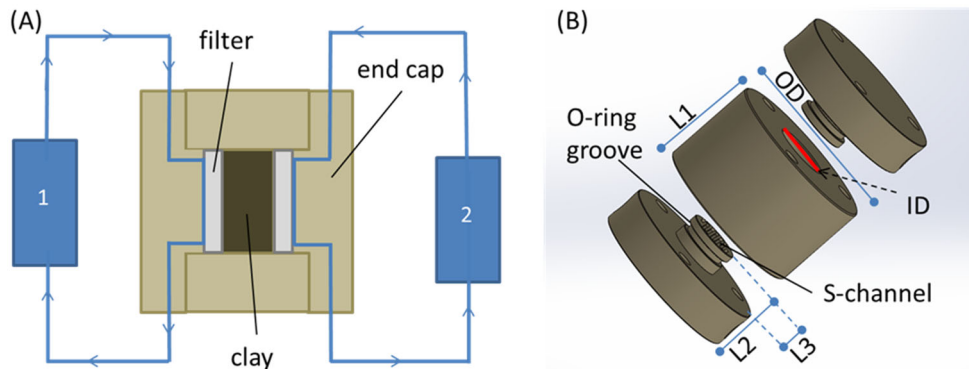
Figure 6.1-30. Schematic of diffusion cells machined in house. (A) Cross-sectional view of the diffusion cell showing the clay plug, filters and two solution reservoirs. During saturation and ^{3}H diffusion, both reservoirs are used, and during U(VI) in-diffusion, reservoir 2 is removed and the cell is plugged at that end. (B) Detailed schematic of the cell design, with groves for the o-rings and an S-shaped channel which allows the solution to distribute evenly over the entire filter of the diffusion cell. The dimensions for the cell are as follows: OD=30 mm, ID=9.5 mm, L1=17.8 mm, L2=12.2 mm, L3=4.9 mm. O-rings measure 7.5 mm ID and 9.5 mm OD.

6.1.2.7.2. *Experimental Results and Modeling Analysis*

The diffusion results were evaluated by calculating a normalized mass flux across the sample, as a function of time. Results obtained for selenium diffusion were compared to tritium as a conservative tracer. Normalized flux for Se(VI) (Figure 6.1-31) reached steady state after approximately 300 hours, with the Ca cell showing the greatest normalized flux. Notably, the differences in the normalized flux between the cells for Se are much greater than was observed for tritium and therefore are not due to differences in total porosity alone. Rather, differences in aqueous Se speciation, clay swelling, and effective porosity in the presence of Na and Ca are expected to play a large role in the diffusive flux of Se(VI).

LBNL also looked at clays slices to analyze selenium clay profile concentrations from HCl extractions at the end of the diffusion experiments, as shown in Figure 6.1-32. Clay slices ranged in thickness from 0.3 to 0.9 mm. The Se concentrations are expressed in terms of the total porewater volume, and follow the trend Na<Na-Ca<Ca. This trend is consistent with the Se diffusion data which suggest that the Ca-saturated clay has the highest effective porosity for Se(VI). Se concentrations in the clay slice closest to the high concentration reservoir (at ~4.5-5.0 mm) are 0.18, 0.25, and 0.77 mM for the Na, Na-Ca, and Ca cells, respectively. The profiles in all three cells are linear with depth as expected for steady-state conditions. These data were then used in conjunction with diffusion data to model adsorption and effective porosity under the different electrolyte conditions.
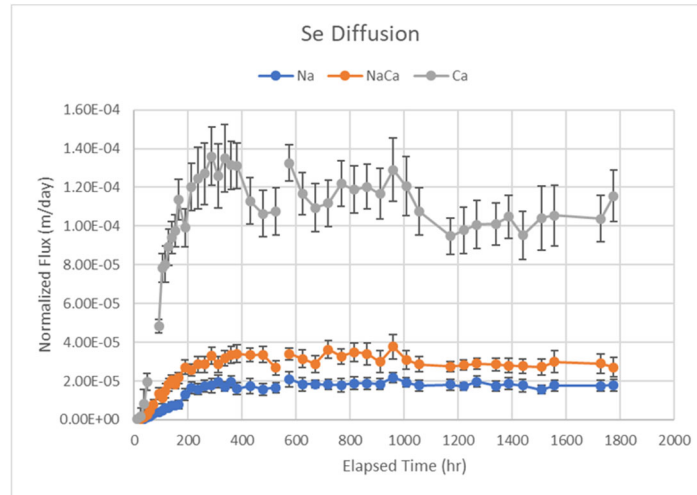
Figure 6.1-31. Normalized Se flux in the three diffusion cells. Error bars represent analytical error (Zheng et al., 2021).
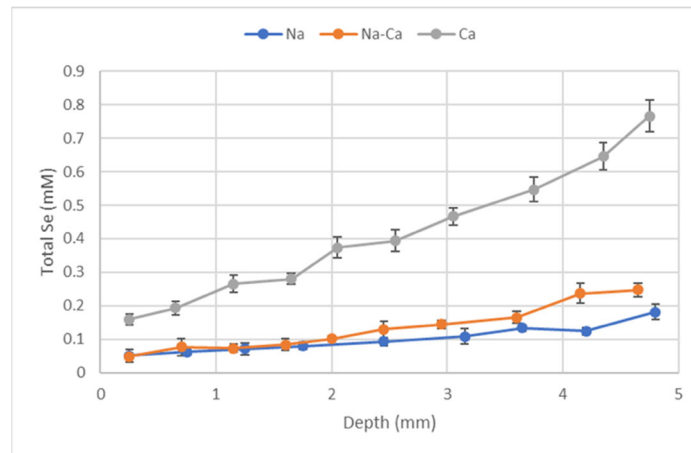
Figure 6.1-32. Se profiles extracted from clay using 0.5 M HCl at the end of diffusion experiments. Se concentrations are expressed as a concentration in the total porewater volume (Zheng et al., 2021).

Modeling of diffusion experiments was carried out using CrunchClay (Steefel et al., 2015; Tournassat and Steefel, 2019a), which is currently one of only two codes that can handle diffusion processes in the diffuse layer, when the solution is not electroneutral, and for which coupled interdiffusion processes must be taken into account to model diffusion properties with a mechanistic approach (Tournassat and Steefel, 2019b). CrunchClay has the ability to treat both electrical double layer and bulk porosity with differing anion and cation diffusivities, which makes it possible to simulate the diffusion of a range of tracers with different charges in a single run, and with the same input parameters. CrunchClay also has surface complexation and cation exchange modeling capabilities, thus making it possible to couple mechanistic adsorption models with diffusion models in clay media. The goal of modeling is to derive consistent diffusion and adsorption parameters for Se, ^{3}H and other trace elements as a function of ionic strength and electrolyte composition, which will be probed experimentally in this project. A summary of the diffusion cell parameters, including an average normalized flux at steady state (>100 hr) is shown in Table 5.1 of the report by Zheng et al. (2021).

In a first step, HTO diffusion data were modeled considering that the whole porosity was accessible to HTO (Figure 6.1-33). These calculations evinced differences of connectivity in the diffusion pathways (tortuosity parameter) as a function of pore water composition. In order to model diffusion through the clay, the diffusion through the filters at either end of the cell must also be considered. Notwithstanding the error in the parameters estimation because of the filter effects, diffusion experiments and simulation results showed a clear increase

of the connectivity with a change of electrolyte from Na dominated to Ca dominated pore water composition. This change is interpreted as a consequence of differences in microstructure driven by pore water composition differences, and hence surface composition differences: Ca dominated surfaces have the tendency to stack clay layers, and so to open larger inter particles pores compared to Na dominated surfaces. This finding is consistent with SeO42- diffusion results, showing a large increase of SeO42- steady state flux value with increasing Ca concentration in the system. As Ca concentration increases, the volumetric proportion of porosity water influenced by the vicinity of charged clay surfaces decreased because of clay layer stacking (Tournassat and Appelo, 2011). Consequently, the proportion of porosity accessible to SeO42- increased, leading to larger steady state fluxes. Reactive transport simulations with CrunchClay are on-going to quantify this phenomenon.
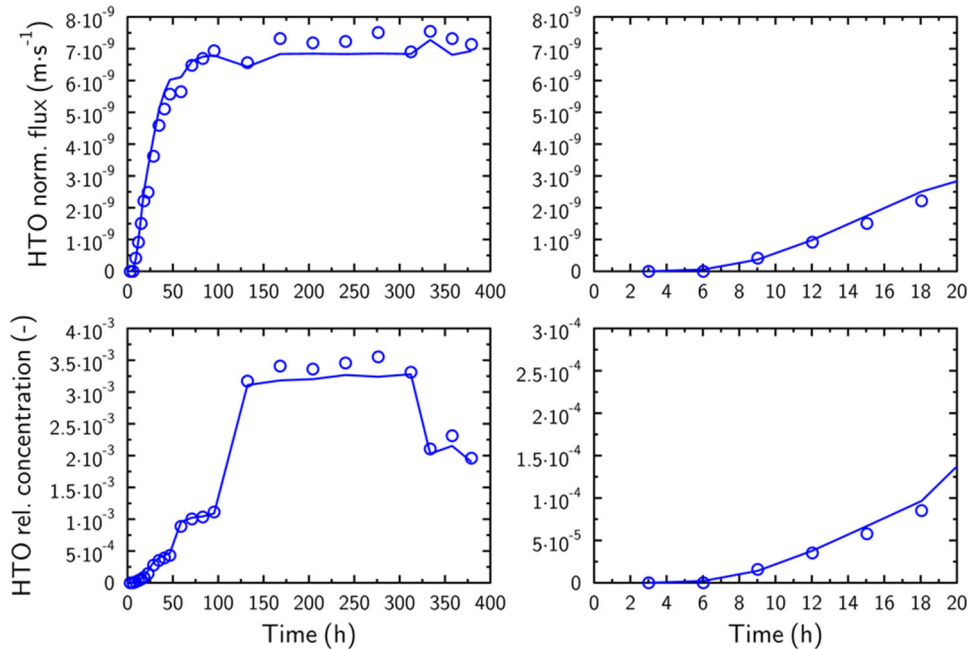
Figure 6.1-33. Modeling (lines) of ³H (HTO) diffusion in experiment (circles) with 0.1 M NaCl background electrolyte composition. Top: HTO normalized flux. Bottom: HTO relative concentration (Clow/Chigh).

6.1.2.7.3. Summary and Future Work

In FY21, ³H and Se(VI) through-diffusion experiments were conducted with compacted montmorillonite at a bulk density of approximately 1.3 kg/L. The experiments were conducted under a single ionic strength (0.1 M) and three different electrolyte compositions: 0.1 M NaCl, 0.033 M CaCl2, and 0.085 M NaCl + 0.005 M CaCl2, representing pure Na, pure Ca, and a Na-Ca mixture, respectively. Results showed that both ³H and Se diffusion was greatest in the pure Ca system and lowest in the pure Na system. These results are consistent with an increase in pore connectivity from Na dominated to Ca dominated pore water composition. This change is interpreted as a consequence of differences in microstructure driven by pore water composition differences: Ca dominated surfaces have the tendency to stack clay layers, and so to open larger inter particles pores compared to Na dominated surfaces. Differences in Se diffusion as a function of electrolyte composition are even greater, with Se normalized fluxes approximately 6 times higher in the pure Ca system compared to the pure Na system. This suggests that the accessible (or effective) porosity for Se in the Ca system is higher than for the Na system, likely due to differences in clay stacking, electrical double layer, and Se(VI) aqueous speciation.

Future work will focus on refining the ³H diffusion model, including the filter diffusion model, and modeling the Se(VI) diffusion through montmorillonite in the three different electrolyte compositions. The study will also include investigations of redox transformations of Se in clay systems and the effect on Se transport.

6.1.2.7.4. *Microbial Analysis of FEBEX Bentonite Samples*

Understanding the fate of microbial communities in EB materials is important for a variety of reasons, for example because of microbial controls on canister corrosion and because the capability of microbes to metabolize H_2 affects gas pressure behavior. In FY21, LBNL scientists continued experimental microbial investigations of materials collected from the FEBEX experiment, using samples representative of high heat, intermediate heat, and control temperature zones (Villar, et al., 2020; Bárcena, 2015). The microbial experiments were designed to determine if these materials possess microbial communities capable of metabolizing H_2 or other substrates, and how the FEBEX treatment impacted those capabilities. In FY19, two sets of materials were tested from a 'heater zone' (BD-48-6) and from a 'cold zone' (BD-59-10). In FY20, two samples were added: from a 'mid high temperature' (BD-48-5) and a 'mid low temperature' (BD-48-4). In FY21, the experiments were continued to completion and the samples were disassembled to perform a final analysis (Zheng et al., 2021).

The experimental procedure was as follow. Bentonite samples were placed horizontally on a rocking table and incubated at 35°C. To monitor activity, gas composition of the serum bottle headspace was analyzed periodically. Gas analysis was performed on a Shimadzu GC-8AIT with Ar carrier gas, which allowed for simultaneous quantitative determination of H_2, O_2, N_2, and CO_2. GC conditions were as follows: Ar flow 0.4 kg/cm2, detector and injection temperature 150°C, Column temperature 35°C, 80 mA current, CTRI packed column. Calibration of H_2, O_2, N_2, and CO_2 was completed prior to sampling bottles with known concentrations of gases. Samples were analyzed immediately after removing from the incubator and replaced after sampling. The experimental procedure included the sample incubation, DNA extraction, measurements of O_2, H_2, CO_2, pH, solids content, DNA sequencing showing Taxonomy by Phylum, and cation and anion analytical analyses. A detailed description of the sample preparation is given in Chapter 11 of Rutqvist et al. (2020) and Chapter 6 of Zheng et al. (2021, Section 6).

Four experiments were completed. Experiment 1 focused the development of the experimental protocols. Experiment 2 consisted testing the high heat samples (48-6) and the control, non-heated sample (59-10). On Day 150, the samples were re-gassed to the original gas composition due to low H_2 in the 59-10 samples, and again with the H_2 mix only for the 59-10 samples only on day 350, which lowered percent CO_2 content from 8% to 4%. Gas consumption was only observed in the 59-10 samples, and was not evident until Day 50, when loss of H_2 and O_2 was observed. Note that the rate of H_2 consumption in the replicates was not consistent, with a range of consumption rates observed. No significant loss of gas was seen in the controls and 48-6 sample. Example results of the DNA microbial analysis are given in Figure 6.1-34. The 48-6 sample had very low DNA extraction amounts, but results show a variety of species present. In contrast, the 59-10 samples show enrichment of a specific organisms which have the potential for hydrogen metabolism, including Actionbacerium, Firmucutes, and Acidobaceria (Giguere et al., 2020; Greening, 2015; Piche-Choquette, 2019; Kalam et al., 2020). The results of the DNA extraction indicate that certain organisms existing on the clay can become active in the non-heated clay.

Experiment 3 included testing two intermediate heated samples, 48-5 and 48-4, and showed the important role of solid to solution ratio in the rate of community development. Experiment 4 had the same sample set as Experiment 3, with the addition of groundwater (GW) media based on pore water composition from compacted MX-80 clay (Bradbury and Baeyens, 2003). Contrary to the 2nd experiment incubations, the gas consumption showed more consumption of oxygen and production of CO_2, and only two of the four 59-10 replicates demonstrated H_2 consumption, one much more than the other. This clearly indicates that the capacity for H_2 oxidation is retained in the FEBEX samples, with the possible exception of the hottest and direst samples. It also indicates that other metabolisms are also possible. The consumption of O_2 and increase in CO_2 are clear evidence for an active microbial community. At this point it is unclear what other metabolisms are, but it further supports the importance of considering the metabolic potential of barrier materials. One of the reasons that H_2 metabolism was less frequent within the individual samples as that the oxygen levels at setup may have played a role selecting for particular organisms, or simply that a different community developed in these sets of samples. The results of geochemical measurements of Experiment 4 showed that there was no significant difference between the samples (pH 6.60) and sterile controls (pH 6.63), and there no correlation of solids

content was seen with CO_2, O_2, or H_2 composition. There are differences in the cation and anion content in the GW samples, notably higher sulfate, Na, and Cl. Some of the cations were affected by the solids content.

Overall, the results from these experiments indicate that clay materials maintain microbial communities with potential for microbial growth. However, the material from the hot zone did not show that potential for the time scales in these experiments. Whether this is due to the heating or the drying or both is unknown at this point. Furthermore, the specific communities that develop appear sensitive to the gas composition and solids content. Because no growth was observed in the control sample this observed enrichment of communities is derived from bacteria existing in the clay prior to the start of incubation. While long by laboratory standards, these experiments are clearly extremely short by the time scales of repository dynamics. At that time scale it is clear that microbial activity within the barrier material is likely to be significant. Given the limitations in moisture and other chemical species, it is reasonable to assume that this microbial activity is most likely to be concentrated along fractures and at the formation boundaries. Further work should focus on the variety of metabolisms possible from the inoculate community present within the barrier material and how specific chemical and physical conditions control its rate of growth.
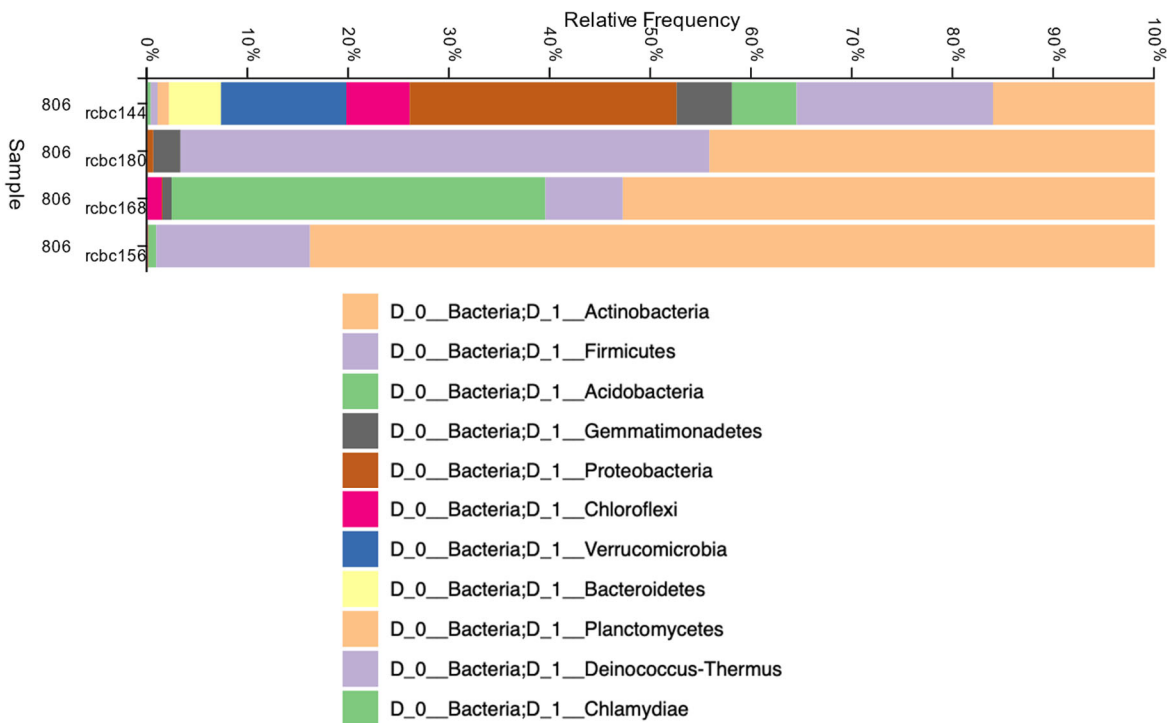
Figure 6.1-34. DNA sequencing results showing Taxonomy by Phylum. ID -144 is 48-6; IDs 180, 168,156 are 59-10 samples.

6.1.3. Research Activities Related to HotBENT Field and Lab Experiments

6.1.3.1. Introduction to the HotBENT Experiment

The HotBENT experiment, a full-scale high-temperature heater test (with a target maximum temperature of 175°C to 200°C) in a fractured crystalline rock environment, is currently being installed in the same tunnel where the FEBEX *in-situ* test was performed at the GTS. The key objective of the experiment is to test whether clay-based barriers can withstand temperature much higher than the 100°C threshold and to evaluate whether strongly elevated temperature would trigger mechanisms compromising various engineering barrier functions and the host rock. The HotBENT project, involving a large-scale test and accompanied by a systematic laboratory program and modeling effort, will evaluate the temperature effects under realistic conditions of strong thermal, hydraulic and density gradients, which cannot be reproduced in the laboratory (Section 3.3.3).

As of writing this report, installation has been finalized and the heating activities just started on September 9, 2021. The experiment is constructed in a modular fashion, whereby a module represents a heater rested on a bentonite block pedestal and encapsulated by a granular bentonite backfill. Modules differ in their design temperature, bentonite type, experimental duration, and whether a liner is used or now. The two modules deepest in the drift are separated from the others by an insulation plug to enable excavation of part of the experiment with minimal perturbations to the remaining modules. The THM evolution of the HotBENT experiment is monitored with ~1200 instruments, including temperature, mechanical pressure, hydraulic pressure, water content, saturation, humidity, displacements, gas concentration, and gas pressure.

LBNL scientists participated on the HotBENT project since the very beginning, including the initiation of the idea of a large-scale high temperature field test (Vomvoris et al., 2015), and conducted numerical modeling to support the experimental design. For example, Zheng et al. (2018) developed models with a simple geometric setup, both 1D or 2D, with consideration of coupled thermal, hydrological, mechanical and chemical (THMC) processes. Zheng et al. (2019a) developed a 3D THM model to further understand the evolution of all the design components. However, these simulations were conducted based on bentonite parameters that are similar to those of the FEBEX bentonite in the *in-situ* test (ENRESA, 2000). In April 2020 (Kober, 2020), the design for HotBENT was completed and LBNL scientists recently adapted their previous models to account for the final design and conduct a new set of predictive THMC modeling for the experiment. A summary of these revised design simulations is given in Section 6.1.3.2 below. In addition, LBNL conducted several bench-scale mock-up laboratory experiments featuring a cylindrical bentonite column with a 200ºC heater in the middle (Section 6.1.3.3). These provide complementary data on high-temperature effects, using geophysical imaging techniques to interrogate the bentonite samples during the test and allowing for detailed post-mortem examination of heated bentonite. LANL researchers meanwhile initiated hydrothermal autoclave experiments probing the thermally-induced reactions to be expected in the full-scale HotBENT test at GTS. The experiments include Wyoming bentonite (FE) and/or Czech bentonite (BCV) + low carbon steel + Grimsel Granodiorite synthetic groundwater (Section 6.1.3.4).

SFWD scientists from several National Labs are expected to work on different aspects of the HotBENT field and lab activities for years to come. As described in Section 3.3.3, the field experiment will run for multiple years and will provide extremely important data on barrier performance in high-temperature repositories.

6.1.3.2. Predictive Modeling of HotBENT

6.1.3.2.1.   Model Development

Zheng et al. (2020) developed a 1D axi-symmetric THC model to study the geochemical changes of MX-80 bentonite in HotBENT. This model was initially based on the THMC model for the FEBEX *in-situ* test, with a few major differences: the temperature is now fixed at 200ºC at the heater, the bentonite is Wyoming bentonite (MX-80) instead of FEBEX bentonite, and the hydraulic pressure in granite is 2 MPa which is the design choice in order to ensure a speedy hydration of bentonite in HotBENT. Note that the natural hydraulic pressure surrounding the FEBEX tunnel is 0.7 MPa (ENRESA, 2000), thus this will require artificial saturation of the host rock. In FY18, the coupling of codes TOUGHREACT V2 and FLAC was upgraded with

TOUGHREACT V3.0-OMP (Xu et al., 2014), which has several major advantages: one of the them is the OpenMP parallelization of chemical routines on multi-core shared memory computers, which significantly decreases the computation time. Modeling was performed using the existing axi-symmetrical model domain and mesh from the previous simulations (see Figure 6.1-27 of the FY20 International report by Birkholzer et al., 2020).

Based on the results of the sensitivity analysis of the THMC model for the FEBEX *in-situ* test, the key parameters affecting the hydration of bentonite are permeability of granite, permeability and water retention curves of bentonite, and the vapor diffusion coefficient of bentonite. As in previous models for *in-situ* tests (Samper et al., 2008; Sánchez et al., 2012), the fractured granite is represented as a homogeneous porous medium with an equivalent permeability of 2×10^{-18} m^2 was used (Zheng et al., 2020, Table 7-1). The model also takes into account the effect of thermal osmosis on a fluid flux (Zhou et al., 1999a; Dirksen, 1969), and the liquid flux caused by thermal osmosis term can be added to the Darcian terms (Ghassemi and Diek, 2002; Zhou et al., 1999a). In the current model, a kT of 1.2×10^{-12} m^2/K/s is used.

6.1.3.2.2. *Model Predictions*

TH Modeling Results

With the temperature fixed at 200°C at the heater, the thermal perturbation of the bentonite and host rock in HotBENT will be significant. For example, a point located 3 cm away from the heater quickly reaches 190°C (Figure 6.1-33). In the middle of the bentonite barrier, the temperature will reach about 128°C, and 6 cm away from the granite host rock, the bentonite temperature will reach about 97°C. The temperature at the bentonite/granite interface will rise to roughly 87°C (not shown in the figure). The temperature in the granite host rock decreases to 75°C about 1.6 m away from the heater, and to 40°C about 4 m away from the heater (Figure 6.1-35). At 10 m depth into the granite host rock (R = 11 m), the temperature is about 20°C. The thermal disturbance penetrates about 25 m into the granite.

Typically, bentonite near the heater goes through desaturation/re-saturation cycling: evaporation due to high heat dries the bentonite, and re-saturation occurs once the hydraulic pressure overcomes the vapor pressure. However, the time span of such a cycle depends on the temperature, the permeability of bentonite, and the hydraulic pressure in the granite host rock. Model results show that re-saturation for HotBENT is much faster than in the FEBEX *in-situ* test (Zheng et al., 2019a,b), because the permeability of the bentonite is higher and the hydraulic pressure in granite is higher, despite the higher temperature.

Figure 6.1-36 shows the evolution of liquid saturation and relative humidity at several radial distances from the heater. Most parts of the bentonite barrier become fully saturated in about 3 years, but an area about 3 cm away from the heater remains slightly unsaturated (95% to 98% liquid saturation) until the end of the simulation period, because hydraulic pressure cannot exceed the high gas pressure in this region.
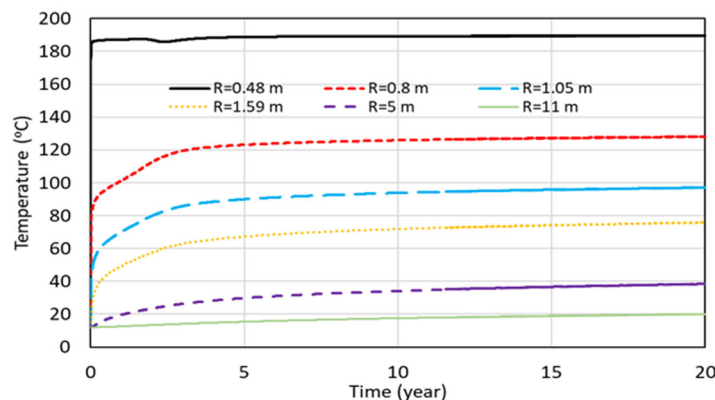
Figure 6.1-35. Temporal evolution of temperature at several radial distances. Note that points at R = 0.48 m, 0.8 m, and 1.05 m are located within the bentonite barrier, and the rest of the points are located in granite.
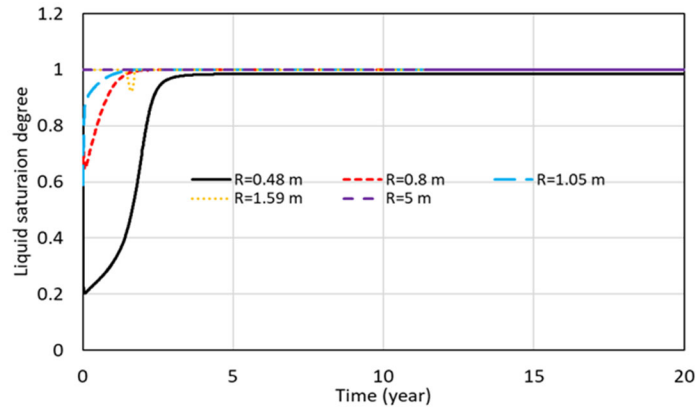
Figure 6.1-36. Temporal evolution of liquid saturation at several radial distances. Note that points at R = 0.48 m, 0.8 m, and 1.05 m are located within the bentonite barrier, and the rest of the points are located in granite.

Chemical Modeling Results

Zheng et al. (2020) found that the evolution of Cl, which represents conservative chemical species is controlled by three processes: water displacement/advective transport, diffusion, and evaporation/condensation. As a result of the combination of these processes, the Cl profile can be divided into three areas: from radial distance of 0.45 m to 0.48 m, a narrow area (referred as "evaporation zone") with a high concentration due to continuous evaporation, and from radial distance of 0.48 m to 0.8 m, a condensation area (referred as "condensation zone"), which are shown in Figure 6.1-37. Despite other chemical reactions are involved in the transport of sulfate, its radial and temporal distributions are similar to those of chloride. The MX-80 bentonite contains a small amount of gypsum that quickly dissolves uniformly along the entire bentonite barrier, leading to a uniform rise of the sulfate concentration shortly after the simulation starts, but later it behaves just like chloride, and the spatial distribution is dominated by transport processes including displacement by penetration of granite water, evaporation/condensation, and diffusion.
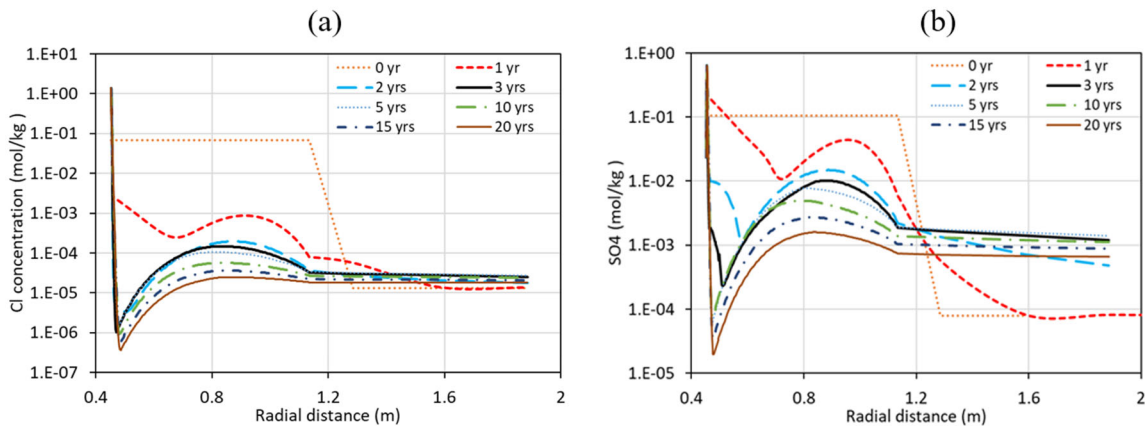
Figure 6.1-37. Radial profiles of Cl (a) and SO4 (b) concentrations at several times. Note that the bentonite/granite interface is located at R = 1.13 m.

Though calcium is involved in many chemical reactions related to calcite and gypsum dissolution/precipitation as well as cation exchange, the radial trend of calcium (Figure 6.1-38a) is identical to that of chloride: an "evaporation zone" that is characterized by high concentration, a "condensation zone" that features low concentration, and a "diffusion zone" with a decreasing concentration from bentonite to granite. Calcite dissolution/precipitation and precipitation of the anhydrite are the major reactions that affect the concentration of calcium. The model shows precipitation in the "diffusion zone." In the "condensation zone," dissolution

150

dominates, but precipitation appears at the boundary between the "diffusion zone" and the "condensation zone." There is re-precipitation in the "evaporation zone," i.e., calcite dissolves in the first 5 years and then re-precipitates, although the volume fraction therein is still lower than the initial value (negative value in Figure 6.1-38b). Precipitation of the anhydrite is also observed in the model. Both gypsum and anhydrite are calcium sulfate minerals, but gypsum is the hydrous form, with two water molecules in the chemical formula. Anhydrite is more stable when the temperature is higher than 43ºC (Zheng et al., 2011), which is why precipitation of anhydrite is usually expected under the conditions of HotBENT.
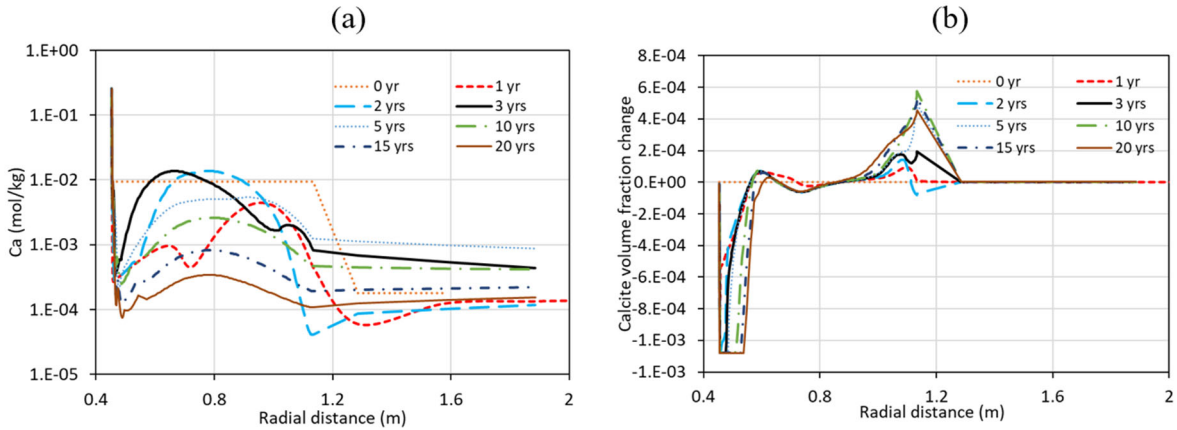
Figure 6.1-38. Spatial profiles of calcite concentration (s) and calcite volume fraction (b) at different time). Negative values indicate dissolution and positive values–precipitation. Note that the bentonite/granite interface is located at R = 1.13 m.

Most important is the question whether mineral alterations will affect swelling of clays due to the presence of smectite. Based on the results of the FEBEX *in-situ* test (Zheng et al., 2018), comparison of smectite mass fraction in bentonite samples that were collected after 18 years of heating and hydration with reference bentonite (reserved, represent the state of bentonite before the test) did not show a clear difference, because the data were too scattered. But the model for the FEBEX *in-situ* test (Zheng et al., 2018) showed bentonite in the narrow area close to heater would experience a loss of about 1% of its smectite. The current model for HotBENT predicts a significant dissolution of smectite in the area about 3 cm thick next to the heater because of strong and continuous evaporation near the heater, meanwhile illite precipitates in the same area (Figure 6.1-39).
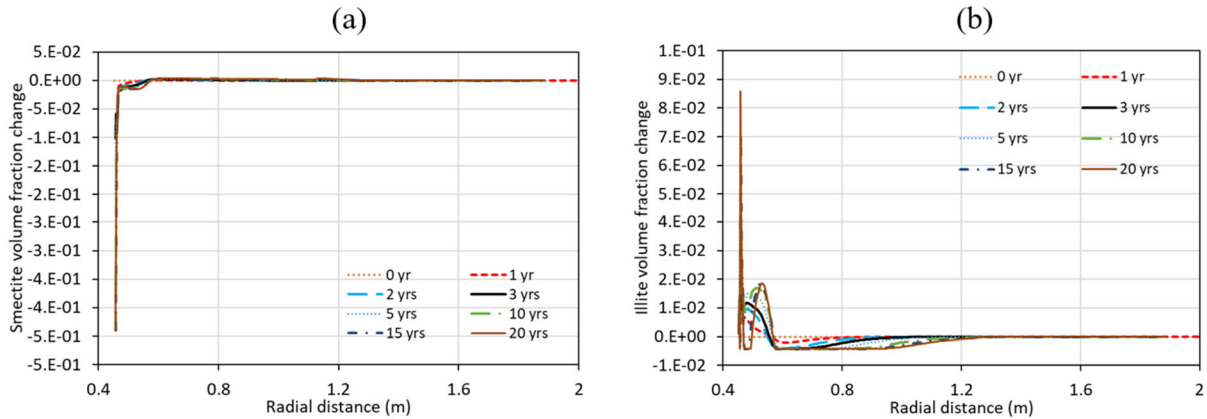
Figure 6.1-39. Radial profiles of smectite (a) and illite (b) volume fraction change at different times. Note that bentonite/granite interface is located at R = 1.13 m.

151

Based on the results of modeling, changes in minerals phases are expected to occur mostly in areas very close to the heater, about 3 cm thick with radial distance from 0.45 m to 0.48 m, by the end of the planned test period of 20 years. The model shows the dissolution of smectite, and the precipitation of illite, anhydrite, quartz and cristobalite. Calcite, muscovite, and plagioclase dissolve initially, but stard to precipitate at a later time, although the volume fractions of these minerals at the 20 years are still lower than their perspective initial values. Changes of siderite, ankerite, albite, and anorthite have not been shown by the model.

6.1.3.2.3.   *Summary of Predictive Modeling Results and Future Work*

A one-dimensional radial-symmetric THC model was developed and deployed to predict the evolution of the HotBENT experiment. Modeling of coupled THC processes affected by high temperature, relatively high permeability and high hydraulic pressure, combined with the effect of artificial hydration, generated results that have not been observed in FEBEX *in-situ* test (Zheng et al., 2018). With a heater temperature of 200ºC, the temperature at the bentonite/granite interface is expected to reach 87ºC. In about three years, most of the bentonite would become fully saturated, but a narrow zone about 3 cm thick in the close vicinity of heater would remain unsaturated with a water saturation degree from 95% to 98% until 20 years. The narrow unsaturated zone is where the most prominent chemical changes are expected to occur, because of the continuous strong evaporation (referred as "evaporation zone" in this report). Ion concentrations are expected to increase up to 2-3 mol/kg due to the dissolution of smectite, precipitation of illite, anhydrite, quartz and cristobalite, very high exchange Na and Mg and very low exchange of Ca and K at the cation exchangeable sites. Modeling showed the development a chemically active area a little further away from the heater and right next to the narrow unsaturated zone. It is referred to as the "condensation zone," in which chemical changes are induced by continuous condensation of vapor that is generated in the "evaporation" zone. In this area, the model showed a significant dilution of the bentonite pore water, dissolution of most aluminum-silicate minerals, except muscovite, very high exchange of Ca and K, and very low exchangeable Na and Mg at the cation exchangeable sites. Measurement of chemical concentrations in bentonite in a narrow zone close to the heaters may become a challenging problem, when modules H3 and H4 in HotBENT are dismantled after 5 years of operation.

In FY22 and beyond, HotBENT modeling activities will move from a predictive phase to an interpretative phase, as experimental data will start being generated soon with the onset of heating. LBNL will expand the 1-D model by adding new secondary minerals and refining the thermodynamic and kinetic databases to resolve the discrepancies between measured aqueous concentration and model results, and by introducing the effect of changing porosity on tortuosity and diffusion coefficients to understand the effect of mineral dissolution/precipitation on the transport process at the interface. LBNL's research activities will also be focused on developing a 3D TH model for the field test as part of the collaborative HotBENT Modeling Platform launched by the HotBENT project. In this modeling platform, modeling groups associated with the individual partner organizations are working on predictive and interpretative modeling of the test data. The multi-institutional group will be structured as to (a) increase the support provided to the HotBENT experiment and its interpretative evaluation, (b) broaden questions being addressed to advance fundamental understanding, and (c) address modeling issues, specifically the quantification of conceptual uncertainties. All partners encourage the Modeling Platform to pursue a broad spectrum of alternative conceptual models that address a common question or support a decision to be made jointly by the HotBENT participants. In addition, specific expertise and skills of the modeling groups can be used to examine particular aspects raised by the data collected as part of the HotBENT experiment or to make specific predictions.

6.1.3.3. HotBENT-Lab Experiment

6.1.3.3.1.   Objectives of the Experiment

Two benchtop-scale laboratory experiments, HotBENT-Lab, have been conducted at LBNL to provide a laboratory analog of the HotBENT field experiment. These experiments have provided a comprehensive set of characterization and monitoring data (Zheng et al., 2020, 2020a; Zheng et al., 2021, Section 7). The primary objectives of the laboratory experiment are to (1) improve understanding of bentonite THMC processes under heating and hydration for model parameterization and benchmarking, (2) compare the HotBENT-Lab data with HotBENT field-scale test results, and (3) develop a prototype of an experimentation platform for future studies of bentonite under conditions of high temperature.

6.1.3.3.2.   Column Design

The HotBENT-Lab experiments comprise a cylindrical pressure column to reproduce realistic heating and hydration conditions of the field-scale experiment (Figure 6.1-40). The design of the experimental apparatus and monitoring tools are based on estimated ranges of temperature and pressure, ability to accommodate characterization methods, i.e., X-ray computed tomography (CT) and ERT, and safety. The results of the baseline CT imaging can be found on Figures 7.5 through 7.8 of the report by Zheng et al. (2021).

In order to better understand the effects of heating and hydration, two identical test columns were used, with the control column undergoing only hydration, and the experiment column experiencing both heating and hydration. The chemical composition of the artificial groundwater used to saturate the column is given in Table 7.1 of the report by Zheng et al. (2021). Starting in June 2019, the column tests were run for over 1.5 years and both columns were dismantled with bentonite samples collected in December 2020.
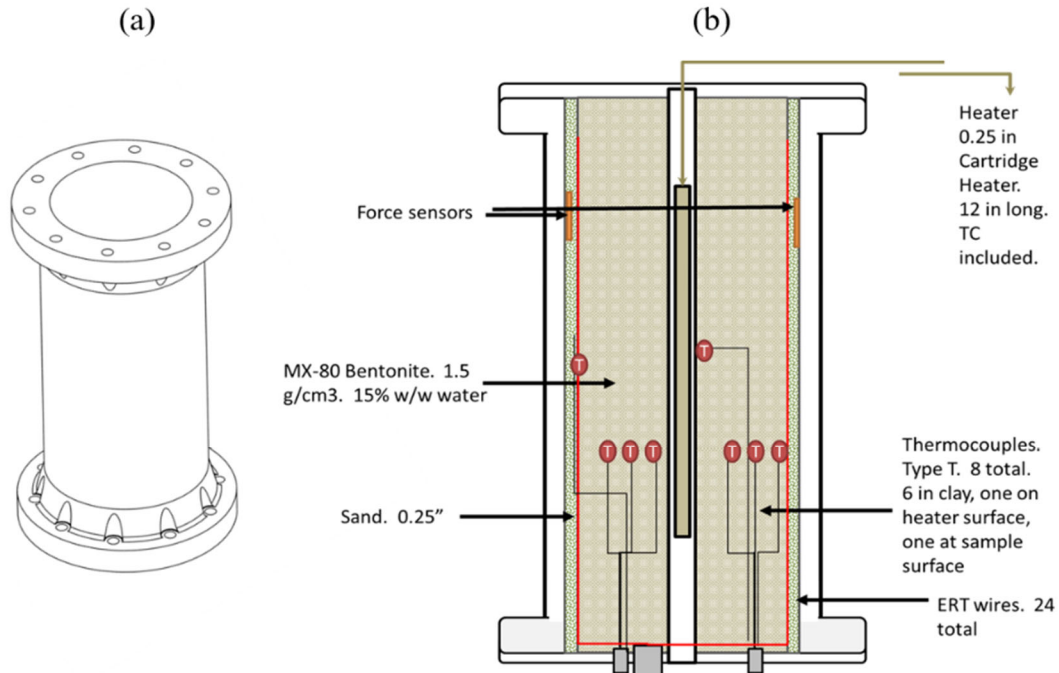
Figure 6.1-40. Schematic diagram of the column design for HotBENT-Lab experiment. (a) 3D rendering of the column exterior; (b) interior design of the bentonite column, showing locations of sensors and the heater.

6.1.3.3.3.   Experimental Operation and Monitoring Methods

The system operation started in June 2019. A schematic diagram of the experimental setup with the column and supporting components is shown in Figure 7.4 of the report by Zheng et al. (2021). After the baseline scan

and testing other components, hydration and heating were started. The experiments were running until December 2020, when both columns were dismantled and subsequent analysis of the clay has been completed including hydration, mineralogy, and chemical analysis. Column 1 was subject to both hydration and heating, and Column 2 was subject to hydration. Comparison of the results of testing of these columns is used to understand (1) the temporal changes of 2D and 3D clay density distributions due to water intrusion, swelling and structural deformation during hydration in the non-heated column, and hydration and heating in the heated column, (2) the swelling and deformation of clay subject to hydration and heating by image-tracking the transit movement of the thermocouple sensors, and (3) the density averaged over the entire clay column and its changes as a function of time.

The two experimental columns were monitored for hydration, temperature distribution, effluent chemistry, and density changes, using the following techniques. X-ray CT imaging was used to provide a 3D visualization of the density distribution in the column using a GE Lightspeed 16 medical CT scanner. The post processing and analysis of the obtained CT scan images was conducted using self-developed codes. Continuous temperature monitoring was conducted using eight thermocouples (acquired from Conax Technologies, with an accuracy of 0.1°C) installed in each column between the heater shaft and the column wall. Time-lapse electrical resistivity tomography (ERT) monitoring was done using a DAS-1 ERT system (Multi-phase Technologies), combining electrodes used to send electrical current or measure electrical potential. A total of ~2600 data points were collected for a single resistivity survey in each column, which takes ~ 40 minutes. The open software BERT (boundless ERT, Günther and Rücker, 2012) and Paraview (Kitware, NY) were used for data inversion and visualization. Geochemical analysis of the fluid used to hydrate the bentonite and effluent was conducted using the standard Ion Chromatography (IC) and Inductively Coupled Plasmas–Mass Spectrometry (ICP-MS) protocols. (Geochemical composition of the fluid used for hydration is given in Rutqvist et al., 2021a, Table 7.1.) Pre- and post-experiment mineralogical clay analysis was conducted with X-ray Diffractometry (XRD). Example of results from the experimental data set are given below.

6.1.3.3.4. Monitoring Results

Bentonite Hydration without Heating

Figure 6.1-41 depicts the 3D orthogonal view of CT density distribution and temporal changes in the non-heated column. The color bar bounds density changes from 1.2 to 2.4 g/cm^3, and a brighter color indicates a higher density. The image at T=0 day shows the initial conditions and density distribution after packing, including the heater and heater shaft in the center (white color), the sand layer surrounding the clay (orange color), the ERT bars emplaced at the sand-clay boundary (white line in the top slice, the other ERT bar was emplaced in the opposite position that cannot be directly seen in the figure), and clay packed between the sand layer and the central shaft (blue to orange color). The density variations, bedding layers and the dark fracture patches (bounded by the white dotted lines) close to one end of the column are attributed to uneven packing. The uneven packing, especially the fracture patches, affect the hydration process and induce preferential brine flow pathway. The CT density of clay averaged over the entire column is 1.46 g/cm^3, similar to the measured value of 1.44 g/cm^3 by weighing the clay mass used for packing and the column volume. The measured water content was 0.17, the dry density and porosity were then calculated as1.23 g/cm^3 and 0.53, respectively. The swelling of clay at the boundary may compact the interior clay, resulting in the sharp density increase ahead of the hydration front.

Deformation Due to Hydration

The bentonite swelling and compaction during column experiments caused the transient movement of the thermocouple sensors. Figure 6.1-44 shows the results of measurements by six thermocouple sensors that are used for tracking clay displacement at different locations. A negative displacement value represents displacement towards the center shaft, and a positive value denotes the displacement is away from the center shaft.
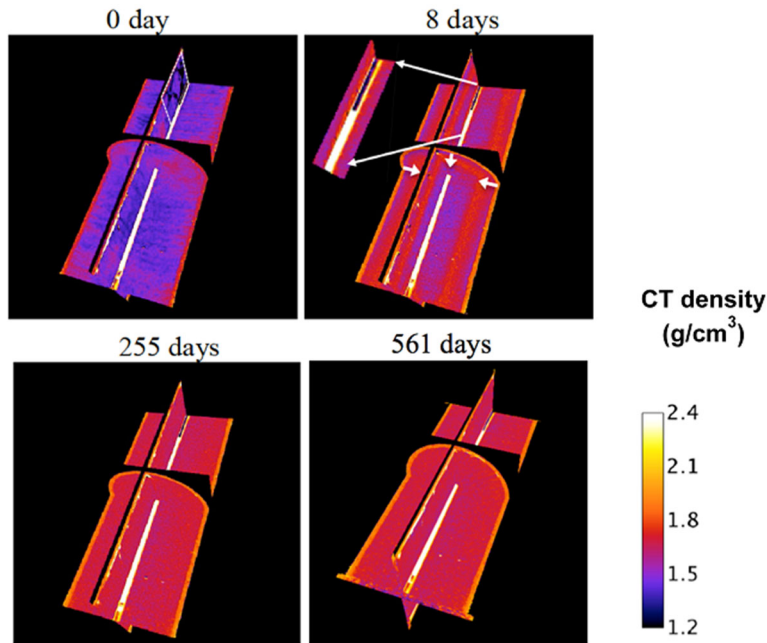
Figure 6.1-41. The CT 3D imaging of density distribution during the experiment of hydration in the non-heated column. The image at T=0 day shows the initial condition after packing, with the uneven-packing induced fracture marked by the white dotted box. The white arrows at T=8 days depict the continuous hydration from the surrounding sand layer, while the magnified image at T=8 days presents the preferential water intrusion along the center shaft at early time. At T=561 days, the column was dismantled.
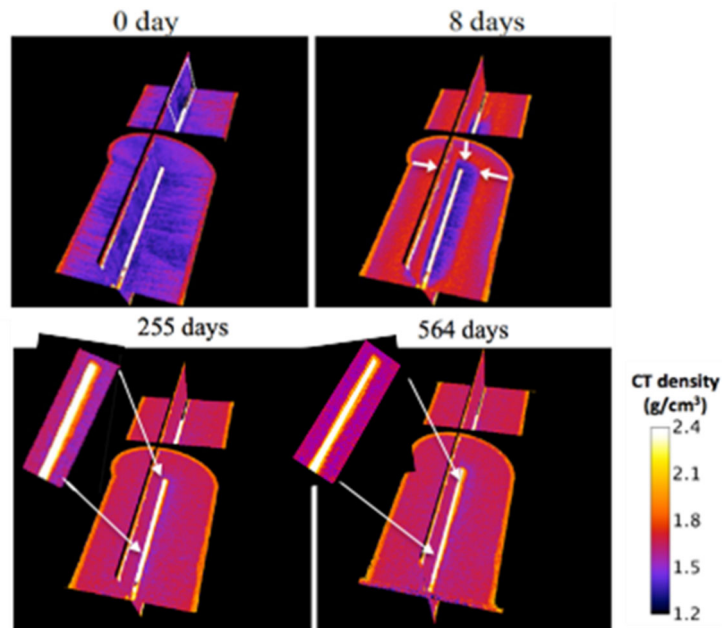
Figure 6.1-42. The 3-D clay density map and temporal variations in the heated column. The sub-image at T=0 day shows the initial condition after packing, with the uneven-packing induced fracture marked by the white dotted box. The white arrows at T=8 days depict the continuous hydration from the surrounding sand layer. The magnified image at T=255 and 564 days presents the bright high-density deposition on the heater shaft subject to heating and water vaporization. At T=564 days, the column was dismantled with bentonite sample collected at different locations.
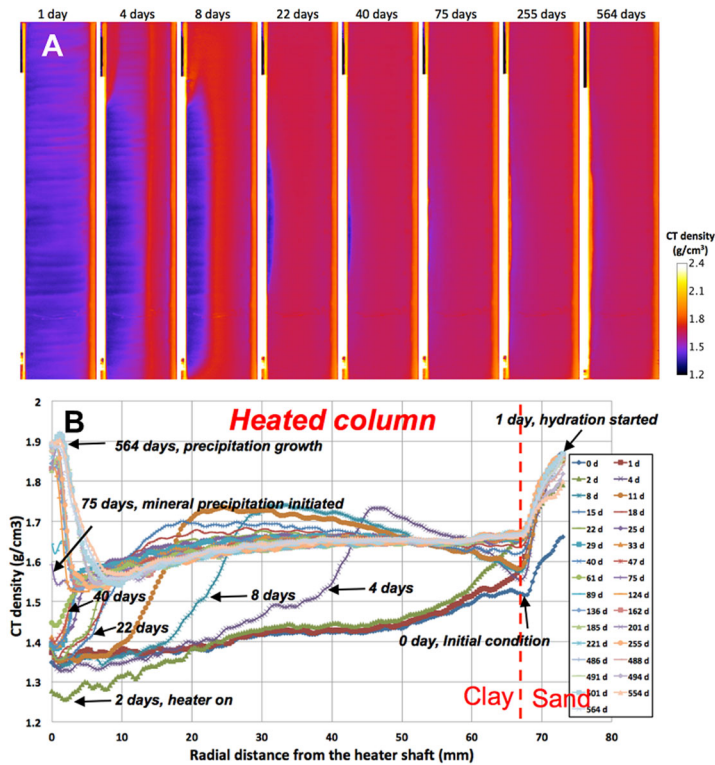
Figure 6.1-43. (A) The radially averaged density map and changes with time for the heated column subject to heating and hydration. (B) The average density profile vs. radial distance from the heater shaft along the white dotted line in (A).
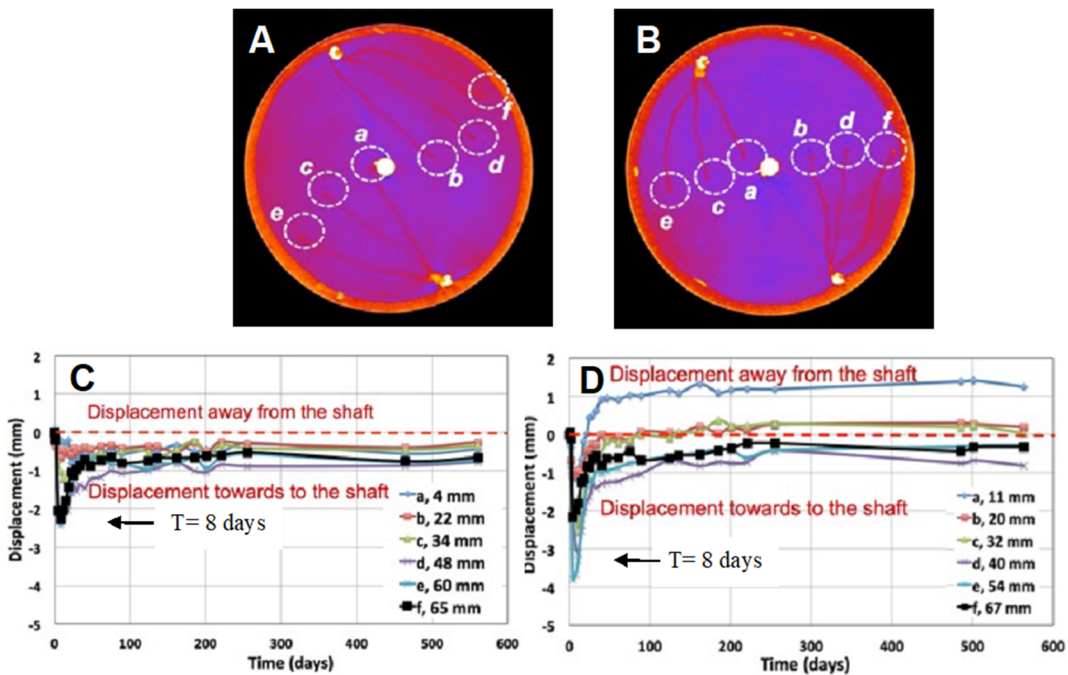
Figure 6.1-44. The six thermocouple sensors that are used for tracking clay displacement at different locations in the non-heated (A) and heated (B). (C) and (D) present the displacement changes relative to their original positions vs. time for the six thermocouple sensors. A negative displacement value represents displacement towards to the center shaft, while a positive value represents displacement away from the center shaft.

156

Geochemistry

Within the influent mixture, the effluent of the heated column showed sulfur reduction (also identified observed through the smell of sulfide), excess of silicon and retention of calcium and magnesium. Detailed results of the geochemical analyses are given in Section 7.4.2 of the report by Zheng et al. (2021).

Electrical Resistivity Tomography

The ERT setup included (1) an electrical impedance tomography system (MPT DAS-1) and (2) 24 square copper electrodes (0.5 by 0.5 cm) evenly spaced on a pair of fiberglass rods (12 electrodes on each rod, with a 3.8 cm inter-electrode distance), which were used for automatic measurements of both columns A python-based algorithm BERT (Günther and Rücker, 2012) was used for simulating ERT data and generating a 3D electrical resistivity distribution in the clay volume. Joint ERT-CT calibration was used to determine the material-specific relationship between resistivity and water content. The calibration results show that ERT can be used to capture local and temporal moisture variation given temperature, chemistry and porosity estimation inputs. The results of the calibration are given in Section 7.4.3 of the report by Zheng et al. (2021).

Post-Experimental Sampling and XRD analysis

After dismantling, multiple samples were collected from the two ends of each column at the same time to minimize exposure of sample to air and any potential changes. In total, over 800 bentonite samples were collected from the two columns at different locations and depths. In the heated column bentonite was fully water saturated at 40-70 mm away from the heater shaft. The values gradually decreased to 0.90 at 40 mm and were constant at 7-40 mm away from the heater shaft. Similar to the non-heated column, no variations occurred along the depth. The bulk wet densities, however, showed a large decrease in values from 1.65 to 1.57 g/cm³, at sampling depths of 21 and 23 cm and at 10-20 mm away from the heater shaft. On the contrary, water content increased from 0.45 to 0.55 at the same sampling locations. Note that at the depths of 21 and 23 cm, the two sampling layers are normal to the middle heater shaft, where the most pronounced heating effect is expected. These differences imply the impacts of heating and hydration on bentonite structure that were not observed in the non-heated column. The porosity in the heated column was 0.60 at 10-20 mm away from the heater shaft, higher than that of the neighboring clay (0.56) and bentonite at the same location in the non-heated column (0.57). Correspondingly, the dry density at 10-20 mm away from the heater shaft is smaller. This increased clay porosity and decreased dry density indicate more pronounced swelling of clay at 10-20 mm away from the heater shaft than that in the non-heated column. Note that thermocouple a located at 11 mm away from the heater shaft indicated larger swelling of clay close to the clay dry-out zone, which is consistent with changes in the porosity and dry clay density measured from *in-situ* bentonite samples. A detailed description of the results can be found in Section 7.5 of the report by Zheng et al. (2021).

To characterize the crystalline phases in the "HotBENT" samples, X-ray powder diffraction was conducted using a Rigaku SmartLab working in a theta-theta Bragg-Brentano configuration, equipped with a spinning sample holder (to improve data collection statistics), and a D/teX Si strip linear detector. Filtered Cu Kα radiation was used, and an interval between 3° and 68° of 2θ was measured. The data were analyzed via the Rietveld method using the MAUD software, which is equipped with advanced tools for modeling both lattice preferred orientation and turbostratic disorder, two very important factors when working with materials containing smectites (Lutterotti et al., 2010). The results are summarized in Table 7.2 and Figure 7.34 of the report by Zheng et al. (2021). For example, there are three types of montmorillonites, representing the three different hydration states found in the samples. In the samples collected from the heated vessel all samples contain montmorillonite with three water molecules per reduced unit cell, except for the sample closer to the heating element where about 45% of the total montmorillonite amount is dehydrated (montmorillonite 16A), showing a loss in moisture as compared to the montmorillonite 19A. No mono-hydrated structure, as the starting dry material, have been found anywhere. The amount of quartz was largely variable, which is likely due to the presence of sand grains in the sample, left from the outer buffer sand layer of the vessels.

In addition to LBNL's sample characterization, SNL (Jové-Colón et al., 2021) obtained samples from sieved size fractions of <38 microns of both heated and unheated columns. Two types of samples were prepared: air-dried (AD) and ethylene glycol (EG) saturated samples. Jové-Colón et al. (2021, Figure 21) showed XRD

spectra of bentonite sampled in region R3 (closer to the heater) for both heated and unheated columns. As expected, there is a close correspondence of montmorillonite peaks with PDF cards for the EG saturated samples. Strong peaks such as those for quartz were identified. The appearance of a 10 Angstrom peak at 2-theta of ~9 degrees in both heated/unheated EG samples may be indicative of potential interstratified illite in the clay but this needs much further evaluation of the XRD spectra. The study of Gomez-Espina and Villar (2016) suggested the presence of interstratified illite in heated column experiments using MX-80 bentonite.

Other features in the XRD spectra are peak broadening at 2-theta 6-9-10 degrees in the AD samples with increasing distance from the column center axis (regions R1 and R2) as observed in Figures 22 and 23. The regions R1 and R2 are closer to the sand layer which are expected to be more hydrated in the heated (V1) column. Such peak broadening of the 2-theta range of 6-9-10 degrees has been observed from *in-situ* XRD measurements under controlled temperature and moisture conditions. Again, more work is needed to evaluate the structural data to assess the changes in bentonite hydration/dehydration under variable temperature and moisture conditions. The XRD spectra shows close correspondence to the montmorillonite peaks, as expected, for AD and EG samples. Although there are some commonalities in the XRD spectra for samples from both heated and unheated columns, there are also some differences such as peak broadening in samples radially farther from the column central axis.

6.1.3.3.5. *Summary and Future Work for HotBENT-Lab*

The HotBENT-lab experiments were successfully conducted between June 2019 and December 2020, when both columns were dismantled and subsequent analysis of test samples was conducted of the clay has been completed including hydration, mineralogy, and chemical analysis. The time-lapse sensing and monitoring during the test and the post-mortem analysis have provided the following major findings:

- CT imaging clearly showed the hydration front moving radially inward. Density measurements from CT images also indicated clay swelling upon hydration, which caused swelling at the clay/sand interface, localized compaction, and fast flow paths created from column packing heterogeneities.

- In the center of the column, the bentonite showed lower water saturation, but higher CT density due to mineral precipitation. XRD analysis demonstrated that this precipitation was 100% anhydrite.

- Bentonite was compacted before the arrival of the hydration front (e.g., at the early time) due to swelling in areas where the clay had already hydrated, and then swelled after the arrival of the hydration front. Spatially the test column exhibits a displacement first moving inwards towards the heater and then moved back to its initial location as hydration propagated to the center.

- The hydration of bentonite was delayed in the heated-column in comparison with the non-heated column, whereas the former presented larger compaction of inner bentonite under heating, followed by larger and sustained swelling near the heater shaft.

- Heated and non-heated columns differed in the chemical composition of effluent water with the heated column showing lower sulfate, calcium, and magnesium concentration, but higher silicon, potassium and manganese concentration. XRD results show differences in the hydration of the clays and accumulation of soluble mineral phases from the influent water.

In FY22, LBNL plans to start two new column experiments with bentonite collected from the HotBENT field site. More ERT arrays and thermocouple sensors will be emplaced to improve the ERT monitoring and temperature profiles. New strain gauges will be implemented on the vessel shell for clay swelling pressure measurements. More markers will be emplaced in the column for more detailed characterizations on the spatio-temporal deformation. Tests will be provided with water analogous to the Grimsel groundwater, which is significantly lower in salt content. The number of thermocouples will be increased to measure a more detailed temperature distribution. These activities will provide valuable controlled experiments complementing the larger HotBENT field test. Meanwhile, LBNL has initiated development of a THMC model to interpret the data from the HotBENT Column Tests (see Section 8.3 in Zheng et al., 2021). These modeling activities will continue in FY22.

6.1.3.3.6. *Hydrothermal Experiments with HotBENT Bentonite*

This section presents LANL's research efforts focused on the initiation of an experimental hydrothermal testing program to complement the full-scale HotBENT test at the GTS (Caporuscio et al., 2021). The experiments include mixtures of Wyoming bentonite (FE) and/or Czech bentonite (BCV) + low carbon steel + Grimsel Granodiorite synthetic groundwater. Eight-week autoclave experiments were run at the planned maximum temperature of the HotBENT test (200°C). The three completed experiments so far demonstrate the potential for mineralogical and geochemical changes in the FE and BCV bentonite at 200ºC and water saturated conditions:

- The main observed effects of heating for the eight-week period are the slight reduction in montmorillonite swelling, formation of carbonate phases in experiments that contained BCV, and the lack of formation of silicate minerals such as zeolites. Reaction fluids in the mixed BCV-FE system remained around a pH of 6.

- Low carbon steel coupons included in the experiments were variably corroded and provided a substrate for Fe-rich mineral precipitation. Fe-oxides and phyllosilicates were observed in the experiment with FE only. In experiments with BCV, Fe-rich carbonates (siderite) were observed on the reacted steel surface in addition to oxides and Fe-saponite (see Figure 6.1-45).

Future research will consider the low-pH shotcrete mixture, which has a complicated formula, and potentially lower temperatures (90°C, the predicted temperature at the buffer/rock interface). In addition, the experimental campaign may be expanded with experiments of different duration, varying water/rock ratio, and comparison of tests done with granulated vs compacted vs powdered bentonite.
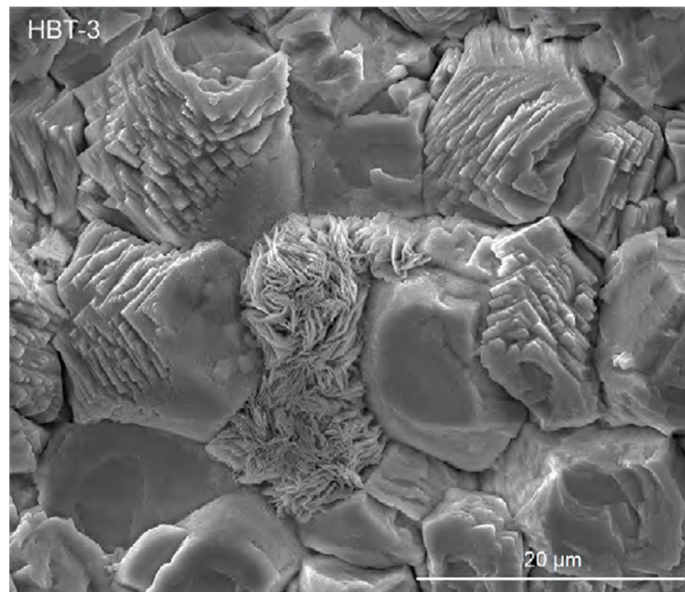
Figure 6.1-45. Example of in-step dislocation of siderite crystal structure observed in hydro-thermal experiments (Caporuscio et al., 2021).

6.1.4. Experimental Studies of Clay Colloid Transport at Elevated Temperature and Bentonite Swelling

6.1.4.1. Introduction

As part of the Colloid Formation and Migration Project (CFM, Section 3.3.1 of this report), LANL scientists have been involved in various activities to quantify radionuclide transport associated with bentonite colloids. Although DOE's formal partnership in CFM ended in 2015, SFWD researchers have continued to collaborate with their international partners. For example, in FY18 and FY19, LANL scientists performed batch sorption and column transport studies to interrogate the effects of colloid aging on colloid-facilitated transport of ^{137}Cs through crushed analcime columns (Viswanathan et al., 2019). These studies demonstrated that the colloids in a specific type of groundwater from the Nevada Test Site will sorb and transport radionuclides more effectively than a synthetic colloid solution of comparable chemistry (Viswanathan et al., 2019). Unlike freshly prepared colloid solutions typically used in laboratory experiments, groundwater at the test site experienced temperatures up to 75°C and was in place for several decades prior to collection. Therefore, experiments were designed to test whether these effects (i.e., aging and heating the colloids with sorbed radionuclides) might increase colloid-facilitated transport of radionuclides. Most recently, LANL showed that aging FEBEX colloids spiked with ^{137}Cs for 1200 hours increased the colloids' ability to transport ^{137}Cs through a series of columns by 10% (Telfeyan et al., 2020). The correlation between aging and sorption capacity was attributed to the increased time allowed for ^{137}Cs to migrate to the strong, less abundant sites (i.e., frayed edge sites) on the colloids.

Increasing temperature is expected to cause less stable colloidal suspensions due to reducing the diffuse electrical double layer thickness which is responsible for stabilizing the electrostatic repulsion, and increasing particle collision frequency and, therefore, aggregation rate. García-García et al. (2009), Tari et al. (2000) and Lu et al. (2003) studied the effects of temperature on colloid stability assuming the peak repository temperatures of ~80°C. The effect of heat on colloid stability and sorption capacity is less straightforward, however, in particular for higher temperature ranges from 100-200°C. This higher temperature range may cause much lower dielectric constant of water and the potential for mineralogical and morphological alteration to the bentonite, which would affect its sorption capacity, both by potentially increasing its surface area and through transformation to a potentially more sorptive phase, and affecting bentonite swelling, anisotropy, and erosion.

Another challenging factor potentially affecting the long-term stability of EB material is bentonite swelling and erosion. Many studies have investigated the swelling of bentonite clays in the micro-scale by observing them under Environmental Scanning Electron Microscopy (ESEM) and Transmission Electron Microscopy (TEM) or have investigated constrained swelling pressure measured via oedometer as a proxy for the unconstrained volumetric swelling of bentonite (Herbert et al., 2008; Komine, 2004; Komine and Ogata, 1994; Laird, 2006; Zhang et al., 2016). They have found among other things that the ionic strength and valence of electrolyte solutions strongly affects the swelling rate, swelling pressure, and final volume of bentonite (Komine and Ogata, 1994; Zhang et al., 2016). Recent efforts in modeling bentonite swelling indicate that varying swelling rate may introduce anisotropy of a bentonite pellet. Anisotropy in swelling could have implications for modeling the erosion of a bentonite barrier, especially in the context of safety assessment.

Erosion of the bentonite barrier poses a risk for transport of radionuclides from the near-field repository to the far-field environment. The ability of bentonite to adsorb radionuclides onto its large surface area is part of what makes it attractive as a barrier material, preventing the release of dissolved radionuclides into the environment. However, that same property poses a risk of enhanced transport of those radionuclides should bentonite with sorbed radionuclides erode (Reimus and Boukhalfa, 2014). The behavior and interactions of various radionuclides when adsorbed onto bentonite colloids are the subject of numerous past and ongoing studies (Birgersson et al., 2009; Missana et al., 2003, 2008, 2018). Understanding the conditions under which bentonite erodes and the extent of that erosion are vital to predicting bentonite behavior in both the repository and surrounding environments.

In FY20 and FY21, LANL scientists conducted laboratory experiments to address two potential alterations to bentonite that could have strong impact on colloid transport (Viswanathan et al., 2020; 2021): (1) high temperature impacts on bentonite colloids, and (2) swelling and/or erosion of bentonite pellets. Both are important for the safety assessment of bentonite as a barrier material in high-level radioactive waste repositories, and both are linked to international collaboration efforts conducted in the CFM and FEBEX projects at the GTS.

6.1.4.2. *Column Studies of Colloid Transport at Elevated Temperature*

Column experiments were conducted to investigate the effect of heating on cesium sorption and transport in association with colloids and colloid transport under thermal conditions. The experiments were designed to simulate the transport of colloids generated under thermal conditions in the near-field repository to the far-field environment. All experiments employed a synthetic solution of Chancellor groundwater with FEBEX bentonite at a concentration of approximately 100 mg/L as was described previously (Viswanathan et al., 2019; 2020). A concentrated solution of FEBEX colloids in synthetic Chancellor groundwater was spiked with ^{137}Cs $(7.3 \cdot 10^{-13}$ M) and subsequently heated in autoclaves for two weeks at 200°C, was diluted and settled to remove large particles, and was injected via a 60 mL MonojectTM syringe at a rate of 0.5 mL/hr into the first analcime column. Eluents from the column were combined and injected into a second identical column. The solution was spiked with ^{3}HHO used as a conservative tracer. Select samples from the first and second columns were analyzed for ^{137}Cs, ^{3}HHO, and colloid concentrations. The column experiments were interpreted using the colloid-facilitated transport models described in Reimus (2017) and Reimus et al. (2017). A separate series of column studies was conducted to test the difference between pre-heating the colloids, and heating the colloid solution *in-situ* using a heated column apparatus. The temperature was increased from 100°C to 150°C and 200°C under constant pressure of 1000 PSI, and eluent was collected from each interval. The eluent was analyzed for colloid concentration, colloid surface charge, and by Energy Dispersive X-ray Spectroscopy (EDS) and Scanning Electron Microscopy (SEM) for morphological and mineralogical changes.

Following the characterization of colloids subjected to high temperatures, the columns were packed with crushed granodiorite from the Grimsel Site (75-200 nm). A FEBEX solution similar to the above experiments was prepared. Non-radiological CsCl was added to 140 mL of FEBEX colloid solution (~100 mg L^{-1}) to a concentration of $2.6 \cdot 10^{-7}$ M Cs. Although a lower concentration of Cs was desired in order to compare with previous experiments, non-radiological Cs was required for the laboratory with the high temperature furnace. The concentration was prepared to be 100 times of the detection limit of the mass spectrometer, which is $3.0 \cdot 10^{-9}$ M. The solution was then left to equilibrate for approximately 6 months, as it was previously shown that aging the colloids after spiking with Cs allows for Cs to diffuse to the strong adsorption sites on the colloids. The solution was spiked with 10 ppm Br, as LiBr, to serve as a conservative tracer prior to injection through the granodiorite column. The flow rate was set to 3 mL/hr, and samples were collected every 20 min for the first 2 hours and every hour thereafter. The column maintained a temperature of 200°C and a pressure of 1000 PSI for the duration of the experiment.

Selected results from these experiments are discussed below, starting with experiments conducted at ambient temperature using FEBEX colloids spiked with ^{137}Cs and previously heated for 2 weeks at 200°C. Earlier work reported in Viswanathan et al. (2020) found that only about 60% of the colloid concentration relative to the starting pre-injection broke through the column initially indicating the filtration of the colloids by the analcime. The colloid concentration increased to 100% by the end of the experiment. The breakthrough of ^{137}Cs followed a similar trend but only about ~10% of the initial ^{137}Cs elutes initially, increasing to 40% by the conclusion of the experiment. All ^{137}Cs was transported in association with the colloids. The breakthrough results from the repeat injections reported in Viswanathan et al. (2021) showed colloid concentrations reaching 80% of the injected concentration after a few pore volumes (Figure 6.1-46). However, the concentration of ^{137}Cs was below a detection limit indicating complete desorption of ^{137}Cs from the bentonite colloids. This could indicate the destruction of the high affinity low density sites reported in the previous milestone with unheated colloids.
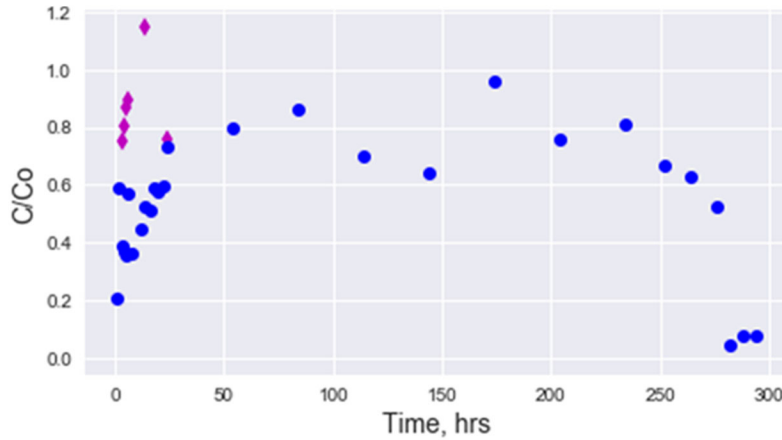
Figure 6.1-46. Breakthrough data from the first column injection run at ambient temperature. FEBEX colloids were spiked with ^{137}Cs and heated for two weeks at 200°C. A [3]HHO tracer was used.

The alternative tests consisted of injecting the FEBEX colloids that were aged in the presence of non-radiological Cs through a column filled with granodiorite heated to 200°C. The column was equipped with a back pressure regulator to maintain the column pressure at 1000 PSI to prevent evaporation and drying. Bromide was used as a conservative tracer. The breakthrough curves showing colloid concentration, Br concentration and the Cs are given in Figure 6.1-47. There is discrepancy in the initial colloid counts which is attributed to the large dead volume in the tubing of the heating setup. However, the colloid concentration drops to about 40% and to about 10% towards the end of the run. The drop in the colloid concentration is consistent with the drop in colloid concentration observed in the empty column. Analysis of a limited number samples for Cs showed elevated Cs breakthrough.
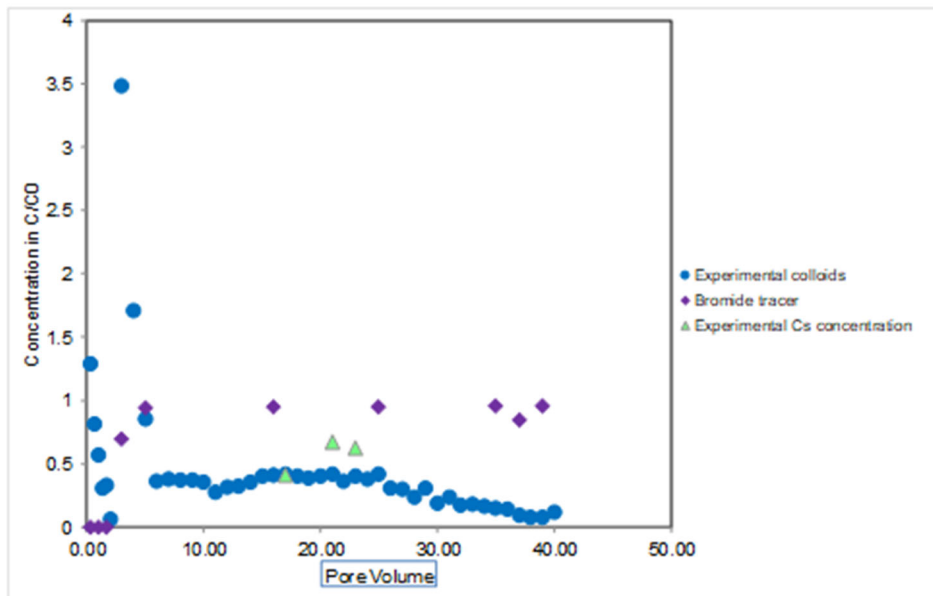
Figure 6.1-47. Breakthrough of FEBEX colloids and conservative tracer (Br) through a granodiorite column heated *in-situ* to 200°C.

The objective of the high-temperature colloid experiments conducted by Viswanathan et al. (2021) was to interrogate the effects of temperature on both the electrokinetic properties of colloids as well as mineralogical and morphological changes to the bentonite. The colloids subjected to high temperatures either in the column or in the autoclave experiments showed significant morphological changes. From the spectroscopic data that

was available, the presence of Ca-O spheres was apparent, and, combined with the visual observations of the clay, may suggest minor formation of calcium silicate hydrate (C-S-H) or calcium aluminate silicate hydrate (C-A-S-H). Such phases are the main cement hydration products formed at the interface between cement and bentonite in a repository setting (e.g., Fernández et al., 2017; Missana et al., 2018). However, it is unclear how such phases could form as the only addition of Ca to the system is the minor amount added from the Chancellor water. The SEM analysis performed on the colloids injected into a heated column show similar results to the colloids heated in an autoclave. At 100°C, some fraying of the bentonite edges occurs, but the mineralogy largely indicates clay. At 200°C, however, the morphology of the clay is largely different, and the EDS analysis indicates some conversion to a Ca-O dominant mineral. Additional SEM and potentially X-Ray Diffraction are planned to better identify these new phases. The repeat injection column showed complete loss of Cs during the second column. This suggests that the thermal alterations completely changed the nature of the low-density slow desorption sites. These preliminary results need to be complemented with more rigorous sorption and desorption experiments to characterize the partitioning coefficient of Cs to the colloids and to check on the need for a two-site model.

6.1.4.3. Bentonite Swelling and Erosion Experiments

Experiments were conducted to visually analyze the swelling of small pellets of MX80 bentonite in two dimensions under different ionic strength salt solutions. In order to test the swelling properties of the small bentonite pellets as a 2D object, an apparatus was designed that allows the pellet to swell in the radial direction but not the axial direction. This apparatus uses a 3D printed spacer that is the same vertical height as the bentonite pellet sandwiched between the bottoms of two clear plastic petri dishes. Preliminary investigations showed that the inclusion of the venting hole significantly reduced inconsistency in the evaluation of the swelling rate and pellet shape caused by air bubbles escaping the pellet. The swelling apparatus is placed on the stage of a Zeiss Stemi 2000-C inspection microscope with a canon Rebel 3t digital camera attached. Swelling was tested using deionized water as a control alongside NaCl solutions at concentrations of 0.02 mMolL-1, 0.2 mMolL-1, 2.0 mMolL-1, and 20 mMolL-1. Images were analyzed using the open-source ImageJ software developed by the National Institute of Health. The shape descriptors used in this method are the circularity and aspect ratio, which are used to measure the features which are inbuilt into the particle analyzer in ImageJ (Viswanathan et al. 2021, Figure 2.10). Farther in the future, experiments for measuring erosion of the bentonite pellet as it swells will be devised and performed.

Two principal types of data were generated: one is the change in area of the pellet over time, and the other is the change in shape descriptors, mainly the aspect ratio of the pellet, over time. These data are used to assess a relationship between swelling rate and the shape of the pellet, and to determine the swelling anisotropy. Figure 6.1-48 demonstrates a correlation between the swelling rate and the aspect ratio of the swelling pellet does exist. Figure 6.1-49 shows a graph of the averaged per-second change in area for each of the tested solutions. Note that the deionized (DI) and 0.02 mM/L solutions have similar initial swelling rates, with 2.0 mM/L showing a higher initial swelling rate, and 20 mM/L showing the highest initial swelling rate.

Average Areas and Aspect ratios
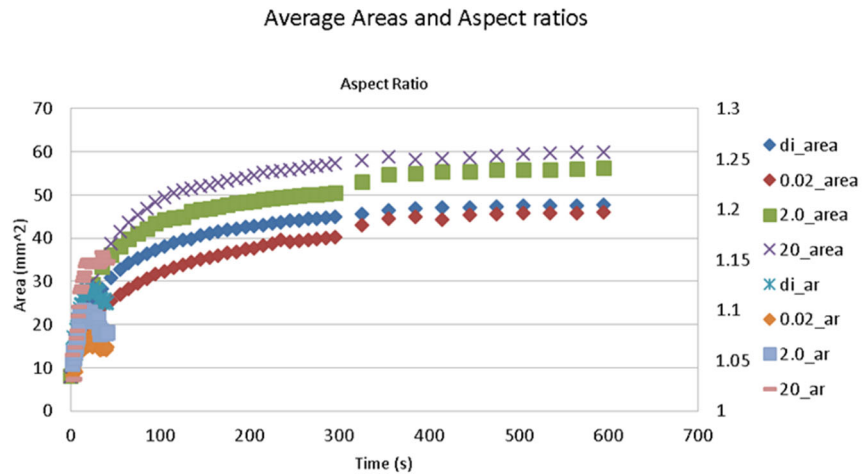
Figure 6.1-48. Graph comparing the averaged swelling area and averaged aspect ratios of each of the swelling tests with deionized water, 0.02 mM/L, 2.0 mM/L, and 20 mM/L NaCl solutions.
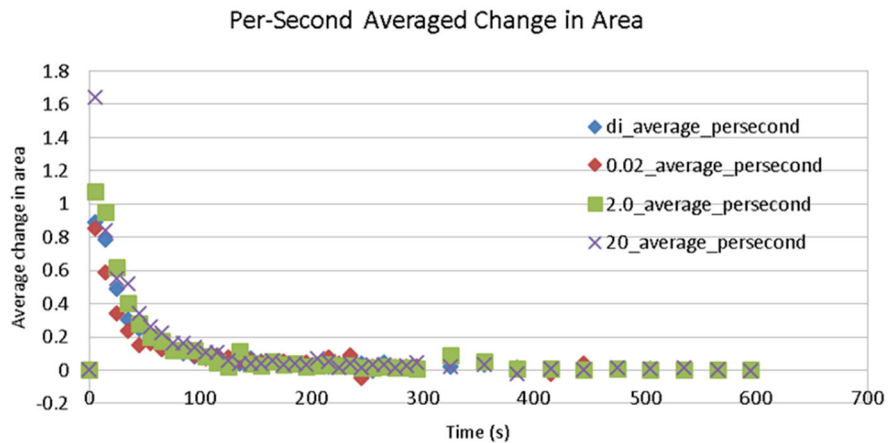
Figure 6.1-49. Graph showing the average per-second change in area for each of the tested solutions.

The bentonite swelling and erosion experiments used new experimental methods and image processing tools for visual evaluation of the swelling of bentonite pellets. This work was conducted to gain an understanding of the parameters that control bentonite swelling and colloid generation. Interestingly, the swelling rates do not follow the expected pattern of which solutions should swell quickly or slowly which has been extensively demonstrated by many workers, (Alonso et al., 2017; Komine, 2004; Komine and Ogata, 1994; Zhang et al., 2016) which indicates that increasing solution strength will decrease swelling capacity. This is near the opposite of what did transpire. The only solution which caused bentonite to swell more slowly and to a smaller size than the deionized water was the 0.02 mM/L solution. The 2 and 20 mM/L solutions both swelled more quickly and to large sizes than the deionized water control. It is possible that at concentrations higher than tested, the expected relationship between swelling rate and solution strength may reassert itself. It is also possible that the small volume of bentonite used, and comparatively short timescale used in this test contributed to this deviation from expected behavior. Between the different solution strengths, the most obvious differences in the speed of swelling occur in the initial 90 seconds of swelling. Swelling beyond the initial 90 seconds of swelling seems to occur at roughly the same rate regardless of solution chemistry. One possible explanation for this could be that there are two different processes controlling the initial 90s of swelling and the subsequent swelling, one that is more sensitive to solution chemistry and another that is less sensitive.

More work is needed to characterize the impact of the solution chemistry conditions on the morphological and mineralogical changes observed in the colloids. The alteration of the nature of the sorption sites and their density could have a significant impact on the buffer properties of bentonite and their performance as an EB. This will allow assessing the ability of colloids to mediate radionuclides transport to the far field.

6.2. Experimental and Modeling Studies of Engineered Barrier and Host Rock Interactions

This section comprises summaries of SFWD's international activities conducted to better understand interactions between EB and host rock materials. The goal of the experimental and modeling studies described below is to provide insights as to how repository performance may be affected by these interactions, which are most prominent early in the lifetime of a repository when EBS materials such as bentonite, metal containers, and cementitious materials have just been added to the natural environment and when thermal and hydrological perturbations remain strong.

Section 6.2.1 summarizes hydrothermal autoclave laboratory experiments designed to study geochemical and mineralogical interactions between EBS and host rock components, for both an argillite-hosted repository using Mont Terri samples (Sauer et al., 2021, Chapter 1) and a crystalline-hosted repository using GTS rock samples (Caporuscio et al., 2021, Chapter 1). Section 6.2.2 includes the results of investigations, conducted in a collaboration with Israel, of the processes occurring near interfaces between cement and carbonate rocks (limestone and marl), demonstrating how laboratory testing can be used as input to reactive transport simulations (Matteo et al., 2021, Chapter 4). Finally, Section 6.2.3 provides first results from recently started reactive transport modeling studies to interpret the evolution of the *in-situ* CI-D experiment at Mont Terri, which focuses on the long-term interaction between cement, bentonite and Opalinus Clay.

6.2.1. Hydrothermal Laboratory Experiments of EBS and Host Rock Interactions

6.2.1.1. Background and Objective

LANL scientists (Caporuscio et al., 2021; Sauter et al., 2021) continued experimental studies focused on the evaluation of high-temperature impacts on EBS materials, with special attention given to the interaction between host rock, bentonite, cement, and steel. Two parallel experimental campaigns have been conducted, one with argillite host rock using samples from Mont Terri (Section 6.2.1.2) and one with crystalline host rock using samples from the GTS (Section 6.2.1.3).

With regards to argillite host rock, the LANL report by Sauer et al. (2021) focuses on understanding geochemical and mineralogical changes in the EBS, consisting of waste canister, bentonite buffer, and cementitious materials, in a high temperature repository. In FY21, a series of new hydrothermal experiments were completed in the rocking autoclaves at LANL including the following types of media: EBS30 (Opalinus Clay + Wyoming bentonite + cured ordinary Portland cement + Opalinus Clay synthetic groundwater, 316SS, 200ºC/150 bar, 8 weeks), and EBS-31 (Opalinus Clay + Wyoming bentonite + cured ordinary Portland cement + Opalinus Clay synthetic groundwater, 304SS, 300ºC/150 bar, 8 weeks). In addition, LANL continued characterization of the reaction products of experiments conducted in FY20, namely experiments EBS-23 through EBS-29.

LANL's progress on EBS interactions with crystalline host rock is described in Caporuscio et al. (2021, Chapter 1). Three new hydrothermal experiments were completed in the rocking autoclaves at LANL in FY21: IEBS-7 (Grimsel Granodiorite + Wyoming bentonite + Grimsel Granodiorite synthetic groundwater, 250ºC/150 bar, 6 months), IEBS-8 (Grimsel Granodiorite + Wyoming bentonite + cured ordinary Portland cement + Grimsel Granodiorite synthetic groundwater, 316SS, 250ºC/150 bar, 8 weeks) and IEBS-0 (Wyoming bentonite + Grimsel Granodiorite synthetic groundwater, 250ºC/150 bar, 8 weeks). In addition. LANL finalized characterization of one earlier experiment conducted in FY20: IEBS-6, using Grimsel Granodiorite + Wyoming bentonite + cured ordinary Portland cement + Grimsel Granodiorite synthetic groundwater, under temperature of 250ºC and pressure of 150 bar.

In both experimental campaigns, the reaction products of experiments conducted in FY20 and FY21 were analyzed using the following methods: Mineral Characterization using Quantitative X-ray diffraction (OXRD) analyses, X-ray diffraction analyses (XRD), Bulk X-ray Fluorescence (XRF) Spectroscopy analyses, imaging using a FEI™ Inspect F scanning electron microscope (SEM), Aqueous Geochemical Analyses, as well as mineral and water chemistry data. The experimental methods are described in Appendix A through F of the report by Sauter et al. (2021) and in the report by Caporuscio et al. (2021).

6.2.1.2. *Hydrothermal Interaction of EBS Components and Opalinus Clay*

LANL's experimental program in FY21 aimed to further develop concepts for a high-temperature, argillite-hosted repository with respect to: (1) bentonite-cement interaction, (2) bentonite-steel interaction, and (3) novel EBS additives. Characterization of a 6-month experiment and two 8-week experiments were completed (EBS-27, EBS-28, and EBS-29) and two new 6-week experiments were conducted (EBS-30 and EBS-31). Results and interpretations from experiments with Opalinus Clay, Wyoming bentonite, and ordinary Portland cement (EBS-23 through EBS-28, EBS-30, EBS-31), from new measurements of mineral (e.g., Fe-saponite, zeolite) growth rates on the surface of reacted steel coupons, and results from a first experiment investigating the use of apatite as a radionuclide isolating additive material are summarized below (Sauer et al. 2021):

- With regards to bentonite stability in argillite, montmorillonite is stable over the experimental time period (6 weeks to 6 months). Zeolite formation is observed at 300ºC but not 200ºC, and zeolite/aluminosilicate mineral reactions buffer the solution chemistry and pH. Recrystallization of montmorillonite to illite is not observed; apparently zeolite forming reactions are kinetically favorable.

- The addition of uncured Portland cement powder to the Wyoming bentonite + Opalinus Clay experimental system in EBS-23 through EBS-27 at 200ºC resulted in the formation of abundant aluminosilicate phases (phyllosilicates, feldspar, and zeolites), calcium silicate hydrate minerals, and amorphous material, coupled with the dissolution of clay phases. Structural degradation of the smectite mineral structure from within Wyoming bentonite, due to the formation of interlayered illite, silica cementation, and/or CSH mineral intergrowth, resulted in ~10% reduction in expandability. The composition of analcime determined by electron microprobe reveals a wide range of Ca and Na compositions and lower Si/Al values than observed in previous EBS experiments. See example images in Figure 6.2-1.

- One experiment was conducted with Wyoming bentonite + Opalinus Clay + uncured Portland cement powder at 300ºC for 6 weeks (EBS-28). Aqueous chemistry and solid reaction products were notably different from the experiments conducted at 200ºC. Feldspar and zeolite formation was observed as well as significant degradation to the smectite structure and formation of interlayered illite-smectite and chlorite-smectite.

- Two experiments (EBS-30 and EBS-31) were completed that contained a cured cement chip instead of uncured powder. Alteration to the bentonite was less extensive than in the experiments with the uncured powder. Zeolite, feldspar, and CSH formation was still observed but to a lesser extent. Smectite was observed to remain stable; detailed clay mineral structural analyses are in progress. Measured pH values reached near-neutral values by the second week of experiment time.

- The new characterization efforts related to the interaction of stainless-steel coupons and bentonite clay focused on thickness and mineralogy of phases that formed at the steel surface. The mineral phases observed were dependent on the pH of the system (i.e., bulk chemistry). For example, in the Wyoming bentonite + Opalinus Clay experiments, layered alteration products were observed on the surface of coupons that included alteration of the outermost steel edge to Fe,Cr-oxide phases, followed by Fe-rich phyllosilicates (Fe-saponite, chlorite) and interbedded Fe,Cr,Ni-sulfide phases (pentlandite). In contrast, under the alkaline solution conditions in the experiments with uncured cement powder, zeolite and CSH phases are observed attached to the steel surface; no Fe is transferred to the bentonite groundmass. In experiments with the cured cement chip, solutions

evolved to neutral pH values and corrosion of steel coupons and the formation of Fe-rich clay phases was observed.

- An experimental program was initiated in exploring apatite as an additive to the bentonite buffer. Objectives were to: (1) assess apatite interaction with bentonite clay under hydrothermal conditions and (2) apatite solubility at relevant geochemical and pressure-temperature conditions. One experiment was completed with Wyoming bentonite, apatite from Durango, Mexico, and Stripa brine at 250ºC/150 bar for 8 weeks. Characterization efforts revealed minimal apatite dissolution and the absence of newly formed phosphate phases. In the bentonite, XRD analyses reveal a reduction in smectite abundance and formation of muscovite. Future work will confirm these results and will be used to inform experiments on apatite retention of radionuclides in the EBS.

Future research will emphasize the following areas:

- Detailed geochemical modelling of the effects of cement on aqueous geochemistry of the experimental system.

- Incorporation of low-pH cement materials into the argillite experimental system.

- Clay mineral analyses of experiment products with cured cement.

- Conduct investigation into the physical properties of Fe-saponite and other mineral products observed at the steel-bentonite interface.

- Apatite stability in different geochemical EBS environments (i.e., cementitious).

- Incorporate results into generic modeling codes.
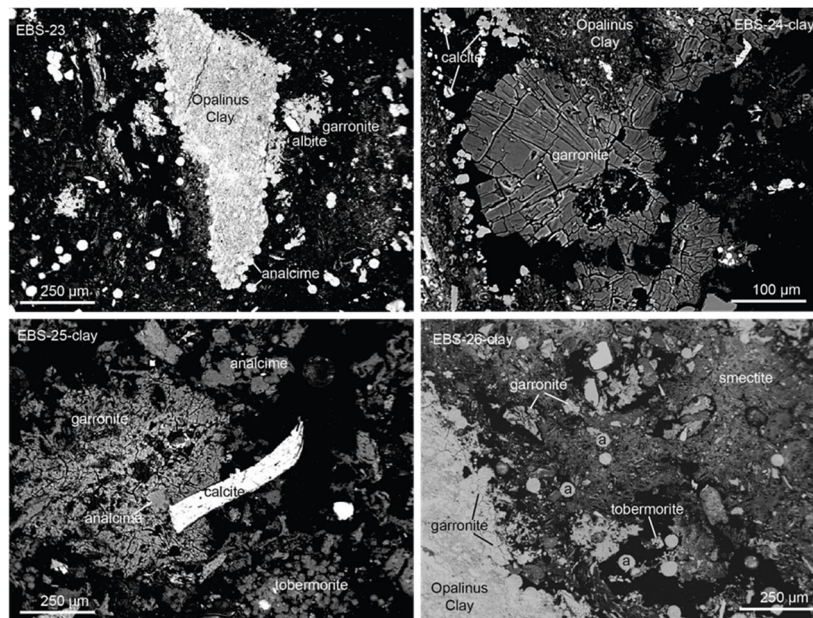
Figure 6.2-1. Thin sections from EBS-23, EBS-24, EBS-25, and EBS-26 showing the petrographic context of authigenic zeolite and CSH minerals (tobermorite). Analcime (a) and garronite crystals form at the interface of the Opalinus Clay fragments and the Wyoming bentonite.

In addition, as part of the international collaboration, LANL scientists are planning to mimic the full-scale EBS test that is currently underway at the Honorobe URL in Japan and is also a modeling task in the current DECOVALEX-2023 Project, Task D (Section 3.2.3.4). The full-scale test focuses on EBS behavior in an argillite-type host rock (Sauter et al., 2021, Figure 1). The proposed experiments will contain combinations of the following components: Kunigel bentonite (EBS buffer material) + quartz, Wakkanai Formation wall rock

from the Horonobe site, synthetic Wakkanai groundwater (formulated after Hama et al., 2007), and low carbon steel (waste canister material). The experiments will be conducted between 125°C to 200°C and at hydrostatic pressure (~150 bar). The Kunigel bentonite shipment was already received at LANL. The mineralogy and geochemistry of the reaction products will be evaluated by a variety of characterization methods (e.g., scanning electron microscopy, X-ray diffraction, electron microprobe, aqueous geochemistry analyses, and modelling). These experiments are expected to provide further insight into mineralogical and geochemical changes that may occur in the EBS region under high-temperature conditions.

6.2.1.3. *Hydrothermal Interaction of Wyoming Bentonite and Grimsel Granodiorite*

Hydrothermal experiments were designed and conducted to understand geochemical and mineralogical changes that may occur in the EBS of a high-temperature crystalline repository. Different combinations of materials found in typical repository settings, including wall rock (Grimsel Granodiorite from GTS), bentonite buffer (unprocessed Wyoming bentonite), waste canister overpack (316SS, 304SS, LCS), cement liner (cured ordinary Portland cement), and groundwater (synthetic Grimsel Granodiorite groundwater) were included in the experiments. Results and interpretations are summarized below (Caporuscio et al. 2021):

- Interaction of Wyoming bentonite and synthetic Grimsel groundwater was documented in IEBS-0. QXRD results show a decrease in clinoptilolite and plagioclase and increase in smectite. XRD results show that smectite structure is not altered during the 6- to 8-week experiment. Locally, analcime crystals are observed. Observed pH values are around 6. Overall, at 250ºC smectite appears to remain stable, and form from the alteration of minerals such as plagioclase feldspar during the experiment. In experiments that included Wyoming bentonite, Grimsel Granodiorite, and a synthetic brine (IEBS-1 through IEBS-5), reaction products include a fine-grained, recrystallized clay matrix with phenocrysts derived from the starting Grimsel Granodiorite and accessory minerals in Wyoming Bentonite, such as feldspars, micas, and quartz. Newly formed mineral phases include calcite, quartz, and gypsum. Montmorillonite remained stable in the 250ºC hydrothermal experiments (6-8 weeks), indicating the bulk composition of the system likely prevented smectite illitization. Preliminary findings suggest that the clay barrier may only experience slight alteration in the initial thermal pulse in a repository setting, but this finding should be supported by longer term experiments and full-scale demonstrations (e.g., HotBENT).

- The formation of bentonite colloids is likely significant for process models of repository function, as colloid-facilitated transport of radionuclides may occur in a crystalline system (e.g., Missana and Geckeis, 2006). Moderately stable colloids were observed in re-suspensions of gel formed in IEBS-5, and likely are present in the other experiments that are yet to be characterized. Colloid stability at the high temperatures utilized in this experimental study is not well known. According to theoretical considerations, colloids are likely not stable in solution at the temperature of the experiment (250ºC) due to reduction in surface charge density and electric double layer thickness of the colloid particles (Garcia-Garcia et al., 2009). Therefore, in our reaction products, colloids were likely stabilized in solution to form a gel phase upon experiment cooling. Future work will investigate if colloids are present in aqueous samples extracted while the experiment is at temperature and the effects of hydrothermal treatment on the physical properties of bentonite colloids.

- Two experiments containing a cured chip of ordinary Portland cement in addition to other EBS and host rock materials have been completed (IEBS-6 and IEBS-8). The inclusion of the cured cement chip introduced multiple mineral phases and chemical species that were reactive at the temperature and pressure conditions of the experiment. The cement chip represented ~18 wt.% of the total solid reactants and resulted in slightly increased solution pH values and diverse mineral reaction products in comparison to the results from IEBS-1 through IEBS-5 and IEBS-7 described above. Caporuscio et al. (2021) concluded that the experimental results provide insight into changes that may be expected at higher temperatures, i.e., the formation of zeolite minerals, pH effects. Characterization that is still in progress includes the observation of local changes in mineralogy of the cement piece included in the experiment and chemistry from the edge to the interior of the cement chip of a thin

section of a cross section of the cement chip. These analyses will reveal important information on the stability of cement phases such as portlandite on the exterior and interior of the cement chip.

- Experiments incorporating steel coupons reveal insights into mineral precipitation and corrosion processes at the steel-bentonite interface. The results from these experiments show a dynamic environment in the experimental systems at the bentonite-metal interface (Figure 6.2-2). The bulk chemistry likely controls the alteration mineralogy, as demonstrated by the similarities in mineral precipitation in the experiments. The new growth of surface-bound minerals is likely due to direct crystallization in the localized environments surrounding the metal with the steel material acting as a substrate for mineral growth in response to corrosion. Future work is needed to address the extent these mineral precipitants influence the EB performance or the repository system as a whole, and to whether these minerals (e.g., Fe- saponite) will act as a passive protecting layer against further corrosion of the waste containers.
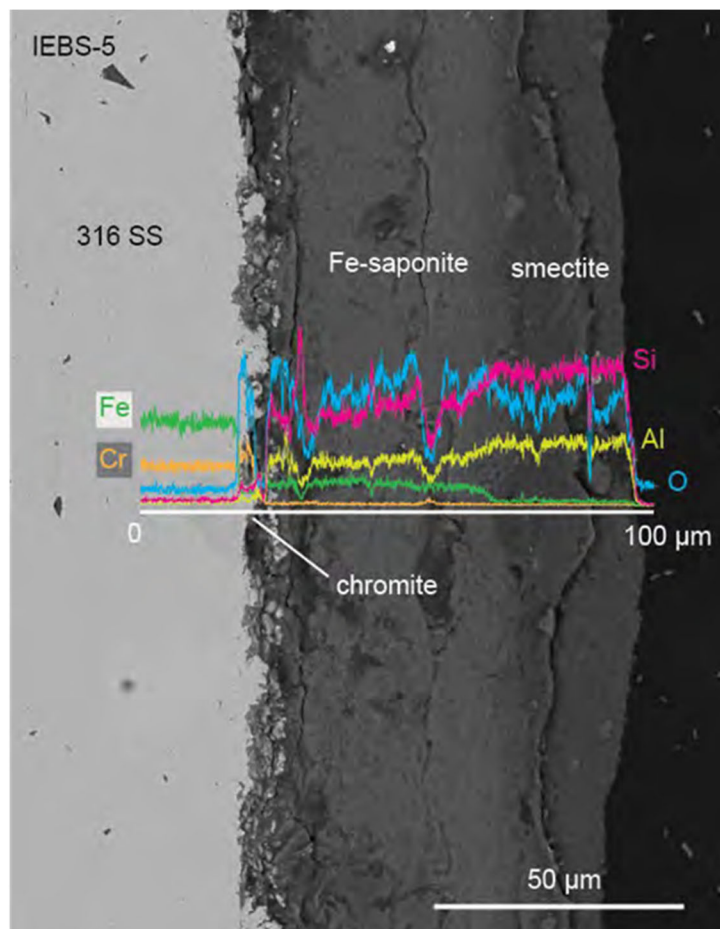
Figure 6.2-2. Energy dispersive X-ray spectroscopy (EDS) chemical results from a line scan (white line) across the steel-clay boundary. A layer of chromite followed by Fe-saponite is observed attached to the steel surface. A layer of unaltered smectite is observed outboard of the Fe-saponite layer.

6.2.2. Cement-Carbonate Rock Interaction Under Saturated Conditions: Laboratory and Modeling Studies

6.2.2.1. Background, Objectives and Approach

Carbonation of the cement hydration products (e.g., portlandite, C-S-H, and ettringite) and changes in rock mineralogy from alkali interaction are expected in the case of an interface between cement paste and carbonate rocks. Carbonation is the formation of calcium carbonate ($CaCO_3$) solid phases at the expense of hydrated cement products. As a result of carbonation, the mobility of some radionuclides may increase or decrease in response to changes in pH, porosity, and mineralogical gradients. Furthermore, the distinct pH and chemical composition of the cement's pore solution compared to the rock pore water results in etched surfaces of solid phases in the rock (e.g., calcite), which increases the chemical reactivity of these phases (Monteiro and Mehta, 1986). The application of existing reactive transport models is limited because of the uncertainties in scaling up model parameters determined under laboratory conditions to field scale for various future scenarios.

As briefly described in Section 4.4 of this report, the Israel Atomic Energy Commission is examining the possibility of locating a geological waste disposal site (Matteo et al., 2021, Figure 4-1) within the carbonate Ghareb and Nezer Formations in the northern Negev, Israel (Klein-BenDavid et al., 2019). In the context of a recently established international collaboration between SNL and Israeli researchers, Matteo et al. (2020, Chapter 4) simulated the long-term performance of interfaces between cementitious materials (CEM I and a low pH cement) with carbonate geologic strata (limestone, chalk, marl, oil shale, low organic phosphorite and high organic phospharite) of the northern Negev, Israel. The performance is being evaluated with respect to (1) changes in abundance of major phases for primary constituents, (2) the anticipated reaction front depths as a function of time for each material, and (3) changes in physical, mass transport and mechanical properties. In this report, the interface between Ordinary Portland Cement (OPC) paste (CEM I) and two carbonate rock types, limestone and marl, were chosen to illustrate the methodology developed to-date and observations regarding the specific cases. CEM I was selected as a bounding case for alkali cement-rock interactions because of its highly alkaline pore water (pH≈13).

Matteo et al. (2020, Section 4) conducted research to: (1) demonstrate how laboratory characterization methods results are used as input data in reactive transport simulations; (2) simulate short-term scenarios (5 years) of interfaces between carbonate rocks (limestone and marl) and OPC paste; and (3) provide a preliminary of long-term PAs (100 and 1,000 years) of these interfaces based on simulations results.

6.2.2.2. Materials and Experimental Methods

Large bulk samples of limestone and marl, approximately 48 cm by 20 cm, were obtained from the carbonate-rich Judea Group and Mount Scopus Group, respectively, in the northern Negev desert in Israel. The samples are from depths of several hundred meters below surface, and above the regional water table and outcrops at the margins of the Plateau. X-Ray diffraction (XRD) was used to provide limestone and marl crystallographic characterization, including clay fractions–illite-smectite, kaolinite, illite, and chlorite. The mineralogical compositions of samples are given in Matteo et al. (2020). U.S. EPA Method 1313 (U.S. EPA, 2017a), which is a pH-dependence leaching test method, was used to determine the liquid-solid partitioning (LSP) of species under near equilibrium conditions. These results are used to select a reaction set of minerals and related parameters to represent the material by fitting LSP curves of constituents as a function of pH at equilibrium (Matteo et al., 2021) in conjunction with other material information. EPA Method 1315 was used to evaluate a mass transfer rate (U.S. EPA, 2017b). The LeachXS (Van der Sloot et al., 2008) with ORCHESTRA (Meeussen, 2003) embedded for geochemical speciation and reactive mass transport (hereafter LeachXS/Orchestra, LXO) was used to develop a geochemical reactive transport model that considers geochemical speciation, liquid/solid partitioning, and multi-ionic diffusion (Arnold et al., 2017; ECN, 2019; Meeussen, 2003). Geochemical speciation modeling was used to simulate the equilibrium liquid-solid partitioning (LSP) of constituents obtained from EPA Method 1313 (i.e., pH-dependent LSP model) and the mass transfer release of constituents in EPA Method 1315 (i.e., monolith diffusion-controlled leaching model).

The resulting geochemical speciation model and mass transfer model were used to simulate rock-cement interface behavior.

A conceptual model for simulating cement-rock interfaces is shown in Figure 6.2-3. A multi-ionic diffusion approach (Arnold et al., 2017) was used to model constituent specific diffusivity in both monolith diffusion-controlled leaching and rock-cement interface models. The approach uses free liquid diffusivity coefficients, Di^0, for specific constituents are summarized in Matteo et al. (2020). A 1D LXO model (Figure 6.2-3b) was used to simulate the interface between carbonate rocks and cement. The model was set up with one interface (rock-cement) and 2-materials (limestone or marl and OPC paste). Measured porosity and calibrated tortuosity were used to describe the physical properties of the solid materials.
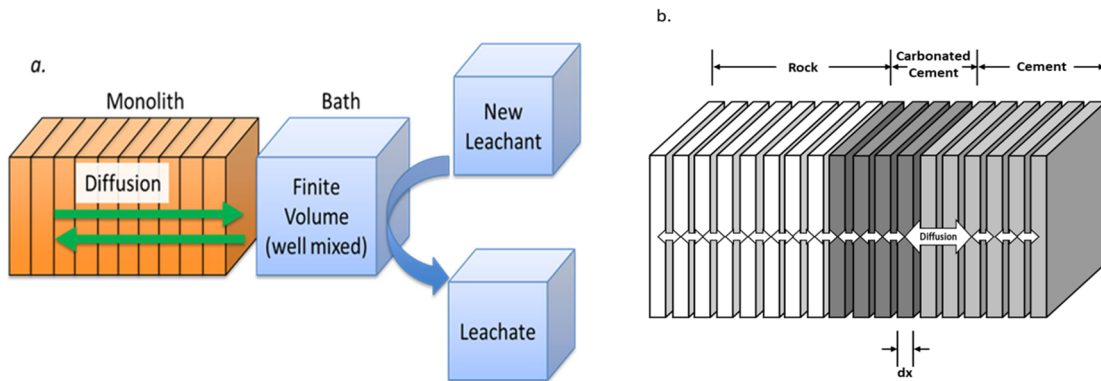
Figure 6.2-3. Conceptual models for (a) modeling EPA Method 1315 and (b) rock-cement interface

6.2.2.3. Chemical Characterization of Limestone, Marl and OPC Paste Samples and Calibration of Mineral Reaction Set

The pH of the OPC paste sample is controlled by the formation of portlandite in the cement. The solubility curves of various constituents from EPA Method 1313 can be classified into two categories: reactive and conservative. Solubility curves of aluminum, calcium, magnesium, and silicon show a reactive behavior as a function of pH, which reflects reactions of these constitutes with solid materials. Aluminum and silicon do not show a minimum for the OPC paste as they are both tied to major cement phases, such as C-S-H and have low solubility under highly alkaline pH conditions of 9 to 13. Constituents that show a conservative (not reactive) behavior are potassium, sodium, and boron, which were used to quantify the diffusion-controlled transport in the porous media and used to calibrate the tortuosity of the solid materials.

The diffusion of constituents in these materials and during EPA Method 1315 testing is strongly dependent on tortuosity. Potassium was used as a conservative constituent for calibrating tortuosity by fitting the predicted potassium flux calculated using the LXO model to the measured flux from EPA Method 1315 test. Tortuosity values range for OPC cements varies between 30 and 80 (Branch, 2018). For both interfaces, after a simulated time of 5 years, most of the change in the phase distributions occurred in calcium bearing. The dominant calcium-bearing phase(s) in both rocks is calcite (100%) and in the OPC paste are portlandite (60%), C-S-H phases (20%), and ettringite (20%).

The carbonation front advanced from the interface 1 mm in 5 years when the rock was limestone compared to 4.5 mm for marl. Regardless of the difference in predicted carbonation depths, the overall redistribution of calcium bearing phases is nearly the same. In both scenarios, calcite precipitation replaced cementitious phases (portlandite, C-S-H, and ettringite). However, in the marl/OPC paste scenario, the maximum depth of calcite precipitation was significantly deeper (4.5 mm), where in the case of limestone it was closer to the interface (~1 mm). Within the carbonated layer in the limestone/OPC paste scenario, the cementitious phases were slightly depleted and still dominated the carbonated cement layer. In contrast, after 5 years of interaction with marl, most of the OPC paste carbonated layer was depleted of cementitious phases that were replaced with calcite and dolomite. Dolomite formed in the simulation with marl and not with limestone. While the available

content of magnesium is similar for both rocks, it is most likely that the formation of dolomite in the limestone scenario happens after longer interaction periods with the OPC paste. As the available content of calcium, magnesium, and carbonate of the two rocks are very similar, it is reasonable that the results of marl/OPC paste interface scenario are a reflection of advanced carbonation that may happen to the OPC paste after longer interaction periods with the limestone. Moreover, the differences between the two interfaces long-term performances are likely due to physical differences between the two rocks and not chemical differences.

The main differences between the physical parameters of limestone and marl are in porosity and tortuosity. These parameters control the fluxes of constituents through diffusion across the interface. As the cement pore water is relatively enriched in calcium, the thickness of the carbonated cement layer may be controlled by bicarbonate flux from the rock's pore water to the cement's pore water. Constituent fluxes are controlled by (1) the ratio of porosity to tortuosity ($\emptyset/\tau 2$) and (2) concentration gradients. For both interfaces, the concentration of bicarbonate in the rock's pore water is six orders of magnitude greater than in the cement and about 40% higher in the limestone pore water compared to the marl pore water. Thus, the concentration gradient cannot account for most of the difference in thickness of the carbonate layer between the two interfaces. As both concentration gradients are steep, the resistance ($\emptyset/\tau 2$) of the carbonate rock to bicarbonate diffusion can account for differences in the flux. The value of $\emptyset/\tau 2$ is about 4.6 times greater for the marl than the limestone (0.0032 compared to 0.0007). The factor of 4.6 is almost the ratio between the thicknesses of the two carbonated layers (4.5). The relative ratios of $\emptyset/\tau 2$ factors can account for most of the difference between the two rock-cement interface results.

As the carbonation layer thickness is almost independent of the chemical composition of the carbonate rock, it is possible to use the ratio of porosity to tortuosity ($\emptyset/\tau 2$) to estimate the extent of the carbonated layer in other carbonate rich rocks and OPC paste interface. Other common carbonate rocks are chalk, oil shale and phosphorite. Assuming typical porosity values for the rock of 40%, 33%, and 35% for chalk, oil shale, and phosphorite, respectively) and tortuosity of 10, the thickness of the carbonated cement layer will be after 5 years of interaction 6 mm, 5 mm, and 5 mm for chalk, oil shale, and phosphorite respectively. The aforementioned mechanistic model is complex, but it can be simplified to represent carbonation as a sharp moving front. A simple analytical expression for the location, XC (m), of the moving carbonation front as a function of cement composition and conditions. Using this expression, it is possible to estimate the location of carbonation front as a function of time (Figure 6.2-4). After 100 and 1,000 years, the carbonation front within the cement will be 166 mm and 507 mm from the initial location of the interface between marl and the OPC paste and for limestone OPC paste interface the carbonation front will be 17 mm and 63 mm after 100 and 1,000 years, respectively.
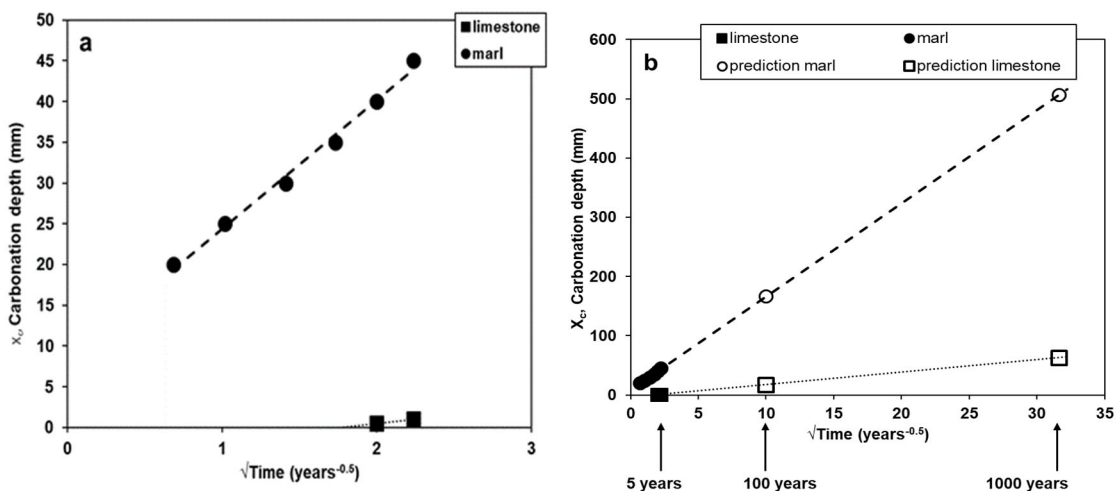
Figure 6.2-4. (a) The location (XC) of carbonation front as a function of square root of time. The lines are fitting lines based on the carbonation results from the LXO model; (b) extrapolation of equation to estimate carbonation depths after 100 and 1000 years.

6.2.2.4. Conclusions and Future Work

In parallel with simulations, interface experiments of carbonate rocks with cements are being carried out in the laboratory. Samples from these experiments are in early stages of chemical and physical characterization, using the following methods: (1) interface characterization using LA-ICP-MS, SEM EDS, and micro-CT, and (2) nano-indentation to measure changes in material mechanical properties as a result of interface reactions. Based on simulation results, the porosity to tortuosity ratio ($\emptyset/\tau^2$) was found to control the thickness of the carbonated cement layers. It is recommended to choose a rock formation for geological disposal site with the lowest $\emptyset/\tau^2$ ratio. However, in this study, host rock macro-scale features, such as fractures and karst, were not considered, which may potentially dominate bicarbonate and other constituent fluxes from the rock to cement and vice versa. The findings of this work are not limited to EBs in geological waste disposal sites, but may also be useful for assessing the long-term performance of cement used in wellbores for oil/gas and geological carbon sequestration.

6.2.3. Modeling of CI-D Experiment at Mont Terri

In FY21, LBNL scientists initiated a modeling effort in collaboration with the CI-D Experiment at Mont Terri. As described in Section 3.1.4, the Cement Interaction (CI) experiment comprises two vertical boreholes that have multiple segments with bentonite and concrete/cement materials. Since start of the experiments in 2007, sampling campaigns have been conducted in 2009, 2012, 2015, and 2017 using slanted boreholes, which were carefully drilled into the vertical boreholes to retrieve core materials at interfaces between bentonite, concrete/cement, and the argillite host rock. The objective of these campaigns was to characterize interfacial regions with regards to time-dependent mineralogical, chemical or textural changes. The current experimental phase, referred to as CI-D, goes beyond characterization of interfaces with various imaging approaches to direct *in-situ* testing of transport properties and processes across the interfaces. Starting in May 2019, a cocktail of water with radionuclide tracers was released in a pilot borehole drilled into the vertical borehole in a Portland cement/concrete section. The tracer cocktail has since been allowed to migrate outwards mainly by diffusion across the interface and into the argillite host rock. The scope of LBNL's modeling task is to perform predictive simulations of the hydro-chemical-mechanical couplings occurring during the *in-situ* Cl-D experiment at Mont-Terri (Rutqvist et al., 2021a, Section 10).

6.2.3.1. Model Development

The numerical simulations of the CI-D experiment have been conducted using the code CrunchClay, which is an evolving branch of the code CrunchTope/CrunchFlow (Steefel et al., 2015). The code considers electrostatic effects associated on chemical transport (Tournassat and Steefel, 2019a,b; Steefel and Tournassat, 2021). The model is based on a dual continuum formulation to account for diffuse layer and bulk water pore space. The diffuse layer model is obtained by volume averaging ion concentrations in the Poisson-Boltzmann equation, but includes the treatment of longitudinal transport within this continuum. The calculation of transport within the bulk and diffuse layer porosity is based on a new formulation for the Nernst-Planck equation that considers averaging of diffusion coefficients and accumulation factors at grid cell interfaces.

The CrunchClay simulator, which is able to model simultaneously the transport of anions, cations/, and uncharged solutes in charged media, is now coupled to flow and reaction taking place in the bulk water (electrically neutral) porosity and has been demonstrated on a single discrete fracture-clay matrix problem in 2D (Tournassat and Steefel, 2019a,b; Steefel and Tournassat, 2021). It was necessary to add new capabilities to the code to fully take into account the complexity of the Cl-D simulation objectives. These developments are still on-going. To simulate the mechanical behavior of the clay rock, which is attributed to the swelling properties of clay mineral compounds, a new mathematical model has been developed (see Equations 10-1 through 10-9 in Chapter 10 of the report by Rutqvist et al., 2021a). The model is based on the same working hypothesis a thermodynamic equilibrium between the various types of porosity. The values of the Ionic strength and water activity have been added in the set of primary variables in order to be able to couple their changes in the swelling properties during the Newton iteration cycle. Speciation results are currently

benchmarked with results obtained with the previous version of the code. Once this benchmarking is completed, the newly developed transport equations will be implemented.

In order to simulate the Cl-D experiment at Mont Terri, it will eventually be necessary to have a full 3D treatment of the system. LBNL scientists are currently extending the simulation methods and the model geometry to 3D, working first with the legacy version of CrunchClay. Once completed, the changes will be migrated to the newer version of CrunchClay described above. Future work will consist of completion of the tasks described in Sections 10.1.1-10.1.4 of the report by Rutqvist et al. (2021a). To get early insights into the predicted behavior of CI-D, LBNL conducted preliminary 2D simulations in FY21 as summarized below.

6.2.3.2. Preliminary 2D Calculations

Preliminary calculations were performed using the dual-continuum version of the CrunchClay simulator (Steefel and Tournassat, 2021). These simulations make use of ad hoc parameters, not definitive ones (see Table 10.3 of the report by Rutqvist et al., 2021a), with the purpose of viewing the approximate system behavior while at the same time demonstrating that the problem in 2D is tractable. Simulations for the period of 1,000 days require about 24 hours. The total size of the system is 1.5 m × 0.8 m with mesh discretization down to 0.002 m (3,000 cells in total). All boundary conditions are treated as no-flux, and only diffusive transport via the Nernst-Planck equation is considered. Initial conditions and self-diffusion coefficients for the aqueous species are given in Tables 10.1 and 10.2 of Rutqvist et al. (2021a), respectively. For the Opalinus Clay, sorption on the clays was simulated with a specific surface area of 790 m^2/g and a volume fraction of 0.12%. The site density for surface hydroxyls on the clays of 4.59×10^{-6} mol/m^2 was used in the simulations. The following tortuosity values were taken into account: a value of 1 for the high porosity fracture zone, a value of 0.12 for the Opalinus Clay (OPA), and a value of 0.10 for the concrete (OPC). Initial conditions for the simulation are shown in Figure 6.2-5.
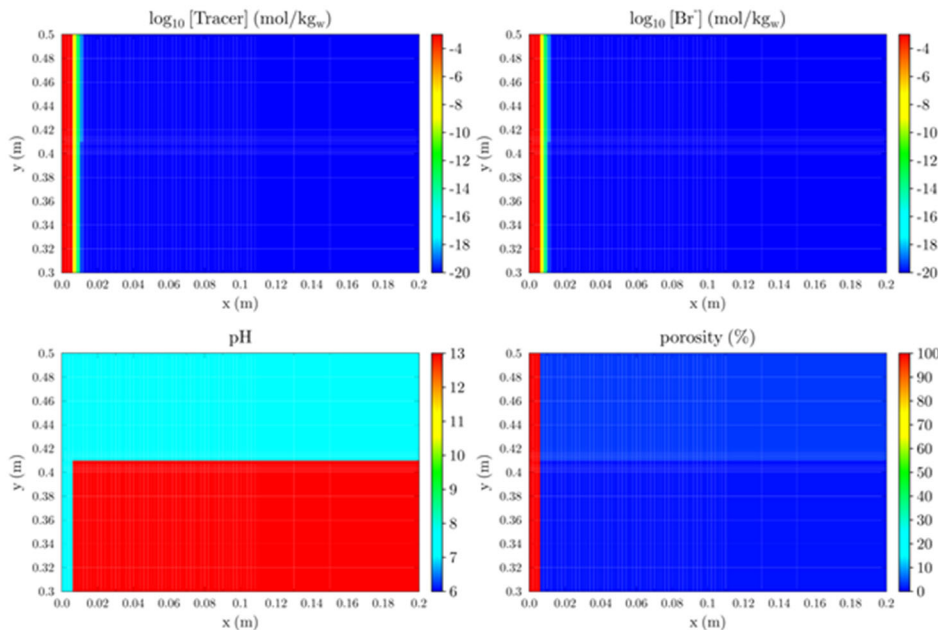
Figure 6.2-5. Initial conditions for a 2D simulation of system with a borehole or fracture on the left of the simulation domain, and a horizontal interface between OPA (Opalinus Clay) and concrete materials (OPC) on the right of the simulation domain. The concrete domain can be visualized with the high pH value resulting from the solubility of portlandite (pH = 13.39). OPA and concrete positions correspond to the low porosity domain. The system is discretized with 3000 cells with a dimension refinement down to 0.002 m at the interfaces between the three domains. The tracer is a neutral molecule (such as HTO). Br⁻ serves as an anionic tracer for the simulation, similar in behavior to ^{36}Cl⁻.

Although preliminary, the 2D reactive transport simulations display some of the expected behavior of a concrete-Opalinus Clay system within which a single higher porosity zone is developed within otherwise lower porosity clay rock. Only diffusive transport is considered and is treated with the dual porosity approach outlined above, with a Nernst-Planck rather than Fickian treatment of diffusion in all cases.

The relatively high ionic strength of 0.3 m results in less difference between the anionic and uncharged tracer distributions than would be expected at lower ionic strength, but some difference can be seen if the results are examined closely (Figure 6.2-6). Between 100 and 1,000 days (still a period of time less than the experiment), the high pH front propagates into the Opalinus Clay via diffusion, with greater advancement in the y-direction within the high porosity zone on the left (Figure 6.2-7).
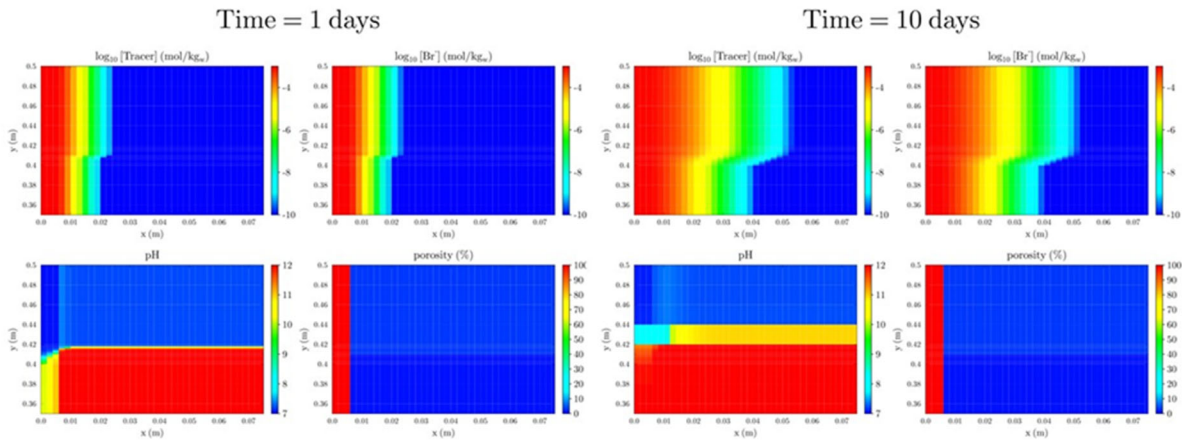
Figure 6.2.-6. Early time behavior (1 day to 10 days). Note the retardation of the pH front relative to the tracer and the slight retardation of the anion front relative to the uncharged tracer. The relatively high ionic strength of the background electrolyte (0.3 m) minimizes to some extent the anion retardation compared to a more dilute case.
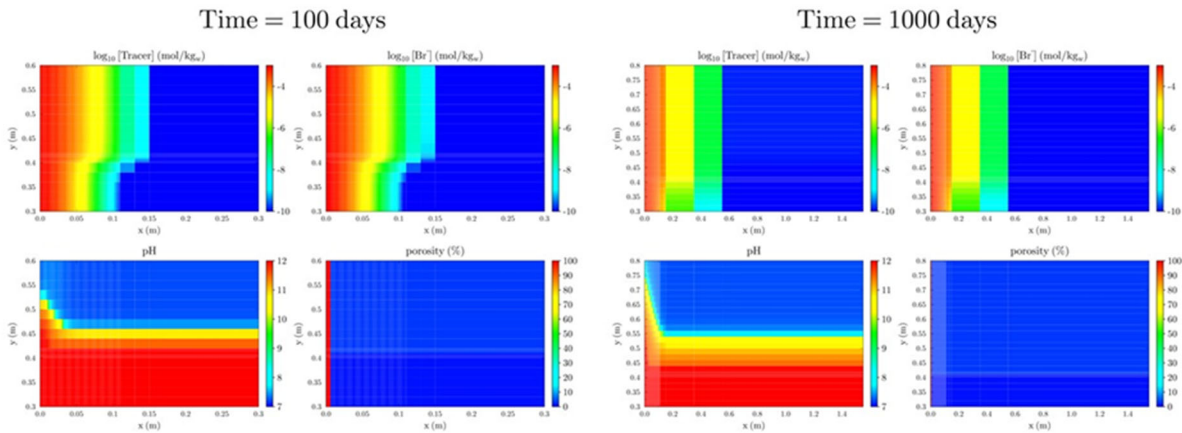
Figure 6.2-7. Diffusion-reaction simulation results from 100 to 1,000 days. The high pH front propagates both within the micro-fracture zone on the left via diffusion and within the Opalinus Clay close to the concrete contact. Note the change in horizontal scales in comparison with Figure 6.2-6.

6.2.3.3. Summary and Future Work on Cl-D Experiment at Mont Terri

The performed investigations included (1) the development of a new model that includes a set of new master variables, including the electrical potential and the ionic strength, (2) conversion of the CrunchClay simulator to 3D, and (3) preliminary scoping calculations of a 2D system containing a single higher porosity zone, in which diffusive transport is enhanced compared to typical Opalinus Clay (no flow is considered). The results

of preliminary simulations suggest the propagation of uncharged tracer, anion, and pH fronts over the time period of 100-1,000 years.

Future work will include 3D modeling of the Cl-D experiment at Mont Terri, using the 3D capability in CrunchClay. Figure 6.2-8 provides a schematic illustration of fluid circulation, sampling, and tracer dosing system in the Cl-D experiment at Mont Terri, which will be simulated when the 3D CrunchClay code is ready. Electrostatic effects on transport in the clay-rich Opalinus will be considered, and reaction-induced changes in porosity and permeability due to the reaction of the high pH cement and the OPA will be calculated.

While not described here, LBNL scientists also attempted to use a pore- to mesoscale model based on the Lattice Boltzmann Model (LBM) approach to simulate the cement-bentonite interface area, as an alternative approach to the CrunchClay continuum modeling. In FY21, LBNL scientists started with capability development adding a reactive transport module to an existing LBM simulator for multiphase flow (see Chapter 9 in Rutqvist et al., 2021a). The next step will be to verify the LBM model against the continuum reactive transport model.
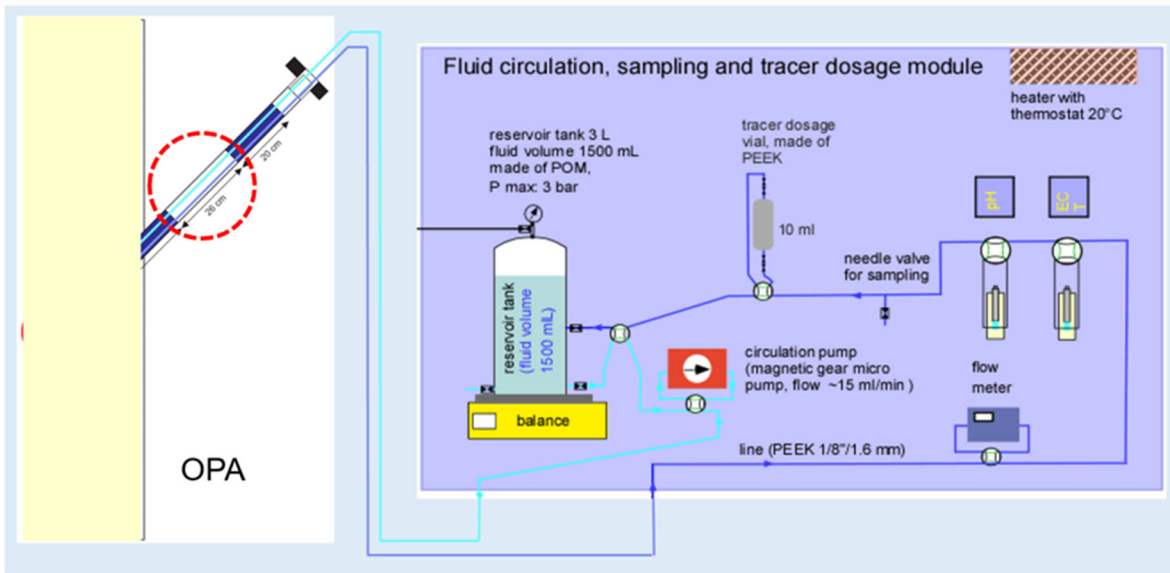
Tracers: ^{3}H, ^{36}Cl

Water tracer and anion (conservative, electrostatic effect)

Tracer	Activity conc.	LL	Activity (1.5 L)	LA (1.5 L)
^{3}H (HTO)	$2 \cdot 10^5$ Bq/kg	2	$3 \cdot 10^5$ Bq	0.001
^{36}Cl	$4 \cdot 10^4$ Bq/kg	40	$6 \cdot 10^4$ Bq	0.06

LL: clearance limit / Befreiungsgrenze; LA: licensing limit / Bewilligungsgrenze

Figure 6.2-8. Schematic illustration of fluid circulation, sampling, and tracer dosing system in the Cl-D experiment at Mont Terri. The data from this recirculation system will be used in 3D modeling when the 3D code is ready.

6.3. Modeling of THM Processes in Heater Experiments in Argillaceous Rock

This section provides a summary of international SFWD R&D activities focused on modeling of THM processes taking place in large-scale heater experiments conducted in argillaceous host rock—the Mont Terri FE Experiment in Switzerland (see Section 6.3.1), and the Thermal Fracturing Experiment at the Bure URL in France (see Section 6.3.2). As opposed to the experimental and modeling described in Sections 6.1 and 6.2, the emphasis in these experiments is more on the host rock than on the EB.

6.3.1. Modeling of the Mont Terri FE Experiment

6.3.1.1. *Status of the Mont Terri FE Experiment*

The full-scale Mont Terri FE experiment in the Mont Terri URL provides experimental data needed for understanding THM coupled processes taking place in the host rock and in the emplacement tunnel under realistic environmental conditions, such as representative ranges of temperature, saturation, swelling pressure, and stress gradients (see Section 3.1.2). Processes examined in the test include many aspects of the expected repository evolution, such as creation and desaturation of the EDZ during tunnel excavation and operation (including ventilation), reconsolidation of the EDZ, resaturation, thermal stress, and thermal pore-pressure increase after backfilling and heating. The heater test was constructed and instrumented in 2011 and 2012. In 2012, the tunnel was opened for a one-year ventilation period. Then, the heaters, bentonite buffer, and a concrete plug were emplaced. In the fall of 2014 and early 2015, the heaters were gradually turned on, and starting in February 2015, the full heat power of 1,350 W was established at all three heaters (H1, H2, H3). The heating is expected to last for at least 15 years, with continuous monitoring of THM processes in both the bentonite buffer and surrounding rock. Since the planning phase for the FE Experiment, LBNL scientist have been involved in the predictive and interpretative modeling of the experimental data collaborating with other international; modeling teams associated project partners.

6.3.1.2. *FE Experiment as a Modeling Task in DECOVALEX-2023*

In Spring 2020, the FE Experiment was selected as a new modeling task in the international DECOVALEX-2023 Project. The goal of the comparative modeling task is to understand the pore pressure development in the Opalinus Clay, which is affected by heating, engineering factors (e.g., shotcrete, tunnel shape) and damage due to tunnel construction and thermal effects. The task is divided into the following steps, as defined in the task specification:

- **Step 0 - Preparation phase:** Benchmarking of participating teams computing methods against some simple, tightly defined 2D test cases, which are designed to obtain consensus across the modeling teams and to test modeling capabilities. The modeling cases are:

  - **Step 0a:** 2D Thermal-only simulations with saturation dependent thermal properties and saturation held at initial values.

  - **Step 0b:** 2D Thermal-hydrological simulations with vapor transport simulations. TH model with partial saturation in the bentonite and Opalinus Clay close to the tunnel.

  - **Step 0c:** 2D THM simulations which include rock mechanics. Linear elastic models for bentonite and Opalinus clay to be used.

- **Step 1 - FE heating phase:** Modeling the change in pore pressure in the Opalinus Clay because of heating in the FE experiment, which will require 3D THM simulations of partially saturated media.

- **Step 2 - FE ventilation phase:** Modeling of absolute pressures in the Opalinus Clay, which will require representation of the ventilation of the FE tunnel prior to heating. Modeling teams can choose the complexity of the representation of excavation and EDZ development.

Researchers from LBNL and SNL are participating in this modeling task together with several other international modeling groups. In Section 6.3.1.3, we present the current status of LBNL's modeling of the FE Experiment at Mont Terri, followed by SNL's modeling results in Section 6.3.1.4.

6.3.1.3. TOUGH-FLAC Modeling of the Mont Terri FE Experiment Conducted by LBNL

6.3.1.3.1. Conceptual Model and Numerical Grids

LBNL's modeling of the multiphase coupled THM processes observed in the FE is conducted with the TOUGH-FLAC simulator developed at LBNL (Rutqvist et al. 2002; 2011; 2014; Zheng et al. 2015; 2016). The original TOUGH-FLAC version was modified over the years to be better suited for applications related to bentonite-backfilled repositories in clay host formations (Rutqvist et al., 2014a; Rutqvist, 2016). Major improvements include implementation of the Barcelona Basic Model (BBM) for the rigorous THM modeling of swelling behavior of materials and applied to modeling of bentonite backfill behavior (Alonso et al., 1990). Recently, the BBM was extended to a dual-structure model, referred to as the Barcelona Expansive Model— BExM (Vilarrasa et al., 2015).

Using TOUGH-FLAC, the host rock surrounding the FE tunnel is modeled taking into account the anisotropic properties considering bedding planes of the Opalinus Clay. To accurately model anisotropic thermal and hydrological behavior, LBNL created an inclined mesh. For the bentonite, the mechanical behavior of the buffer was not considered because (a) no significant swelling stress has been developed at the experiment, and (b) the DECOVALEX-2023 project is focused on the THM processes in the host rock rather than the bentonite buffer. LBNL's current simulation model for the FE Experiment is based on previous work reported in Rutqvist et al. (2018; 2019; 2020). In FY21, the existing 3D model was considering a bedding dip of 34º compared to the previous model that assumed a dip of 45º. In addition, a new 2D model was developed for benchmarking within the DEOVALEX-2023 project.

Figures 6.3-1 and 6.3-2 show the numerical grids of the FE experiment developed for the DECOVALEX-2023 modeling. Figure 6.3-1 presents a new simplified 2D grid that was applied in the initial benchmark simulations for the DECOVALEX-2023. Figure 6.3-2 presents an updated 3D TOUGH-FLAC numerical grid of the FE experiment, which includes all material components used for modeling of the FE experiment, such as the layered Opalinus Clay host rock, excavation disturbed zone, tunnel, three heaters, bentonite buffer, concrete liner, and a concrete plug. The following initial conditions for the model simulations were selected: pore-fluid pressure of 2 MPa, temperature of 15ºC, and σ_x = 4.5 MPa, σ_y = 2.5 MPa, σ_z = 6.5 MPa for the host rock. Because the 2 MPa pore pressure does not represent hydrostatic conditions, simulations were first running to model an open tunnel at the atmospheric pressure for one year, creating a pressure drop and hydraulic gradient around the tunnel. Afterward, heating simulations included instantaneous emplacement of the heater and the buffer. Outer boundary conditions of the model were a fixed zero displacement and no heat of fluid transfer. Simulations confirmed that these boundaries are placed far enough from the heat source so that there is no heating effect on the outer boundaries. In the 2D model simulation a heat load of 293 W/m was assumed. This number was calculated as the total heat decay power for one canister (1,350 W) divided by the length of the canisters (4.6 m).
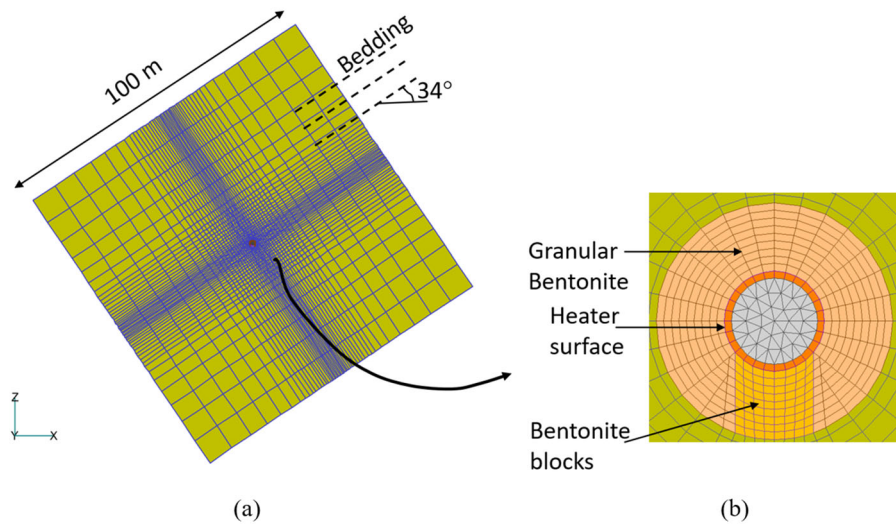
Figure 6.3-1. TOUGH-FLAC 2D numerical grid of the FE experiment for DECOVALEX-2023 benchmarking: (a) entire model, and (b) materials and gridding of the EBS.
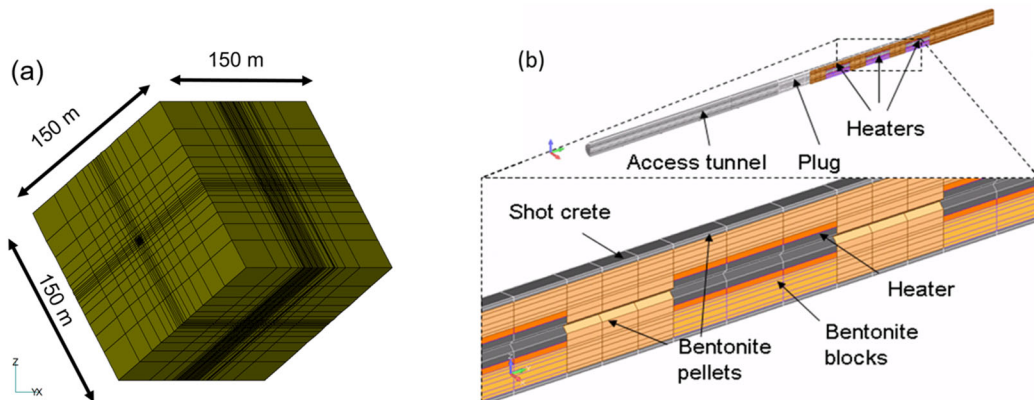
Figure 6.3-2. TOUGH-FLAC 3D numerical grid of the FE experiment: (a) entire model, and (b) materials and gridding of the EBS.

6.3.1.3.2.   Simulation Results

The simulations for the DECOVALEX-2023 modeling task focus on the pressure evolution in the host rock surrounding the tunnel. Nevertheless, the evolution of coupled THM processes in the buffer could have an impact on the host rock, in particular, due to the strong capillarity suction from the partially saturated bentonite. Figures 6.3-3 and 6.3-4 present the simulation results of temperature and fluid pressure for the 2D benchmarking simulation. Because both thermal conductivity and permeability are along the bedding higher than across the bedding, the temperature at monitoring points O1 to O3 located along the bedding increases faster than at points O4 through O6. The faster temperature growth causes a stronger thermal pressurization at early stage of heating, followed by a faster pressure decline after the initial pressure pulse. The fluid pressure close to the tunnel is strongly impacted by the capillary suction in the bentonite, which tends to draw water from the surrounding host rock. Figure 6.3-3b shows that the pressure at point O1 falls to near zero at 800 days, because the host rock is desaturated at that location. Figure 6.3-4b illustrates in blue color the zone of very low fluid pressure around the tunnel.
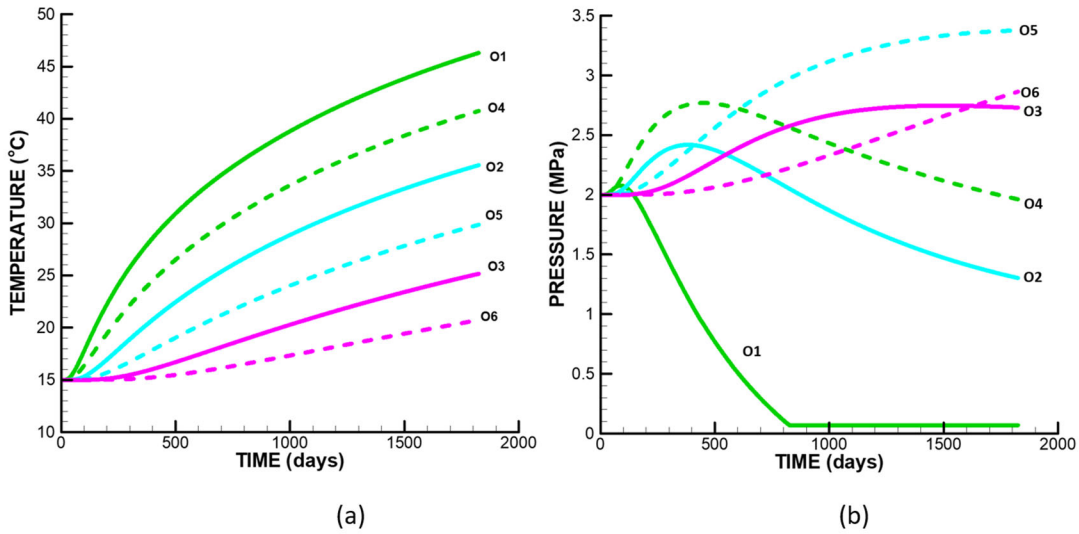
Figure 6.3-3. 2D model simulation result of anisotropic evolution of (a) temperature, and (b) fluid pressure, at monitoring points O1 to O6 located in the Opalinus Clay. See locations O1 to O6 in Figure 6.3-4.
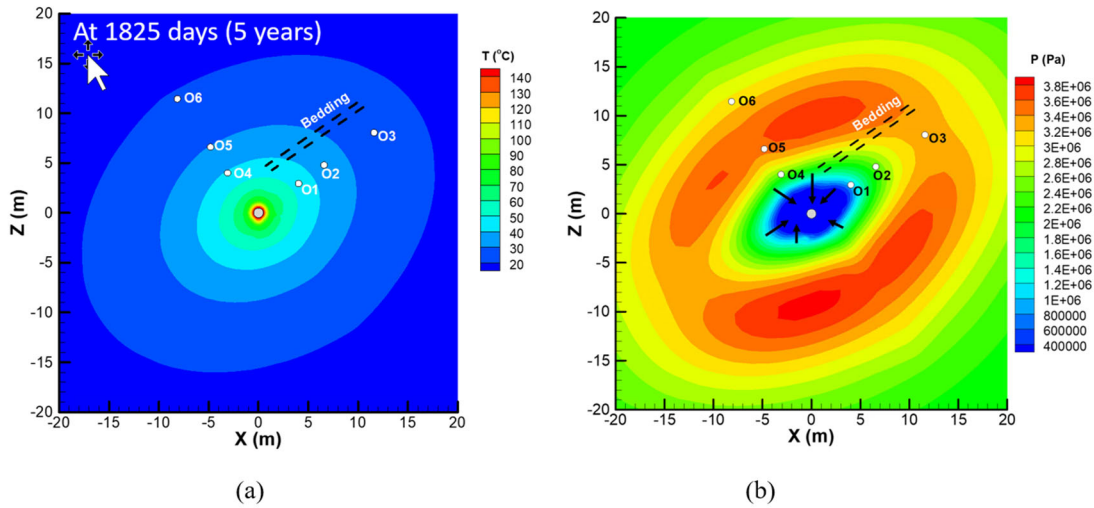
Figure 6.3-4. 2D model simulation result of anisotropic distribution of (a) temperature and (b) pressure after 5 years.

Model comparison with other modeling teams in the DECOVALEX-2023 task revealed a systematic difference in the results of modeling of the fluid pressure. The modeling results from the LBNL's TOUGH simulations tend to result in a lower thermal pressurization compared to the benchmark solution developed in the DECOVALEX-2023 task. The reason for this difference can be explained by the fact that TOUGH used the built-in temperature dependent water properties from steam tables, while in the task description, temperature-independent constant values of water properties were given.

Figure 6.3-5 shows a comparison to the temperature dependent properties and the constant value defined in the DECOVALEX-2023 description. As shown, for the temperature range from 15º to 40ºC, the thermal expansivity defined in the DECOVALEX-2023 is higher than the temperature dependent values used in TOUGH2. The reason for the constant thermal expansivity in the DECOVALEX-2023 was to have a simplified case for comparison and a code-to-code verification between the modeling teams. However, it appears that it will be important to have an accurate model for thermal expansivity of water to improve predictions of thermal pressurization around a repository tunnel.
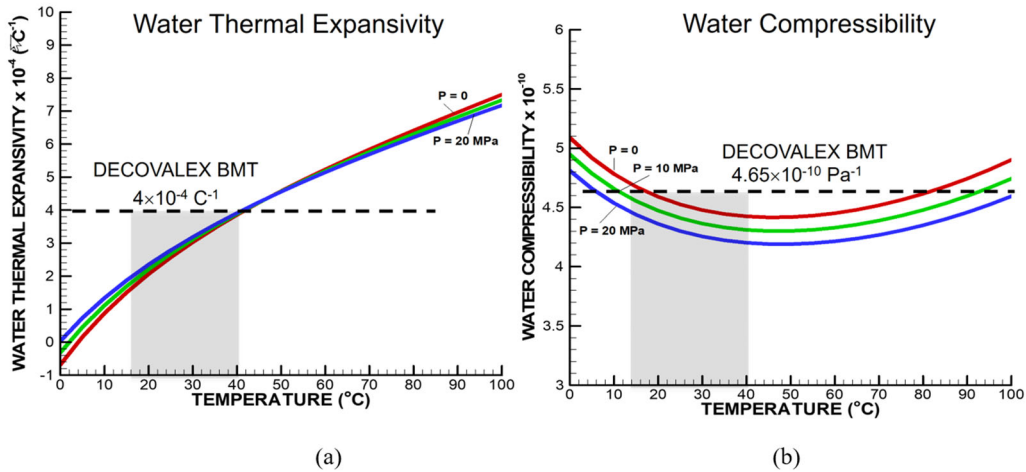
Figure 6.3-5. Comparison of water properties defined in DECOVALEX-2023 task definition with temperature dependent water properties as assumed in the TOUGH2 code: (a) water thermal expansivity, and (b) water compressibility.

Figures 6.3-6 and 6.3-7 depict selected results from full 3D model simulations. Figure 6.3-6 shows that the heater temperature increases to 130ºC. The highest temperature occurs on top of the middle heater (H2), while the temperatures on top of the two outer heaters (H1 and H3) are slightly lower. The simulation results also show that the heater temperature is slightly lower at the bottom of H2 compared to that at its top. The lower temperature at the bottom can be attributed to the higher degree of saturation and a higher thermal conductivity of the bentonite blocks below the heaters. Comparison of the results depicted in Figure 6.3-7 for the 3D model to the results shown in Figure 6.3-3 for the 2D case shows that temperature increased much less for the case of 3D modeling. The lower temperature increase also results in a lower thermal pressurization in the 3D modeling compared to the 2D modeling. The 2D model overestimates temperature as a result of the greater heat load (293 W/m) and the lack of lateral heat loss that is taken into account in a full 3D model. These results indicate that thermal pressurization is quite small.
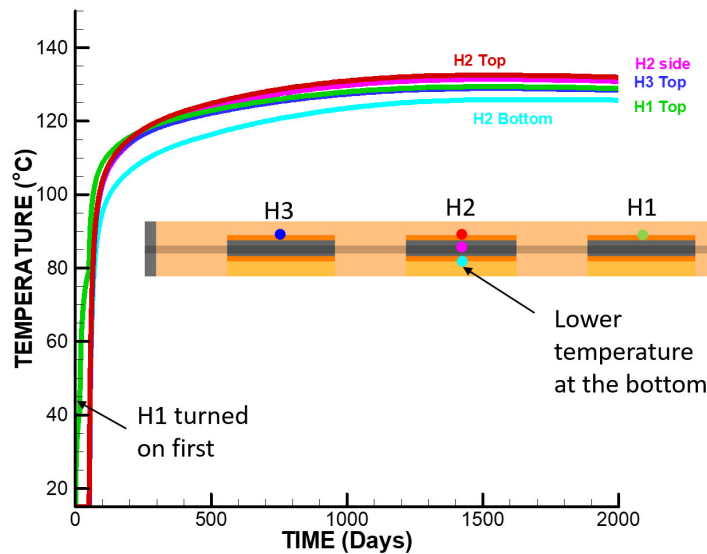
Figure 6.3-6. 3D modeling results of heater temperatures.
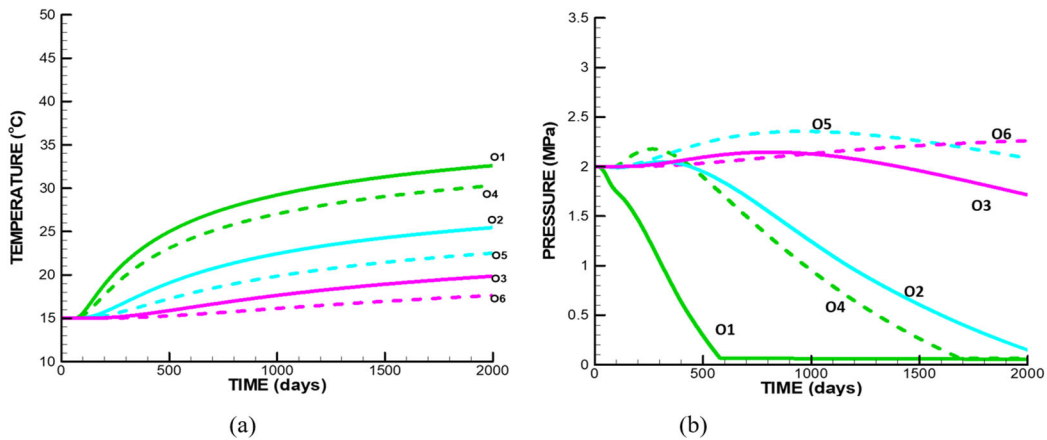
Figure 6.3-7. 3D model simulation result of anisotropic evolution of (a) temperature and (b) fluid pressure at monitoring points O1 to O6 located in the Opalinus Clay. See locations O1 to O6 in Figure 6.3-4.

6.3.1.4. THM Modeling of the Mont Terri FE Experiment Conducted by SNL

6.3.1.4.1. Conceptual Model and Numerical Grids

The SNL team conducted numerical simulations of the FE modeling task using two different numerical codes: PFLOTRAN (Hammond et al., 2014) and COMSOL Multiphysics®. The report by Matteo et al. (2021) describes SNL's modeling results for Step 0 of the DECOVALEX task. The 2D modeling domain represents a cross-section through the center of the middle heater in the FE experiment (Figure 6.3-8). The geometry and mesh used for PFLOTRAN simulations are shown in Figure 6.3-9. The domain size is 50 x 50 m, and the mesh consists of 138,103 grid blocks. Like LBNL's modeling team, SNL conducted the 2D benchmark simulation using the predefined DECOVALEX Task C material properties, as provided by the task leads. In other words, both LBNL's and SNL's simulations were conducted using the same material parameters. The following specified material property equations were added into PFLOTRAN to accommodate the FE modeling task requirements: (1) the thermal conductivity equation as a function of liquid saturation, (2) the heat equation a function of various variables, (3) a water density equation that uses a constant thermal expansion coefficient of water, and (4) the pore compressibility as a function of porosity.
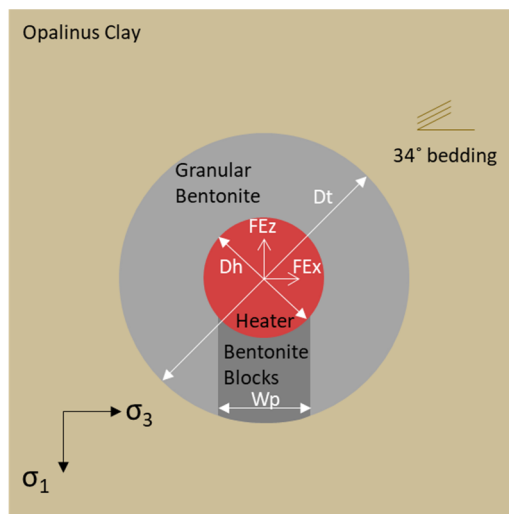
Figure 6.3-8. Model geometry for Step 0 simulations (Task C Specifications).
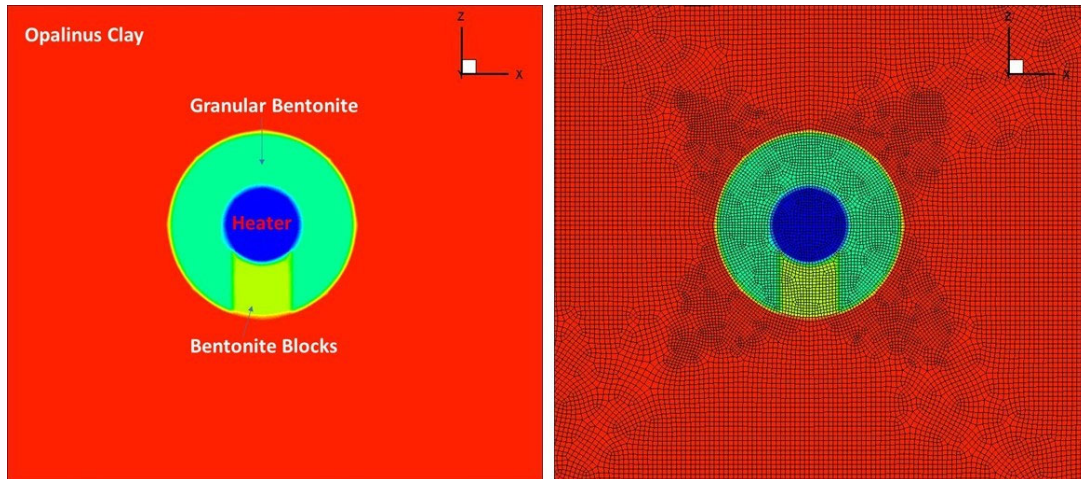
Figure 6.3-9. Geometry and meshing used for Task C, Step 0 PFLOTRAN simulations.

6.3.1.4.2.   *Simulation Results*

Both PFLOTRAN and COMSOL® simulations were conducted for Step 0a (T) and Step 0b (TH) simulations, and the COMSOL® simulations were also conducted for Step 0c (THM). Simulation results are given for the measurement locations, which are summarized in Table 2 of the report by Matteo et al. (2021), and will be shown below on the figures depicting the time trends of modeling variables. The results of PFLOTRAN Step 0b simulations are shown in Figures 6.3-10, presenting a 2D distribution of temperature; and Figures 6.3-11 and 6.3-12, showing the temporal trends of temperature and relative humidity, respectively. Figures 6.3-13 and 6.3-14 show COMSOL® predicted evolution of (a) temperature in the bentonite (both bentonite blocks and granular bentonite), and (b) liquid pressure at specified locations in the Opalinus Clay.
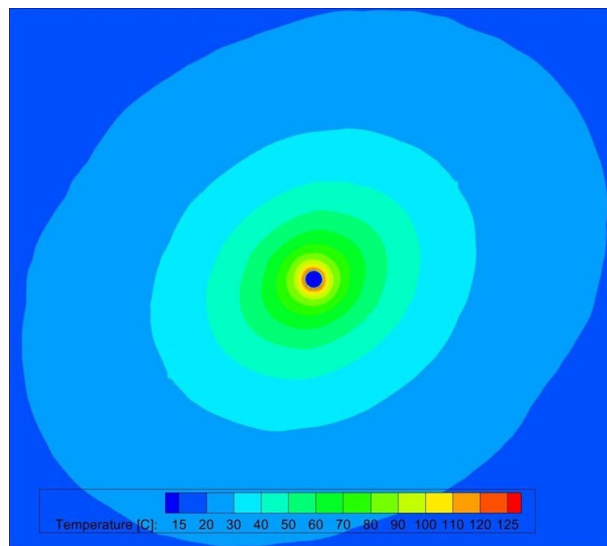
Figure 6.3-10. Step 0b: PFLOTRAN 2D predicted temperature distribution at 1,800 days (with anisotropy).

Predicted temperature trends for the thermal-only case (Step 0a) were about the same for most Task C participating teams. However, predictions for the TH (Step 0b) and THM (Step 0c) modeling cases are different. To evaluate the causation of these differences, two additional TH cases were simulated for Step 0b: the Case b2, a TH model with the Opalinus Clay properties, but zero (or very small) permeability of the Opalinus Clay, and a Case b3, a TH model with the Opalinus Clay properties, but typical permeability of the Opalinus Clay.

SNL's COMSOL® simulation results for Case b2 compared well with the results of other teams that used constant linear thermal expansion coefficient of water. However, SNL's PFLOTRAN liquid pressure simulations were consistently lower because of the use of the built-in equation of state (EOS) that uses temperature varying thermal expansion coefficient (water density). This was also the case with simulations performed by LBNL described in Section 6.3.1.3. SNL also compared the results of modeling using PFLOTRAN and COMSOL® for Case b2, taking into account the temperature variable thermal expansion coefficient of water, but without the effect of anisotropy of Opalinus Clay. The results of simulations using the two codes matched very well.

(a)   (b)
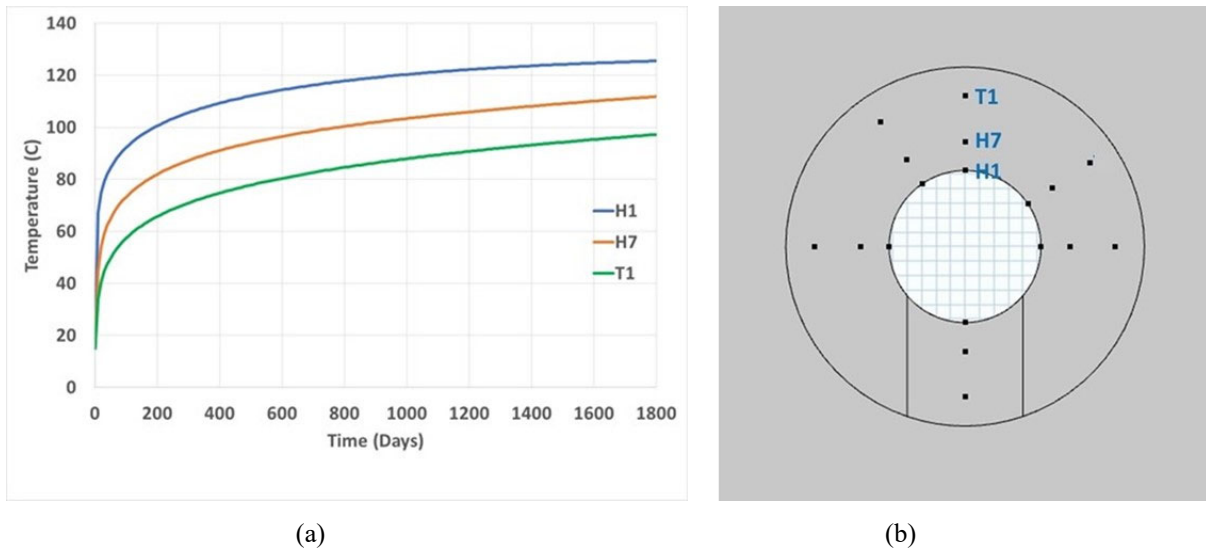
Figure 6.3-11. Step 0b: (a) PFLOTRAN predicted trends of temperature, and (b) a map of locations of measurements.

(a)   (b)
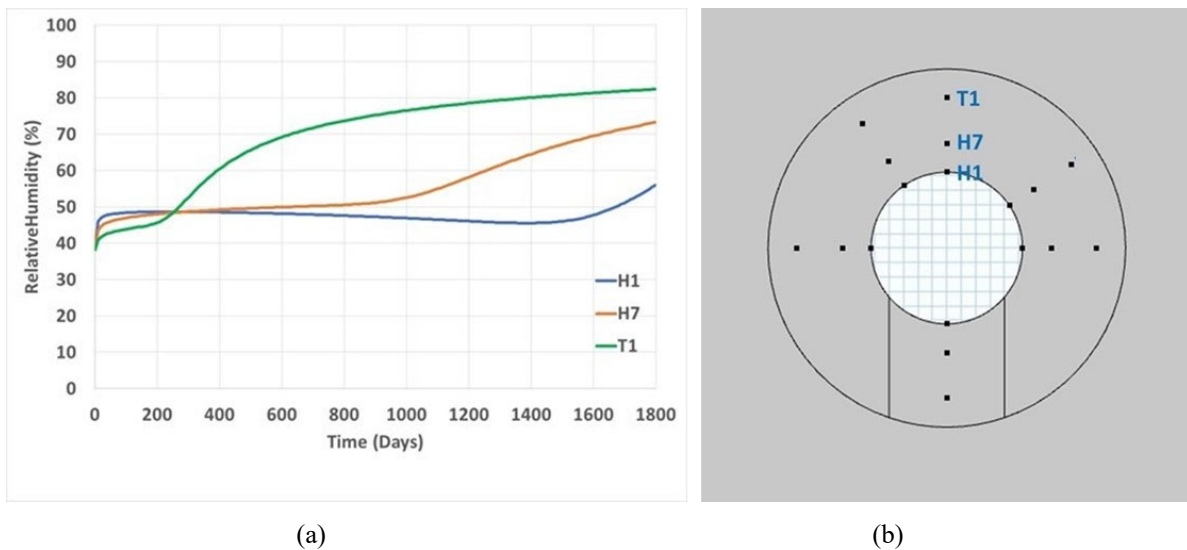
Figure 6.3-12. Step 0b: (a) PFLOTRAN predicted trends of relative humidity, and (b) a map of locations of measurements.
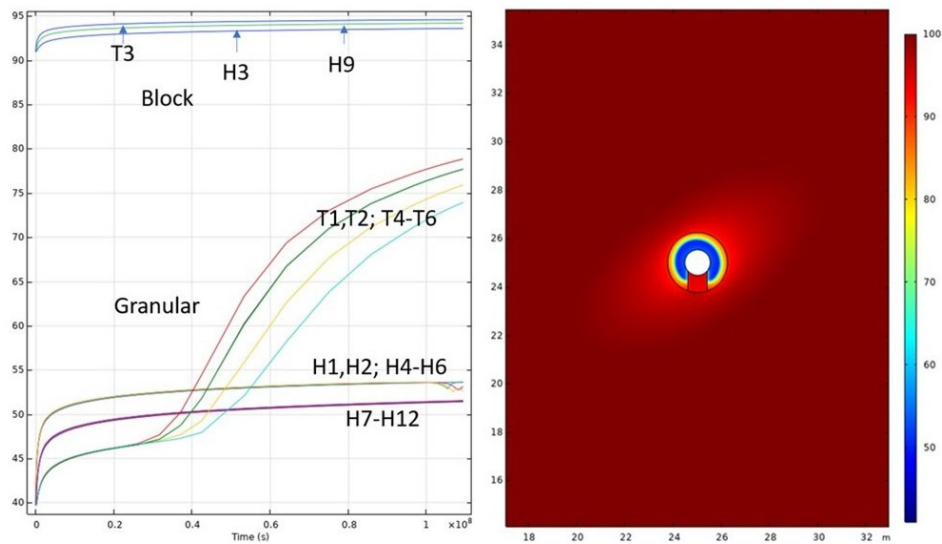
Figure 6.3-13. Step 0b: COMSOL® predicted evolution of relative humidity at specified locations.
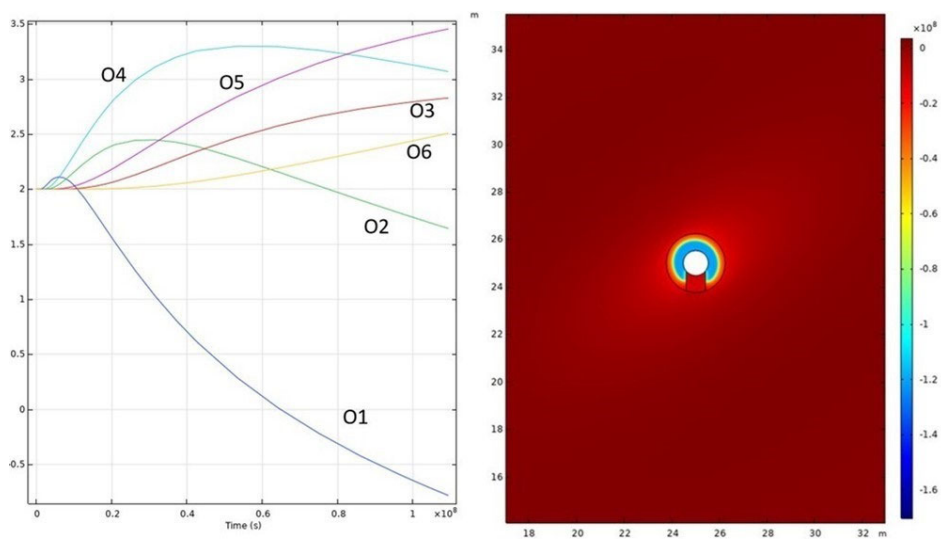
Figure 6.3-14. Step 0b: COMSOL® predicted evolution of liquid pressure at specified locations.

6.3.1.5. Summary and Future Work

Preliminary simulations of DECOVALEX Task C, Step 0, which were conducted at LBNL, using TOUGH-FLAC, and SNLs, using PFLOTRAN and COMSOL® codes, were used to build models for T, TH and THM simulations. Simulations of Step 0 will continue to reduce differences between DECOVALEX modeling teams. Modeling will also start on Task C, Step 1. The next step in the DECOVALEX-2023 task will involve comparison to field data for the first 5 years of the experiment. This will also include comparison of mechanical responses in the host rock such as strain, following by regular Mont Terri project simulations of the field data going beyond 5 years. Modeling will also involve simulations of the excavation and ventilation phase before the heaters were turned on, as well as will focus on simulations of the evolution of the bentonite buffer to understand the stress in the bentonite buffer.

6.3.1.6. Modeling of Thermal Fracturing in COx Claystone at Bure

As described in Section 3.2.3.1, the French nuclear waste disposal agency ANDRA is currently conducting a Thermal Fracturing Experiment in the Bure URL to better understand the processes and mechanisms of fracture initiation and growth in claystone due to a rapid increase of temperature. This experiment and some supporting laboratory studies are now used in a new modeling task of the DECOVALEX-2023 Project (Task A). The concept for deep geological disposal of radioactive waste in France, called Cigéo, is based on the emplacement of exothermic waste packages in long parallel micro-tunnels drilled from access tunnels. The heat emitted by the HLW is expected to cause the temperature rise within the host formation and its surrounding layers. In the water-saturated and low-permeability COx, the temperature rise could cause a pore pressure increase due to the difference between the thermal expansion coefficient of pore water and of solid skeleton, causing the formation of diffuse fractures or damage due to transient THM loading. The DECOVALEX-2023 Task A started in FY21 with benchmark simulations of laboratory experiments of thermal pressurization with fracturing. This initial step involved modeling of a series of thermal extension tests performed on COx samples taken from the Bure URL. LBNL scientists are participating in Task A and in FY21 performed TOUGH-FLAC modeling of the thermal pressurization laboratory experiments (Rutqvist et al., 2021a). According to the Task A planning, the initial benchmarking step will later be followed by numerical modeling of the thermal fracturing *in-situ* experiment and by application of these models at the repository scale.

6.3.1.7. Laboratory Experiments on Thermal Pressurization of COx Claystone

Braun (2019) conducted a series of laboratory investigations using samples of the COx. The samples were subjected to different thermal loads, but lateral deformations were constrained, and the vertical total stress on the top of the sample remained constant. Three samples (EXT1, EXT2, and EXT3) were collected at the Bure URL, and tested under different initial conditions to investigate the effect of the initial stress state and the initial temperature on the stress-strain behavior and the tensile strength of the COx. Figure 6.3-15 shows the conceptual design of the experiments which are described in detail in Braun (2019). The sample fluid pressure was measured through drainage lines connected to a geotextile, wrapped around the specimen inside a jacket. The jacket, a neoprene membrane was put over the specimen and the geotextile, providing isolation between the confining fluid and the pore fluid. An internal aluminum force sensor measured the axial total stress. Axial and radial strains were recorded through the strain gages glued on the sample at mid-height (Braun, 2019). The samples were first loaded under different confining pressure, σ_0, and then were saturated under a fluid pressure of $P = 0.1$ MPa; swelling strains stabilized after about two days (Figure 6.3-15). After hydration, different initial conditions for each sample were set prior to heating.
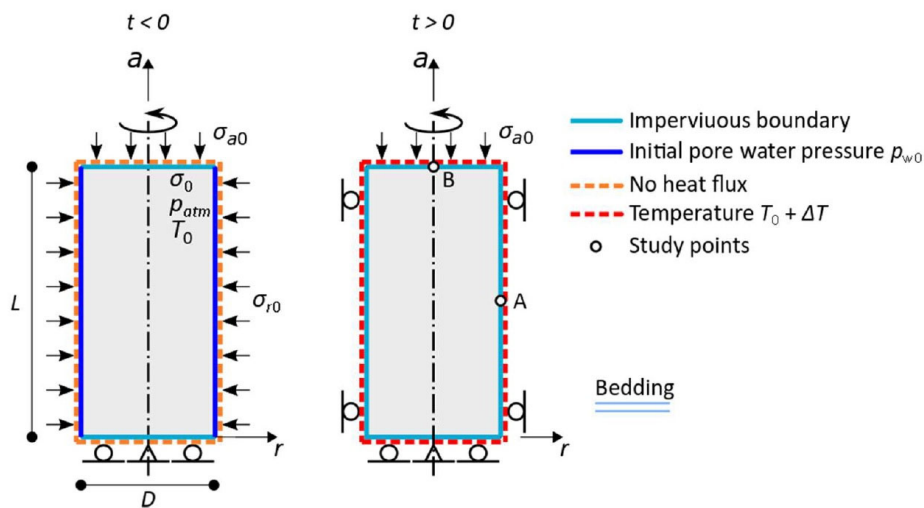
Figure 6.3-15. Conceptual model of the thermal-fracturing experiments that were conducted by Braun (2019).

6.3.1.8. Comparison of Experimental and Simulation Results

Figure 6.3-16a shows a comparison of the experimental and modeling trends of the applied thermal load, which cause variations of the fluid pressure (Figure 6.3-16b), total stresses (Figures 6.3-16c, d), axial strain (Figure 6.3-16e), and effective stresses (Figure 6.3-16f). The main processes occurring during the thermal extension tests can be summarized as follows: (1) an increase in pore pressure due to thermal pressurization, (2) an increase of axial extension and radial total stress due to lateral constrained deformations, and (3) an eventual failure, once the specimen reached its tensile strength. The axial total stress remained almost constant, with some variations due to the friction of the piston. The radial total stress and the pore pressure experienced a continuous increase due to heating (Rutqvist et al., 2021a).

The model simulation results provide a good qualitative agreement with the experimental results, but significant quantitative deviations. The agreement is the best for sensor EXT1, where the pressure is accurately modeled, axial strains are fairly well modeled, while stresses show a more significant deviation. For EXT2 and EXT3, the pressure is not as well modeled, while the total stress is closer to the experimental results. Overall, it was not possible to obtain a good match to all three experiments with the same input material properties. A calibration of the material properties was performed and some of the disagreements between modeling and experimental results were reduced, but a consistent parameter set was not obtained. One cause of the disagreement between modeling and experiments is the application of a constant axial stress at the top boundary for modeling, while it was not constant in experiments. The other reason of disagreement could be related to the fact the tensile failure process is ignored in the current TOUGH-FLAC model.

6.3.1.9. Summary and Future Work on DECOVALEX-2023 Task A

Numerical modeling of the laboratory tests of thermal pressurization of COx claystone, which were conducted by Braun (2019), showed that the main processes occurring during the thermal load tests are: (1) an increase in pore pressure due to thermal pressurization, (2) an increase of axial extension and radial total stress due to lateral constrained deformations, and (3) an eventual failure, once the specimen reached its tensile strength. Comparison of the experimental and modeling data indicated a good qualitative agreement between experimental and modeling data, while some quantitative discrepancies remain.

In the near future, LBNL plans to improve its modeling of the thermal pressurization laboratory tests considering tensile failure by applying the FLAC3D ubiquitous joint model. Together with other DECOVALEX Task A modeling teams, LBNL will then start modeling the *in-situ* experiment at Bure, an activity that will carry through most of FY22.

As described in Section 3.2.3.1, the DECOVALEX-2023 Task A comprises a parallel modeling activity with focus on the potential for gas fracturing in the COx claystone. This second activity is slightly behind; benchmark simulations related to gas fracturing have just started. Results from these simulations have not available at the time of preparation of the current report. It is intended to perform modeling of gas fracturing using a set of constitutive models that are similar for both the thermal and gas fracturing experiments.
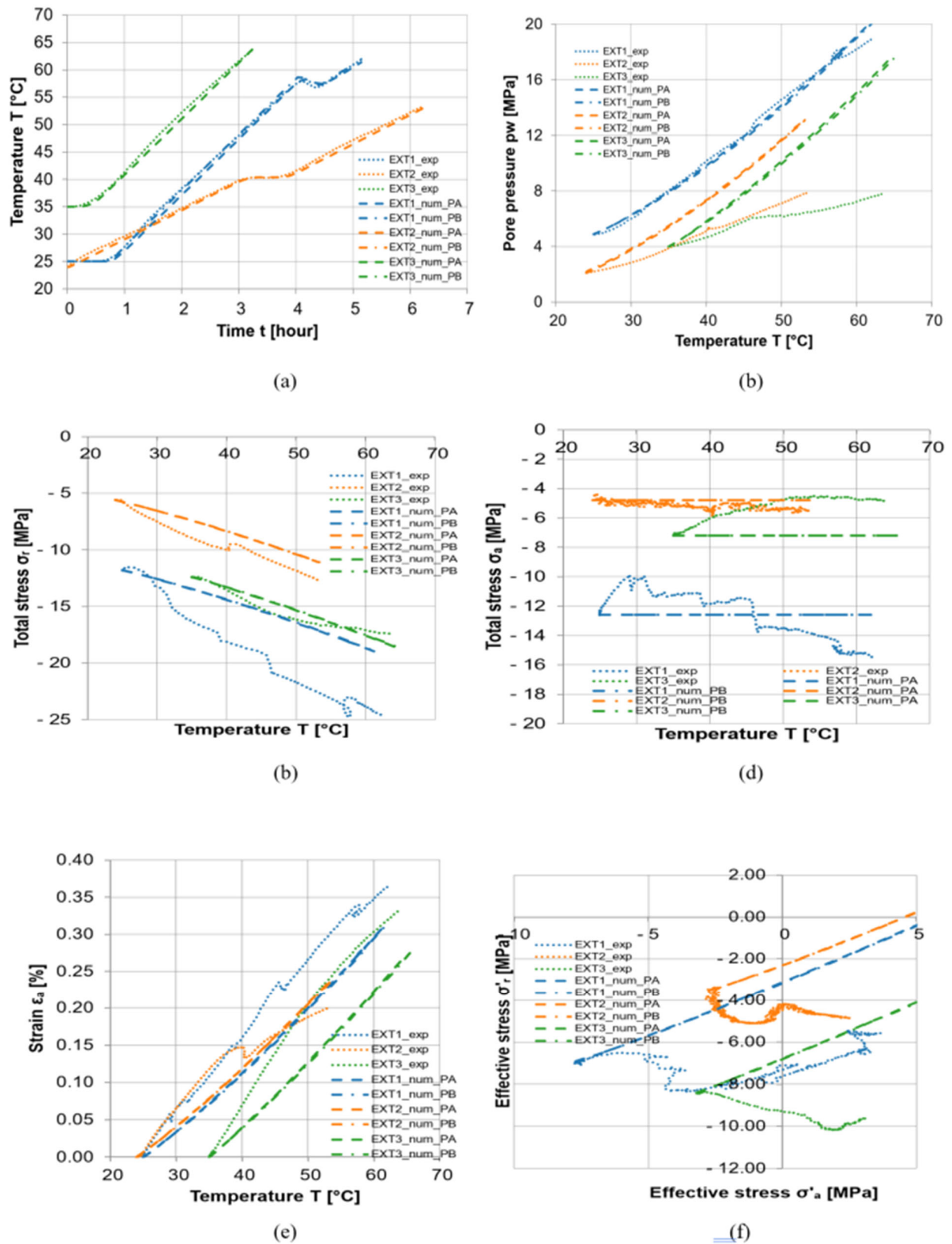
Figure 6.3-16. Experimental and numerically simulated data of the thermal extension tests: (a) temperature evolution applied during the thermal extension tests, (b) pressure, (c) radial stress, (d) axial total stress, (e) axial strain, and (f) effective stress evolution. Experimental results are from Braun (2019).

6.4. Modeling of Gas Migration in Clay-Based Materials

6.4.1. Introduction to Gas Migration

In a nuclear waste repository, hydrogen and other gases may be generated due to the corrosion of metallic materials under anoxic conditions, the radioactive decay of waste, the radiolysis of water (Christensen and Sunder, 2000), and microbial activities (Pedersen, 1996; 1999). Depending on the repository concept, the production of these gases may span in excess of 100,000 years, following emplacement of the waste. As gas is produced, it will accumulate, moving away from its source through the processes of molecular diffusion and bulk advection. The gas-water interfaces serve as an important vehicle for the transport of radionuclides and microorganisms due to preferential flow and preferential sorption (Wan and Wilson, 1994), whereas trapped gas bubbles can cause immobilization of radionuclides. In addition, local pressure build-up due to gas production and accumulation can trigger mechanical responses in low-permeability materials like bentonite and clays that reshape pore spaces by deformation or fracturing. Understanding these processes, the long-term fate of the gas, and its impact on the surrounding materials is therefore important in the development of a geological disposal facility for radioactive waste.

Upon introduction of gas into a water-saturated clay-based material (bentonite or clay rock), a discrete gas phase is expected to form and accumulate until its pressure becomes large enough to exceed the entry gas pressure of the surrounding material, at which point advective flow of gas is expected to occur. The nature of such advective flow is complex and likely affected by deformation processes such as pathway dilation. Special attention needs to be given to the mechanisms of controlling processes such as gas entry and flow, as well as pathway distribution, stability and sealing, which will impact the long-term performance of the natural and engineering barriers. Therefore, new numerical conceptual and numerical models for the quantitative prediction of gas fluxes are needed. These models are to be tested against controlled laboratory tests and/or field experiments. It is expected that the development of these models will provide a valuable tool to assess the impact of gas flow on barrier and host materials, providing information which could be used to support future repository design.

SFWD's activities aimed at predicting gas migration in compacted clay have been related to modeling tasks in the international DECOVALEX Project. In past years, LBNL and SNL scientists participated in Task A of the DECOVALEX-2019 phase, which was focused on comparative modeling of a series of laboratory experiments on gas migration in bentonite. More detail on these research activities is given in Section 6.4.2 below. Starting in FY21, SFWD researchers migrated to Task B of the current DECOVALEX-2023 phase, which in addition to new laboratory experiments comprises modeling of a full-scale field experiment referred to as LASGIT (Section 6.4.3).

We note that the ongoing DECOVALEX-2023 Project comprises another task of relevance to gas generation in geologic repositories and potential impacts on performance. As described in Section 3.2.3.1, ANDRA has conducted a series of gas fracturing injection task at their URL in Bure, France. SFWD scientists are considering participation in this task, but to date no related activities have occurred.

6.4.2. DECOVALEX-2019 Activities

Task A of the international DECOVALEX-2019 project was coordinated by BGS. The purpose of this task was to better understand the fundamental processes governing the advective movement of gas in compacted bentonite. The scope of work included testing numerical models against the results obtained from a series of controlled laboratory tests of various complexity (Section 6.3.2 of the report by Birkholzer et al., 2020).

6.4.2.1. Laboratory Experiments on Gas Migration in Bentonite

Two laboratory experiments were at the center of Task A: a 1D gas flow test through a saturated bentonite sample, and a 3D spherical gas flow test in a saturated bentonite sample.

- The 1D gas flow test was conducted on a cylindrical sample of MX-80 bentonite. The sample was hydrated and equilibrated at a pressure of 1 MPa, resulting in swelling and development of swelling

stress within the sample, followed by the helium gas injection. When the injection pressure reached about 10 MPa, an abrupt increase in pressure was observed at monitoring points along the sample. Modeling teams focused on matching the observed trends in the pressure behavior, the related gas flow patterns, and the changes in stress conditions as a function of time.

- The 3D spherical gas flow test examined gas flow from an injection point in the center of a saturated sample of MX-80 bentonite over 700 days. Modeling teams were asked to conduct numerical simulations of coupled gas pressure and stress responses for the period from 735 days to 835 days of gas injection, which is when gas breakthrough occurred from the center injection point to monitoring points along the sample. Figure 6.4-1 shows that the peak in gas pressure occurred at day 768, following by a protracted negative pressure transient leading to a quasi-steady state by around day 825. During this period, the change in injection pressure is crudely mirrored by stress which exhibits none of the apparent chaotic patterns observed at earlier breakthrough events. The reduction in the variability of stress from day 768 onwards is accompanied by the development of stable outflow, with flux localized to one drainage array.
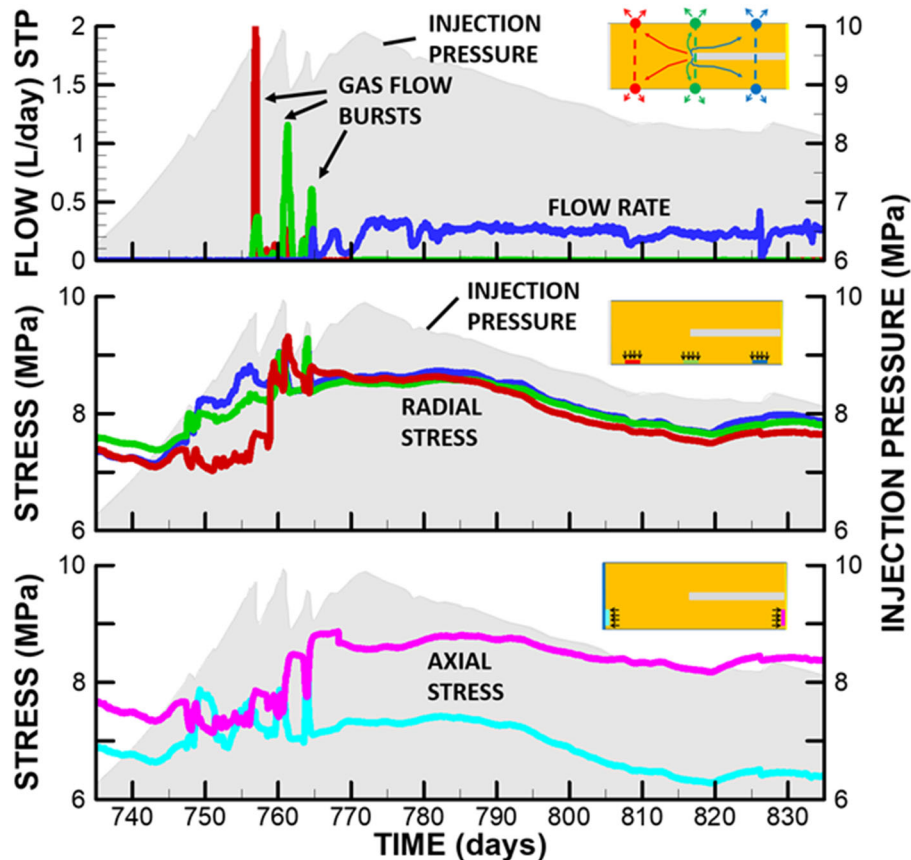
Figure 6.4-1. Observed 3D spherical gas flow test results: (upper) outflow (middle) radial stress and (lower) axial stress with shaded area being injection pressure (data from Harrington et al., 2017).

6.4.2.2. *Modeling of Gas Migration in Bentonite*

6.4.2.2.1. *Approaches and Conceptual Models*

LBNL deployed two complementary approaches for modeling gas migration associated with DECOVALEX-2019 Task A: (1) a continuum modeling approach using TOUGH-FLAC simulator (Rutqvist et al., 2011), and (2) a discrete fracture modeling approach using TOUGH-RBSN simulator (Kim et al., 2017). Figure 6.4-2 presents respective conceptual models of these approaches. The continuum modeling approach was designed

for simulations of water-gas flow in heterogeneous media, in which dilatant flow paths or stain dependent permeability in individual cells can be developed (Section 6.4.2.2.2). This approach is based on the application of TOUGH-FLAC for the modeling of long-term THM performance of nuclear waste repositories in clay host rocks. The continuum approach has been extended to include full geomechanics coupling within the framework of TOUGH-FLAC (Zheng et al., 2018b). The discrete fracture modeling approach uses the TOUGH-RBSN simulator, in which the opening of grain boundaries for dilatant gas migration is modeled explicitly using a fracture mechanics approach (Section 6.4.2.2.3). The TOUGH-RBSN has been applied for modeling of fluid driven hydraulic fracturing and complex fracturing in clay host rocks, including dilatant gas migration in clays (Kim et al., 2017).
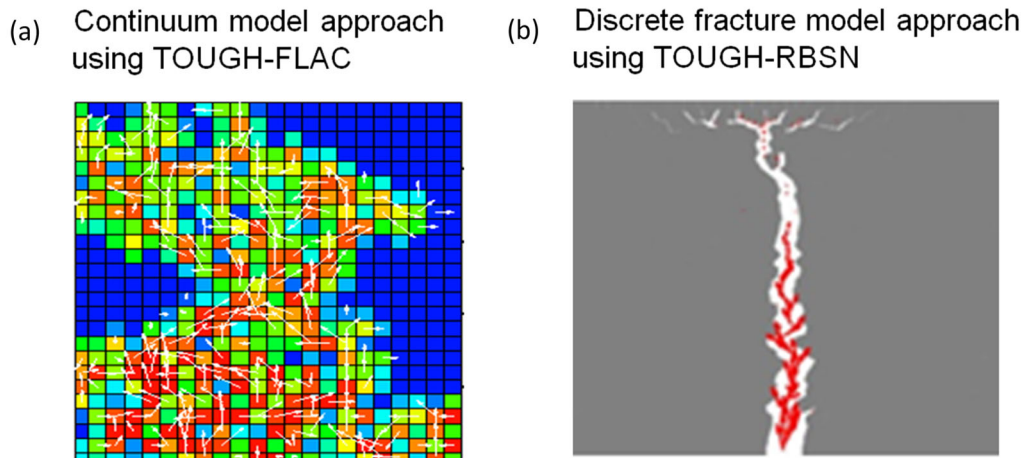
Figure 6.4-2. Schematics of conceptual models of LBNL and SNL scientists, illustrating modeling approaches for gas migration through clay related to DECOVALEX-2019 Task A: (a) the continuum approach using TOUGH-FLAC; and (b) the discrete fracture modeling approach using TOUGH-RBSN (the red color shows the fluid flow vectors and the white color indicates the opening of fracture path).

LBNL and SNL also performed evaluation of diagnostic parameters of nonlinear dynamics and chaos in the complex experimental data to establish the basic principles of a phenomenological experimental data-gathering and a modeling research design (see Section 6.4.2.2.4 below).

6.4.2.2.2. TOUGH-FLAC Continuum Modeling of Gas Migration Experiments

For its continuum modeling approach, LBNL used the TOUGH-FLAC simulator to test two approaches for creating the abrupt changes in gas migration observed in the experiments: (1) evaluation of the effect of a gas-entry pressure below which no gas could enter the sample, and (2) evaluation of pressure-dependent permeability on the formation of a fracture-like flow path. The TOUGH2 sensitivity study was conducted using the axisymmetric numerical model. Rutqvist et al. (2020b) concluded that the continuum modeling of gas migration could capture the general pattern of processes observed in the laboratory experiments. LBNL also employed a full hydromechanical coupling scheme using TOUGH-FLAC, involving the initial hydration, the development of swelling pressure, applying permeability values dependent on stress and strain, and also using heterogeneous material properties for potential creation of localized dilation-induced flow paths. The continuum model was updated based on the comparison with experimental data, using a large number of simulation scenarios and several types of models: (1) multiphase (gas and liquid) flow, (2) linear poro-elastic model, (3) a linear moisture swelling model, and (4) a gas permeability model related to minimum effective compressive stress. A full 3D model was developed to model heterogeneous material properties. However, modeling simulations were conducted assuming homogeneous properties of the MX-80, with additional elements added at the top and bottom in the TOUGH2 fluid flow domain to simulate the injection and back-pressure filters.

6.4.2.2.3.   TOUGH-RBSN Modeling of Gas Migration Experiments with Mechanical Deformation and Fracture/Damage Processes

The TOUGH-RBSN simulator was used as an alternative conceptual model for modeling two-phase flow with mechanical deformation and localized fracture/damage processes. The TOUGH-RBSN coupling modules have been substantially modified to account for the fluid flow through discrete fractures (Asahina et al., 2014; Kim et al., 2017). A discrete fracture network (DFN) approach was applied to represent enhanced gas flow through discrete fracture paths. Comparison of fracture patterns and pressure distributions during fracturing processes were used for a qualitative analysis of gas pressure-induced fracture propagation and fracture-assisted flow.

A 3D Voronoi mesh of a cylinder with dimensions of 120 mm height and 60 mm diameter was used, and the model was composed of 7,856 Voronoi cells and 33,316 element connections. A constant injection rate of 2.75×10^{-9} m^3/s at STP was maintained throughout the simulation. Outflow values were measured at the connections between the circumferential elements and the backpressure boundary elements. Model parameters are listed in Table 7.1 of Rutqvist et al. (2020). The TOUGH-RBSN model included the baseline parameters suggested from the DECOVALEX Task A coordinator. It was found that the simulated pressure trend followed the trend of experimental data, although the simulation did not match accurately pressure oscillations observed in the experiment (Figure 6.4-3).

(a)   (b)
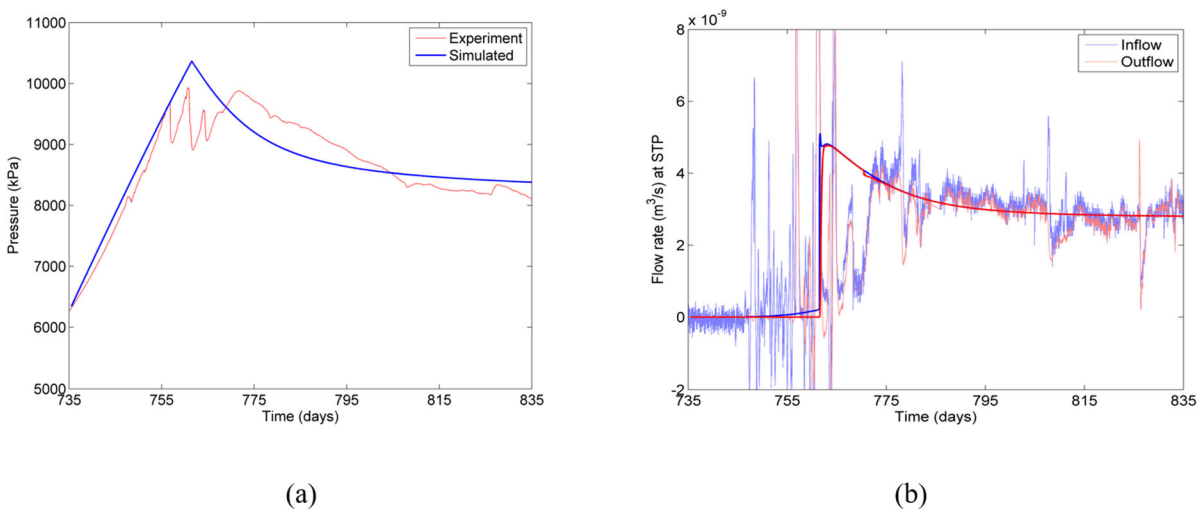
Figure 6.4-3. Comparison of simulated and experimental (a) injection pressure trends, and (b) inflow and outflow rates evolutions.

Overall, the RBSN modeling showed good agreement between simulated and experimental data prior to the gas breakthrough. The applied modeling approach with Bishop's equation for the effective stress calculation worked well before discrete fractures occur, but it needs to be improved to model the two-phase pressure in the fractured elements. Modeling was also conducted to simulate the development of the fracture network during the gas injection into the sample. Simulations showed that fractures were initiated at the center of the sample, where the gas injection occurred, followed by the main fracture cluster grows into a spherical shape toward the lateral surface of the sample. After the fracture cluster reaches the lateral surface, near-surface fractures propagate in the longitudinal direction. Examples of the 3D modeling illustrating the fracture development during gas injection are shown in Figure 6.3-9 of the FY20 report by Birkholzer et al. (2020).

6.4.2.2.4.   Nonlinear Dynamics Modeling of Gas Migration in Compacted Clay

The gas-injection laboratory experiments in bentonite demonstrated a strong coupling between stress, gas pressure and flow, which takes place during multiple discrete propagation events, with strong spatial variability and time-dependency of bentonite permeability. Harrington et al. (2019) concluded that characterization of the

gas network distribution is of fundamental importance in predicting gas dissipation rates and understanding the long-term fate of gas in radioactive waste repositories. In light of the complexity and randomness of the observed spatial and temporal patterns, Faybishenko et al. (2020) analyzed the results of these experimental studies with nonlinear dynamics models and developed a phenomenological model of nonlinear dynamics and deterministic chaos for gas flow in bentonite. A conceptual model of the gas transport given by Cuss et al. (2014) is shown in Figure 6.4-5 (upper row) along with the results of time series observations of gas inflow and outflow (lower row). The onset of gas inflow in the bentonite core, which occurs before the gas breakthrough through the core outlet (Segments A and B), is characterized by the process of chaotic diffusion and dilatant pathways. After the breakthrough, when gas reached the backpressure end of the sample, with end-to-end movement of gas, the prevailing process is chaotic gas advection taking place along microscopic and macroscopic tensile fractures (Segment E). The final relaxation/recovery stage of gas outflow, with no inflow to the Mx80 sample, is characterized by a combination of chaotic diffusion and chaotic advection (Segment H). On Figure 6.4-5, green lines on the schematics of the gas transport indicate the randomly generated gas flow paths within porous media; the yellow dashed lines and red arrows indicate that the overall volume of affected porous media is expanding prior and post breakthrough; and then the volume shrinks during the recovery; and black lines for the period of the chaotic advection indicate dilatant pathways originating at the inlet and ending up at the outlet.

The types of data analysis and the proposed phenomenological model, not derived from first principles, can be used to establish the basic principles of a phenomenological experimental data-gathering and a modeling research design. The proposed concept provides a new perspective for modeling gas migration in low-permeability materials and is of direct relevance to other clay-based scientific and engineering issues associated with advective gas flow, such as shale gas, hydrocarbon migration, carbon capture and storage, gas storage and landfill design.
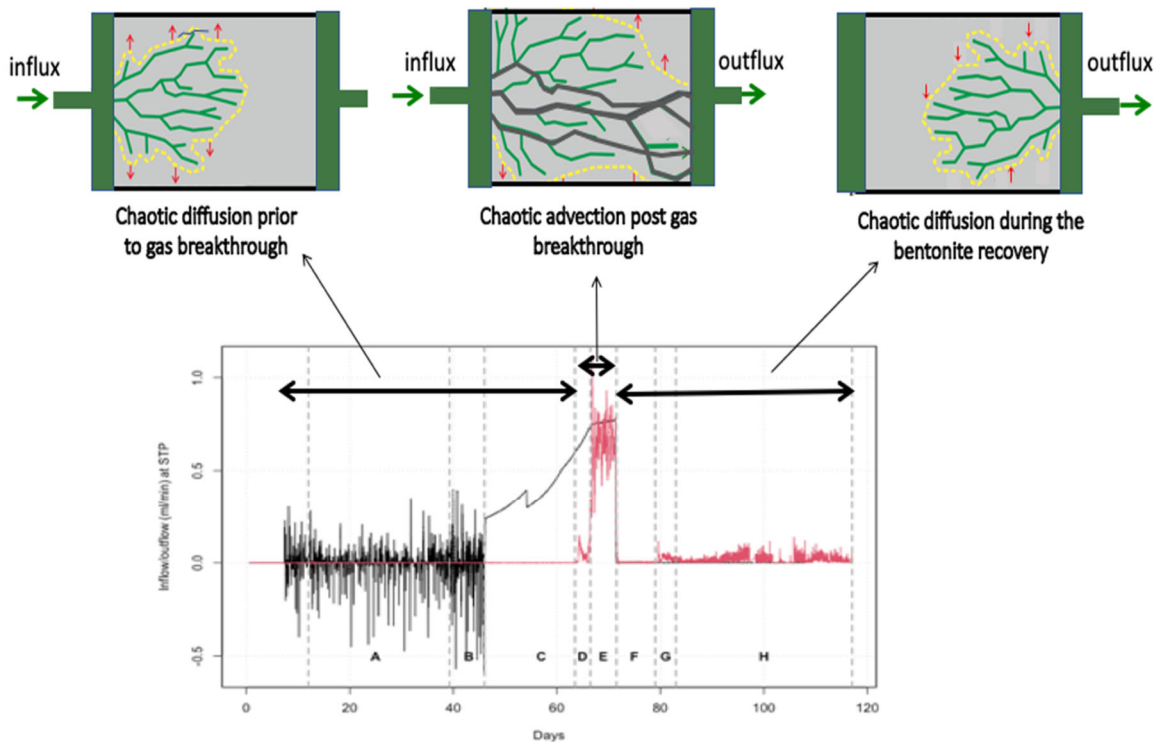
Figure 6.4-5. Phenomenological model of gas flow in Mx80-D. The upper row shows the schematics of the fracture development (modified from Cuss et al., 2014), which are representative for different stages of gas transport through bentonite. The lower row is the time series of the gas outflux. (Explanation of the meaning of lines in the upper row is given in the text.).

6.4.2.3. Summary and Lessons Learned from DECOVALEX-2019 Task A

LBNL's modelling of gas migration processes using alternative approaches, in the context of other international teams using multiple approaches and simulators, has created valuable lessons for simulation of these complex processes. Application of these numerical models shows that continuous strategies are capable of obtaining a good fitting with respect to experimental stress measurement and bulk gas flow results. However, these models require substantial calibration of fitting parameters and focus on the deterministic features rather than representing the stochastic behavior observed in the experiments. Continuous approaches with preferential pathways have fewer constraints within the models and while they are largely unable to represent some experimental details, the phenomenological processes are better represented. Similarly, discrete models, whose basis reflects the underlying physics of gas flow, also struggle to capture some of the key experimental features of the data such as stress or pore pressure distributions. The 1D and the 3D gas injection tests exhibited a combination of stochastic and deterministic behaviors, which led some teams to explore the development of stochastic or nonlinear dynamics models. Overall, calibration, constraints and parameterization of the codes emerge as key considerations in the modeling of advective gas, as well as the understanding of the key repeatable processes from gas flow experiments. The models did also provide a valuable service in aiding the interpretation of the experimental data and highlighted potential alternative interpretations of the experimental boundaries. Most importantly, the comparison of multiple approaches and simulation results clearly demonstrated that explicit representation of the injector is very important in order to produce a robust model, as the vast majority of the gas in the experimental system is held in the injector vessel and not in the clay sample itself.

The DECOVALEX-2019 Task A has now been completed, and investigations of gas flow have migrated towards a new task in DECOVALEX-2023 (see next section). The results of the DECOVALEX-2019 Task A research studies were published in the following publications: Bond et al. (2018), Daniels and Harrington (2017), Tamayo-Mas and Harrington (2020), and Kim et al. (2021).

6.4.3. DECOVALEX-2023 Task B Gas Migration Modeling

6.4.3.1. Objectives, Approach, and Participating Organizations

As mentioned before, Task B of DECOVALEX-2023 is a continuation of the earlier gas migration modeling work conducted in the previous project phase. The plan of this ongoing Task B includes three stages. The objective of the 1st Stage is the development of a conceptual model and assessment of team's modelling capabilities, originally developed within the DECOVALEX-2019 Task A. The 2nd Stage includes a blind prediction test, with the objective to assess the developed models and to analyze whether the key features of the experiments are captured. Special emphasis will be placed on modeling of mass-balance, inflow and outflow time series, gas migration, gas saturation, and mechanical coupling (see Section 6.4.3.2 below). The 3rd stage, which as not yet started, will include modeling of the Large-Scale Gas Injection Test (LASGIT) conducted at the Äspö Hard Rock Laboratory in Sweden (see Section 3.2.3.2). LASGIT is a full-scale *in-situ* test conducted in the assembly hall area in Äspö HRL at a depth of 420 m. A deposition hole, 8.5 m deep and 1.8 m in diameter, was drilled into the gallery floor. A full-scale mockup waste canister (without heater) was emplaced in the hole. Thirteen circular filters of varying dimensions have been placed on the surface of the canister to provide point sources for the injection of gas to mimic canister defects. Pre-compacted bentonite blocks with high initial water saturation were installed in the deposition hole. The test program of LASGIT included several gas injection experiments conducted from a number of filters embedded at the canister-bentonite interface.

6.4.3.2. Blind Prediction of a New Gas Migration Experiment

LBNL scientists (and other international modelling groups) are currently working on the blind prediction phase of DECOVALEX-2023 Task B (Rutqvist et al., 2021a). Based on the experience from past comparative models during the DECOVALEX-2019 phase, the selected approach is a continuum model taking into account: (1) multiphase (gas and liquid) flow; (2) a linear poro-elastic model; (3) a linear moisture swelling model; and (4)

a gas permeability model related to minimum effective compressive stress. The blind prediction exercise involves a new gas migration experiment using MX-80 bentonite, with the gas injection conducted from a gas injector at the center of the sample (Figure 6.4-6a). Gas flow rate was measured at the outlet filter on the top of the sample. Before commencing the gas injection, a sample was first hydrated to full saturation. The injection rate of helium gas into an injection chamber was 180 µL/hour. A constant pressure of 1 MPa was applied at the outflow filter. Before injection, the gas pressure at the injector was increased to 2 MPa, while the initial fluid pressure in the sample was 1 MPa. The experiment is still ongoing in the laboratory at BGS and no interim results have been made available to the modeling teams. LBNL performed initial predictive modeling was conducted using a simplified axisymmetric model (Figure 6.4-6b). The conceptual model of gas migration and the material properties were the same as in the 1D gas migration modeling described in the Section 6.4.2.2.2.

(a)

(b)
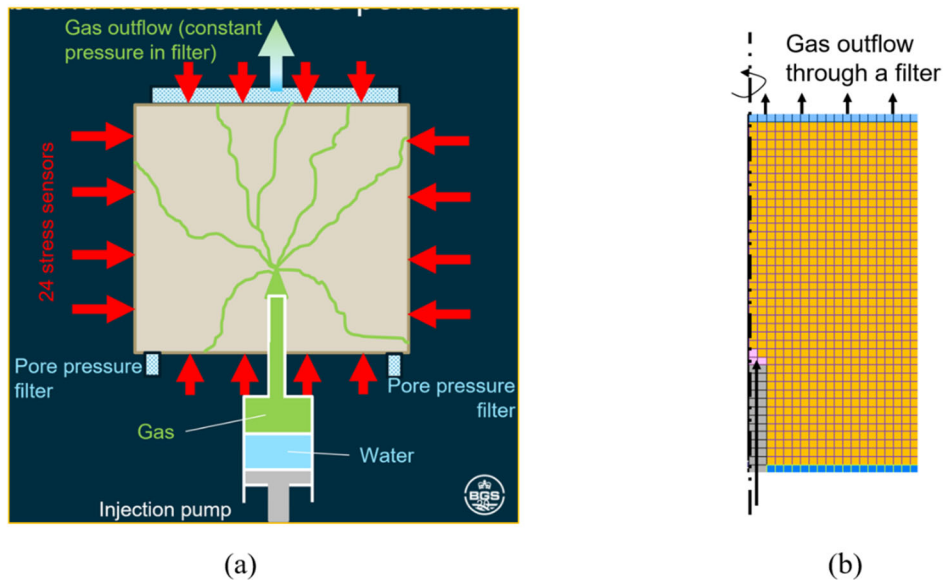
Figure 6.4-6. Setup and model of the gas migration experiment. (a) Conceptual model from BGS, and (b) axisymmetric numerical model for TOUGH-FLAC simulations. The sample size is 60 mm vertically and 60 mm in diameter. The red arrows in figure (a) indicate the layout of 24 sensors used for measuring total stress.

Figures 6.4-7a,b present the blind-prediction simulation results of pressure and flow rate as a function of time. At a constant injection rate, the injection pressure increases gradually starting from the 22nd day of the injection (Figure 6.4-7a). At 40 days, there is an indication of a limited gas breakthrough at the injector. After 50 days, there is a sharp increase in injection rate, and about 5 days thereafter, there is a sharp increase in outflow rate. At the same time, pressure within the sample increases sharply. The gas breakthrough occurred at an injection pressure of about 7.5 MPa (Figure 6.4-7b). The gas injection rate peaks at 6e-9 m^3/s at standard temperature and pressure (STP). The injection rate then declined especially after the injector was shut-in.

6.4.3.3. Next Steps in Task B of DECOVALEX-2023

Modeling of gas injection will be conducted as part of DECOVALEX-2023 Task B. LBNL scientists are going to develop a heterogeneous continuum model and a double structure approach for simulations of gas migration, involving the interaction between micro- and macro-porosity of the clay. Modeling of heterogeneous media will require an application of a 3D numerical model. Scientists from SNL will also join the Task B efforts. After careful analysis and comparative evaluation of the blind prediction laboratory test, the participating modelling teams will move to the simulation of the full-scale LASGIT experiment. The expansion of the numerical approaches to a full-scale test will provide an invaluable tool to help inform the modelling approaches and assess the impact of upscaling of gas flow on repository layout and therefore the design of any future facility.
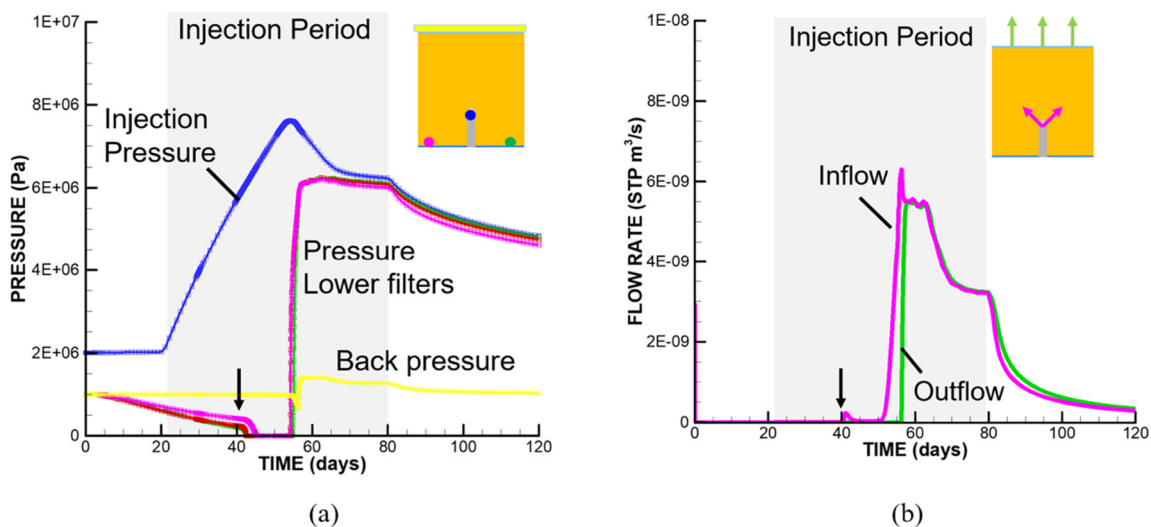
Figure 6.4-7. Modeling results of (a) pressure and (b) flow rate trends during the blind-prediction gas injection test.

6.5. Modeling Coupled Processes, Fluid Flow and Transport in Fractured Crystalline Rock

Crystalline rocks/granite formations are considered as a host rock throughout the world (e.g., Sweden, Korea, Japan, China) and are being studied at several Underground Research Laboratories (URLs)—for example at the Äspö HRL, Sweden, at the GTS, Switzerland, and in the Beishan area, China. The most advantageous features for crystalline/granite rock with respect to radioactive waste isolation include mechanical stability, low permeability (unfractured rock), and high thermal conductivity. As hard competent rocks, crystalline formations are often fractured; thus, repository PA studies require an understanding of (1) fracture properties may be affected by stress changes and other perturbations related to repository induced processes, and (2) reactive transport of radionuclides potentially migrating from the repository to the biosphere.

This section summarizes two international collaboration activities that address above research needs. Section 6.5.1 describes hydromechanical modeling of fracture contact mechanics upon shearing, an effort related to the DECOVALEX-2023 Project (Guglielmi et al., 2021; Hadgu et al., 2021). Section 6.5.2 highlights discrete fracture network (DFN) modeling efforts to characterize the impact of fracture network structure on flow, transport, and fluid-fluid reactive transport (Viswanathan et al., 2021). These fracture network modeling activities provide new understanding and capabilities to support international collaboration under the umbrella of the SKB Task Forces, namely the GWFTS task force and its ongoing Task 10 work.

6.5.1. Modeling of Rock Fractures Under Shear Stress

6.5.1.1. Introduction of DECOVALEX Task G

As described in Section 3.2.3.7, Task G of the DECOVALEX-2023 Project strives to improve our understanding of shear reactivation of pre-existing discontinuities in brittle host rocks used for radioactive waste disposal. In particular, the potential for existing features to undergo shear displacements and related changes in permeability as the result of coupled THMC effects can have significant impacts on repository safety functions (e.g., creating permeable pathways or, for very large displacements, mechanical damage of waste packages). The focus of the collaborative research in Task G is the modeling of laboratory-scale experiments that are currently being conducted to link micro-scale THMC effects acting on fracture surfaces and asperity contacts with emergent fracture properties such as permeability. These experiments are conducted on typical granite samples with pre-existing well-characterized discontinuities. It is expected that DECOVALEX research teams will apply and develop existing constitutive models for fracture characterization, and, hence, will improve fundamental physical understanding of these complex processes as well as improving modeling predictive capabilities.

In FY21, task participants from multiple international modeling groups started with a benchmark simulation (Step 1 in Task G), to set the stage for more complex blind-prediction modeling of laboratory experiments. The Step 1 benchmark investigates the mechanical behavior rough fractures before and after mechanical shear. Shearing of a single fracture in a rectangular domain exposed to a differential (shear) load is simulated and the results are compared with the analytical solution by Pollard and Segall (1987). The fractured sample is under mechanical loading as illustrated in Figure 6.5-1. Modeling teams were asked to assume various inclinations (0º, 30º, 45º, 90º) of the fracture with an initial length of 0.17 m, which means that the fracture will not fully penetrate the specimen. Observation points are set evenly along the fracture length and are rotated with the fracture inclination, correspondingly. Simulations were done for two cases of a planar and a rough fracture with asperities. The fracture roughness data are from experiments conducted at TU BA Freiberg in Germany (Kolditz et al., 2020), as shown in Figure 6.5-2. SFWD scientists from LBNL and from SNL are participating in Task G activities. Their respective modeling approaches and results are briefly described below.
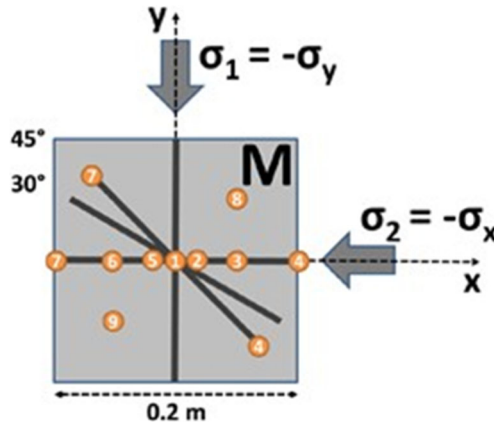
Figure 6.5-1. Modeling specification including observation points.
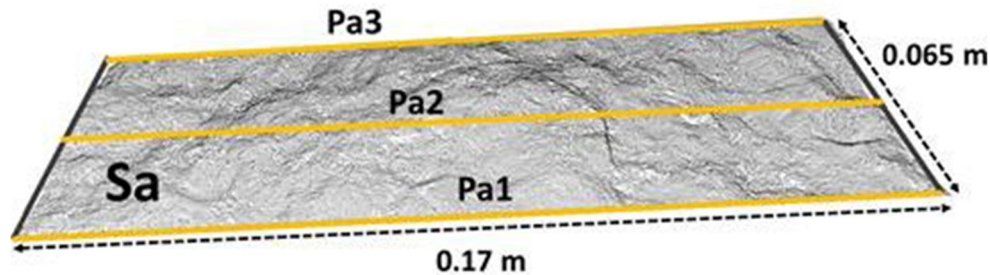
Figure 6.5-2. Fracture surface (Freiberg experiment) and specification for the rough fracture

6.5.1.2. Multi-Physics Modeling of Step 1 with the NMM Method

The numerical manifold method (NMM) (Shi, 1992) is based on the concept of "manifold" in topology. In the NMM, independent meshes for interpolation and integration are defined separately. Based on this approach, an initially one-time generated, non-conforming mesh (not necessarily conforming with the physical boundaries) can be used, and flexible local approximations can be constructed and averaged to establish global approximations for both continuous and discontinuous analyses. Based on the NMM, LBNL has developed comprehensive modeling capabilities to simulate coupled processes in fractured rocks by considering fractures as finite-thickness porous zones, discrete interface networks and granular systems at different scales. For stressed fractures with complex asperities, LBNL scientists built a rigorous framework with multi-step contact calculations to simulate dynamic contacts with possible large deformation and large displacements with explicit geometric representation of the complex structures (Hu and Rutqvist, 2020a,b). LBNL used these new capabilities to simulate DECOVALEX Task G, Step 1. More information on the NMM and Step 1 deployment, including governing equations, constitutive relationships, HM couplings, and challenges associated with intersections and shearing of fractures, are described in Guglielmi et al. (2021, Section 4).

In FY212, LBNL conducted several simulation scenarios addressing different research questions related to the single-fracture shearing problem defined in Task G. Examples results are presented below. As shown in Figure 6.5-3, the LBNL team first investigated domain size effects and selected a size that is large enough to avoid boundary effects and small enough to capture near fracture changes without the need of a very fine mesh. The team then used three different models with different geometric representations to simulate a 45° oriented single fracture, where the fracture is represented with a continuous representation as a finite-thickness porous zone, with a discontinuous representation as a smooth and planar interface, and with a discontinuous representation as a rough and non-planar interface. The meshes used for the calculations are shown in Figure 6.3-4.
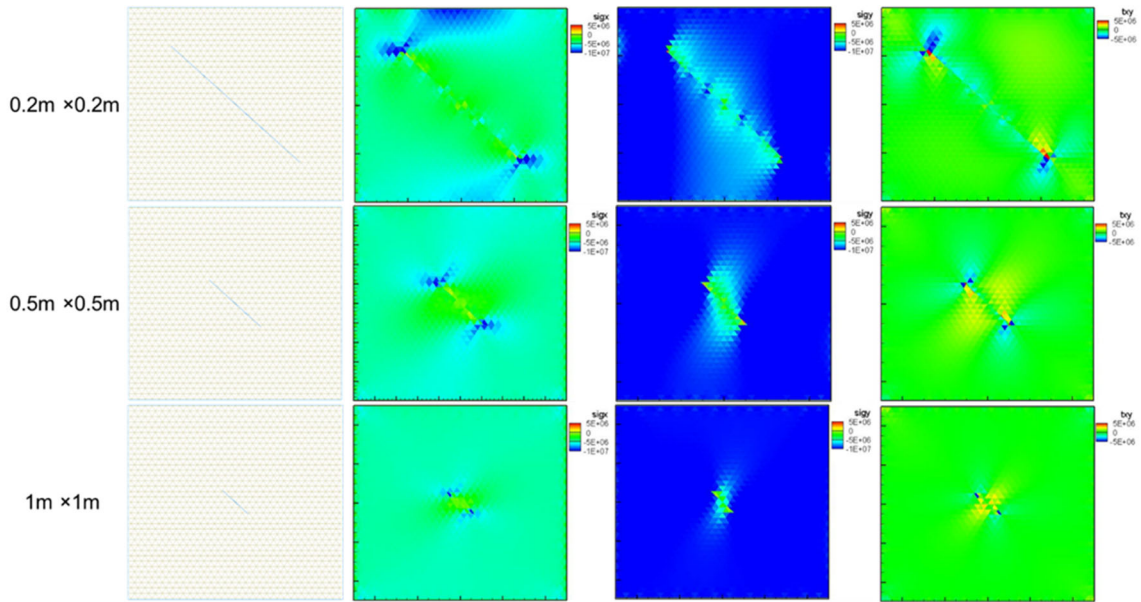
Figure 6.5-3. Stress calculated with different domain sizes with the same single planar fracture.
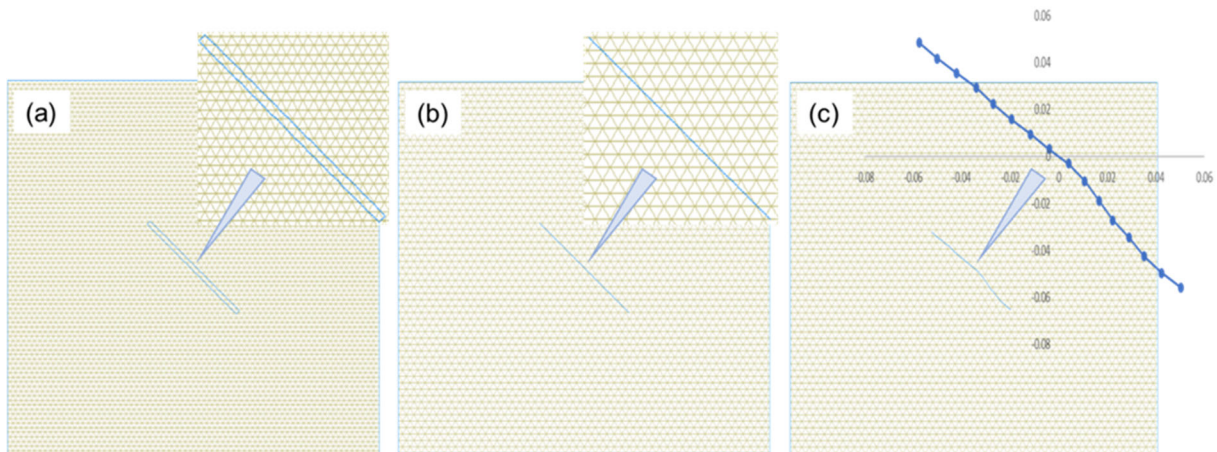
Figure 6.5-4. Modeling a single fracture slip with three different geometric representations: (a) a finite-thickness porous and deformable zone of a planar fracture, (b) discontinuous interfaces of a planar and smooth fracture, and (c) discontinuous interfaces and asperities of a non-planar and rough fracture.

Simulation results for the shearing problem in Task G are shown in Figure 6.4-5 in comparison with the analytical solution. The plot displays the shear displacements along the fracture in a localized 1D coordinate system of the crack. In this localized 1D coordinate system, the crack center is the origin. The negative and positive values denote the distances to the center from the upper left and lower right regions, respectively. Good agreement is achieved with the analytical solution for both shear displacements and stress using all three different models: the continuous solid element model, the discontinuous interface model, and the discontinuous asperity model. Such validation builds up confidence for applying these models for studies of crystalline rock. Using three different geometrical models shows the important effect of non-planar fracture geometry on the shear behavior of a single fracture (Figure 6.4-5c). The reduced shearing seen on the left end of the non-planar fracture can be attributed to the lower dip angle of that left section of the fracture. Thus, for rough fractures and networks of rough fractures, the accurate calculation of contact dynamics is important for analyzing the geometric and multi-physical evolution of fractured rock, in particular when rough fractures are not filled with minerals and when a number of rough fractures form a blocky system.
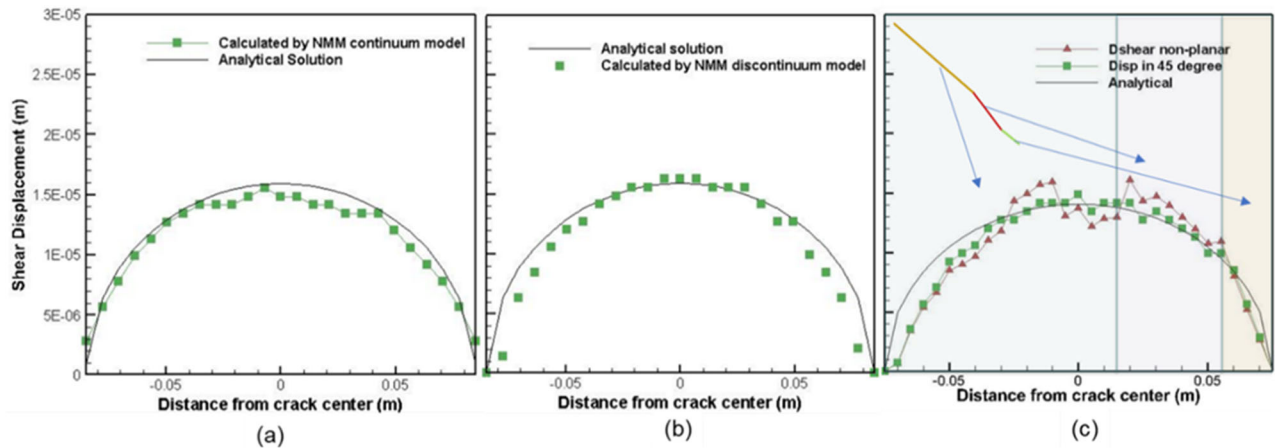
Figure 6.5-5. Calculated shear displacements and comparison with the analytical solution by three different models: (a) the continuous finite-thickness porous zone model, (b) the discontinuous planar interface model, and (c) the discontinuous rough interface model.

To further study the impact of asperities on shearing, LBNL compared the stress calculated for the perfectly smooth and planar fracture with that of the rough, non-planar fracture as shown in Figure 6.5-6. In the case of the perfectly planar frictionless fracture, the stresses are concentrated at the two ends of the fractures, whereas in the case of non-planar (rough) fracture, some shear stress is transmitted across the fracture at asperity contact points/areas. In the case of a non-planar rough fracture, the stress disturbance affects a wider area around the crack tips and across the fracture as a result of local asperity contacts. Locally, the asperities introduce concentration of both vertical and shear stress. In general, these concentrated contact stresses could cause formation of new cracks, fracture plasticity, or pressure solution when fluid chemistry condition is satisfied. If considering non-zero friction, local highly stressed asperity contacts could be interpreted as a result of high frictional resistance significantly impacting the overall fracture shear deformations.
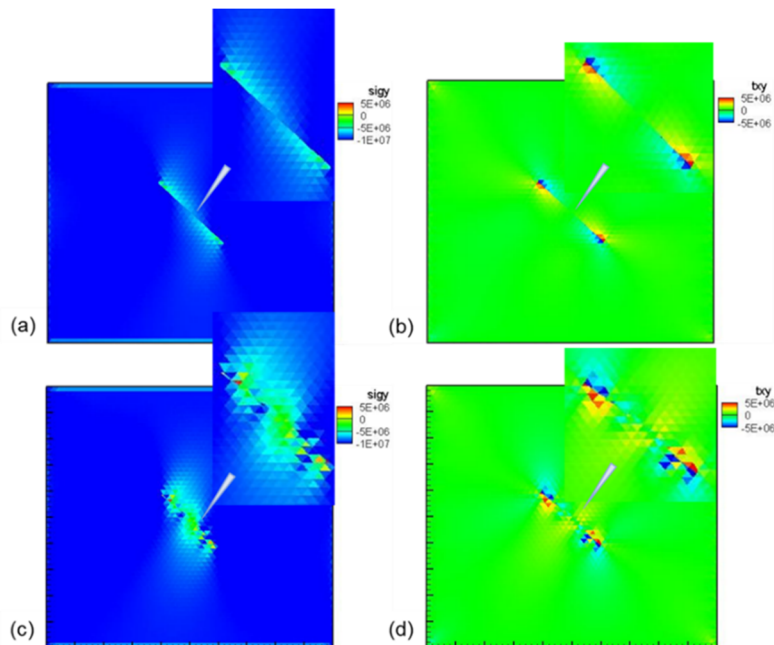
Figure 6.5-6. Impact of asperities on shearing: comparison of vertical and shear stresses (Unit: Pa) calculated by the discontinuous planar interface model (a-b) and by the discontinuous rough interface model (c-d).

6.5.1.3. Modeling of Step 1 with Comsol Multiphysics Software

Complementing LBNL's activities, a team of researchers at SNL simulated the same Step 0 benchmark problem with the Comsol Multiphysics Software (Hadgu et al., 2021). The simulations assumed an embedded planar fracture in an elastic material. The simulation mesh and selected results are shown, respectively, in Figures 6.5-7 and 6.5-8. Similar to LBNL's results, significant stress concentration can be seen at the fracture tips. While not shown here, the shear displacements simulated with Comsol showed an excellent agreement with the analytical solution by Pollard and Segall (1987). In FY21, SNL did not yet simulate fractures with complex geometries and asperity contacts. Future work will use the Comsol Multiphysics to conduct Step 1 modeling for rough fractures in an elastic and/or elastoplastic matrix.

6.5.1.4. Next Steps in DECOVALEX Task G Modeling

In alignment with the Task G plans and schedule, both LBNL and SNL teams will in FY21 move to more complex benchmarking, followed by targeted modeling of the advanced laboratory experiments brought into this DECOVALEX task. As mentioned in Section 6.2.3.7, these evaluation of mechanical (M) results derived from constant normal load (CNL) direct shear tests and constant normal stiffness (CNS) direct shear tests as well as high-resolution fracture surface scans (TU BA Freiberg) with focus on mechanics of rough fractures and how they are affected by shear and normal displacement (Step 1), investigation of hydro-mechanical (HM) results obtained with the GREAT cell (University of Edinburgh) with focus on fundamental shear processes under complex 3D stress states (Step 2), and finally investigation of thermo-mechanical (TM) results obtained from tri-axial tests (KICT) with focus on shear processes triggered by thermal stresses (Step 3).

6.5.2. Reactive Transport in Three-Dimensional Fracture Networks

6.5.2.1. Introduction

Over the past years, researchers at LANL have been involved in international collaboration with the SKB GWFTS Task Force, focusing on studies of advection, diffusion, and sorption in fractured rock. Between FY15 and FY18, LANL was involved in a diffusion and sorption modeling task in the GWFTS Task Force, referred to as Task 9 (Section 3.4.2.1), which centered on two *in-situ* matrix diffusion experiments, the LTDE-SD test at the Äspö HRL in Sweden and the REPRO project at Onkalo URL in Finland. LANL's ultimate aim was to develop a realistic DFN model to represent matrix retardation in the natural rock matrix at depth (Viswanathan et al., 2019). More detail on this past work is given in Viswanathan et al. (2019) and Birkholzer et al. (2019).

In FY20, LANL shifted its international collaboration effort under the umbrella of the GWFTS Task Force to a new Task 10 that is focusing on flow channelization in fractured media (Viswanathan et al., 2020). As pointed out in Section 3.4.2.1, this new task officially started in May 2020 and currently ramping up its activities. LANL conducted preparatory investigations of the transport of waterborne substances in subsurface fractured bedrock, taking into account rough surface asperities, assuming textures with different connectivity structures. This study was in direct alignment with the goal of GWFTS Task 10, which is to improve our understanding of multi-scale flow channelization of fractured crystalline rock.

In FY21, LANL scientists started including reactions to their discrete fracture network transport calculations since repository PA studies will require considering reactive transport of radionuclides potentially migrating from a repository (Viswanathan et al., 2021). Using the discrete fracture network modeling tool dfnWORKS combined with PFLOTRAN for the flow and transport solution with multi-component reactive transport capability, LANL scientists conducted preliminary simulations to model irreversible kinetic reactions in a 3D DFN. The simulations explored the behavior of an irreversible kinetic reaction during the interaction of two solute plumes within a three-dimensional DFN, which marks the first simulations and study of this type. It was found that the interplay of network connectivity with the chemical properties of the reactive solutes is the principal control for reactive transport processes. The network structure drives the reactive species into the same regions of the network (the principal pathways). Their chemical properties then dictate whether and how quickly a reaction occurs. These results provide initial insights into how an irreversible fluid-fluid reaction occurs within a fracture network and how such reactions are influenced by network topological and chemical

properties. More details are given below. Again, this work is closely aligned with the goals defined in the ongoing Task 10 of the international SKB GWFTS Task Force.

6.5.2.2. Discrete Fracture Network Representation and Simulations

First, a 3D fracture network was created using the dfnWORKS simulator (Hyman, et al., 2015), which is open-source software that can be obtained at https://github.com/lanl/dfnWorks_LA-UR-20-26548. Network generation and meshing are performed using the feature rejection algorithm for meshing (FRAM) (Hyman et al., 2014), which produces a conforming Delaunay triangulation of the fracture network. The dual meshes of the triangulation, the Voronoi control volumes, were then used by the massively parallel subsurface flow and transport code PFLOTRAN (Lichtner et al., 2015) to determine the steady state pressure solution within the network. An extension of the WALKABOUT particle tracking method (Makedonska et al., 2015; Painter et al., 2012) was used to determine pathlines through the DFN and simulate solute transport.

The generic 3D fracture network created for this study is composed of several disc shaped fractures with a radius of 1 m in a cubic domain of size 5 x 5 x 5 m (Figure 6.5-7). Fracture apertures are uniform and equal to $b = 10^{-4}$ m. Flow in the fracture network is modeled using the Reynolds equation (Zimmerman and Bodvarsson, 1996), which provides volumetric flow rates and pressure values throughout the network (Figure 6.5-7a). Despite the fracture apertures are uniform within each fracture plane, the in-fracture velocity field can be highly non-uniform due to the complex network topology and boundary conditions imposed by the intersections with other fractures (Figure 6.5-7b).

Transport through the network is simulated using purely advective-particle tracking. A pulse injection of two separate plumes (*A* and *B*) is considered, which have equal masses (i.e., each consisted of $O(10^6)$ particles) and are placed into the steady-state flow field within the DFN. Species *A* and *B* are initially injected into separate regions of the DFN, but later converge via the flow network and react to form Species C. The questions raised are: (1) how does spatial variability in the velocity field alter behavior relative to a pure diffusive system; (2) how does the relative interplay of transport and reaction kinetics alter such behaviors, and (3) where do the majority of reactions occur?

(a)   (b)
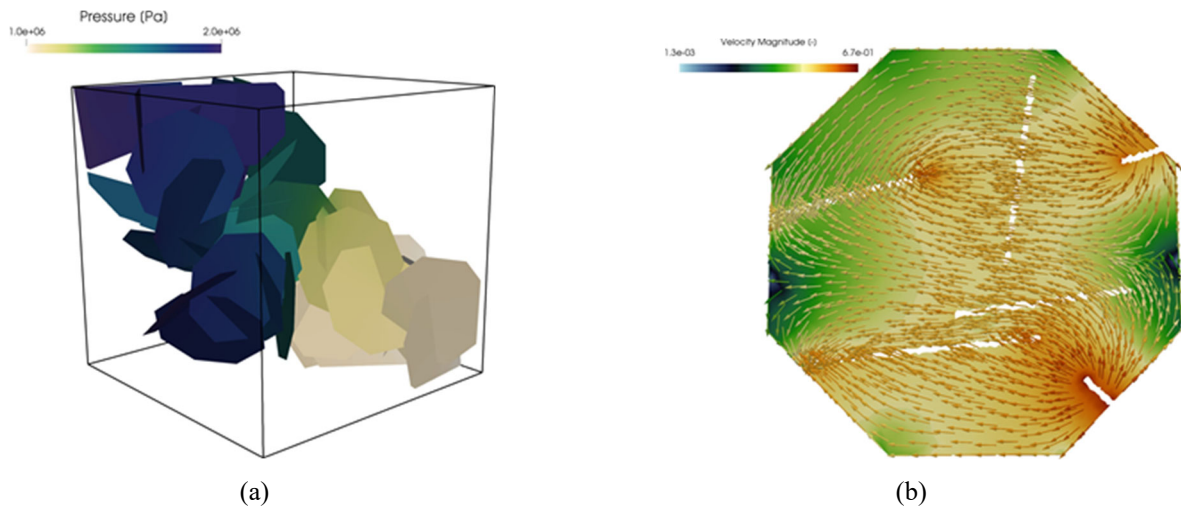
Figure 6.5-7. (a) Steady state pressure field in the entire DFN, and (b) the velocity vector field on a single fracture.

Reactive transport was modeled from a Lagrangian perspective, using the particle trajectories obtained in the steady-state flow field and with chemical reactions implemented in a probabilistic framework. Simulations of transport were conducted for a wide range of Damköhler numbers *Da* from 10^2 to 10^6. The Damköhler number is a non-dimensional number characterizing the ratio of diffusive to reactive time scales. The evolution of solute plume characteristics is tracked by measuring Lagrangian statistics at control planes throughout the

domain. The effective tortuosity between two control planes is defined as a flow-dependent parameter that naturally aligns with the particle tracking approach.

In additional to the transport observables discussed in the previous section, LANL also considered the fracture network structure. The topology (connectivity) of the network is characterized using a graph-based method where nodes in the graph correspond to fractures in the DFN and an edge between two nodes indicates that the corresponding fractures intersect (Huseby et al., 1997; Hyman et al., 2018). The graph-representation of the DFN topology presented in Figure 6.5-8 shows that there are multiple paths from the inflow fractures (input nodes are colored red and blue) to the outflow fractures (the output node is colored in green). There are also a few dead-end regions of the DFN, which are represented as trees in the sub-graphs. Edge-sizes in the graph in Figure 6.5-8 are proportional to the percentage of particles that pass between the corresponding intersection in the DFN with thicker lines indicating a larger number of particles. This graph representation is referred to as a flow topology graph (FTG) as it embeds the dynamics of the particle transport, which in this case represents the pathlines in the flow field, into the graph representation of the DFN (Aldrich et al., 2017).
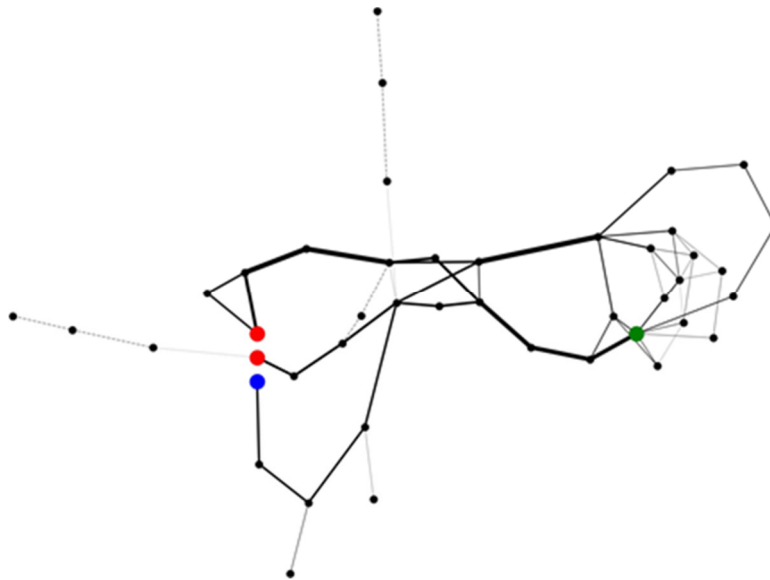
Figure 6.5-8. Topological (graph) representations of the DFN. Every node in the graph corresponds to a fracture in the DFN, and an edge between two nodes indicates that the corresponding fractures intersect; the inflow fractures are colored blue and red; the outflow fracture is green; and the edge thickness is proportional to the volumetric discharge.

Figure 6.5-9 gives an example of the simulated temporal evolution of the reactive solute plumes for a given Damköhler number ($Da = 10^6$). Again, the simulations consider two Species A and B injected into separate regions of the DFN. These later converge via the flow network and react to form Species C. At early times, the particle A and B plumes are separate and have yet to converge, so no reactions occur. By $t = 50$s, the fastest A and B particles strive in the center fractures where plumes mix and C particles are produced. After particles channelize through the fractures, the network topology expands and branches, creating many possible pathways from the convergence fracture to the network outlet. Both A and B particles traverse these pathways, enabling reactions to occur across the transverse spatial domain at later times.

The influence of network topology on particle channelization and reactive transport becomes evident in topological representations of the network. Figure 6.5-10 displays the possible paths for A (left), B (middle), and C (right) particles. A few primary pathways, depicted by thick lines, control the majority of particle plume transport. Plumes A and B have separate primary pathways. However, when the A and B pathways converge, reactions become more probable, shown by green lines in the right subfigure. Reactions are limited to regions of the network where both A and B particles visit, e.g., reactions are not permitted in the far upper right of the network (Figure 6.5-10) because only A particles visit this network section.

Figure 6.5-11 provides another form of displaying the simulation results, further demonstrating particle channelization. The figure shows the transverse breakthrough position distribution (TBPD) of particles, illustrated in a color code. Bright colors, corresponding to higher probability values, indicate regions of greater particle channelization. The network regions with the highest reaction probability are also regions with high TBPD values, demonstrating that reactions preferentially occur in primary pathways, where particles are channelized. Reactions become less likely near the network outlet. There is a reduced number of *A* and *B* particles that reach the outlet, because many particles react earlier in the domain, thereby reducing the probability of reaction near the network outlet, i.e., particle reaction probability decreases as there are less particles available for reaction. One key finding is that the majority of reactions are confined to a small percentage (< 10%) of the fractures in the network, which make up the network backbone.

Additional reactive transport simulations were conducted for a range of *Da* spanning several orders of magnitude, from $Da = 10^2$ to $Da = 10^6$. Some general behavioral trends emerge:

(1) When *Da* increases, more reactions occur.

(2) When *Da* increases, particles tend to react in high velocity channels. *A* and *B* particles with higher velocities are more likely to react, manifesting as faster *C* outlet breakthrough times for higher *Da*.

(3) When *Da* increases, reactions tend to occur closer to the network inlet, as quantified with topological distance.
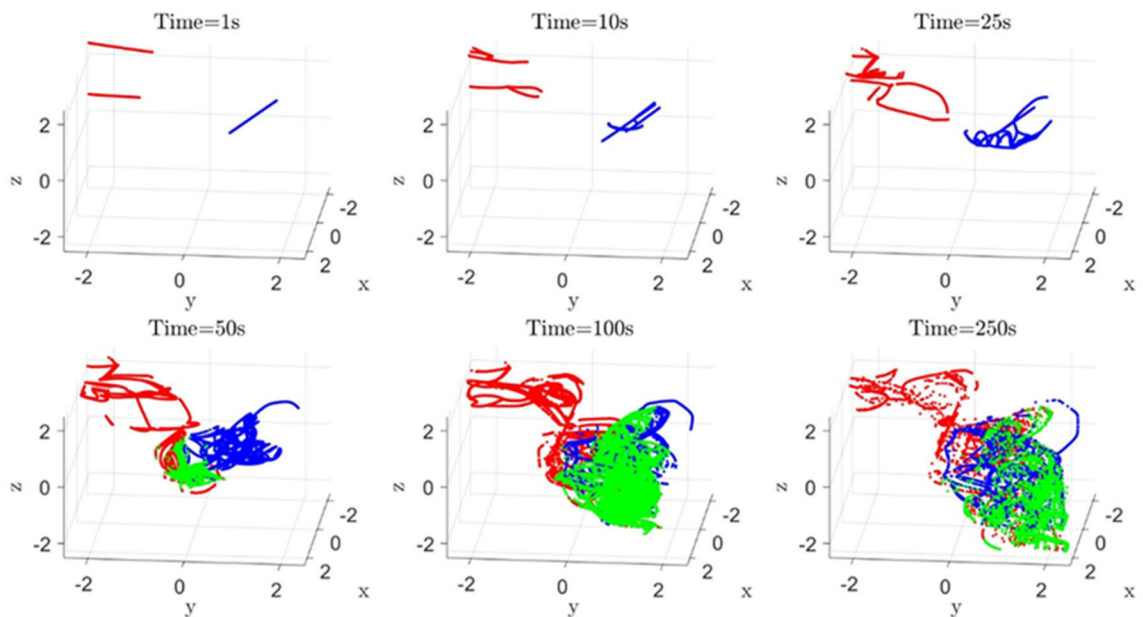
Figure 6.5-9. Snapshots of the solute plume at times for the *Da*=10^6. *A* (red) and *B* (blue) particles react to form *C* (green) particles, showing that after sufficient time, the network topology channels particles to fractures, in which the flow field converges and reactions occur.
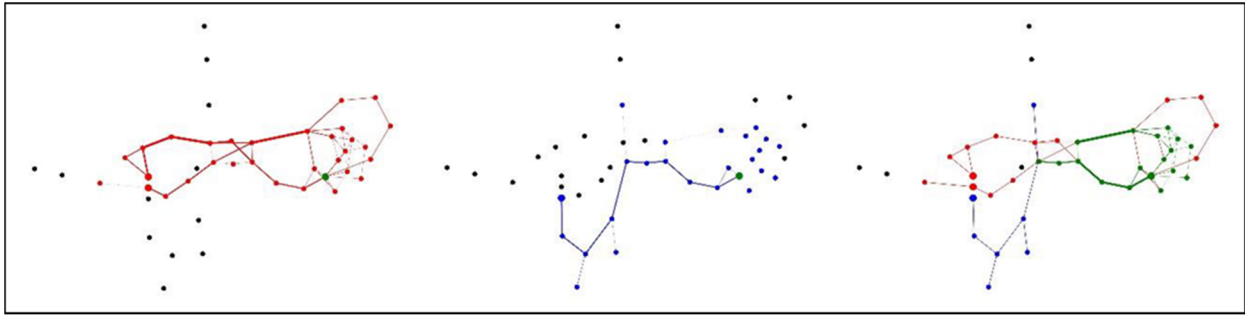
Figure 6.5-10. Topological representations of where particles pass through the DFN. Every node is a fracture and edges indicate particles pass between the two corresponding fractures. Left: *A* particles: Nodes and edges are colored red to show the paths of *A* particles. Middle: *B* particles: Nodes and edges are colored blue to show the paths of *B* particles. Right: Nodes and edges are colored green if both *A* and *B* particles pass through those fractures and intersections.
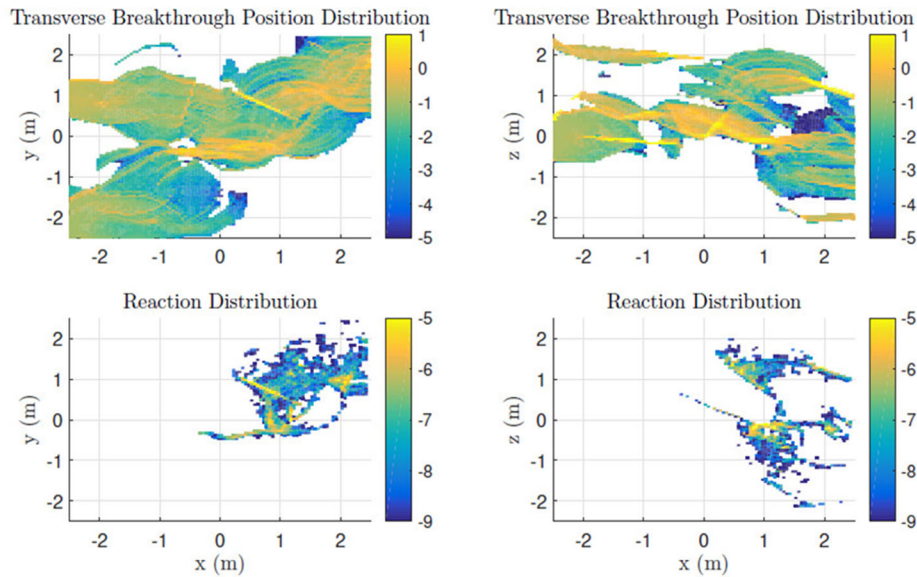
Figure 6.5-11. TBPD and reaction location for $Da = 10^6$ and flux weighted boundary condition. Colors correspond to log probabilities.

6.5.2.3. Summary and Future Work

The study reported above is a first step towards understanding how an irreversible kinetic reaction influences the migration of a solute plume in a discrete fracture network framework (Viswanathan et al., 2021). The reactive transport simulations conducted on discrete fracture networks suggest that the interplay of network topology and solute chemical properties are the principal controls on reactive transport behavior. It was determined that reactions are most probable in high velocity pathways, where particles are channelized and therefore more likely to interact with other chemical species, and that the local chemical properties dictate whether a reaction will occur. Such findings improve current characterization of reactive transport processes in subsurface fractured media and provide important implications for developing the next generation of upscaled reactive transport models. Future studies will consider the range of network properties, e.g., fracture density, connectivity, permeability, as well as a variety of initial and boundary conditions for different chemical reactions at different temporal and spatial scales. The capability to include reactions within a DFN modelling framework aligns well with the goals of international collaboration in the context of SKB's GWFTS Task Force.

6.6. Salt Coupled Processes, Geomechanics and Brine Migration

6.6.1. Introduction to International Collaboration Activities on Salt as Host Rock

In FY21, several international collaboration activities related to salt as host rock for nuclear waste disposal have been conducted by LBNL and SNL in a cooperation with German research institutions. A bilateral MoU was signed in 2011 between DOE and the German Federal Ministry of Economics and Technology (BMWi) to cooperate in the field of geologic disposal of radioactive waste, and a variety of joint R&D projects have been conducted over the years. Three of the most prominent active U.S.-German research activities are described in more detail in Sections 6.6.2 to 6.6.4 below.

- Section 6.6.2—Summary of the Drift Closure Analysis and Simulations conducted as part of the Joint Project WEIMOS, based on the report by Kuhlman et al. (2021a,b),

- Section 6.6.3—Summary of research activities as part of the collaborative project RANGERS, which focuses on EB in salt (Kuhlman et al., 2020a,b; 2021a,b),

- Section 6.6.4—Summary of research activities related to the U.S.-German KOMPASS project, which seeks to improve THM models for crushed salt (Kuhlman et al., 2020a,b; 2021a,b),

In addition, institutions from countries continued their long history of information exchange in US-German workshops. In FY21, the 11th US/German Workshop on Salt Repository Research, Design and Operation was held virtually and distributed over several days throughout the year. The workshop was co-hosted by Wilhelm Bollingerfehr (BGE TECH), Michael Bühler (PKTA), Philipp Herold (BGE TECH), and Kris Kuhlman (SNL). The first day of the meeting (Tuesday February 2, 2021) involved a presentation of the progress and intentions of international radioactive disposal programs in the United States, Germany, the Netherlands, and the United Kingdom. The second day of meeting (Thursday June 17, 2021) was on the topic of granular salt reconsolidation, including presentation of laboratory, modeling, field, and microstructural work in the KOMPASS and GESAV-II projects. The final two days of the meeting were held Wednesday and Thursday of September 8-9, 2021. The final days of the meeting were on the topics of EBS, materials and backfilling, and modeling in salt.

SFWD researchers are also involved in two broader international initiatives involving multiple nations, through the new salt-related task in DECOVALEX-2023 and through the NEA, which are described in the following sub-sections:

- Section 6.6.5—Summary of the BATS conducted as a modeling task in the DECOVALEX-2023 Project (Kuhlman et al., 2020a,b; 2021a,b).

- Section 6.6.6—Summary of FY21 activities conducted under the auspices of the NEA.

6.6.2. Drift Closure Analysis and Simulations – Joint Project WEIMOS

Joint Project WEIMOS is a collaboration of German and U.S. researchers aimed at improving thermo-mechanical modeling of salt repositories (Section 4.2.1.1). The WEIMOS partners include Hampel Consulting (Mainz, Germany), Institute für Gebirgsmechanik (IfG, Leipzig, Germany), Leibniz University (Hannover, Germany), Technical University of Braunschweig (Braunschweig, Germany), Technical University of Clausthal (TUC, Clausthal, Germany), and SNL (Albuquerque, USA). The WEIMOS project is planned to be completed on March 31st, 2022. The joint project is organized into five work packages; updates in each work package are given below followed by an additional note on WEIMOS-related model development, based on the report by Kuhlman et al. (2021a,b).

WP 1. Deformation Behavior at Small Deviatoric Stresses

Salt creep is the driving force for room closure in salt repositories. The precursor to WEIMOS, Joint Project III, confirmed that salt undergoes a creep mechanism change between intermediate and low stresses. Low stress creep occurs below about 8 MPa, but methods to accurately measure low stress steady-state creep strain

rates, low stress creep's temperature dependence, and the underlying micromechanical mechanism behind low stress creep have not been fully established. Measurements of low-stress creep are very challenging because the axial strain rates are small, sensitive to small temperature and humidity fluctuations, and can be convolved with volumetric consolidation strain rates. The IfG in Germany has recently developed a test procedure to accurately measure the steady-state strain rate at low stresses for a long (>100 days) hydrostatic consolidation phase at an elevated temperature of >100°C. Next, a low equivalent shear stress is applied and held constant while the temperature is decreased in a stepwise fashion over a year or more. The high temperatures cause the sample to accrue more creep strain and reach the steady-state microstructure more quickly. Once the temperature is close to room temperature, the equivalent shear stress is returned to zero to confirm the volumetric strain rate is virtually zero. Finally, the non-zero equivalent shear stress is reapplied to confirm the same axial strain rate as observed. This process has been successfully applied to a WIPP salt sample at 4 MPa equivalent shear stress, and further tests on WIPP salt are underway to test the equivalent shear stress.

WP 2. Damage Reduction and Healing

Healing of cracks in salt is important for the long-term safety case because cracks in the disturbed rock zone (DRZ), as well as broken pieces of rubble that fall into a room, serve as flow pathways for radionuclides. Although shear-induced damage has been studied in the past, the influence of temperature and stress state on healing is not well understood. Accordingly, an experimental program has been underway at TUC in Germany to characterize these dependencies. Although TUC's preliminary healing tests produced inconclusive results, new high precision equipment combined with innovative testing procedures have produced a clean set of results on Asse salt samples. Some of the WEIMOS partners have simulated these tests and, for the first time, a given model is able to reasonably capture all test results with one unique parameter set. In addition, a new set of healing tests was started on WIPP salt using the same test conditions applied to the Asse salt. Although the WIPP salt creeps and damages substantially faster than Asse salt, the fundamental dependencies on temperature and stress state appear to be the same. Consequently, the partners expect the same model formulation should be able to capture the healing of both salt types with different parameter sets.

WP 3. Tensile Stresses

Cracks, which are developed due to tensile stress, can play important roles in creation of the DRZ and subsequent roof fall events. However, limited data exist on tensile failure. In 2019, the IfG in Germany performed first tensile test experiments on 90 x 180 mm cylindrical WIPP salt samples. The samples were first damaged (dilated) to different degrees in a triaxial compression cell, and then tensile tested to determine the tensile strength. The triaxial compression was conducted by utilizing the confining pressure from 0.2 MPa to 5 MPa to generate the volume strain ranging from 0.5% to 3%. Experiments were conducted using multiple confining pressures. The tensile strengths exhibited a large degree of scatter and did not appear to directly depend on the amount of damage for a given confining pressure. More recently, the TUC performed a similar test series on WIPP and Asse salt. Although Asse salt has fewer impurities than WIPP salt, no clear difference between the two salt types was discernable and no trends could be determined. The lack of trends may have been caused by orientation of the microcracks induced during the triaxial compression phase. Triaxial compression under low confining pressures causes microcracks that open perpendicular to the subsequent tensile stress axis. Future studies of the tensile strength's dependence on microcracking should attempt to apply tensile stresses that tend to open the microcracks. Unfortunately, such a test program is unlikely to be completed during the WEIMOS project due to limited resources.

WP 4. Layer Boundaries

The mechanical behavior of clay seams between layers of salt can substantially affect room closure rates and roof falls, yet experimental data on clay seam behavior does not exist in the literature. To characterize the mechanical behavior of clay seams between layers of salt, SNL sub-contracted RESPEC during 2018 through 2020 to perform a series of shear tests extracted from a mine near the WIPP site and artificially manufactured clay seams. The natural clay seam cohesion strength and friction angle were nearly the same as pure salt without any interfaces because salt crystals spanned much of the clay seam interface (Sobolik et al., 2019). The artificial clay seam cohesion strength and friction angle, on the other hand, were like a saturated, highly

consolidated, clay (Sobolik et al., 2020). The behavior of actual clay seams from the WIPP is expected to be somewhere in-between these two bounding cases. Efforts to obtain actual clay seams from the WIPP have been unsuccessful so far. For example, sliding along Clay G has been observed in the underground, but extracting Clay G cores would require an angled approach because Clay G is close to the drift ceiling on WIPP's upper horizon. Clay F is more easily accessible, but it is a less uniform and distinct layer and not known to slide in the underground. Despite these difficulties, SNL will continue to investigate ways to procure WIPP clay seams.

WP 5. Virtual Demonstrator

The WEIMOS partners are currently at work on two demonstrations of the modeling capabilities developed in the other work packages. One demonstration involves a simulation of unrestrained open drift closure for 30 years, introduction of a sealing system, and continued simulation of the subsequent 70 years. The closure of the open drift exercises low stress creep and tensile damage, while the compaction of the seal deactivates damage evolution and activates healing. The second demonstrator scenario involves a clay seam, an 8×8 m drift, and a 5 m × 5 m parallel drift. Preliminary results show the influence of the low equivalent stress creep, as well as the considerable damage and tensile failures around the larger drift. Further simulations with both demonstration models are in progress.

Model Development Related to WEIMOS Activities. SNL currently utilizes the Munson-Dawson (M-D) model for rock salt, but the M-D model does not include the evolution of damage or healing. It also fails to capture the damage-free mechanical response at moderate strain rates (10^{-6} to 10^{-4} 1/s), which is particularly problematic, as the degree of damage is usually inferred from the difference between the damaged and damage-free behavior. As such, SNL developed a new constitutive model that captures both damage-free creep tests with slow steady-state strain rates (10^{-11} to 10^{-8} 1/s) and moderate constant strain rate tests (10^{-6} to 10^{-4} 1/s) (Reedlunn, 2020). The model was implemented in Sierra/Solid Mechanics (2021) and the implementation was verified against analytical solutions during the past year. Future work will focus on adding damage and healing to this new constitutive model. These model changes must be completed before SNL can fully take part in Work Packages 2, 3, and 5.

6.6.3. International Collaborative Project RANGERS

As described in Section 4.2.1.2, RANGERS is a collaborative project SNL and BGE Technology on the "Design and Integrity Guideline for EBS for a HLW Repository in Salt." The aim of the project is to develop a guideline for the design and verification of geotechnical barrier systems in repositories in salt formations that incorporates the existing knowledge and experience about geotechnical barriers. Recommendations for the design and verification of geotechnical barriers are being formulated based on the state of the art in science and technology and an overview of new concepts, building materials and technologies is being developed. The project is divided into six work packages, which are described in detail in the report by Kuhlman et al. (2021a,b).

- WP 1. State of the Art in Science and Technology.

- WP 2. Basics and Requirements.

- WP 3. Development of a Guideline Based on State-of-the-Art Science and Technology for Design and Verification of Geotechnical Barriers.

- WP 4. Preliminary Design and Verification of the Geotechnical Barrier System

- WP 5. Comparison of Design Results According to New Guideline with Results of Previous Design and Assessment.

- WP 6. Documentation and Final Report.

Significant progress was made in FY21 in the first two work packages; brief summaries of these and the respective progress made are given below.

WP 1. State of the Art in Science and Technology

This work package includes the development of a State of the Art (SOTA) Report including:

- Extensive description of the state of the art in science and technology for sealing structures: drift seals construction in the German Asse Mine, drift seal prototype at the Morsleben Repository in Germany, design and verification of shaft systems of the preliminary safety case of the Gorleben Repository (VSG) in Germany, shaft seals work done for WIPP, SNL closure concepts.

- Summary of all relevant findings for the design, construction and integrity verification of sealing structures.

- The international status of the design and construction of geotechnical barriers, which are different from currently being pursued in Germany and the US. The research includes new building materials, such as polymer concretes, as well as *in-situ* experiments, pre-stressing techniques or thermal elements for faster creep that are relevant for geotechnical barriers.

The SOTA Report is nearly complete and consists of activities centered on updating previous reviews and reports of seal tests in salt. By creating a comprehensive review of prominent seal materials (e.g., cementitious materials, crushed salt, and asphalt), the SOTA provides a firm basis for developing the Design Guidelines in WP 3, 4, and 5.

WP 2. Basics and Requirements

This Work Package includes:

- Evaluation and comparison of the regulatory requirements for the design and construction of sealing structures for salt mines and for repositories in Germany and the US.

- Determination of site- and repository-specific boundary conditions for the design of sealing structures using the example of repository concepts such as KOSINA and the WIPP.

- Compilation of relevant Features, Events and Processes (FEPs) and scenario developments for geotechnical barriers based on international and national FEP catalogues.

- Compilation of further basics and requirements from the findings of research projects and from practical experience.

BGE Technology has generated a seals-focused FEPs analysis that will be cross-checked against previous work on the US-German Salt FEPs Catalogue.

6.6.4. International Collaborative Project KOMPASS

Joint Project KOMPASS is a collaboration of German and American researchers seeking to improve thermo-hydro-mechanical models for crushed salt (i.e., run-of-mine or granular salt). The project is similar to the Joint Project WEIMOS, but focuses on crushed salt rather as a backfill material (see Section 4.2.1.3). Partners conduct experiments to understand crushed salt behavior and further develop, calibrate, and validate models for crushed salt. After translating to English, the acronym KOMPASS stands for "Compaction of Crushed Salt for Safe Enclosure". The KOMPASS partners are Bundesgesellshaft für Endlagerung Technology (BGE) (Peine, Germany), Institute für Gebirgsmechanik (IfG) (Leipzig, Germany), Technical University of Clausthal (TUC) (Clausthal, Germany), Gesellschaft für Anlagen-und Reaktorsicherheit (GRS) (Koeln, Germany), Bundesanstalt für Geowissenschaften und Rohstoffe (BGR) (Hannover, Germany), and SNL. Progress made in this project is summarized below; further details can be found in Kuhlman et al. (2021a,b)

The first phase of the KOMPASS project was completed in 2020, with a comprehensive final report by Czaikowski et al. (2020). During this phase, experimental techniques for consolidation were thoroughly evaluated to produce adequate pre-compacted and compacted samples under various conditions, which included characterizing sufficient reference material. A total of 34 different samples were produced, and several underwent microstructural investigations to document associated deformation mechanisms. In addition

to laboratory testing and analysis, model benchmarking initiatives revealed that while most models are capable of reproducing results, they still require a well-founded laboratory database to predict functional relationships to further characterize the THM-coupled compaction behavior of crushed salt. Various constitutive model approaches were compared in the first phase to determine the main influencing factors or properties of each and identify specific lab tests needed for sufficient validation.

The second phase of the project officially began in July 2021. Based on results from the first phase, a systematic test series has been planned to further establish reproducible and predictable correlations between stress, duration of compaction, moisture states, and respective target porosity. Figure 6.6-1 shows the main factors contributing to the behavior of crushed salt and the type of experimental tests needed to improve predictions of those parameters. It is also desired to perform sensitivity analysis across all methods for measuring low porosity and low permeability of long-term compacted samples to reduce errors and uncertainties. SNL plans to contribute to KOMPASS Phase 2 by performing additional microstructural investigations on past and future samples, as well as continuing model validation against the expanded experimental results.
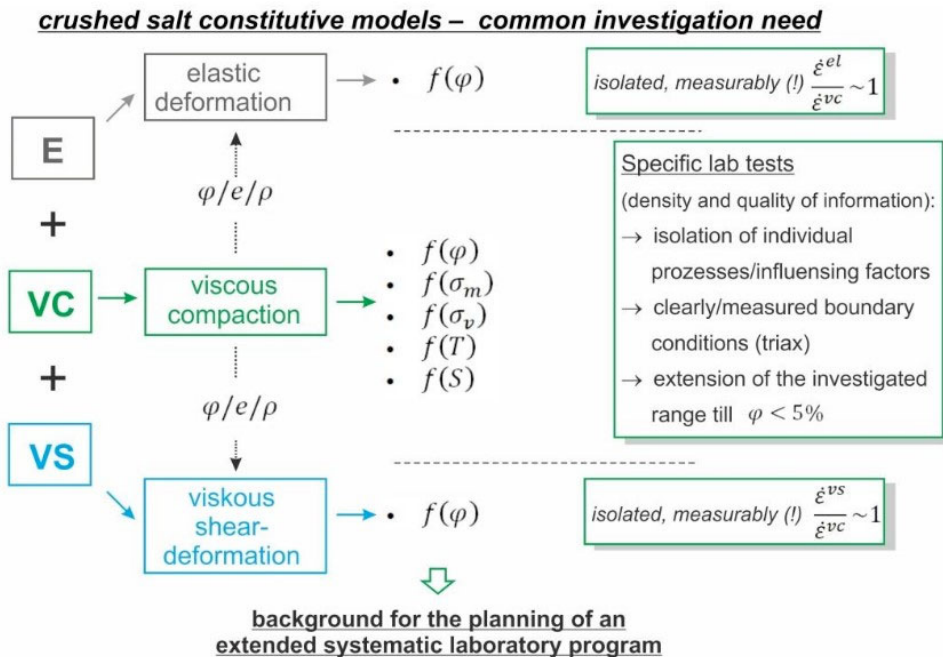
Figure 6.6-1. Schematic describing the factors contributing to crushed salt behavior and further laboratory tests needed to evaluate them (Czaikowski et al., 2020).

6.6.5. BATS in DECOVALEX 2023 – Task E

BATS is a field test that is currently conducted in the bedded salt formations at the WIPP facility in New Mexico (Kuhlman et al., 2020a,b). As pointed out in Section 3.2.3.5, the field test is now at the center of a modeling task (Task E) in the ongoing DECOVALEX 2023 project. Teams participating in Task E include: a U.S. team consisting of the organizations conducting the BATS test (SNL, LANL, LBNL), COVRA (Netherlands), RWM/Quintessa (United Kingdom), and GRS/BGR (Germany). Kris Kuhlman from SNL serves as the task lead. Since the start of the DECOVALEX Project in April 2020, Task E has progressed through three formal virtual semi-annual project meetings. Between each of the formal meetings, three informal Task-E kickoff or status meetings have occurred.

The objective of Task E is to observe and predict the coupled processes governing the availability of water to heated excavations in geologic salt. Brine availability strongly impacts the long-term performance of salt repositories for heat-generating radioactive waste. Important questions asked in Task E are as follows: (1) Is

two-phase flow in the excavation damage zone in salt important? (2) How to simulate brine flow after heating? (3) How confident can one be in brine pulse predictions? While Task E focuses on the field test data from BATS, the task lead designed a few introductory tasks with benchmarking exercises as a 'warm-up' to more complicated field -test models. In total, Task E includes four modeling and analysis steps (see schedule in Table 6.5-1). The four steps allow tackling the effects of high temperature coupled processes on brine accessibility and migration in a stepwise manner adding complexity with each step.

- Step 0: Single-process H1 and T benchmarks,

- Step 1: TH1 benchmark & H2M/H2 unheated brine inflow test case,

- Step 2: TH2M heated brine inflow test case (BATS), and

- Step 3: Possible additional tasks (ERT/AE joint inversion, seals, TH2MC, creep)

Note that H1 refers to single-phase brine flow and H2 to two-phase brine and vapor flow.

Table 6.6-1. High-level DECOVALEX-2023 Task E Schedule

	Apr.	Nov.	Apr.	Nov.	Apr.	Nov.	Apr.	Nov.
	2020		2021		2022		2023	
Step 0								
Step 1								
Midterm Report → (Nov 2021)								
Step 2								
Step 3								
Papers and Final Report → (Nov 2023)								

Brief updates on the elements and status of Step 0 and Step 1 are provided in Sections 6.5.5.1 and 6.5.5.2 below. The updates are based on the report by Rutqvist et al. (2021). Task E modeling teams are just starting to work on Step 2 in earnest, which is the most complex step involving BATS field test data. Instead of discussing early modeling for Step 3, Section 6.5.5.3 provides some highlight examples of monitoring data from the BATS test.

6.6.5.1. Step 0: Single Process H1 and T Benchmarks

The benchmarking exercises conducted in Step 0 comprise three tasks. The first two are simulations of brine inflow into unheated boreholes drilled at WIPP as part of small-scale brine inflow experiments conducted at WIPP (Finley et al., 1992), and the third task is the simulation of the measured temperature distribution in Phase 1a of the BATS experiment. All of these benchmark tests feature simplified physical representations of the processes.

6.6.5.1.1. Unheated Single-Phase Brine Migration into Room L4 Boreholes

In the 1991 small-scale brine inflow experiment at WIPP, 17 boreholes were drilled from three different underground rooms/drifts, which were continuously monitored for brine accumulation beginning from 1987. Room L4 and Room D, which were not heated, were selected for simulations in Task E Step 0 to characterize single flow processes. Figure 6.6-2 shows a schematic illustration of WIPP stratigraphy and layout of the brine inflow boreholes.
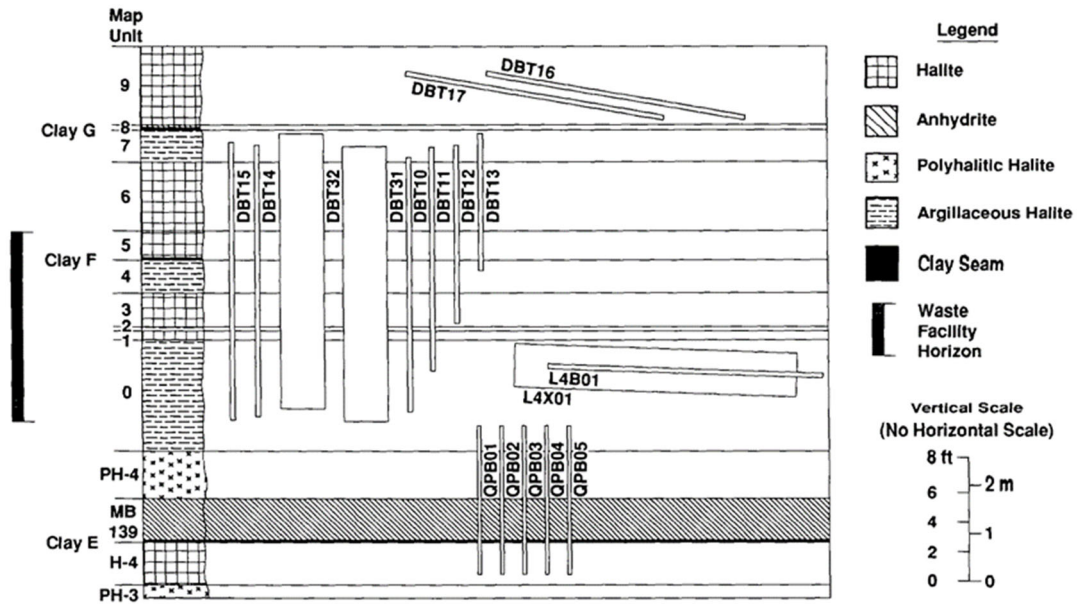
Figure 6.6-2. Schematic illustration of WIPP stratigraphy and small-scale brine inflow boreholes (Finley et al., 1992).

For the Room L4 modeling, brine inflow data were provided from a 10-cm diameter and 5.6 m long horizontal borehole (L4B01). The LBNL modeling team used a simple 1D axisymmetric model to calculate the inflow per meter length of borehole (Rutqvist et al., 2021b). This per meter value was then multiplied by 5.6 m to calculate the total inflow for comparison against field data. A schematic of the model and model parameters are given in Figure 6.6-3. Figure 6.6-4 shows a good agreement of experimental and simulations results, using parameters that are in good agreement with values found in the literature about the salt host rock at WIPP. The influence of different parameters such as permeability, porosity, initial pore pressure and borehole relative humidity was presented in a previous milestone report (Rutqvist et al., 2017), related to pre-test modeling of the BATS experiment at WIPP.
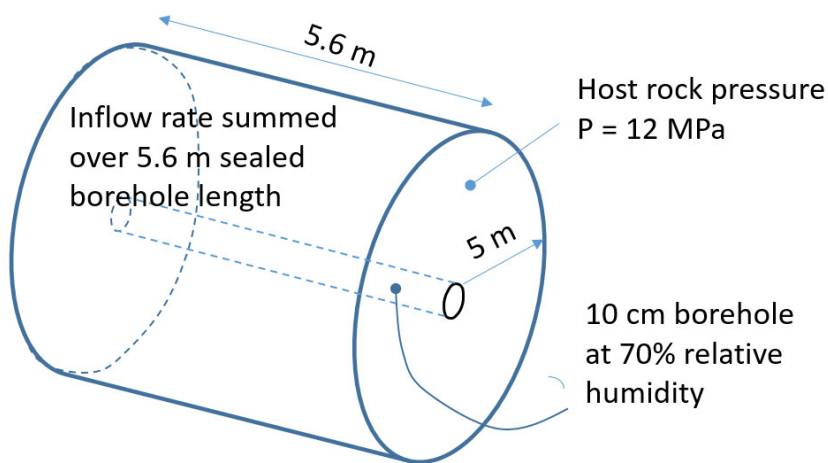
Figure 6.6-3. Schematic of model approach for simulating brine inflow into a horizontal borehole at WIPP.

(a)   (b)
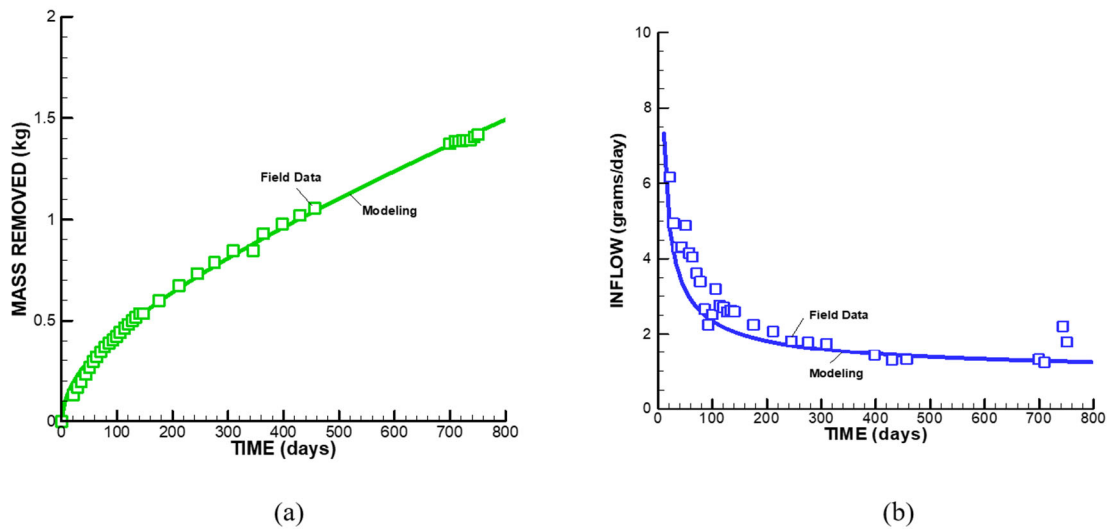
Figure 6.6-4. Comparison of modeling and field data on brine inflow into borehole L4B01. (a) Cumulative inflow mass, and (b) inflow rate.

6.6.5.1.2.   *Unheated Single-Phase Brine Migration into Room D Boreholes*

As to the second modeling exercise in Step 0, boreholes in Room D intersect at least three different geological units of the Salado formation: a halite, argillaceous halite and a clay seam, which allowed for the evaluation of the effect of host rock vertical anisotropy on brine accumulation. Brine flow modeling was conducted using a 3D model as shown in Figure 6.4-5; thermal and mechanical effects were neglected. The model with the XZ plane of symmetry represents a horizontally stratified lithological domain, which is 40 m long, 5 m wide, and 10 m deep. The model domain includes four boreholes DBT10, DBT11, DBT12, DBT13 (10 cm in diameter and 5.3 m, 4.6 m, 3.7 m and 2.8 m in length, respectively), which were selected for their relevancy to Step 0 objectives and other considerations related to the quality of brine inflow measurements. The model domain contains 514,805 mesh elements and it is refined around the boreholes as shown in the closeup view. Because the boreholes in Room D were drilled 3.5 years after the completion of Room D excavation, initial modeling was performed for the period of 3.5 years to assess the impact of Room D excavation on the distribution of pore pressure. The resulting pore pressure distribution after 3.5 years was used as the initial state for simulations of brine inflow into the boreholes. Figure 6.6-6 shows the distribution of pore pressure 850 days after drilling of the boreholes. A comparison of experimental data and numerical modeling of brine inflow into the boreholes as a function of time (Figure 6.6-7) shows good agreement between simulated and measured data. In all boreholes, the highest inflow rate occurs immediately after the drilling and decreases exponentially with time to reach a quasi-steady-state value.
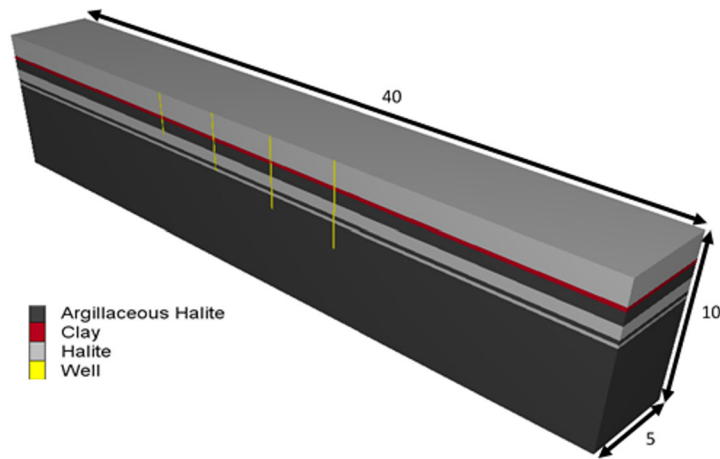
Figure 6.6-5. 3D Geometry used to simulate Room D brine inflow experiment.
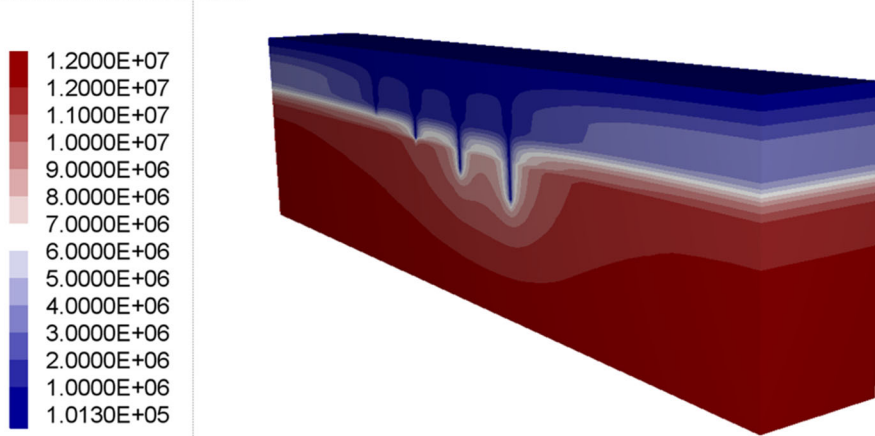
Figure 6.6-6. Distribution of pore pressure (in Pa) 850 days after drilling of the boreholes.
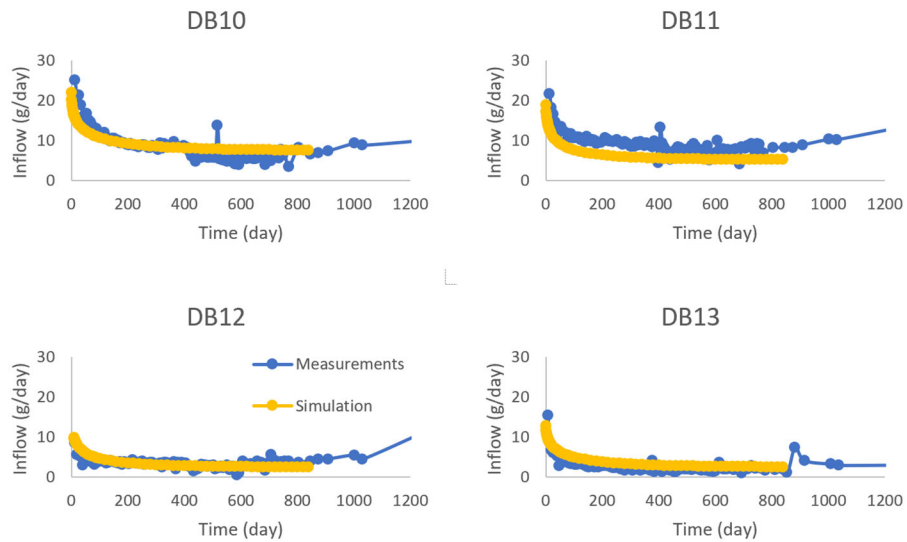
Figure 6.6-7. Comparison between experimental data and predicted brine inflow in DBT10, DB11, DB12 and DBT13. Pore compressibility is 3×10^{-9} Pa^{-1} and initial pore pressure at the bottom boundary is 8 MPa.

6.6.5.1.3.   Heat Conduction Near BATS Heated Borehole

The last benchmarking task in Step 0 is focused on the simulation of heat transfer in salt around a heated borehole. Experimental data used for modeling of heat conduction were obtained from one of the borehole heating experiments related to the BATS campaign at WIPP (Mills et al., 2019). The objective of this task is to simulate temperature distribution due to heat conduction during the January to March 2020 BATS heating and cooling cycles. The DECOVALEX teams were provided with time-varying temperature data, laboratory estimates of thermal properties, and relevant coordinates and distances between the source and measurement points. LBNL's simulations were performed using a 2D axisymmetric model with the application of the TOUGH code, which was previously developed for modeling of thermal responses at the BATS experiments (Rutqvist et al., 2020a). The modeling of a previous BATS experiment resulted in good agreement with the results of an alternative 3D model analysis (Guiltinan et al., 2020). Figure 6.6-8 gives an example of the temperature distribution calculated by the LBNL model along with the locations of temperature sensors in the axisymmetric geometry. The model simulations demonstrate that it is very important to use an accurate model for the temperate dependent thermal conductivity. Figure 6.6-9 shows a good agreement between simulated and measured temperature evolution at the monitoring points, except at HT2CT4.
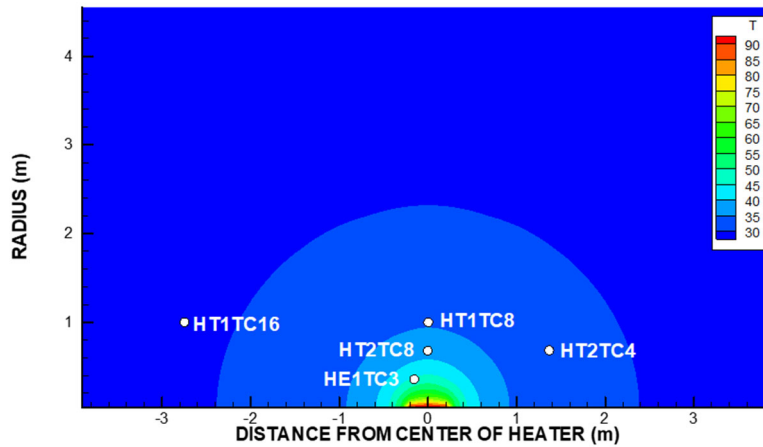
Figure 6.6-8. Simulation result of temperature contours in the axisymmetric model centered around the heater with marked locations of temperature monitoring sensors.
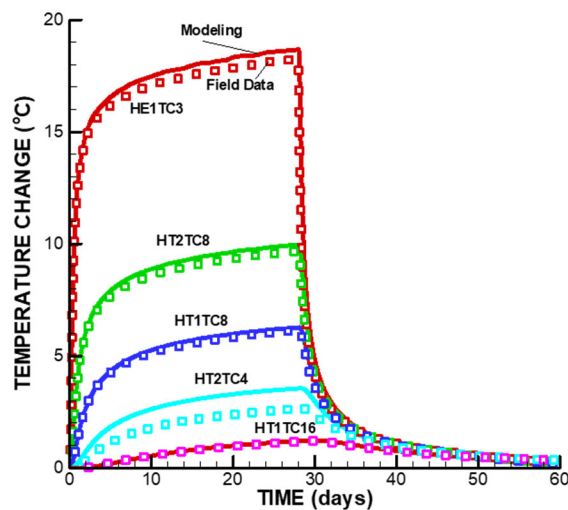
Figure 6.6-9. Comparison of simulated and measured temperature evolution during the heated borehole tests.

216

6.6.5.2. Step 1: TH1M Benchmark and H2M/H2 Unheated Brine Inflow Test case

6.6.5.2.1. Single-phase Brine Inflow into Heated Borehole

Simulations were conducted to compare the results of numerical modeling with the analytical solution of McTigue (1990). The McTigue (1990) analytical solution was derived to predict the thermally induced fluid flow around a heated borehole drilled in an infinite, homogeneous, isotropic, linearly elastic and fully saturated medium, which is not subjected to any pressure gradient or external stress. The modeling approach adopted in these simulations is based on the model of thermo-poroelasticity in order to account for the coupled interaction between thermally-induced fluid flow and porous matrix deformation. Simulations were carried out using TOUGH3-FLAC7 and COMSOL Multiphysics, the latter of which is a Finite Element Method (FEM) commercial code. Contrary to TOUGH-FLAC that uses a sequential coupling scheme, COMSOL allows users to solve models using a fully coupled approach that solves for all of the unknowns and includes all of the couplings between the unknowns within a single iteration.

The numerical predictions of temperature, pressure and flux obtained using TOUGH-FLAC and COMSOL agree very well with the analytical solutions. The minimal disagreement between the analytical solution and the TOUGH3 simulations for pressure after one week, shown in Figure 6.6-10, may be due to the fact that fluid density is constant in the analytical solution, whereas it varies linearly with pressure and temperature in TOUGH3. If the fluid density is kept constant in TOUGH3, a good agreement of experimental and modeling results is achieved. In order to evaluate the contribution of coupling with geomechanical processes, thermo-hydraulic simulations were performed using TOUGH3 and COMSOL.
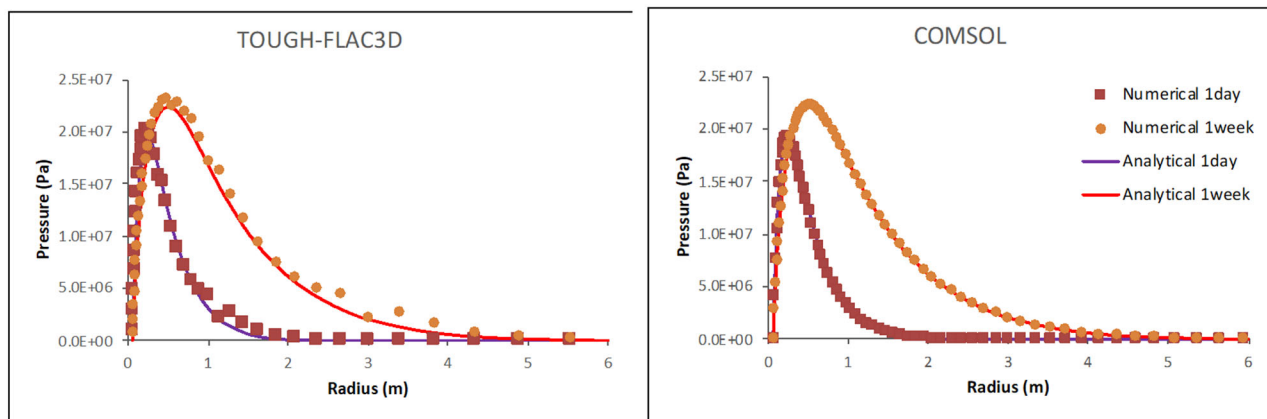
Figure 6.6-10. Pressure versus radius profiles after 1 day and 1 week.

6.6.5.2.2. Two-Phase Flow in Drift EDZ

This Step 1 benchmark takes into account the fact that a damage zone around newly excavated drifts in salt rock, characterized by an increase in permeability and porosity and by partial desaturation. That is why brine flow around an excavation should be treated as a variably saturated flow problem even in the absence of any heating leading to pore-water evaporation. This modeling task therefore compares different modeling approaches for two-phase flow around a BATS access drift at WIPP. The LBNL model (Rutqvist et al., 2021b) assumes that the EDZ forms immediately after the excavation and extends 2.5 m into the salt formation, which is initially fully saturated under a pressure of 12 MPa. Initial simulations were conducted using a 1D flow domain including the EDZ and intact salt (Figure 6.4-18). The choice of the formation pressure, permeability and porosity are based on experimental observations at the WIPP site (Beauheim and Roberts, 2002). Atmospheric pressure and a relative humidity of 75% are specified at the left boundary of the model representing the air and water vapor in the drift. Figures 6.6-11 displays predicted pressure and saturation profiles for the case where the two-phase flow parameter P_0 in the EDZ is set 100 times lower than that in

intact salt. The figures shows that the presence of the EDZ results in a gradual partial desaturation of the near-drift salt rock.
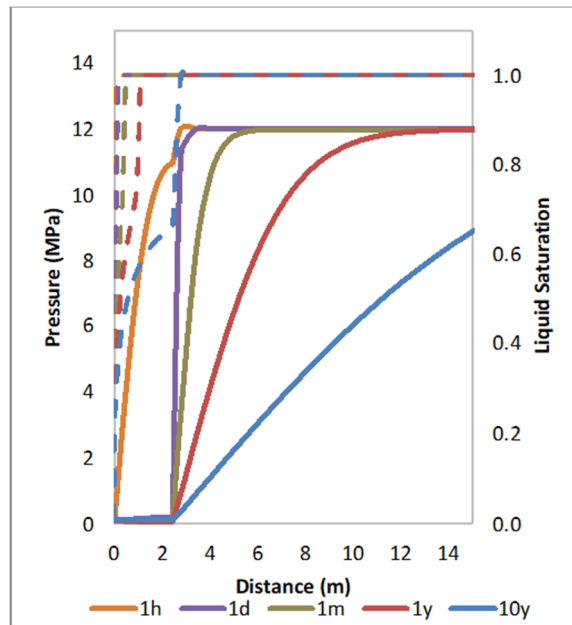
Figure 6.6-11. Pressure and saturation profiles for different times until 10 years after the drift excavation for the case when P_0 in the EDZ is 100 times lower than in the host rock.

6.6.5.3. BATS Progress

Despite Covid related testing and travel restriction, the BATS experimental program and analysis has made good progress in the past year. After conducting the preliminary "shakedown" test in 2018/2019, the BATS Phase 1a heater testing occurred from January to March 2020. BATS Phases 1b and 1c began in January 2021 and involved addition of gas (1b) and liquid (1c) tracers in the same heated and unheated boreholes of the BATS Phase 1a location (Kuhlman et al., 2020a,b; 2021a,b . Together, these tests have provided a wealth of data, a subset of which is now being used for Step 2 of DECOVALEX-2023 Task E. A few selected highlights of the BATS data set are provided below. The configuration of the test is described in Section 3.2.3.5.

Figures 6.6-12 shows temperature data in multiple boreholes of BATS as well as the water inflow data into same boreholes (Kuhlman et al., 2020a,b). As shown in Figure 6.6-13, acoustic emissions monitoring was used to measure and locate damage in the salt due to heating, cooling, and brine migration (Figure 6.4-13). Results from gas tracer tests conducted during Phase 1b are illustrated in Figure 6.6-14 for the unheated and in Figure 6.6-15 for the heated test array (Kuhlman et al., 2021a,b). As a final example, Figure 6.6-16 provides ERT (electrical resistivity topography) data that have been acquired daily throughout the last year (Rutqvist et al., 2021b). For ERT measurements, a current is injected through one pair of electrodes, and the resulting voltage is measured across a separate pair of electrodes. By using numerous different combinations of current injection and voltage measurement dipoles, the subsurface resistance is densely sampled. The ERT figure illustrates the differences between the heated and unheated BATS testbeds, pointing to differences in the moisture content and other relevant parameters affecting ERT response.
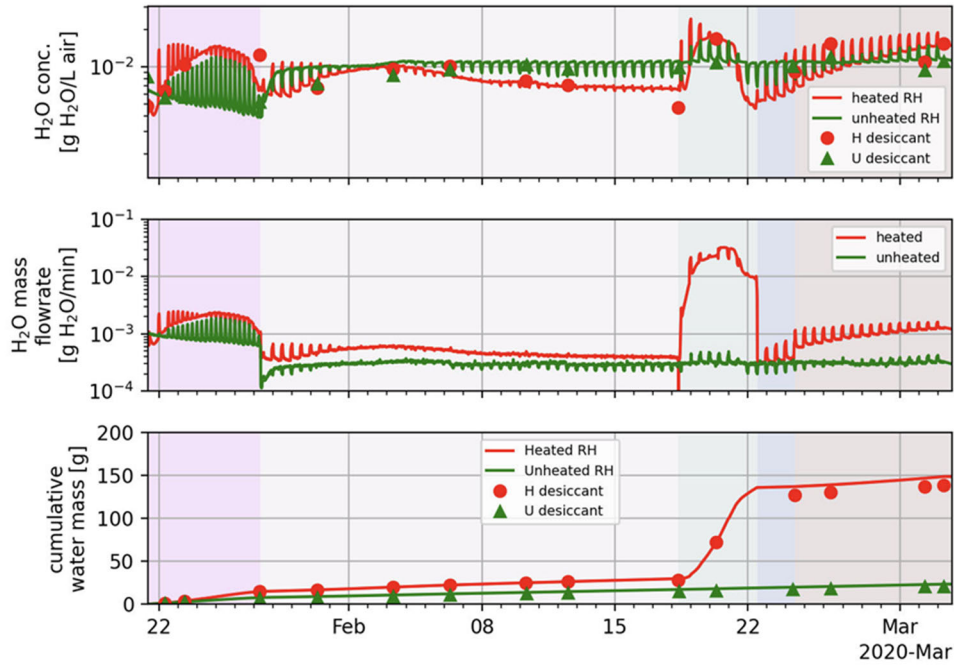
Figure 6.6-12. Water production computed from RH and gas flowrate compared to desiccant-based observations.
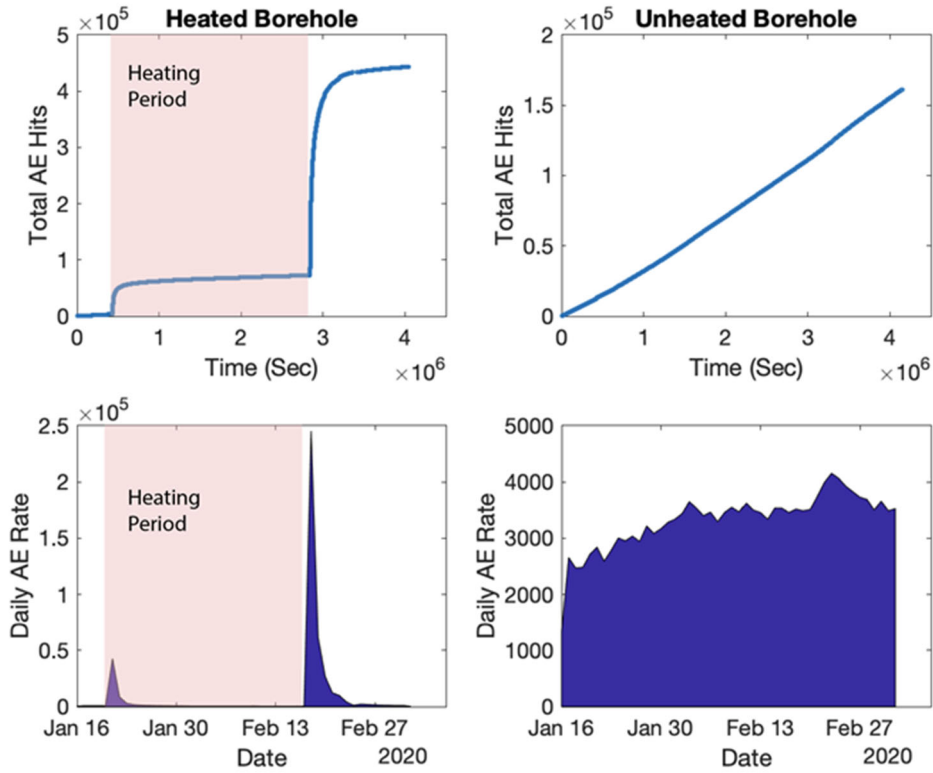
Figure 6.6-13. Total number of AE hits and daily rate per array during BATS 1.
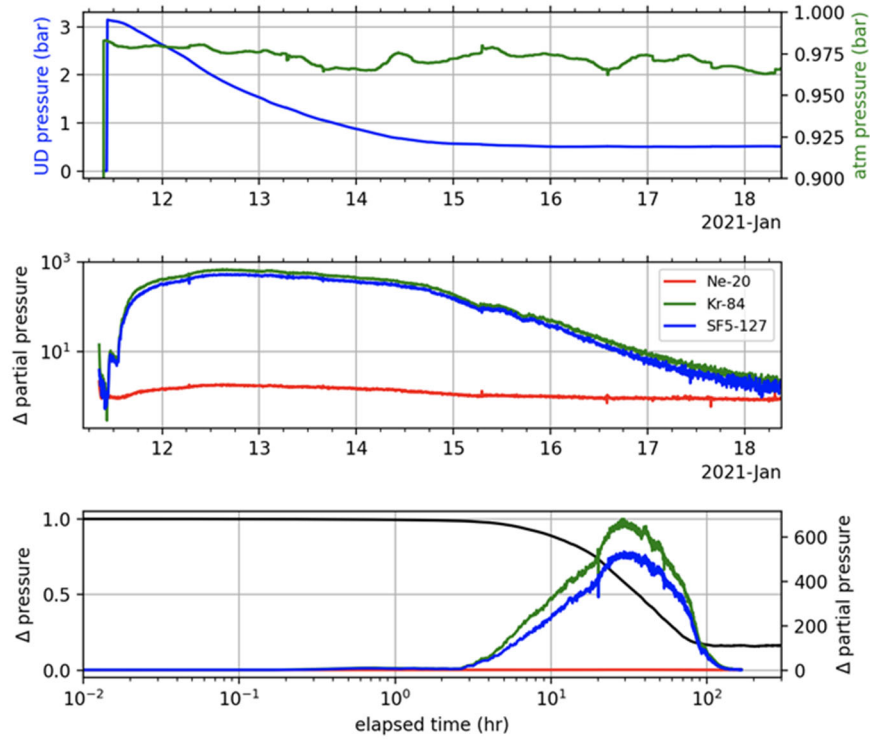
Figure 6.4-14. Gas tracer Test 1 results in unheated array.
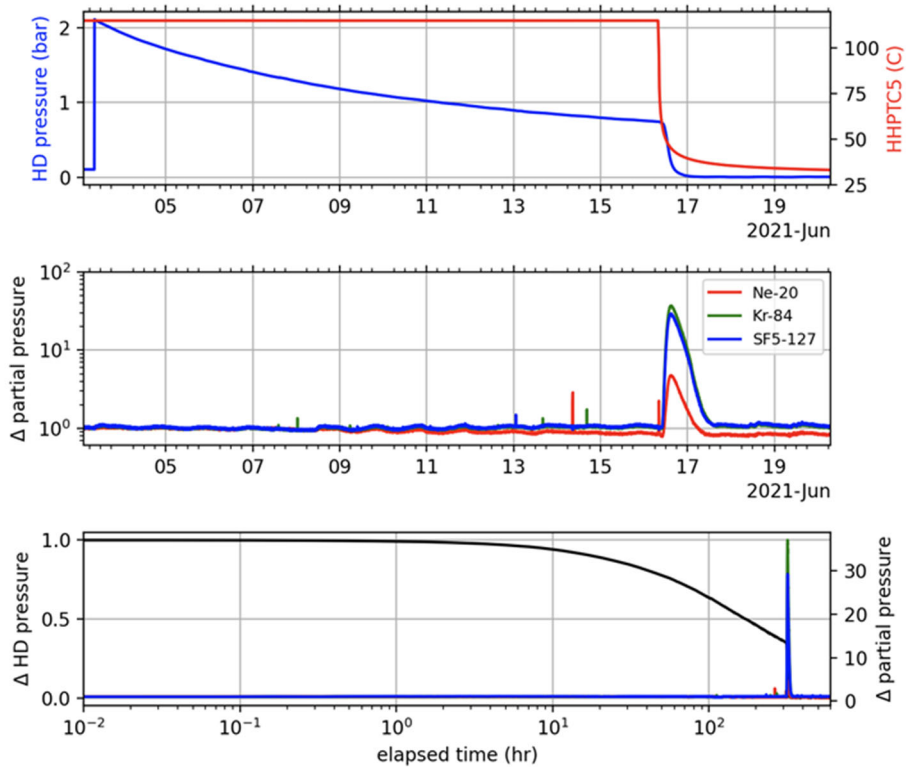
Figure 6.6-15. Gas tracer Test 5 results in heated array.
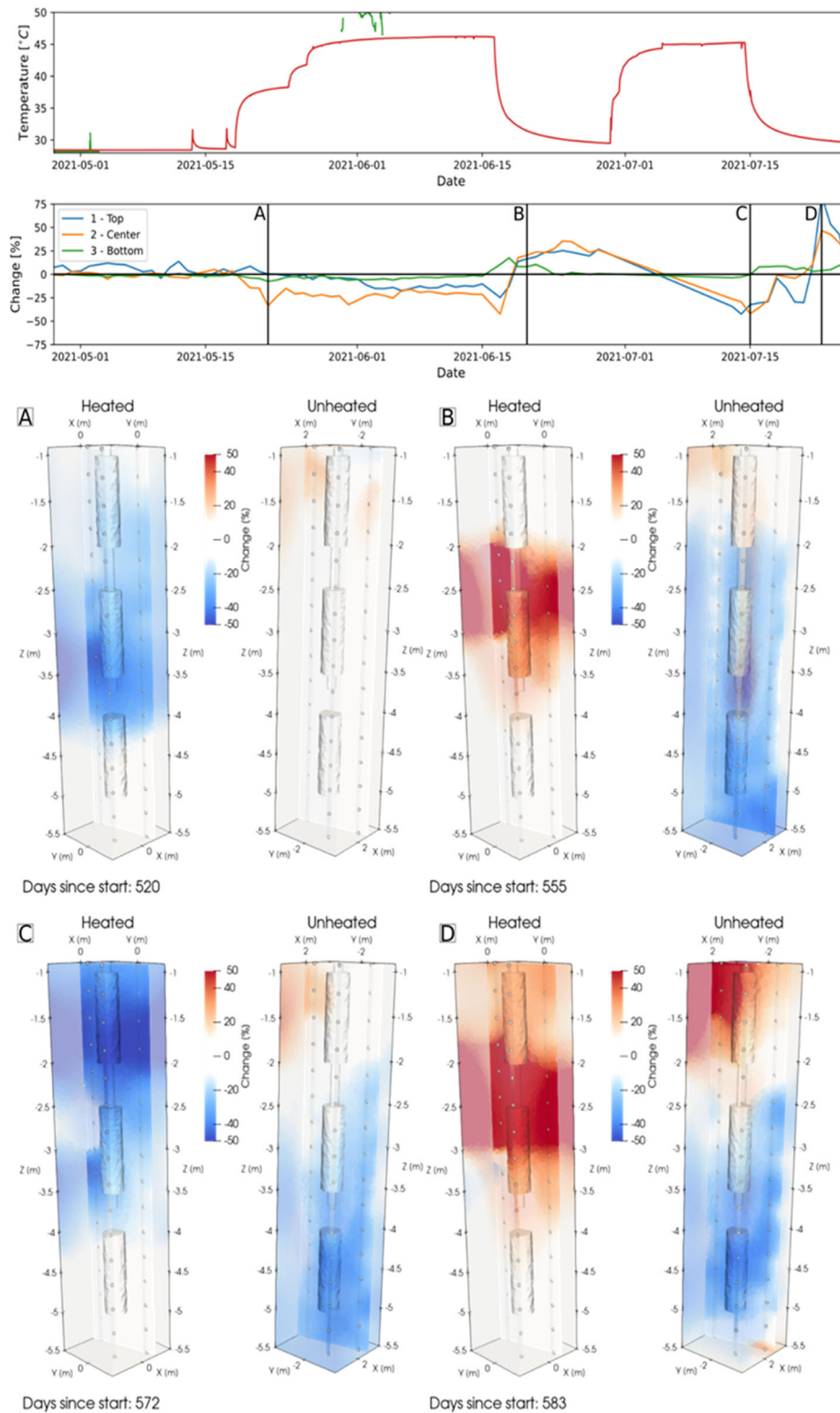
Figure 6.6-16. 3D resistivity modeling results showing the change in both plots during heating and tracer tests in Summer 2021. Top panel shows the resistivity variation in the heated plot for three different areas within the studied domain, as well as temperature recorded in the heated borehole. Note that the other temperature sensors failed during this experiment. Figures (a)-(d) show 3D changes in resistivity.

6.6.6. NEA Activities

6.6.6.1. NEA Salt Club

In FY21, SNL researchers continued and expanded their involvement in the NEA Salt Club activities (Section 3.5.2). The 10th Salt Club meeting was held virtually via Zoom on December 8, 2020. At that meeting, Kris Kuhlman from SNL was elected the new chair and Michael Bühler from the German PKTA the vicechair. In his first role as Salt Club chair, Kris Kuhlman attended the virtual NEA International Group for the Safety Case (IGSC) meeting (April 27 to 29 2021), presenting on the ongoing activities of the NEA Salt Club. The 11th NEA Salt Club meeting was held Ma 11-12, 2021 via Zoom. The topical session was focused on PA and included presentations on geochemistry aspects, scenario development, and PA modeling with RANGERS and DECOVALEX Task F, characterization of halite deposits in the UK, and Dutch PA modeling in DECOVALEX Task F. Next year, both the 12th US/German Workshop and 12th NEA Salt Club meetings are planned to be in person in Braunschweig, Germany, the week beginning May 9, 2022. This was the planned location of the 2020 US/German Workshop, before it was canceled due to the COVID-19 pandemic

6.6.6.2. Salt FEP Catalog and Salt Scenarios

In FY20, SNL and GRS finalized the development of a comprehensive Features, Events and Processes (FEPs) catalogue and FEP database to the development of a generalized approach to scenario development for a high-level waste repository at a generic salt site (see Section 4.2.1.4). Freeze et al. (2020) issued a final report on the bilateral US-German Salt FEPs project, which is now linked to from the NEA Salt Club website. An effort was made since then to broaden this FEP work and publish it as an NEA report. To achieve this objective, an international virtual Salt Scenarios Workshop was held on August 11-13, 2020. The workshop included contributions from US, German, UK, and Dutch colleagues and summarized the history of the scenario development process. The Workshop was coordinated with both the development of a salt reference case as part of Task F of DECOVALEX 2023 project (see Section 3.2.3.6), and the discussion of FEPs and modeling associated with the EBs as part of the RANGERS project. The work that began with the 2020 Salt Scenarios Workshop has continued in FY21 with several virtual large-group meetings and a small group. The goal of the larger group is to produce an NEA-publishable report summarizing the transition from FEPs to scenarios in several countries. The goal of the smaller group is to draft a journal manuscript on "best practices" in radioactive waste disposal related to scenarios

6.7. Hydromechanical Behavior of Faults in Response to Repository-Induced Perturbation

6.7.1. Introduction

Repository-induced effects such as creation of an EDZ, gas generation from canister corrosion, and thermally-induced pore pressure perturbations may result in the reactivation of pre-existing features (fractures, faults or bedding planes). Understanding such reactivation due to pressure and stress changes, the possible formation of permeable pathways, and their potential long-term sealing is critical in assessing the performance of radioactive waste repositories, in particular in shale formations. A few years ago, SFWD researchers started collaboration with the *in-situ* fault testing activities conducted at the Mont Terri URL, as described in Section 3.1.3. A first controlled-injection fault activation experiment was conducted in 2015 by injecting high-pressure synthetic pore water in a fault zone intersecting the Opalinus Clay formation; this experiment is referred to as FS experiment. Starting in 2018, a new experimental testbed was being prepared in the same fault, to conduct a follow-up experiment with a larger activated fault patch and improved monitoring. As part of these preparations, the permanent installation of new sensors provided measurements of the long-term evolution of fault pore pressure and three-dimensional displacements in response to excavation work for a new Mont Terri gallery ~40 to 50 m away from the fault. Finally, in November 2020, a new controlled-injection injection experiment was conducted in the larger fault testbed; this 2020 experiment, referred to as FS-B, included time lapse seismic imaging of fault movements and leakage.

In FY21, LBNL researchers continued their international collaboration efforts with the FS and FS-B experiments to better understand the conditions that could cause fault activation and instability based on *in-situ* testing at the Mont Terri URL, and to test new predictive models for simulating the complex coupling processes between fault slip, pore pressure, permeability creation, and fluid migration (Rutqvist et al., 2021a). The following activities were conducted:

- LBNL scientists continued their advanced numerical analysis of the 2015 FS experiment to explore the link between fault zone complexity, size of the leakage volume, and induced seismicity (Section 6.7.2 below).

- The team conducted a more complete analysis of the remote fault activation induced by the excavation of a new Mont Terri gallery in 2018, using data from the extensive array of distributed fiber optic strain monitoring deployed in several boreholes crosscutting the fault to understand long-term fault behavior (Section 6.7.3 below).

- Finally, LBNL scientists started collecting and analyzing the results of the new 2020 fluid injection experiment that was conducted in November 2020 (Section 6.7.4 below).

High-level findings of the fault-related research conducted to date are as follows: (1) Complex opening and slip was measured on the fault at fluid activation pressures close to the normal stress applied on the fault; (2) High-transmissivity flow paths developed at least temporarily and "local" (~meters from the injection point); (3) Fault reactivation and leakage produced mainly aseismic movements and a limited number of small magnitude seismic events; (4) When pore pressures in the fault drop after injection ceases, an instantaneous mechanical closing of the fault is observed. Nevertheless, a long-term residual hydraulic permeability is measured. Since 2015, the pressure in the ruptured patch slowly increased but did not fully recover, remaining ~0.45 MPa below its initial value. This may highlight slow sealing of the activated fault patch.

6.7.2. Modeling the Effects of Fracture Interactions on Fault Behavior and Induced Seismicity Based on the 2015 FS Experiment

Continued simulations of the FS experiment explore the link between the fault zone complexity, the size of the leakage volume and the induced seismicity (Rutqvist et al., 2021a). Results highlight that a complex fault zone, where multiple fractures are activated, produces a small amount of seismicity and local channeling. This is related to fracture stress interactions, as seismicity occurs predominantly at these fracture intersections.

6.7.2.1. Model Setting

Modeling of fluid injection and seismicity in a fault network representative of the FS experiment was conducted using the 3D Distinct Element Code (3DEC) (Itasca, 2016). The code can be used to model the interaction between fluid flow with two-way hydromechanical coupling, aseismic slip and seismic rupture in a system of discrete faults intersecting impervious elastic rocks. The location and magnitude of seismic events are estimated from the seismic slip and the ruptured area. Further information on the numerical method can be found in Wynants-Morel et al. (2020).

The earthquake rupture model falls into the class of "inherently discrete models" (Rice, 1993). The model is based on using the cubic law to describe the coupling between fluid flow, pressure and the hydraulic aperture change. A system of equations implemented for modeling is given in Rutqvist et al. (2021a, Equations 8.2 through 8.5). Fluid injection is modeled as a point source in the fault, with fluid pressure increasing step by step from 0.5 MPa to 5.4 MPa (Figure 6.7-1). The total time of injection is 650 seconds. In the model, fluid flow occurs in the activated parts in shear failure of the fault plane; the model prevents flow from occurring in the remaining elastic parts (Guglielmi et al., 2015a,b; 2020a). The sensitivity of the calculated seismicity to different levels of fault criticality is estimated by including a deviatoric component to change the shear stress without modifying the normal stress among the tests.
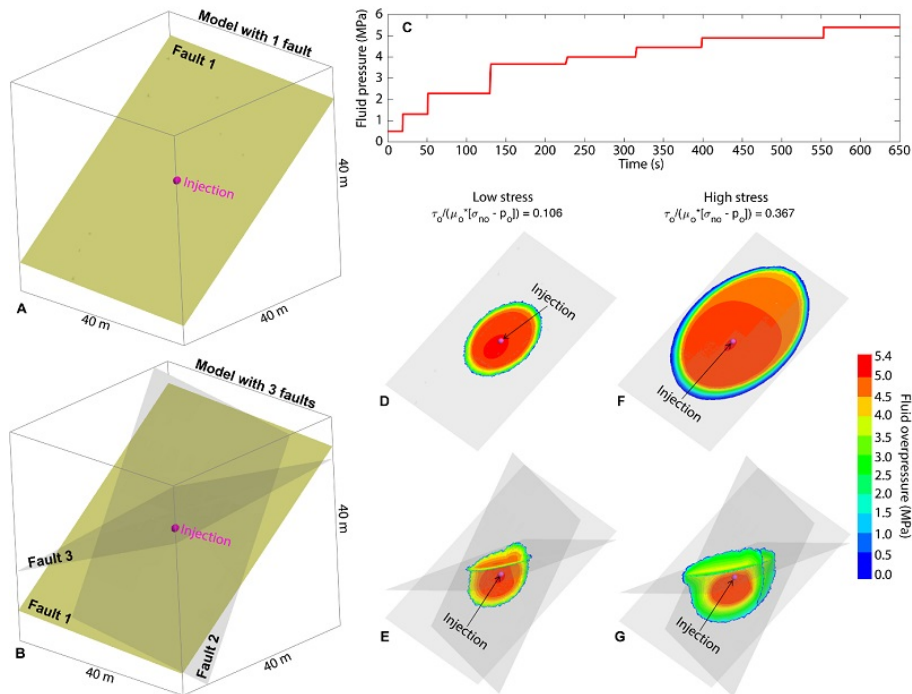
Figure 6.7-1. 3D view of the different model geometries, including (a) a single fault, and (b) three faults. The yellow fault, labeled "Fault 1," is the fault where the fluid injection is applied (magenta dot). (c) Fluid pressure history applied at the injection point. (d) Spatial distribution of the fluid overpressure at the end of injection (650 s) for low and high background stress ratios.

6.7.2.2. Model Results

Modeling results show that a local fluid injection can produce a different fluid pressure distribution depending on a number of faults and the initial stress conditions (Figures 6.7-2d-g). High-fluid pressure is distributed over a larger patch on a single fault, while it is concentrated around the injection interval in the case of a fault network.

The fluid injection also induces significant aseismic slip near the injection that then contributes to trigger micro-seismicity within a fault volume, especially on the secondary structures and fault intersections at a distance from injection in the main fault plane (Figure 6.7-2).

The seismic events are aligned along the intersection between the faults, and the moment magnitude (M_w) of seismic events depends on the initial stress state. Figure 6.7-3 indicates that the seismicity is triggered at a distance from injection of about 3 m for a single fault, and about 2 m for a fault network model. The pressure and shear stress fronts affect a zone of about 10 to 20 m for the fault network model, and of about 10 to 33 m for the single fault model at the end of the simulation.
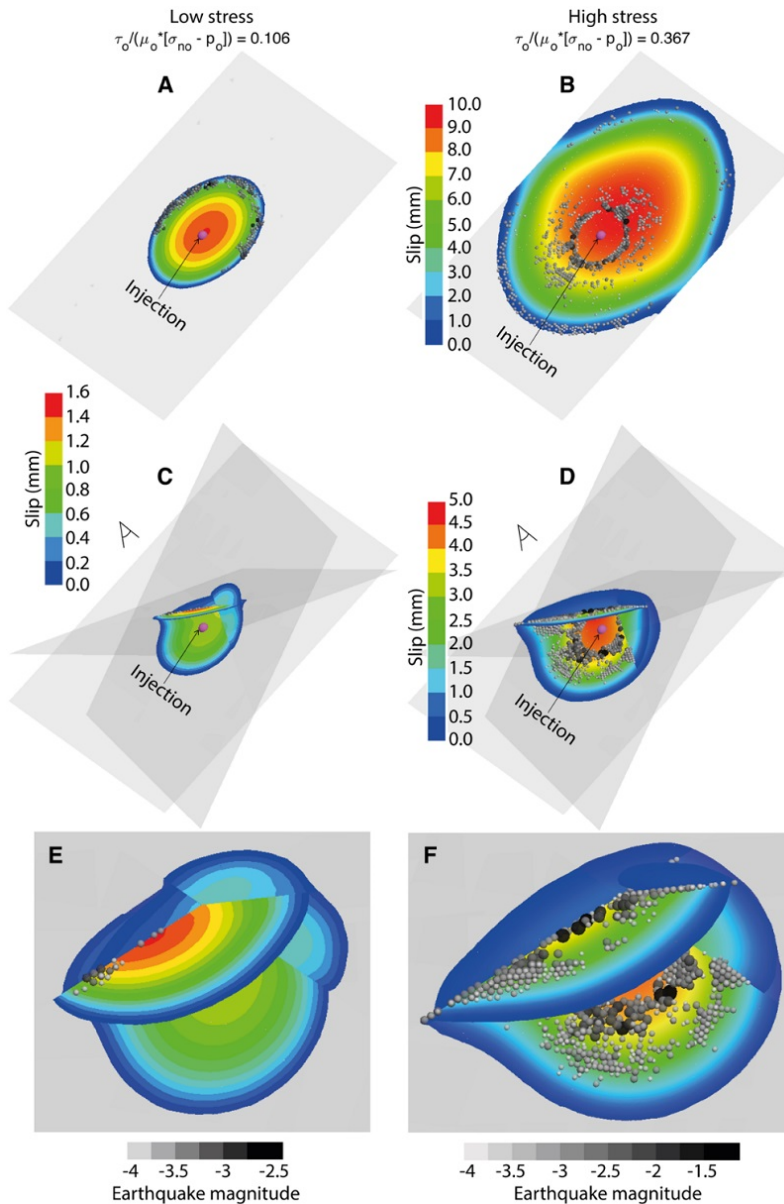
Figure 6.7-2. (a)(b): Spatial distribution of fault slip and seismicity at the end of injection for the single fault model; (c)(d): the fault network model; (c)(d): Close-up view of the fault network model with a different viewing angle (upper view). Left column represents the low stress conditions, and the right column--high stress. The sphere diameter is correlated to the size of events.
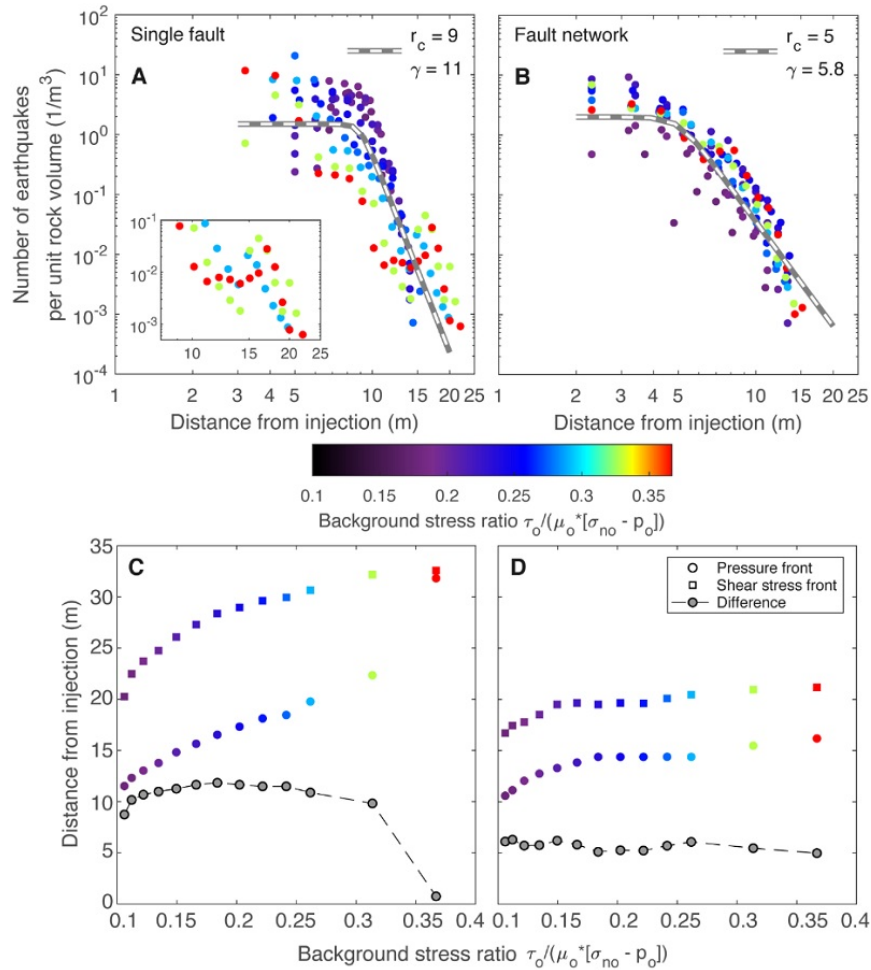
Figure 6.7-3. Number of earthquakes per unit rock volume as function of distance from injection for the model with (a) a single fault and (b) three faults. Position of the fronts of fluid pressure and shear stress at the end of injection for the model with (c) a single fault and (d) three faults. The difference between the shear and pressure fronts is plotted with the gray dot and the dashed line.

6.7.2.3. Conclusion

The 3D modeling study shows that the architecture of the fault zone, the initial state of stress, and the fault permeability evolution are affecting the fluid pressure diffusion, the growth of aseismic slip and the triggering and distribution of seismicity during fluid injection. Modeling results indicate that interaction of secondary fractures within the fault zone and the competition between fluid pressurization and stress transfer associated both to pressurization and co-seismic rupture are mechanisms affecting induced seismic events in low permeability host rock, and can cause multiple seismic ruptures together or separately at individual fault segments. The resulting induced seismic sequence exhibits a heterogeneous distribution in space and complex spatial-temporal characteristics. During fluid injection, the size and timing of pressurization and associated stress perturbation may vary significantly between faults zones.

Further studies of fault stability by means of controlled fluid injection experiments are needed to investigate the physical processes controlling the interplay between the fault network, frictional properties, stress perturbation and permeability evolution. The developed approach will be extended to analyze the seismicity induced during the FS-B experiment.

6.7.3. Long-Term Fault Behavior of Reactivated Faults

In May and June of 2019, prior to the controlled-release fault activation planned FS-B experiment at Mont Terri, the exhaustive multi-parameter monitoring network installed for FS-B captured significant pore pressure changes coupled to fault displacements triggered by ongoing excavation work for a new Mont Terri gallery. This unexpected hydromechanical response of a fault ~40 to 50 m away from an excavation, thus at distances significantly farther than a few tunnel diameters, is of crucial importance in assessing the long-term loss of faulted host rock integrity. This section presents a synthesis of measurements from a suite of six boreholes intersecting the fault (Rutqvist et al., 2021a). Each borehole is instrumented with a loop of single-mode fiber optic cable, grouted behind casing. The boreholes also contain separate strain (extensometer) and displacement (SIMFIP) sensors, co-located with the Distributed Optical Fiber System (DOFS), which allowed LBNL scientists to validate the Distributed Brillouin Strain Sensing (DSS) measurements.

6.7.3.1. Monitoring Setup for Long-Term Fault Behavior

Figure 6.7-4 illustrates the tunnel and fault geometry as well as the monitoring boreholes installed in 2018 to prepare for the 2020 FS-B fault reactivation experiment. The Mont Terri Main Fault consists of a thrust zone, 1 to 3 m in width, bounded by two major fault planes characterized by a strike of N066º to N075º and a dip of 45º to 65ºSE. A 70 x 70 x 70 m block, crosscut by the Main Fault, was instrumented with 23 boreholes hosting various monitoring systems recording pressure, flow rate into multiple injection intervals, active and passive-source seismicity, and geomechanical strain/displacement/tilt sensors. The monitoring system was installed between August and December 2018. Excavation of Gallery 18 began on March 14, 2018, and lasted for more than one year. In the first half of 2019, the excavation was completed. Excavation passed along the strike of the Main Fault at a distance of 23 m from the upper fault zone interface. The fiber optics DSS (Distributed Brillouin Strain Sensing) monitoring system detected the first fault movement in response to excavation on May 22, 2019, when the excavation front was 26 m from the SIMFIP. (The DSS concept is based on the following: a laser pulse is sent along the optical fiber, but some amount of light is scattered backwards, including three components relevant to Distributed Optical Fiber System (DOFS): one is elastic (Rayleigh), and two are inelastic (Raman and Brillouin). The Brillouin component arises from an incident photon's interaction with crystal lattice vibrations that holds some of the optical fiber's heat. As the interaction is inelastic, the backscattered light is frequency shifted by some amount that depends linearly on temperature and strain.) Breakthrough of the excavation into the existing tunnels occurred adjacent to monitored fault segment on May 27, 2019 (red color in Figure 6.7-4)

LBNL research focused on monitoring using instruments deployed in seven boreholes (BCS-D1 through BCS-D7) drilled through the Main Fault zone (Figure 6.7-4). A detailed description of the monitoring well setup is given in the report by Rutqvist et al. (2021a, Section 8). Boreholes BCS-D1 through BCS-D6 contain a single 3.2 mm-diameter loop of BRUsensTM strain sensing cable comprising a single optical fiber hermetically sealed and strain-locked within a metal tube and an outer nylon sheath. Continuous measurements were provided along the entire length of boreholes BCS-D3, D4, D5, and D6, using the fiber (BRUSens 3.2 mm V9 grip) cemented behind the PVC casing (green color in Figure 6.7-4). Fiber loops in each borehole are connected into a multi-borehole circuit and interrogated by an Omnisens DITEST temperature and strain unit, using the Brillouin Optical Time Domain Analysis technique (Horiguchi and Tateda, 1989). A chain of 12 potentiometers was cemented behind casing alongside the fiber-optic loop in borehole BCS-D5 (Zappone et al., 2020; Rinaldi et al., 2020). This chain of potentiometers provides co-located measurements of displacement with respect to the optical fibers, which is needed to directly verify the DSS measurements. In borehole BCS-D7, a combined 3D-displacement, pressure, fluid electrical conductivity probe and the SIMFIP (Guglielmi et al., 2019) were installed above and below the Main Fault. The clamps are 6.3 meters apart allowing the SIMFIP to measure the relative displacement across the entire Main Fault zone. The 3D fault displacement measurements were compared to the DSS data.
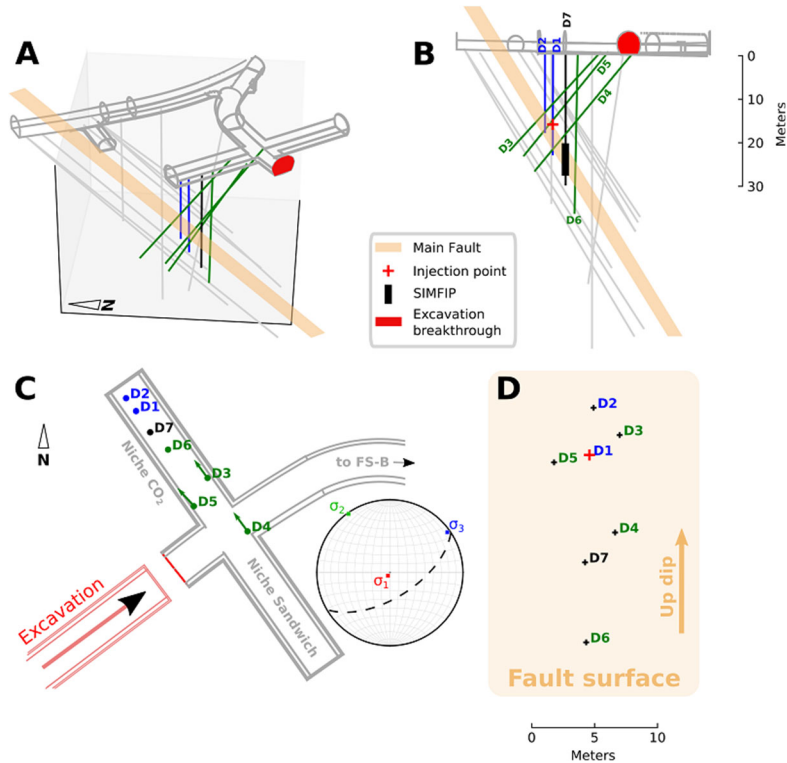
Figure 6.7-4. (a) 3D perspective of the FS-B/CS-D project layout. Boreholes D1 and D2 (blue color) are injection and pressure monitoring boreholes. Boreholes shown in green contain monitoring systems, and Borehole D7 (show in in black) contains the SIMFIP displacement sensor. Light gray symbols in the background indicate the FS-B boreholes. All boreholes are instrumented with distributed fiber optic sensors except D7. (b) Cross-section along Niche CO_2 with the injection point in D1 indicated by a red cross. (c) A map view of the borehole collar locations in Niche CO_2 and lower hemisphere stereonet projection of the principal stress axes estimated by Guglielmi et al. (2020). A dotted line shows the approximate orientation of the Main Fault (d) intersection points for each well with the top of the Main Fault.

6.7.3.2. Distribution of Deformation Induced by the Remote Gallery Excavation

6.7.3.2.1. Correlation of DSS Strains with Geological Features Observed in Boreholes

The results of DSS measurements in Figure 6.7-5 show that strains localize on some discrete fractures outside of the fault zone and at fault zone boundaries. The deformations in the excavation-damage zone near the tunnels are up to one order of magnitude larger than in deeper zones. Figure 6.7-5 illustrates the measured strains in the upper 7 m of each borehole. Boreholes D3 and D5 show contractions of >800 and 600 µE, respectively. In contrast, D4 and D6 show two smaller magnitude peaks of extensional strain, each 200 µE. The discrete spikes in the strain shown in Figure 6.7-5B suggest that deformations were probably concentrated on preexisting fractures intersecting the gallery and niches, and these strains resulted from complicated interactions between a new gallery and the existing galleries and niches. In Boreholes D3, D4, and D5, located off the Main Fault, deformations exceed 100 µE, which are comparable to and exceeding the strain measured within the Main Fault zone. Approximately 18% of the off-Main Fault fractures identified in core logs correspond to the features indicated by arrows in Figure 6.7-2A. Geological interpretation of the core classifies the deepest non-fault feature in BCS-D3 (16 m depth) as an interval of scaly clay layers. The single shallow feature in D4, as identified in OTV logs, corresponds to a single fracture striking of N052°, dipping SE69°. The 15–16 m depth interval in BCS-D5 is classified as a distinct fault zone, four meters above the Main Fault (strike N014–060°, dip 20–70°SE). The 8-meter anomaly in D5 corresponds to either 'bedding' or 'fracture planes' in the core (strikes N053–082°, dips 54–74°SE). Unfortunately, due to the 1-m spatial resolution, DSS anomalies cannot be assigned to any single feature where fracture density is >1 per meter. Figure 6.7-5C shows the strains measured within the Main Fault zone for all boreholes.
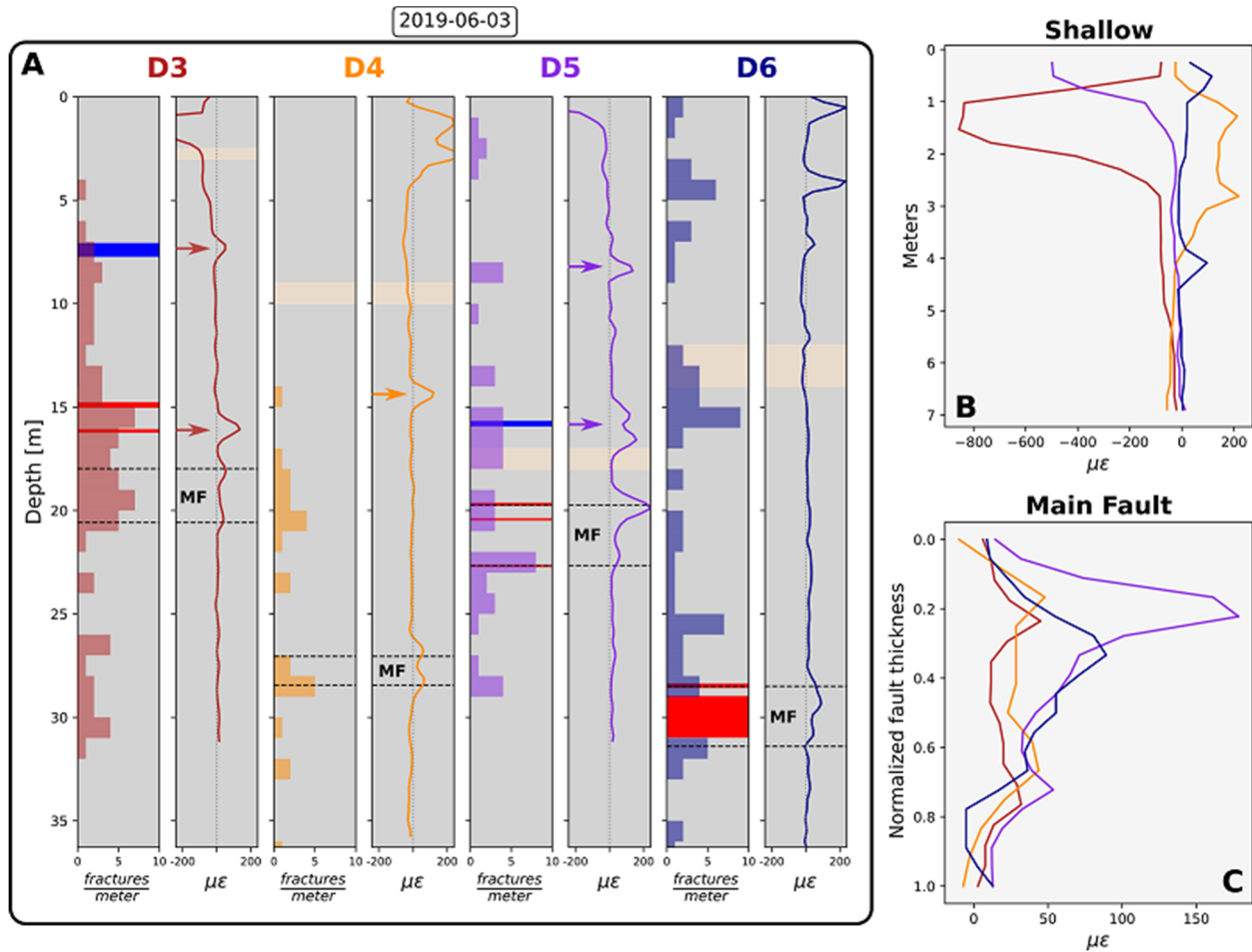
Figure 6.7-5. (a) Measured strain and fracture density estimated from core. Solid red lines indicate depths of scaly clay, blue color indicates a fracture zone. The fracture density in D4 was determined from optical televiewer logs. Resin plugs are in beige color, fault top and bottom are indicated by horizontal dotted lines. Arrows show above-fault features recorded on both the up and down-going fibers. (b) Strains for the upper 7 m of each borehole. (c) Strains within the fault zone for each borehole. Depths are normalized to the fault zone thickness in each borehole.

6.7.3.2.2. *Temporal Evolution of DSS Strains*

Figure 6.7-6A summarizes the Main Fault deformation with time as observed by DSS in Boreholes D3, D4, D5, and D6, and by the SIMFIP in D7. The DSS data are integrated across the Main Fault zone to better compare to the SIMFIP, which is measuring relative displacement across the entire zone. These data reveal two distinct modes of Main Fault activation: shear deformation before the excavation breakthrough, followed by opening-mode deformation after the breakthrough. When the excavation front is still at a distance from the sensors, the loading vector is oblique to the fault and results in mostly shear slip. At breakthrough, the force of the overburden removal is approximately normal to the fault, resulting in mostly fault opening. Figure 6.7-6Bb shows the evolution of displacement on the features above the Main Fault, with a pattern that is similar to that of the Main Fault zone.
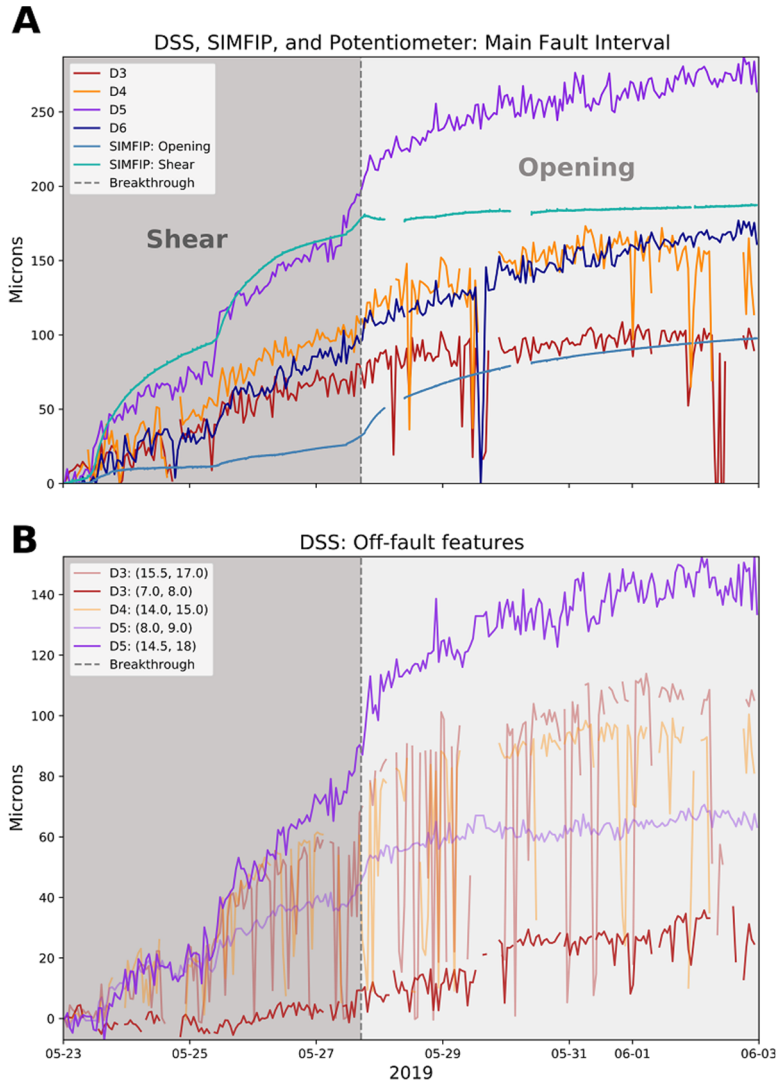
Figure 6.7-6. (a) Main Fault displacement throughout the excavation for all boreholes. DSS measurements have been integrated over the Main Fault depth interval, as identified by core and logging. The displacements measured by the SIMFIP have been decomposed into two components: one parallel to the Main Fault (green) and one normal to the fault (blue). (b) Displacement for each of the anomalies indicated with and arrow in Figure 6.7-5A. The legend indicates the depth range over which strain was integrated. The time of the breakthrough is identified with a vertical dotted line.

6.7.3.2.3. *DSS Strain Evolution Compared to the Orientation of the Excavation Front*

Figure 6.7-7 shows the observed 3D deformations on May 26, 2019, before the breakthrough, and on June 1, 2019, after breakthrough. The data analysis shows a clear negative gradient in fault zone displacement from left to right (SW to NE) and top to bottom (shallower to deeper), which is consistent with the orientation of the excavation front, approximately indicated by the red arrow. The black arrow is the projection of the SIMFIP displacement onto the fault plane for the preceding hour. This displacement represents an oblique reverse sense of shear across the fault zone, pointing in the direction of greatest strain perturbation, in good agreement with the deformation gradient. Once breakthrough occurs, little shear occurs. The Main Fault interfaces, defined by their logged depths, are figured in dotted gray. The peaks in the strain curves are not present at all boreholes suggesting the presence of local reactivation of the bedding planes. The strain on the Main Fault (whose orientation and depth are well constrained) was observed in all boreholes.
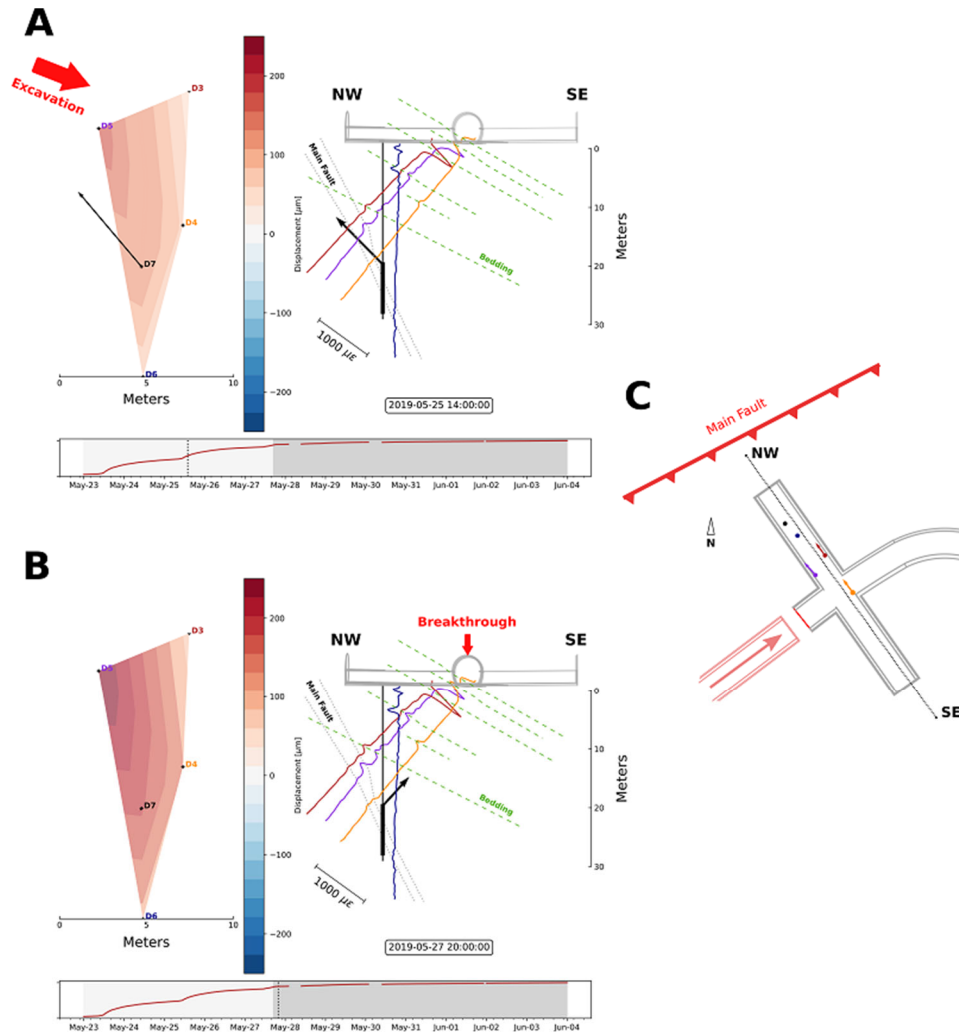
Figure 6.7-7. (a) Deformation before the excavation breakthrough on May 26, 2019, and (b) after the excavation on June 1, 2019. The left columns show displacement along the fault plane, linearly interpolated between boreholes. (c) Layout of Niche CO_2 showing the excavated gallery, Main Fault, and boreholes.

6.7.3.2.4. *Features Controlling Fault Strain Tens of Meters Away from the Excavation Front*

Effect of the Main Fault Architecture

The DSS measurements indicate that the two Main Fault zone interfaces accommodate most of the fault slip related to the gallery excavation, with no single, central slip surface. This is particularly evident in the inclined boreholes D3, D4, and D5. In all cases, strain declines quickly away from the fault interfaces, suggesting that a damage zone was not developed and no gradient of deformation from the principal slip zone towards the intact host rock was observed.

Fault zones are commonly conceptualized as a fault core, where the majority of the slip concentrates, and a surrounding damage zone that accommodates progressively less slip with distance from the core (Caine et al., 1996; Shipton and Cowie, 2003). The Main Fault, however, has a different architecture, with a thick, heterogeneous layer bounded by two weak interfaces. SIMFIP measurements from a previous experiment at the Mont Terri URL indicate that the fault zone's Young's modulus is 2 to 5 times less than that of the host rock (Jeanne et al., 2017). Thus, the Main Fault can be treated as a thick layer with weak boundaries and no surrounding damage zone, shown in Figure 6.7-8.
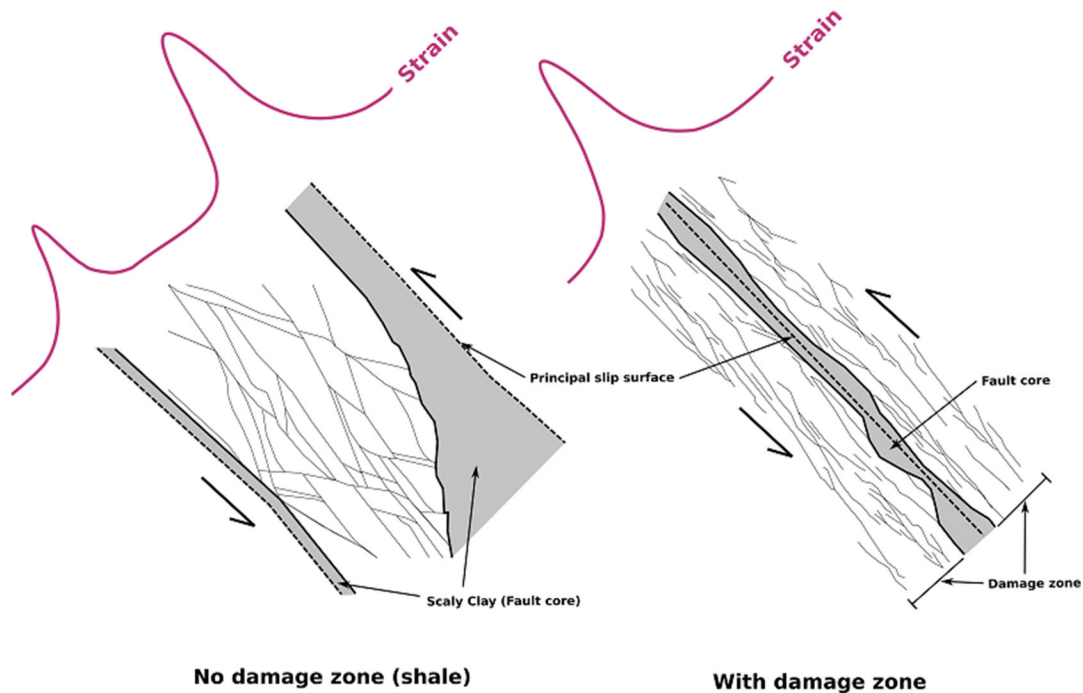
Figure 6.7-8. Schematic representations of the Main Fault: left--the canonical fault zone model (adapted from Jaeggi et al., 2017), and right -- the relationship between fault core/gouge, principal slip surfaces, and the 'fault damage' zone (adapted from Shipton and Cowie, 2003). Theoretical DSS measurements are shown in purple for slip on either type of fault.

Effects of Stress Versus Intrinsic Mechanical Properties

In many cases, the strain that accumulated on secondary (i.e., non-Main Fault) fractures exceeded that of the Main Fault interfaces. For example, the 16-m anomaly in D3 displays nearly twice the displacement of the top or bottom interfaces of the Main Fault. In addition, the anomalies in D4 and D5 display similar deformation magnitudes to the Main Fault zone. Although a number of these secondary structures were activated, the vast majority of those identified in logs were not. For a given fracture, activation is controlled by its orientation in the local stress state and its intrinsic properties, i.e., cohesion, coefficient of friction (Handin, 1969; Freed, 2005), but identifying which will activate for given stress perturbation is difficult.

To investigate what distinguished the active fractures from the non-active ones, all OTV-picked fractures were grouped into three groups: fractures inside the fault zone, active fractures outside the fault zone, and inactive fractures outside the fault zone. Figure 6.7-9 shows each plane identified in the BCS-D4, -D5, and -D6 optical televiewer logs colored by slip tendency (increasing from blue to red) when subjected to the stress field (Guglielmi et al., 2020b). Wenning et al. (2020) showed that the Main Fault zone includes a variety of fracture sets of varying orientations, including fault-zone parallel fractures and WNW-dipping fractures, which are the most prone to slip of any of the identified features (red color in Figure 6.7-9). However, slip localized on the upper and lower fault zone interfaces, which are further from failure in the *in-situ* stress conditions (dashed black lines and adjacent green lines in Figure 6.7-9).

Characterization of the core indicates that most of the activated structures are associated with either (1) a lens of scaly clay, consisting of shear-realigned grains, or (2) highly fractured zones where core was either lost or fragmented. It is possible that the fractured zones contain small amount of scaly clay that was not recovered during coring. The presence of scaly clay can be considered one of the main factors affecting the fracture weakness. At the Mont Terri URL, scaly clay may have developed on both bedding parallel secondary faults and on the Main Fault-parallel structures, despite their somewhat distinct orientations. This makes both sets of features susceptible to reactivation and fluid flow within the Opalinus Clay.

232
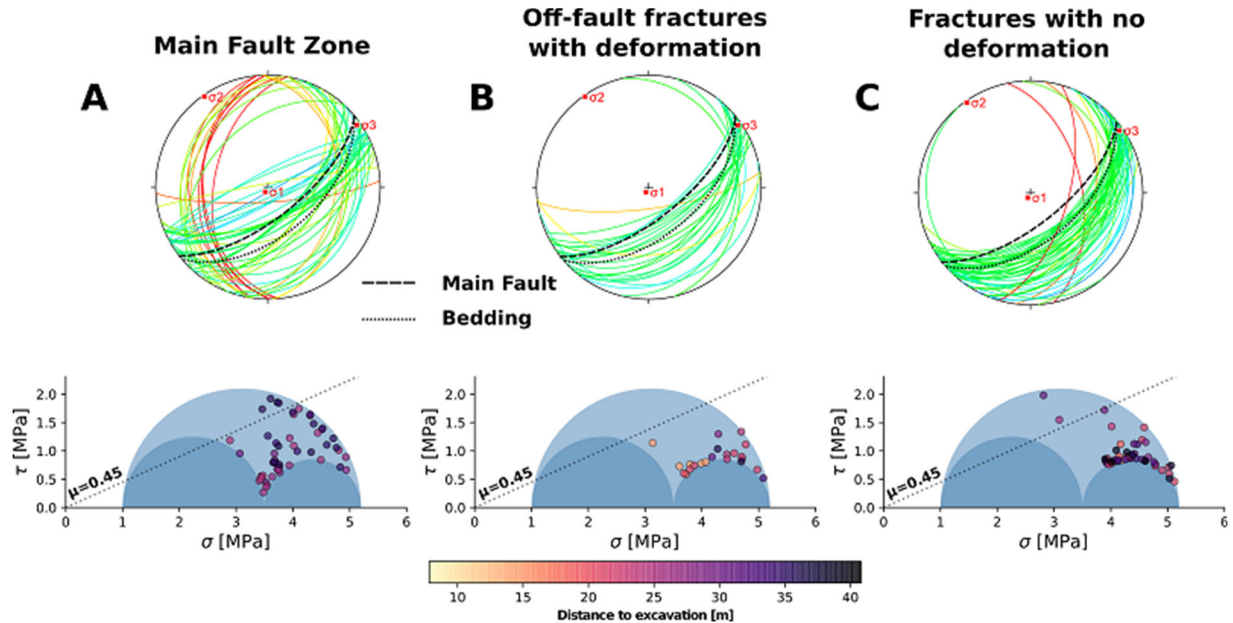
Figure 6.7-9. Fractures identified in optical televiewer logs in BCS-D4, D5, and D6: (a) Within the Main Fault zone, (b) outside of the Main Fault, but displaying deformation on DSS, and (c) All other fractures. The upper plots are lower hemisphere projections of poles and planes, colored by slip tendency in the local stress regime (blue = low, red = high tendency). Dotted line shows the orientation of bedding at the Mont Terri URL, the dashed line shows the approximate orientation of the Main Fault. The lower row plots show the state of stress on each fracture relative to a Mohr Coulomb failure envelope for cohesionless fractures. The color of each dot corresponds to the distance from the feature to the excavation front (light = closer, dark = farther).

6.7.3.3. Conclusions

During the excavation of the gallery, located about 30 m away from the instrumented boreholes, strains ranging from 50 to 240 µE were measured mainly at the top and bottom of the fault zone. Outside of the EDZ, the DSS measurements show that deformation in the rock mass has been localized on several discrete fractures identified in core and logs. No strain gradient was observed from the excavation front showing a strongly anisotropic response of the shale formation. Within the Main Fault, deformation concentrated on the upper and lower fault zone interfaces, with relatively little deformation occurring inside the fault zone. Core samples revealed zones of fault gouge on these interfaces, indicating past episodes of slip and present-day mechanical weakness. The DSS measurements support a fault model consisting of a single, thick fault zone with no surrounding damage zone. Slip occurs at both interfaces between the fault zone and the undisturbed host rock, possibly due to bulk deformation of the relatively compliant fault zone geology. Since there is no fault damage zone, there is no strain gradient developing from the main slip zone. This is in contrast to the canonical fault model for harder rocks where most slip occurs on a central fault core, while a strain gradient extends away from the core within the surrounding fault damage zone. Outside the fault zone, deformation concentrated at depths associated with lenses of scaly clay or highly-fractured intervals, likely on bedding parallel fractures. Most fractures identified in OTV logs were not reactivated, despite nearly all having a similar orientation. Therefore, the fracture reactivation during the excavation was controlled by the intrinsic properties of the fractures, likely the presence or absence of scaly clay and fault gouge resulting in a low-cohesion, low-friction surface. Identifying these signs of past slip and weakness in the drilling core could be a means for predicting prime structures for activation during future experiments.

6.7.4. Continuous Active-Source Seismic Monitoring of the Loss of Integrity Induced by the FS-B Fault Reactivation

The FS-B experiment at Mont Terri aims at imaging long-term fluid flow, permeability and stress variations through a ruptured minor fault to assess the performance of radioactive waste repositories in shale formations (Section 3.1.3). The first of several fault stimulations planned in this new larger fault testbed took place on November 21, 2020. Injection was conducted in a borehole at 40.4 m depth below the Mont Terri galleries, through a 1 m long interval set across the top of the Main Fault zone (Figure 6.7-10). Six consecutive injections were performed at constant flowrates of 2 l/min (Injection 1), 6 l/min (Injection 2), 9.8 l/min (Injection 3), 9.94 l/min (Injection 4), 9.55 l/min (Injection 5) and 10 l/min (Injection 6). The first five injections lasted 10 minutes. Injection 6 was conducted for 20 minutes. The injection interval was shut-in for some time between the injections. The fault hydraulically opened when injection pressure was between 5 and 6 MPa. At some point during the injection cycles, when the cumulated injected volume reached 178 liters, a hydraulic connection was established between the injection and a monitoring borehole in Gallery 2008, a distance of 15 to 18 m away along the strike of the fault. No clear hydraulic connection was observed in boreholes intersecting the fault in the nearby CS-D niche, located 8 to 10 m up-dip from the injection point. These results show an apparent heterogeneity in the fault leakage behavior, with preferential flow initiated parallel to the fault strike where leakage of about 26% of the injected flowrate was measured. Ten times smaller signals were observed in the CS-D zone, indicating this zone deformed during the stimulation, but was not hydraulically connected.
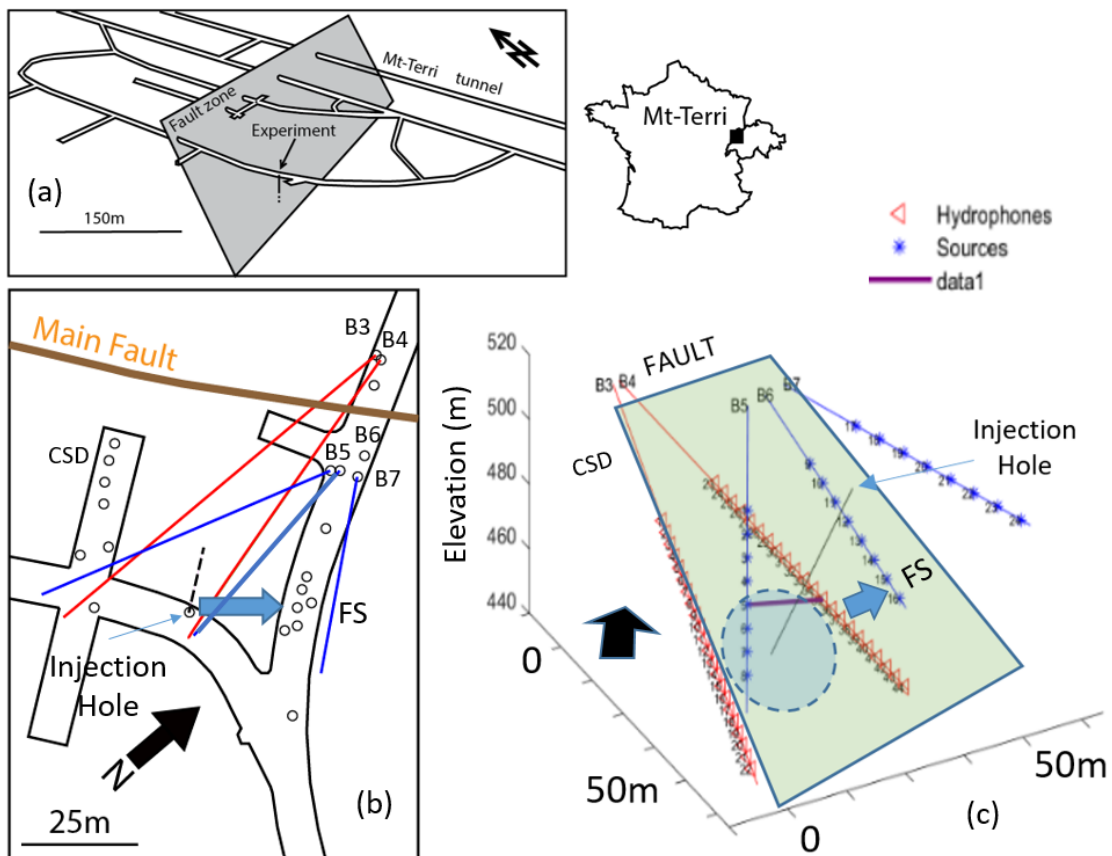
Figure 6.7-10. Continuous Active-Source Seismic Monitoring (CASSM) geometry surrounding the main fault of Mont Terri: (a) Experiment location in the Mont Terri underground laboratory. (b) Map view of the FS-B experiment (circles indicate vertical boreholes crosscutting the fault). Colored lines are the inclined boreholes instrumented with CASSM. Blue arrow shows the hydraulic connection between injector and monitor during the experiment. (c) 3D view of the CASSM setting (fault is simplified as the green plane). The receiver boreholes, B3, B4, are in the footwall and the source boreholes, B5, B6, B7, are in the hanging wall. The Dinjection borehole is 30-40° inclined with the fault plane.

Preliminary results of the time-lapse seismic imaging (CASSM = Continuous Active-Source Seismic Monitoring) conducted during the FS-B experiment are presented below. Although processing of the data is ongoing, first results confirm that changes in p-wave velocities across the fault are measurable, and that such changes correlated to changes in effective stress and deformations induced during and after the injection. The seismic imaging confirms that the leakage volume is local within the fault zone. Instantaneous changes in the seismic signals relate to fracture opening while delayed changes might highlight some irreversible shear damage following activation.

The CASSM technology (Daley et al., 2007; Silver et al., 2007; Marchesini et al., 2017) is based on monitoring using a large array of instruments including DAS-DTS-DSS fibers, pressure and 3D fault displacement sensors, tiltmeters, passive acoustic and seismic sensors. The CASSM system includes five dedicated monitoring wells straddling the fault from above and below (Figure 6.7-10). The acquisition process cycles through all sources to generate a single CASSM epoch. An example of a source-gather is shown in Figure 6.7-11. The time to complete each full sequence is about 8 minutes, which is the temporal resolution of this system.
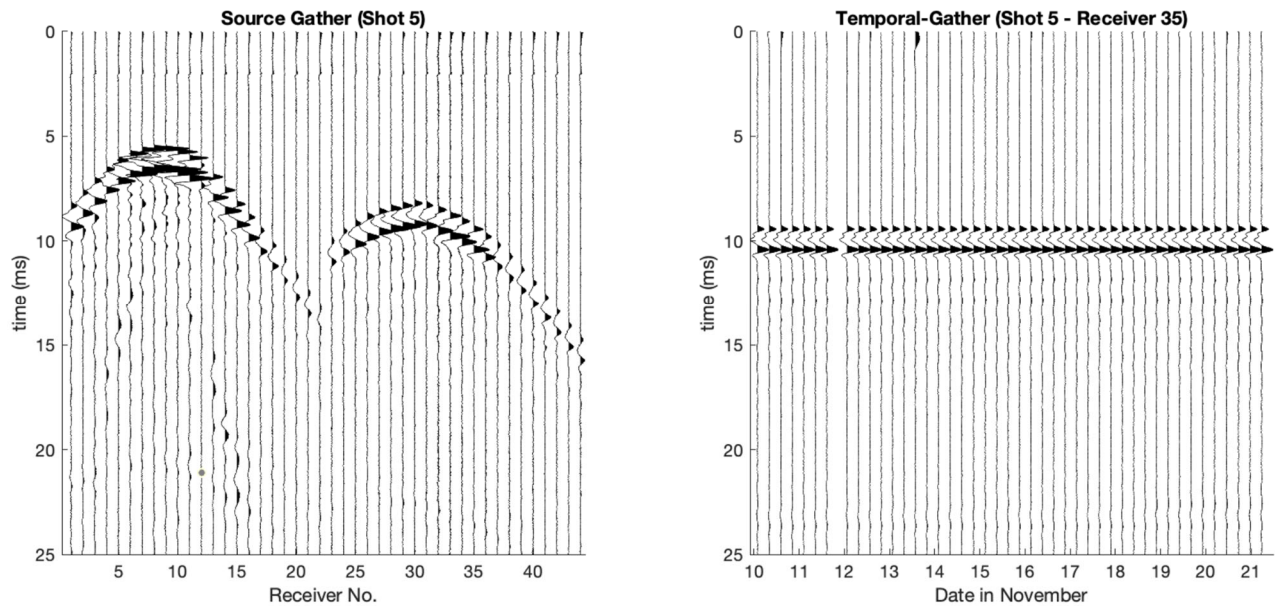
Figure 6.7-11. (a) An example of a source-gather for shot 5 (located in B4) at the beginning of November 10th, 2020. Receiver numbers 1-22 and 23-44 correspond to boreholes B3 and B4. (b) An example of a temporal-gather prior to injections for shot 5 and receiver 35.

The system provided information about background noise prior to the injections. It is important to measure the velocity change rather than absolute velocity, because the difference in travel time along fixed ray paths is the primary measurable. Temporal gathers are used to determine changes in waveforms as a function of time for a single source-receiver pair (Figure 6.7-12B). To evaluate the precision of the CASSM system, the values of the delay time δt were calculated for epochs prior to the injections between November 10th and November 21st, 2020). The results shown in Figure 6.7-12 reveal that the CASSM system is stable, and the standard deviation of the delay time is 895 ns, close to previous estimates of a similar system (Silver et al., 2007).
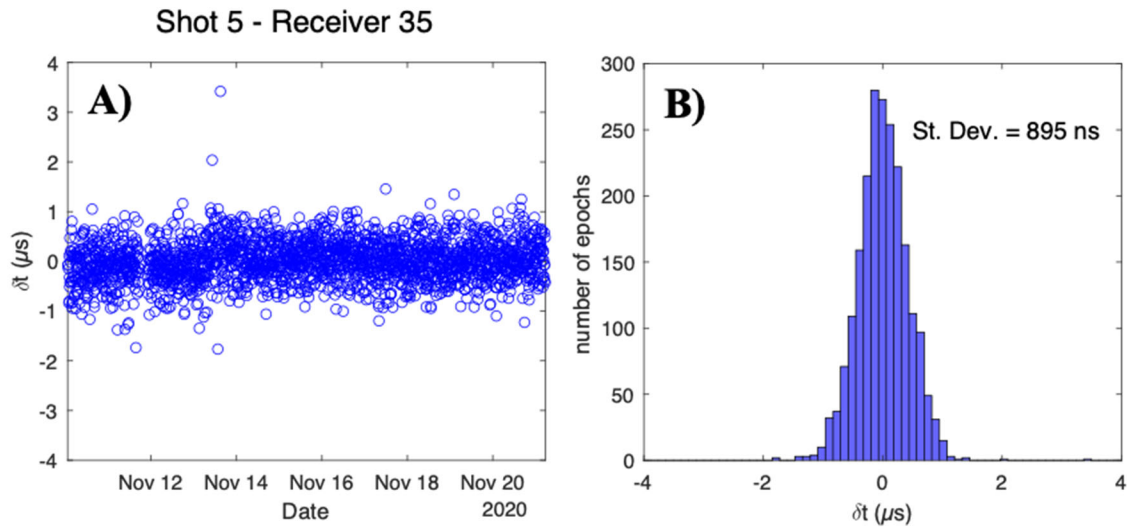
Figure 6.7-12. (a) Plot of δt for a single source-receiver pair (5/35) between the dates of November 10th and November 21st (prior to injections). (b) The corresponding histogram, showing the delay time standard deviation of 895 ns, which confirms the stability of the CASSM system.

An example of a δt curve for a source-receiver pair is shown in Figure 6.7-13. Also plotted is the injection pressure during the experiment. From this curve, Injections 2 through 6 show clear signals with δt values ranging from 8 to 15 μs. The first injection was not detected by any source-receiver pair, likely due to the small injection volume. Travel time variations almost instantaneously follow the injection pressure variations, decreasing when pressure increases and increasing when the injection is shut-in. After the last injection, the delays do not return to background noise, suggesting that a long-term change in the fault occurred. The "instantaneous" variations in delay time with injection pressure can be related to mechanical opening and closing of compliant fractures within the fault zone. A decrease in P-wave velocity (increase in delay time) as a function of injection pressure is consistent with laboratory data showing similar reductions as a function of decreased normal stress (e.g., Pyrak-Nolte et al., 1990). Likewise, similar signatures are observed during hydraulic fracturing operations, albeit at lower accuracies in the context of time-lapse VSP studies (e.g., Binder et al., 2018; 2020). The apparent long-term change in travel times match the irreversible fault deformations recorded on the strain monitoring array. It might relate to fault zone shear-induced damage or to delayed leakage of the injected fluid volume in this low permeability clay fault environment.

In addition to the δt response, the LBNL processing team calculated the percent change in RMS amplitude and centroid frequency during the same period for the source-receiver pair, 5 and 35, respectively (Figure 6.7-14). Changes in RMS amplitude were measured during the last four brine injections, while changes in centroid frequency occurred during the last five brine injections. While the amplitude and centroid estimates have higher noise levels than our phase delay measurements, they are consistent and suggest that P-wave attenuation is increasing as a function of injection pressure.
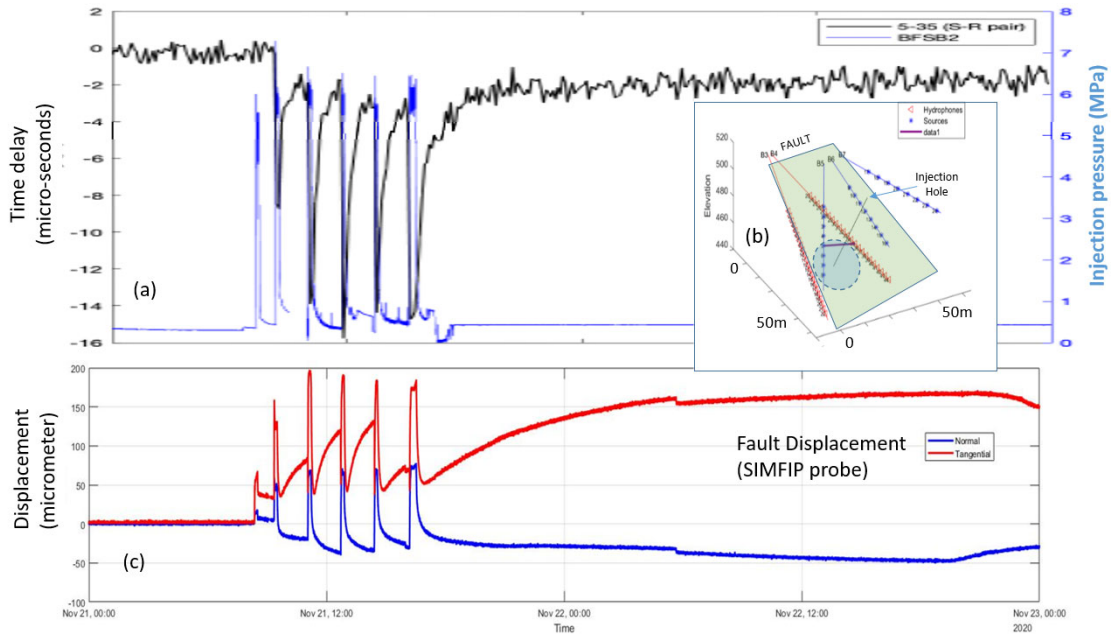
Figure 6.7-13. Variations of p-waves time delay related to injection pressure and fault movements (November 2020 FS-B fault activation experiment). (a) p-waves time delay (black) and injection pressure (blue); (b) Location of the seismic ray path considered in figure a (blue dashed circle figures the pressurized fault zone); (c) Fault tangential (red) and opening (blue) displacement measured at the injection borehole.
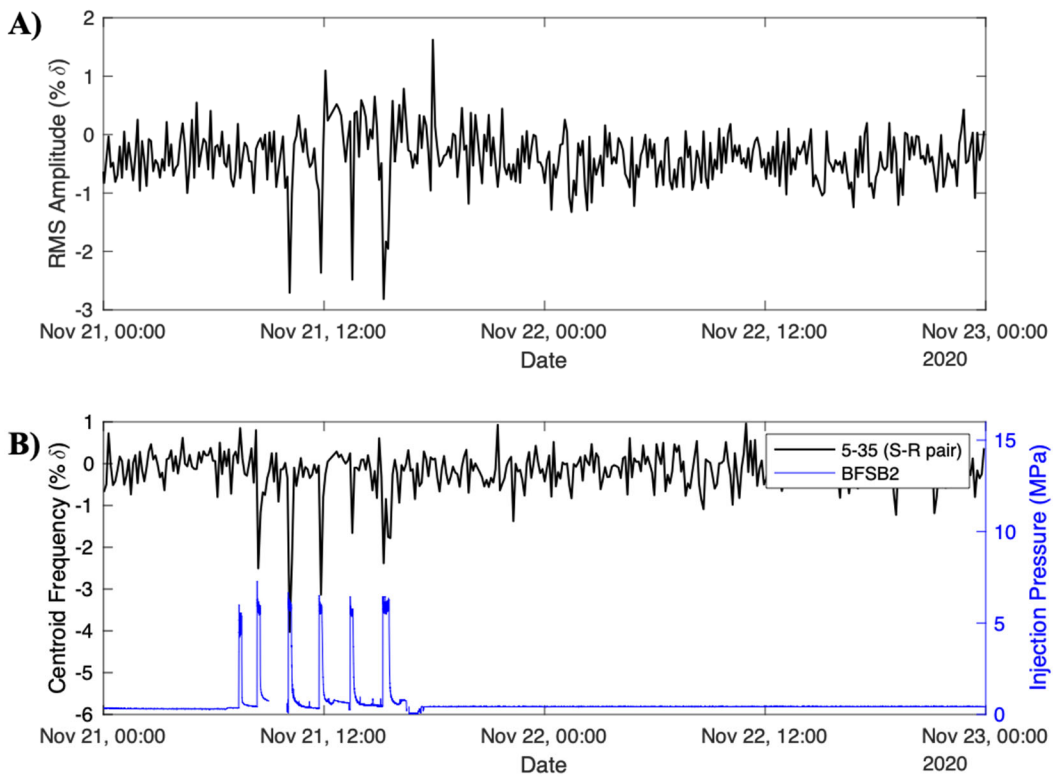
Figure 6.7-14. (a) Percent change (%δ) in RMS amplitude, and (b) percent change in centroid frequency for source-receiver pair 5/35 with injection pressure (blue).

The CASSM approach was successfully used to detect the injection and movement of fluids in the Mont Terri Main Fault and its subsequent reactivation. These processes were detected by small changes in P-wave travel time (i.e., 8 to 15 µs) as well as amplitude reductions and a decrease in first arrival centroid frequency. A small number of receivers were able to detect the injections suggesting that the fault activated patch was localized. Further tomographic imaging will be conducted to determine the size of this patch and the temporal dynamics of fault healing.

6.7.5. Summary and Directions for Future Fault Research

Activations of the Mont Terri fault zones are characterized by a high strain localization at the fault zone "boundaries." These faults evidently display a reduced fracture damage zone, and a thick highly deformable and heterogeneous core "layer" with abrupt contact with the surrounding intact rock. The result is that deformation and leakage may be "contained" within the "layer," with the possibility for preferential slip at the layer's interface. Second order fracture interactions within the fault zone and the fact that leakage relates to rupture favor local stress concentrations at fracture intersections. This may reduce the possibility for a large stress change at rupture, limit the number and magnitude of seismic events, favor aseismic movements and local fluid channeling, and potentially slow potential post-activation sealing processes (because of high dilation eventually occurring at fracture intersections).

Future research will include continued processing of the rich data set from the most recent 2020 experiment at Mont Terri (FS-B). The LBNL team will use the time-lapse p-waves tomographic images to further explore the intricate relationships between aseismic flow paths and seismic volumes within a thick fault zone. The velocity images will be analyzed using a 3DEC fully coupled hydromechanical model in terms of leakage and ruptured areas. Numerical modeling will be conducted to explore the effects of different fault zone complexity on induced seismicity, and to compare with measured seismic events and strains (DSS, DAS and SIMFIP) from the experiment. Results from these monitoring and modeling efforts will be used to inform PA investigations for repositories in clay host rock.

6.8. Field-Scale Characterization of Fractures in Crystalline Rock

6.8.1. Introduction

Low-permeability crystalline rocks have long been considered an important geologic environment for long-term disposal of nuclear waste (e.g., Witherspoon et al., 1981; Bredehoeft and Maini, 1981). However, a key concern relating to this geologic disposal option is the presence of hydraulically conductive fractures that could serve as pathways for rapid transport of radionuclides in the subsurface (Cherry et al., 2014). The 2020 SFWST Disposal Research 5-Year Plan (Sassani et al., 2020) and its 2021 update (Sassani et al., 2021) identified that improved geophysical, geochemical, geomechanical and hydrological techniques for site characterization are needed for crystalline repository systems, especially to characterize fractures and their hydrogeologic properties. These provide important input for the development of better constrained discrete fracture network (DFN) models (e.g., Follin et al., 2014; Hadgu et al., 2017).

This section summarizes international field-based collaboration activities to better understand how flow and transport evolve in initially low permeability fractures in crystalline rocks under fluid pressure or stress variations, including the effects of normal deformation, shear displacement, dilation, and propagation. Though a number of modeling, laboratory and field investigations have been conducted across many international programs, there is a lack of data on coupled hydromechanical and chemical processes, particularly at kilometer-scale depths relevant for the design and safety assessment of nuclear waste repositories. Therefore, over the past seven years, LBNL has been engaged in a research cooperation with the "Collisional Orogeny in the Scandinavian Caledonides" (COSC) project, a deep drilling project in Sweden in Sweden (Section 4.3). Investigations were conducted using the COSC-1 borehole as a testbed to characterize and evaluate the H-M processes in a crystalline basement environment. Section 6.8.2 provides a description of LBNL's FY21 efforts on field characterization of transmissive fractures in crystalline rocks as part of the COSC collaboration (Guglielmi et al., 2021, Sections 3.1-3.5). Section 6.8.3 summarizes the results of laboratory studies to establish a correlation between flowing fracture zones in the field and their characteristics as measured in respective core samples (Guglielmi et al., 2021, Section 3.6), and Section 6.8.4 describes the development of a new numerical model to reproduce the results of previously conducted fracture-flow laboratory experiments (Guglielmi et al., 2021, Section 3.7).

6.8.2. Characterization of Transmissive Fractures in Crystalline Rocks: Field Testing Campaign and Interpretation

6.8.2.1. Introduction

LBNL has been collaborating with the COSC scientific team to use the COSC-1 borehole, located in central Sweden (Figure 6.8-1), as a testbed to evaluate fracture transmissivity within a crystalline basement environment. The borehole was drilled to a depth of 2.5 km, and encountered a sequence of high-grade metamorphic rocks, such as felsic gneisses, amphibolite gneisses, calc-silicate gneisses, amphibolite, migmatites, and garnet mica schists, with discrete zones of mylonite and microkarst (Lorenz et al., 2015). Analysis of localized borehole failures such as breakouts and drilling-induced tensile fractures (DITF) showed an average maximum horizontal stress, SHmax, with an orientation of 127°±12°, in agreement with the general trend in Scandinavia (Figure 6.8-1b). This study highlighted the scarcity of breakouts and DITF, and their absence in the uppermost 600 meters of the borehole, concluding that this is due to the elastically stiff and high strength metamorphic rocks, an assumption that is often considered in the estimation of stress tensor magnitudes in continental-crustal areas such as the Fennoscandian Shield.

LBNL's initial work focused on logging using the Flowing Fluid Electrical Conductivity (FFEC) tool to identify hydrologically transmissive fractures in the COSC-1 borehole (Tsang et al., 2016; Doughty et al., 2017), and linking these fractures to potential flow zones. A new comprehensive field campaign was conducted in the summer of 2019. This time, the LBNL team deployed the Step-rate Injection Method for Fracture *In-situ* Properties (SIMFIP) tool (Guglielmi et al., 2015), shown in Figures 6.8-1c and d, to test the hydromechanical behavior of a suite of selected fractures within the COSC-1 borehole. Based on the results of

the 2019 field study (Guglielmi et al., 2020), LBNL identified three representative intervals within the borehole for further analysis and interpretation (Figure 6.8-2): (1) an unfractured interval located at a depth of 485.2 m (Case 1), (2) a gently dipping transmissive fracture at a depth of ~504.5 m that is subparallel to foliation (Case 2); and (3) a steeply dipping cemented fracture located at a depth of ~515.1 m (Case 3).
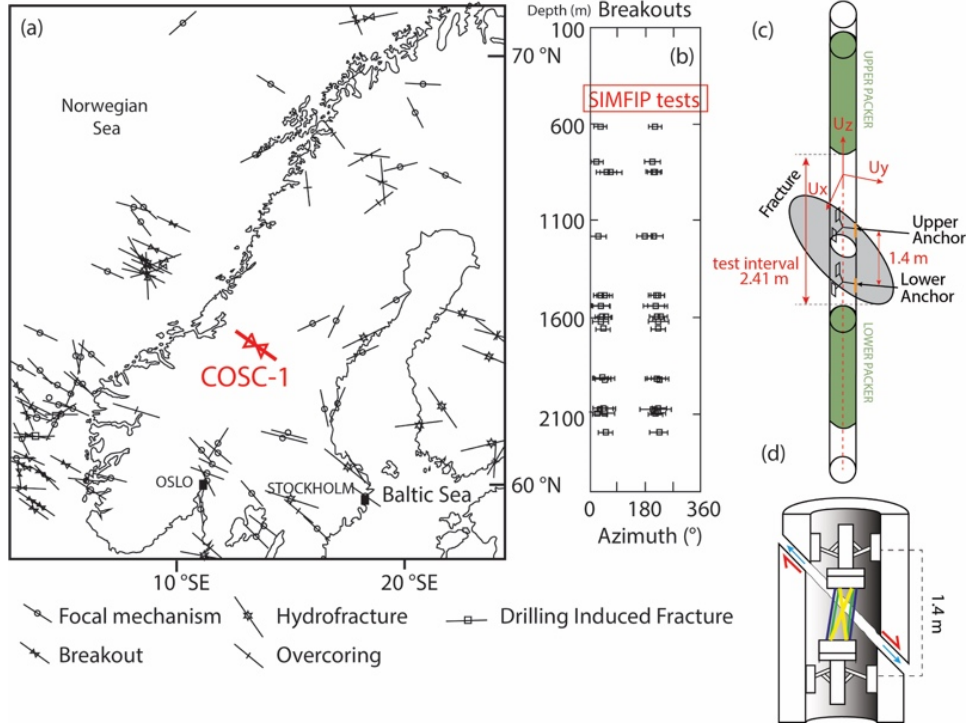
Figure 6.8-1. (a) Location of the COSC-1 borehole on the stress map of Fennoscandinavia (stress indicators from the World Stress Map after Heidbach et al., 2010), (b) Schematic location of the SIMFIP tests along the vertical profile of the COSC-1 borehole with the log of breakouts mapped by Wenning et al. (2017), (c) Schematic of the SIMFIP probe deployed at COSC-1, and (d) Schematic of the SIMFIP cage.
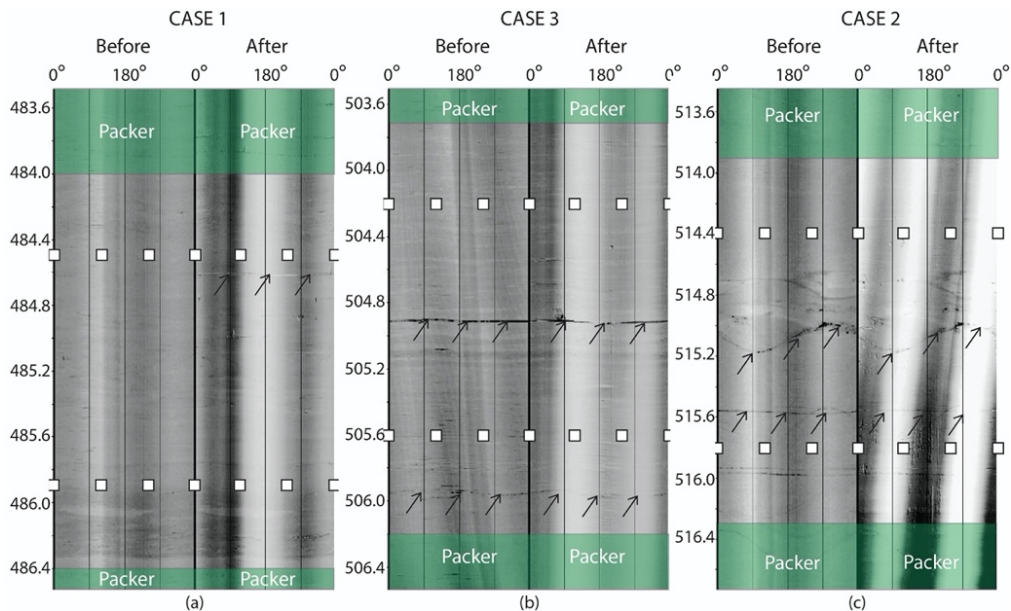
Figure 6.8-2. Acoustic images of the geological logs: (a) – Case 1, (b) –Case 3, (c) – Case 2; white squares are the locations of the SIMFIP sensor's clamps; black arrows show the main geological structures of the fractured intervals.

In FY20, LBNL used the SIMFIP data to evaluate continuous measurements of displacements oriented in geographical coordinates - East, North, and vertical upward (Guglielmi et al., 2020), and conducted three types of analyses of the SIMFIP measurements:

- Identification of the activated fractures and their activation modes,

- Full stress tensor estimation (orientation and magnitude), and

- Preliminary analysis of the effects of fracture properties on injection test pressure and displacement measurements using 3D fully coupled forward numerical modeling.

In FY21, the LBNL team continued its analysis and interpretation of the COSC-1 SIMFIP data, including a detailed interpretation of the observed fracture displacements during stimulation (Section 6.8.2.2), an evaluation of stress perturbations and their impact on fracture aperture at the borehole scale (Section 6.8.2.3), and finally a study on stress perturbations and their impact on fracture flow at the network scale (Section 6.8.2.4). This work is described in detail in Guglielmi et al. (2021) and summarized below.

6.8.2.2. In-situ Fracture Activation Displacements

The LBNL team first conducted a comparison of new televiewer data from the COSC-1 borehole conducted after the stimulation with the pre-stimulation images to identify which fractures appeared to have undergone stimulation within each of the tested intervals.

- Case 1 – An interval of intact rock between 484 m and 486.4 m depths was selected from the acoustic image log (Figure 6.8-2a). The core observations showed two flat-lying fractures at 484.9 m and 486.2 m, with orientations roughly 247°/13°. These fractures appear to be sub-parallel to foliation: one is between the SIMFIP clamps, and the other is below the lower clamp. Comparison of the acoustic image logs before and after the tests shows that a new flat-lying fracture parallel to foliation might have been created at 484.5 m, which is distinct from the "pre-existing" fractures seen on cores.

- Case 2 – Initially closed fractures between 513.9 m and 516.3 m depths (Figure 6.8-2c). FFEC logging showed no flow in this interval (Doughty et al., 2017). This interval is defined as a zone with initially closed (non-flowing) fractures, with one feature parallel to foliation (260-280/2-13) and the other representing a steeply dipping mineralized fracture (110/59). No new fractures were identified after the tests, suggesting that the preexisting ones were reactivated. However, this interval started leaking at a very low pressure, indicating that some fractures might not be initially closed.

- Case 3 – Initially flowing fractures between 503.7 m and 506.2 m depths (Figure 6.8-2b). FFEC logging showed flowing fractures at 504.9 m and 505.9 m depths (Doughty et al., 2017), with flow emanating from multiple entries within this region. The fractures are relatively flat, more or less parallel to the foliation with dip direction and dip of 281/5 to 288/12, respectively. No new fractures were seen in the televiewer images after the tests.

Second, the team analyzed how the fracture displacements evolved during the entire series of stimulation cycles conducted with the SIMFIP probe. Figure 6.8-3a shows that fracturing of the intact rock interval (Case 1) appeared in four successive leak-off tests from 10:47 to 11:46 on June 18, 2019. During the leak-off tests, the injection flowrate was kept constant. During cycles, borehole displacements showed a variation correlated to the injection chamber pressure increase up to a peak value (Figure 6.8-3b). At the peak, a new fracture was created in the interval. The analysis shows that the fracture first activated in a pure opening mode (Mode 1), then started shearing and growing away from the borehole, while the injected fluid volume was increasing.

The initially closed fractures (Case 2) were stimulated by applying two cycles of increasing pressure steps (Cycles 0 and 1 in Figure 6.8-4) until a clear hydraulic opening was observed, characterized by a pressure transient decay at these steps. Then, a constant flowrate step cycle was applied (Cycle 2). Note that pressure transients initiated at 8 MPa, which was only 3.5 MPa above the borehole fluid pressure (Figure 6.8-4a). This could mean that the fractures of this interval were not initially fully closed. When pressure was elevated

241

significantly above 8 MPa (Cycle 1), pressure dropped faster. The pressure drop was associated with a significant vertical displacement (Figure 6.8-4b). At the end of the test, there was a limited residual displacement.
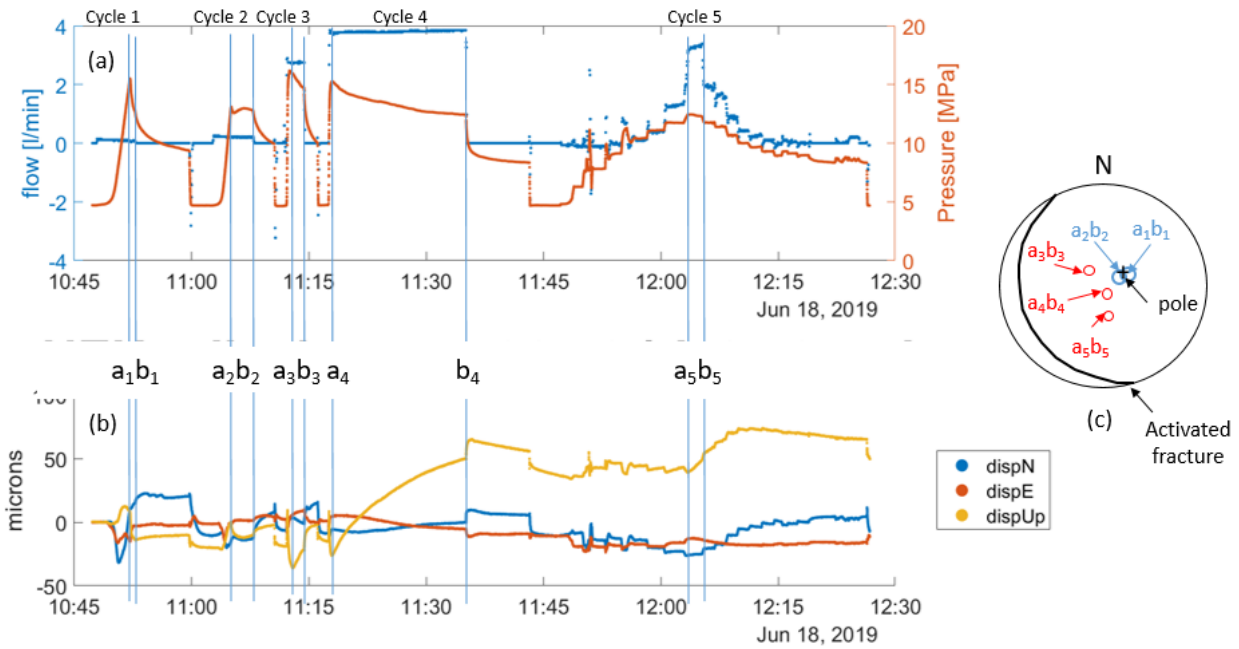
Figure 6.8-3. Hydromechanical response of the tested interval for Case 1: (a) Pressure-flowrate variations vs time; (b) SIMFIP upper anchor displacement vs time; and (c) Stereographic projection of borehole displacement vectors a_1b_1 to a_5b_5 during fracture activation and growth periods.
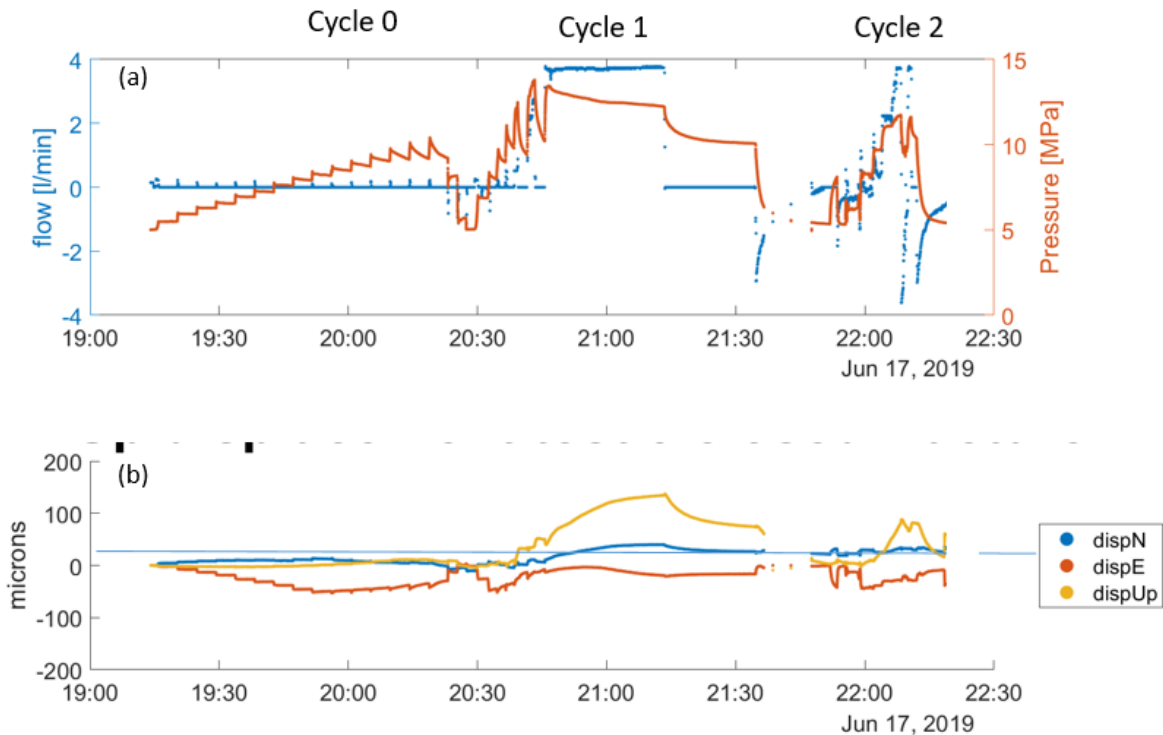
Figure 6.8-4. Hydromechanical response of tested interval for Case 2: (a) Pressure-flowrate variations vs time; and (b) SIMFIP upper anchor displacement vs time.

Activation of the initially flowing fracture (Case 3) was conducted in three cycles, same as for Case 2, with two pressure-controlled Cycles 0 and 1, and a flow-controlled Cycle 2 (Figure 6.8-5a). The pattern of the changing pressure during the first pressure step cycle from 14:00 to 15:30 on June 17, 2019 (Figure 6.8-5a) indicate the presence of the initial hydraulic opening of fractures in this interval. A slight residual displacement was identified at the end of the test (Figure 6.8-5b). Displacement was subvertical and in good accordance with the quasi-reversible opening and closing of a sub-horizontal fracture. Nevertheless, some shear occurred at high pressure of 12.3 MPa to 12.5 MPa during Cycle 1, characterized by the vector KL that significantly deviated from the vertical, and appeared as an outlier to the group of all other lower pressure vectors. KL may thus indicate a limited fracture slipping event at high pressure.
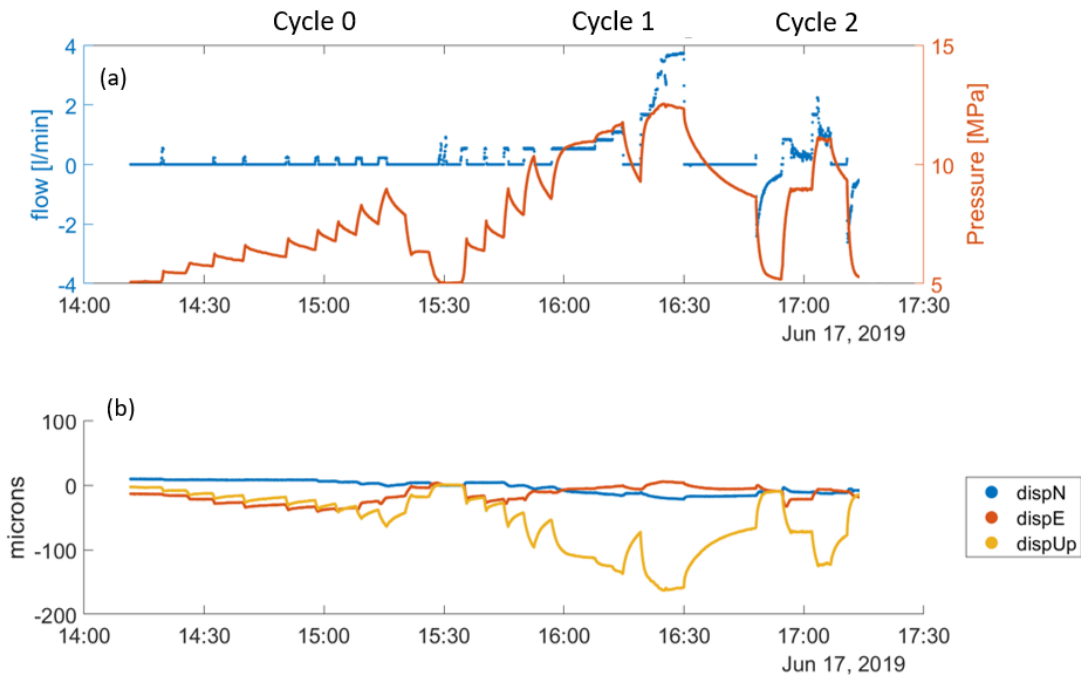
Figure 6.8-5. Hydromechanical response of interval for Case 3: (a) Pressure-flowrate variations vs time; and (b) SIMFIP upper anchor displacement vs time.

The main conclusions of the displacement analyses conducted on the three different borehole intervals are as follows: Flat-lying fractures subparallel to foliation open under variations of the normal effective stress in a slightly reversed stress regime. Planes are hydraulically opening at injection pressures as low as 9.3 MPa, about 3.7 MPa below the sub-vertical minimum principal stress. This opening precedes a slight reactivation in reverse shear that occurs at higher injected pressure. Normal opening of fractures explains most of the flow leakage while shearing does not correlate with any change in the leakage flowrate. The naturally flowing fracture appear more deformable than the closed ones for the same injection pressure. Sealed (mineralized) non-flowing fractures apparently do not display additional strength to behave differently from the closed fractures. They activate as easily as the other fractures given their orientation towards stress. The geology of the three different intervals gives roughly the same leakage pressure and flow response under a comparable state of stress. The estimated stress tensor orientation is consistent with the general N120° trend in the Scandinavian Caledonides with some deviation related to the approach and to some shallow depth conditions influencing stress. Borehole displacements highlight the role of foliation planes in creating a shallow crust significantly weaker than usually considered in isostatic and tectonic models. The SIMFIP measurement method proved to be successful to capture borehole displacements at large (~0.5 km) borehole depths, thus opening a new perspective for an accurate estimation of the full stress tensor in the crust.

6.8.2.3. Influence of Stress Perturbations on Fracture Aperture at the Borehole Scale

A 3D model of fractures intersecting a vertical borehole was developed using the distinct element code 3DEC (Itasca, 2016) to investigate the impact of borehole-scale stress perturbations on fracture aperture. The hydromechanical model explicitly represents the borehole as a hollow 12 m long and 0.14 m diameter cylinder located in the center of the crystalline rock mass (Figure 6.8-6). The model domain dimensions are 4.3 m x 4.3 m x 12 m. The borehole is intersected by a single fracture with a dip direction and dip angle respectively of 247°and 13°. This geometry is typical for the geometry of field Cases 1 and 3.
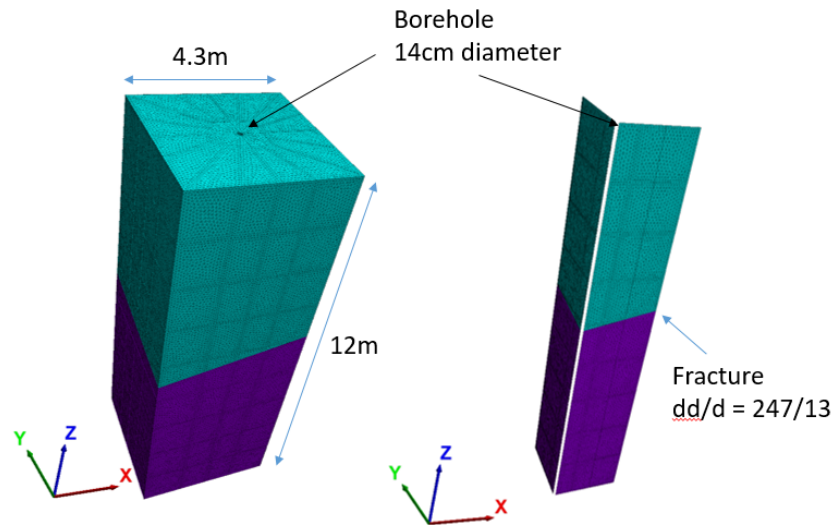
Figure 6.8-6. 3DEC model geometry of a vertical borehole intersecting a sub-horizontal natural fracture.

The model parameters and the fluid domain network structure were the same as those reported in FY20 (Guglielmi et al., 2020). A variable permeability model was used for the fracture, based on the cubic law equation with a value of hydraulic aperture that changed with the evolution of fault normal displacement. The fracture and intact rock properties used for modeling are given in Table 3-1 of the report by Guglielmi et al. (2021). The host rock is assumed to be linear elastic, with the impermeable rock matrix. Fracture stiffness values (K_n, K_s) were estimated from matching model results to the initial reversible parts of the measured displacement-vs-pressure curves. A hydraulic aperture was incrementally actuated during calculation iterations. The stress magnitude pattern is the same as that in the FY20 inverse analysis of the COSC data (Table 3-2 of the report by Guglielmi et al., 2021). A stress boundary condition was applied to the top and the four vertical model faces. A no-displacement boundary is applied to the bottom face. Figure 6.8-7 demonstrates a model-loading protocol that represents the *in-situ* SIMFIP test protocol:

- 1 – The model with open hole is first consolidated under gravity and stress conditions,

- 2 – The inflation of the probe's packer is represented by applying a 21.4 MPa hydrostatic stress at the borehole wall over a 1 m length, which corresponds to the length of the SIMFIP packer. This hydrostatic stress was applied at two depths separated by the length of the SIMFIP probe injection chamber,

- 3 – A 16.15 MPa hydrostatic stress is applied at the borehole wall in the injection chamber. The value of 16.15 MPa corresponds to the fracture activation pressure measured during the Case 1 intact-rock test. No flow is allowed into the fracture.

- 4 – A fluid pressure of 16.15 MPa is applied to calculate flow leakage into the opening model fracture.

Selected results are presented below.
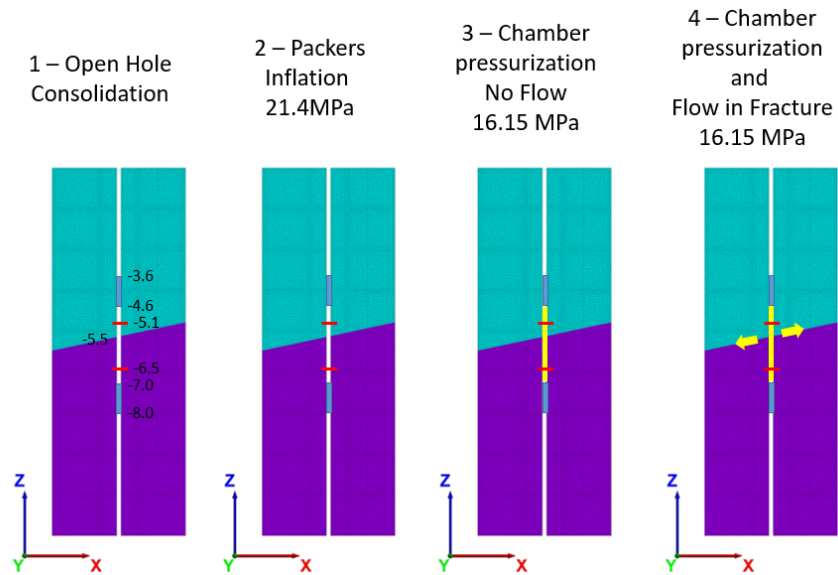
Figure 6.8-7. 3DEC model-loading protocol (numbers are the depths of the SIMFIP probe elements). The red markers indicate the locations of probe's anchors. Note that the SIMFIP sensor was used to measure the relative displacement of the upper anchor relative to the lower one.

Borehole Stress and Displacement Perturbation During the Hydraulic Opening of a Fracture

Figure 6.8-8 shows the maximum horizontal stress S_H variation in a vertical plane of the model (S_H is parallel to Ox in the model). After consolidation, there is a stress decrease from 18 MPa (far field stress) to 14 MPa in a zone of about one borehole radius from the borehole. The inflation of the packers and the chamber pressurization strongly affects the local stress. The stress perturbation that is observed at the fracture intersection is related to the chamber inflation, and the strongest stress variation is caused by the hydraulic opening of the fracture.
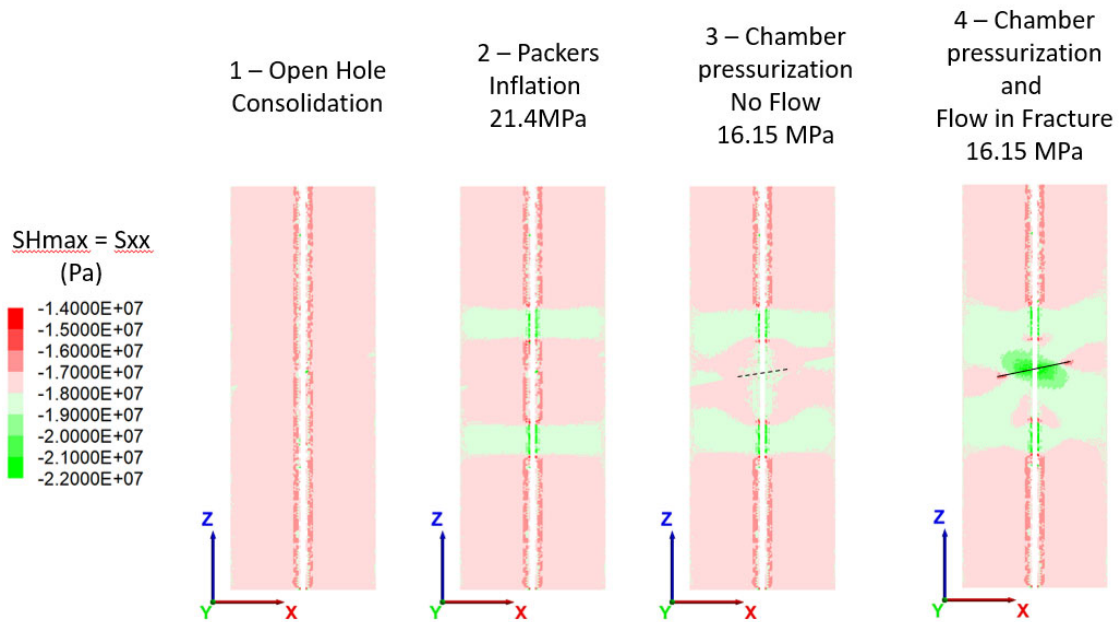
Figure 6.8-8. Maximum horizontal stress distribution.

Figure 6.8-9 shows the displacements calculated for Steps 1 to 4. Inflation of packers does not generate displacements at the SIMFIP measuring zone around the fracture. Fracture activation induces displacements in a large (several meter) volume around the borehole. The displacement field is asymmetric, but is significantly less extended in the fracture footwall than that in the hanging wall.
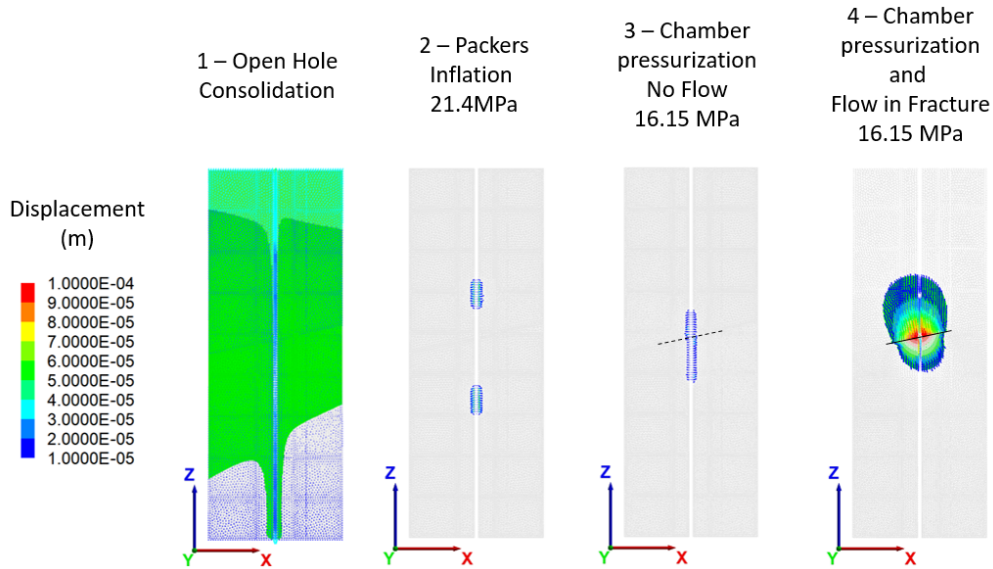
Figure 6.8-9. Model grid point displacement for Steps 1 to 4.

Displacements correspond to a pure opening of the stimulated fracture (Figure 6.8-10). Indeed, no significant shear displacement is calculated in the fracture plane during activation (and after 10,000 calculation cycles). Figure 6.8-10 shows that the lower anchor displacement is less than the upper anchor displacement. It also clearly appears that the borehole axis is not parallel to the axis of the displacement field (which is perpendicular to the fracture activated patch in that example).
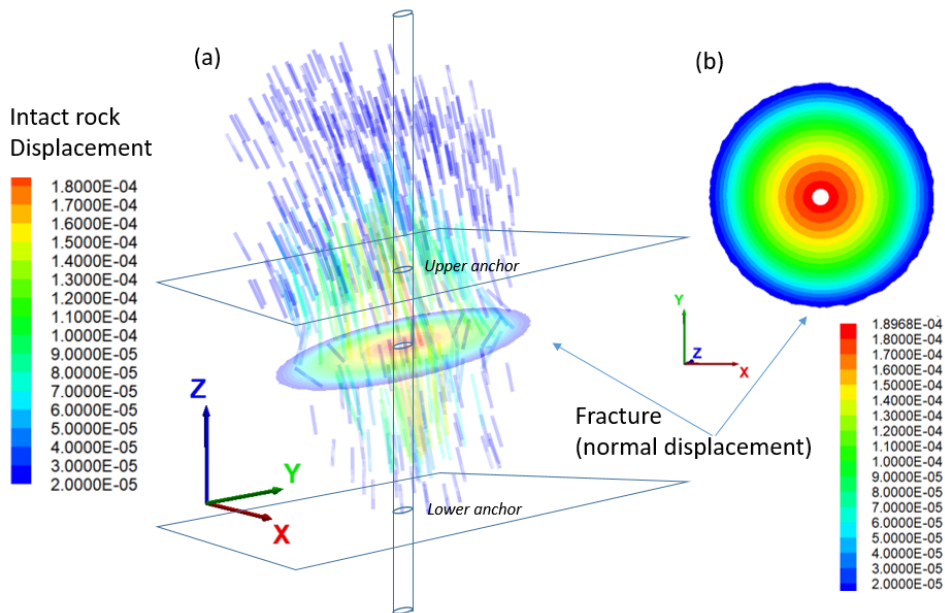
Figure 6.8-10. Three-dimensional displacement field produced by the fracture Mode 1 activation: (a) Intact rock displacement vectors, and (b) Activated fracture wall normal displacement map.

246

Borehole Stress and Displacement Perturbation During a Mixed Mode Fracture Activation

Figure 6.8-11 demonstrates a comparison of the stress perturbation caused by the Mode 1 opening of the fracture with the stress perturbation induced by fracture opening and slip. To produce the second "mixed mode" (Mode 2) rupture, the same borehole geometry was used, but with a reduced fracture friction of 5° and the cohesion and tensile strength to zero. To initiate shear failure and slip, the number of calculation cycles was increased from 10,000 (Figure 6.8-11a) to 20,000 (Figure 6.8-11b). Figure 6.8-12 shows that the displacement at the anchors is dominated by normal fracture opening, while a slight migration of the displacement vector orientation shows the initiation of slip from initial injection time t_1 to t_3 (when the model was stopped). This result is consistent with the migration of the displacement vector observed during Case 1, from perpendicular to the fracture plane (a_1b_1 in Figure 6.8-3c) to oblique (a_5b_5 in Figure 6.8-3c). The magnitude of the shear component is also in the range of the Case 1 shear. The dominant opening compared to slip displacement component is explained by the fact that this fracture is poorly oriented for failure in shear. The results show that the fracture strike is almost perpendicular to S_{Hmax}, and there is no significant difference between the maximum and the minimum principal stresses to bring the fracture to a critical Coulomb stress failure.
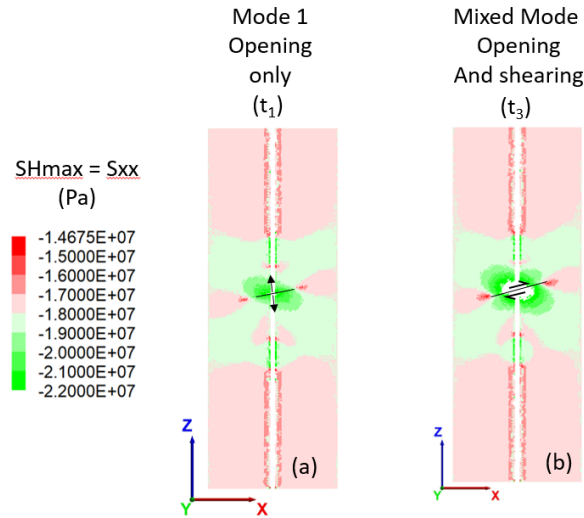
Figure 6.8-11. Evolution of the maximum horizontal stress perturbation due to the transition from (a) pure opening to (b) opening and slip on a fluid-driven fracture.
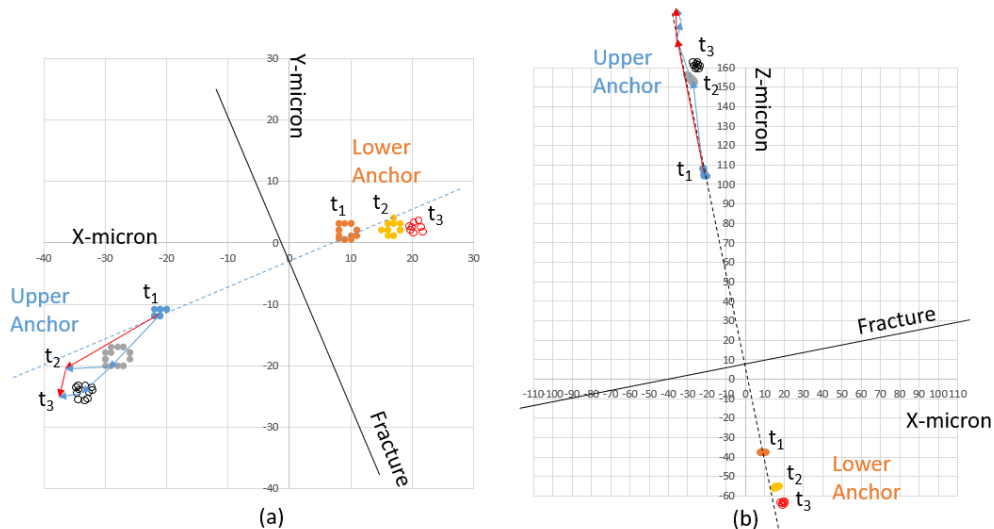
Figure 6.8-12. Calculated horizontal (a) and vertical (b) displacements at times t_1 to t_3 of the slipping fracture model.

247

Activated Fracture Stress and Aperture Evolution

Figure 6.8-13 shows the normal and shear stress distribution within the activated fracture, and the corresponding fracture aperture evolution. The open hole induces a perturbation of the stress gradient in the fracture plane (Figures 6.8-13a-d), which, in turn, causes a perturbation of the initial fracture aperture by a ~2 micron closing in the direction perpendicular to S_{Hmax} (Figure 6.8-13g). The chamber pressurization to 16.15 MPa tends to attenuate the borehole stress perturbation, while the fracture aperture perturbation remains within about the same magnitude (Figure 6.8-13b,e,h). The injection in the fracture strongly modifies the normal stress, and the stress gradient disappears (Figure 6.8-13c), which generates a complex shear stress gradient (Figure 6.8-13f) and creates an axisymmetric opening of the fracture (Figure 6.8-13i). Thus, the high injection pressure required to open the sub-horizontal fracture is "canceling" most of the initial internal stress and aperture heterogeneity. It is possible that the initial stress induced aperture heterogeneity may potentially influence the leakage in the fracture at lower injection pressures.
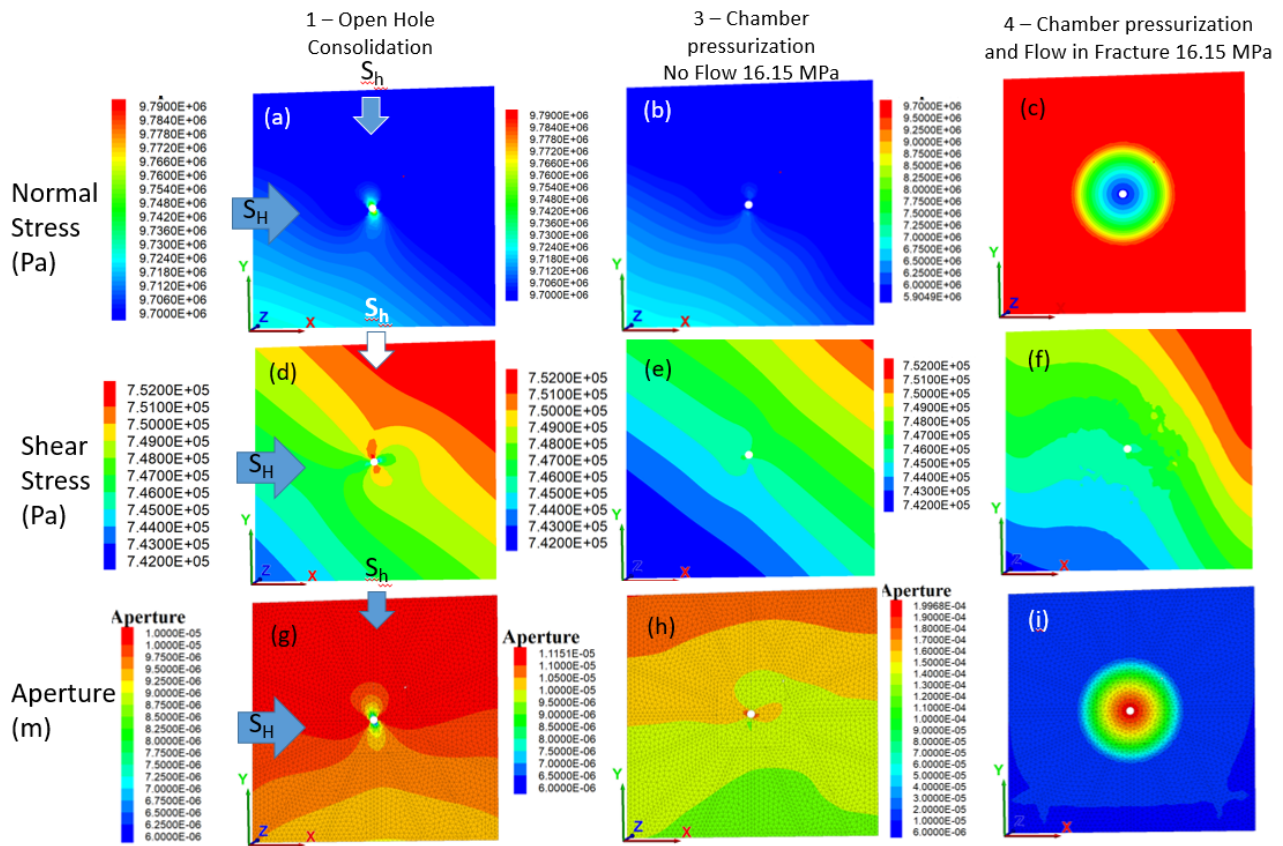
Figure 6.8-13. Pure opening fracture calculated stress and aperture variation during the SIMFIP hydraulic test protocol for the cases of the open hole consolidation (left column), chamber pressurization with no flow under the pressure of 16.15 MPa (middle column), and chamber pressurization and in fracture under pressure of 16.15 MPa (right column).

Findings From Borehole-Scale Fracture Modeling

A fracture that is poorly oriented for slip versus the ambient stress, such as the one selected for the numerical study, will first open, then progressively start slipping while fluid pressure is penetrating the fracture. Such a fracture requires a high injection pressure (close to the normal stress or larger if the fracture has some initial tensile strength) to activate. The main consequence is that most of the measured displacement is perpendicular to the fracture plane with little shear component. The second main consequence is that opening of the fracture may be large enough to overcome the effects of fracture's surface heterogeneity on fluid channeling. This might be true at least in the borehole nearfield.

The results of numerical modeling are consistent with the field observations from the SIMFIP hydromechanical testing. Modeling shows that the simulated 3D fracture displacements transfer well to the measured displacement orientations. The magnitude of the anchors' displacements is less than the true magnitude of the fracture wall displacement, because it is attenuated due to the intact rock stiffness. It was found that displacements of the anchors correspond to 50% of the fracture wall displacement. The model shows that the migration of fluid in the activated fracture generates displacement gradients that induce local and measurable rotations of the SIMFIP anchors. To obtain a better match between the modeling and observation data, the model is supposed to take into account the intact rock elastic properties deduced from borehole logging, as well as the rotations measured by the field sensor.

6.8.2.4. Influence of Stress Perturbations on Fracture Aperture at the Fracture Network Scale

Using the same 3DEC model characteristics as those above, the model geometry was extended to a domain size of 10 m x 10 m x 50 m in order to simulate the borehole length of all three SIMFIP tests (Figure 6.8-14). As observed by Wenning et al. (2017), there are mainly two families of fractures, low dipping ones subparallel to foliation, and >30° dipping tectonic fractures. The tested 50-m interval is characterized by two fracture zones separated by a distance of 10 m within the intact rock. The initially flowing and non-flowing fracture tests are located in the lower fracture zone (Cases 2 and 3 in Figures 6.8-14a,b).
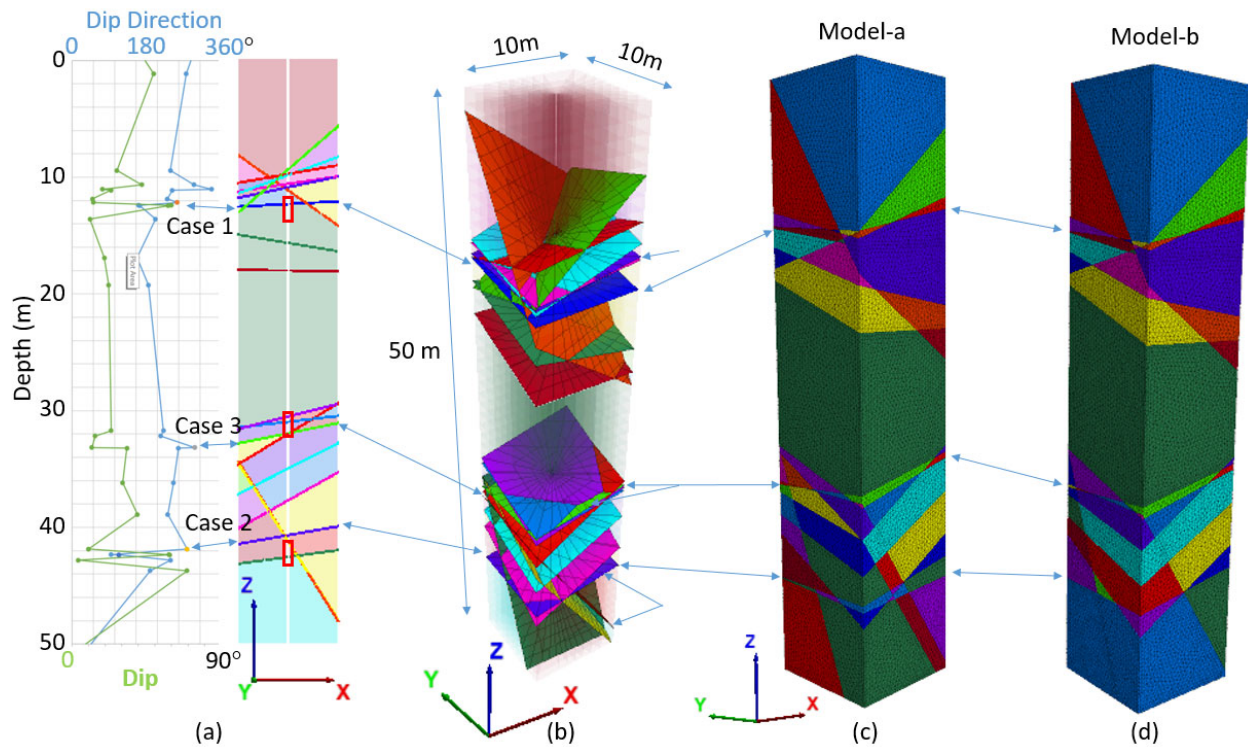
Figure 6.8-14. Fracture network model centered on a 50 m long section of the COSC model including the three SIMFIP tests: (a) Location of the natural fractures picked on the acoustic televiewer log, (b) Fracture network considered in the 3DEC model, (c) Model-a with all the fractures picked on the log, and (d) Model-b where some fractures were removed or merged with nearby ones.

The simulations are fully hydromechanically coupled, and the stress tensor is calculated from the inversion of all the SIMFIP tests on all the model faces. Modeling is conducted to compare the effects of the network geometry, the regional loading stress and the mechanical properties of the fractures on the stress perturbations and the fracture apertures. Simulations are conducted until equilibrium is reached. No additional injection is simulated at this step of the work.

Figure 6.8-15 shows model results obtained considering the high strength properties deduced from the Case 1 analysis. The stress magnitude in the model was adjusted to match the modeling results with the values estimated from the SIMFIP field tests. A reasonable match of principal stresses was obtained for Cases 1 and 3, while the model overestimated σ_1 and σ_2 in Case 2. A possible reason of the discrepancy is that multiple fractures may have been activated in the field in Case 2, which could lead to a lower accuracy of the stress inversion. Figures 6.8-15b,c show large variations of 10 MPa and 3 MPa of the normal and shear stress, respectively, calculated on the fractures. If, in general, the normal stress is higher on the large dipping fractures because they are the most perpendicular to S_H (S_{xx} in the model), the influence of the intersections between fractures is also inducing a large stress variability within some fractures. Figures 6.8-15d,e,f show the horizontal and vertical stress perturbations in the intact rock.
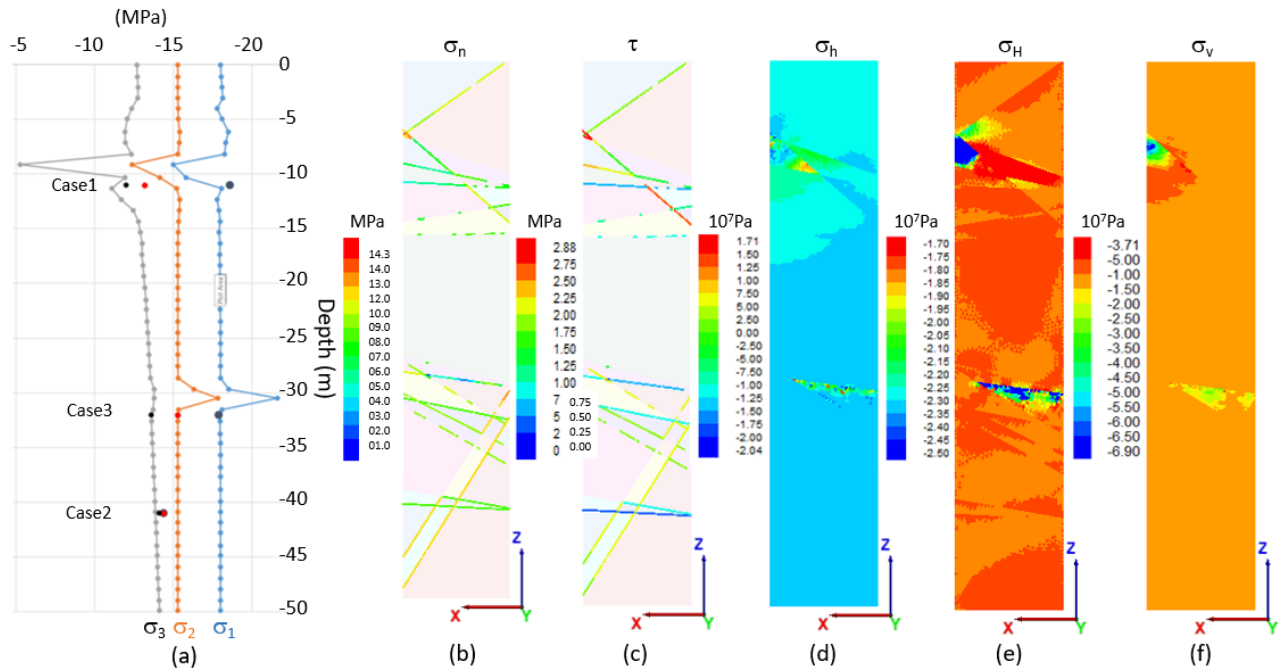
Figure 6.8-15. Stress perturbations in the COSC fracture network: (a) Vertical principal stress profile calculated along the model's central axis, (b) Fracture normal stress, (c) Fracture shear stress, (d) Intact rock minimum horizontal stress (parallel to Oy in the model), (e) Intact rock maximum horizontal stress (parallel to Ox in the model), and (f) Vertical stress.

Model results suggest that stress heterogeneity may disturb fracture apertures, as demonstrated here for the case of Model-a (see Figure 6.8-16). It is clearly observed that where the stress concentrations occur there is a significant closing of the fracture aperture. In the upper fracture zone, a fracture aperture closes below a micrometer along the axis of the borehole (white color in Figure 6.8-16). In the Case 1 test, it could mean that the fracture could have existed, but was closed and not detected due to limited resolution of the logging techniques. This could explain why the "ultra" closed fracture opened at a pressure close to the two other cases, and why the numerical modeling did not have to affect such a large initial strength to explain measured fracture displacements. Thus, a healed natural fracture could have been reactivated, rather than a new one was created due to propagating rupture along a foliation plane. In Cases 2 and 3, initial hydraulic apertures in the lower fracture zone are 10-micron at the borehole wall. The aperture distribution in the Case 3 fracture is perturbed by the nearby stress perturbation. In detail, there is a fracture aperture gradient increasing towards the positive x direction. It means that when activating, this fracture may preferentially open in the positive x direction. This may create a rotation of the borehole anchors roughly along the y direction. Case 2 appears to represent the most "homogenous" fracture aperture. The fact that we did not detect flow in this case, although the activation pressure is lower than in the other tests may require reconsidering this assumption, may be related to non-local

stress perturbation in this zone. Of course, other considerations such as a fracture filling are not considered in our modeling approach.
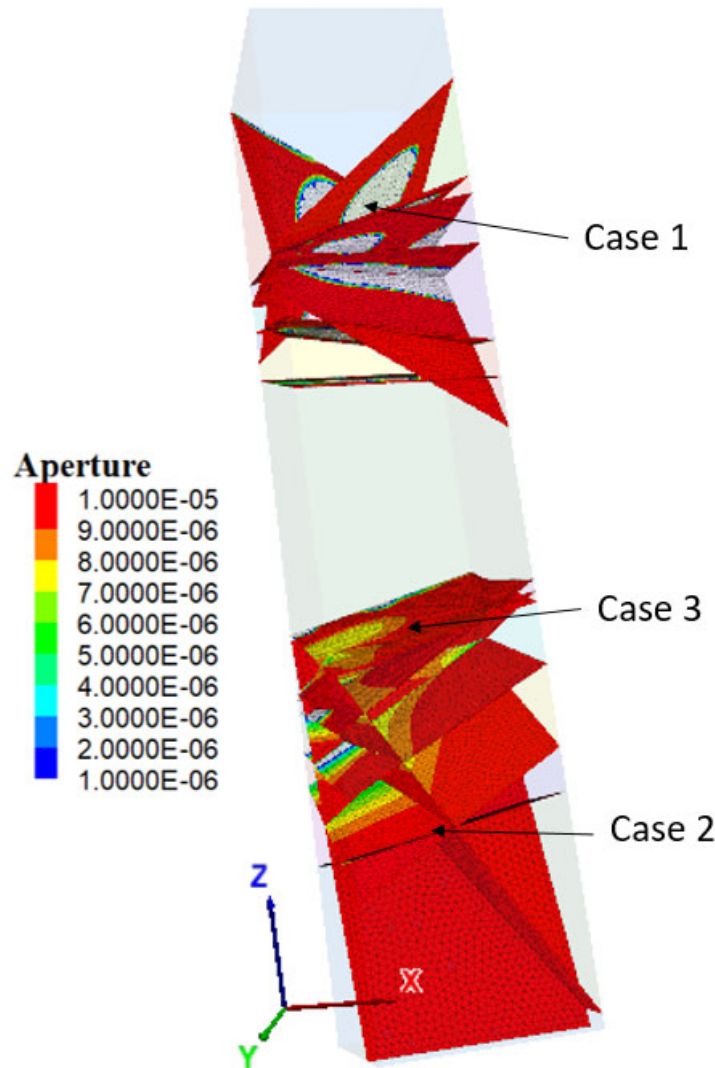
Figure 6.8-16. Variation of fracture aperture simulated using Model-a

Overall, the fracture-network model based on a stress model was validated using the SIMFIP field test data. The results of modeling are as follows:

- There may be a relationship between stress concentrations and the size of the minimum block volume in a fractured zone. This minimum block volume is usually limited when running geomechanical models based on DFN. Thus, the development of a DFN must be done with great care.

- The relationship between intact rock stress concentrations and fracture properties plays a significant role in dissipating stress perturbations. Larger compliant fractures tend to increase stress heterogeneity in the DFN, because more stress is transferred to the intact rock.

- Stress heterogeneity is causing stress and aperture gradients in fractures, which can impact the orientation of flow and transport paths in the fracture network.

6.8.2.5. Conclusions and Directions for Future Research

LBNL scientists developed a method to calculate the stress heterogeneity in a fracture network by using a profile of SIMFIP hydromechanical tests and numerical modeling using the 3DEC fully coupled hydromechanical model. The method consists of the following steps:

- Selecting a borehole segment within which all field tests are conducted,

- Populating this segment with natural fractures identified on borehole image logs,

- Adjusting the model stress boundary conditions obtaining a reasonable match is obtained with the tensors estimated from the inversion of measured fracture displacement vectors, and

- Running the model to equilibrium in order to calculate stress perturbations and to compare the associated fracture aperture perturbations with the continuous displacements measured in the field.

The end product of the developed approach is a refined estimate of the variability of fracture apertures within a DFN. These findings are important for simulations of flow and transport in discrete fracture networks for PA studies, such as those described in Sections 6.5.2 and 6.9.2.

The orientation of the vectors measured by a SIMFIP sensor reflects the true orientation of the activated fracture movement. One limitation is that the tested interval must be as simple as possible, i.e., initially intact or crosscut by one fracture. This approach could be coupled with stress profiling deduced from the analysis of borehole breakouts on image logs, if such data are available. However, in the COSC borehole, no breakouts were identified in the test area, which might be typical for the shallow crust, in which nuclear repository sites are planned to be located.

The data analysis confirmed that the fracture opening dominates displacement and flow in fractures that are not "critically" oriented versus stress. In case some shear initiates later, after initial opening; however, the shear component remains small compared to opening, and does not seem to have much impact on fracture flow. It was also observed that high pressure activation of the non-critically oriented fractures is required to cause sufficient SIMFIP displacement. When large fracture opening dominates the fracture hydromechanical response, the response to smaller pressure injections cannot be observed.

Future research will include a detailed analysis of the initial chamber elastic response and understanding of the rotations measured by the SIMFIP. Additional modeling and analysis will be conducted to simulate:

- The case of an inclined large dipping fracture,

- A pure shear slip activation of a critically stressed fracture,

- The rotation of the borehole,

- Local deviation of the stress tensor orientation, and

- The SIMFIP test injections at the fracture network model scale.

6.8.3. Core Tensile Strength Tests on COSC Samples

6.8.3.1. Introduction

In-situ fracturing experiments conducted within a borehole at the COSC site produced horizontal fractures instead of typically observed borehole-parallel fractures. Such fractures are typically induced when the vertical, overburden stress is less than horizontal, borehole–perpendicular principal stresses. However, the strong texture anisotropy in the foliated gneiss can also lead to tensile strength of the rock, which is much weaker in the borehole-perpendicular direction, and which is approximately aligned with the foliation plane. The objective of the core tensile laboratory experiments conducted by LBNL in FY21 is to examine a possible correlation between the anisotropic rock texture and the tensile strength of the rock (Guglielmi et al., 2021, Section 3.6).

6.8.3.2. Experimental Setup and Results

A well-preserved Core A-137-2 was obtained from the unfractured interval in the COSC-1 borehole. This core was collected at the depth that was tested using the SIMFIP, as described in the previous sections of the report. From this core, eight disc-shaped test samples were produced with the axis aligned along the borehole. Additionally, two smaller samples were produced by subcoring the host core in a direction perpendicular to the borehole axis, along an approximate foliation plane (Figure 6.8-17). The rock density of these samples (after overnight drying under 60°C) varied in a narrow range from 2.93 to 2.99 g/cm^3 (Guglielmi et al., 2021, Table 3.3).

The tensile strength of the rock was evaluated via Brazilian Loading Tests (Ulusay and Hudson, 1978). To avoid fracturing initiated by loading-point cracking and crushing, which could result in premature failure and underestimation of the rock tensile strength, an ISRM-recommended method was used, involving loading platens with a curved surface (Figure 6.8-18). Following this method, the surface radius R and the platen thickness T were chosen, so that R=1.5×D and T=H, where D is the diameter, and H is the thickness of a disc-shaped sample. Although ISRM recommends very fast loading rate (e.g., ~200 N/s for our larger samples), the LBNL loading system was not able to achieve this rate. Therefore, a slower loading rate of ~200 N/min was used for large samples, and ~73 N/min for small samples. Because the load-bearing capability of the sample is not necessarily lost after a tensile fracture is formed in a rock sample, the fracturing load P was determined as the first clear drop in the applied load. The tensile strength of the sample was determined using the formula (Ulusay and Hudson, 1978).

During the tests, tensile force was induced in the disc in the directions of 0, 15, 30, 45, 60, 90, 120, and 150° from the reference direction, for samples 1 through 8, respectively. For the smaller cores perpendicular to the borehole, the tensile stress was induced along the foliation plane for both samples. Photographs from an experiment in progress and a failed sample are shown in Figure 6.8-19. During loading, a single prominent tensile fracture initiated from the center of a sample. However, typically, this was followed by additional fractures near the loading points, subparallel to the initial fracture. A photograph of all the samples after the experiments is shown in Figure 6.8-20.

Figure 6.8-17. Disc-shaped subcores from Core A-137-2 produced for Brazilian tensile strength tests. Larger cores were cut directly from the original core (top photograph), while smaller cores were made by subcoring the original core in a direction that is perpendicular to the borehole.
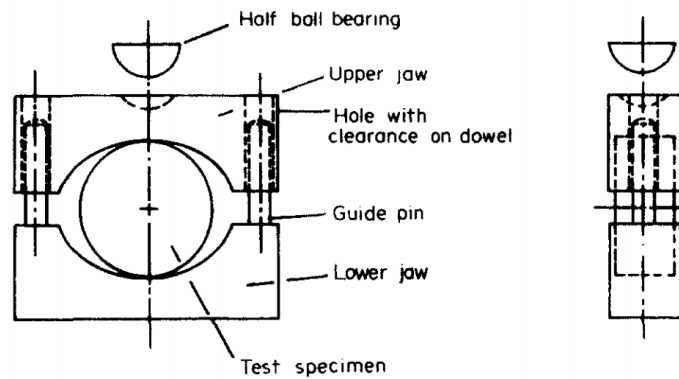
Figure 6.8-18. ISRM-recommended method, which uses loading platens with a curved surface (Ulusay and Hudson, 1978).
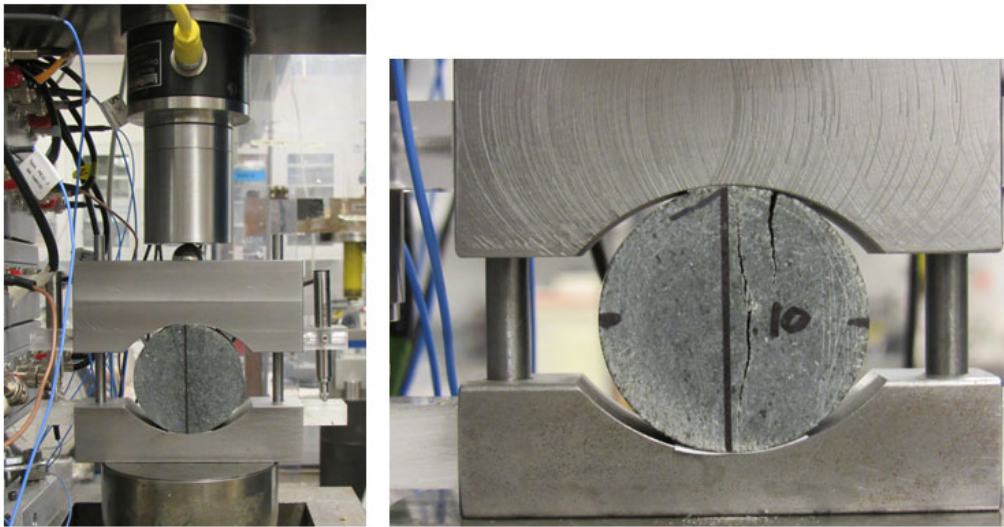
Figure 6.8-19. Photographs of the Brazilian tensile strength test conducted in the laboratory. A single tensile fracture forms first from the center of a disc sample, typically followed by additional fractures near the loading points.

Figure 6.8-20. A photograph of all the samples after the experiment. Note that the black line along a diameter of each core indicates the plane on which the tensile stress was induced (see Figure 6.8-19).

The tensile strengths measured from the experiments are summarized in Figure 6.8-21 and Table 6.8-1. The tensile strengths along the borehole axis (i.e., perpendicular to the foliation plane) show somewhat systematic changes with the angle. This may indicate the effect of tilting of the foliation plane against the borehole-perpendicular direction or presence of a weaker section along the host core due to heterogeneity. In contrast, the two test results for the tensile strength parallel to the foliation plane are nearly the same. The averaged tensile strength of the rock in the direction parallel to the foliation plane is 11.4 MPa, and in the direction perpendicular to the foliation plane is 20.1 MPa.
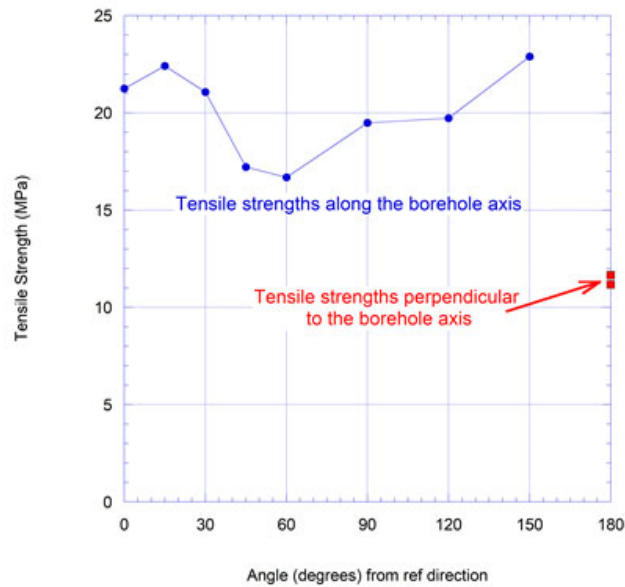
Figure 6.8-21. Brazilian tensile strength of Core A-137-2 subcores. The data for direction perpendicular to the foliation plane (i.e., along the borehole axis) are shown in blue, and for the direction parallel to the foliation plane (i.e., perpendicular to the borehole axis) are shown in red.

Table 6.8-1. Brazilian tensile strength of subcores

Sample	Fracturing angle (degrees)	Tensile strength (MPa)	Average (MPa)	Std. Dev. (MPa)
1	0	21.253		
2	15	22.415		
3	30	21.079		
4	45	17.218		
5	60	16.690	20.1	2.3
6	90	19.488		
7	120	19.726		
8	150	22.902		
9	Perpendicular to core	11.654	11.4	_____
10		11.176		

6.8.3.3. Summary

Brazilian tensile strength tests were conducted on rock samples recovered from the COSC-1 borehole. The test results indicate that the tensile strength of the rock parallel to the borehole-perpendicular foliation plane was significantly (~50%) smaller than in the direction perpendicular to the foliation plane. These results are consistent with the results of the *in-situ* field tests, which showed preferential opening of fractures perpendicular to the borehole. However, the estimated tensile strength of the *in-situ* rock was as little as ~0.5 MPa, which is far smaller than the laboratory-obtained strengths. This discrepancy could have occurred because *in-situ* fracturing was initiated by reactivation of healed, weakly-cemented cracks along the foliation.

6.8.4. Modeling Transmissivity Tests on COSC Core Samples

6.8.4.1. Introduction

In previous years, laboratory fracture flow-through experiments were conducted by imposing flow Q between pairs of ports surrounding a fractured rock core, and measuring the pressure difference DP. This was done at a series of confining pressures between 200 and 4500 psi. Typical flow rates used are 5, 10, 15, 20 cm^3/s. Then Darcy's Law was used with DP and Q to determine the transmissivity T of the flow paths between different port pairs. The main objective of these core measurements at LBNL were to determine fracture transmissivity as a function of controlled stress under laboratory conditions, to complement findings from the *in-situ* field testing (Guglielmi et al., 2020). Details of the experimental apparatus were described in previous reports (e.g., Dobson et al., 2017; Zheng et al., 2018c). In FY20, LBNL initiated a modeling study to investigate the nature of the observed anisotropic of flow transmissivity in the tested fracture cores (Guglielmi et al., 2020). Numerical simulations were conducted using the TOUGH3 code with the equation of state package EOS1, which considers flow of a single-phase liquid/water under isothermal conditions. This year, LBNL continued and improved this this modeling analysis (Guglielmi et al., 2021, Section 3.7).

6.8.4.2. Modeling Setup and Results

In FY20, a numerical model of the fracture in Core 211-2 was developed by taking an *x*-ray CT scan, which provided a fine-scale presentation of the aperture distribution, and using the cubic law to relate local fracture aperture to local transmissivity T (Guglielmi et al., 2020). The lab experiments imposing flow between pairs of ports were then simulated, and the specified Q and modeled dP were used to determine T of the flow paths. The modeled results agreed with some experimental results, but not all. In particular, the model identified the port pair that provided the largest T, but not the smallest, and the range of modeled T was too small. Examining the modeled flow paths across the fracture suggested that heterogeneity rather than anisotropy caused variations in T between port pairs.

In FY21, several model shortcomings were addressed in order to improve the model's ability to reproduce laboratory experimental results. Because the *x*-ray CT scan, while excellent at illustrating aperture variations, does not clearly identify the radial extent of the core, a new model was developed to simulate a flow domain with slightly smaller radial extent of cores. This model eliminated large aperture regions that provided fast flow paths around the perimeter of the core (i.e., the so-called wall flow). The experimental flow setup, an example of an *x*-ray CT scan of the fracture aperture, and a numerical representation of the fracture were adopted from prior modeling work by Guglielmi et al. (2020), and are depicted in Figure 6.8-22.

In comparison with the original version of the model, in which all ports were assigned continuously high permeability, the new model was designed to have variable permeability of ports with time. High permeability (~100 times larger than the fracture) was assigned to one pair of ports (1 and 5, 2 and 6, 3 and 7, 4 and 8) during the period when the port is active allows for injecting fluid to easily spread throughout the port and then into the fracture, rather than just emanating from a single source point. Low permeability was assigned during the period when the port was inactive, to prevent the port itself to act as a preferential flow path. A negative flow rate of -0.01 kg/s was assigned at the sink port, with all other ports having at low permeability (~1,000 times smaller than the fracture), and zero flow rates for that time period.

Numerical modeling was conducted using several model variations, in which a constant value of either 100 or 200 microns was subtracted from each fracture aperture value, to represent a partially shut fracture. This resulted in producing more channelized flow paths and a greater range of calculated T between different port pairs. This qualitatively improved the agreement between the model and experiments. Because the original goal of the lab experiments was to identify transmissivity anisotropy, a series of simulations were conducted using a uniform aperture and a stochastic heterogeneous aperture distribution, with various amounts of anisotropy. Figures 6.8-23 and 6.8-24 illustrate the results of modeling homogeneous and heterogeneous, anisotropic fractures (a 5:1 anisotropy, $k_x = 5k_y$, for both cases), respectively. (More details can be found in Section 3 of the report by Guglielmi et al., 2021). These results demonstrate that the permeability distribution is dependent on the combined effect of local heterogeneity, converging/diverging flow paths, and anisotropy.
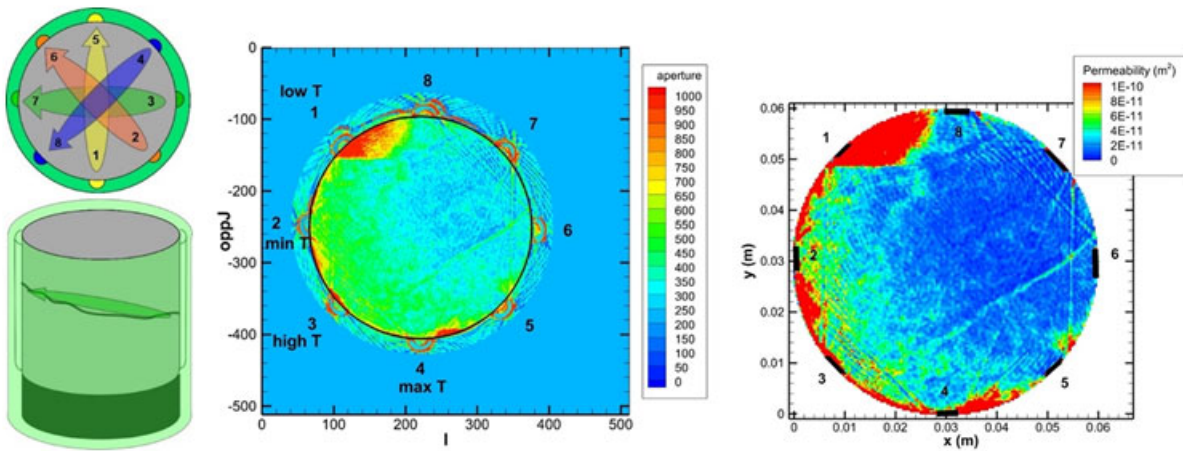
Figure 6.8-22. Left – schematic illustration of core fracture flow experiment with eight ports; Center – Scanned fracture aperture distribution of Core 211-2, with labeled ports; Right – permeability distribution based on numerical modeling of Core 211-1, using the modeling scheme Guglielmi et al. (2020).
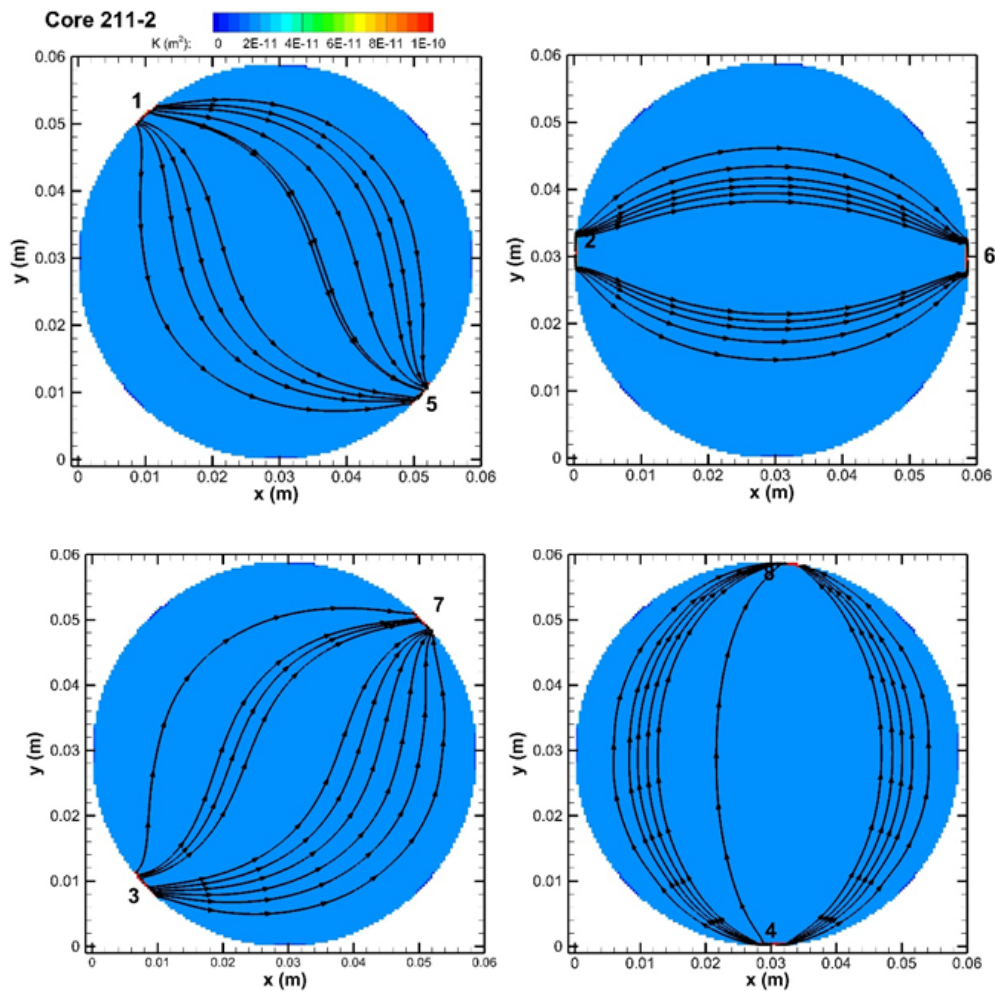
Figure 6.8-23. Modeled flow in a homogeneous, anisotropic fracture, with $k_x = 5\ k_y$. The black lines represent streamlines between source and sink ports.

257
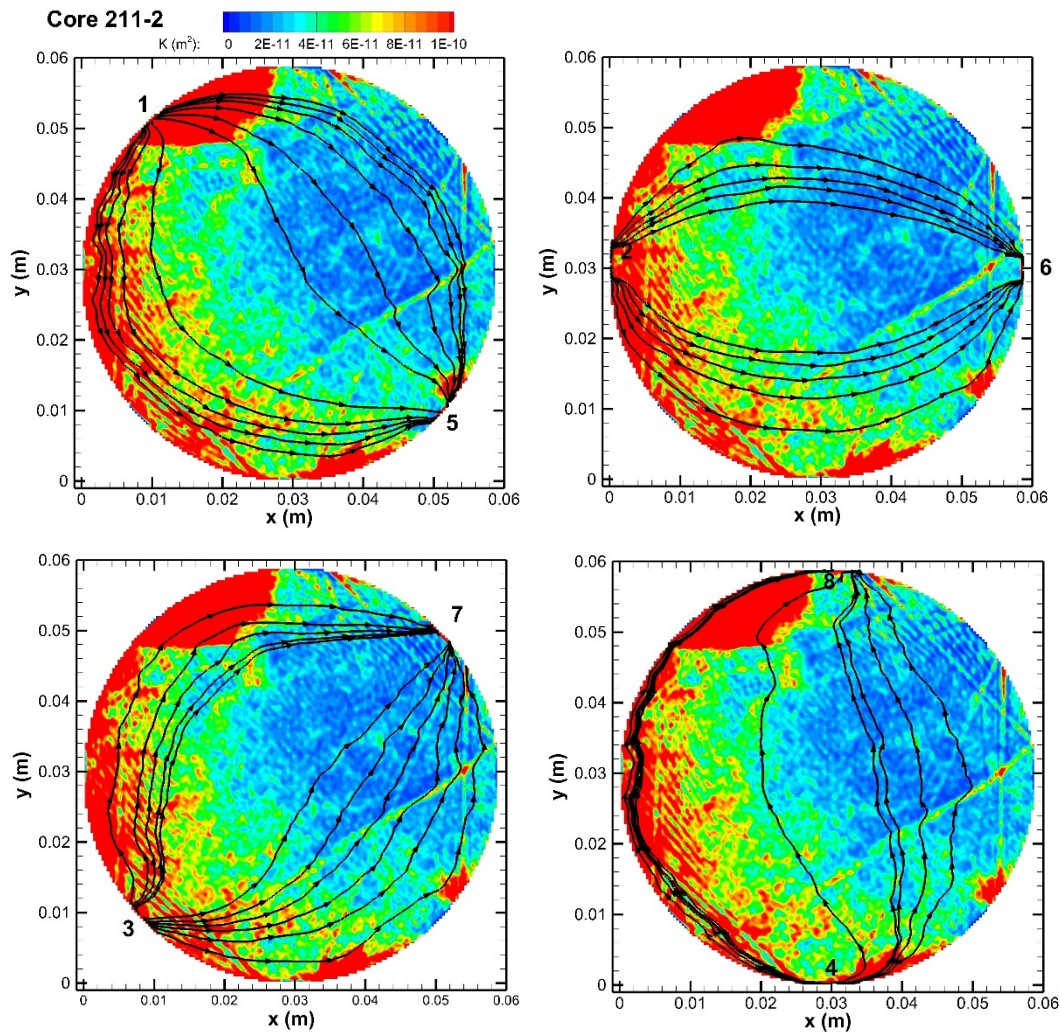
Figure 6.8-24. Modeled flow in a heterogeneous, anisotropic fracture, with $k_x = 5 \, k_y$. The color variations (calculated permeability) reflect the measured variations in fracture aperture. The black lines represent streamlines between source and sink ports.

6.8.4.3. Summary and Directions for Future Research

The findings of this task suggest that identifying anisotropy should probably not be the primary goal of the laboratory experiments and modeling studies. The combined effect of heterogeneity, converging/diverging flow, and anisotropy makes it very difficult to evaluate the relative impact of anisotropy alone on transmissivity. However, demonstrating the ability to create numerical models that reproduce the key results of fracture-flow laboratory experiments is still valuable, because the models enable flow fields to be visualized and evaluated, which is impossible in the laboratory. The results of simulations of flow fields can provide great insights into the nature of fracture flow through heterogeneous fractures, and in particular into the nature of the fracture/matrix interface area, which is a controlling factor affecting the sorption of radionuclides. This modeling also shows how variations in fracture aperture can result in channelized flow, which could lead to faster flow and transport compared to a case where a uniform fracture aperture is assumed.

In the future, modeling of the 211-2 Core will be performed to examine the hypothesis that some features visible in the *x*-ray CT scan are, in fact, artifacts that should not be incorporated in the permeability distribution in the model. Modeling results will also be compared to other existing laboratory data from Core 211-2. Modeling of Core 401-1 will also be conducted

258

6.9. International Comparison of Performance Assessments Methods

6.9.1. Introduction

The SFWD The SFWD campaign has placed considerable resources into the (1) development of advanced PA methodologies and (2) testing of these on generic deep geologic disposal systems. Generic design (or reference-case) concepts being considered for waste disposal since 2010 include mined repository concepts in bedded salt, argillite (shale), and crystalline rock. An additional option begun three years ago is a potential mined repository in unsaturated alluvium. Activities related to the development and application of PA methods on generic reference test cases reside in the Geologic Disposal Safety Assessment (GDSA) Repository System Analysis (RSA) work package of SFWD (LaForce et al., 2020).

Recognizing the importance of building confidence in the models, methods, and software used for PA of deep geologic repositories, SFWD researchers decided a few years ago to increase its international collaboration in this area (Sassani et al., 2020; 2021). Confidence in PA models can be enhanced by comparison with international standards and data sets; it can also be improved by comparing PA modeling results from multiple international disposal program applied to the same reference cases. The latter approach is at the heart of the new Task F of DECOVALEX 2023, which is led by the GDSA team at SNL and involves ten international PA modeling groups. The task investigates two generic reference cases in parallel: a repository for commercial spent nuclear fuel (SNF) in a fractured crystalline host rock and a repository for commercial SNF in a bedded salt formation. Section 6.9.2 discusses progress of Task F to date, based on LaForce et al. (2021).

Radionuclide transport simulations are a central component of any PA model, as they evaluate transport from the repository to the biosphere for dose calculations. The development and implementation of adequate equilibrium and thermodynamic databases and models across broad physicochemical conditions are an important prerequisite to simulating radionuclide transport. In FY21, SFWD scientists from LLNL have continued to collaborate with the international research community to improve thermodynamic and thermochemical databases and models that evaluate the transport of radionuclides as they interact with EBS materials, host rock and fluids. Progress is reported in Section 6.9.3, based on Zavarin et al. (2021a,b).

6.9.2. Modeling of DECOVALEX Task F Reference Cases

Task F of DECOVALEX-2023 aims at a comparison of models and methods used for post-closure PA. The task provides numerous opportunities for learning new modeling approaches, developing new models for use in PA simulations, testing uncertainty and sensitivity analysis methods, comparing PA methods, and networking with modelers in other programs. Additional information on the structure of and the plans for DECOVALEX-2023 Task F are provided in LaForce et al. (2020; 2021).

Comparative PA modeling centered around two generic disposal concepts (which are called reference cases) for commercial SNF: a generic repository in a fractured crystalline host rock, and a generic repository in a salt formation (bedded or domal). In Year 1, nine teams from six countries participated in a discussion of the crystalline reference case and benchmarking exercises, and three teams (from three countries) participated in the development of the salt reference case. In Year 2 (this year), each reference case has gained the participation of an additional team. Although a direct comparison cannot be made between simulations of a crystalline repository and simulations of a salt repository, it is expected that foundational aspects will be transferable between concepts, such as, for instance, methods of coupling process models, propagating uncertainty, and conducting sensitivity analysis.

A common set of conceptual models and parameters will be provided for each reference case, and teams will be responsible for determining how best to implement and couple the models involved in the PA. The comparison will be conducted in stages, beginning with a comparison of key outputs of individual process models, followed by a comparison of a single deterministic simulation of the full reference case, and moving on to the evaluation of uncertainty propagation and a sensitivity analyses. The Task F Specification (Stein et al., 2021) provides background information, a summary of the proposed reference cases, and a staged plan for the analysis. In the first year of the project, the crystalline teams have been focused on initial benchmarking,

especially comparative simulations of transport in fractured rock, while the salt teams developed a repository reference case and designed a phased modeling approach.

6.9.2.1. *Crystalline Reference Case*

A preliminary description of the DECOVALEX crystalline reference case and the choices to be made regarding features and processes to be simulated is available in Stein et al. (2021). In FY21, teams participating in the Crystalline Task F completed several benchmark cases related to flow and transport through fractured rock. The benchmark cases provide an opportunity to understand differences in model implementation that affect how a problem can be specified, what results can be obtained, and the influence modeling choices have on PA results in relatively simple systems. After initially modeling a simple transport problem involving a single fracture with matrix diffusion, in comparison with an analytical solution, teams moved on to a more complex four-fracture problem in three dimensions. The modeling teams practiced solving the test problem by generating deterministic fractures, upscaling to an Equivalent Continuous Porous Medium (ECPM), and modeling advection and diffusion of a conservative tracer via particle tracking. It is assumed that flow and transport can only occur in fractures, and matrix diffusion is neglected. A few highlights from SNL's GDSA simulations of the test problem are provided below.

LANL's dfnWORKS tool (Hyman et al., 2015; 2021) was used to generate the fractures, and then PFLOTRAN was applied for steady state flow simulations. The four-fracture benchmark case was modeled using the DFN approach and two different methods of upscaling to the ECPM. For comparison, normalized breakthrough curves (determined as the total mass that crossed the east face divided by the initial mass at the west face) over 30 years were generated at the outflow face. The parameters and values used can be found in Table 2.2 of LaForce et al. (2021). Figure 6.9-1 shows the fracture domain pressure solution in the DFN.
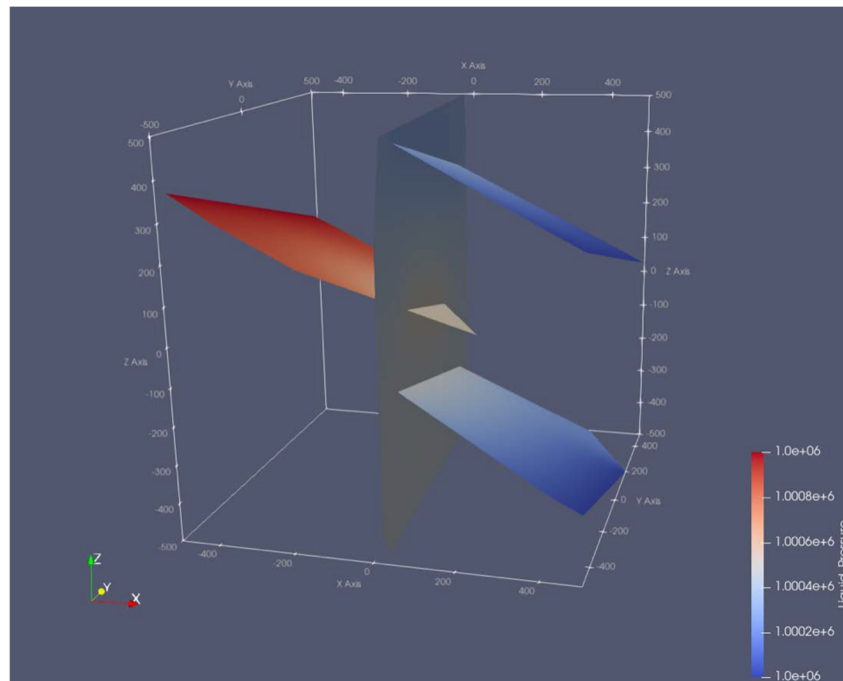
Figure 6.9-1. Steady state fluid pressure for 4-fracture DFN.

Two different transport modeling methods were applied using the DFN approach. The first utilized dfnWORKS particle tracking software dfnTrans (Lagrangian reference frame). The dfnTrans software takes the flow field and fracture information and outputs particle travel times in the domain. The second method uses the advection-dispersion equation (ADE) in PFLOTRAN (Eulerian reference frame) with 175,920 cells in the model domain.

Upscaling was also performed using two methods. The first method used a pythonscript called mapdfn.py (Stein et al., 2017), which creates a uniform grid. Using output from dfnWORKS (apertures, permeabilities, radii, the unit vector defining the normal vector to the fractures, and coordinates of the fracture center) along with user input defining the domain and grid cell size, mapDFN produces upscaled anisotropic permeability, porosity, and tortuosity based on the intersection of fractures within grid cells. A cell length of 20 m was chosen, which resulted in a total of 9,704 active cells. For modeling, the matrix cells were made inactive. The second method is based on using the dfnWORKS octree meshing. This method returns a spatially variable Delaunay tetrahedral mesh, and is refined only where there are fractures (Sweeney et al., 2020). The model domain is 160 m long, representing the largest cell size of the background mesh cells, and three refinement levels, which resulted in ~20 m grid cells for a total of 30,086 cells. Modeling was conducted using the matrix cells being active, but the tracer was only injected into the fracture.

Figure 6.9-2 shows tracer breakthrough curves for the SNL team for the different transport modeling and upscaling options. The results show a good agreement between the models and with the other teams (not shown). Most teams chose to model the tracer via an ECPM. Tracer can first be seen on the outflow face at ~0.5 years and has fully migrated through the domain after ~10 years. Differences between results may be due to mesh size, numerical diffusion, or different upscaling methods.
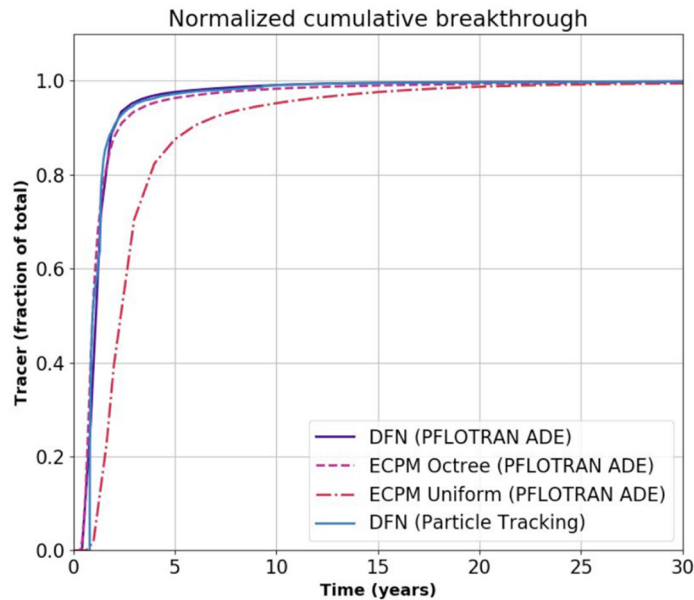
Figure 6.9-2. SNL team breakthrough curves for the Crystalline Task F 4-Fracture DFN.

The four-fracture benchmark case was later extended by adding stochastically-generated fracture sets to the model domain. The stochastic fractures were generated based on input from the Finish waste management organization POSIVA, representative of fracture networks at their repository site in Onkalo, Finland (Hartley et al., 2016, Table 3.1). The resulting fracture set, including stochastically-generated fractures, was provided to the teams. The modeling problem included simulations of advection and diffusion of a conservative, decaying, and adsorbing tracer through the four deterministic fractures and the additional stochastic fractures within a cubic domain. Three fracture families were defined, two subvertical and one subhorizontal. For each fracture family, thje fracture radius was sampled from a truncated power law distribution, and a fracture orientation was sampled from a Fisher distribution. The fractures were generated using LANL's dfnWORKS (Hyman et al., 2015). However, in this case, the DFN was modeled only using the ADE method, and only one upscaling method was applied. The resulting DFN flow field is illustrated in Figure 6.9-3. The DFN used 4,647,375 cells and ran for ~3 hours on 288 processors on a parallel super-computer. The ECPM used 49,685 cells, and ran in ~1.5 minutes on 288 processors.
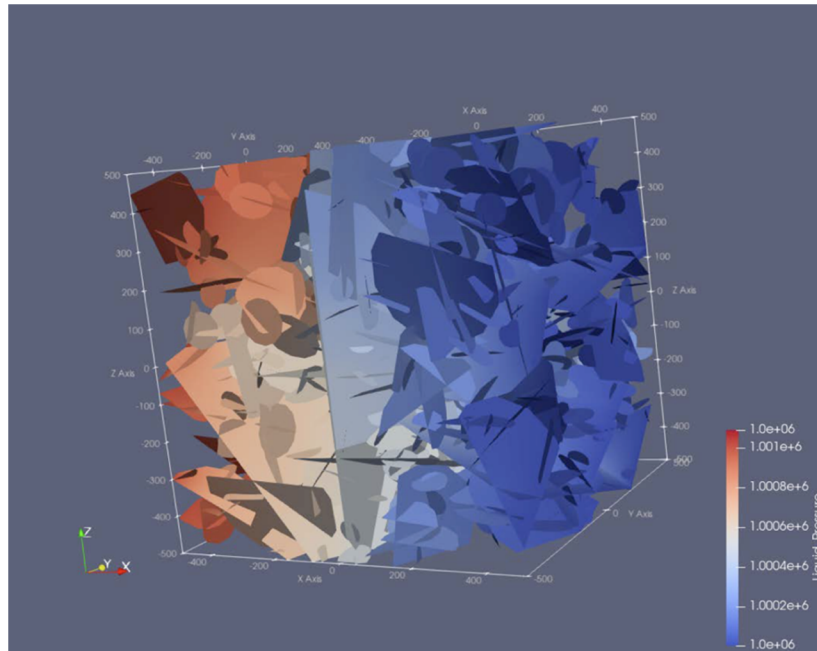
Figure 6.9-3. Steady state fluid pressure distribution for 4-fracture DFN with stochastic fractures.

Tracer breakthrough curves, obtained by the SNL team, are shown in Figure 6.9-4. Adding stochastic fractures to the domain creates a delayed breakthrough time in the four-fracture simulations: the breakthrough occurs at about 2.5 years for the DFN and at about 8 years for the ECPM, where the curves deviate from the four-fractures only breakthrough curve.
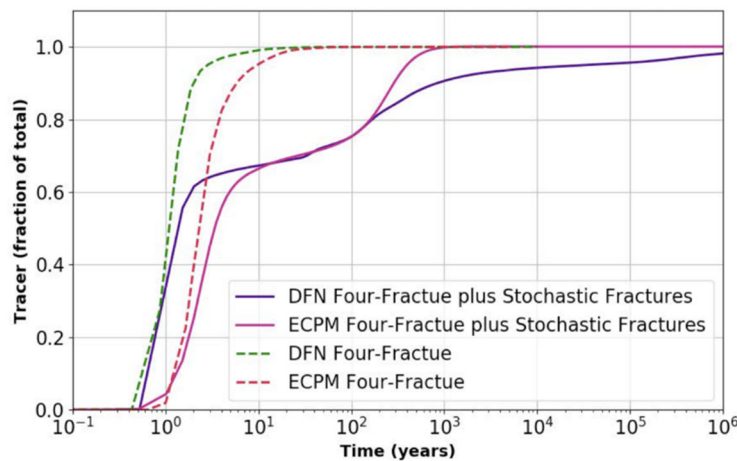
Figure 6.9-4. Breakthrough curve comparison of 4-Fracture DFN and 4-Fracture DFN with stochastic

The next step is for all teams to move on to a full PA model of a geologic repository. Modeling will be conducted for a domain size of 5 x 2 x 1 km^3. The first step will be to model transport with a uniform source term placed across the repository; this will enable teams to identify fast flow paths. Next, waste packages will be placed at the shortest distance to the preferential flow paths. Around 2,500 waste packages will be simulated, and ~50 waste packages will be assumed to fail after a specified amount of time. Vertical emplacement rather than horizontal will be used. Both concentration and flux values will be used to perform a comparison of simulations conducted by different groups.

6.9.2.2. Salt Reference Case

The international teams involved in Task F spent considerable effort in FY21 to define a detailed reference case for a generic repository in a salt formation based on reference cases previously published in the United States (bedded salt), Germany (bedded and domal salt), and the Netherlands (domal salt). PA simulations will be conducted assuming a disturbed scenario in which shaft seals fail 1,000 years after repository closure, allowing an influx of brine down the shafts and into the repository. Teams developed a staged approach for salt PA modeling, building up to a full PA. The following stages are envisioned: (1) flow + radionuclide mobilization and transport, (2) drift convergence added, (3) heat flow and temperature-dependence of drift convergence added, (4) model uncertainty added, and possibly (5) gas transport added. Details are given in LaForce et al. (2021, Section 2.2). Some basic information on the salt reference case are summarized below.

The salt reference case for a domal salt considers a mined repository for spent nuclear fuel and vitrified high-level waste. The repository is mined at a depth of 850 m below the ground surface. The generic geological cross section of a salt dome developed for another project (Bertrams et al., 2020b) was simplified to six homogeneous geologic units to simulate in this reference case (Figure 6.9-5). It is assumed that the salt dome geometry extends for 9 km perpendicular to the plane of the cross section. The ground surface is at about 50 m above mean sea level (absl) and the top of the salt dome is roughly at -150 m absl. The base of the salt dome is at -3,150 m, and is underlain by basement rock, extending to the base of the section at -5,500 m. Hydrologic, mechanical, and thermal properties of the geologic units are given in Section 2.2.4 of the report by LaForce et al. (2021). Modeling teams are expected to consider different conceptual models and parameterization and to choose individual process models for benchmarking and comparison (i.e., salt creep, crushed salt reconsolidation, thermal conduction).
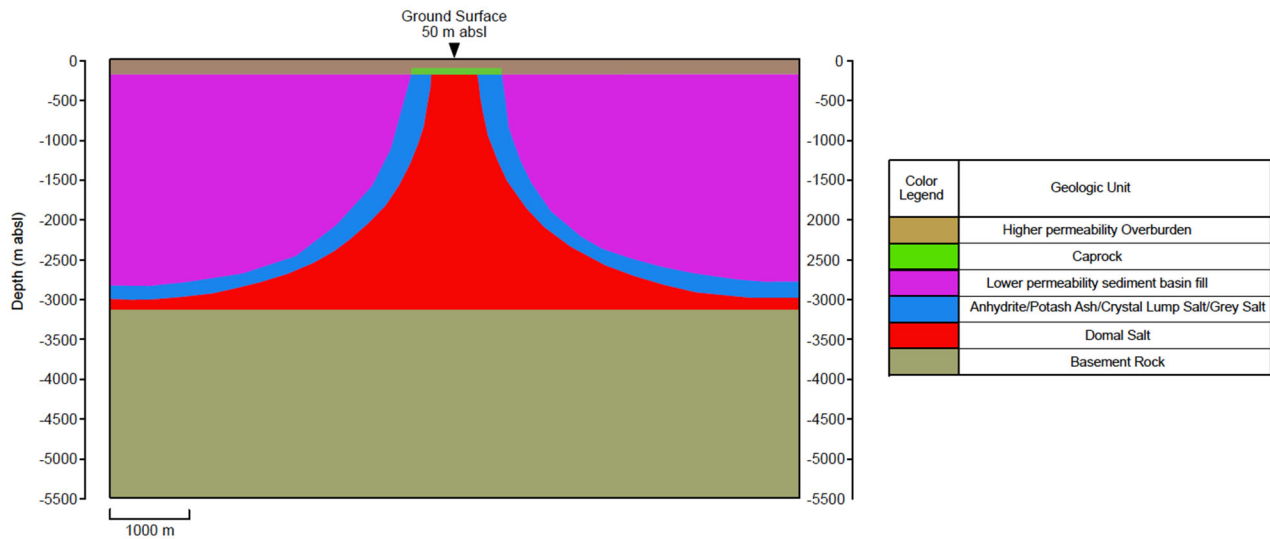
Figure 6.9-5. Geological cross-section with model units for the generic salt reference case. The model units are simplified from Bertrams et al. (2020b). The repository is at a depth of -850 m in the domal salt.

Figure 6.9-6 shows the assumed repository layout for the reference case. The repository is accessed by two vertical shafts extending through the cap rock and to the surface to the salt dome formation. The access shafts are designed based on the design of the shaft seal as it is specifically engineered to be an effective seal within a salt formation. Within the repository there are three sets of 25 emplacement drifts with a drift spacing of 35 m. For heat-generating waste, the waste package spacing is 3 m end-to-end. Each emplacement drift is 90 m long with a total of 10 waste packages per drift, and a total is 500 POLLUX-10 waste packages.

The vitrified waste emplacement area consists of 25 emplacement drifts with 35 m drift spacing, each drift containing 10 vertical boreholes with a center-to-center spacing of 4.5 m in an emplacement drift 45 m long

with two waste packages per borehole, and a total is 500 vitrified waste packages. The spacing of the drifts and waste packages is sufficient to ensure that the peak temperature would not exceed 100°C. The dimensions of drifts within the repository are the same, at 7 m width and 4 m height. The infrastructure has a total volume of 240,000 m³, with dimensions of 240 m × 250 m × 4 m. The infrastructure is utilized during the construction and emplacement phases of disposal. During the post-closure phase, this area is filled with gravel to allow for excess fluid or gas buildup to accumulate. A detailed description of specifications for the reference case, such as spent nuclear fuel waste forms, waste container, vertical emplacement borehole, and a shaft design are provided in Section 2 of the report by LaForce et al. (2021).
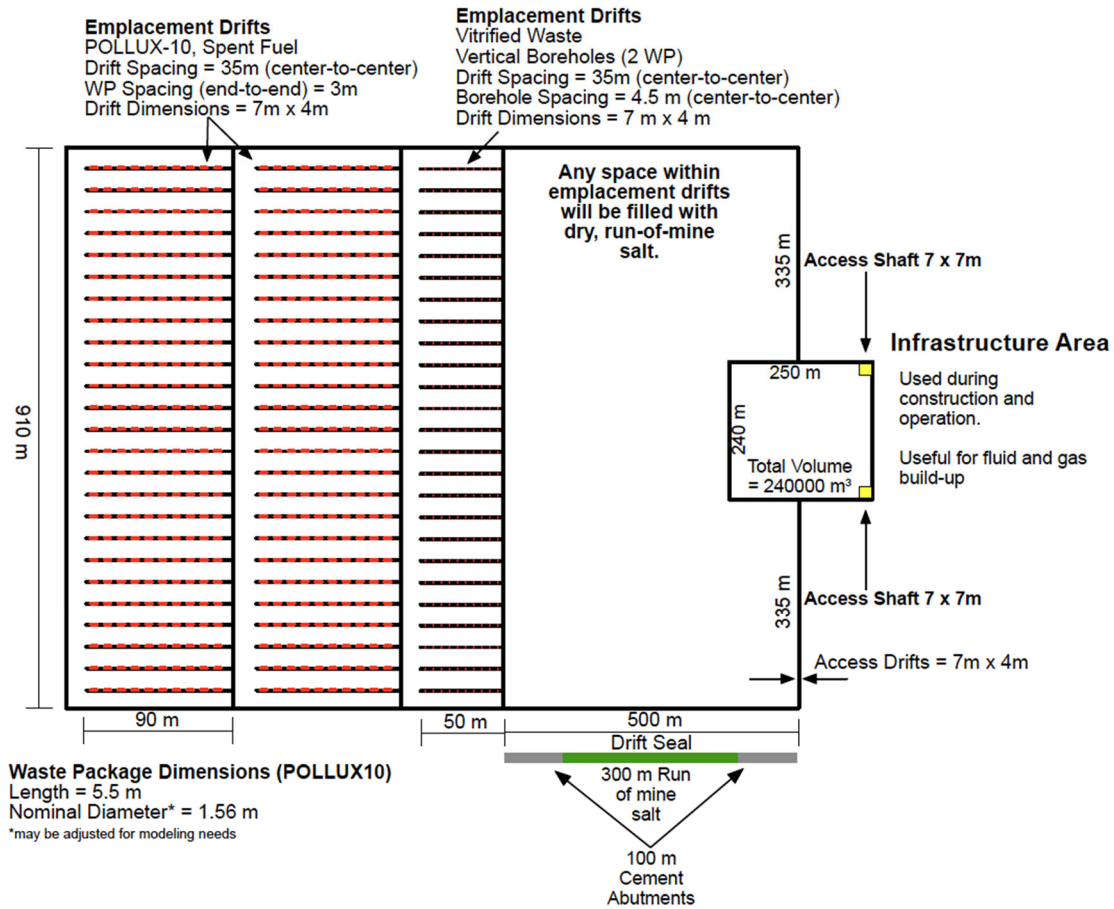
Figure 6.9-6. Schematic of the waste repository layout in a generic salt dome reference case.

6.9.3. Thermodynamic and Thermochemical Database Development

Thermodynamic and thermochemical data are essential for understanding, evaluating, and modeling geochemical processes, such as speciation solubility, reaction paths, or reactive transport. The data are required to evaluate both equilibrium states and the kinetic approach to such states. However, existing thermodynamic databases are often limited and do not span the range of conditions that may exist under the various generic repository scenarios (argillaceous, crystalline, salt, etc.). For example, previously developed thermodynamic data overstate the stabilities of smectites and illites. While this is adequate for both tuff and salt host rock, the databases have some deficiencies with respect to other repository designs, such as those in clay/shale, or those that include a bentonite buffer.

In FY21, SFWD scientists from LLNL have continued to collaborate with the international research community to improve thermodynamic and thermochemical databases across various physicochemical conditions relevant to subsurface repository environments (Zavarin et al., 2021a,b). The development and implementation of equilibrium thermodynamic models are intended to describe relevant chemical and physical processes for radionuclide transport such as solubility, sorption, and diffusion. The following activities were conducted:

- LLNL scientists have continued participating in the international NEA Thermochemical Database (TDB) Project through the support of Dr. Atkins-Duffin as the SFWST representative for international thermodynamic database development effort (Section 6.9.3.1). This effort ensures that PA modeling efforts in the U.S. are aligned with internationally accepted practices for repository PA calculations.

- LLNL continued its effort to produce an interactive software tool to help manage thermodynamic database files as new and improved data become available. A short code was written with the goal of importing new data and exporting formatted databases for use in Geochemists Workbench, PHREEQC, EQ3/6, and other reactive transport codes (Section 6.9.3.2).

- As part of LLNL's international engagement with surface complexation model development, FY21 efforts included the assimilation of sorption data collected by the JAEA. These data are in the process of being incorporated into LLNL's sorption database that will increase to approximately 35,000 individual measurements (Section 6.9.3.3).

- Finally, LLNL scientists continued their collaboration with colleagues from the Helmholtz Zentrum Dresden-Rossendorf (HZDR) in Germany to develop sorption databases with particular focus on radionuclide (e.g., Cs, Sr, U, Np, and Pu) sorption to clay minerals (Section 6.9.3.4).

6.9.3.1. Activities in Support of NEA's Thermochemical Database Program

The NEA-TDB was conceived of and initiated to (1) make available a comprehensive, internally consistent, internationally recognized database of selected chemical elements; (2) meet the specialized modeling requirements for safety assessments of radioactive waste, and (3) prioritize the critical review of relevant data for inorganic compounds and complexes containing actinides. Data from other elements present in radioactive waste are also critically reviewed together with compounds and complexes of the previously considered elements with selected organic ligands.

Phase I of the NEA-TBD program started in 1984. In February 2019, program entered its Phase VI with all participating member parties signing the Framework Agreement. Dr. Atkins-Duffin as the SFWST long-term representative for international thermodynamic database development efforts played an important role in the planning and execution of this new phase. She also serves as the Executive Group (EG) liaison to the TDB Cements team and will help coordinate the completion of the Cements report.

6.9.3.2. *Software Development to Manage Thermodynamic Databases*

To facilitate seamless integration between SFWD's thermodynamic database and international thermodynamic database compilations (e.g., the NEA-TDB radiochemical thermodynamic data), LLNL continued to create software to help manage thermodynamic database files as new and improved data become available (Zavarin et al., 2021a). The software will ensure that new data are added to databases correctly, conveniently, and consistently with existing data, and in a form immediately useful for reactive transport modeling. The product data files will be made available to all users wanting to use the new thermodynamic data in their modeling calculations. For example, the latest NEA data will be made available for most of the widely used modeling codes. The software itself will be made available to users wanting to create a custom data file for their specific needs. The task consists of two main subtasks:

1. Create a method to add thermodynamic data for new species, or replace thermodynamic data for existing species to the existing database, and

2. Produce a new data file for the user-specified reaction path code (e.g., PHREEQC, EQ3/6, GWB) that contains the new or modified data formatted for the reactive transport code of choice.

LNNL completed most of these tasks. The new software tool is built around the original SUPCRT data base and now is referred to as SUPCRTBL. The tool is meant to be used by someone wanting to add new data to SUPCRT and ensure that it is internally consistent with the existing data. The code will produce a new version of the data file needed to run any of several reactive transport codes. The SUPCRT data file is generic and universal in the sense that it contains the most common species (aqueous, solid, and gaseous) for the elements commonly used in modeling aqueous systems. These data were obtained from critically reviewed sources. For most user applications, it is anticipated that these data will not be further modified as they are considered the best available. The next step is to create a graphical user interface (GUI) to allow a user to (1) input new or revised data into the SUPCRT database, and (2) create a data file with a user specified set of species.

6.9.3.3. *Japanese Atomic Energy Agency K_d Database Assimilation Effort*

In an effort to build an open-source database of raw sorption data for use in nuclear waste PA models, LLNL recently reached out to the JAEA colleagues and began the process of assimilating JAEA's large database of sorption data into the LLNL's database. The JAEA K_d database is a web-based open-source database (https://migrationdb.jaea.go.jp/nmdb/db/sdb/search_1.jsp) that contains nearly 70,000 K_d data (Zavarin et al., 2021a, Table 1) and also comprises information on both rock and single mineral sorption data. The database spans a wide range of radionuclides relevant to the nuclear waste programs (Zavarin et al., 2021a, Table 2). However, a number of issues needed to be resolved for use in surface complexation/ion exchange database development being pursued at LLNL. Key issues to resolve included the following:

- Conversion of electrolyte composition into units compatible with the LLNL SCIE (mol/L),

- Conversion of gas composition alphanumeric strings into gas fugacity values,

- Conversion of various alphanumeric strings (value ranges, "<" and ">" values, etc., into numbers,

- Conversion of K_d data into aqueous and sorbed radionuclide concentration.

A Jupiter notebook was developed with ~500 lines of python code to perform the necessary reformatting of the JAEA database and allow for the assimilation of JAEA data into the LLNL database. In this first effort to assimilate JAEA data, nearly 17,000 single mineral data were converted into the LLNL format. This nearly doubles the number of data that are now available to the surface complexation/ion exchange and machine learning database development efforts.

In FY22, LLNL will pursue a more detailed evaluation of JAEA K_d data quality and examine whether additional data can be mined from the JAEA database for other SFWD PA purposes. For example, there are significant amount of data for rock and engineered materials that may be relevant to the SFWD program. LLNL scientists will engage directly with the JAEA database group (Dr. Yukio Tachi, Radionuclide Migration Group lead) to facilitate further data evaluation efforts in FY22.

6.9.3.4. Sorption and Surface Complexation Databases with German Partners

In FY21, LLNL continued its long-term collaboration with international partners on development of sorption and surface complexation databases (Zavarin et al., 2021b). Of particular importance is the collaboration with sorption database development group at the German Helmholtz Zentrum Dresden Rossendorf, HZDR, where the RES³T project is conducted, which is an ongoing effort to develop a digital open-source thermodynamic sorption database.

In FY20, LLNL's activities focused primarily on building out an Access database of raw sorption data and developing a framework for surface complexation/ion exchange data fitting methods and surface complexation/ion exchange database development. LLNL efforts were coordinated with international partners involved in similar database development efforts (e.g., HZRD RES³T). In FY20, ~24,000 data were captured, including literature data, as well as digitized data from the RES³T partners. The focus was on radionuclide (Cs, Sr, U, Np, and Pu) sorption to clay minerals (with particular focus on bentonite/montmorillonite).

In FY21, LLNL pursued several data mining methods to support development of a surface complexation/ion exchange constant database from primary sorption data. A key component of that effort was the automation of commercially available fitting routines (e.g., PEST) that can be linked to surface complexation/ion exchange codes and produce optimized constants/parameters and associated parameter uncertainties. The scripts needed to perform this automation were originally implemented in Access and were translated into R and Python scripts that are much more flexible and adaptable. Of particular interest is the expansion of data interrogation effort by applying modern data science methods (e.g., machine learning). The combination of machine learning approaches with more traditional PEST/PHREEQC data fitting approaches provides flexibility to PA modeling efforts (e.g., use of mechanistic surface complexation/ion exchange models versus smart K_d lookup tables).

A significant challenge to developing a universal approach to surface complexation models (SCM) and associated reaction constants has been the absence of a universal framework to mine, compile, and analyze the massive numbers of sorption data available in the literature, and to test different SCMs across these common datasets. Analyzing these large sorption datasets has also been limited by the lack of access to digitized literature data and the lack of common standards and approaches to archiving these data types (i.e., findable, accessible, interoperable, reusable [FAIR] data, Wilkinson et al., 2016). The materials science community has been on the forefront of applying machine learning to the mining of scientific literature. As data mining approaches are applied to experimental geochemistry, data mining/data driven approaches will fundamentally change how predictive tools quantify uncertainty, impacts, and risks associated with the reactive transport of contaminant and nutrients in Earth systems. LLNL's approach is based on principles of FAIR data that allows a SCM database to evolve with SCM constructs and reactive transport modeling codes. Figure 6.9-7 presents an overview of the data mining/data driven workflow for the SCM database development. Further details on this workflow are given in Zavarin et al. (2021).

In FY22, focus will be on the buildout of a large set of surface complexation and ion exchange reactions constants for radionuclides and minerals of interest to nuclear waste repository PA. Research will also focus on the expansion of the data interrogation effort by applying modern data science methods. The effort will include testing of various surface complexation (non-electrostatic, diffuse layer, etc.) and ion exchange (Vanselow, Gapon, etc.) models, and will provide a path for incorporation of surface complexation/ion exchange reaction constants into the repository PA models. Further refinement of the surface complexation reaction stoichiometries may be warranted in the long-term and can be readily introduced with the inclusion of spectroscopic evidence from the literature.
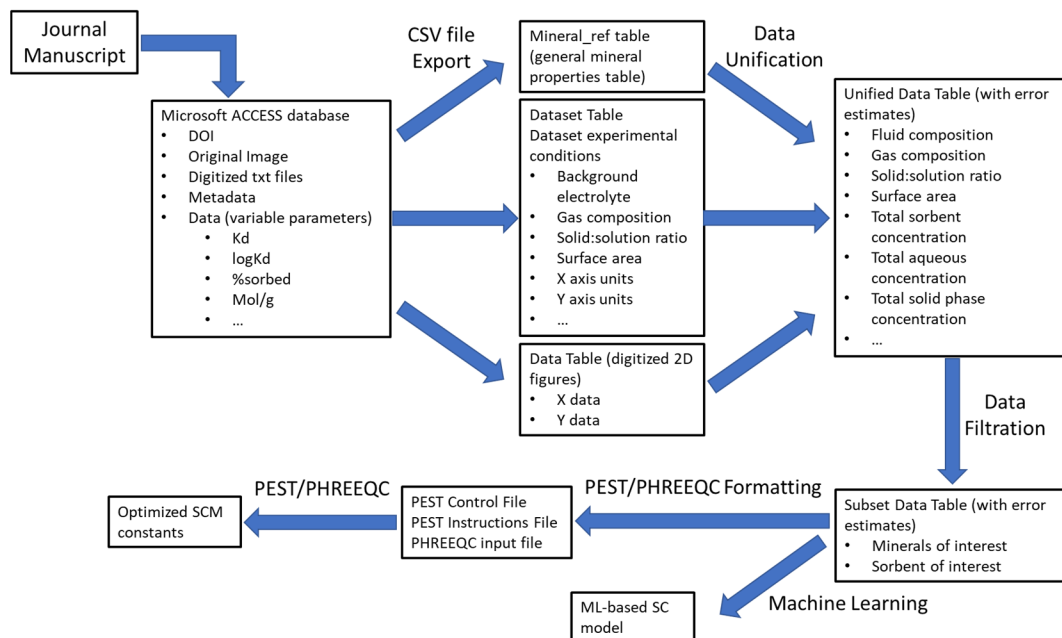
Figure 6.9-7. Workflow describing the process from of data digitization, incorporation into the LLNL SCIE database, unit conversion and data unification, data filtration, data formatting, the SCM reaction constant fitting.

7. SUMMARY AND CONCLUDING REMARKS

This report describes the FY21 status of international collaboration focused on investigations of nuclear waste disposal in geological formations as part of the DOE SFWD Campaign. Since 2012 the SFWD program has been advancing active collaboration with several international geologic disposal programs in Europe, North America, and Asia. The joint research activities with international programs, initiatives, and projects are extremely beneficial to SFWD's disposal research program: (1) they provide first-hand access to the decades of experience that our international partners have gained in various disposal options and geologic environments; (2) they give SFWD scientists a large library of experimental data from many past and ongoing *in-situ* tests conducted in several URLs in different host rocks; (3) they provide a framework for active peer-to-peer research participation in international groups that conduct, analyze, and model performance-relevant processes; and (4) they open the door to conducting SFWD *in-situ* experiments in international URLs not available in the U.S. Last not least, international collaboration allows the SFWD Campaign to benefit from substantial international investments in research facilities (such as underground research laboratory testing and modeling) and achieve cost savings via joint funding of expensive field experiments.

The first part of this report provides an in-depth overview of the various opportunities for active international collaboration available to SFWD researchers, with a primary focus on those opportunities that involve field experiments in international URLs. Section 3 of this report contains a summary of currently existing international opportunities resulting from DOE's formal partnership in collaborative initiatives: the Mont Terri Project, the DECOVALEX Project, the Colloid Formation and Migration Project (CFM), the FEBEX Dismantling Project, the HotBENT Project, and the SKB Task Forces, which are multinational initiatives with emphasis on field experiments in international URLs. Other multinational initiatives, the NEA Clay Club, Salt Club and Crystalline Club, the NEA Thermochemical Database Project, the NEA Repository Metadata Project, the NEA Data and Knowledge Management Group, and some European Union research programs, provide opportunities for information exchange and data assessment. In addition to its extensive cooperation with multiple international organizations under the umbrella of above-listed initiatives, the SFWD program has also explored direct bilateral opportunities for active research collaboration, with institutions from in Korea, Germany, Sweden, Israel, France, Japan, Belgium, Finland, Czech Republic, and China. As described in Section 4, some of these bilateral opportunities (e.g., Republic of Korea, Germany, Sweden, Israel) have already resulted in close collaborative research activities between SFWD scientists and their international counterparts; the others provide opportunities for active research collaboration in the future.

Over the years, as research priorities have changed and new opportunities for collaboration developed, SFWD's international research portfolio has evolved and will continue to evolve. The SFWD program has made a targeted effort to reassess its international collaboration activities on a regular (annual) basis. Section 5 describes the continued planning process that (1) re-evaluates ongoing international research activities, (2) evaluates the technical merit of new collaboration opportunities, and (3) makes revisions to the overall portfolio of international R&D activities as appropriate. Given its importance within the overall portfolio of disposal research activities, any such planning and prioritization is done in tight integration with all other disposal research areas, e.g., the host-rock specific research portfolios, the EBS research portfolio, and the performance assessment research portfolio. The section also gives a brief high-level overview of the major R&D themes and international experiments that SFWD researchers have participated in since 2012, either as active members of the experimental team, or as researchers involved in the interpretative evaluation and modeling of the experimental data.

Section 6 gives a detailed description of specific FY21 research activities in the SFWD campaign that have been conducted under the umbrella of the international collaboration projects introduced earlier. The comprehensive list of research activities described in this section attests to the fact that SFWD researchers have made very good use of these opportunities and that international collaboration activities now form a considerable portion of the campaign's disposal research program. International collaboration is a prominent element of key work packages in the SFWD disposal research program, in particular in the EBS, Crystalline, Argillite, and Salt Work Packages, and more recently also in the GDSA Work Packages. Therefore, international collaboration in a balanced portfolio of relevant R&D challenges addresses such important

research areas as engineered barrier integrity, near-field perturbations, radionuclide transport, integrated system behavior, performance assessment, and methods for characterization and monitoring of engineered and natural barriers.

Substantial scientific and technical advances have been made over the past years. The joint R&D with international researchers, the worldwide sharing of knowledge and experience, and the access to data for field and laboratory experiments from a variety of URLs and host rock have helped SFWD researchers significantly improve their understanding of the current technical basis for disposal in a range of potential host-rock environments. SFWD scientists have utilized data and results from laboratory and field studies that have been and are being conducted with millions of R&D investments provided by international partners. Advanced simulation models have been verified and validated against these experimental data, providing a robust modeling and experimental basis for the prediction of the complex processes defining the performance of a multi-barrier waste repository system. In addition, international scientists have contributed to the analysis and interpretative modeling of laboratory or field studies performed by SFWD, such as the HotBENT Lab Experiment and the BATS field experiment. Comparison of model results with other international modeling groups, using their own simulation tools and conceptual understanding, has enhanced confidence in the robustness of predictive models used for performance assessment. In addition, the possibility of linking model differences to particular choices in conceptual model setup has provided valuable guidance into "best" modeling choices and understanding the effect of conceptual models on predictions. Such advances in the ability to make long-term predictions of complex coupled THMC and flow and transport processes contribute directly to improved post-closure performance assessments (PA) models. In the SFWD campaign, the work packages for international collaboration, for generic research on EBS and host-rock specific topics, and for performance assessment are well integrated to make optimal use of improved process models leading to better safety assessments models. On a general level, international collaboration has allowed for engagement of U.S. researchers with the international waste management R&D community in terms of best practices, new science advances, state of the art simulation tools, and lessons learned, and has provided ample opportunity for training/educating junior staff to move a disposal program forward into the next decades.

Below are brief highlights of selected research areas where international collaboration has resulted in significant scientific advances that are relevant not only to SFWD's disposal program but also to the broader radioactive waste management and disposal community.

Progress Related to Understanding of Coupled Processes and Alterations in Bentonite-Based Engineered Barrier Systems (Section 6.1)

Collaborations with the international FEBEX-DP and HotBENT projects involve experimental and modeling studies to better understand temperature-dependent perturbations and alterations in engineered barrier materials. These activities have provided valuable insights as to how repository performance may be affected by these perturbations and alterations.

- Participation in the large scale FEBEX *in-situ* heater and its comprehensive dismantling effort after 18 years of operation has significantly enhanced the understanding of the thermal alteration of EBS materials at moderate disposal temperatures (up to 100ºC), and has led to the development of validated THMC simulation tools for long-term EBS integrity predictions.

- Two different modeling activities were conducted based on the FEBEX-DP data, including detailed THMC simulations over 18 years of heating to better understand long-term integrity of heated bentonite, and massively parallel TH modeling of the FEBEX test as part of SKB's EBS Task Force acivities.

- Continued analysis of post-mortem FEBEX-DP bentonite samples provided a sound basis for understanding potential EBS property changes as a result of THMC alterations. Microstructural analysis of FEBEX bentonite samples was conducted using thermogravimetric analysis and differential scanning calorimetry. Diffusion and sorption experiments were performed on FEBEX bentonite materials to investigate whether 18 years of heating would lead to changes in radionuclide

transport behavior. Furthermore, microbial experiments were designed and conducted to determine whether bentonite materials collected from the FEBEX experiment possess microbial communities capable of metabolizing H_2, and how thermal alterations impact those capabilities.

- After years of planning, preparation and construction, the full-scale HotBENT field experiment started its heating phase on September 9, 2021. HotBENT will test bentonite behavior at much higher temperatures (up to 200ºC) relative to those that were achieved in the FEBEX heater test, to examine whether the maximum temperature in a bentonite-backfilled repository can be raised to this level without strong performance impact. SFWD scientists continued predictive modeling activities for the HotBENT experiment and also conducted several laboratory column heater experiments called HotBENT-Lab to complement the field study.

- Hydrothermal autoclave experiments were conducted with focus on bentonite alteration, swelling and erosion to better understand implications for colloid transport. These processes are important for the safety assessment of bentonite as a barrier material in high-level radioactive waste repositories, and both are linked to international collaboration efforts conducted in the CFM and FEBEX projects at the Grimsel Test Site.

Progress Related to Understanding Interfacial Processes Between EBS and Host Rock Materials (Section 6.2)

Several international collaboration studies made important progress in evaluating interfacial reactions between EBS components and host rock materials. Materials alterations in the vicinity of these interfaces can affect repository performance in multiple ways, for example by changing the flow and transport properties for radionuclides to migrate from the engineered into the natural barrier systems. Interfacial reactions are most prominent early in the lifetime of a repository, when EBS materials such as bentonite, metal containers, and cementitious materials have just been emplaced and when thermal-hydrological perturbations remain strong.

- Hydrothermal laboratory studies were conducted to evaluate high-temperature impacts on interfacial processes and alterations, considering multiple EBS materials in contact with crystalline rock (Grimsel granodiorite from the Grimsel Test Site), argillaceous rock (Opalinus Clay from Mont Terri), and carbonate rocks (limestone and marl from Israel).

- Reactive transport simulations were initiated to interpret interfacial reactions and their impact across aged bentonite, concrete/cement, and clay rock interfaces. This activity is aligned with the international CI experiment, which probes diffusive transport across materials emplaced in a borehole at the Mont Terri URL about 14 years ago.

Progress Related to Understanding THM Processes in Heated Argillaceous Rock (Section 6.3)

Through international research collaborations and access to several *in-situ* heater experiments, SFWD scientists made significant scientific advances in understanding and predicting the thermo-hydro-mechanical (THM) perturbations occurring in argillaceous host rock after emplacement of heat-emanating radioactive waste.

- The full-scale FE heater test at Mont Terri, now in its 7th year of heating, continues to provide valuable data for comparative THM model testing and validation at a relevant scale.

- High-performance modeling approaches were developed as part of a DECOVALEX-2019 task that allow for simulations of THM processes at the scale of an entire repository while ensuring that the computational load remains manageable.

- The same DECOVALEX-2019 task evaluated upscaling approaches for THM modeling, from small-scale laboratory tests to intermediate- to full-scale field testing all the way to repository-scale predictions. Working with their international partners, SFWD scientists demonstrated that most model input parameters for argillite host rock can be up-scaled from laboratory data, but certain parameters, such as those for the excavation disturbed zone, are best characterized *in-situ*.

- The ability to simulate processes and mechanisms of fracture initiation and growth in claystone, identified as an emerging modelling challenge due to the potential for gas-pressure or thermal damage, is now being tested as a new task in the international DECOVALEX-2023 project. The primary focus of this task is predictive and interpretative modeling of a recent *in situ* experiments conducted at ANDRA's Bure URL.

Progress Related to Gas Transport in Bentonite and Clay-Based Host Rock (Section 6.4)

Gas generation from canister corrosion and other processes can impact the performance of a geological disposal facility in several ways: The gas-water interfaces serve as an important vehicle for the transport of radionuclides and microorganisms due to preferential flow and preferential sorption, whereas trapped gas bubbles can cause immobilization of radionuclides. Local pressure build-up due to gas production and accumulation can trigger mechanical responses such as deformation or fracturing in low-permeability materials like bentonite and clays. Significant progress was made in understanding the short- and long-term processes involved in the generation and migration of repository gases.

- Modeling studies of gas migration laboratory experiments on compacted clay were conducted under the umbrella of the international DECOVALEX-2019 project. The purpose of these studies was to better understand the processes governing the gas migration in low permeability clay barrier materials and developing new numerical representations for the quantitative prediction of gas fluxes.

- International teams including SFWD scientists compared a suite of novel prediction approaches for gas migration and identified which ones could best capture the complex phenomenological behavior of gas flow through bentonite.

- With promising simulation methods developed and tested against laboratory experiments, SFWD scientists and their international partners are now testing their predictive capabilities at the field scale, under the umbrella of a new gas-migration task in the DECOVALEX-2023 project. After conducting a blind prediction exercise, teams will soon move on to modeling of the Large-Scale Gas Injection Test (LASGIT) conducted at the Äspö Hard Rock Laboratory in Sweden.

Progress Related to Modeling Coupled Processes, Fluid Flow and Transport in Fractured Crystalline Rock (Section 6.5)

As hard competent rocks, crystalline formations are often fractured; thus, repository performance assessment studies require an understanding of (1) the impact of stress changes and other perturbations on fracture properties, and (2) the large-scale transport patterns of radionuclides potentially migrating in fracture networks from the repository to the biosphere. Two international collaboration activities have made great progress in addressing these challenges.

- Task G of the DECOVALEX-2023 project involves hydromechanical modeling of fracture contact mechanics upon shearing. International teams are simulating laboratory-scale experiments that are currently being conducted to link micro-scale THMC effects acting on fracture surfaces with emergent fracture properties such as permeability.

- Under the umbrella of the SKB Task Forces, SFWD scientists performed discrete fracture network (DFN) modeling efforts to characterize the impact of network structure on flow, transport, and fluid-fluid reactive transport. The ability to conduct reactive transport simulation at large fracture network scales has been enabled by the development of new high-performance computing methods.

Progress Related to Coupled Processes in Salt (Section 6.6)

A broad portfolio of international collaboration activities has resulted in significant advances regarding the understanding of mechanical, hydrological, thermal and chemical processes in both domal and bedded salt.

- Collaborative research with German institutions included: (1) the analysis of drift closure in the joint project WEIMOS, (2) the assessment of geotechnical barriers in salt in the collaborative project

RANGERS, and (3) the improvement of THM modeling for crushed salt (used as backfill for repository tunnels) in the joint KOMPASS project.

- SFWD scientists are now leading a new task in the international DECOVALEX-2023 project which comprises several modeling steps associated with the Brine Availability Test in Salt (BATS) at WIPP. This will allow SFWD to benefit from the engagement of international partners in the analysis and modeling of brine migration in heated salt.

Progress Related to Characterization of Faults as Potential Transport Pathways (Section 6.7)

Via field-based and simulation-based research, SFWD scientists made important advances in understanding whether faults in low-permeability host rock can become potential radionuclide migration pathways upon activation from thermal pressurization or gas pressure increase.

- SFWD scientists continued their advanced numerical analysis of the 2015 and 2020 fault reactivation experiments conducted at the Mont Terri URL to explore the link between fault zone complexity, fault deformation, and permeability change. The close integration of *in-situ* experiments and modeling resulted in important model improvements and provided a better understanding of the hydromechanical behavior of minor faults and fractures.

- Several international partners contributed to new investigations of fault deformation in the Mont Terri URL to investigate the long-term sealing and healing of faults after an initial activation and permeability increase.

Progress Related to Characterization of Fractured Crystalline Rock (Section 6.8)

A key concern relating to geologic disposal is fractured crystalline rock is the presence of potentially conductive fractures that could result in transport of radionuclides. There is a need for improved hydrological, geophysical, and geochemical site characterization techniques, especially to detect flowing fractures and their hydrogeologic properties, as this will allow for the development of better constrained discrete fracture network (DFN) models.

- In a research cooperation with the "Collisional Orogeny in the Scandinavian Caledonides" (COSC) project in Sweden, a deep borehole was used as a testbed for an advanced downhole probe developed by SFWD scientists/ The probe, referred to as SIMFIP, allows identifying flowing fractures, evaluating their hydromechanical properties, and estimating the state of stress in the subsurface.

- The workflow for the characterization of fractured rock via borehole studies as demonstrated at COSC provides a promising blueprint for *in-situ* testing across various potential repository sites, in particular in crystalline host rock.

Progress Related to Performance Assessment (Section 6.9)

Recognizing the importance of building confidence in the models, methods, and software used for performance assessment (PA) of deep geologic repositories, SFWD researchers have increased their international collaboration in this area.

- In Task F of the DECOVALEX 2023 project, confidence in performance assessment models and methods is enhanced by comparing PA modeling results from ten international disposal programs applied to the same reference cases. The task, which is led by SFWD's GDSA team, investigates two generic reference cases in parallel: a repository for commercial spent nuclear fuel (SNF) in a fractured crystalline host rock and a repository for commercial SNF in a bedded salt formation.

- Radionuclide transport simulations are a central component of any performance assessment model, as these evaluate transport from the repository to the biosphere for dose calculations. Continued collaboration with the international research community led to significant improvement of thermodynamic and thermochemical databases and models that evaluate the stability of EBS

materials and their interactions with fluids at various physicochemical conditions relevant to subsurface repository environments.

SFWD scientists have frequently presented technical highlights from international collaboration activities at international conferences and symposia, to engage with the broader radioactive waste management and disposal sciences community, as well with the other geoscience fields. For example, the DECOVALEX 2019 Symposium on Coupled Processes in Radioactive Waste Disposal and Subsurface Engineering Applications, co-organized by SFWD researchers, was held in Brugg, Switzerland, November 4-5, 2019 (http://decovalex-coupled-processes-symposium.org/). A dedicated session on international collaboration organized during the "International Conference on Coupled Processes in Fractured Geological Media – COUFRAC" (held in Seoul, Korea, November 11-13, 2020) focused on recent advances from the nuclear waste disposal field and many other applications. SFWD's international research activities also presented at a public workshop organized by the U.S. Nuclear Waste Technical Review Board (NWTRB), dedicated to "Recent Advances in Repository Science and Operations from International Underground Research Laboratory Collaborations" (April 24-25, 2019 in San Francisco, see https://www.nwtrb.gov/meetings/past-meetings/spring-2019-workshop-april-24-25-2019). The workshop report developed by the NWTRB provides an excellent summary of international activities and the critical role of underground research laboratories (NWTRB, 2020).

Going forward, international collaboration will continue to be an important cross-cutting campaign activity within the SFWD campaign, in particular with regards to opportunities involving *in-situ* experiments in underground research laboratories across a range of geologic systems. SFWD leadership recently discussed the five-year direction of the campaign and developed a five-year plan that serves as a strategic guide to the work within the disposal research R&D technical areas (i.e., the control accounts), focusing on the highest priority technical thrusts (Sassani et al. 2020, 2021). The plan defines a comprehensive list of near-term to mid-term goals for international collaboration as a central element of the campaign's disposal research (see summary in Section 5). There are ample opportunities to expand on the current portfolio of international research, several of which are mentioned in this report. The five-year plan also discusses the integration of international activities across other control accounts, including performance assessment modeling, where the joint modeling and comparative analysis of complex *in-situ* experiments can ultimately lead to better predictive models and thus directly contribute to confidence building of PA predictions. As long-term topics, the plan identifies the potential value of international collaboration in (1) developing best practices and technologies for site selection and characterization and (2) utilizing international activities for the training/education of junior staff. Both of which are areas the campaign seeks to pursue in the next three to five years.

The five-year plan in Sassani et al. (2020; 2021) furthermore calls for DOE to consider moving from a mostly participatory role in ongoing *in-situ* experiments conducted by other nations to a more active role in conducting its own experimental program in international URLs. The advantage of active planning is obviously that the experimental focus and design can be better tailored to the campaign needs. Some collaborative initiatives like the Mont Terri Project provide their partner organizations with the opportunity of conducting their own experimental work and inviting other partners to join. This option would allow the U.S. disposal program to lead targeted *in-situ* field activities in representative host rocks, even though there are currently no operating underground research laboratories in clay or crystalline host rock environments in the U.S.

While there are no immediate plans for DOE to conduct its own experiments in international URLs, SFWD's disposal program has already started taking a much more active approach in shaping the future R&D portfolio of the international initiatives it has joined as a partner. For example, with Jens Birkholzer of LBNL as Chairman of the international DECOVALEX Project, SFWD scientists have been instrumental in the definition and selection of tasks for the current DECOVALEX-2023 project, and are now leading two of the seven modeling tasks, one focusing on the BATS heater test at WIPP, and one comparing different performance assessment approaches. In addition, DOE has co-developed with international partners the planning and design of the HotBENT Project, the full-scale high-temperature heater experiment at the Grimsel Test Site that after a year of planning and construction just entered its operational phase. Complementing the HotBENT field work, SFWD researchers are also leading a modeling task in the SKB EBS Task Force, which at its center has a high-temperature column experiment conducted at LBNL.

8. REFERENCES

8.1. List of the FY 21 Feeder Reports Used in Preparation of the Current Report

Caporuscio, F.A., Sauer, K.B., and Rock, M.J. (2021), Engineered Barrier System R&D and International Collaborations – LANL – FY21, SF-21LA01030801 Rev. 2, SF-21LA01030802 Rev. 2,Los Alamos National Laboratory, LA-UR-21-28735.

Guglielmi, Y., Hu, M., Chang, C., Cook, P., Dobson, P., Doughty, C., Rutqvist, J., Soom, F., Nakagawa, S., Niemi, A., Juhlin, C., Lorenz, H., Rosberg, J.E., Dessirier, B., Tsang, C.F., Tatomir, A., Basirat, F., Lundberg, E., Almqvist, B., Borglin, S., and Zheng, L. (2021), Crystalline Disposal R&D at LBNL: FY21 Progress Report, Milestone M4SF-21LB010302031, Lawrence Berkeley National Laboratory, SFWD Working Document.

Hadgu, T., Dewers, T., and Wang, Y. (2021), FY21 Report on International Collaboration, M4SF-21SN010302082.

Hyman, J. (2021), GDSA-Modeling and Integration, Los Alamos National Laboratory, M4SF-21LA010304032, Los Alamos National Laboratory Report No. LA-UR-21-27931.

Jové-Colón, C.F., Ho, T.A., Coker, E.N., Lopez, C.M., Kuhlman, K.L., Sanchez, A.C., Mills, M., Kruichak, J., and Matteo, E. (2021), Evaluation of Nuclear Spent Fuel Disposal in Clay-Bearing Rock - Process Model Development and Experimental Studies, M2SF-21SN010301072, SAND2021-6358 R.

Kuhlman, K., M. Mills, R. Jayne, E. Matteo, C. Herrick, M. Nemer, Y. Xiong, C. Choens, M. Paul (2021a), Brine Availability Test in Salt (BATS) FY21 Update, M2SF-21SN010303052 SAND2021-10962 R, Sandia National Laboratories.

Kuhlman, K., Matteo, E.N., Mills, M.M., Jayne, R.S., Reedlunn, B., S. Sobolik, S., Bean, J., Stein, E.R., and Gross, M. (2021b), Salt International Collaborations, M3SF-21SN010303062, SAND2021-9232R, Sandia National Laboratories.

LaForce, T., Basurto, E., Chang, K.W., Jayne, R., Leone, R., Nole, M., Perry, F.V., and Stein, E. GDSA Repository Systems Analysis Investigations in FY2021, M2SF-20SN010304062, Sandia National Laboratories, SAND2021-11691 R.

Matteo, E.N., Dewers, T., and Hadgu, T. (2021), FY21 Report on Activities for EBS InternationalSandia National Laboratories, M4SF-21SN010308062, SAND2021-10756 R.

Nole, M., Leone, R.C., Park, H.D., Paul, M., Salazar, A., Hammond, G.E., Lichtner, P.C. (2021), PFLOTRAN Development FY2021, M3SF-21SN010304072, SAND2021-8709 R, Sandia National Laboratories.

Rutqvist, J., Guglielmi, Y., Hu, M., Sasaki, T., Deng, H., Li, P., Steefel, C., Tournassat, C., Xu, H., Babhulgaonkar, S., and Birkholzer, J. (2021a), Investigation of Coupled Processes in Argillite Rock: FY21 Progress, Lawrence Berkeley National Laboratory, May 28, 2021, LBNL- 2001402.

Rutqvist, J., Hu, M., Tounsi, H., Wu, Y., Steefel, C., Uhlemann, S., Wang, J., and Birkholzer, J. (2021b), Salt Coupled THMC Processes Research Activities at LBNL: FY21 Progress, SFWD Internal Working Document.

Sauer, K.B., Caporuscio, F.A., and Rock, M.J. (2021), Argillite Disposal R&D and Argillite International Collaborations - LANL, SF-21LA01030101 Rev2, SF-21LA01030102, LA-UR-21-26538.

Viswanathan, H., Boukhalfa, H., Chu, S., Hoinville, A.R., Hyman, J., Sweeney, M.R., Telfeyan, K., Morrison, K.D., and Zavarin, M. (2021), M4SF-21LA010302014, Los Alamos National Laboratory Report No. LA-UR-21-26311.

Wang, Y., Xiong, Y., Mills, A., Sanchez, C., Hadgu, T., Kruichak, J.N, Tuan, T.A., Dewers, T., Russo, S., Lopez, C.M. Process Model Development and Experimental Investigation for Spent Fuel Disposal in Crystalline Rocks: FY21 Report. M2SF-21SN010302072.

Zavarin, M., Atkins-Duffin, C., Bourcier, W., Carle, S.F., and Kaukuntla, R. (2021a), M4SF-21LL010302062-Update on NEA-TDB Database Development and Database Formatting Tool.

Zavarin, M., Zouabe, J., Chang, E., and Wainwright, H. (2021b), Rev0 Non-Electrostatic Surface Complexation Database for GDSA, M4SF-21LL010301062.

Zheng, L., Borglin, S., Lammers, L., Whittaker, M., Zarzycki, P., Fox, P., Chang, C., Subramanian, N., Nico, P., Tournassat, C., Chou, C., Xu, H., Singer, E., Steefel, C., Peruzzo, L., and Wu, Y. (2021), LBNL Engineered Barrier System R&D Activities in FY21, Milestone M3SF-21LB010308031, Lawrence Berkeley National Laboratory, SFWD Working Document.

8.2. Other Cited References

Aalto, P., Aaltonen, I., Ahokas, H., Andersson, J., Hakala, M., Hellä, P., Hudson, J.A., Johansson, E., Kemppainen, K., Koskinen, L., Laaksoharju, M., Lahti, M., Lindgren, S., Mustonen, A., Pedersen, K., Pitkänen, P., Poteri, A., Snellman, M., and Ylä-Mella, M. (2009), Programme for Repository Host Rock Characterization in ONKALO (ReRoc), Posiva Oy Working Report 2009-31.

Äikäs, T. (2011), Towards Implementation, Presentation given at the HADES Workshop, "30 Years of Underground Research Laboratory," May 23-25, 2011, Antwerp, Belgium.

Aldrich, G., Hyman, J. D., Karra, S., Gable, C. W., Makedonska, N., Viswanathan, H., Woodring, J., and Hamann, B. (2017). Analysis and visualization of discrete fracture networks using a flow topology graph. IEEE Transactions on Visualization and Computer Graphics, 23(8), 1896–1909. doi: 10.1109/tvcg.2016.2582174

Alonso, E.E., Gens, A., and Josa, A. (1990), A Constitutive Model for Partially Saturated Soils, Geotechnique. 40: 405-430.

Alonso, M.C., García Calvo, J.L., Cuevas, J., Turrero, M.J., Fernández, R., Torres, E., and Ruiz, A.I. (2017), Interaction Processes at the Concrete-Bentonite Interface After 13 years of FEBEX-Plug Operation. Part I: Concrete Alteration, Physics and Chemistry of the Earth, Parts A/B/C, vol. 99, pp. 38–48, Jun. 2017.

Altmann, S. (2008), Geochemical research: A key building block for nuclear waste disposal safety cases. Journal of Contaminant Hydrology 102, 174-179.

Altmann, S., Tournassat, C., Goutelard, F., Parneix, J.-C., Gimmi, T., and Maes, N. (2012), Diffusion-driven transport in clayrock formations. Applied Geochemistry 27, 463-478.

Akesson, M. (2021), Water Transport in Pellet-Filled Slots – Preliminary Evaluation of Subtask B, Presentation at 32th EBS-Task Force Meeting, Virtual, May 10-12, 2021.

ANDRA (2009), http://www.andra.fr/download/andra-international- en/document/355VA-B.pdf

Arnold, J., Duddu, R., Brown, K. and Kosson, D.S. (2017) Influence of multi-species solute transport on modeling of hydrated Portland cement leaching in strong nitrate solutions. Cement and Concrete Research, 100, 227-244.

Asahina, D., Houseworth, J.E., Birkholzer, J.T., Rutqvist, J., and Bolander, J.E. (2014), Hydro-Mechanical Model For Wetting/Drying and Fracture Development in Geomaterials, Computers & Geosciences, 65, 13–23.

Asmussen, S.E., and Hanson, B.D. (2020), PNNL Engineered Barrier Systems International Collaborations, Prepared for U.S. Department of Energy Spent Fuel and Waste Disposition Campaign, SFWD-SFWST-M4SF-20PN010308071, Pacific Northwest National Laboratory, PNNL-30054.

Bárcena, I., García-Siñeriz, J.L. (2015). FEBEX-DP (GTS) Full Dismantling Sampling Plan (in 492 situ Experiment). NAGRA Arbeitsbericht NAB 15-14. 103 pp.

Beauheim, R.L. and Roberts, R.M., 2002. Hydrology and hydraulic properties of a bedded evaporite formation, Journal of Hydrology, 259(1–4):66–68.

Binder, G., Titov, A., Tamayo, D., Simmons, J., Tura, A., Byerley, G., and Monk, D. (2018) Time delays from stress-induced velocity changes around fractures in a time-lapse DAS VSP. SEG Technical Program Expanded Abstracts, Aug. 2018.

Binder, G., Titov, A., Liu, Y., Simmons, J., Tura, A., Byerley, G., and Monk, D. (2020) Modeling the seismic response of individual hydraulic fracturing stages observed in a time-lapse distributed acoustic sensing vertical seismic profiling survey. Geophysics 85 (4), T225-T235.

Birgersson, M., Börgesson, L., Hedström, M., Karnland, O., and Nilsson, U. (2009), Bentonite Erosion - Final Report (TR-09-34), Clay Technology AB: Sweden, SKB (Swedish Nuclear Fuel and Waste Management Company), p. 164.

Birkholzer, J.T. (2011), Disposal R&D in the Used Fuel Disposition Campaign: A Discussion of Opportunities for Active International Collaboration, Prepared for U.S. Department of Energy Used Fuel Disposition Campaign, FCRD-USED-2011-000225, Lawrence Berkeley National Laboratory.

Birkholzer, J.T. (2012), Status of SFWD Campaign International Activities in Disposal Research, Prepared for U.S. Department of Energy Used Fuel Disposition Campaign, FCRD-SFWD-2012-000295, Lawrence Berkeley National Laboratory.

Birkholzer, J.T. (2014), International Collaboration Activities in Different Geologic Disposal Environments, Prepared for U.S. Department of Energy Used Fuel Disposition Campaign, FCRD- SFWD-2015-0000679, Lawrence Berkeley National Laboratory.

Birkholzer, J.T. (2015), International Collaboration Activities in Different Geologic Disposal Environments, Prepared for U.S. Department of Energy Used Fuel Disposition Campaign, FCRD- SFWD-2014-000065, Lawrence Berkeley National Laboratory.

Birkholzer, J.T. (2016), International Collaboration Activities in Different Geologic Disposal Environments, Prepared for U.S. Department of Energy Used Fuel Disposition Campaign, FCRD-UFD-2016-000077, Lawrence Berkeley National Laboratory.

Birkholzer, J., Faybishenko, B., Zheng, L., Rutqvist, J., Dobson, P., Fox, P.M., Reimus, P., Viswanathan, H., Jové-Colón, C.F., Wang, Y., Kuhlman, K., McMahon, K. and Zavarin, M. (2017), International Collaboration Activities in Different Geologic Disposal Environments, Prepared for US Department of Energy, Spent Fuel and Waste Disposition Campaign (SFWD-SFWST-2017-000013). Lawrence Berkeley National Laboratory Report No. LBNL-200106.

Birkholzer, J., Faybishenko, B., Dobson, P.F., Rutqvist, J., Zheng, L., Caporuscio, F.A., Reimus, P., Viswanathan, H., Jové-Colón, C.F., Wang, Y., Kuhlman, K., Matteo, E. , McMahon, K., and Zavarin, M. (2018), International Collaboration Activities in Different Geologic Environments, Prepared for US Department of Energy, Spent Fuel Waste Science and Technology Campaign (SFWST), M2SF-18LB010307012, LBNL-2001178, Lawrence Berkeley National Laboratory, Berkeley, CA USA, Berkeley, California, 236 pp.

Birkholzer, J., Faybishenko, B., Ajo-Franklin, Borglin, S., Deng, H., Dobson, P., Gilbert, B. Guglielmi, Y. Fox, P.M., Kim, K., Nico, P., Rutqvist, J., Sonnenthal, E., Steefel, C., Xu, H., Wu, Y., Zarzycki, P., Zheng, L., Caporuscio, F., Reimus, P., Viswanathan, H., Jové-Colón, C., Wang, Y., Kuhlman, K.L., Matteo, E., McMahon, K., Zavarin, M., Balboni, E., Wolery T. (2019a), International Collaboration Activities in Different Geologic Environments, in Spent Fuel Waste Science and Technology (SFWST), M2SF-19LB010307012, LBNL-2001239, Lawrence Berkeley National Laboratory, Berkeley, CA USA, 321 pp.

Birkholzer, J.T., Tsang, C.-F., Bond, A.E., Hudson, J.A., Jing, L., and Stephansson, O. (2019b), 25 Years of DECOVALEX - Scientific Advances and Lessons Learned from an International Research Collaboration in Coupled Subsurface Processes, Invited Review, International Journal and Rock Mechanics and Mining Sciences, 122, 1-21.

Birkholzer, J., Faybishenko, B., Ajo-Franklin, Borglin, S., Deng, H., Dobson, P., Gilbert, B. Guglielmi, Y. Fox, P.M., Kim, K., Nico, P., Rutqvist, J., Sonnenthal, E., Steefel, C., Xu, H., Wu, Y., Zarzycki, P., Zheng, L., Caporuscio, F., Reimus, P., Viswanathan, H., Jové-Colón, C., Wang, Y., Kuhlman, K.L., Matteo, E., McMahon, K., Zavarin, M., Balboni, E., Wolery T. (2019), International Collaboration Activities in Different Geologic Environments, in Spent Fuel Waste Science and Technology (SFWST), M2SF-19LB010307012, LBNL-2001239, Lawrence Berkeley National Laboratory, Berkeley, CA USA.3), Berkeley, California, 236 pp.

Birkholzer, J., Faybishenko, B., Guglielmi, Y., Rutqvist, J., Zheng, L., Caporuscio, F., Viswanathan, H., Jové-Colón, C., Wang, Y., Kuhlman, K.L., Matteo, E., Zavarin, M., and Asmussen, S. (2020), International Collaboration Activities in Geologic Disposal Research: FY20 Progress, LBNL report LBNL-2001353.

Birkholzer, J., Zheng, L., Stein, E., Camphouse, C. (2021), Developing a Diverse Next Generation Workforce for Radioactive Waste Disposal: A National Lab Pilot Program, Concept Paper, Jointly Developed by LBNL and SNL.

Blechschmidt, I., Schneeberger, R., Lanyon, W., Schaefer, T. (2021), Colloid Formation and Migration Project - Status Update, Presentation at 19th International Steering Committee Grimsel Test Site, Virtual Meeting, September 22-23, 2021.

BMWi (2008), Final Disposal of High-level Radioactive Waste in Germany – The Gorleben Repository Project, Federal Ministry of Economics and Technology (BMWi), Germany, October, 2008.

Bond, A., and Birkholzer, J.T. (2019), Task Proposals for DECOVALEX-2023, Briefing note to potential DECOVALEX future funders, Internal Briefing BN-13-v1, August 2019.

Bond, A., and Birkholzer, J.T. (2020), DECOVALEX-2019 – Executive Summary, Lawrence Berkeley National Laboratory Report, LBNL-2001360.

Bond A., Chittenden N. and Thatcher K. 2018. RWM Coupled Processes Project: First Annual Report for DECOVALEX-2019. Quintessa Report to RWM. QRS-1612D-R1 v1.2. Quintessa Ltd., Henley-on-Thames, UK.

Börgesson, L. and Akesson, M. (2016), Modelling of Water Transport in Pellets Filled Slots, Presentation at 25th EBS-Task Force Meeting in Oxford, UK, November 15-17, 2016.

Bossart, P. (2014), Enclosure – Steering Meeting SM-654, Presentation given at the Mont Terri Steering Meeting SM-65, May 15, 2014, Horonobe, Japan.

Bossart, P. and Thury, M. (2007), Research in the Mont Terri Rock Laboratory: Quo vadis? Physics and Chemistry of the Earth, Parts A/B/C, 32(1-7), 19-31.

Bossart, P., Bernier, F, Birkholzer, J.T., Bruggeman, C., Connolli, P., Dewonck, S., Fukaya, M., Herfort, M., Jensen, M., Matray, J., Mayor. J, Moeri, A., Oyama, T., Schuster, K., Shigeta, N., Vietor, T., and Wieczorek, K. (2017), Mont Terri Rock Laboratory, 20 Years of Research: Introduction, Site Characteristics and Overview of Experiments, Swiss Journal of Geosciences, 110 (1), pp. 3-22.

Bradbury, M. H., and Baeyens, B. (2003), "Porewater chemistry in compacted re-saturated MX-80 bentonite." Journal of Contaminant Hydrology 61(1–4): 329-338.

Bragg-Sitton, S.M., Birkholzer, J.T., MacKinnon, R., McMahon, K., Saltzstein, S., Sorenson, K., and Swift, P. (2014), Update of the Used Fuel Disposition Campaign Implementation Plan, Prepared for U.S. Department of Energy Used Fuel Disposition Campaign, SAND2019-9997 R, Topical Report RSI-2948.

Braun, P. (2019), Thermo-hydro-mechanical behavior of the Callovo-Oxfordian claystone: Effects of stress paths and temperature changes. Thesis, Université Paris-Est, 2019.

Bredehoeft, J.D., and Maini, T. (1981), Strategy for radioactive waste disposal in crystalline rocks. Science 423 (4505), 293–296.

Bruines, P., and Lanyon, W. (2021), Task 10 Way Forward, Presentation given at 39th SKB GWFTS Task Force Meeting (TF 39), Online, March 2021.

Buchholz, S., Keffeler, E., Lipp, K., de Vries, K., Hansen, F. (2019), Proceedings of the 10th U.S/German Workshop on Salt Repository Research, Design, and Operation, Prepared for U.S. Department of Energy Used Fuel Disposition Campaign, FCRD-SFWD-2014-000047.

Camphouse, C. (2020), Personal Communication, September 8, 2020.

Caporuscio, F.A., Sauer K.B., Rock, M.J., Kalintsev, A., Migdissov, A., and Alcorn, C. (2020), Engineered Barrier System R&D and International Collaborations – LANL –FY20, Los Alamos Laboratory, July 24, 2020, SF-02LA01030801 Rev2, SF-20LA01030805, LA-UR-20-25330.

Carter, B., and Nieder-Westermann, G. (2021): China Begins Construction of its First Underground Research Laboratory for High Level Waste Disposal, IAEA Newscenter, Online, July 23. https://www.iaea.org/newscenter/news/china-begins-construction-of-its-first-underground-research-laboratory-for-high-level-waste-disposal

Cherry, J.A., Alley, W.M., and Parker, B.L. (2014), Geologic disposal of spent nuclear fuel – An earth science perspective. The Bridge, Spring 2014, 51–59.

COMSOL Multiphysics® v. 5.6. www.comsol.com. COMSOL AB, Stockholm, Sweden.

Cuadros, J., and Linares, J. (1996), Experimental kinetic study of the smectite-to-illite transformation. Geochimica et Cosmochimica Acta 60, 439-453.

Cuss, R.J., Harrington, J.F., Noy, D.J., Graham, C.C., Sellin, P. (2014), Evidence of Localized Gas Propagation Pathways in a Field-Scale Bentonite Engineered Barrier System; Results From Three Gas Injection Tests In The Large-Scale Gas Injection Test (LASGIT). Applied Clay Science, 102, pp.81-92.

Czaikowski, O., L. Friedenberg, K. Wieczorek, N. Müller-Hoeppe, C. Lerch, R. Eickemeier, B. Laurich, W. Liu, D. Stührenberg, K. Svensson, K. Zemke, C. Lüdelig, T. Popp, J. Bean, M. Mills, B. Reedlunn, U. Düsterloh, S. Lerche, J. Zhao, 2020. *GRS-608*: *KOMPASS- Compaction of crushed Salt for the Safe Containment*. Gesellschaft für Anlagen- und Reaktorsicherheit (GRS) gGmbH.

Daley, T.M., Myer, L.R., Peterson, J.E., Majer, E.L., and Hoversten, G.M. (2007), Time-lapse crosswell seismic and VSP monitoring of injected CO_2 in a brine aquifer: Environmental Geology, http:dx.doi.org/ 10.10071500254-007-0943-2.

Daniels, K.A. and Harrington, J.F. 2017. The Response of Compact Bentonite during a 1D Gas Flow Test. British Geological Survey Open Report, OR/17/067. 19pp.

DECOVALEX, DECOVALEX-2019: The Current Project Phase (2016-2019), www.decovalex.org.

Delay, J., Vinsot, A., Krieguer, J.-M., Rebours, H., and Armand, G. (2007), Making of the underground scientific experimental programme at the Meuse/Haute-Marne underground research laboratory, North Eastern France. Physics and Chemistry of the Earth, Parts A/B/C 32, 2-18.

Dirksen, D. (1969), Thermo-Osmosis through Compacted Saturated Clay Membranes. Soil Sci. Soc. Am. Proc., 33(6): 821-826.

Dobson, P., Tsang, C.F., Kneafsey, T., Borglin, S., Piceno, Y., Andersen, G., Nakagawa, S., Nihei, K., Rutqvist, J., Doughty, C., and Reagan, M. (2016), Deep Borehole Field Test Research Activities at LBNL.

Prepared for U.S. Department of Energy Used Fuel Disposition Campaign, FCRD-UFD-2016-000438, LBNL Report LBNL-1006044.

Dobson, P., Tsang, C.F., Doughty, C., Ahonen, L., Kietäväinen, R., Juhlin, C., Rosberg, J.E., Borglin, S., Kneafsey, T., Rutqvist, J., Zheng, L., Xu, H., Nakagawa, S., and Nihei, K. (2017), Deep borehole field test activities at LBNL 2017. US DOE Spent Fuel and Waste Science and Technology, SFWD-SFWST-2017-000046, LBNL Report 2001043, 118 p.

Doughty, C., Tsang, C.F., Rosberg, J.E., Juhlin, C., Dobson, P.F., and Birkholzer, J.T. (2017), Flowing Fluid Electrical Conductivity Logging of a Deep Borehole During and Following Drilling: Estimation Of Transmissivity, Water Salinity And Hydraulic Head Of Conductive Zones. Hydrogeology Journal 25, 501-517.

ECN (2019) LeachXS User's Guide: LeachXS Pro Version 3.0.10. Energy Research Centre of The Netherlands, Petten, The Netherlands.

ENRESA (2000), Full-scale Engineered Barriers Experiment for a Deep Geological Repository In Crystalline Host Rock FEBEX Project, European Commission: 403.

Faybishenko, B., Wang, Y., Harrington, J., Birkholzer, J., and Jové-Colón, C. (2020), Phenomenological Model of Deterministic-Chaotic Gas Migration in Bentonite: Experimental Evidence and Diagnostic Parameters, LBNL-2001354.

Fernández, A.M., Sánchez-Ledesma, D.M., Melón, A., Robredo L. M., Rey, J.J., Labajo, M., Clavero, M.A., Carretero, S., and González, A.E. (2017). Thermo-hydro-geochemical behaviour of a Spanish bentonite after dismantling of the FEBEX in situ test at the Grimsel Test SitePore water chemistry of the FEBEX bentonite. CIEMAT report, CIEMAT/DMA/2G216/03/16.

Finley, S.J., Hanson, D.J., and Parsons, R. (1992). Small-Scale Brine Inflow Experiments—Data Report Through 6/6/91 (SAND91-1956; UC-721). Albuquerque, AZ: U.S. Sandia National Laboratory.

Follin, S., Hartley, L., Rhén, I., Jackson, P., Joyce, S., Roberts, D., and Swift, B. (2014), A methodology to constrain the parameters of a hydrogeological discrete fracture network model for sparsely fractured crystalline rock, exemplified by data from the proposed high-level nuclear waste repository site at Forsmark, Sweden. Hydrogeology Journal 22, 313–331.

Freeze, G., S.D. Sevougian, K. Kuhlman, M. Gross, J. Wolf, D. Buhmann, J. Bartol, C. Leigh & J. Mönig, 2020. *Generic FEPs Catalogue and Salt Knowledge Archive*, SAND2020-13186. Albuquerque, NM: Sandia National Laboratories, 151 p.

Garcia-Garcia, S., Wold, S., and Jonsson, M. (2009). Effects of temperature on the stability of colloidal montmorillonite particles at different pH and ionic strength. Applied Clay Science, 43(1), 21-26.

Garitte, B. (2010), New In Situ Experiments at Mont Terri, Presentation given at 6th DECOVALEX-2011 Workshop, October 2010, Wuhan, China.

Gaus, I., and Kober, F. (2014), FEBEX-DP Project Plan, NAGRA, Switzerland.

Gens, A., Sánchez, M., Guimaraes, L.D.N., Alonso, E.E., Lloret, A., Olivella, S., Villar, M.V., and Huertas, F. (2009), A full-scale in situ heating test for high-level nuclear waste disposal: observations, analysis and interpretation. Geotechnique 59, 377–399.

Gens A., Alcoverro J., Blaheta R., Hasal M., Michalec Z., Takayama Y., Lee C., Lee J., Kim G.Y., Kuo C.-W., Kuo W.-J., and Lin C.-Y (2021), HM and THM Interactions in Bentonite Engineered Barriers for Nuclear Waste Disposal. Int J Rock Mech Min Sci; 137: 104572.

Gens, A. (2020), DECOVALEX-2019 – Task D Final Report, Lawrence Berkeley National Laboratory Report, LBNL-2001267.

Gens, A. (2021), Task 13 – Unsaturated Homogenization, Presentation at 32th EBS-Task Force Meeting, Virtual, May 10-12, 2021.

Ghassemi, A. and Diek, A. (2002). Porothermoelasticity for swelling shales. Journal of Petroleum Science and Engineering, 34: 123-125.

Giguere, A. Eichorst, S. Meier, D., Herbold, C., Richter, A, Greening, C. Woebken,. D. Acidobacteria are active and abundant members of diverse atmospheric H_2-oxidizing communities detected in temperate soils. 2020. ISME, 15:363-376.

Gómez-Espina, R. and Villar, M. (2016) Time evolution of MX-80 bentonite geochemistry under thermo-hydraulic gradients. Clay Miner 51, 145-160.

Graupner, B., Rutqvist, J., and Gugliemi, Y. (2020), DECOVALEX-2019 – Task B Final Report, Lawrence Berkeley National Laboratory Report, LBNL-2001263.

Greening, C., Constant, P., Hards, K., Morales, S.E., Oakeshott, J.G., Russell, R.J., Taylor, M.C. Berney, M., Conrad, R., and Cook, G.M. (2015), "Atmospheric Hydrogen Scavenging: from Enzymes to Ecosystems." Applied and Environmental Microbiology 81(4): 1190.

Guglielmi, Y., Cappa, F., Lançon, H., Janowczyk, J.B., Rutqvist, J., Tsang, C.F., and Wang, J. (2013a), Estimation of Permeability, Elastic and Friction Properties of Fractured Rock Masses from In Situ Hydromechanical Testing: The High- Frequency Pulse Poroelasticity Protocole (HPPP) Testing Method. Submitted contribution to the ISRM Commission on Testing Methods, Int J Rock Mech Min Sci and Geomech Abstr special issue.

Guglielmi, Y., Henry, P., Cappa, F., and Derode, B. (2013b), Relationships Between Slow Slip, Seismicity and Fluid Leakage During a Pressurized Fault Zone Rupture In Situ Experiment: Importance For Reservoir/Caprock Stimulation Monitoring And Efficiency Assessment. ARMA Symposium Paper N°13- 517, ARMA San Francisco 23-26 June 2013.

Guglielmi, Y., Cappa, F., Avouac, J.-P., Henry, P., and Elsworth, D. (2015), Seismicity Triggered by Fluid Injections Induced Aseismic Slip, Science, 348(6240), 1224–1226, doi:10.1126/science.aab0476.

Guglielmi, Y., Cappa, F., Avouac, J.-P., Henry, P., and Elsworth, D. (2015a), Seismicity Triggered by Fluid Injections Induced Aseismic Slip, Science, 348(6240), 1224–1226, doi:10.1126/science.aab0476.

Guglielmi, Y., Elsworth, D., Cappa, F., Henry, P., Gout, C., Dick, P., and Durand, J. (2015b), In situ Observations on the Coupling Between Hydraulic Diffusivity and Displacements During Fault Reactivation in Shales, J. Geophys. Res., 120, doi:10.1002/2015JB012158.

Guglielmi, Y., P. Henry, C. Nussbaum, P. Dick, C. Gout, and F. Amann (2015c), Underground Research Laboratories for Conducting Fault Activation Experiments In Shales. ARMA Symposium Paper N°15-480, ARMA San Francisco June 2015.

Guglielmi, Y. (2016), In Situ Clay Fault Slip Hydro-mechanical Characterization (FS Experiment), Mont Terri Underground Rock Laboratory, Mont Terri Project Technical Note 2015-60 63 pp.

Guglielmi, Y., Cook, P., Dobson, P., Nakagawa, S., Zheng, L., Niemi, A., Juhlin, C., Lorenz, H., Rosberg, J.-E., Dessirier, B., Tsang, C.-F., Tatomir, A., Vasirat, F., Lundberg, E., Almqvist, B., Borglin, S., and Doughty, C. (2019), Crystalline Disposal R&D at LBNL: FY19 Progress Report, Prepared for US Department of Energy, Spent Fuel and Waste Disposition Campaign M4SF-19LB010302031, Lawrence Berkeley National Laboratory, LBNL-2001221.

Guglielmi, Y., Chang, C., Cook, P., Dobson, P., Soom, F., Nakagawa, S., Niemi, A., Juhlin, C., Lorenz, H., Rosberg, J.-E., Dessirier, B., Tsang, C.-F., Tatomir, A., Basirat, F., Lundberg, E., Almqvist, B., Borglin, S., Doughty, C., and Zheng, L. (2020), Crystalline Disposal R&D at LBNL: FY20 Progress Report, Prepared for US Department of Energy, Spent Fuel and Waste Disposition Campaign, M4SF-20LB010302031, Lawrence Berkeley National Laboratory, LBNL-2001334.

Guglielmi, Y., Nussbaum, C., Jeanne, P., Rutqvist, J., Cappa, F., and Birkholzer, J. (2020a), Complexity of fault rupture and fluid leakage in shale: Insights from a controlled fault activation experiment. Journal of Geophysical Research: Solid Earth, 125, e2019JB017781. https://doi.org/ 10.1029/2019JB017781.

Guglielmi, Y., Nussbaum, C., Rutqvist, J., Cappa, F., Jeanne, P. and Birkholzer, J. (2020b), Estimating perturbed stress from 3D borehole displacements induced by fluid injection in fractured or faulted shales. Geophys. J. Int. (2020) 221, 1684–1695.

Guiltinan, E.J., Kuhlman, K.L., Rutqvist J., Hu, M., Boukhalfa, H., Mills, M., Otto, S., Weaver, D.J., Dozier, B., and Stauffer, P.H. (2020). Temperature response and brine availability to heated boreholes in bedded salt. Vadose Zone Journal, 19. https://doi.org/10.1002/vzj2.20019.

Günther, T. and Rücker, C. (2012). Boundless Electrical Resistivity Tomography (BERT) v. 2.0 - Open Access Software for Advanced and Flexible Imaging. Villar, M. (2017). FEBEX-DP Post-mortem THM-THG Analysis Report.

Guyonnet, D., Touze-Foltz, N., Norotte, V., Pothier, C., Didier, G., Gailhanou, H., Blanc, P., and Warmont, F. (2009), Performance-based indicators for controlling geosynthetic clay liners in landfill applications. Geotextiles and Geomembranes 27, 321-331.

Hadgu, T., Karra, S., Kalinina, E., Makedonska, N., Hyman, J.D., Klise, K., Viswanathan, H.S., and Wang, Y. (2017), A Comparative Study of Discrete Fracture Network and Equivalent Continuum Models for Simulating Flow and Transport in the Far Field of a Hypothetical Nuclear Waste Repository In:Crystalline Host Rock. Journal of Hydrology, 553, 59-70.

Hadgu, T., Dewers, T., Gomez, S., and Matteo, E. (2020), EBS Task Force: Task 9/FEBEX Modeling Final Report: Thermo-Hydrologic Modeling with PFLOTRAN, Sandia National Laboratories, Albuquerque, NM, SAND2020-4195 R.

Hama, K., Kunimaru, T., Metcalfe, R., and Martin, A. J. (2007) The hydrochemistry of argillaceous rock formations at the Horonobe URL site, Japan. *Phys. Chem. Earth*, 32, 170-180.

Hammond, G. E., Lichtner, P. C., and Mills, R. T. (2014), Evaluating the Performance Of Parallel Subsurface Simulators: an Illustrative Example with PFLOTRAN, Water Resources Research. 2014; 50, doi:10.1002/2012WR013483.

Hansen, F., Steininger, W., and Biurrun, E. (2013), Proceedings of the 4th US/German Workshop on Salt Repository Research, Design and Operation. FCRD-SFWD-2014-000335, SAND2013-10592P. U.S. Department of Energy, Office of Nuclear Energy, Used Fuel Disposition Campaign, Washington, D.C.

Hansen, F., Leigh, C.W., Steininger, W., Bollingerfehr, W., and von Berlepsch, T. (2015), Proceedings of the 5th US/German Workshop on Salt Repository Research, Design and Operation. FCRD-UFRD- 2015-00514, SAND2015-0500R. U.S. Department of Energy, Office of Nuclear Energy, Used Fuel Disposition Campaign, Washington, D.C.

Hardin, E., Bryan, C., Ilgen, A., Kalinina, E., Teich-Goldrick, S., Banerjee, K., Clarity, J., Howard, R., Jubin, R., Scaglione, J., Perry, F., Zheng, L., Rutqvist, J., Birkholzer, J.T., Greenberg, H., Carter, J., and Severynse, T. (2014), Investigation of Dual-Purpose Canister Direct Disposal Feasibility, Prepared for U.S. Department of Energy Used Fuel Disposition Campaign, FCRD-UFD-2014-000069 REV 1, Sandia Laboratories.

Harrington, J.F. (2016), Specification for DECOVALEX-2019: Task A: modElliNg Gas INjection ExpERiments (ENGINEER), Task Specification Document for DECOVALEX Project, Ref: BGS-DX-v3, 2016.

Harrington J.F., Graham C.C., Cuss R.J. and Norris S. (2017), Gas network development in a precompacted bentonite experiment: Evidence of generation and evolution in Applied Clay Science. 147, 80-89. DOI: 10.1016/j.clay.2017.07.005.

Harrington J.F, Tamayo-Mas E., Shao H., Dagher E.E., Lee J., Kim K., Lai, S.H., Chittenden N., Wang Y, Damians I.P., Olivella S. (2019), Modelling advective gas flow in a compact clay: Application and assessment of different numerical approaches in the 6th EAGE Shale Workshop, Bordeaux, France. DOI: 10.3997/2214-4609.201900283.

Harrington, J.F., and Tamayo-Mas, E. (2020), Specification for DECOVALEX-2023 Task B: MAGIC (Modeling Advection of Gas in Clays), Task Specification Document for DECOVALEX Project, 17 pp, 2020.

Herbert, H. J., Kasbohm, J., Sprenger, H., Fernández, A. M., and Reichelt, C. (2008), Swelling pressures of MX-80 bentonite in solutions of different ionic strength. Physics and Chemistry of the Earth, 33(SUPPL. 1). https://doi.org/10.1016/j.pce.2008.10.005.

Hesser, J., and Wieczorek, K. (2020), SW-A Sandwich – Measurements in the Rock Mass – Objectives and Instrumentation, Poster Presentation given at the 38th Mont Terri Technical Meeting, Porrentruy, Switzerland, January 29-30, 2020.

Ho, T.A., Wang, Y., Jové Colón, C.F. and Coker, E.N. (2020), Fast Advective Water Flow Through Nanochannels in Clay Interlayers: Implications for Moisture Transport in Soils and Unconventional Oil/Gas Production. ACS Applied Nano Materials 3, 11897-11905.

Horiguchi, T., and Tateda, M. (1989), BOTDA-nondestructive measurement of 763 single-mode optical fiber attenuation characteristics using Brillouin interaction: 764 theory. Journal of Lightwave Technology, 7 (8), 1170–1176. Doi: 10.1109/50.32378.

Horseman, S.T., Harrington, J.F., and Sellin, P. (1999), Gas Migration in Clay Barriers. Engineering Geology, Vol. 54, 139-149.

Hu, M., and Rutqvist, J. (2020a), Finite Volume Modeling of Coupled Thermo-Hydro-Mechanical Processes with Application to Brine Migration in Salt. Computational Geosciences, https://doi.org/10.1007/s10596-020-09943-8.

Hu, M., and Rutqvist, J. (2020b), Microscale Mechanical Modeling of Deformable Geomaterials With Dynamic Contacts Based on the Numerical Manifold Method. Computational Geosciences. https://doi.org/10.1007/s10596-020-09992-z.

Huertas, F.B., de la Cruz, J.L., Fuentes-Cantillana, et al. (2005), Full-Scale Engineered Barriers Experiment for a Deep Geological Repository for High-Level Waste in Crystalline Host Rock – Phase II. EUR 21922.

Hyman, J. D., Gable, C. W., Painter, S. L., and Makedonska, N. (2014), Conforming Delaunay Triangulation of Stochastically Generated Three-dimensional Discrete Fracture Networks: A Feature Rejection Algorithm for Meshing Strategy, SIAM J. Sci. Comput., 36:4, A1871–A1894.

Hyman, J. D., Karra, S., Makedonska, N., Gable, C. W., Painter, S. L., and Viswanathan, H. S. (2015), dfnWorks: A Discrete Fracture Network Framework for Modeling Subsurface Flow and Transport. Comput. Geosci., 84: 10–19.

Hyman, J. D., Hagberg, A., Srinivasan, G., Mohd-Yusof, J., and Viswanathan, H. S. (2017), Predictions of first passage times in sparse discrete fracture networks using graph-based reductions. Physical Review E, 96(1), 013304.

Hyman, J. D. and Jiménez-Martínez, J. (2018), Dispersion and mixing in three-dimensional discrete fracture networks: Nonlinear interplay between structural and hydraulic heterogeneity. Water Resour. Res., 54 (5), 3243-3258.

Itasca (2009), FLAC3D V4.0, Fast Lagrangian Analysis of Continua in 3 Dimensions, User's Guide, Itasca Consulting Group, Minneapolis, Minnesota.

Itasca (2016), 3DEC, 3Dimensional Distinct Element Code. Itasca Consulting Group, Minneapolis, MN.

Iwatsuki, T. (2020), DECOVALEX-2019 – Task C Final Report, Lawrence Berkeley National Laboratory Report, LBNL-2001264.

Jeanne, P., Guglielmi Y., Rutqvist J., Nussbaum C., and Birkholzer J. (2017), Field characterization of elastic properties across a fault zone reactivated by fluid injection, J. Geophys. Res., 122, doi:10.1002/2017JB014384.

Johnson, L., Niemeyer, M., Klubertanz, G., Siegel, P., and Gribi, P. (2002), Calculations of the temperature evolution of a repository for spent fuel, vitrified high-level waste and intermediate level waste in Opalinus Clay. National Cooperative for the Disposal of Radioactive Waste.

Jové-Colón, C.F., Caporuscio, F.A., Levy, S.S., Xu, H., Blink, J.A., Halsey, W.G., Buscheck, T., Sutton, M., Serrano de Caro, M.A., Wolery, T.J., Liu, H.-H., Birkholzer, J.T., Steefel, C.I., Rutqvist, J., Tsang, C.-F., and Sonnenthal, E. (2010), Disposal Systems Evaluations and Tool Development - Engineered Barrier System (EBS) Evaluation, Prepared for U.S. Department of Energy Used Fuel Disposition Campaign, Used Fuel Disposition Campaign.

Jové-Colón, C.F., Payne, C., and Knight, A. (2018), International Collaboration Activities on Disposal in Argillite R&D: Progress Report, Prepared for US Department of Energy, Spent Fuel and Waste Disposition Campaign M4SF-18SN010301092, Sandia National Laboratories, SAND2018-9718 R.

Jové-Colón, C.F., Payne, C., Coker, E., Boisvert, L., Sanchez, A., Knight, A., and Hadgu, T. (2019a), Argillite Disposal R&D International Collaborations interim report – 2019, M4SF-19SN010301091, SAND2019-6731 R, 2019.

Jové-Colón, Ho, T., Coker, Weck, P., Payne, C., Knight, A., Sanchez, A., Boisvert, L., Rutqvist, J., Guglielmi, Y., Kim, K., Xu, H., Deng, H., Li, P., Hu, M., Steefel, C., Gilbert, B., Rinaldi, A., Nico, P., Borglin, S., Fox, P., Birkholzer, J., Caporuscio, F.A., Sauer, K.B., Rock, M.J., Houser, L.M., J.Jerden, Lee, E., Gattu, V.K., Ebert, W., Zavarin, M., and Wolery, T. J. (2019b), Evaluation of Nuclear Spent Fuel Disposal in Clay-Bearing Rock - Interim report 2019, M2SF-19SN010301051, 2019.

Jové-Colón, C.F., Ho, T., Coker, E., Hadgu, T., Lopez, C.M., Kruichak, J., Mills, M., and Sanchez, A. (2020), International Collaborations Activities on Disposal in Argillite R&D: Bentonite Barrier Characterization Studies and Modeling Investigations (2020) SF-20SN01030109, M3SF-20SN010301091, SNL Tracking Number: 1128444, May 2020.

KAERI (2011), KURT–KAERI Underground Research Tunnel, Brochure, Korea Atomic Energy Research Institute, Division of Radioactive Waste Technology Development.

Kalam, S. Basu, A. Ahmad, I., Sayyed, R. El-Enshasy, H. Dailin, D., Suriani, N. Recent Understanding of soil Acidobacteria and their ecological significance: A critical review. 2020. Frontiers in Microbiology. Vol 11, Article 580024.

Kim, K., Rutqvist, J., Nakagawa, S., and Birkholzer, J. (2017), TOUGH-RBSN simulator for hydraulic fracture propagation within fractured media: Model validations against laboratory experiments, Computers & Geosciences, 108, 72–85.

Kim, K., Rutqvist, J., Harrington, J.F., Tamayo-Mas, E., and Birkholzer, J.T. (2021), Discrete dilatant pathway modeling of gas migration through compacted bentonite clay. International Journal of Rock Mechanics and Mining Sciences. 137, 104569 (2021). https://doi.org/10.1016/j.ijrmms.2020.104569.

Klein-BenDavid, O., Harlavan, Y., Levkov, I., Teutsch, N., Brown, K.G., Gruber, C., and Ganor, J. (2019), Interaction between spent fuel components and carbonate rocks. Science of The Total Environment 689, 469-480.

Kober, F. (2017a), FEBEX-DP Dismantling and Analysis of the FEBEX (Full-Scale Engineered Barrier EXperiment) during 2015/2016, Executive Summary of the presentation made at the 15th ISCO Meeting GTS Phase VI, Hotel Handeck, Grimsel, Switzerland.

Kober, F. (2017b), FEBEX (Full-scale Engineered Barrier Experiment), Presentation given at 15th International Steering Committee Meeting, Grimsel Test Site Phase IV, Hotel Handeck, Grimsel, Switzerland.

Kober, F. (2020), HOTBent (High Temperature Bentonite), Presentation given at 18th International Steering Committee Meeting (ISCO 2020), Grimsel Test Site Phase IV, Virtual Meeting, June 3, 2020.

Kober, F. (2021), HOTBent Experiment (Effects of High Temperature on Bentonite), Presentation given at 19th International Steering Committee Grimsel Test Site, Virtual Meeting, September 22-23, 2021.

Kolditz, O., McDermott, C., and Yoon, Y.-S. (2020), DECOVALEX-2023 Task G Specifications: Planning Document, Task Specification Document for DECOVALEX Project, 45 pp., 2020.

Komine, H. (2004). Simplified evaluation for swelling characteristics of bentonites. Engineering Geology, 71(3–4), 265–279. https://doi.org/10.1016/S0013-7952(03)00140-6

Komine, H., and Ogata, N. (1994). Experimental study on swelling characteristics of compacted bentonite. Canadian Geotechnical Journal, 31(4), 478–490. https://doi.org/10.1139/t94-057

Kuhlman, K. (2020), DECOVALEX-2023, Task E Specification, Task Specification Document for DECOVALEX Project, prepared for U.S. Department of Energy Spent Fuel and Waste Disposition Campaign, SAND2020-4289, Sandia National Laboratories, 32 pp., 2020.

Kuhlman, K., Mills, M., Jayne, R., Matteo, E., Herrick, C., Nemer, M., Heath, J., Xiong, Y., Choens, C., Stauffer, P., Boukhalfa, E., Guiltinan, E., Rahn, T., Weaver, D., Dozier, B., Otto, S., Rutqvist, J., Wu, Y., Hu, M., Uhlemann, S., and Wang, J. (2020a), *FY20 Update on Brine Availability Test in Salt*, SAND2020–9034R. Albuquerque, NM: Sandia National Laboratories.

Kuhlman, K., Matteo, E., Mills, M., Jayne, R., Reedlunn, B., Sobolik, S., Bean, J., Stein, E., and Gross, M. (2020), International Collaborations on Radioactive Waste Disposal in Salt, M4SF-20SN010303062 SAND2020-7440 R, 2020.

Kunimaru, T., Reinicke, A., and Schneeberger, R. (2020), GSET – The Borehole SEAling Test: New GTS Project, Objective, Concept and Timeline, Presentation given at 18th International Steering Committee Meeting (ISCO 2020), Grimsel Test Site Phase IV, Virtual Meeting, June 3, 2020.

LaForce, T., Chang, K. W., Perry, F. V., Lowry, T. S., Basurto, E., Jayne, R., Jordan, S., Stein, E., Leone R., and Nole M. (2020), GDSA Repository Systems Analysis FY 2020 Update Albuquerque, New Mexico, Sandia National Laboratories.

Lanaro, F. (2016), DECOVALEX-2019 Task G – EDZ Evolution, Reliability, Feasibility and Significance of Measurements of Conductivity and Transmissivity of the Rock Mass for the Understanding of the Evolution of a Repository of Spent Nuclear Fuel, Presentation given at 1st DECOVALEX-2019 Workshop, May 2016, Berkeley, USA.

Lanyon, G.W. and Gaus, I. (2013), Review of the FEBEX In Situ Experiment and The Mock-Up After 15 Years of Operation and Monitoring. NAGRA NAB 13-096.

Lanyon, W. (2021), Task 10 Status and Overview, Presentation given at 39th SKB GWFTS Task Force Meeting (TF 39), Online, March 2021.

Lebon, P. (2011), Large-scale Experiment at Bure, Presentation given at the HADES Workshop, "30 Years of Underground Research Laboratory," May 23-25, 2011, Antwerp, Belgium.

Li, X. (2011), Design and Status of the PRACLAY Seal and Heater Test, Presentation given at the HADES Workshop, "30 Years of Underground Research Laboratory," May 23-25, 2011, Antwerp, Belgium.

Lichtner, P., Hammond, G., Lu, C., Karra, S., Bisht, G., Andre, B., Mills, R., and Kumar, J. (2015), PFLOTRAN user manual: A Massively Parallel Reactive Flow and Transport Model for Describing Surface and Subsurface Processes, Tech. rep., Report No. LAUR-15-20403, Los Alamos National Laboratory, 2015.

Lorenz, H., Rosberg, J.E., Juhlin, C., Bjelm, L., Almqvist, B.S.G., Berthet, T., Conze, R., Gee, D.G., Klonowska, I., Pascal, C., Pedersen, K., Roberts, N.M.W., and Tsang, C.F. (2015), COSC-1 – Drilling of a Subduction-Related Allochthon in the Palaeozoic Caledonide Orogen of Scandinavia, Scientific Drilling 19, 1–11.

Los Alamos Grid Toolbox, LaGriT, Los Alamos National Laboratory, ⟨http:// lagrit.lanl.gov⟩, 2018.

Lu, N., Reimus, P. W., Parker, G. R., Conca, J. L., and Triay, I. R. (2003), Sorption kinetics and impact of temperature, ionic strength and colloid concentration on the adsorption of plutonium-239 by inorganic colloids. Radiochimica Acta, 91(12), 713-720.

Lutterotti, L., Voltolini, M., Wenk, H.R., Bandyopadhyay, K. and Vanorio, T. (2010), Texture analysis of a turbostratically disordered Ca-montmorillonite. American Mineralogist, 95(1), pp.98-103.

Maeder, U., and Martin, L. (2020), CI-D – Diffusion Across a 12-Year-Old Cement-Clay Interface (36Cl, 3H), Presentation given at the 38th Mont Terri Technical Meeting, Porrentruy, Switzerland, January 29-30, 2020.

Maes, N., Weetjens, E., Aertsen, M., Govaerts, J., and Van Ravestyn, L. (2011), Added Value and Lessons Learned from In Situ Experiments – Radionuclide Migration, Presentation given at the HADES Workshop, "30 Years of Underground Research Laboratory," May 23-25, 2011, Antwerp, Belgium.

Makedonska, N., Painter, S. L., Bui, Q. M., Gable, C. W., and Karra, S. (2015), Particle tracking approach for transport in three-dimensional discrete fracture networks. Computational Geosciences, 19(5), pp. 1123-1137.

Marchesini, P., Ajo-Franklin, J.B. and Daley, T. (2017), In situ measurement of velocity-stress sensitivity using crosswell continuous active-source seismic monitoring. Geophysics, Vol 82, N° 5 (September-October 2017), 319-326.

Martin, A. (2021), MaCoTe – Materials Corrosion Test, Presentation given at 19th International Steering Committee Meeting (ISCO 2021), Meeting, September 22, 2021.

Marty, N.C.M., Bildstein, O., Blanc, P., Claret, F., Cochepin, B., Gaucher, E.C., Jacques, D., Lartigue, J.E., Liu, S.H., Mayer, K.U., Meeussen, J.C.L., Munier, I., Pointeau, I., Su, D.Y. and Steefel, C.I. (2015), Benchmarks for Multicomponent Reactive Transport Across a Cement/Clay Interface. Computational Geosciences, 19(3): 635-653.

Matteo, E.N., Dewers, T.A., Jové-Colón, C., Hadgu, T., Gruber, C., Steen, M., Brown, K., Delapp, R., Brown, L., Kosson, D., and Meeussen, J.C.L. (2019), FY19 Progress of EBS International Collaborations, M4SF-19SN010308082, SAND2019-10787 R, 2019.

Matteo, E.N., Dewers, T.A., Gomez, S., Hadgu, T., Klein-Ben David, O., Bar-Nes, G., Meussen, J.C.L., Gruber, C., Steen, M., Brown, K., Delapp, R., Brown, L., Taylor, A., Ayers, J., and Kosson, D.S. (2020a), FY20 Report on Activities for EBS International, M4SF-20SN010308082.

Matteo, E.N., Hadgu, T., Zheng, L., Xu, H., Wainwright, H., Subramanian, N., Voltolini, M., Lammers, L., Gilbert, B., MacDonwell, A., Nichol, J., Lisabeth, H., van Hartesveldt, N., Migissov, A., Strzelecki, A.C., Xu, H., Caporuscio, F., Roback, R., White, J., Buck, E.C., Yu, X.-Y., Yao, J., Reilly, D.D., Son, J., Chatterjee, S.D., McNamara, B.K., IIton, E.S., Claret, F., Gaboreau, S., Ermakova, D., and Gabitov, R. (2020b), Evaluation of Engineered Barrier Systems FY19 Report, SNL, M2SF-20SN010308043, SF-20SN01030808, January 2020.

McMahon, K. (2017), Report on the Status of the SFWST Campaign International Activities in Disposal Research at SNL, Prepared for US Department of Energy, Spent Fuel and Waste Disposition Campaign SFWD-SFWST-2017-000111, Sandia National Laboratories, SAND2017-9048 R.

McMahon, K.A. (2018), Report on the Status of the SFWST Campaign International Activities in Disposal Research at SNL, Prepared for US Department of Energy, Spent Fuel and Waste Disposition Campaign M4SF-18SN010307022, SAND2018-9025 R.

McMahon, K.A. (2019), Report on the Status of the SFWST Campaign International Activities in Disposal Research at SNL, Prepared for US Department of Energy, Spent Fuel and Waste Disposition Campaign M4SF-19SN010307022, SAND2019-8869 R.

McTigue, D.F. (1990), Flow to a heated borehole in porous, thermoelastic rock: Analysis. Water Resources Research, 26(8), 1763-1774.

Meeussen, J.C.L. (2003), ORCHESTRA: An Object-Oriented Framework for Implementing Chemical Equilibrium Models. Environmental Science & Technology 37, 1175-1182.

Meier, T., and Backers, T. (2020), DECOVALEX-2019 – Task G Final Report, Lawrence Berkeley National Laboratory Report, LBNL-2001266.

Mills, M., Kuhlman, K., Matteo, E., Herrick, C., Nemer, M., Heath, J., Xiong, Y., Paul, M., Stauffer, P., Boukhalfa, H., Guiltinan, E., Rahn, T., Weaver, D., Dozier, B., Otto, S., Rutqvist, J., Wu, Y., Ajo-Franklin, J., and Hu, M. (2019), Salt Heater Test (FY19), M2SF-19SN010303031, SAND2019-4814R, Albuquerque, NM: Sandia National Laboratories.

Missana, T., and Geckeis, H. (2006), Grimsel Test Site–Investigation Phase V. The CRR Final Project Report Series II: Supporting Laboratory Experiments with Radionuclides and Bentonite Colloids NAGRA Technical Report Series NTB, 03-02.

Missana, T., Alonso, Ú., and Turrero, M. J. (2003), Generation and stability of bentonite colloids at the bentonite/granite interface of a deep geological radioactive waste repository. Journal of Contaminant Hydrology, 61(1-4), 17-31.

Missana, T., Alonso, U., García-Gutiérrez, M., and Mingarro, M. (2008), Role of bentonite colloids on europium and plutonium migration in a granite fracture. Applied Geochemistry, 23(6), 1484-1497.

Missana, T., Alonso, U., Fernández, A. M., and García-Gutiérrez, M. (2018), Colloidal properties of different smectite clays: Significance for the bentonite barrier erosion and radionuclide transport in radioactive waste repositories. Applied Geochemistry, 97(December 2017), 157–166. https://doi.org/10.1016/j.apgeochem.2018.08.008

Monteiro, P.J.M. and Mehta, P.K. (1986), Interaction between carbonate rock and cement paste. Cement and Concrete Research 16, 127-134.

NAGRA (2010), Grimsel Test Site – Research on Safe Geologic Disposal of Radioactive Waste, Brochure in Recognition of 25 Years of Research at Grimsel Test Site, NAGRA, July 2010.

NAGRA (2014), FEBEX-DP Kick-Off Meeting, Presentation given at the kick-off meeting for the FEBEX-DP project, Thun, Switzerland, June 2014.

NAGRA (2017), Agreement between The US Department of Energy (US DOE) and The National Cooperative for the Disposal of Radioactive Waste (NAGRA), Switzerland on the Phase VI International Experiment HOTBENT (High Temperature Effects on Bentonite), Wettingen, Switzerland, 2017.

NAGRA (2019), Implementation of the Full-scale Emplacement Experiment at Mont Terri: Design, Construction and Preliminary Results. nagra Technical Report 15-02.

NEA, Nuclear Energy Agency (2018), Metadata for Radioactive Waste Management, NEA No. 7378, 2018.

NEA, Nuclear Energy Agency (2019), Preservation of Records, Knowledge and Memory (RK&M) Across Generations, Final Report of the RK&M Initiative, NEA No. 7421, 2019.

NEA, Nuclear Energy Agency (2019a), Preservation of Records, Knowledge and Memory (RK&M) Across Generations, Compiling a Set of Essential Records for a Radioactive Waste Repository, NEA No. 7423, 2019.

NEA, Nuclear Energy Agency (2019b), Preservation of Records, Knowledge and Memory (RK&M) Across Generations, Developing a Key Information File for a Radioactive Waste Repository, NEA No. 7377, 2019.

Nutt, M. (2011), *Used Fuel Disposition Campaign Disposal Research and Development Roadmap, Prepared for U.S. Department of Energy Used Fuel Disposition Campaign*, FCRD-USED-2011- 000065 REV0, Argonne National Laboratory.

NWTRB (2020), Filling the Gaps: The Critical Role of Underground Research Laboratories in the U.S. Department of Energy Geologic Disposal Research and Development Program, A Report to the U.S. Congress and the Secretary of Energy, U.S. Nuclear Waste Technical Review Board, NWTRB, January 2020.

Painter, S. L., Gable, C. W., and Kelkar, S. (2012), Pathline tracing on fully unstructured control-volume grids. Computat. Geosci., 16(4), 1125–1134.

Pedersen, K. (1996), Investigations of subterranean bacteria in deep crystalline bedrock and their importance for the disposal of nuclear waste, Canadian Journal of Microbiology, 42(4), 382-391.

Pedersen, K. (1999), Subterranean microorganisms and radioactive waste disposal in Sweden, Engineering Geology, 52(3-4), 163-176.

Piché-Choquette S, Constant P. Molecular Hydrogen, a Neglected Key Driver of Soil Biogeochemical Processes. Appl Environ Microbiol. 2019 Mar 6;85(6):e02418-18. doi: 10.1128/AEM.02418-18. PMID: 30658976; PMCID: PMC6414374.

Plúa, C., Vitel, M., Seyedi, D.M., and Armand, G. (2020), DECOVALEX-2019 – Task E Final Report, Lawrence Berkeley National Laboratory Report, LBNL-2001265.

Plúa, C., and Armand, G. (2020), DECOVALEX-2023 Task A Specifications: Heat and Gas Fracturing (HGFrac), Task Specification Document for DECOVALEX Project, 20 pp., 2020.

Plúa, C., Vu, M., Armand, G., Rutqvist, J., Birkholzer, J., Xu, H., Guo, R., Thatcher, K., Bond, A., Wang, W., Nagel, T., Shao, H., and Kolditz, O. (2021), A reliable numerical analysis for large-scale modelling of a high-level radioactive waste repository in the Callovo-Oxfordian claystone. Int J Rock Mech Min Sci., 140: 104574.

Pollard, D., and Segall, P. Theoretical displacements and stresses near fractures in rock: With applications to faults, joints, veins, dikes, and solution surfaces. In *Fracture Mechanics of Rock*. Academic Press Inc. (London) Ltd., 1987, ch. 8, pp. 277–349. ISBN 0-12-066265-5

Posiva (2011), Olkiluoto Site Description 2011, Posiva Oy, Report POSIVA 2011.

Pyrak-Nolte, L.J., Myer, L.R. and Cook, N.G.W. (1990), Transmission of seismic-waves across single natural fractures. Journal of Geophysical Research-Solid Earth and Planets 95, 8617–8638.

Ragoussi, M.E., and Brassinnes, S. (2015), The NEA Thermochemical Database Project: 30 Years of Accomplishments. Radiochimica Acta, 2392.

Reedlunn, B. (2020), Status of a New Thermomechanical Constitutive Model for Rock Salt. Memorandum. SAND2020-11023 CTF, Sandia National Laboratories, Albuquerque, NM, USA.

Reimus, P.W. (2012), Preliminary Interpretation of a Radionuclide and Colloid Tracer Test in a Granodiorite Shear Zone at the Grimsel Test Site, Switzerland, Prepared for U.S. Department of Energy Used Fuel Disposition Campaign.

Reimus, P. W., and Boukhalfa, H. (2014), Chancellor Water Colloids : Characterization and Radionuclide Associated Transport (No. LA-UR-14-2). Los Alamos National Laboratory (LANL) Los Alamos, NM (United States).

Reimus, P. W. (2017), Mathematical Basis and Test Cases for Colloid-Facilitated Radionuclide Transport Modeling in GDSA-PFLOTRAN Intended for. Los Alamos National Laboratory, LA-UR-26560. Retrieved from https://permalink.lanl.gov/object/tr?what=info:lanl-repo/lareport/LA-UR-17-26560

Reimus, P.W., Zavarin, M., and Wang, Y. (2016), Colloid-Facilitated Radionuclide Transport: Current State of Knowledge from a Nuclear Waste Repository Risk Assessment Perspective, Prepared for U.S. Department of Energy Used Fuel Disposition Campaign, FCRD-SFWD-2016-000446.

Reimus, P. W., Zavarin, M., and Wang, Y. (2017), Colloid-Facilitated Radionuclide Transport: Current State of Knowledge from a Nuclear Waste Repository Risk Assessment Perspective (No. LA-UR-16-26638). Los Alamos National Laboratory (LANL), Los Alamos, NM (United States).

Reinicke, A., Manukyan, E., Lanyon, B., Finsterle, S., Romero, E., Gisiger, J., Kontar, K., and Roesli, U. (2020), GAST Field and Lab Experiment, Presentation given at 18th International Steering Committee Meeting (ISCO 2020), Grimsel Test Site Phase IV, Virtual Meeting, June 3, 2020.

Reinicke, A., Stopelli, E., Manukyan, E., Lanyon, B., Finsterle, S., Romero, E., Gisiger, J., Kontar, K., and Roesli, U. (2021), GAST Field and Lab Experiment, Presentation given at 19th International Steering Committee Meeting (ISCO 2021), Virtual Meeting, September 22, 2021.

Rice, J.R. (1993), Spatio-temporal complexity of slip on a fault, J. Geophys. Res., 98, 9885–9907.

Rinaldi, A. P., Guglielmi, Y., Zappone, A., Soom, F., Robertson, M., Cook, P., Kakurina, M., Wenning, Q., Rebscher, D., and Nussbaum, C. (2020), Coupled processes in clay during tunnel excavation, EGU General Assembly Vienna, Austria, 4-8 May 2020, EGU2020-184, doi:10.5194/egusphere-egu2020-18041, 2020.

Romero, E., Gonzalez-Blanco, L., Dieudonne, A.C., Marschall, P. (2017), EBS-Task Force: Hydro-mechanical Processes Associated with Gas Transport in MX-80 Bentonite, SKB Task Force, trask Description for Task 7.

Rutqvist, J., Wu, Y.S., Tsang, C.F., and Bodvarsson, G. (2002), A Modeling Approach for Analysis of Coupled Multiphase Fluid Flow, Heat Transfer, and Deformation in Fractured Porous Rock, Int. J. of Rock Mechanics & Mining Sciences, 39, 429–442.

Rutqvist, J., Ijiri, Y., and Yamamoto, H. (2011), Implementation of the Barcelona Basic Model into TOUGH-FLAC for simulations of the geomechanical behavior of unsaturated soils. Computers & Geosciences, 37, 751–762.

Rutqvist, J., Blanco-Martín, L., Mukhopadhyay, S., Houseworth, J., and Birkholzer, J.T. (2014), Modeling Coupled THMC Processes and Brine Migration in Salt at High Temperatures, LBNL-6718E, Lawrence Berkeley National Laboratory.

Rutqvist, J., Zheng, L., Chen, F., Liu, H.-H., and Birkholzer, J.T. (2014a), Modeling of Coupled Thermo-Hydro-Mechanical Processes with Links to Geochemistry Associated with Bentonite-Backfilled Repository Tunnels in Clay Formations. Rock Mechanics and Rock Engineering, 47, 167–186.

Rutqvist, J., Blanco Martin, L., Molins, S., Trebotich, D., and Birkholzer, J.T. (2015), Modeling Coupled THMC Processes and Brine Migration in Salt at High Temperatures. Prepared for U.S. Department of Energy, Used Fuel Disposition, FCRD-UFD-2015-000366, LBNL-191216, Lawrence Berkeley National Laboratory.

Rutqvist, J., Blanco-Martin, L., Hu, M., Molins, S., Trebotich, D., and Birkholzer, J.T. (2016), Modeling Coupled THMC Processes and Brine Migration in Salt at High Temperatures. Prepared for U.S. Department of Energy, Used Fuel Disposition, FCRD-UFD-2016-000439, LBNL-1006308, Lawrence Berkeley National Laboratory.

Rutqvist, J., Hu, M., Blanco-Martín, L., and Birkholzer, J.T. (2017), Coupled THM Modeling In Support of a Phased Salt Field Test Plan, Prepared for US Department of Energy Spent Fuel and Waste Disposition, SFWD-SFWST-2017-000103, Lawrence Berkley National Laboratory, LBNL-2001023

Rutqvist, J., Kim, K., Xu, H., Guglielmi, Y., Birkholzer, J.T. (2018), Investigation of Coupled Processes in Argillite Rock: FY18 Progress, M3SF-18LB010301031, Lawrence Berkeley National Laboratory, LBNL-2001168.

Rutqvist, J., Wu, Y., Hu, M., Commer, M., Wang, J., and Birkholzer, J.T. (2019), Salt Coupled THMC Processes Research Activities at LBNL: FY2019 Progress, Lawrence Berkeley National Laboratory, 2019, LBNL-2001230.

Rutqvist, J., Guglielmi, Y., Xu, H., Tian, Y., Zarzycki, P., Deng, H., Li, P., Hu, M., Nico, P., Borglin, S., Fox, P., and Birkholzer, J.T. (2020), Investigation of Coupled Processes in Argillite Rock: FY20 Progress, M4SF-20LB010301031, SF-20LB01030103 /SF-20LB01030107, LBNL-2001324, May 2020.

Rutqvist, J., Wu, Y., Hu, M., Uhlemann, S., Wang, J., and Birkholzer, J. (2020a), Salt Coupled THMC Processes Research Activities at LBNL: FY20 Progress, Milestone M3SF-20, LB010303022.

Rutqvist J., Graupner B., Guglielmi Y., Kim T., Massmann J., Nguyen T.S., Park J.-W., Shiu W., Urpi L., Yoon J.S., Ziefle G., Birkholzer J. (2020b), An international model comparison study of controlled fault activation experiments in argillaceous claystone at the Mont Terri Laboratory. Int J Rock Mech Min Sci; 136: 104505.

Samper, J., Zheng, L., Montenegro, L., Fernández, A.M., and Rivas, P. (2008), Coupled thermo-hydro-chemical models of compacted bentonite after FEBEX in situ test. Applied Geochemistry 23(5): 1186-1201.

Sánchez, M., Gens, A., and Olivella, S. (2012), THM analysis of a large-scale heating test incorporating material fabric changes. International Journal for Numerical and Analytical Methods in Geomechanics 36(4): 391-421.

Sassani, D., Birkholzer, J.T., Camphouse, C., Freeze, G., and Stein, E. (2020), SFWST Disposal Research 5-Year Plan, Prepared for U.S. Department of Energy, Spent Fuel and Waste Science and Technology Campaign, M2SF-20SN010304045, Sandia National Laboratories, SAND2020-9053R.

Sassani, D., Birkholzer, J.T., Camphouse, C., Freeze, G., and Stein, E. (2021), SFWST Disposal Research 5-Year Plan – FY21 Update, Prepared for U.S. Department of Energy, Spent Fuel and Waste Science and Technology Campaign, M2SF-21SN010304054, Sandia National Laboratories, SAND2021-XXXR.

Seyedi D., Plua C., Vitel M., Armand G., Rutqvist J., Birkholzer J., Xu H., Guo R., Thatcher K., Bond A., Wang W., Nagel T., Shao H., Kolditz O. (2021), Upscaling THM modeling from small-scale to full-scale in-situ experiments in the Callovo-Oxfordian claystone. Int J Rock Mech Min Sci, 144: 104582.

Sevougian, S.D., Mariner, P.E., Connolly, L.A., MacKinnon, R.J., Rogers, R.D., Dobson, D.C., Prouty, J.L. (2019), DOE SFWST Campaign R&D Roadmap Update, Prepared for U.S. Department of Energy, Spent Fuel and Waste Science and Technology Campaign, M2SF-19SN010304042, Sandia National Laboratories, SAND2019-9033R.

Shao, H., Wang, Y., Kolditz, O., Nagel, T., and Bruning, T. (2019), Approaches to Multi-scale Analyses of Mechanically and Thermally-driven Migration of Fluid Inclusions in Salt Rocks, Physics and Chemistry of the Earth, 113, p1-13.

Shi, G. (1992), Manifold method of material analysis. Transaction of the 9th army conference on applied mathematics and computing. U.S. Army Research Office.

Shipton, Z.K., and Cowie, P.A. (2003), A conceptual model for the origin of fault damage zone structures in high-porosity sandstone. Journal of Structural Geology, 25 (3), 333–344. 831.

Sierra/Solid Mechanics, 2021. Sierra/Solid Mechanics User's Guide. 5.0. SAND2021- 2961. Sandia National Laboratories. Albuquerque, NM, USA; Livermore, CA, USA.

Silver, P.G., Daley, T.M., Niu, F., and Majer, E.L. (2007), Active source monitoring of cross-well seismic traveltime for stress-induced changes: Bulletin of the Seismological Society of America, 97, 1B, 281–293; http://dx•.doi.org/10.1785/0120060120.

SKB (2011), Äspö Hard Rock Laboratory Annual Report 2010, SKB Technical Report TR-11-10, February 2011.

Sobolik, S.R., Buchholz, S.A., Keffeler, E., Borglum S., and Reedlunn, B. (2019), "Shear Behavior of Bedded Salt Interfaces and Clay Seams". ARMA 19-040, In: *Proceedings of the 53rd US Rock Mechanics/Geomechanics Symposium*.

Sobolik, S.R., Keffeler, E. and Buchholz, S. (2020), *Shear Behavior of Artificial Clay Seams within Bedded Salt Structures*, Technical Report SAND2020-11959, Sandia National Laboratories, Albuquerque, NM, USA.

Sonnenthal, E. L., Smith, J. T., Cladouhos, T., Kim, J., and Yang L. (2015), Thermal-Hydrological-Mechanical-Chemical Modeling of the 2014 EGS Stimulation Experiment at Newberry Volcano, Oregon. PROCEEDINGS, 40th Workshop on Geothermal Reservoir Engineering. Stanford University, Stanford, California, January 26-28.

Sonnenthal, E., Pettitt, W., Smith T., Riahi, A., Siler D., Kennedy, M., Majer, E., Dobson, P., Ayling, B., Damjanac, B., and Blankenship D. (2018), Continuum Thermal-Hydrological-Mechanical Modeling of the Fallon FORGE Site. GRC Transactions, Vol. 42.

Steefel, C.I., Appelo, C.A.J., Arora, B., Jacques, D., Kalbacher, T., Kolditz, O., Lagneau, V., Lichtner, P.C., Mayer, K.U., Meeussen, J.C.L., Molins, S., Moulton, D., Shao, H., Šimůnek, J., Spycher, N., Yabusaki, S.B., and Yeh, G.T. (2015), Reactive transport codes for subsurface environmental simulation. Computational Geosciences 19, 445-478.

Steefel, C.I. and Tournassat, C. (2021), A model for discrete fracture-clay rock interaction incorporating electrostatic effects on transport. Computational Geosciences, 25, 395-410.

Stein, E. (2020), DECOVALEX-2023, Task F Overview, Presentation given at the DECOVALEX-2023 Spring 2020 Virtual Meeting, April 30, 2020.

Stein, E., Leone, R., and Nguyen, S. (2020), DECOVALEX-2023, Task F Specification, Task Specification Document for DECOVALEX Project, Prepared for U.S. Department of Energy Spent Fuel and Waste Disposition Campaign, SAND2020-8494, Sandia National Laboratories, 54 pp., 2020.

Sugita, Y. (2020), DECOVALEX-2023, Task D: Full-scale Engineered Barrer System Experiment at Horonobe URL, Task Specification Document for DECOVALEX Project, 2020.

Tamayo-Mas E., Harrington J.F., Bruning T., Shao H., Dagher E.E., Lee J., Kim K., Rutqvist J., Kolditz O., Lai S.H., Chittenden N., Wang Y., Damians I.P. and Olivella S. (2021), Modelling advective gas flow in compact bentonite: lessons learnt from different numerical approaches. Int J Rock Mech Min Sci; 139: 104580.

Tarì, G., Olhero, S. M., Ferreira, J. M. F. (2000), Influence of temperature of electrostatically stabilized alumina suspensions. Journal of Colloid and Interface Science, 231, 221-227. https://doi.10.1006/jcis.2000.7112.

Telfeyan, K., Reimus, P. W., Boukhalfa, H., and Ware, S. D. (2020), Aging effects on Cesium-137 (^{137}Cs) sorption and transport in association with clay colloids. Journal of Colloid and Interface Science, 566, 316-326. https://doi.org/10.1016/j.jcis.2020.01.033

Thatcher, K., and Graupner, B. (2020), DECOVALEX-2023, Task C Specification: THM Modelling of the FE Experiment, Task Specification Document for DECOVALEX Project, 25 pp., 2020.

Tournassat, C., and Appelo, C.A.J. (2011), Modelling approaches for anion-exclusion in compacted Na-bentonite. Geochimica et Cosmochimica Acta 75, 3698-3710.

Tournassat, C., Steefel, C.I., Bourg, I.C., and Bergaya, F. (2015), Natural and engineered clay barriers. Elsevier.

Tournassat, C., and Steefel, C.I. (2019a), Modeling diffusion processes in the presence of a diffuse layer at charged mineral surfaces: a benchmark exercise. Computational Geosciences.

Tournassat, C., and Steefel, C.I. (2019b), Reactive Transport Modeling of Coupled Processes in Nanoporous Media. Reviews in Mineralogy and Geochemistry 85, 75-109.

Tsang, C.F., Stephansson, O., Jing, L. and Kautsky, F. (2009), DECOVALEX Project: from 1992 to 2007, Environmental Geology, 57, 1221–1237, 2009.

Tsang, C.F., Rosberg, J.E., Sharma, P., Berthet, T., Juhlin, C., and Niemi, A. (2016), Hydrologic Testing During Drilling: Application of the Flowing Fluid Electrical Conductivity (FFEC) Logging Method To Drilling of a Deep Borehole. Hydrogeology Journal 24, 1333–1341.

Turrero, M.J. and Cloet, V. (2017), FEBEX-DP Concrete ageing, concrete/bentonite and concrete/rock interaction analysis. Arbeitsbericht NAB 16-18.

UFD (2012), Office of Used Nuclear Fuel Disposition International Program – Strategic Plan, April 2012, U.S. Department of Energy.

Ulusay, R. and Hudson, J.A. (1978), Suggested methods for determining tensile strength of rock materials. Part 2: Suggested method for determining indirect tensile strength by the Brazil test. Int J Rock Mech Min Sci Geomech Abstr 15 99-103.

U.S. EPA (2017a), Method 1313, Liquid-solid partitioning as a function of extract pH using a parallel batch extraction procedure.

U.S. EPA (2017b), SW-846 Test Method 1315: Mass Transfer Rates of Constituents in Monolithic or Compacted Granular Materials Using a Semi-Dynamic Tank Leaching Procedure, Washington, D.C.

Van der Sloot, H., Seignette, P., Meeussen J., Hjelmar, O., and Kosson, D. (2008), A database, speciation modelling and decision support tool for soil, sludge, sediments, wastes and construction products: LeachXS™-Orchestra, Second international symposium on energy from biomass and waste, Venice.

Van Loon, L.R., Soler, J.M., and Bradbury, M.H. (2003), Diffusion of HTO, 36Cl− and 125I− in Opalinus Clay samples from Mont Terri: Effect of confining pressure. Journal of Contaminant Hydrology 61, 73-83.

Van Marcke, P. and Bastiaens, W. (2010), Construction of the PRACLAY Experimental Gallery at the Hades URF, Clay in Natural and Engineered Barriers for Radioactive Waste Confinement, 4th International Meeting, March, 2010, Nantes, France.

Vilarrasa, V., Rutqvist, J., Blanco-Martin, L., and Birkholzer, J. (2015), Use of a Dual Structure Constitutive Model for Predicting the Long-Term Behavior of an Expansive Clay Buffer in a Nuclear Waste Repository. Int. J. Geomech., D4015005.

Villar, M., García-Siñeriz, J.L., Bárcena, I., and Lloret, A. (2005), State of the Bentonite Barrier after Five Years Operation of an inSitu Test Simulating a High Level Radioactive Waste Repository. Engineering Geology. 80. 175-198. 10.1016/j.enggeo.2005.05.001.

Villar, M.V., Fernandez, A.M., Romero, E., Dueck, A., Cuevas, J., Plotze, M., Kaufhold, S., Dohrmann, R., Iglesias, R.J., Sakaki, T., Voltolini, M., Zheng, L., Kawamoto, K. and Kober, F. (2017a), FEBEX-DP Post-mortem THM/THG Analysis Report, NAGRA Arbeitsbericht NAB 16-17. NAGRA, Wettingen, Switzerland, pp. 187 pp.

Villar, M.V., Iglesias, R.J., Abós, H., Martínez, V., de la Rosa, C., Manchón, M.A. (2017b), FEBEX-DP on-site analyses report. Nagra NAB 16-12, Wettingen, Switzerland.

Villar, M.V., Iglesias, R. J., and Luis, G.-S. J. (2020), State of the in situ FEBEX test (GTS, Switzerland) after 18 years: a heterogeneous bentonite barrier. Environmental Geotechnics 7(2): 147-159.

Viswanathan, H., Chu, C., Dittrich, T., Hyman, J., Karra, S., Makendonska, N., and Reimus, P. (2016), Crystalline and Crystalline International Disposal Activities, prepared for U.S. Department of Energy Used Fuel Disposition Campaign, FCRD-SFWD-2016-000626, Los Alamos National Laboratory.

Viswanathan, H., Boukhalfa, H., Chu, S., Makendonska, N., Hyman, J., Karra, S., Reimus, P., Telfeyan, K. (2019), Crystalline and Crystalline International Disposal Activities (LA-UR-19-24954). Los Alamos National Laboratory (LANL).

Viswanathan, H., Chu, S., Hoinville, A.R., Hyman, J., and Karra, S. (2020), Crystalline and Crystalline International Disposal Activities, LANL, M4SF-20LA01032021, SF-20LA01030202, Los Alamos National Laboratory Report No. LA-UR-20-24944, July 2020.

Vomvoris, S., Birkholzer, J.T., Zheng, L., Gays, I., and Blechschmidt, I. (2015), THMC Behavior of Clay-Based Barriers Under High Temperature – from Laboratory to URL Scale, Proceedings, International High-Level Radioactive Waste Management Conference, Charleston, NC, USA, April 12-16, 2015.

Wan, J.M., and Wilson, J.L. (1994), Visualization of rhe Role of the Gas-Water Interface on the Fate and Transport of Colloids in Porous-Media, Water Resources Research, 30(1), 11-23.

Wang, Y. (2010), Natural System Evaluation and Tool Development – FY10 Progress Report, Prepared for U.S. Department of Energy Used Fuel Disposition Campaign, August 2010, Sandia National Laboratories.

Wang, J. (2014), On Area-Specific Underground Research Laboratory for Geological Disposal of High-Level Radioactive Waste in China, Journal of Rock Mechanics and Geotechnical Engineering, 6, pp. 99-104.

Wang, Y. (2016), On Subsurface Fracture Opening and Closure, J. Petroleum Sci. Eng., 155, 46-53.

Wang, Y., Gardner, P., Kuhlman, K.L., Kim, G.-Y., and Ji, S.-H. (2014), International Collaborations on Fluid Flow in Fractured Crystalline Rocks: FY14 Progress Report, Prepared for U.S. Department of Energy Used Fuel Disposition Campaign, FCRD-UFD-2014-000499, Sandia National Laboratories.

Wenning, Q.C., Berthet, T., Ask, M., Zappone, A., Rosberg, J.-E., and Almqvist, B.S.G. (2017), Image Log Analysis of In Situ Stress Orientation, Breakout Growth, And Natural Geologic Structures to 2.5 km Depth in Central Scandinavian Caledonides: Results from the COSC-1 borehole. Journal of Geophysical Research Solid Earth 122, 3999–4019.

Wenning, Q.C., Madonna, C., Zappone, A., Grab, M., Rinaldi, A.P., Plotze, M., and Wiemer, S. (2020), Shale fault zone structure and stress dependent anisotropic permeability and seismic velocity properties (Opalinus Clay, Switzerland). Journal of Structural Geology, 104273.

Wersin, P., Johnson, L.H., and McKinley, I.G. (2007), Performance of the Bentonite Barrier at Temperatures Beyond 100°C: A Critical Review. Physics and Chemistry of the Earth, 32, 780-788.

Wilson, J.C., Benbow, S., Sasamoto, H., Savage, D. and Watson, C. (2015), Thermodynamic and Fully-Coupled Reactive Transport Models of a Steel-Bentonite Interface. Applied Geochemistry.

Witherspoon, P.A., Cook, N.G.W., and Gale, J.E. (1981), Geologic Storage of Radioactive Waste: Field Studies in Sweden. Science 211 (4485), 894–500.

Wynants-Morel, N., Cappa, F., De Barros, L., and Ampuero, J.P. (2020), Stress Perturbation from Aseismic Slip Drives The Seismic Front During Fluid Injection In A Permeable Fault, J. Geophys. Res., doi:10.1029/2019JB019179.

Xie, M.L., Mayer, K.U., Claret, F., Alt-Epping, P., Jacques, D., Steefel, C., Chiaberge, C. and Simunek, J. (2015), Implementation and Evaluation of Permeability-Porosity and Tortuosity-Porosity Relationships Linked to Mineral Dissolution-Precipitation. Computational Geosciences, 19(3): 655-671.

Xu, T., Spycher, N., Sonnenthal, E., Zhang, G., Zheng, L., and Pruess, K. (2011), TOUGHREACT Version 2.0: A Simulator for Subsurface Reactive Transport under Non-Isothermal Multiphase Flow Conditions. Computers & Geosciences 37(6): 763-774.

Xu, T., Sonnenthal, E., Spycher, N., and Zheng, L. (2014), TOUGHREACT V3.0-OMP Reference Manual: A Parallel Simulation Program for Non-Isothermal Multiphase Geochemical Reactive Transport, LBNL Report.

Zappone, A., Rinaldi, A.P., Grab, M., Wenning, Q., Roques, C., and Madonna, C. (2020), Fault sealing and caprock integrity for CO_2 storage: an in-situ injection experiment. Solid Earth Discussions, 1–51.

Zavarin, M., Wolery, T., and Atkins-Duffin, C. (2016), Thermodynamic Database Development and Sorption Database Integration, Prepared for U.S. Department of Energy Used Fuel Disposition Campaign, M4FT-16LL080302051, Lawrence Livermore National Laboratory.

Zavarin, M., Balboni, E., Booth, C., Wolery, T., and Atkins-Duffin, C. (2018), Thermodynamic Database Development and Identification of Actinide Sequestration in Corrosion Products, M4SF-18LL010302082, LLNL.

Zavarin, M., Atkins-Duffin, C., Bourcier, W., and Carle, S. F. (2019), International Thermodynamics Activities, M4SF-19LL010302082, LLNL-TR-778561, 2019.

Zavarin M., Atkins-Duffin, C., Bourcier, W., and Carle, S.F. (2020), Thermodynamic Database for Generic Disposal System Assessment, LLNL, M4SF-20LL010302082, SF-20LL010301081, LLNL-TR-812024, June 2020.

Zhang, F., Ye, W. M., Chen, Y. G., Chen, B., and Cui, Y. J. (2016), Influences of salt solution concentration and vertical stress during saturation on the volume change behavior of compacted GMZ01 bentonite. Engineering Geology, 207, 48–55. https://doi.org/10.1016/j.enggeo.2016.04.010

Zheng, L., Samper, J., and Montenegro, L. (2011), A Coupled THC Model of the FEBEX In Situ Test with Bentonite Swelling and Chemical and Thermal Osmosis. Journal of Contaminant Hydrology 126(1–2): 45-60.

Zheng, L., Rutqvist, J., Kim, K., and Houseworth, J. (2015), Investigation of Coupled Processes and Impact of High Temperature Limits in Argillite Rock. Prepared for U.S. Department of Energy, Used Fuel Disposition, FCRD-UFD-2015-000362. LBNL-187644, Lawrence Berkeley National Laboratory.

Zheng, L., Kim, K., Xu, H., and Rutqvist, J. (2016), DR Argillite Disposal R&D at LBNL, Prepared for U.S. Department of Energy Used Fuel Disposition Campaign, FCRD-SFWD-2016-000437, Lawrence Berkeley National Laboratory.

Zheng, L., Rutqvist, J., Xu, H., Kim, K., Voltolini, M., Cao, X. (2017), Investigation of Coupled Processes and Impact of High Temperature Limits in Argillite Rock: FY17 Progress, Prepared for U.S. Department of Energy, Used Fuel Disposition SFWD-SFWST-2017-000040, Lawrence Berkeley National Laboratory, 2017.

Zheng, L., Xu, H., Fox, P., Nico, P., and Birkholzer, J. (2018), Engineered Barrier System Research Activities at LBNL: FY18 Progress Report. SFWD-SFWST-2018-000040, LBNL-200117. Lawrence Berkeley National Laboratory.

Zheng, L., Xu, H., and Birkholzer, J.T. (2018a), THMC Modeling in Support of HotBENT, an Experiment Studying the Effects of High Temperatures on Clay Buffers/Near-field, NAGRA Working Report, NAB 18-032, 2018, Switzerland.

Zheng, L., Xu, H., Fox, P., Nico, P., and Birkholzer, J.T. (2018b), Engineered Barrier System Research Activities at LBNL: FY18 Progress Report, M3SF-18LB010308022, Lawrence Berkeley National Laboratory, LBNL-200117.

Zheng, L., Deng, H., Nakagawa, S., Kim, K., Kneafsey, T., Dobson, P., Borglin, S., Doughty, C., Tsang, C-F., Dessirier, B., Wenning, Q., and Juhlin, C. (2018c), Crystalline Disposal R&D at LBNL, M4SF-18LB010302031.

Zheng, L., Fox, P., Zarzycki, P., Sonnenthal, E., Borglin, S., Chang, C., Chou, C., Wu, Y., Xu, H., Nico, P., Gilbert, B., Kneafsey, T., Cheng, Y., and Birkholzer, J. (2019a), Engineered Barrier System Research Activities at LBNL Via International Collaboration: FY19 Progress Report, M3SF-19LB010308061, LBNL-2001210, 2019.

Zheng, L., H. Xu, J. Rutqvist, M. Reagan, J. Birkholzer, M. V. Villar, and A. M. Fernández (2019b), The hydration of bentonite buffer material revealed by modeling analysis of a long-term in situ test. Applied Clay Science, 105360.

Zheng, L., Lammers, L., Fox, P., Chang, C., Xu, H., Borglin, S., Whittaker, M., Chou, C., Tournassat, C., Subramanian, N., Wu, Y., Nico, P., Gilbert, B., and Kneafsey, T. (2020), Engineered Barrier System Research Activities at LBNL via international collaboration: FY19-FY20 progress report, LBNL M3SF-20LB010308062, SF-20LB01030806, LBNL-2001331, June 2020.

Zheng, L., Xu, H., Rutqvist, J., Reagan, M., Birkholzer, J.T., Villar, M.V., and Fernández, A.M. (2020a), The Hydration of Bentonite Buffer Material Revealed by Modeling Analysis of a Long-Term In Situ Test, Applied Clay Sciences, 185, 105360.

Zimmerman, R. W. and Bodvarsson, G.S. (1996), Hydraulic conductivity of rock fractures. Transport Porous Med., 23 (1), 1–30.

Zoback, M., Kohli, A., Das, I., and McClure, M. (2012), The Importance of Slow Slip on Faults During Hydraulic Fracturing Stimulation of Shale Gas Reservoirs. Society of Petroleum Engineer, SPE155476, The Americas Unconventional Resources Conference, Pittsburgh, Pennsylvania, USA, 5-7 June 2012.

Zhou, Y., Rajapakse, R.K.N.D., and Graham, J. (1999), Coupled Field in a deformable unsaturated medium. International Journal of Solid and Structures, 36: 4841-4868.

Zuidema, P. (2007), Advancements in Deep Geological Disposal of Radioactive Waste through International Cooperation: The Role of Underground Laboratories – Mont Terri Project, Proceedings of the 10 Year Anniversary Workshop, pp 69-71, Rep. Swiss Geol. Surv. 2.